Vol. 64 November, 1960 No. 11

THE JOURNAL OF PHYSICAL CHEMISTRY

(Registered in U. S. Patent Office)

CONTENTS

Stanley Bruckenstein and L. M. Mukherjee: Equilibria in Ethylenediamine. I. The Relative Dissociation Constants of Silver Salts and Alkal Metal Halides 1601
David White, Thor Rubin, Paul Camky and H. L. Johnston: The Virial Coefficients of Helium from 0 to 300 K. 1607
Robert R. Mod, Frank C. Magne and Ewald L. Skau: Freezing Point Data for a Portion of the Ternary System: Acetamide-Palmitic Acid-Stearic Acid 1613
Marjorie J. Vold: The Sediment Volume in Dilute Dispersions of Spherical Particles 1616
M. J. Vold and D. V. Rathnamma: The Subsidence Rates of Suspensions of Lithium Stearate in *n*-Heptane with *n*-Alcohols as Additives 1619
Thomas J. Hardwick: The Reactivity of Hydrogen Atoms in the Liquid Phase 1623
D. L. Leussing and P. K. Gallagher: The Heats and Entropies of Formation of the Copper (II) Pyridine Complexes 1637
Jean H. Futrell: Gas Phase Radiolysis of *n*-Pentane 1634
K. U. Ingold: Inhibition of Oil Oxidation by 2,6-Di-*tert*-butyl-4-substituted Phenols 1636
R. H. Aranow and L. Witten: The Environmental Influence on the Behavior of Long Chain Molecules 1643
Franklin J. Wright: Flash Photolysis of Carbon Disulfide and its Photochemically Initiated Oxidation 1648
H. H. Hyman, Arlene Kaganove and J. J. Katz: The Basicity of Amino Acids in D_2O 1653
Lowell G. Tensmeyer, Reinhard W. Hoffmann and G. W. Brindley: Infrared Studies of Some Complexes between Ketones and Calcium Montmorillonite 1655
Assa Lifshitz and B. Perlmutter-Hayman: The Kinetics of the Hydrolysis of Chlorine. I. Re-investigation of the Hydrolysis in Pure Water 1663
Elias Klein, J. Keith Bosarge and Irwin Norman: Spectrophotometric Determination of Fast Xanthate Decomposition Kinetics 1666
J. R. McNesby: Kinetic Isotope Effects in the Reaction of Methyl Radicals with Ethane, Ethane-d_6 and Ethane-1,1,1-d_3 1671
J. A. Van Lier, P. L. de Bruyn and J. Th. G. Overbeek: The Solubility of Quartz 1675
J. F. Ditter, E. B. Klusmann, J. C. Perrine and I. Shapiro: Mass Spectra of Deuterated Diboranes 1682
Henry F. Bartolo and Frederick D. Rossini: Heats of Isomerization of the Seventeen Isomeric Hexenes 1685
J. R. Sams, Jr., G. Constabaris and G. D. Halsey, Jr.: Second Virial Coefficients of Neon, Argon, Krypton, and Xenon on a Graphitized Carbon Black 1689
Thaddeus L. Kolski and George W. Schaeffer: Etherates of Lithium Borohydride. IV. The System Lithium Borohydride-Tetrahydrofuran 1696
Herbert A. Pohl, Robert Bacskai and William P. Purcell: Steric Order and Dielectric Behavior in Polymethyl-methacrylates. 1701
Ralph A. Zingaro and W. B. Witmer: Infrared Studies of Amine-Halogen Interactions 1705
Meyer M. Markowitz, Daniel A. Boryta and Robert F. Harris: The Differential Thermal Analysis of Perchlorates. V. A Spurious Heat Effect 1711
Harry P. Leftin: Electronic Spectra of Adsorbed Molecules: Stable Carbonium Ions on Silica Alumina 1714
D. Mackay: The Tortuosity Factor of a Water-Swollen Membrane 1718
K. R. Lynn and Peter E. Yankwich: Kinetics of the Reactions of Sodium Cyanide with Some Alkyl Iodides 1719
W. D. Johnston, R. R. Heikes and J. Petrolo: The Preparation of Fine Powder Hexagonal Iron Carbide and its Coercive Force 1720
Dimitrios M. Speros and Frederick D. Rossini: Heats of Combustion and Formation of Naphthalene, the Two Methyl-naphthalenes, *cis* and *trans* Decahydronaphthalene, and Related Compounds 1723
Eli S. Freeman, David A. Anderson and Joseph J. Campisi: The Effects of X-Ray and γ-Ray Irradiation on the Thermal Decomposition of Ammonium Perchlorate in the Solid State 1727
Edwin M. Larsen and Donald R. Vissers: The Exchange of Li^+, Na^+ and K^+ with H^+ on Zirconium Phosphate 1732
Linda Warner Diller, Raymond L. Orr and Ralph Hultgren: Thermodynamics of the Lead-Antimony System 1736
Leonard I. Katzin and Elsie Gulyas: Dissociation Constants of Tartaric Acid with the Aid of Polarimetry 1739
R. R. Irani and C. F. Callis: Metal Complexing by Phosphorus Compounds. II. Solubilities of Calcium Soaps of Linear Carboxylic Acids 1741
Jeff C. Davis, Kenneth S. Pitzer and C. N. R. Rao: Nuclear Magnetic Resonance Studies of Hydrogen Bonding. II. Alcohols 1744
Robert G. Charles: Copper Chelate Polymers Derived from Tetraacetylethane 1747
D. J. Currie and A. R. Gordon: Transference Numbers for Concentrated Aqueous Sodium Chloride Solutions ..... 1 ·1
Morton Z. Hoffman and Richard B. Bernstein: Isotope Effects in $Hg(6^3P_1)$-Photosensitized Reactions: $H_2 + N_2O$ and $H_2 + NO$ 1753
Fred Cartan and Charles N. Caughlan: Electric Moments of the Simple Alkyl Orthovanadates 1756

Notes

Louis Watts Clark: The Decarboxylation of the Trichloroacetate Ion in *n*-Butyl Alcohol, *n*-Hexyl Alcohol and *n*-Caproic Acid 1758
R. W. Nicholls: On the Nature of Ultraviolet Light which Accompanies the Decomposition of Some Azides 1760
J. W. Nielsen and E. F. Dearborn: The Growth of Large Single Crystals of Zinc Oxide 1762
Robert T. Grimley and John L. Margrave: The High Temperature Heat Content of Sodium Oxide 1763
Karl H. Gayer and Rudy M. Haas: Hydrolysis of Cadmium Chloride at 25° 1764
Norman Sutin: The Absorption Spectrum of Ferric Perchlorate and the Rate of the Ferrous-Ferric Exchange Reaction in Isopropyl Alcohol 1766

(Continued on inside cover)

THE JOURNAL OF PHYSICAL CHEMISTRY

(Registered in U. S. Patent Office)

Published monthly by the American Chemical Society at 20th and Northampton Sts., Easton, Pa.

Second-class mail privileges authorized at Easton, Pa. This publication is authorized to be mailed at the special rates of postage prescribed by Section 131.122.

The *Journal of Physical Chemistry* is devoted to the publication of selected symposia in the broad field of physical chemistry and to other contributed papers.

Manuscripts originating in the British Isles, Europe and Africa should be sent to F. C. Tompkins, The Faraday Society, 6 Gray's Inn Square, London W. C. 1, England.

Manuscripts originating elsewhere should be sent to W. Albert Noyes, Jr., Department of Chemistry, University of Rochester, Rochester 20, N. Y.

Correspondence regarding accepted copy, proofs and reprints should be directed to Assistant Editor, Allen D. Bliss, Department of Chemistry, Simmons College, 300 The Fenway, Boston 15, Mass.

Business Office: Alden H. Emery, Executive Secretary, American Chemical Society, 1155 Sixteenth St., N. W., Washington 6, D. C.

Advertising Office: Reinhold Publishing Corporation, 430 Park Avenue, New York 22, N. Y.

Articles must be submitted in duplicate, typed and double spaced. They should have at the beginning a brief Abstract, in no case exceeding 300 words. Original drawings should accompany the manuscript. Lettering at the sides of graphs (black on white or blue) may be pencilled in and will be typeset. Figures and tables should be held to a minimum consistent with adequate presentation of information. Photographs will not be printed on glossy paper except by special arrangement. All footnotes and references to the literature should be numbered consecutively and placed in the manuscript at the proper places. Initials of authors referred to in citations should be given. Nomenclature should conform to that used in *Chemical Abstracts*, mathematical characters be marked for italic, Greek letters carefully made or annotated, and subscripts and superscripts clearly shown. Articles should be written as briefly as possible consistent with clarity and should avoid historical background unnecessary for specialists.

Remittances and orders for subscriptions and for single copies, notices of changes of address and new professional connections, and claims for missing numbers should be sent to the American Chemical Society, 1155 Sixteenth St., N. W., Washington 6, D. C. Changes of address for the *Journal of Physical Chemistry* must be received on or before the 30th of the preceding month.

Claims for missing numbers will not be allowed (1) if received more than sixty days from date of issue (because of delivery hazards, no claims can be honored from subscribers in Central Europe, Asia, or Pacific Islands other than Hawaii), (2) if loss was due to failure of notice of change of address to be received before the date specified in the preceding paragraph, or (3) if the reason for the claim is "missing from files."

Subscription Rates (1960): members of American Chemical Society, $12.00 for 1 year; to non-members, $24.00 for 1 year. Postage to countries in the Pan-American Union $0.80; Canada, $0.40; all other countries, $1.20. Single copies, current volume, $2.50; foreign postage, $0.15; Canadian postage $0.05; Pan-American Union, $0.05. Back volumes (Vol. 56–59) $25.00 per volume; (starting with Vol. 60) $30.00 per volume; foreign postage, per volume $1.20, Canadian, $0.15; Pan-American Union, $0.25. Single copies: back issues, $3.00; for current year, $2.50; postage, single copies: foreign, $0.15; Canadian, $0.05; Pan American Union, $0.05.

The American Chemical Society and the Editors of the *Journal of Physical Chemistry* assume no responsibility for the statements and opinions advanced by contributors to This Journal.

The American Chemical Society also publishes *Journal of the American Chemical Society, Chemical Abstracts, Industrial and Engineering Chemistry*, International Edition of *Industrial and Engineering Chemistry, Chemical and Engineering News, Analytical Chemistry, Journal of Agricultural and Food Chemistry, Journal of Organic Chemistry, Journal of Chemical and Engineering Data* and *Chemical Reviews*. Rates on request.

Aimery Caron and Jerry Donohue: The X-Ray Powder Pattern of Rhombohedral Sulfur 1767
Elmer J. Huber, Jr., Earl L. Head, and Charles E. Holley, Jr.: The Heat of Combustion of Lutetium 1768
Morton Z. Hoffman and Richard B. Bernstein: Note on the $Hg(6^3P_1)$-Photosensitized Decomposition of Nitric Oxide 1769
H. Edelhoch: The Properties of Thyroglobulin. III. The Titration of Thyroglobulin in Sodium Dodecyl Sulfate 1771
C. C. McCune, F. Wm. Cagle, Jr., and S. S. Kistler: The Effect of Hydrostatic Pressure on the Rate of Racemization of *l*-6-Nitro-2,2′-carboxybiphenyl 1773
D. G. Tuck: The Polarizability of Radon 1775
Ronald M. Milburn and Henry Taube: The Reduction of Oxalate by Chromium(II) 1776
George T. Armstrong and Sidney Marantz: The Heat of Combustion of Dicyanoacetylene 1776
A. A. Maryott and G. Birnbaum: Non-resonant Microwave Absorption and Relaxation Frequency at Elevated Pressures 1778
James P. Hoare: Note on the Solution of Hydrogen in Palladium Wires 1780
Kurt H. Stern and Marijon Bufalini: Mechanism of the Isothermal Decomposition of Potassium Perchlorate 1781
George S. Hammond, Albrecht W. Moschel and Wilfred G. Bordium: Chelates of β-Diketones. IV. Acidity of Dibenzoylmethanes 1782
Peter Rentzepis, David White and Patrick N. Walsh: The Reaction between $B_2O_3(l)$ and $C_{(s)}$: Heat of Formation of $B_2O_{2(g)}$ 1784
J. D. Vaughn and E. L. Muetterties: Thermochemistry of Sulfur Tetrafluoride 1787
H. Bradford Thompson and Craig W. Lawson: Electric Moments and Rotational Conformations of Halogenated Propanes and Related Compounds 1788
L. J. Hughes and W. F. Yates: Pyrolysis of Allyl Chloride 1789

Communications to the Editor

I. R. Miller: Polyelectrolyte Concentration on Polarized Mercury Surface 1790
Gerald Perkins, Jr., R. B. Escue, James F. Lamb and J. Wayne Wimberley: Self-Diffusion in Molten $PbCl_2$ 1792

THE JOURNAL OF
PHYSICAL CHEMISTRY

VOLUME 64 DECEMBER 1, 1960 NUMBER 11

EQUILIBRIA IN ETHYLENEDIAMINE. I. THE RELATIVE DISSOCIATION CONSTANTS OF SILVER SALTS AND ALKALI METAL HALIDES

BY STANLEY BRUCKENSTEIN AND L. M. MUKHERJEE

School of Chemistry, University of Minnesota, Minneapolis, Minnesota

Received December 7, 1959

The relative dissociation constants of a series of silver salts and alkali metal halides has been determined potentiometrically in ethylenediamine using cells of the type Reference electrode//AgX(C_1)/Ag and Reference electrode//AgX(C_1). MX(C_2)/Ag. Silver chloride was found to exhibit typical weak electrolyte behavior and the absolute value of its dissociation constant is estimated to be less than 10^{-5}. The values of $pK_{AgCl} - pK_{MX}$ for the specified MX are: LiCl, −0.33; NaCl, −0.18; KCl, −0.01; RbCl, +0.03; CsCl, +0.22; AgBr, −0.63; LiBr, −0.67; NaBr, −0.50; KBr, −0.72; RbBr, −0.69; CsBr, −0.60; AgI, −1.35; LiI, −0.46; NaI, −0.24, KI, −0.23; RbI, −0.42; CsI, −0.36; $(n\text{-}C_4H_9)_4NI$, −0.44; AgOAc, +0.88; AgSCN, +1.03 and $AgNO_3$, 1.34. Silver iodide reacts with both sodium potassium, rubidium and cesium iodides according to the reaction AgI + MI ⇄ AgI·MI. The equilibium constants for the reaction as written are 1.33, 1.13, 1.60 and 1.58 for sodium, potassium, rubidium and cesium iodides, respectively. Silver cyanide is monomeric in ethylenediamine and dissociates into silver and argentocyanide ($Ag(CN)_2^-$) ions.

Introduction

This study was undertaken with the ultimate goal of calculating acid–base protolysis (neutralization) curves in anhydrous ethylenediamine (EDA) as a solvent. EDA is a strongly basic liquid with a freezing point of 11.0°,[1a] a boiling point of 117.2°[1b] and a dielectric constant of 12.9[1a] It is extremely hydroscopic, reacts rapidly with atmospheric carbon dioxide in the presence of water to form a carbamate,[1c] and must be manipulated under an inert atmosphere.

Moss, Elliot and Hall[2a] were the first to recognize the potentialities of EDA as a solvent for the titration of weak acids, and numerous practical applications[2b,c,d,e,f] for the determination of extremely weak acids have been reported since their work. Only two previous studies dealing with equilibria of uni-univalent salts in EDA have been made, both by conductance methods; Bromley and Luder[3a] studied silver nitrate and iodide and potassium iodide while Hibbard and Schmidt[3b] studied the nitrates and iodides of silver, sodium and tetra-*n*-butylammonium ions. In these studies the Fuoss–Kraus method was used to obtain the dissociation constant and the limiting equivalent conductance of the salts, and it was found that most salts have dissociation constants less than 10^{-3}.

Hibbard and Schmidt's[3b,4] quantitative interpretation of their data leads to two unusual results: (1) Kohlraush's law of independent mobility of ions is not obeyed by nitrate and iodide ions; (2) The observed and calculated Onsager slopes do not agree.

There is no obvious explanation for these two results. As a first step towards explaining the shapes of protolysis curves in EDA, it was decided to investigate a series of silver and alkali metal salts, including some of the compounds studied by Hibbard and Schmidt using potentiometric methods. The results of this potentiometric study using cells with liquid junction are reported below.

Theoretical

Equilibria in AgX Solutions.—It is possible to explain the potentiometric results that have been obtained on the basis of the equilibrium.

$$AgX \rightleftharpoons Ag^+ + X^- \qquad (1)$$

(1) (a) L. F. Audrieth and J. Kleinberg, "Non-Aqueous Solvents," John Wiley and Sons, Inc., New York, N. Y., 1953, p. 119; (b) "Lange's Handbook of Chemistry," Handbook Publishers, Inc., Sandusky, Ohio, 1949, p. 516; (c) E. Schering, German Patent 123,138 (July 30, 1901).

(2) (a) M. L. Moss, J. H. Elliot and R. T. Hall, *Anal. Chem.*, **20**, 874 (1948); (b) J. S. Fritz, *ibid.*, **24**, 674 (1952); (c) M. Katz and R. A. Glenn, *ibid*, **24**, 1157 (1952); (d) H. Brockmann and E. Meyer, *Naturwiss.*, **40**, 242 (1953); (e) R. A. Glenn and J. T. Peak, *Anal. Chem.*, **27**, 205 (1955); (f) A. J. Martin, *ibid.*, **29**, 79 (1957).

(3) (a) W. H. Bromley and W. F. Luder, *J. Am. Chem. Soc.*, **66**, 107 (1944); (b) B. B. Hibbard with F. C. Schmidt, *ibid.*, **77**, 225 (1955).

(4) B. B. Hibbard, Ph.D. Dissertation, Indiana University, p. 83, 1951.

using the thermodynamic dissociation constant of the silver compound, K_{AgX}

$$K_{AgX} = a_{Ag^+} a_{X^-}/a_{AgX} \quad (2a)$$

Assuming that the activity coefficient of undissociated AgX is one

$$K_{AgX} = a_{Ag^+}a_{X^-}/C_{AgX} \quad (2b)$$

If we also assume that the activity coefficients of $[Ag^+]$ and $[X^-]$ are the same, equation 2c is obtained

$$a_{Ag^+} = \sqrt{K_{AgX}C_{AgX}} = \sqrt{K_{AgX}\{(C_{AgX})_t - [Ag^+]\}} \quad (2c)$$

where $(C_{AgX})_t = C_{AgX} + [Ag^+]$.

K_{AgX} Very Small.—When K_{AgX} is very small, $(C_{AgX})_t >> [Ag^+]$ and the simple expression

$$a_{Ag^+} = \sqrt{K_{AgX}(C_{AgX})_t} \quad (2d)$$

is applicable. Equation 2d is analogous to the relation between hydrogen ion concentration and the dissociation constant or concentration of a weak acid in aqueous solution.

The e.m.f. of a cell with liquid junction, such as Cell I

Cell I: Ref. Elect. (EDA)//AgX($C = (C_{AgX})_t$)(EDA)/Ag

may be written as

$$E_{AgX} = E^0_{Ag,Ag^+} + E_{lj} + E_{Ref.\ Elect.} + \frac{RT}{F} \ln a_{Ag^+} \quad (3a)$$

where E_{lj} is the liquid junction potential. If it is assumed that E_{lj} is independent of AgX or $(C_{AgX})_t$, equation 3b results.

$$E_{AgX} = E^{0\prime} + \frac{RT}{F} \ln a_{Ag^+} \quad (3b)$$

where $E^{0\prime} = E^0_{Ag,Ag^+} + E_{lj} + E_{Ref.\ Elect.}$ Substitution of equation 2d into 3b yields equation 4a.

$$E_{AgX} = E^{0\prime} + \frac{RT}{2F} \ln K_{AgX}(C_{AgX})_t \quad (4a)$$

This expression predicts that the e.m.f. of a silver electrode in a solution of a weakly dissociated silver salt will decrease 0.0296 volt per ten-fold dilution at 25.0°. We find that silver iodide, bromide and chloride belong to this class of very weakly dissociated silver salts in EDA.

K_{AgX} Very Large.—Qualitatively it is seen that as K_{AgX} becomes very large, the equilibrium concentration of silver ion will approach the analytical concentration of AgX and that $a_{Ag^+} \approx (C_{AgX})_t$. Thus a plot of E *vs.* log $(C_{AgX})_t$ will approach a limiting slope of 0.05916 volt at 25°, as compared to a slope of 0.0296 volt when K_{AgX} is very small. We find the slopes obtained for silver nitrate, thiocyanate and acetate to be intermediate between these two extremes, indicating that K_{AgX} lies somewhere between the two extreme cases.

K_{AgX} Intermediate in Value.—Only semi-quantitative conclusions can be drawn concerning the silver nitrate, thiocyanate and acetate data. The primary difficulty is estimating the single ion activity coefficient of the silver ion at the relatively high concentrations necessary to obtain reproducible potentiometric results. If one assumes that the limiting Debye–Hückel law is valid, the single ion activity coefficient of Ag^+ at 25° may be calculated from equation 4b.

$$-\log f_{Ag^+} = 7.61\ (\mu)^{1/2} \quad (4b)$$

and equation 2c, for any assumed value of K_{AgX}. It is then possible to calculate a_{Ag^+} and construct a plot of log a_{Ag^+} *vs.* log $(C_{AgX})_t$ for the particular assumed value of K. This curve may then be superimposed on the actual experimental data plotted as E *vs.* log $(C_{AgX})_t$. After a series of trials, a value of K can be found which produces a theoretical curve which superimposes on the experimental data fairly well. The data for silver nitrate have been treated this way and the detailed results given in the Discussion.

Pseudo Strong Electrolyte Behavior.—Another possible equilibrium scheme which will yield a slope of RT/F volt when E *vs.* ln $(C_{AgX})_t$ is plotted is

$$2AgX \rightleftharpoons Ag^+ + AgX_2^- \quad (5a)$$

This yields equation 5b

$$a_{Ag^+} \cong (C_{AgX})_t\sqrt{K} \quad (5b)$$

if the activity coefficients of Ag^+ and AgX_2^- are assumed equal and $(C_{AgX})_t >> [Ag^+]$, where $K = a_{Ag^+}a_{AgX_2^-}/a^2_{AgX}$. We find that silver cyanide dissociates according to the equilibrium scheme shown in equation 5a. If silver cyanide were present in EDA primarily as a dimeric species, *i.e.*, Ag_2CN_2 or $Ag^+AgCN_2^-$, the predicted E *vs.* $\ln(C_{AgCN})_t$ slope would be $RT/2F$.

Relative pK Values of Silver Salts.—The difference in the pK values at 25° of two slightly dissociated silver salts, AgX and AgX′, is found directly from equation 4a to be

$$pK_{AgX} - pK_{AgX'} = (E_{AgX'} - E_{AgX})/0.0296 \quad (6)$$

when $(C_{AgX})_t = (C_{AgX'})_t$.

Equilibria in Solutions of AgX and MX.—In an EDA solution containing both a silver salt, AgX, and the corresponding alkali metal salt, MX, the rule of electroneutrality is

$$[Ag^+] + [M^+] = [X^-] \quad (7a)$$

assuming that no complications such as the formation of ion triplets, etc., occurs. We shall assume that the activity coefficient of these three ions are all identical, therefore equation 7a yields equation 7b

$$a_{Ag^+} + a_{M^+} = a_{X^-} \quad (7b)$$

We define the dissociation constant of MX in the same way as for AgX and make similar assumptions concerning species present and activity coefficients; *i.e.*, $K_{MX} = (a_{M^+}a_{X^-})/C_{MX}$. Eliminating a_{M^+} and a_{X^-} from equation 7b by using K_{AgX} and K_{MX}, the silver ion activity in a mixture of AgX and MX is given by equation 7c

$$(a_{Ag^+})_{AgX,MX} = \sqrt{\frac{K_{AgX}C_{AgX}}{1 + \dfrac{K_{MX}C_{MX}}{K_{AgX}C_{AgX}}}} \quad (7c)$$

The e.m.f. of Cell II

Cell II: Ref. Elect. (EDA)//AgX($C = (C_{AgX})_t$), MX ($C = (C_{MX})_t$)(EDA)/Ag

is

$$E_{AgX,MX} = E^{0\prime} + \frac{RT}{F} \ln \sqrt{\frac{K_{AgX}C_{AgX}}{1 + \dfrac{K_{MX}C_{MX}}{K_{AgX}C_{AgX}}}} \quad (7d)$$

The e.m.f. of an EDA solution containing only AgX with an equilibrium concentration C_{AgX} of the silver salt is given by equation 7e

$$E_{AgX} = E^{0\prime} + \frac{RT}{F} \ln \sqrt{K_{AgX} C_{AgX}} \qquad (7e)$$

Thus the difference in e.m.f. between a pure solution of silver salt and a solution of a silver and alkali metal salt is

$$\Delta E = E_{AgX} - E_{AgX,MX} = \frac{RT}{F} \ln \sqrt{\left\{1 + \frac{K_{MX} C_{MX}}{K_{AgX} C_{AgX}}\right\} R} \qquad (7f)$$

where R is the ratio of equilibrium concentration of AgX in a solution of AgX to the equilibrium concentration of AgX in a solution of AgX and MX. Usually R is one and equation 7g results

$$\Delta E = \frac{RT}{F} \ln \sqrt{1 + \frac{K_{MX} C_{MX}}{K_{AgX} C_{AgX}}} \qquad (7g)$$

In the case where both the alkali metal salt and the silver salt are extremely slightly dissociated, one may use the analytical concentrations, $(C_{AgX})_t$ and $(C_{MX})_t$ in the place of the equilibrium concentrations to calculate the ratio K_{MX}/K_{AgX} from ΔE using equation 7g. Equation 7g has been used successfully with silver chloride and Li, Na, K, Rb and Cs chlorides, silver bromide and Li, Na, K, Rb, Cs bromides. It was found that it was not possible to explain the behavior of the alkali metal iodides in this simple fashion.

In the case of Na, K, Rb and Cs iodides, it was assumed that the reaction

$$AgI + MI \rightleftarrows AgI \cdot MI \qquad (8a)$$

occurred. ($K_{MI \cdot AgI} = C_{AgI \cdot MI}/C_{AgI}C_{MI}$). Thus, while, equation 7d is still valid

$$C_{AgI} = (C_{AgI})_t - C_{AgI \cdot MI} \qquad (8b)$$

and

$$C_{MI} = (C_{MI})_t - C_{AgI \cdot MI} \qquad (8c)$$

It is possible to obtain values for K_{AgI}/K_{MI} and $K_{MI \cdot AgI}$ which fit the experimental results quite closely. The method of calculation used is described below.

Equation 7d gives the e.m.f. of a solution containing C_{AgI} and C_{MI} in terms of the equilibrium concentration of silver and alkali metal halide. If $E^*_{AgI,MI}$ is defined as the e.m.f. of a solution containing the same analytical concentration of AgI, but an analytical concentration $(C_{MI})^*_t$ of alkali iodide, then

$$\Delta E^* = E_{AgI,MI} - E^*_{AgI,MI} = \frac{RT}{F} \ln \sqrt{\frac{C_{AgX}}{C^*_{AgX}} \left[\frac{1 + K_{MX} C^*_{MX}/K_{AgX} C^*_{AgX}}{1 + K_{MX} C_{MX}/K_{AgX} C_{AgX}}\right]} \qquad (8d)$$

where the superscript asterisks signify equilibrium concentrations in the solution containing $(C^*_{MI})_t$ M alkali metal iodide.

A further simplification is possible if $1 << K_{MX} C^*_{MX}/K_{AgX} C^*_{AgX}$ and $K_{MX} C_{MX}/K_{AgX} C_{AgX}$. Under these conditions equation 7f reduces to

$$\Delta E^* = \frac{RT}{F} \ln \frac{C_{AgX}}{C^*_{AgX}} \sqrt{\frac{C^*_{MX}}{C_{MX}}} \qquad (8e)$$

In our experiments, the concentration of alkali metal iodide is normally much larger than that of the silver iodide, so it is convenient to assume as a starting point that $C_{MX}/C^*_{MX} \approx (C_{MX})^*_t/(C_{MX})_t$ and calculate an approximate value for C_{AgX}/C^*_{AgX} from equation 8e and ΔE^*.

This value of C_{AgI}/C^*_{AgI} may be related to $K_{MI \cdot AgI}$ using equation 8b. Substituting for $C_{AgI \cdot MI}$ in equation 8b from $K_{MI \cdot AgI}$, the following expression is obtained

$$\frac{C_{AgI}}{C^*_{AgI}} = \frac{1 + K_{MI \cdot AgI} C^*_{MI}}{1 + K_{MI \cdot AgI} C_{MI}} = \frac{1 + K_{MI \cdot AgI}[(C^*_{MI})_t - C^*_{MI \cdot AgI})]}{1 + K_{MI \cdot AgI}[(C_{MI})_t - C_{MI \cdot AgI})]} \qquad (8f)$$

Equation 8f can be expressed approximately as

$$\frac{C_{AgI}}{C^*_{AgI}} \approx \frac{1 + K_{MI \cdot AgI}(C^*_{MI})_t}{1 + K_{MI \cdot AgI}(C_{MI})_t} \qquad (8g)$$

and a first approximation to $K_{MI \cdot AgI}$ obtained.

Using the approximate value of $K_{MI \cdot AgI}$ obtained as described above, $C^*_{MI \cdot AgI}$, C^*_{MI}, $C_{MI \cdot AgI}$ and C_{MI} were calculated and equations 8e and 8f used to obtain a better value for $K_{MI \cdot AgI}$. This procedure was used until a constant value for $K_{MI \cdot AgI}$ was obtained. In all cases only two approximations were needed. $K_{MI \cdot AgI}$ was calculated from equation 7f using the equilibrium concentrations derived from $K_{MI \cdot AgI}$. The values of $K_{MI}C_{MI}/K_{AgI}C_{AgI}$ were always much greater than one, justifying the use of equation 8e rather than 8d. If this were not the case, it would be necessary to recalculate all our constants using equation 8d and a successive approximation technique. The e.m.f. data obtained for Na, K, Rb and Cs iodides were treated in this manner and values of K_{MI}/K_{AgI} and $K_{MI \cdot AgI}$ obtained.

Experimental

Reagents. EDA.—Commercially available EDA, both Dow 98% and Eastman Kodak 95–100%, contains at least two impurities which absorb in the ultraviolet region. For example, the Dow product when dissolved in ethanol has an absorption maximum in the vicinity of 265 mμ and a distinct absorption band at about 311 mμ. In a two-cm. cell, liquid EDA as supplied by Dow or Eastman Kodak will not transmit appreciably below 340 mμ. Conventional purification of EDA by preliminary drying over KOH, BaO and finally distillation over sodium in a CO_2-free nitrogen atmosphere did not significantly improve the spectra. This product was treated with sodium borohydride, activated alumina, silica gel, cation and anion exchange resins, silver oxide and potassium permanganate in an attempt to decrease the ultraviolet absorbance. No significant change in spectrum was noted after any of these treatments. Multiple extraction of EDA with purified cyclohexane indicated that the impurities could be extracted with difficulty. This approach was not pursued further, since probably only trace amounts of highly absorbing materials are present, and would not interfere in our potentiometric measurements. We did not note any difference in our potentiometric results for EDA samples which contained widely different concentrations of the absorbing impurities. Fractional crystallization did not appear to be more satisfactory than fractional distillation on the basis of the spectra of the EDA obtained.

Fractional distillation of EDA over sodium metal in a dry, carbon dioxide-free nitrogen atmosphere yielded progressive improvement in the ultraviolet spectrum of EDA. In our early work, the fraction boiling between 114–117° was collected, shaken with freshly baked Alcoa F-20 activated alumina (20 g./l. EDA), the alumina allowed to settle, the supernatant EDA transferred to a distilling flask and fractionated in a dry, carbon dioxide-free nitrogen atmosphere at a reflux ratio of 1:20. The fraction boiling at 117.2° was used. In our later work, the preliminary sodium treatment was omitted as there was no significant difference

TABLE I

LEAST-SQUARES CONSTANTS FOR EQUATION 9

Anion	E^*, v.	A	E (0.01 M)	$pK_{AgCl} - pK_{AgX}$
Nitrate	0.1763 ± 0.0020	0.0378 ± 0.0008	0.1008 ± 0.0006	1.34
Thiocyanate	.1640 ± .0045	.0361 ± .0028	.0918 ± .0017	1.03
Acetate	.1528 ± .0016	.0329 ± .0009	.0870 ± .0005	0.88
Chloride	.1192 ± .0009	.0290 ± .0006	.0611 ± .0007	.00
Bromide	.1087 ± .0016	.0331 ± .0012	.0424 ± .0011	− .63
Iodide	.0787 ± .0015	.0287 ± .0009	.0213 ± .0007	−1.35
Cyanide	.1424 ± .0027	.0603 ± .0018	.0218 ± .0012	

in water contents obtained with and without sodium treatment. Kaiser KA 101 activated alumina is also satisfactory. It is supplied as small pellets, and minimizes bumping during the fractionation.

The purified EDA was stored in a sealed reservoir under a nitrogen atmosphere, and dispensed under nitrogen pressure as needed. The moisture content of this EDA was checked periodically by Karl Fischer titration.[5] It was found necessary to cool the methanol–acetic acid mixture in which the EDA is dissolved in an ice–salt mixture. The Karl Fischer titration was carried out while the EDA solution was cooled in this same ice–salt mixture. If these precautions were not taken, erroneously high water contents were found. Presumably, the heat evolved when acetic acid reacts with EDA or the pyridine in the Karl Fischer reagent increases the rate of esterification of methanol with acetic acid, with the subsequent production of water. The water content of the EDA used in this investigation varied between 0.055 and 0.075 M.

The specific conductances of two samples of purified EDA with water contents of 0.0538 and 0.0390 M water were, respectively, 1.46×10^{-6} ohm^{-1}cm.$^{-1}$ and 0.96×10^{-6} ohm^{-1}cm.$^{-1}$. Typical values obtained by other workers are 1.4×10^{-6} to 2.6×10^{-6},[6] 9×10^{-8} [3a] and 2×10^{-7} [3b] at 25°. The specific conductance is not a precise measure of the water content. For example, two different samples of EDA, one containing 0.054 M water and the other 0.12 M water had the same specific conductance of 1.7×10^{-6}.

Silver Salts.—Silver bromide, iodide, cyanide, thiocyanate and acetate were all prepared by reacting reagent grade silver nitrate with a slight excess of the corresponding alkali metal salt. The precipitates were thoroughly washed with hot distilled water. Silver acetate was recrystallized twice from hot water. The salts were dried at approximately 110° *in vacuo* for 10 to 12 hours.

The silver chloride used was Mallinckrodt A. R. reagent. All silver compounds were protected from light during storage.

Alkali Metal Compounds.—All were of A.R. or C.P. grade and dried for 10–12 hours *in vacuo* at approximately 110° before use. The compounds are listed below with their source. A. D. Mackay: LiI, RbCl, RbBr, CsCl, CsBr and CsI; Coleman and Bell: LiBr; Mallinckrodt: NaCl, NaBr, KCl; J. T. Baker: LiCl, NaI; Baker and Adams: KI; Merck: KBr; and Fisher: RbI.

Tetra-*n*-butylammonium Iodide.—An Eastman Kodak product was recrystallized twice from ethanol and dried overnight at 50°.

Preparation of Solutions.—Solutions were generally prepared immediately before use in a dried volumetric flask using a technique described earlier.[4] When solutions were not used immediately, they were stored in dry, carbon dioxide-free atmosphere in a tightly stoppered volumetric flask. In some cases all manipulations had to be carried out in a dry box free of carbon dioxide in order to obtain reproducible results.

Potentiometric Methods. Indicator Electrode.—The indicator electrode consisted of platinum wire freshly coated with silver by electrolysis of aqueous $KAg(CN)_2$ and washed free of cyanide with conductivity water. Normally, six such electrodes were short-circuited together while submerged in a dilute aqueous silver nitrate solution. Just before use they were washed thoroughly with water, then acetone and allowed to air-dry.

Reference Electrode.—A calomel electrode could not be prepared in EDA because mercurous chloride instantaneously reacts with EDA to give a black precipitate. The reference electrode used consisted of a mercury pool in contact with an EDA solution saturated with respect to both *mercuric* chloride and lithium chloride. The lithium chloride was added to decrease the resistance of the reference electrode. Peacock, Schmidt, Davis and Schaap[7] reported that mercuric chloride reacts with EDA, opposite to our observations. Isbin and Kobe[8] determined the solubility of mercuric chloride in EDA and make no mention of any reaction with EDA, even though they reported a reaction between mercuric chloride and ethanolamine. This electrode is termed a saturated corrosive sublimate electrode (SCSE). Duplicate reference electrodes agreed to within several tenths of a millivolt.

Half-cells.—The indicator and reference half-cell have been described previously.[9] The salt bridge contained an EDA solution saturated with respect to both mercuric and lithium chlorides.

E.M.F. Determination.—The apparatus described previously[9] was used with one modification. A Radiometer TTla Titrator replaced the Beckman Model H-2 *p*H meter as the null indicator. Using a 30 microampere meter (internal resistance 167 ohms) across the recorder output terminals of the Radiometer Titrator, an unbalance of 10 microvolts is detectable.

The silver half-cells were allowed to equilibrate in air thermostat (T = 25.0 ± 0.1°) for 10 to 12 hours before forming the liquid junction. 10 to 15 minutes after the liquid junction was formed, e.m.f. readings were taken. Successive readings were made at 10- to 15-minute intervals. Ordinarily, the mean of the first four readings was taken as the e.m.f. The average deviation of the mean was usually about ±0.2 mv. The reproducibility of duplicate experiments is not nearly as good as 0.2 mv. because of the difficulties in handling and preparing EDA solutions.

Results

The results obtained with silver nitrate, acetate, thiocyanate, chloride, bromide, iodide and cyanide using Cell I are given in Table I. In all cases the data can be represented by a straight line of the form

$$E = E^* + A \log (C_{AgX})_t \qquad (9)$$

Using the method of least squares, E^* and A of equation 9 were obtained and are given in Table I along with the standard deviations of both these constants. (E^* is the e.m.f. when $(C_{AgX})_t = 1\ M$). Also listed are e.m.f. values at $(C_{AgX})_t = 0.0100\ M$ calculated from the least-square lines, and $pK_{AgCl} - pK_{AgX}$ calculated from equation 9 using the e.m.f. value at $(C_{AgX})_t = 0.0100\ M$.

The dissociation constants of the chlorides, bromides and iodides of lithium, sodium, potassium, rubidium and cesium and tetra-*n*-butylammonium iodide with respect to the dissociation constant of silver chloride were determined using Cell II. Tables II, III and IV list the experimen-

(5) J. Mitchell and D. M. Smith, "Aquametry," Interscience Publishers, Inc., New York, N. Y., 1948, p. 126.

(6) G. L. Putnam and K. A. Kobe, *Trans. Electrochem. Soc.*, **74**, 609 (1938).

(7) J. Peacock, F. C. Schmidt, R. E. Davis and W. B. Schaap, *J. Am. Chem. Soc.*, **77**, 5829 (1955).

(8) H. S. Isbin and K. A. Kobe, *ibid.*, **67**, 464 (1945).

(9) S. Bruckenstein and I. M. Kolthoff, *ibid.*, **78**, 2974 (1956).

tal results obtained with the various chlorides, bromides and iodides, respectively. The mean values of $pK_{AgCl} - pK_{MX}$, as calculated in Tables II, III and IV are listed in Table VI.

TABLE II

ΔE OF SILVER CHLORIDE AND ALKALI METAL CHLORIDE MIXTURES

Alkali metal	C_{AgCl}[a]	C_{MCl}[a]	ΔE, v.	Log K_{MCl}/K_{AgCl}[c]	Mean $pK_{AgCl} - pK_{MCl}$
Lithium	0.01000	0.01105	0.0245	−0.28	
	.00170	.00940	.0170	− .30	
	.00100	.00550	.0150	− .40	−0.33 ± 0.05
Sodium	.00338	.0352	.0270	− .16	
	.00340	.0176	.0185	− .20	− .18 ± .02
Potassium	.00100	.00190	.0135	− .01	
	.00100	.00180	.0130	− .01	− .01 ± .00
Rubidium	.000530	.000960	.0135	+ .04	
	.000522	.000995	.0144	+ .03	
	.000522	.000995	.0144	+ .03	+ .03 ± .00
Cesium	.000530	.000710	.0150	+ .23	
	.000466	.000595	.0145	+ .21	+ .22 ± .01

[a] Moles/liter. [b] ΔE = e.m.f. difference between Cell I and Cell II, both containing same $(C_{AgCl})_t$. [c] Calculated from equation 7f.

TABLE III

ΔE OF SILVER BROMIDE AND ALKALI METAL BROMIDE MIXTURES

Alkali metal	C_{AgBr}[a]	C_{MBr}[a]	ΔE,[b] v.	Log K_{MB}/K_{AgBr}[c]	Mean $pK_{AgCl} - pK_{MBr}$
Lithium	0.0105	0.0930	0.0280	−0.05	
	.0105	.0280	.0160	− .03	−0.67 ± 0.04
Sodium	.0105	.1220	.037	+ .16	
	.0105	.0610	.027	+ .09	− .50 ± .04
Potassium	.00475	.00830	.0110	− .11	
	.00475	.00744	.0110	− .06	− .72 ± .03
Rubidium	.000705	.00222	.0200	+ .06	
	.000705	.00075	0070	+ .17	− .69 ± .12
Cesium	.00705	.00188	.0195	+ .12	
	.000705	.00102	.0105	− .06	− .60 ± .09

[a] Moles/liter. [b] ΔE = e.m.f. difference between Cell I and Cell II, both containing same $(C_{AgBr})_t$. [c] Calculated from equation 7f.

Discussion

From Table I it is seen that the order of the over-all dissociation constants of the silver salts are $AgNO_3 > AgCNS > AgOAc > AgCl > AgBr > AgI$. (Silver cyanide is discussed below and is omitted from the present discussion.) Within the experimental error the slopes obtained indicate that silver chloride, silver bromide and silver iodide are all very weakly dissociated in EDA. Silver nitrate, acetate and thiocyanate have dissociation constants sufficiently large to yield slopes significantly greater than the theoretical value for weak electrolytes, 0.0296. This fact must be kept clearly in mind when the relative dissociation constants of these compounds referred to silver chloride are calculated from equation 6, as was done to obtain the final column of Table I.

In an attempt to obtain potentiometric estimates of the over-all dissociation constants of silver nitrate we have calculated the silver ion activities for various analytical concentrations of silver nitrate, assuming values for K_{AgNO_3} of 4×10^{-4}, 5×10^{-4}, 6×10^{-4} and 10×10^{-4}. In the manner described in the Theoretical section, a_{Ag^+} is calculated and a plot of $\log a_{Ag^+}$ *vs.* $\log (C_{AgNO_3})_t$ made and superimposed upon the experimentally determined E *vs.* $\log (C_{AgNO_3})_t$ plot. As is seen in Fig. 1 and 2, none of the calculated curves fit the experimental data at the higher concentrations of silver nitrate. However, below 0.02 M silver nitrate there is rather good agreement for a calculated curve based upon a dissociation constant of 5×10^{-4}. This result is in surprisingly good agreement with Hibbard and Schmidt's conductometric value of 5.74×10^{-4}.[3b]

It must be emphasized that the reliability of the dissociation constant of silver nitrate obtained in this manner depends entirely upon the validity of the Debye–Hückel limiting law. As an example of the numerical value of silver ion activity coefficients predicted at the concentrations of silver nitrate for which the calculated results are in

TABLE IV

SILVER IODIDE AND ALKALI METAL AND TETRA-*n*-BUTYLAMMONIUM IODIDE MIXTURES

Cation	$(C_{AgI})_t$[a]	$(C_{MI})_t$[a]	ΔE,[b] v.	$K_{MI \cdot AgI}$	Log K_{MI}/K_{AgI}[c]	Mean $pK_{AgCl} - pK_{LiI}$
Lithium	0.0251	0.2600	0.0595		0.98	
	.0251	.1280	.0494		.95	
	.00840	.0667	.0544		.94	
	.00840	.0334	.0433		.84	
	.00840	.0167	.0343	..	.83	−0.46 ± 0.06
$(C_4H_9)_4N$	.1000	.2980	.0410		.88	
	.1000	.1990	.0375		.94	
	.05175	.1985	.0455		.94	
	.05175	.0992	.0362		.91	
	.05175	.0397	.0226	..	.79	− .44 ± .05
Sodium	.05075	.4810	.0740		1.13	
	.05075	.2405	.0600		1.11	
	.05075	.0962	.0440		1.13	
	.05075	.0600	.0355	1.33	1.06	− .24 ± .02
Potassium	.05185	.4770	.0730		1.15	
	.05185	.2385	.0590		1.14	
	.05185	.0954	.0435	1.13	1.09	− .23 ± .02
Rubidium	.0509	.0411	.0273		0.94	
	.0509	.1028	.0395		.93	
	.04175	.4450	.0725		.94	
	.0251	.1200	.0526		.86	
	.0251	.2540	.0667	1.60	.94	− .42 ± .03
Cesium	.04175	.4550	.0720		1.01	
	.0251	.2460	.0661		0.98	
	.0251	.1528	.0570		.95	
	.0096	0374	.0480	1.58	.98	− .36 ± .02

[a] Moles/liter. [b] ΔE = e.m.f. difference between Cell I and Cell II, both containing same $(C_{AgI})_t$. [c] Calculated from equation 7f, corrected for MI·AgI formation in the case of Na, K, Rb and Cs.

TABLE V

COMPARISON BETWEEN OBSERVED AND CALCULATED ΔE AT VARYING CONCENTRATIONS OF SILVER IODIDE IN 0.5875 M POTASSIUM IODIDE

Initial concn. (M) KI	Initial concn. (M) AgI	ΔE (v) Obsd.	ΔE (v) Calcd.
0.5875	0.2065	0.0595	0.0574
.5875	.1032	.0505	.0485
.5875	.0516	.0410	.0425
.5875	.0258	.0315	.0335

TABLE VI

MEAN VALUES OF $pK_{AgCl} - pK_{MX}$ IN ETHYLENEDIAMINE

Anion	Cation Li	Na	K	Rb	Cs
Cl	−0.33	−0.18	−0.01	+0.03	+0.22
Br	− .67	− .50	− .72	− .69	− .60
I	− .46	− .24	− .23	− .42	− .36

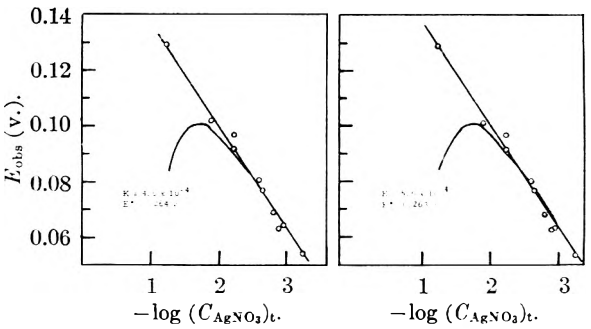

Fig. 1.—Comparison of experimental and calculated E *vs.* log $(C_{AgNO_3})_t$ plots. The assumed value of K_{AgNO_3} and the value of E^0 which gives the best fit is indicated in the figure, *i.e.*, $K = 4.0 \times 10^{-4}$ and $E^0 = 0.264$ v. and $K = 5.0 \times 10^{-4}$ and $E^0 = 0.263$ v.

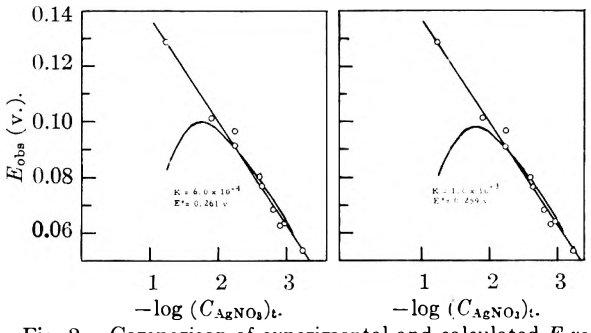

Fig. 2.—Comparison of experimental and calculated E *vs.* log $(C_{AgNO_3})_t$ plots. The assumed value of K_{AgNO_3} and the value of E^0 which gives the best fit is indicated in the figure, *i.e.*, $K = 6.0 \times 10^{-4}$ and $E^0 = 0.261$ v. and $K = 1.0 \times 10^{-3}$ and $E^0 = 0.259$ v.

agreement with the experimental curve, we calculate

$$f_{Ag^+} = 0.1735 \text{ when } (C_{AgNO_3})_t = 0.01602\ M$$
$$f_{Ag^+} = 0.6759 \text{ when } (C_{AgNO_3})_t = 0.000730\ M$$

The values of $(C_{AgNO_3})_t$ used represent the extreme limits for which theory and experiment agree when $K_{AgNO_3} = 5 \times 10^{-4}$. Since there is some uncertainty in this approach, all dissociation constants were referred to that of silver chloride rather than assigning an absolute value.

The value of pK_{AgCl}–pK_{AgX} for the various silver salts does not depend on the validity of the Debye–Hückel limiting law, but only on equation 6 and the assumption that $f_{Ag^+} = f_{X^-}$. In the case of AgCl, AgBr and AgI there is no good reason to question either of these assumptions.

The observed order of dissociation constants for silver chloride, bromide and iodide indicate that a simple ion pair picture cannot explain the results. At least two approaches to interpret the observed order are possible. In the first one, we may invoke the possibility of polarization (covalent overlap). In the second, one may assume that more than one type of undissociated species may exist at equilibrium, *i.e.*, an ion pair with at least one solvent molecule between the silver and halide ions and the other a species with no solvent between the silver and halide ions. These two species correspond to the solvent separated and the intimate ion pairs.[10] One might expect the bonding in the intimate ion pair to be described qualitatively in terms of the electronegativity difference between the cation and anion composing the intimate ion pair, *i.e.*, the per cent, ionic or covalent character.[10d] Either approach results in agreement with experiment. The potentiometric method is not capable of deciding which approach is correct in this case.

Davies[11] has tabulated the dissociation constants of silver nitrate and silver chloride in aqueous solutions. This tabulation indicates that the pK_{AgAc} is about 0.9 pK unit larger than pK_{AgNO_3} in aqueous solution as compared to 0.5 unit in EDA. As a first approximation one would expect the difference in pK's of these compounds to be the same in water and EDA since there should be no effect of dielectric constant when comparing the dissociation constant of compounds with identical charge.

Jonte and Martin[12] have calculated K_{AgCl} in aqueous solutions to be 5.1×10^{-4}. Combining this value for K_{AgCl} with Davies' tabulated value for K_{AgNO_3}, $pK_{AgCl} - pK_{AgNO_3} = 3.4$ in water, as compared to 1.3 in EDA. The comparison in this case shows only qualitative agreement.

Silver cyanide displays a pseudo strong electrolyte behavior in that the plot of E *vs.* log $(C_{AgCN})_t$ is a straight line with slope 0.060 (see equation 5b). This compound cannot be a strong electrolyte because the e.m.f.'s observed for all experimental concentrations of silver cyanide are lower than that of the e.m.f. of a corresponding silver nitrate solution; *i.e.*, the activity of silver in silver cyanide solutions is always less than the activity of silver in a corresponding silver nitrate solution. Since silver nitrate is a weak electrolyte with a dissociation constant of the order of 5×10^{-4}, silver cyanide must be a still more weakly dissociated compound. The observed slope is predicted by equation 5b if silver cyanide dissociates into silver ions and $AgCN_2^-$ ions. This result is in accord with the well-known high stability of the $AgCN_2^-$ ion in aqueous solution.

In the alkali metal chloride experiments (Table II), as the size of the alkali metal ion increases, K_{MCl} also increases. This is the result expected on the basis of a simple ion pair picture assuming the sizes of the solvated alkali metal ions increase continuously with atomic number.

In the alkali metal bromide series, no clear trend is obvious from Table III.

Table IV presents the data obtained for lithium, sodium, potassium, rubidium, cesium and tetra-*n*-butylammonium iodides. Lithium and tetra-*n*-butylammonium iodides appear to show normal behavior, while sodium, potassium, rubidium and cesium iodides seem to form the species MI·AgI. Using the method described in the Theoretical section, $K_{MI\cdot AgI}$ values for sodium, potassium, rubi-

(10) (a) E. Grunwald, *Anal. Chem.*, **26**, 1696 (1954). (b) S. Winstein, E. Clippinger, A. H. Fainberg and G. C. Robinson, *Chemistry and Industry*, 664 (1954). (c) S. Winstein, E. Clippinger, A. H. Fainberg, R. Heck and G. C. Robinson, *J. Am. Chem. Soc.*, **78**, 328 (1956). (d) L. Pauling, "Nature of the Chemical Bond," Second Edition, Cornell University Press, Ithaca, N. Y., 1941, p. 73.

(11) C. W. Davies, "The Structure of Electrolytic Solutions," edited by W. J. Hamer, John Wiley and Sons, Inc., New York, N. Y., 1959, p. 26.

(12) J. H. Jonte and D. S. Martin, *J. Am. Chem. Soc.*, **74**, 2052 (1952).

dium and cesium iodides were found to be 1.33, 1.13, 1.60 and 1.58, respectively.

In order to test the validity of our treatment of alkali metal iodide–silver iodide mixtures, solutions containing varying concentrations of silver iodide were studied at fixed potassium iodide concentration (0.5875 M) and ΔE calculated from the values of K_{KI}/K_{AgI} and $K_{MI\cdot AgI}$ obtained from the data in Table IV. As is seen in Table V, the agreement between observed and calculated values of ΔE is excellent even though the concentration of potassium iodide in these solutions is greater than in any solution used to evaluate the various constants.

The $pK_{AgCl} - pK_{MI}$ values given in Tables IV and VI are corrected for the formation of MI·AgI. The value of $pK_{AgCl} - pK_{MI}$ increases in going from lithium to potassium and then decreases for rubidium and cesium. This trend indicates that some unknown effect in addition to polarization or intimate ion pair formation is operative.

Comparing the effect of anion on pK_{MX} when M is fixed, it is seen from Table VI that the order of dissociation constants is $K_{MCl} > K_{MI} > K_{MBr}$ for all the alkali metal ions. An explanation of these results on the basis of only polarization effects does not seem possible. However, invoking the possibility of the existance of intimate and solvent separated ion pairs in EDA, it is apparent that the predicted lower stability of an alkali metal chloride intimate ion pair might lead to greater dissociation than for the alkali metal iodides and bromides.

Hibbard and Schmidt[3b] calculated K_{AgNO_3}, K_{AgI}, K_{NaI} and K_{Bu_4NI} from their conductance data. The values of $pK_{MX} - pK_{NaI}$ are 1.51, 0.11 and 0.03 for silver iodide, tetra-*n*-butylammonium iodide and silver nitrate, respectively. Our potentiometric data yield + 1.11, +0.20 and −1.6 for $pK_{MX} - pK_{NaI}$ for silver iodide, tetra-*n*-butylammonium iodide and silver nitrate, respectively. The agreement between our results and Hibbard and Schmidt's results is not very good.

Our calculation of the absolute value of K_{AgNO_3} is in very good agreement with Hibbard and Schmidt's value, but we cannot offer an explanation for the lack of agreement among the other values.

Acknowledgment.—This work was sponsored by the Office of Ordnance Research.

THE VIRIAL COEFFICIENTS OF HELIUM FROM 20 TO 300°K.[1]

BY DAVID WHITE, THOR RUBIN, PAUL CAMKY AND H. L. JOHNSTON

Cryogenic Laboratory of the Chemistry Department, The Ohio State University, Columbus 10, Ohio

Received January 27, 1960

The compressibility of gaseous helium from the boiling point of liquid hydrogen to 300°K. in the pressure range one to 33 atmospheres, has been determined. The 22 experimental PV isotherms are represented by an equation of state containing three virial coefficients. The second virial coefficients are compared with those calculated from various intermolecular potential functions for helium suggested in the literature. The agreement is fair.

Introduction

The compressibility of gaseous helium, from the boiling point of liquid hydrogen to room temperature, has been investigated with particular emphasis on the low pressure region. The purpose of the research was twofold; first, to measure deviations from the ideal gas law which could be used for the establishment of a temperature scale in this Laboratory from helium gas thermometry data; second, to determine the second virial coefficients, B's, over an extended temperature range at sufficiently small intervals as to permit a reliable test of a number of suggested intermolecular potential functions for the interaction of two helium atoms. Admittedly, the use of second virial coefficients to establish in any detail, the form of intermolecular potentials is not a satisfactory one, nevertheless, one can obtain some indication of at least two of the parameters, namely, the depth of the potential well and the distance of separation at the minimum. We say some indication since these parameters of the potential functions are not separable. In any calculation of the intermolecular potential function from second virial coefficients, one finds that the effect of increasing the depth of the potential well usually can be offset by a decrease in equilibrium distance of approach without serious deviation from the experimental results. Some of the uncertainty in the relation of the depth of the potential well to the equilibrium distance can be removed if a self consistent set of B's over a wide temperature range are available. Although a large amount of experimental work on the equation of state of helium has been done in the past, there, unfortunately, does not exist a set of data in the accessible temperature range (say 1 to 1200°K.) which to date can be judged self consistent. In the temperature range 20 to 300°K., the work prior to that reported here does not yield B's which join smoothly those of Schneider and Duffie[2] from 300 to 1473°K. It is very difficult to ascertain whether the second virial coefficient in the liquid helium range are consistent with the B's at higher temperature where measurements begin at approximately 14°K. Although the temperature gap is small, there is such a rapid change in the magnitude of B that it is difficult to make any reliable comparison. The present work does not resolve all of the above mentioned problems, however, it does present a consistent set of B's over a wide temperature

(1) This work was supported in part by the Air Material Command, Wright Field.

(2) W. G. Schneider and J. A. H. Duffie, *J. Chem. Phys.*, **17**, 751 (1949).

interval which joins without discontinuity those of Schneider and Duffie.

Apparatus and Procedure

The experimental apparatus used in this research has been described briefly.[3] A further account of it can be found in the work of Friedman.[4] The important difference in this apparatus from those in use by earlier workers consisted of the pipet valve which allowed isolation of the noxious volume from the pipet volume. A similar device was subsequently used by Keller[5] for PV determinations of helium below 4°K. Pipet pressures above two atmospheres were measured by means of an M.I.T. type dead weight gauge, the lower pressures by mercury manometers. The pipet temperatures were determined by two standardized[6] copper–constantan thermocouples. The amount of gas in the pipet was determined by expansion of the sample into calibrated evacuated thermostated tanks connected to a manometer.

In a typical experiment, the pipet pressure and temperature were measured together over a time interval long enough to obtain thermal equilibrium. Heat leaks were minimized by evacuating the volume inside of the can and by maintaining the auxilliary block temperatures at the pipet temperature. When the apparatus was operated in this manner the pipet temperature drift was less than 0.001 degree per half hour,[7] further, this drift was always consistent with the pressure–time variation.

At the end of the pressure–temperature measurements, the pipet valve was closed and the gas in the noxious volume was removed. The gas sample in the pipet was then expanded into the calibrated tanks at 25°. At least three successive expansions were employed in order to reduce the remaining gas in the pipet to a pressure of 50 mm. or less. Accurate measurement of the tank pressures were made with a calibrated cathetometer. The pipet temperatures of the runs in a given isotherm were not identical but did not vary by more than a few thousandths of a degree. Small corrections were applied to the PV products to bring them to a common temperature. The dead weight gauge used in the experiments was accurate to one part per 10,000 and precise to one part in 50,000 or better. All manometer readings were accurate to 0.01 mm. These were corrected for capillarity[8] to the standard gravity and to the density of mercury at 0°. The expansion tanks calibrated with water, were known to one part in 15,000 or better. The pipet volume of 120 cc. calibrated with mercury, at room temperature was known to one part in 25,000 or better. The pipet volume at other temperatures was calibrated using thermal expansion data for nickel samples[9] cut from the same billet as the pipet.

The amount of gas in the expansion tanks was computed by an iterative procedure using, at first, trial second virial coefficients at 25.00°, and finally the values derived from this work. The amount of gas left in the pipet after expansion was similarly corrected by the iterative procedure for the second virial coefficients finally derived from this work. The temperature of the gas left in the noxious volume between the pipet and tanks after the last expansion was taken as the mean of several thermocouple station measurements. Since this noxious volume was only of the order of 2 cc., the perfect gas law was used in the calculation of the number of moles in the space.

Purification of the Helium.—The helium used in this research was obtained from the Air Reduction Company and was purified by first passing it over a high-pressure charcoal trap at the boiling point of liquid nitrogen. The gas was then liquefied and triply distilled before storage in a cylinder. The purity of the gas was determined by means of a mass spectrometer and found to be 99.99%. The impurities consisted of traces of nitrogen and oxygen which were probably introduced while filling the evacuated storage cylinder.

(3) H. L. Johnston and D. White, *Trans. of A.S.M.E.*, **72**, 785 (1950).

(4) A. S. Friedman, Thesis, The Ohio State University, 1950.

(5) W. E. Keller, *Phys. Rev.*, **97**, 1 (1955).

(6) T. Rubin, H. L. Johnston and H. Altman, *J. Am. Chem. Soc.*, **73**, 3401 (1951).

(7) D. White, A. S. Friedman and H. L. Johnston, *J. Am. Chem. Soc.*, **72**, 3927 (1950).

(8) Cawood and Patterson, *Trans. Faraday Soc.*, **29**, 514 (1933).

(9) T. Rubin, H. Altman and H. L. Johnston, unpublished.

Experimental Results

The experimental results are shown in Table I. The data consist of 22 isotherms between 20.58 and 299.99°K. These data were fitted to the three term equation of state

$$PV = A(T) + B(T)P + C(T)P^2 \qquad (1)$$

TABLE I

P–V–T DATA FOR GASEOUS HELIUM

P, atm.	PV, cc. atm. mole^{-1}	PV(calcd.) − PV(obsd.) cc. atm. mole^{-1}
	Temp. = 299.99°K.	
4.5149	24,670.6	2.4
9.9769	24,738.4	−0.2
14.9050	24,805.3	−8.1
20.9709	24,879.8	−9.5
26.5339	24,946.5	−10.5
33.2163	25,016.2	0.5
	Temp. = 273.16°K.	
4.6677	22,480.1	−1.9
9.8100	22,541.8	−1.5
14.8556	22,597.0	4.3
21.1120	22,681.2	−4.4
26.8544	22,744.2	2.0
33.1539	22,820.8	1.5
	Temp. = 249.99°K.	
4.6702	20,572.1	2.2
10.5414	20,635.3	9.7
15.6522	20,713.0	−6.4
20.7861	20,774.8	−5.3
26.5900	20,843.3	−4.9
33.0182	20,921.3	−5.4
	Temp. = 200.11°K.	
4.6920	16,482.4	2.2
5.3862	16,493.9	−8.4
10.3046	16,551.3	1.9
11.0990	16,559.3	3.6
14.7136	16,610.8	−3.6
20.7363	16,678.8	2.0
26.7631	16,755.0	−0.5
32.8367	16,826.2	2.6
	Temp. = 175.02°K.	
4.6452	14,425.8	−0.1
10.0888	14,492.0	0.3
14.6037	14,548.0	−0.4
20.8028	14,623.3	0.1
26.4976	14,693.9	−0.8
32.2868	14,762.9	1.1
	Temp. = 150.04°K.	
4.5926	12,368.8	1.2
9.7597	12,434.7	−1.9
14.5789	12,491.4	0.0
20.8465	12,570.0	−2.5
26.4396	12,634.5	8.0
32.8310	12,711.0	2.1
	Temp. = 125.03°K.	
4.5670	10,313.0	3.6
9.7922	10,379.6	0.7
14.7720	10,440.2	0.7
20.2545	10,510.9	−3.2
26.5302	10,582.2	1.9
33.1357	10,668.4	−3.8

TABLE I (*Continued*)

P, atm.	PV, cc. atm. mole^{-1}	PV(calcd.) − PV(obsd.) cc. atm. mole^{-1}
	Temp. = 100.02°K.	
4.7092	8,264.55	−1.39
10.2396	8,329.81	−1.62
15.9445	8,393.52	−1.83
20.7658	8,451.51	0.75
25.7881	8,515.43	−4.01
32.6609	8,596.63	−3.13
	Temp. = 90.04°K.	
4.5869	7,439.44	1.54
9.6796	7,497.27	1.15
14.9762	7,559.25	1.00
20.1910	7,618.79	1.50
25.8985	7,687.04	−1.07
31.8234	7,755.21	−0.84
	Temp. = 80.02°K.	
4.7353	6,618.37	−0.92
9.5004	6,665.01	4.98
14.8323	6,730.12	−0.67
19.4208	6,779.63	0.72
26.2664	6,855.14	1.88
29.2778	6,898.14	−7.25
	Temp. = 75.01°K.	
4.5877	6,202.37	1.43
9.7942	6,258.02	2.37
14.6939	6,314.94	−0.71
19.8699	6,374.62	−2.89
24.9626	6,427.57	−1.34
30.5448	6,493.84	−1.54
	Temp. = 69.00°K.	
4.5815	5,708.03	−1.38
10.2984	5,766.48	0.52
14.5849	5,812.16	0.82
19.2922	5,861.82	2.39
24.3462	5,921.12	−1.06
29.7154	5,981.62	−1.26
	Temp. = 60.03°K.	
3.7087	4,960.46	0.74
4.5097	4,969.67	− .68
9.0293	5,014.43	− .93
12.5493	5,047.32	1.45
15.0393	5,074.13	−0.07
20.2008	5,127.85	−0.52
	Temp. = 55.09°K.	
0.98985	4,530.97	0.80
1.94156	4,545.12	−4.75
3.6128	4,556.07	−0.51
3.8748	4,557.26	0.70
5.7183	4,576.20	−2.87
8.2170	4,595.28	2.84
8.9897	4,601.03	4.34
12.1679	4,636.77	−1.31
12.3209	4,636.14	0.78
	Temp. = 50.09°K.	
1.05823	4,122.46	−0.88
3.6228	4,142.44	.29
5.1015	4,154.56	.61
5.8284	4,161.26	.09
9.0043	4,188.89	− .06
11.0025	4,206.57	− .04
	Temp. = 45.10°K.	
0.96827	3,712.61	−5.53
1.93306	3,711.93	2.56
3.7090	3,728.46	0.02
4.9968	3,740.00	−1.11
5.7705	3,743.65	1.61
5.8514	3,743.00	2.93
8.8762	3,771.11	0.57
12.0745	3,801.32	−1.03
	Temp. = 40.09°K.	
1.03425	3,298.42	−0.52
1.99666	3,304.99	−0.52
1.99968	3,306.42	−1.93
3.7347	3,315.15	1.60
5.6241	3,330.52	0.16
6.8053	3,340.15	−0.45
8.8665	3,355.73	0.29
11.6206	3,377.62	1.35
	Temp. = 35.10°K.	
1.01995	2,887.73	−0.78
1.97597	2,891.75	0.31
1.99698	2,891.87	0.30
3.8634	2,902.91	−0.48
5.8795	2,913.55	0.38
6.0746	2,914.94	0.13
8.5398	2,930.24	−0.46
12.3549	2,953.25	0.50
	Temp. = 33.00°K.	
0.99736	2,710.99	0.03
1.87998	2,714.85	0.01
1.97717	2,714.87	0.43
3.7467	2,722.53	1.09
5.9826	2,734.83	0.41
6.1212	2,738.30	−2.30
9.1316	2,753.58	0.11
12.1595	2,773.52	0.21
	Temp. = 28.82°K.	
0.95165	2,366.95	−0.45
1.92391	2,368.04	1.38
2.09017	2,370.28	−0.40
3.7585	2,374.32	1.57
5.7035	2,382.06	2.08
6.3433	2,387.95	−0.78
8.25155	2,396.72	0.37
11.60812	2,421.62	−3.74
	Temp. = 24.65°K.	
0.96549	2,025.52	−2.99
1.94976	2,024.75	−0.94
1.99145	2,024.36	−0.49
3.7522	2,026.81	0.20
5.0155	2,030.85	−0.94
5.3707	2,028.97	1.86
6.7835	2,035.35	−0.45
8.7033	2,034.55	6.97
9.7909	2,042.10	3.72
	Temp. = 20.58°K.	
1.07801	1,685.47	−0.49
1.95987	1,684.53	−1.24
3.7017	1,682.60	−1.61
3.8445	1,678.34	2.53
5.0244	1,682.05	−1.87
6.2025	1,675.96	4.18
6.6123	1,683.53	−3.26
8.9292	1,680.71	1.77

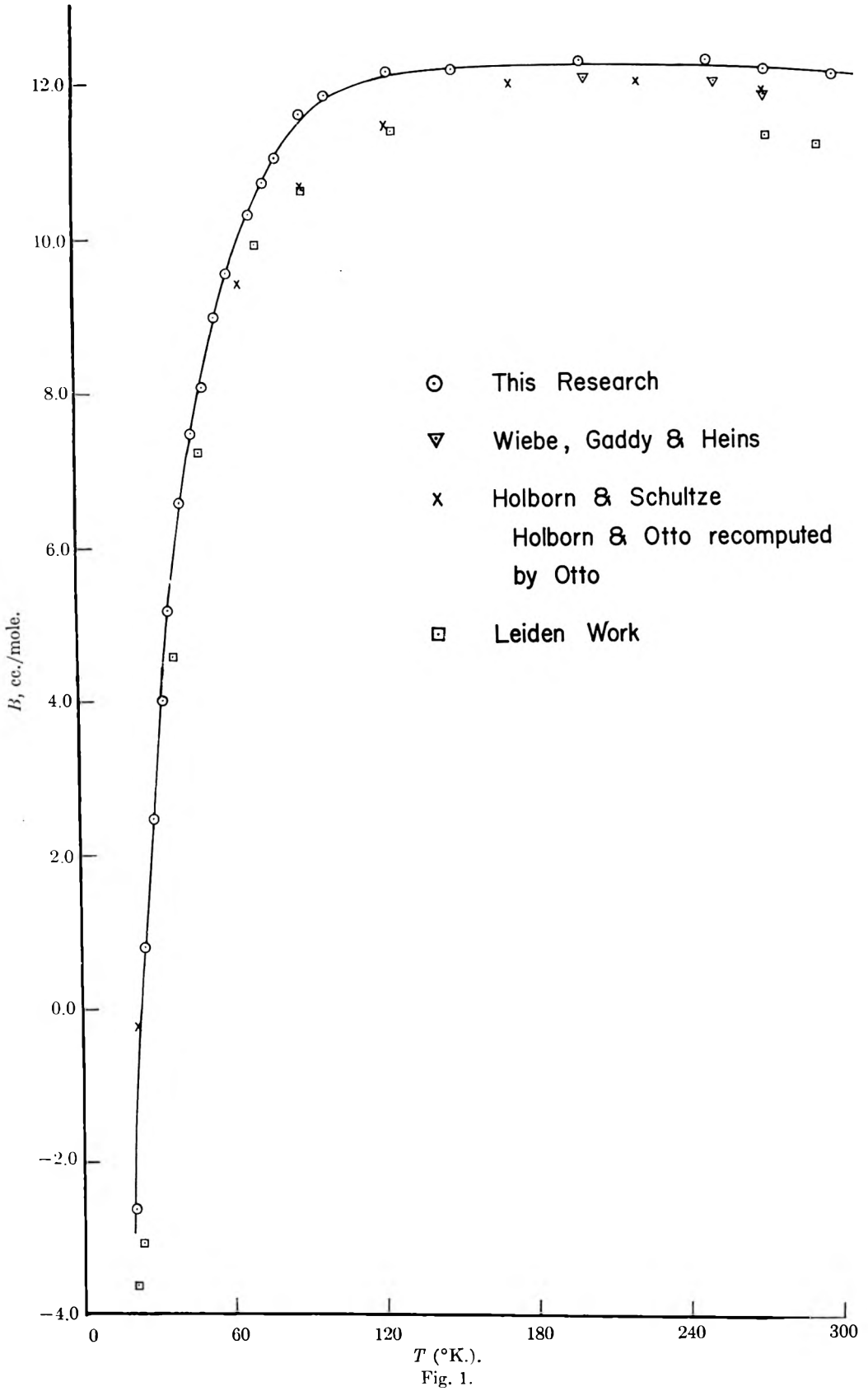

Fig. 1.

where P is the pressure in atmospheres, V is the volume in cc./mole, T is the absolute temperature, and $A(T)$, $B(T)$, $C(T)$ are, respectively, the first, second and third virial coefficients.

The number of significant figures shown in this table are consistent with the precision previously

given. The differences, $PV_{calcd} - PV_{obsd}$ are the deviations obtained for each data point of the experimental values from the values calculated from relation 1 using the virial coefficient values given in Table II. The second and third virial

TABLE II

VIRIAL COEFFICIENTS FOR GASEOUS HELIUM

T, °K.	$\frac{A(T)}{RT}$	$B(T)$, cc.	$C(T)$, cc. atm.$^{-1}$
299.99	1.00009	11.99	−0.000
273.16	1.00032	12.08	−0.000
249.99	1.00023	12.15	−0.000
200.11	1.00041	12.23	−0.000
175 02	1.00050	12.24	+0.000
150 04	1.00020	12.15	+0.000
125 03	1.00015	12.18	+0.000
100 02	1.00006	11.85	0.0009
90 04	0.99963	11.60	0.0015
80.02	.99982	11.01	0.0040
75.01	.99990	10.70	0.0118
69.00	.99951	10.30	0.0172
60.03	.99991	9.55	0.0219
55.00	1.00053	8.96	0.0240
50.09	1.00068	8.06	0.0400
45.10	0.99972	7.48	0.0700
40.09	1.00040	6.57	0.0860
35.10	1.00049	5.18	0.0540
33.00	0.99963	4.00	0.1230
28.82	.99963	2.46	5.1880
24.65	.99946	0.80	0.1710
20.58	.99932	−2.62	0.2300

coefficients were determined using a method first developed by Cragoe.[10] It is as follows: from a set of points constituting an isotherm, one point is chosen as a reference, designated by P_0 and V_0. Now since

$$P_0V_0 = A(T) + B(T)P_0 + C(T)P_0^2$$

on subtraction from (1), one obtains

$$\frac{\frac{PV}{P_0V_0} - 1}{\frac{P}{P_0} - 1} = \frac{B(T)}{V_0} + \frac{C(T)}{P_0V_0}\left(\frac{P}{P_0} + 1\right) \qquad (2)$$

It is obvious that the determination of $B(T)$ and $C(T)$ do not depend upon the temperature scale, chosen, providing the set constitutes a true isotherm. Because of the nature of equation 2 in which differences are being used, it is only applicable to rather precise data.

The ranges of experimental pressure were so chosen, that in nearly all of the cases a straight line was obtained on plotting the left-hand side of equation 2 *vs.* $(P/P_0 + 1)$. Within the experimental error, no higher virial than the third can be justified whether relation 2 or a least squares method is employed.[5] After evaluation of $B(T)$ and $C(T)$, $A(T)$ was calculated from relation 1. All the virials calculated appear in Table II, the graph of the second virial coefficients with temperature is Fig. 1.

The consistency of these coefficients with the temperature scale is shown by the value of the ratio $A(T)/RT$ (Table II) where R is the gas constant, 82.0567 cc. atm./mole deg., T is the absolute temperature of the isotherm measured by the pipet thermocouple in terms of the temperature scale previously mentioned. It is obvious that these data are in accord with this scale to four parts in 10,000 except at 20.58 and 50°K. where the agreement is about 7 parts in 10,000. The second virial coefficient calculated in terms of relation 1 appears to have random errors of about ±0.2–0.3 cc./mole at high temperature and about ±0.5 cc./mole at the lowest temperature.

A comparison of the individual results for the second virial coefficients given by other authors with the present work are shown in Fig. 1.[11–14] It is evident that the results of this research does not reconcile any differences among the earlier investigations. It is even questionable whether these differences in B are real since these researches, in the main, were carried out in pressure ranges where the effect of the higher virial terms could influence the choice of the B. This is not the case in the present work where the pressure range was so chosen as to minimize this effect. It is interesting that the B's of this research compare favorably with the earlier values only at temperatures where the third virial coefficients are similar. The values for $B(T)$, of Wiebe, Gaddy and Heins agrees with our results to within 0.3 cc./mole between 200 and 273°K., where those authors found a value for $C(T)$ of about −0.009 compared to −0.000 from our data. The data of Holborn and Otto and Holborn and Schultze yield $B(T)$'s 0.3 cc./mole smaller in value than those of this research, with fair agreement among the $C(T)$ values above 170°K. Below this temperature the values of both $B(T)$ and $C(T)$ of these sets of data diverge. The Leiden data of Nijhoff and Keesom near 70°K., agrees the best with our results for both $B(T)$ and $C(T)$.

Comparison of Second Virial Coefficients Computed from Intermolecular Potentials with Experimental Values.—The determination of the parameters in the intermolecular potential function of helium has been attempted several times by correlations with experimental second virial coefficient and or with transport properties of the gas. An exhaustive review of this work will not be made here since that has already been done by Hirschfelder, *et al.*,[15] as well as by the authors to whom reference is made below.

The most detailed calculations are those of Kilpatrick, *et al.*,[16–18] who accounted for the quantum effects on the second virial coefficients using a number of different potential functions. Their first

(10) C. S. Cragoe, "Temperature, Its Measurement and Control in Science and Industry," Reinhold Publ. Corp., New York, N. Y., 1941, p. 89.

(11) W. H. Keesom, "Helium" Elsevier Publication, 1942.

(12) L. Holborn and H. Schultze, *Ann. Physik*, [4] **47**, 1089 (1915) and L. Holborn and J. Otto, *Z. Physik*, **10**, 367 (1922); **23**, 77 (1924).

(13) C. W. Gibby, C. C. Tanner and I. Mason, *Proc. Roy Soc. (London)*, **A122**, 283 (1929).

(14) R. Wiebe, V. L. Gaddy and C. Heins, Jr., *J. Am. Chem. Soc.*, **53**, 1721 (1931).

(15) J. Hirschfelder, C. F. Curtiss and R. B. Bird, "Molecular Theory of Gases and Liquids," John Wiley and Sons, New York, N. Y., Chapman and Hall (1954).

(16) J. E. Kilpatrick, W. E. Keller, E. F. Hammel and N. Metropolis, *Phys. Rev.*, **94**, 1103 (1954).

(17) J. DeBoer and A. Michels, *Physica*, [VI] **5**, 409 (1939).

(18) J. E. Kilpatrick, W. E. Keller and E. F. Hammel, *Phys. Rev.*, **97**, 9 (1955).

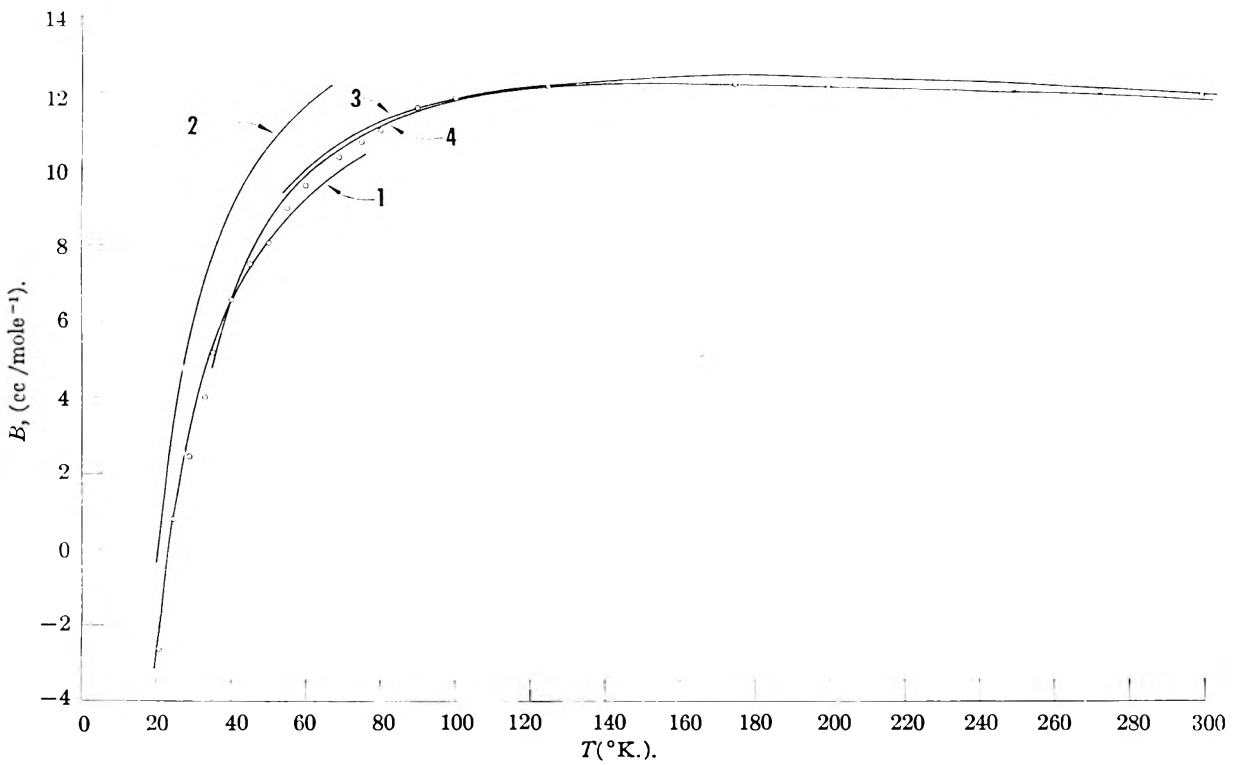

Fig 2.—Comparison of second virial coefficients for various intermolecular potentials with experimental values: curve 1, 6–12 Lennard–Jones potential; 2, MR-5 potential of Kilpatrick, *et al.*; 3, Exp-six function of Kilpatrick, Keller and Hammel; 4 Yntema and Schneider potential (classical).

paper,[16] contains calculations based on a 6 to 12 Lennard-Jones function using constants proposed by DeBoer and Michels.[17] This work is summarized by curve 1 of Fig. 2. For temperatures above 60°K., the calculated results are lower than the experimental data of the present work. This is expected since the constants were chosen to fit the data of the Leiden workers and the results of Holborn and Otto.[17] This potential function, although empirical, permits a qualitative estimation of the second virial coefficient values over an unusually wide temperature range. Kilpatrick, Keller and Hammel[18] also computed the second virial coefficients using an exp-Six potential function. This is a form previously suggested by Slater and Kirkwood,[19] Buckingham[20] and by Mason and Rice.[21] Using this form together with constants suggested by Mason and Rice,[21] good agreement with the higher temperature results of Schneider and Duffie is achieved (curve 3 of Fig. 2) as well as the B's presented here. The agreement with the lowest temperature virial data however is very poor.[5] To improve agreement with the low temperature data, Kilpatrick, *et al.*,[18] selected a new set of constants (MR5). The results are shown in Fig. 2 as curve 2. The agreement of experimental B's with the calculations from the (MR5) potential function is worse than the Lennard-Jones potential function at temperatures above 20°.

It is obvious from the discussion and the comparisons given in Fig. 2 that neither the form nor the choice of constants for the potential function of helium made so far, have given satisfactory quantitative agreement with all of the experimental virial coefficients. It is questionable whether the form or choice of constants in the potential function can ever be resolved from virial data alone. There is considerable merit, however, in providing an empirical function so that a compact form may be used to express indirectly the second virial coefficients.

We suggest the use of Yntema and Schneider's function for this purpose, it is

$$\epsilon(\nu) = \infty \quad \nu < 1 \text{ Å.}$$
$$\epsilon(\nu) = 0 \quad \nu > 12 \text{ Å.} \qquad (4)$$
$$10^{+12} \times \epsilon(\nu) = 1200\, e^{-\nu/0.212} - \frac{1.24}{\nu^6} - \frac{1.89}{\nu^8}$$
ergs, 1 Å. $< \nu <$ 12 Å.

where ν is the interatomic distance between two helium atoms in Ångstroms. This set of expressions substituted in the classical formula

$$B(T) = 2\pi N \int_0^\infty \left(1 - e^{\frac{-\epsilon(\nu)}{RT}}\right) \nu^2 d\nu$$

where ν has the meaning of relation 4, N is Avogadro's number, k is Boltzmann's constant (the other terms have their usual meaning), is simple to use. The agreement with the present results, shown in Fig. 2 as curve 4, is good.

Acknowledgments.—The authors wish to express their thanks to Mr. H. Altman for assistance in some of the measurements, to Mr. L. E. Cox for some of the modifications of the apparatus and to Dr. A. Friedman for calibration of the pipet volume.

(19) J. C. Slater and J. G. Kirkwood, *ibid.*, **32**, 349 (1928); **37**, 682 (1931).

(20) H. S. W. Massey and R. A. Buckingham, *Proc. Roy. Soc. (London)*, **A168**, 378 (1936).

(21) E. A. Mason and W. E. Rice, *J. Chem. Phys.*, **22**, 522 (1956).

FREEZING POINT DATA FOR A PORTION OF THE TERNARY SYSTEM: ACETAMIDE–PALMITIC ACID–STEARIC ACID

By Robert R. Mod, Frank C. Magne and Evald L. Skau

Southern Regional Research Laboratory,[1] *New Orleans, Louisiana*

Received February 15, 1960

Freezing point data were obtained for stable, metastable and unstable crystalline phases in binary mixtures of the 1:1 molecular compounds acetamide–palmitic acid (AP) and acetamide–stearic acid (AS) and for a portion of the ternary system: acetamide–palmitic acid–stearic acid. The equimolar mixture of AP and AS exhibited three freezing points, representing stable equilibrium with the high-melting modification of acetamide, metastable equilibrium with crystals of AS, and unstable equilibrium with a crystalline phase of unknown composition, respectively. X-Ray long spacing measurements of these solidified 1:1 mixtures indicate the presence of the "C" forms of palmitic and stearic acids and the "A" forms of their 1:1 acetamide compounds. The long spacings were essentially the same whether solidification started from stable or from unstable equilibrium, but the X-ray short spacings and the infrared spectra showed slight characteristic differences.

It has been shown in previous publications[2,3] that acetamide forms 1:1 molecular compounds with long chain saturated fatty acids. X-Ray long spacings of the crystals proved to be equal to the sum of the lengths of two acid and two acetamide molecules.[4] This is similar to the arrangement in crystals of the long chain fatty acids, which are made up of double layers of acid molecules, their carboxyl groups being in juxtaposition with their hydrocarbon chains extending in opposite directions.[5] The double molecules are also present in the liquid state as associated molecules.[6] It is not surprising therefore that a fused equimolar mixture of palmitic and stearic acids should contain double molecules made up of one molecule of palmitic acid and one molecule of stearic acid and that crystals of this 1:1 molecular compound can separate on chilling.[7]

By analogy it might be assumed that there would be a similar 1:1 molecular compound between the 1:1 acetamide-palmitic acid compound (AP) and the 1:1 acetamide-stearic acid compound (AS). Binary freezing point data were obtained which at first seemed to confirm this assumption but the supposed molecular compound melted over a temperature range, instead of at constant temperature as required. The reason for this apparently anomalous freezing point behavior was revealed by construction of the pertinent part of the freezing point diagram for the ternary system acetamide–palmitic acid–stearic acid.

Experimental

The 1:1 compounds, AS and AP, were prepared by fusing equimolar portions of pure acetamide and pure acid, each of which had been dried in a vacuum desiccator over phosphorus pentoxide. The solidified mixture was ground in a mortar, remelted, resolidified and reground to ensure homogeneity of the sample. Since nitrogen analysis of the AS indicated an appreciable loss of acetamide by sublimination during the fusion, the required amount of acetamide was added and the process repeated. The final freezing point for the AP was 59.2° and for the AS, 65.7°. *Anal.* Calcd. for AP: N, 4.44; neut. equiv., 315.5. Found: N, 4.36; neut. equiv., 314.7. Calcd. for AS: N, 4.09; neut. equiv., 343.2. Found: N, 4.10; neut. equiv., 343.5. The freezing points were determined with an estimated precision of ±0.2° by the thermostatic sealed-tube method previously described,[2] which involves finding two temperatures a few tenths of a degree apart, one at which the last crystals just disappeared and the other at which a few crystals remained undissolved after prolonged agitation. The heating curves were obtained by an apparatus and technique previously described.[8] The X-ray measurements were made by the powder method.[4] The infrared spectra were obtained with a double-beam infrared spectrophotometer with sodium chloride optics employing the technique of O'Connor, *et al.*[9]

Results and Discussion

The primary freezing point data for the binary system AS–AP are given in Table I and represented graphically in Fig. 1. All compositions are expressed in mole %. The compositions containing between 12 and 58% of AS exhibited two, and in some instances three freezing points, depending upon the previous treatment of the samples. The solid line in this range represents the temperatures of stable equilibria obtained on samples which had been heated for a few minutes at about 80° and shock-chilled in an acetone–Dry Ice mixture. The corresponding metastable equilibria, obtained on samples solidified by spontaneous crystallization of the melt, are represented by the broken lines, which are obviously extensions of the AP and AS branches of the diagram. The mixtures from 29 to 50% AS were later shown to exhibit a still lower freezing point, between about 47 and 50°, involving an unstable crystalline phase which was usually the first to form on spontaneous crystallization of the melt. The exact equilibrium temperature could not be determined because of a gradual transition to the metastable crystalline phase before equilibrium could be established.

On the basis of this freezing point diagram and the precision of the freezing point determinations it might be assumed that this is a binary system in which a congruently melting 1:1 compound, AS·AP, forms. However, it was observed that freezing of the 50–50 mixture initiated at the upper (stable) equilibrium temperature took place over a

(1) One of the laboratories of the Southern Utilization Research and Development Division, Agricultural Research Service, U. S. Department of Agriculture.

(2) F. C. Magne and E. L. Skau, *J. Am. Chem. Soc.*, **74**, 2628 (1952).

(3) F. C. Magne, R. R. Mod and E. L. Skau, *J. Am. Oil Chemists' Soc.*, **34**, 127 (1957).

(4) R. T. O'Connor, R. R. Mod, M. D. Murray and E. L. Skau, *J. Am. Chem. Soc.*, **77**, 892 (1955).

(5) K. S. Markley, "Fatty Acids," Interscience Publishers, Inc., New York, N. Y., 1947, p. 85.

(6) A. W. Ralston, "Fatty Acids and Their Derivatives," John Wiley and Sons, New York, N. Y., 1948, p. 287.

(7) L. E. O. de Visser, *Rec. trav. chim.*, **17**, 182 (1898).

(8) E. L. Skau, *Proc. Am. Acad. Arts Sci.*, **67**, 551 (1933).

(9) R. T. O'Connor, E. F. DuPré and E. R. McCall, *Anal. Chem.*, **29**, 998 (1957).

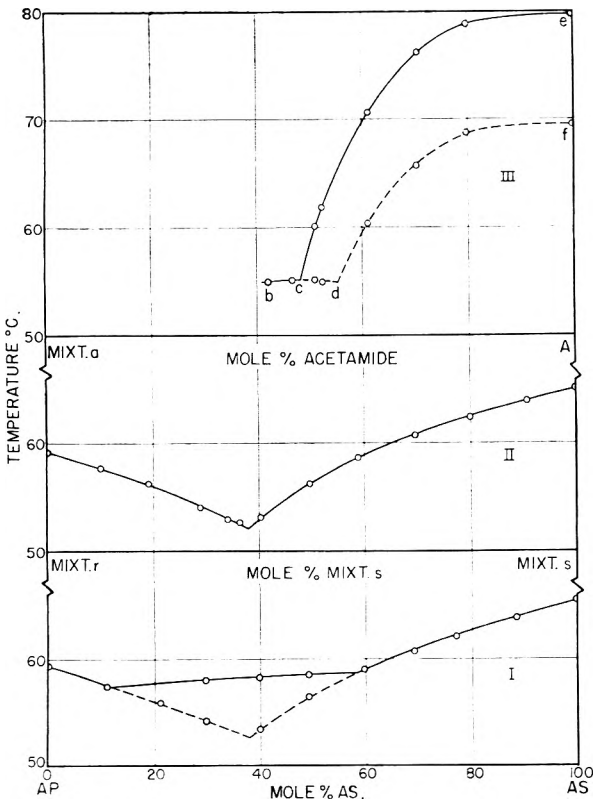

Fig. 1.—Binary freezing point diagrams for I, the acetamide compounds of palmitic and stearic acids; II, Mixture r with Mixture s; III, acetamide with Mixture a. Broken lines represent metastable equilibria.

wide temperature range. The same was true of the mixture containing 39.98% AS, supposedly close to a eutectic, when crystallization started at the lower (metastable) equilibrium temperature. Heating curves were run on two completely solidified samples of 1:1 AS–AP mixture, one prepared by shock-chilling and the other by spontaneous crystallization. Their primary freezing points as determined by the thermostatic sealed-tube method were known to be 58.4 and 56.5°, respectively. The first sample started to melt at about 49°, at which temperature the time–temperature curve showed a typical eutectic halt. The eutectic halt for the second sample came at about 46.5° instead of 52.6° as would be expected from Fig. 1, I. It is obvious, therefore, that the system must be considered as part of the ternary system formed from acetamide (A), palmitic acid (P) and stearic acid (S).

Freezing point measurements were made on pertinent mixtures of acetamide with *Mixture a*, a mixture consisting of 0.4422 mole of stearic acid and 0.5578 mole of palmitic acid. The results are included in Table I and shown in Fig. 1, III. Here ce and df represent solid–liquid equilibria for the stable (high-melting) and the metastable (low-melting) modifications of acetamide, respectively.

Similar freezing point data obtained for mixtures of *Mixture r* (43.29% A, 56.71% P) with *Mixture s* (44.69% A, 55.31% S) are represented in Fig. 1, II. Here again the molten mixtures between about 20 and 50% tended to supercool to give an unstable crystalline phase for which the equilibrium temperatures were between about 47 and 50°.

Table I

Freezing Point Data[a,i]

Mole %[b]	F.p., °C. Stable	F.p., °C. Metastable	Mole %[b]	F.p., °C. Stable	F.p., °C. Metastable
		AS–AP system			
0.00	59.2		49.49	58.4	56.5[c]
11.16	57.3		53.01	58.6	
(11.8)[d]	(57.2)[d]		(58.3)[d]	(58.6)[d]	
20.68	57.7	55.8	59.71	59.1	
29.85	57.9	54.1[c]	69.35	60.6	
(38.0)[d]		(52.6)[d]	77.26	61.8	
39.98	58.1	53.3[c]	88.52	63.8	
44.2[e]		55.2[e]	100.00	65.7	
		A–Mixture a system[f]			
42.12	54.9[c]		(55.2)[d]		(54.9)[d]
46.65	55.1		60.94	70.6	60.3
(48.2)[d]	(55.1)[d]		70.43	76.2	65.7
50.91	60.1	55.2	79.66	79.0	68.7
52.34	61.7	54.9	100.00	79.7	69.5
		Mixture s[g]–Mixture r[h] System			
0.00	59.1		43.9[c]	55.0[c]	
10.17	57.6		49.64	56.3[c]	
19.21	56.3[c]		58.77	58.6	
28.86	54.0[c]		69.63	60.6	
33.98	52.9[c]		79.95	62.4	
36.32	52.7[c]		90.78	64.0	
(38.0)[d]	(52.1)[d]		100.00	65.1	
40.15	53.2[c]				

[a] The values in parentheses were obtained by graphical extrapolation or interpolation. [b] Mole % of first-mentioned component. [c] A lower freezing point was observed lying between about 47 and 50°, but could not be accurately determined, because of gradual transition to the next more stable form before equilibrium could be established. [d] "Eutectic" composition and temperature. [e] Interpolated from A–Mixture a system. [f] Mixture a = 44.22% S, 55.78% P. [g] Mixture s = 44.69% A, 55.31% S. [h] Mixture r = 43.29% A, 56.71% P. [i] The ternary mixture containing 53.55% A, 27.90% P and 18.55% S gave three freezing points: 63.1°, 53.2°, and approximately 49°, corresponding to stable, metastable and unstable equilibria, respectively.

On the basis of the data obtained by interpolation in the freezing point diagrams of Fig. 1 and those for the systems acetamide–stearic acid and acetamide–palmitic acid,[2] it is possible to construct the pertinent part of the primary freezing point diagram for the ternary system acetamide–stearic acid–palmitic acid (A–S–P).

Figures 2 and 3 show the primary freezing point behavior for this system when the metastable (low-melting) and stable (high-melting) forms of acetamide are involved, respectively. The broken lines jk Aa and rs represent the compositions in the systems AP–AS, A–Mixture a, and Mixture r–Mixture s, respectively. The solid lines are isotherms showing the temperatures at which crystalline AS, AP or A are in equilibrium with the liquid.

The black circles in Fig. 3 represent compositions from which an unstable crystalline phase separated when the melt was allowed to supercool and crystallize spontaneously (see Table I, footnote *c*). Although the corresponding equilibrium tem-

peratures could not be determined accurately it was estimated that they all lay between about 47 and 50°.

The metastable form of acetamide (Fig. 2) or the stable form (Fig. 3) can be caused to crystallize from any molten mixture within area Amno. The curve mn represents the eutectic groove formed by the intersection of the A and AP crystallization surfaces, and no and np represent the corresponding intersections between the A and AS surfaces and between the AP and AS surfaces, respectively.

The curves mn and no in Fig. 2, as well as all the isotherms or portions of isotherms on the A, AP and AS surfaces in Fig. 2 lying within the compositional area Amno of Fig. 3 represent metastable equilibria.

These ternary diagrams make it possible to identify the solid phase in equilibrium with the various branches of the diagrams in Fig. 1. For compositions along jk (*i.e.*, the system AP–AS), it is apparent that the crystals in equilibrium with the liquid along the almost horizontal mid-section of Fig. 1, I are crystals of the stable modification of acetamide and not of a 1:1 AP:AS molecular compound. Similarly, the ternary diagrams show that the curve bd in Fig. 1, III represents temperatures of equilibrium between crystalline AS and the liquid phase. Between c and d this is a metastable equilibrium. At c and d a second crystalline phase, the high-melting or the low-melting modification of acetamide, respectively, is also present in the equilibrium. In the system Mixture r–Mixture s (Fig. 1, II) AP and AS are the solid phases in stable equilibrium with the liquid along the left and right branches of the diagram, respectively.

While the ternary diagrams are sufficiently complete to explain the primary freezing point behavior observed when stable and metastable equilibria are involved, additional data would be necessary to account for the specific eutectic temperatures found for the equimolar mixture of AP and AS by heating curves. It can be concluded, however, that these "eutectic halts" can be attributed to eutectic or peritectic points involving one or more unstable crystalline phases of undetermined composition.

The marked tendency for supercooling until an unstable crystalline phase appears affords a plausible explanation. Consider for example, the freezing of a melt having the composition at the mid-point of jk (Fig. 2) in which crystals of AS have started to form. As the temperature falls, more AS would separate and the composition of the liquid would change along jk toward j until the intersection of the AP and AS crystallization surfaces, np, is reached. At this point the melt would be saturated with respect to both AP and AS and if crystals of AP formed, complete solidification should take place without further temperature change since a "saddle point" in the diagram is involved. If, however, supercooling with respect to AP took place; *i.e.*, if the AS surface extended into the metastable region below the AP surface, the temperature would continue to fall as more AS separated. Eventually an unstable crystalline

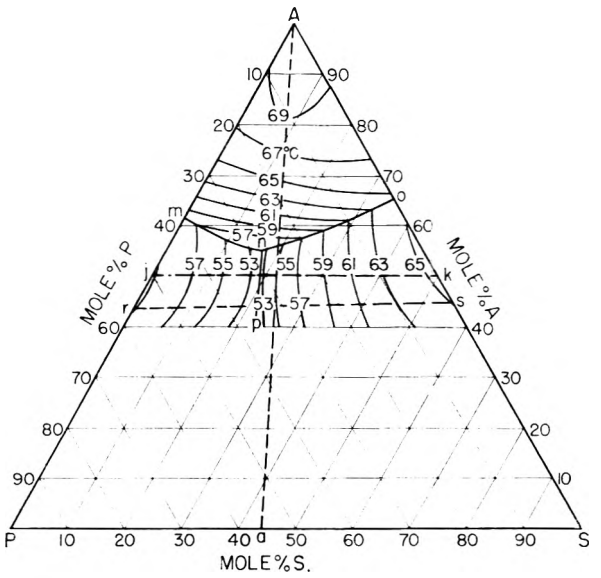

Fig. 2.—Solid–liquid equilibrium isotherms in the ternary system acetamide–palmitic acid–stearic acid. The 55 and 53° isotherms on the acetamide crystallization surface are not shown. In this diagram the equilibria for all compositions in the area Amno of Fig. 3 are metastable.

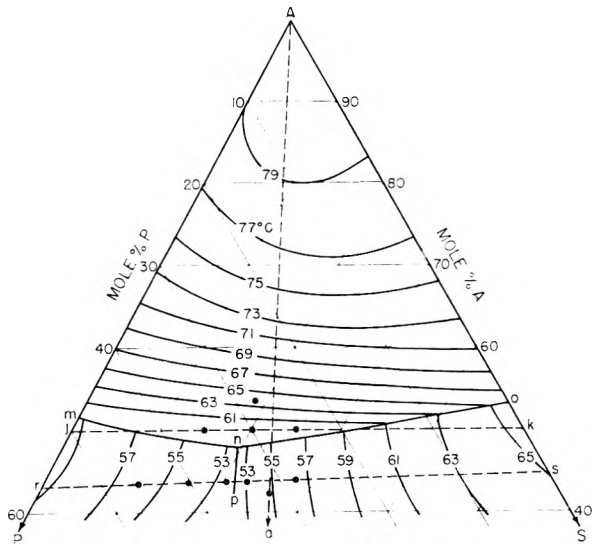

Fig. 3.—Stable solid–liquid equilibrium isotherms in the ternary system acetamide–palmitic acid–stearic acid. The 59, 57, 55 and 53° isotherms on the acetamide crystallization surface are not shown. The black circles represent compositions showing unstable solid–liquid equilibria.

phase would appear at the intersection of the unstable crystallization surface and the metastable AS surface. The subsequent behavior would depend upon the composition of the unstable crystalline phase. The heating curve of the sample so solidified would be expected to show a halt at a temperature below that which would be predicted from the diagram in Fig. 1, I.

Similarly, the apparent anomaly in the heating curve for the 58.4°-melting equimolar mixture of AP and AS can also be attributed to supercooling. In this instance, there is the added possibility that the crystallization surface of the high-melting form of acetamide may extend into a metastable region below the AS surface.

X-Ray diffraction measurements were made on the completely solidified high-melting (f.p. 58.4°) and low-melting (f.p. 56.5°) equimolar mixtures of AP and AS. Each had the same two long spacings, 29.1 and 38.8 Å. However, they had distinctive short spacings which can be used for identification: for the 58.4° form, 5.80(M), 4.14(S), 3.72(MS), 3.56(MS), 2.20(F); and for the 56.5° form, 7.95(F), 5.29(F), 4.49(S), 4.13(S), 3.72(MS) and 3.51(M).

The 38.8 Å. long spacing can be considered as that of a roughly equimolar mixture of the "C" forms of palmitic and stearic acids, of which the long spacings are 36.0 and 40.0 Å.[10] Piper, *et al.*,[11] showed that an equimolar mixture of two such homologs gives a long spacing considerably higher than the average of their long spacings. Similarly the 29.1 Å. spacing can be attributed to the presence of a roughly equimolar mixture of the "A" forms of AP and AS, of which the reported long spacings are 27.6 and 29.9 Å., respectively.[12] It should be noted that the long spacings for the "A" forms of AP and AS are usually accompanied by the long spacings of the "C" form of the corresponding acids.[4]

There was no significant difference between the infrared spectra of the completely solidified 58.4 and 56.5° forms of the 1:1 AS-AP mixtures. Except in the region between 7.8 and 8.4 μ, where a progression of absorption bands of uniform spacing and intensity characteristic of carbon chain length is observed in the spectra of long-chain fatty acids in the solid state, only minor differences were observed between these spectra and those of the "A" forms of AP and AS separately.[4] For the 1:1 mixture slightly less intense absorption was observed at 6.25, 6.70 and 11.10 μ and a considerably less intense band was observed at 7.10 μ. The absorption band at about 10.50 μ had shifted to 10.75 μ.

Acknowledgments.—The authors are indebted to Mildred D. Murray for the X-ray diffraction measurements, to Elsie F. DuPré for the infrared absorption curves, to Robert T. O'Connor for assistance in interpretation of the X-ray and infrared data, to Lawrence E. Brown for the nitrogen analyses, and to George I. Pittman for drawing the figures.

(10) E. Stenhagen and E. von Sydow, *Arkiv Kemi.*, **6**, 309 (1953).

(11) S. H. Piper, A. C. Chibnall and E. F. Williams, *Biochem. J.*, **28**, 2175 (1934).

(12) R. T. O'Connor, R. R. Mod, M. D. Murray, F. C. Magne and E. L. Skau, *J. Am. Chem. Soc.*, **79**, 5129 (1957). More recent X-ray diffraction measurements in this Laboratory show that the 27.6 Å. long spacing for the "A" form of the acetamide–palmitic acid compound is really a second-order spacing and that the first order and the odd-numbered orders are usually absent.

THE SEDIMENT VOLUME IN DILUTE DISPERSIONS OF SPHERICAL PARTICLES

BY MARJORIE J. VOLD[1]

Department of Chemistry, The University of Southern California, Los Angeles, California

Received March 23, 1960

A digital computer has been used to simulate the formation of a sediment by successive deposition of equally sized spherical particles. The sediment density depends critically on the probability that two spheres cohere on contact, provided that the cohesion probability is lower than about 0.35. For higher cohesion probabilities, sediment density is not a sensitive measure of particle interaction. Although the properties of a sediment generated in this way are in good accord with physical model systems such as micron sized glass beads, colloidal systems with at least nearly spherical particles yield sediment densities almost 10 times lower than this model allows. A model is needed which takes both flocculation and sedimentation into account simultaneously.

The sediment volume of a suspension is an accepted qualitative measure of its caducity (tendency to flocculate in a time comparable to the period of observation), large volumes corresponding to caducous suspensions and *vice versa*. In previous work[2] it was shown that observed sediment volumes for suspensions of spherical particles in which each particle cohered rigidly to each other sphere that it contacted could be derived from a computer-generated statistical model. The present work extends this model calculation to the case in which two particles have a given probability of rigid cohesion varying between 0 and 1. The model is applicable only to dilute systems since each of the equally sized spheres is allowed to interact only with particles already located in the sediment. The variable cohesion probability provides a measure of flexibility for interpretation of the results. For spheres with non-homogeneous surfaces containing both cohesive and inert spots it can be looked on as the probability of contact between cohesive sites and hence as the square of the fractional area of the spheres covered by such sites. Alternatively, cohesion requires that the particle resist the continued downward pull of gravity so that the cohesion probability is a measure of the relative magnitudes of the particle interaction and particle weight. The predictions of the model are compared with existing data on the effect of water on the behavior of glass spheres in organic solvents.

The Model System.—Particles are chosen with x and y coördinates selected at random from numbers between 0 and 100 (using a random number generator designed by D. Moore and G. Mitchell, Western Data Processing Center. Careful statistical tests of randomness have been carried out).[3] Each one is given an essentially

(1) This work has been supported by the Office of Ordnance Research, Contract DA-04-495-ORD-1296.

(2) M. J. Vold, *J. Colloid Sci.*, **14**, 168 (1959).

infinite z coördinate which is then diminished continuously (corresponding to vertical fall) until it either reaches the value R, the sphere radius, (corresponding to reaching the bottom of the container), or until, for some $z > R$, contact is established with a particle or particles previously processed. At this point an integer lying between 0 and 99 is generated from the random number generating program. If the integer is less than the selected cohesion probability (0 = no cohesion, 99 = cohesion probability unity), the particle is considered permanently embedded in the sediment at this value of its position. If not, it is continuously displaced in a circular path, still in a vertical plane, and still maintaining contact with the particle it first encountered until it either reaches the same z value as that of its contact, or encounters a second member particle of the sediment. In the former case the particle being processed is again allowed to fall freely. In the latter, the random number generator is again interrogated, and if falling is to continue, the path of the particle is again along the arc of a circle determined by the conditions that contact be maintained with both member particles of the sediment and that the z value decrease continuously. If a third member particle of the sediment is encountered in this process and interrogation of the random number generator prescribes continued fall a test is made to see whether any further fall is possible or whether instead the particle is now firmly nested on three others. Further fall, if allowed, proceeds along a circular path defined by maintenance of contact with the lower two of the three particles which the particle being processed had contacted briefly, but which did not form a nest on which it could rest. Provision is made in the program for the special cases in which the falling particle may contact two or more sediment members simultaneously, but no restriction is placed on values of x or y coördinates that may be reached as it slides over other particles. Figure 1 shows the logical flow chart for the entire process. The details are purely an exercise in analytic geometry. The computations[4] were carried out on the IBM 709 of the Western Data Processing Center at the University of California at Los Angeles.

The operation of the model process generates a truncated roughly conical pile of spheres with the coördinates of the center of each, and the total number of others with which it is in contact recorded. This number can be as low as zero corresponding to a sphere lying on the bottom of the container with a bridge work of other spheres over it, and as high as twelve, since the program records both the contacts which the nth particle makes during its own processing and contacts made with it by succeeding particles. The quantities to be derived from further examination of the pile are the mean density and numbers of interparticle contacts.

With the model system involving only a relatively small number of particles (125), the upper

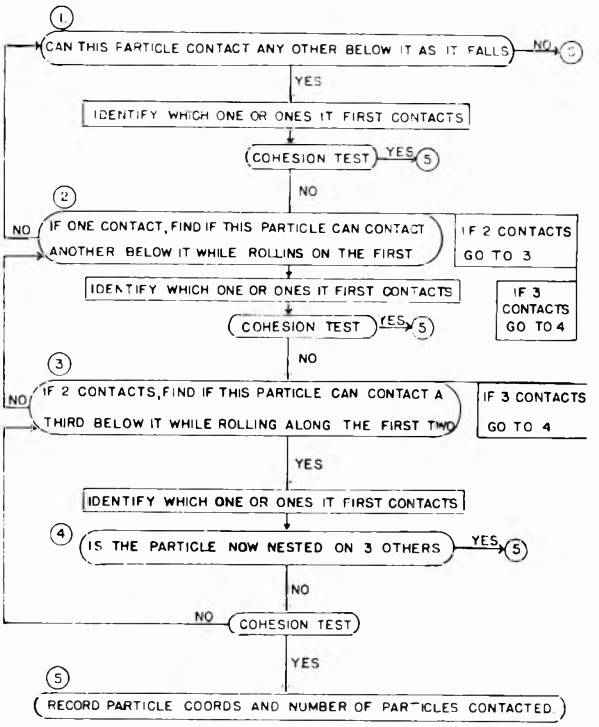

Fig. 1.—Schematic flow sheet for sediment formation. Rectangular boxes indicate operations. Oval ended boxes indicate tests determining the next operation. Input/output and iteration are not shown.

layers of the sediment will be quite dilute, containing many holes into which additional particles might fall if the process were to be continued. A correct value for the particle density corresponding to a given cohesion probability can be obtained only by excluding the incomplete upper layers. The quantity of sediment to be excluded from the density calculation was determined by examining the sediment after each 25th particle had been processed and using only the volume into which none of the last 25 had penetrated. Similarly in counting numbers of contacts only those particles were considered which were embedded on all sides in sediment having the mean density.

The process of deriving information from the results of a model calculation is illustrated by reference to Table I prepared from the computer's output for a run with 125 particles of radius 10.0 arbitrary units and a cohesion probability of 0.5. After the first 25 particles were processed, there were still many large holes accessible in the sediment as shown by the fact that after 25 more had been processed the numbers penetrating to low values of z had increased. However, after 125 had been processed, the numbers in each 20 unit increment of z between $z = 20$ and $z = 140$ had become nearly constant. Thus 69 particles of radius 10 have centers in a $100 \times 100 \times 120$ volume. Particles with their centers in a 100×100 space require a space $(100 + R) \times (100 + R)$ to accommodate the whole particle, allowing for the particle radius. This correction does not apply to the vertical dimension since there are just as many particles projecting into the 120 unit depth at $z = 20$ as

(3) D. Moore, private communication.

(4) The complete program, coded in Fortran language, may be obtained from the author.

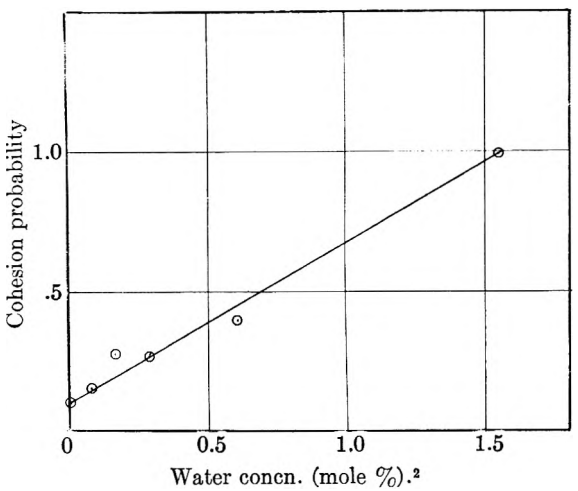

Fig. 2.—Dependence of cohesion probability for glass spheres in nitrobenzene on water content. The data are those of Bloomquist and Shutt.[5] Conversion from sediment volume to cohesion probability was made using the results of Table II.

there are projecting out of it at $z = 140$. Accordingly the density is 19.9 volume %.

TABLE I

SEDIMENT FORMATION AT COHESION PROBABILITY = 0.5

Height in sediment[a]	Numbers of particles[b]				
1	18	22	22	23	23
2	4	14	16	16	16
3	1	4	7	10	11
4		4	8	10	10
5		3	7	11	12
6			5	8	10
7			4	7	10
8				4	8
9				2	7
10				2	5
11				1	3
No. of particles processed	25	50	75	100	125

[a] The given number H stands for $2(H-1)R \leq z < 2HR$ where R is the particle radius. [b] Only those particles are counted whose final center coördinates are within the limits $0 \leq x < 100$, $0 \leq y < 100$.

The computer output included the number of other particles which each of these 69 was touching. One had 5 neighbors, 3 had 4 neighbors, 14 had 3 neighbors, 33 had 2 neighbors and 18 made contact with only one other particle, for a mean constant number of 2.07.

Table II summarizes the results obtained in this way for all runs. For low values of the cohesion probability, the sediment is so dense that only one or two 20 unit layers are filled so that with only 125 particles it is difficult to be sure that the density has really become constant. More reliable values for the sediment density here would have required processing many more particles. Inasmuch as the numbers obtained lie on a smooth curve with those for higher cohesion probability, the machine time needed to process the larger number of particles needed for more precise results was not considered worthwhile.

TABLE II

SEDIMENT DENSITY AND STRUCTURE AS A FUNCTION OF COHESION PROBABILITY

Cohesion probability, %	Particle radius[a]	No. in region of constant density	Density vol., %	Mean contact no.
0	12.5	28	71.1	8.4
3	15.0	18	64.0	6.7
5	14.0	37	60.0	6.7
10	12.5	73	47.2	4.7
25	12.5	82	35.4	3.2
35	10.0	61	26.4	2.5
50	10.0	69	19.9	2.1
50	15.0	64	18.9	2.4
75	10.0	61	15.2	2.0
100	15.0	81	16.5	2.0
100	10.0	94	13.6	2.0

[a] Arbitrary units "container" area = 100 × 100. One hundred and twenty-five particles processed in each case.

Discussion

Inspection of Table II shows immediately that the sediment structure for the present model is very insensitive to the short range interaction of individual particles if this interaction is sufficient to lead to a cohesion probability of 0.35 or more. To the extent to which real systems conform to the model, it follows that sediment volume itself is a more potentially useful procedure for studying suspensions in which the contact cohesion probability is less than 0.35 than for more stable suspensions.

According to Bloomquist and Shutt[5] glass spheres in water and in water miscible liquids sediment to a volume density of close to 55%, which corresponds on the present model to a cohesion probability of only 7%. Very nearly the same results were obtained in dry organic solvents. In one set of experiments these workers determined sediment volume in nitrobenzene containing added water. The apparent cohesion probability obtained from the reported sediment volumes and Table II of this work is in good accord with the idea that the cohesion probability should vary with the square of the concentration of water at such low concentrations that the amount adsorbed on the glass varies linearly with the concentration. These results are shown in Fig. 2.

The most severe limitation of the present model is the restriction that the sedimenting particles interact only with particles already in the sediment. For the *ca.* micron sized glass beads in the above application this is not too serious since their Stokes law sedimentation rate (0.03 cm./sec.) is substantially larger than their random thermal diffusion velocity.

A second limitation has been pointed out to the author by the referees. After contact, even though the random number generator decrees that two particles will not cohere, their rolling over each other could very well bring cohesive spots into contact. Accordingly a more realistic model could make an auxiliary cohesion probability proportional to the length of the path over which

(5) C. R. Bloomquist and R. S. Shutt, *Ind. Eng. Chem.*, **32**, 829 (1940).

the particles roll on each other. The effect of this improvement would be to give slightly looser packing, particularly at small values of the cohesion probability.

Preliminary experiments with non-porous colloidal silica in the millimicron size range has given sediments as dilute as 1.5% by volume, which cannot be accounted for on the present model.

Acknowledgment.—The author is grateful to Mr. N. Hakansson for assistance in "debugging" the computer program and to the Western Data Processing Center for the use of its computing facility (IBM 709).

THE SUBSIDENCE RATES OF SUSPENSIONS OF LITHIUM STEARATE IN *n*-HEPTANE WITH *n*-ALCOHOLS AS ADDITIVES

BY M. J. VOLD[1] AND D. V. RATHNAMMA[2]

Department of Physical and Inorganic Chemistry, The Indian Institute of Science, Bangalore, India

Received March 30, 1960

Suspensions of lithium stearate in *n*-heptane are highly unstable, undergoing gelation even at concentrations as low as 1 g./l. The rate of subsidence of these weakly gelled suspensions is decreased at first by the addition of *n*-alcohols, but passes through a minimum in some cases. The minimum subsidence rate occurs while the adsorption of the alcohol is still below its saturation value. One possible explanation of the effect is that the solvent layer between particles at the junction points in the gel becomes simultaneously more polar, tending toward an increased gel strength, and also thicker, tending toward a decreased gel strength.

Suspensions of lithium stearate in hydrocarbons are "unstable" in the sense that loose aggregates of the primary particles form spontaneously. Electron microscopy[3] shows that the primary particles retain their identity over long periods of time. The aggregates sediment to form a weak gel which can be destroyed by gentle shaking. The contrast between this ready redispersibility and the rigidity of soap aerogels prepared by Peterson and Bondi[4] suggests that the interparticle bonds in the hydrocarbon medium occur between solvated particles. The very large gel volume (as high as 800 ml./g. lithium stearate) requires that end-to-end contacts predominate in the gel.[5] X-Ray work[6] shows that the ends of the particles contain primarily lithium carboxylate groups. Accordingly, the strength of the gel is dependent on the magnitude of the attractive forces between these surfaces as modified both by the thickness and chemical nature of the "solvate" layer intervening at "contact."

The investigations reported in this paper were designed to study this dependence through measurement of the subsidence rate of dilute suspensions of lithium stearate in *n*-heptane to which small amounts of alcohols (ethanol, *n*-butyl alcohol, *n*-heptyl alcohol, *n*-octyl alcohol and *n*-dodecyl alcohol) were added, coupled with measurements of the apparent adsorption of the first three additives. Smellie and La Mer[7] have presented an analysis of subsidence behavior in flocculating suspensions according to which the process is divisible into two stages. Flocculation occurs first, accompanied by an increasing sedimentation rate. The growing flocs then form a weak gel which compacts uniformly at a diminishing rate, finally reaching a limiting volume. Garner, Nutt and Mohtadi[8] point out that the initial gel may have free particles or small flocs in its interstices. In this case, the subsidence rate may continue to increase even after gelation. Smellie and La Mer derived a general equation for the compaction phase of the subsidence based on continuity and conservation conditions which can be put in the form

$$\frac{t}{V_L} = \alpha + \beta t \qquad (1)$$

where V_L is the volume of supernatant liquid at time t and α and β are constants of the system whose reciprocals are the initial subsidence rate and the final liquid volume, respectively. This equation is of the same form as that found empirically by Farrington and Humphreys[9] for expression of liquid by compaction of a lubricating grease under pressure.

The mechanism of subsidence of a flocculated gelled suspension is complex. We visualize particles or particle aggregates loosening themselves from the gel, falling into residual interstitial spaces and displacing liquid therefrom. Both the frequency of release of particles and the degree of compaction that can result will be functions of the existing degree of compaction as well as of the strength of the interparticle bonds. Accordingly, comparisons between the subsidence rates of different suspensions can be related to the strength of the interparticle bonds most significantly at a constant degree of compaction, rather than by comparison of the parameters of equation (1), with a

(1) Department of Chemistry, University of Southern California, Los Angeles 7, California.

(2) This work is part of a dissertation submitted by D. V. Rathnamma to Mysore University for the Ph.D. degree under the guidance of Professor M. R. A. Rao.

(3) M. J. Vold, D. L. Bhattacharya and D. V. Rathnamma, *J. Ind. Inst. Sci.*, *XL*, 97 (1958).

(4) W. H. Peterson and A. Bondi, THIS JOURNAL, **57**, 30 (1953).

(5) M. J. Vold, *ibid.*, **63**, 1608 (1959).

(6) A. Bondi and 11 colleagues, Proc. Third World Petr. Cong. Section VII, p. 373 (1951).

(7) R. H. Smellie, Jr., and V. K. La Mer, *J. Colloid Sci.*, **4**, 720 (1956).

(8) F. H. Garner, C. W. Nutt and M. F. Mohtadi, *J. Inst. Petroleum*, **39**, 677 (1953).

(9) B. B. Farrington and J. Humphreys, *Ind. Eng. Chem.*, **31**, 230 (1939).

small rate associated with strong binding and *vice versa*.

Experimental Part

Materials.—Lithium stearate was prepared by neutralization of stearic acid in ethanol with an aqueous solution of Rideal and de Haen C.P. grade LiOH from which Li_2CO_3 had been removed by centrifugation of a saturated solution. The precipitate was washed in aqueous alcohol and dried to constant weight at 105°. Two "stearic acids" were employed without significant effect on the results. One was obtained by recrystallization of Armour Neofat 66 from acetonitrile to reduce the iodine value to 0.2. The other was prepared by complete hydrogenation of a technical triple pressed acid. Exploratory experiments with a third lithium stearate prepared from the technical acid directly led to considerably lower subsidence rates.

Technical 95% ethanol was first refluxed over caustic potash to remove aldehydes, then distilled from calcium oxide, and finally purified by the method of Lund and Bjerrum.[10] The higher alcohols were all of reagent grade, the *n*-octyl alcohol from the Fischer Scientific Co. and the remainder from the British Drug Houses.

Preparation of Suspensions.—Gels were first prepared by quick cooling solutions of 2 g. of dry lithium stearate in 18 g. of mineral white oil (Nujol) sealed in 1 × 8 pyrex glass tubes, from 230 to −15°. The gel was gradually diluted with *n*-heptane to about 1% concentration and centrifuged. The supernatant liquid containing Nujol was decanted and replaced with fresh *n*-heptane. The process was repeated until the supernatant layer was oil-free. The crystalline particles were shown by electron microscopy to be lath-like in shape with mean dimensions of the order of 0.6 × 0.06 × 0.01 μ.[3]

The stock suspension was analyzed by evaporating the heptane from a weighed portion, first in air and finally by heating to constant weight at 105°. Suspensions containing the desired weights of lithium stearate were prepared in cylindrical glass stoppered graduated cylanders of 50-cc. capacity, 2 cm. in diameter.

Adsorption Measurements.—The adsorption results reported are net adsorptions, $V\Delta c/m$ where V is the volume of solution containing m grams of adsorbent whose concentration diminished by Δc as a result of the adsorption. Analysis of the solutions was performed both by oxidation of the alcohol to the corresponding acid by $K_2Cr_2O_7$ and iodimetric determination of the excess reagent[11] and by means of a Brice–Phoenix differential refractometer.

Subsidence Measurements.—The measurement involves only observation of the position of the demarcation line between supernatant liquid and suspended material as a function of time. The results were found to depend erratically upon temperature fluctuations and on the inadvertent presence of trapped air bubbles. Hence, the suspensions were de-aerated with suction, kept in a draft-free air thermostat at 30 ± 0.5°, and homogenized at the beginning of each settling period by prolonged rather than violent agitation. Despite these precautions, the subsidence rates were somewhat erratic as can be seen in Fig. 1, which shows complete results for a typical experiment consisting of many individual runs.

The subsidence rate also depends critically upon the concentration of the suspension. Suspensions more concentrated than 2 g./l. are initially gelled and compact isotropically only very slowly. Suspensions more dilute than 0.5 g./l. form gelled macroscopic clumps within minutes which stir up gross convection currents as they settle, preventing establishment of any reproducible subsidence behavior. Suspensions with 1 g./l. settled regularly at a conveniently observable rate. Accordingly, all measurements were made at this concentration.

Results and Discussion

Adsorption.—Adsorption isotherms at 30° for the three alcohols on lithium stearate are shown in Fig. 3. The rather large scattering is believed due more to lack of complete reproducibility of the specific surface area of the suspended lithium stearate than to lack of analytical precision. Langmuir plots of the smoothed data are somewhat curved and are useful principally to obtain reliable values of the saturation values which are 1.9, 2.2 and 1.1 mmoles per gram of lithium stearate for the ethyl, butyl and heptyl alcohols, respectively. Estimation of the total surface area from the mean particle dimensions is, of course, very crude because of the poly-dispersity. Nevertheless, its order of magnitude, which works out to 236 sq. m./g., when compared with the limiting adsorption (*i.e.*, surface excess) corresponds to 20.5, 17 and 36 Å.[2] per "adsorbed" alcohol molecule, respectively, meaning that the surface excess is of the order of magnitude of a statistical monolayer.

The lithium stearate crystal surfaces present at least two types of planes,[3] the larger of which is presumably composed of the exposed methyl groups, and the smaller, at the particle ends, and edges, having exposed COOLi groups. It seems likely that the –COOLi groups present more favorable adsorption sites which could build up a substantial thickness of adsorbed alcohol before much adsorption occurs on the less favorable sites.

Subsidence Rates.—Table I shows the mean times required for suspensions of the indicated concentrations of additive to separate 13 ml. of free solvent, or to reach a volume concentration of lithium stearate of 50 mg./37 ml. (*i.e.*, 740 ml./g. of suspended material) for each of the 5 alcohols studied. Where available, the adsorption of the additive is given as per cent. of its saturation value. The subsidence times were obtained from curves such as Fig. 1. Figure 2 shows a complete set for ethanol with the individual points omitted.

In all cases, the first effect of a small amount of additive is to increase the subsidence time substantially. With increasing amounts of additive the subsidence time appears to pass through a maximum and then decrease again for ethanol, butanol and heptanol, although the experimental data do not conform to a smooth curve with any precision. The same is true for dodecanol as an additive but the behavior of octyl alcohol is very erratic.

For the three cases for which results are available, the adsorption has not reached its apparent limit or maximum at the additive concentration giving the largest subsidence time.

London–Van der Waals Interaction.—Quantitative calculation of the London–van der Waals interaction for rod shaped particles is quite cumbersome, and not really justifiable at present because only very crude estimates of the van der Waals constants can be made. The qualitative features of the possible results of replacing solvent molecules (heptane) with adsorbed molecules (alcohol) can be explored by using calculations based on spheres with a diameter of the mean of the average width and thickness of the particles (about 400 Å.)

An expression for the interaction of two such spheres, each surrounded by an inner shell of 4 Å. thickness, and an outer shell of thickness δ, distant about 3 Å. from each other has been derived from the general expression derived by one of us,[12]

(10) A. Weissberger, "Technique of Organic Chemistry," Vol. VII, Interscience Pub. 1955, p. 341.

(11) P. Szeberengi, *Z. anal. Chem.*, **54**, 409 (1915).

(12) M. J. Vold, *J. Colloid Sci.*, submitted.

TABLE I

SUBSIDENCE DATA FOR SUSPENSIONS OF LITHIUM STEARATE[a] IN *n*-HEPTANE WITH ADDITIVES

Concn. of additive, mg./100 mg. list.	Time to separate 13 ml. solvent	Surface saturation, %
	Ethanol	
32	172	34
96	166	68
128	239	74
160	284	79
320	N400	90
640	183	95
1280	166	97
1600	150	99
3200	126	100
0[b]	116	..
	n-Butyl alcohol	
1.5	240	<10
6.1	110	20
12.3	170	35
24.6	235	50
49.3	365	59
147	298	77
296	198	88
0[b]	82	..
	n-Heptyl alcohol	
2.4	184	9
4.8	212	18
9.7	390	40
19.4	450	50
38.7	270	65
116	136	81
232	136	90
0[b]	136	..
	n-Octyl alcohol	
2.7	200	
5.4	128	
10.8	190	
21.6	220	
43.2	180	
86.4	243	
260	98	
0[b]	122	
	n-Dodecyl alcohol	
7.7	196	
31.1	200	
62	170	
124	204	
373	252	
970[b]	160	
0[b]	122	

[a] Concentration 1.00 g./liter. [b] Blank runs were made on each batch of suspension and are listed with the additives employed for that suspension.

incorporating some reasonable assumptions about the van der Waals constants.

In the absence of any additive, with roughly a monolayer of heptane ($\delta + 4 = 10$ Å.) the total interaction is given by

$$-12V = (A_P^{1/2} - A_M^{1/2})^2 \frac{H(23, 1)}{400} \qquad (1)$$

where H is a function of the particle separation ($2 \times 10 + 3$ Å.) and the particle diameter (400 Å.), derived by Hamaker

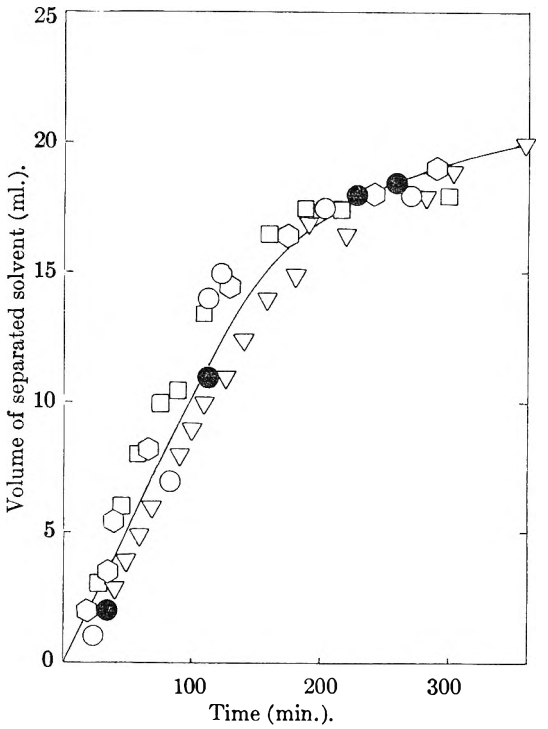

Fig. 1.—Subsidence of lithium stearate suspensions in *n*-heptane; runs 1–5, respectively.

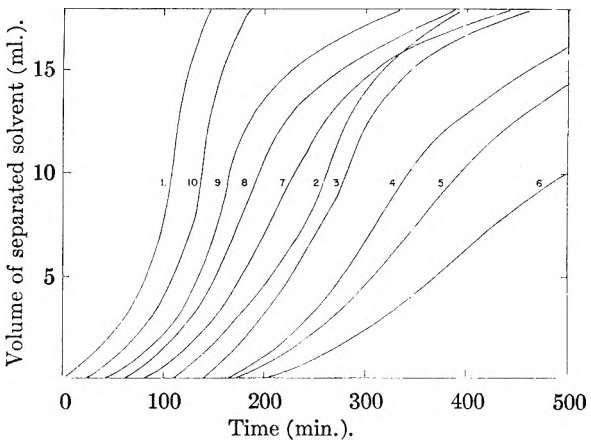

Fig. 2.—Effect of ethanol on the subsidence of lithium stearate in *n*-heptane. Concentration of ethanol (mg./100 ml.) 1, 0.0; 2, 32; 3, 96; 4, 128; 5, 160; 6, 320; 7, 640; 8, 1280; 9, 1600; 10, 3200. The curves have been shifted along the time axis by the amounts indicated by the times at 0 ml. separated solvent. Table I gives points read from the graphs at 13.0 ml.

$$H(X,Y) = \frac{Y}{X^2 + XY + X}\,\frac{Y}{X^2 + XY + X + Y} + 2 \ln \frac{X^2 + XY + X}{X^2 + XY + X + Y} \qquad (2)$$

where X is the ratio of the particle separation to the diameter of the smaller particle and Y is the ratio of the particle diameters which is unity in this case. The A's are van der Waals constants for particle (P), medium (M) and sorbate (S).

The experimental fact that the systems gel means that the interaction energy must be larger than kT by a substantial factor, but the fact that they can be easily redispersed means that the maximum *force* required to separate them cannot be

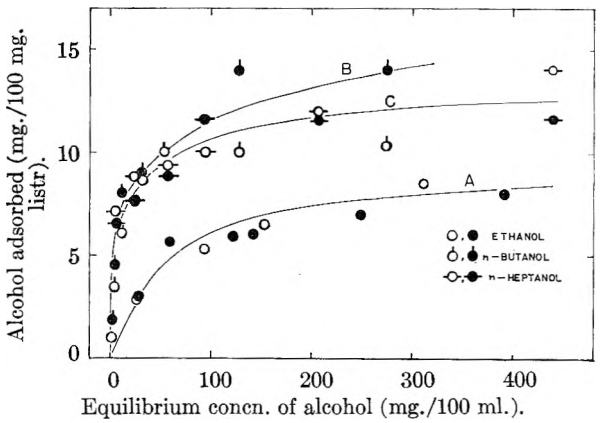

Fig. 3.—Adsorption of various alcohols on lithium stearate in *n*-heptane: O, ethanol; O,●, *n*-butyl alcohol; O,●, *n*-heptyl alcohol; -O-,-●-, open points, analytical; solid points, refractometric.

larger than could be reasonably expected to be exerted by hand shaking. These two conditions may be used to estimate a range of values for

$$(A_P^{1/2} - A_M^{1/2})^2$$

If the liquid moves relative to the container during hand shaking at a maximum speed of the order of 100 cm./sec., and the separation between a layer of liquid adhering to the container surface and one moving with this speed is in some regions at least as small as 10^{-4} cm., the local shear rate can reach 10^6 sec.$^{-1}$ and the corresponding force/unit area 10^4 dynes/cm.^{2}, if the viscosity is of the order of one centipoise. Acting over the cross-sectional area of a particle such a shear rate corresponds to a force of 10^{-6} dynes. The force acting (radially of course) is obtained by differentiating the energy expression. One obtains for the assumed layer thickness, contact separation, and particle radius.

$$V = 0.40(A_P^{1/2} - A_M^{1/2})^2 \text{ ergs}$$
$$F = -2.5 \times 10^6 (A_P^{1/2} - A_M^{1/2})^2 \text{ dynes}$$

Accordingly, values of van der Waals term lying between 5×10^{-13} and 5×10^{-12} are quite plausible.

Each of the quantities $A_P^{1/2}$ and $A_M^{1/2}$ is in turn given by expressions of the form

$$\frac{1}{\pi} A_P^{1/2} = \Sigma q_P(c)\, \lambda_C^{1/2} + q_P(0)\lambda_0^{1/2}$$
$$\frac{1}{\pi} A_M^{1/2} = \Sigma q_M(c)\lambda_C^{1/2}$$

where the q's are the numbers of the indicated atoms per cc. and the λ's are the London–van der Waals constants for the indicated atoms. It has been assumed that the contributions of the hydrogen atoms and lithium ions are negligible. Using the known densities of the two substances, one finds

$$A_P^{1/2} = 3.72 \times 10^{22} \lambda_C^{1/2} + 4.14 \times 10^{21} \lambda_O^{1/2}$$
$$A_M^{1/2} = 2.9 \times 10^{22} \lambda_C^{1/2}$$

In the presence of adsorbed additive equation 1 no longer applies. Instead the net interaction is given by

$$-12V = (A_S^{1/2} - A_M^{1/2})^2 H\left(\frac{2\delta + 3}{408}\right) +$$
$$(A_P^{1/2} - A_S^{1/2})^2 H\left(\frac{2\delta + 11}{400}, 1\right) +$$
$$2(A_S^{1/2} - A_M^{1/2})(A_P^{1/2} - A_S^{1/2}) H\left(\frac{2\delta + 7}{400}, 1.02\right) \quad (3)$$

if it is assumed that the oxygen atoms in the alcohol will all go into the 4 Å. thick shell immediately surrounding the particle, and that the hydrocarbon portion will have the same Van der Waals constant as the heptane it replaces in the layer of thickness δ.

As adsorption proceeds both $A_S^{1/2}$ and δ may be expected to change in monotomic fashion. Since λ_0 is presumably greater than λ_C, $A_S^{1/2}$ will increase, eventually probably surpassing $A_P^{1/2}$ when adsorption is nearly complete since its limiting value may be near $2.9 \times 10^{22} \lambda_O^{1/2}$. It can be shown by differentiating equation 3 with respect to $A_S^{1/2}$ that such a change can result only in a continuously increasing interaction energy, corresponding to the observed increasing times required for a given extent of subsidence. Any increase occurring in the thickness of the adsorbed layer can result only in a decreasing interaction energy, and *vice versa*.

It is clear that a judicious choice of values for the four parameters involved in equation 3 can give rise to a maximum interaction energy at incomplete adsorption. One such arbitrary choice and its results are given in Table II. However, it is equally clear that such a result is insufficient to determine any of the parameters uniquely or even to guarantee that this explanation of the effects observed is the correct one.

Koelmans and Overbeek[13] observed a maximum settling time for suspensions of ferric oxide in xylene with various fatty acids as stabilizing additives occurring when adsorption was still incomplete. Both the interpretation of the experimental observations and the explanation of the effect are quite different for this case. These suspensions do not gel and the particles settle more or less independently, so that maximum settling time corresponds to smallest flocculation tendency. The factor which is probably dominant here is the entropy effect pointed out by Mackor and Van der Waals[14] which increases in importance as the chain length of the acid increases and decreases as the adsorbed layers approach close packing since less configurational entropy is available to be lost by flocculation.

TABLE II

DEMONSTRATION THAT A MAXIMUM INTERACTION ENERGY CAN BE CALCULATED

Quantity[a]	No additive	Additive concn., C_1	Additive concn., $C_2 > C_1$
$A_S^{1/2} \times 10^{-6.5}$, ergs$^{1/2}$	2.9	5.5	5.7
Adsorbed hydrocarbon layer thickness, Å.	6	10	14
Interaction energy multiples of RT	4.5	5.0	4.4

[a] Additional quantities common to the three calculations were chosen as $kT = 4 \times 10^{-14}$ ergs, particle radius 200 Å., $A_P^{1/2} = 5 \times 10^{-6.5}$, $A_M^{1/2} = 2.9 \times 10^{-6.5}$, separation at contact = 3 Å., polar layer thickness, 4 Å.

(13) H. Koelmans and J. Th. G. Overbeek, *Disc. Faraday Soc.*, **18**, 52 (1954).

(14) E. L. Mackor and J. H. Van der Waals, *J. Colloid Sci.*, **7**, 535 (1952).

THE RADIOLYSIS OF LIQUID *n*-HEXANE

BY THOMAS J. HARDWICK

Gulf Research & Development Company, Pittsburgh, Pennsylvania

Received April 5, 1960

The continuous decrease in hydrogen gas yield during the radiolysis of *n*-hexane is attributable to the addition of H atoms to the hexenes concurrently being produced. Unsaturation in the C_7–C_{12} products arises from the addition reaction of alkyl plus alkenyl radicals; the alkenyl radicals are derived from hydrogen abstraction from hexenes by H atoms. The overall kinetics of radiolysis are satisfactorily explained by invoking free radical mechanisms; ion–molecule reactions appear to play little or no part. Both "hot" and thermal H atoms are produced, the former invariably forming hydrogen gas. An explanation for the mechanisms of formation of the so-called "molecular" products is given. The yield of products can be explained quantitatively by a relatively simple reaction scheme.

Introduction

The radiolysis of liquid *n*-hexane has been studied by several investigators. Dewhurst[1] found the hydrogen yield from *n*-hexane to be constant up to doses of 100 j./g. (G_{H_2} = 5.0 mol./100 e.v.). In the presence of free radical scavengers, the hydrogen yield dropped to a limiting value of 3.0. Davison[2] reported a lower hydrogen yield (G_{H_2} = 4.0 mol./100 e.v.). Recently, Allen and Schuler[3] showed that there was no effect of linear energy transfer (l.e.t.) on the hydrogen yield.

We have previously reported that a decrease in hydrogen yield occurs on irradiating cyclohexane.[4] When a similar experiment with *n*-hexane resulted in the same behavior, it became desirable to investigate further into the *n*-hexane system to explain this phenomenon and to reconcile it with published data. Accordingly, a varied program was undertaken to determine the primary processes and subsequent reactions which occur on the radiolysis of liquid *n*-hexane. In view of the discrepancies in previous results, it was felt that a quantitative investigation was necessary in which accurate yields of primary processes could be determined and the rates of subsequent reactions measured. In a practical sense, such data would enable one to alter reaction sequences and thus predictably modify the product spectrum.

Experimental

Materials.—Phillips Pure Grade *n*-Hexane was used throughout. The concentration of unsaturated material, presumably some C_6 isomer, was 0.25 millimolar or 0.003%. It will be shown later that the small amount of this impurity does not affect the various yields.

Analytical. Determination of Unsaturation.—The hydrocarbon sample (5–50 ml.) was added to 20 ml. of glacial acetic acid. About 25% excess bromine was added as a 1.5 *M* solution in acetic acid. After two minutes, 25 ml. of water containing excess KI was added, converting the excess bromine to iodine. The whole mixture was titrated with 0.05 *M* sodium thiosulfate in the usual iodometric manner. Titrations with pure olefins gave theoretical values of the unsaturation. This method is considered satisfactory for light ($<C_{18}$) hydrocarbons which are free of aromatic components.

Other analytical methods will be described in connection with individual experimental procedures. These include mass spectrometric and gas chromatographic analyses plus certain techniques specific to hydrocarbon analysis.

It is convenient to report the results in several sections, each section being dependent on a particular radiation technique and requiring different analytical procedures.

(1) H. A. Dewhurst, THIS JOURNAL, **62**, 15 (1958).

(2) W. H. T. Davison, *Chemistry and Industry*, 662 (1957).

(3) A. O. Allen and R. H. Schuler, *J. Am. Chem. Soc.*, **77**, 507 (1955).

(4) W. S. Guentner, T. J. Hardwick and R. P. Nejak, *J. Chem. Phys.*, **30**, 601 (1959).

Section I

Irradiation of Pure *n*-Hexane

Irradiation Facility.—A 4-liter volume of hexane was irradiated by electrons from a Van de Graaff accelerator (Model KS, High Voltage Engineering Corp.). The liquid was placed in a circulating loop, the details of which are published elsewhere.[5] Briefly, the liquid was circulated through a loop consisting of an irradiation cell, a degassifier, a heat exchanger and a pump. Gases produced by radiolysis were stripped from the liquid in the degassifier and were removed from the system through a condenser maintained at 0°. A dry test meter placed in series with this condenser measured the total volume of gas evolved. Provision was made for sampling the gas without interrupting the flow.

The rate of energy absorption for the particular electron energy and beam current used was measured using the sodium formate dosimeter.[6] Values were considered accurate to the reproducibility of machine operation (±2%).

Using the gas collection arrangements described above, the rate of gas evolution could be measured at a constant power input. The ratio of these two quantities, d(gas)/d*t*/(power input), expressed in appropriate units, is the yield (*G*-value) of the gas evolved: furthermore, this yield can be measured continuously throughout the experiment.

In a typical run the hexane was put into the loop and brought to 25°. Nitrogen was passed through the degassifier to purge oxygen from the system. For a total of 1500 j./g. energy absorption about 40 l. of gas was evolved during radiolysis. The power absorption in the liquid was usually in the range 500–700 watts.

Samples of gas were taken about every 80 j./g. of energy absorbed and were analyzed mass spectrometrically. By interpolating the analytical results, a continuous measurement of the individual gas yields was obtained as a function of energy absorbed.

Gas Production.—With increasing energy absorption, the yield of total gas decreased from a high initial value and finally leveled off to a reasonably constant value in much the same manner as was found with cyclohexane. This change in yield was found to be due entirely to hydrogen. In Fig. 1 the hydrogen yield is plotted as a function of energy absorption (unbroken line).

Making allowances for the holdup of higher hydrocarbon gases in hexane due to increased solubility, the yields of those hydrocarbons in the C_1-C_5 range are reasonably constant throughout the radiolysis. The yields are shown in Table I together with those of Dewhurst[1] and Davison.[2] Differences exist in the values in the C_3-C_5 range, but with C_1 and C_2 hydrocarbons there is no significant over-all disagreement. It may be worth noting that in our experiments the gases were removed from solution almost immediately, whereas in previous experiments it appears that gas stripping occurred only after completion of the experiment. The yields of C_4 and C_5 hydrocarbons are somewhat less reliable than the others, due to mechanical problems of separating these components from the mother liquid.

Liquid Products.—The remaining liquid was separated by fractional distillation. All of the hexane and hexenes were removed by preliminary distillation to 72°. The remaining material was analyzed for unsaturation and then

(5) W. S. Guentner and T. J. Hardwick, *Ind. Eng. Chem.*, in press.

(6) T. J. Hardwick and W. S. Guentner, THIS JOURNAL, **63**, 396 (1959).

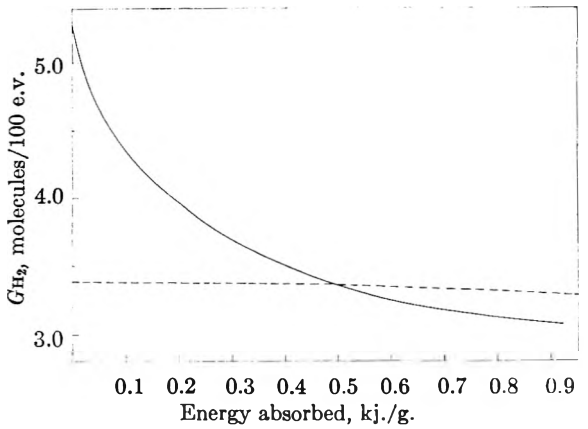

Fig. 1.—Differentially measured hydrogen gas yield as a function of energy absorbed during *n*-hexane radiolysis: solid line, hexane pure initially; dotted line, hexane containing 4% hexene-1 initially.

TABLE I

YIELDS OF LIGHT HYDROCARBONS FROM *n*-HEXANE RADIOLYSIS

	Yield, molecules/100 e.v.			
Product	Dewhurst[1]	Davison[2]	This work	*n*-Hexane + 4% hexene-1
Hydrogen	5.0	4.0	Decreases from 5.28	3.4
Methane	0.15	0.12	0.10	0.11
Ethane	.30	.22	.21	.22
Ethylene	.30	.36	.23	.16
Propane	.42	.36	.13	.08
Propylene	.13	.20	.07	.06
Butane	.53		.05	.06
Butenes				
C_6	.20		.02	

fractionated, cuts being made at the temperatures expected for *n*-alkanes. The unsaturation in each fraction was determined by bromination and by fluorescence indicating absorption analysis.[7] Each sample was submitted for mass spectrometric analysis to determine the homogeneity of the distillation cuts. Generally, 80% of the product was found to be in the expected alkane range, with 10% each of higher and lower alkanes. Suitable corrections were made when computing yields.

The total unsaturation in the hexane fraction, *i.e.*, hexene, was determined. In a second sample these hexenes were separated from the hexane by absorption on silica gel. These absorbed hexenes were released from the absorbent and passed through a suitable gas chromatographic column which separated the five hexenes, allowing a percentage determination of the individual hexenes. From these data, the yields of individual hexenes were calculated.

The yields of hexenes and of products heavier than hexane are shown in Table II. The yields of C_{12} products and of the C_7-C_{11} products are lower than those found by Dewhurst and by Davison. With the large volumes which were used in these experiments, yields were determined by direct weighing and probably represent a maximum value. The discrepancy between these results and those previously published may arise from difficulty in calibrating absolutely gas chromatographic units or mass spectrometers for the highly branched materials resulting from radiolysis.

One noticeable result is the extent of unsaturation in all product groups. A high degree of unsaturation has been noted before in *n*-hexane radiolysis by Dewhurst,[1] and by Keenan, *et al.*,[8] on liquid butane radiolysis. Further experiments were made to determine the role of unsaturation in the radiolytic reactions.

(7) A.S.T.M. Method D-1319-58P.

(8) V. J. Keenan, R. M. Lincoln, R. L. Rodgers and H. Burwasser, *J. Am. Chem. Soc.*, **79**, 5125 (1957).

TABLE II

LIQUID PRODUCTS FROM *n*-HEXANE RADIOLYSIS

Product	Total yield, mol./100 e.v.	% unsaturated
C_7	0.06	0
C_8	.26	13
C_9	.23	17
C_{10}	.27	19
C_{11}	.02	40
C_{12}	1.70	21
Hexene-1	0.45	
Hexene-2	0.96	
Hexene-3	0.35	
Total hexene	1.76	

Section II

Production of Unsaturation

Irradiation of Pure Hexane.—The irradiation technique used in the experiments reported in this section involved irradiating a 200-ml. sample of hydrocarbon in an aluminum cup (3″ diameter × 2.5″ high) with a 10–20μ amp spot beam. The cup sat in a constant temperature water-bath and its contents were stirred magnetically. A thin (7 mg./cm.^{2}) polyethylene cover was placed over the cup to prevent ingress of air and to decrease evaporation of the hydrocarbon. The over-all temperature of the irradiated liquid was never more than 5° above that of the bath (21°).

The energy absorbed in the liquid was determined by calorimetric measurements of the beam under the same operating conditions.[6]

Samples of *n*-hexane were irradiated in this manner to various total doses up to 2000 j./g. The unsaturation was determined by bromination, and the amount produced plotted as a function of energy absorbed (Fig. 2). Total unsaturation is reasonably proportional to the dose, at least up to 1500 j./g. Similar results have been reported for other *n*-alkanes.[9,10]

If, however, a separation is made by distillation of the hexenes from the unsaturation products containing seven carbon atoms or more, the results on the lower two curves of Fig. 2 are obtained. Hexenes are produced with an initial yield of 3.10 molecules/100 e.v., but the yield decreases with increased energy absorption. The unsaturation yield in the heavier products is less than 0.005 mol./100 e.v. initially but gradually increases as more energy is absorbed. It would seem reasonable to assume that hexenes are precursors of the unsaturation in the heavier products. Subsequent experiments reported in this section are based on this premise.

Irradiation of Hexane–Hexene-1 Mixtures.—Experiments were made in which 200-ml. samples of hexane containing small amounts of hexene-1 were irradiated. For low doses, up to 200 j./g., the production of hexenes and of higher unsaturates was proportional to the energy absorbed.

The yields of the products are shown in Fig. 3. At higher hexene-1 concentrations, a net decrease in total hexenes is found. The yield of higher unsaturation products appears to level off at high hexene-1 concentrations. Similar results are obtained with the system hexane + an isomeric mixture of hexene-2. Both the decrease in hexene yield and the increase in higher unsaturation yield are smaller for hexene-2 than for hexene-1.

From the above evidence it appears fairly clear that hexenes are intermediates in the formation of unsaturation in heavier products ($>C_7$).

A 4-liter volume of hexane containing 4%/vol. hexene-1 was irradiated at 25° in the circulating loop. The method of radiolysis and the analytical procedures were identical with those described in Part I. The yields of lower hydrocarbons are shown in the last column of Table I. The values are essentially the same as those found for pure *n*-hexane. The product distribution in the range C_7-C_{12} was found to be about the same with and without the presence of hexene-1, although the yield of unsaturation was increased by about 20% throughout.

(9) H. A. Dewhurst, THIS JOURNAL, **61**, 1406 (1957).

(10) A. M. Brodsky, Yu A. Kolbanovsky, E. D. Filatova and A. S. Tchernyskeva, *Inter. J. Applied Rad. and Isotopes*, **5**, 57 (1959).

The great difference in results from the radiolysis of hexane and hexane–4% hexene-1 was found in the hydrogen yield. This yield was constant for the first 500 j./g. of energy absorbed ($G_{H_2} = 3.4$) and gradually decreased with increasing dose. The results are plotted as the dotted line in Fig. 1.

The presence of hexene in *n*-hexane during radiolysis has two effects: (1) the hexene acts as an intermediate in the formation of higher unsaturated hydrocarbons and (2) reduces the hydrogen yield to a constant value over a wide range of energy absorption.

From these and other unreported results it becomes obvious that one key to understanding the mechanism of hexane radiolysis was to determine quantitatively the effects of addition of small amounts of hydrogen atom scavengers; *e.g.*, hexene, on the hydrogen yield. The development of this investigation is reported in Section III.

Section III

Hydrogen Production in the System: Hexane + Scavenger

Experimental—Irradiations were carried out in an irradiation cell of the design which permitted removal of dissolved gases prior to irradiation and of hydrogen after exposure. This cell (~250 ml.) was filled with 100 ml. of liquid, a connecting tube containing a stopcock was added through which the cell was attached to a vacuum system. Gases were removed by conventional chilling and pumping techniques.

The liquid was irradiated at room temperature (23°) by X-rays from a Van de Graaff accelerator. The irradiation cell was placed at a 45° angle to the beam with the bottom bulb in the area of maximum flux. The dose was kept small, about 0.3 j./g., in order that the composition of the solution remain essentially unchanged during radiolysis. In the usual experiment, about 5–10 μmoles of hydrogen was produced.

After irradiation, the cell was connected to a gas analysis apparatus, where the hydrogen was removed and measured quantitatively in a McLeod gage. Details of this apparatus appear elsewhere,[11] but it is pertinent to mention that the analytical procedure is based on differential absorption on charcoal at −196°. Small amounts of oxygen, nitrogen or hydrocarbons in the gas removed from the irradiation cell do not interfere with the analytical accuracy.

The output of X-rays in the forward direction from high energy electrons varies approximately as the cube of the incident electron energy. Since the accuracy of reproducing a given voltage in a sequence of irradiations is about ±2%, there will be a significant variation of total energy absorbed in successive experiments. The extent of this variation was monitored by placing beside the irradiation cell an identical cell containing 100 ml. of ferrous sulfate dosimeter solution. From a comparison of the ferric ion produced the measured gas yields could then be corrected for small variations in energy absorption. Absolute energy absorption was measured by replacing the organic liquid with an identical volume of the ferrous sulfate solution and determining the energy absorbed from the ferric yield ($G_{Fe^{+++}} = 15.5$ mol./100 e.v.). The necessary corrections for density of the organic fluid, and for differences in attenuation between liquids of different densities were made. The over-all variation in results on successive determinations of the hydrogen gas yields was ± 2%.

Kinetics of Hydrogen Gas Formation.—Hydrogen gas production from irradiated hexane occurs by two general processes, one influenced by scavengers, the other, not. One process may be represented by the inclusive reaction

$$C_6H_{14} \xrightarrow{G_1} H_2 + \text{Products} \qquad (1)$$

In the other process, the first step is hydrogen atom formation

$$C_6H_{14} \xrightarrow{G_2} C_6H_{13} + H \qquad (2)$$

When small amounts of a scavenger S are present in solution the reaction of this hydrogen atom takes place in the competitive reactions

(11) T. J. Hardwick, to be published.

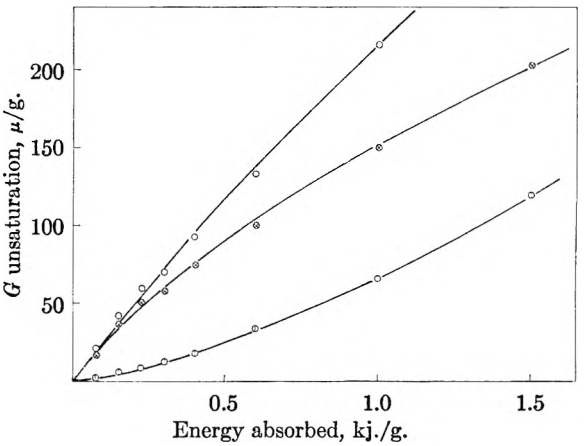

Fig. 2.—Production of unsaturation in irradiated hexane: ○, total unsaturation; ⊗, hexenes; ⊙, unsaturation in C_7–C_{12} hydrocarbons.

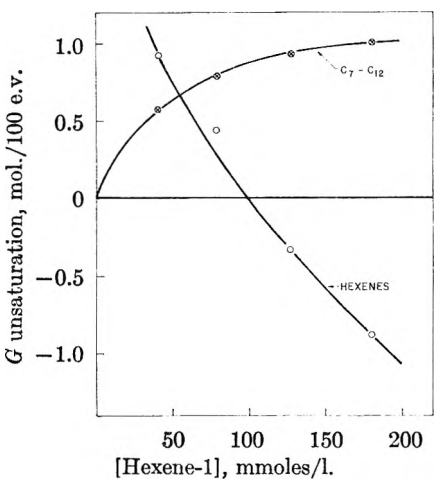

Fig. 3.—Unsaturation yields in the radiolysis of hexane–hexene-1 mixtures: ○, net yield of hexenes; ⊗, yield of unsaturated hydrocarbons C_7–C_{12}.

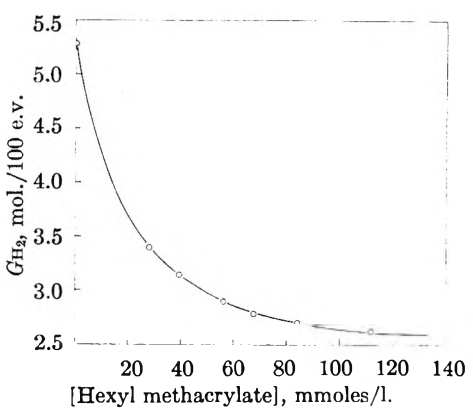

Fig. 4.—Hydrogen yield in hexane radiolysis as a function of scavenger concentration (hexyl methacrylate).

$$H + C_6H_{14} \xrightarrow{k_3} H_2 + C_6H_{13} \qquad (3)$$

$$H + S \xrightarrow{k_4} HS \qquad (4)$$

where the nature of S is such that hydrogen gas is not produced in reaction 4. In the absence of a scavenger (*i.e.*, pure hexane) the total hydrogen yield, $G_{H_2(0)}$, equals $G_1 + G_2$. With S present a decrease in hydrogen yield is observed, the extent of which depends on the scavenger concentration. Figure 5 shows the decrease in hydrogen yield

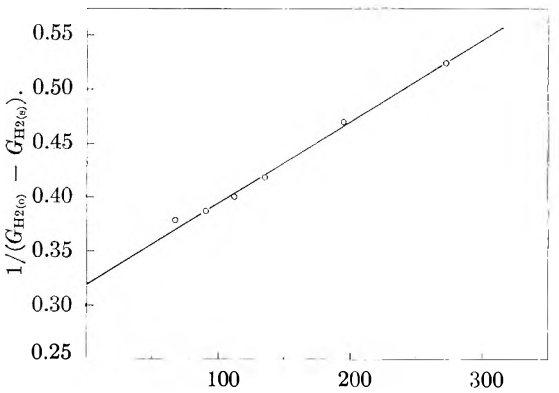

Fig. 5.—Kinetic plot of data in Fig. 5 to determine hydrogen atom yield.

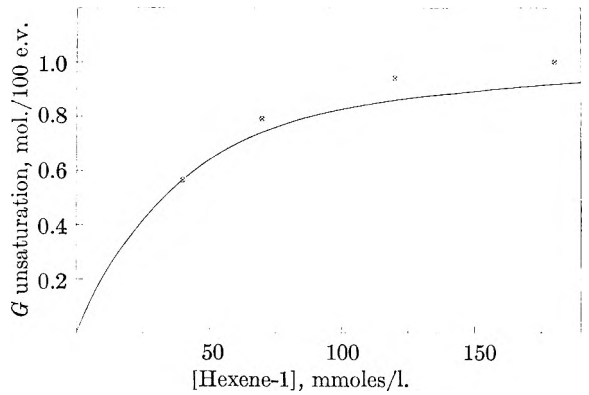

Fig. 6.—Comparison of hexenyl radical formation and unsaturation yield in C_7–C_{12} range from irradiated hexane–hexene-1 solutions: ⊗, unsaturation in C_7–C_{12}; —, hexenyl formation calculated from k_3/k_6 data.

found with various concentrations of hexyl methacrylate scavenger. The hydrogen yield from pure hexane is 5.28 mol./100 e.v., somewhat higher than had been reported previously.

If we apply a steady-state kinetic treatment for hydrogen atoms, and measure the hydrogen gas production for the system hexane + scavenger, $G_{H_2(S)}$, the following equation is obtained

$$\frac{1}{G_{H_2(0)} - G_{H_2(S)}} = \frac{1}{G_2} \times \frac{k_3}{k_4} \frac{[\text{Hexene}]}{[S]} + \frac{1}{G_2} \qquad (I)$$

This equation states that if we measure the hydrogen yield in pure hexane, and in hexane containing small concentrations of scavenger, the reciprocal of the difference in the hydrogen yield without and with scavenger, plotted against the ratio [Hexane]/[S], gives a straight line, the intercept of which is $1/G_2$ and the slope $1/G_2 \times k_3/k_4$. If different scavengers are used, the same value of the intercept should be obtained, but the slope would be different due to a different value of k_4.

Experiments to test this postulate were made using five scavengers: methyl methacrylate, hexyl methacrylate, carbon tetrachloride, tetrachloroethylene and iodine. The kinetic plot for the scavenger hexyl methacrylate is shown in Fig. 6; the other scavengers show like results. The values of G_2 obtained from the intercept are shown in Table III.

The mean value of G_2 is 3.16 atoms/100 e.v. By difference, the hydrogen gas yield unaffected by scavengers, (G_1), equals 2.12 mol./100 e.v.

Kinetic expressions of this type are quite general. Baxendale[12] has used similar equations to determine scavenging effects in methanol radiolysis. Historically, competitive reactions in gas phase reactions have been treated in the same general fashion.

(12) G. E. Adams, J. H. Baxendale and R. D. Sedgwick, THIS JOURNAL, **63**, 855 (1959).

TABLE III

THERMAL HYDROGEN ATOM YIELDS IN IRRADIATED *n*-HEXANE

Scavenger	Hydrogen atom yield (G_2), atoms/100 e.v.
Methyl methacrylate	3.18
Hexyl methacrylate	3.15
Tetrachloroethylene	3.16
Carbon tetrachloride	3.13
Mean	3.16

If, from the data of Burton, *et al.*,[13] on the radiolysis of the cyclohexane–iodine system, the kinetic plot ($1/\Delta G_{H_2}$ *vs.* [cyclohexane]/[I_2]) is made, a straight line is found. Similar results are found on using the data reported on the cyclohexane–methyl iodide system[13] and the isopropyl alcohol-acetone system.[14]

When considering the more natural case of hydrogen atom scavenging by hexenes, an extra reaction must be considered. As well as adding across the double bond, the hydrogen atom may abstract hydrogen to produce a hydrogen molecule and an allyl radical. Darwent and Roberts[15] have shown this to happen in propylene and butene-1; Back[16] has shown it to occur in the case of pentene-1. There seems to be no reason to expect that such a reaction would not be general.

The reactions for the disappearance of hydrogen atoms in hexane containing small amounts of hexene are

$$H + C_6H_{14} \xrightarrow{k_3} H_2 + C_6H_{13} \qquad (3)$$

$$H + C_6H_{12} \xrightarrow{k_5} C_6H_{13} \qquad (5)$$

$$H + C_6H_{12} \xrightarrow{k_6} H_2 + C_6H_{11} \qquad (6)$$

Reaction 5 is the addition of hydrogen to the olefin bond to give an alkyl radical; reaction 6 is the abstraction of hydrogen from an olefin to give an alkenyl radical, in this case a hexenyl radical.

With the addition of reaction 6 to the kinetic scheme equation I becomes

$$\frac{1}{G_{H_2(0)} - G_{H_2(S)}} = \frac{1}{G_2} \times \frac{k_3}{k_5} \frac{[\text{Hexene}]}{[\text{Hexene}]} + \frac{1}{G_2} \times \left(\frac{k_6}{k_5} + 1\right) \qquad (II)$$

A plot similar to that from equation I gives a straight line, with the difference that the intercept is now $1/G_2 \times (k_6/k_5 + 1)$. However, since G_2 has already been determined, the ratios k_3/k_5, k_6/k_5, etc., may be determined.

Experiments were made using as scavengers pure hexene-1, cyclohexene and a mixture of hexene-2 isomers. In all cases a straight line was obtained on the kinetic plot. The values of the relative rate constants are (a) for hexene-1, $k_5/k_3 = 173$, $k_6/k_5 = 0.50$; (b) for hexene-2 (83% *cis*), $k_5/k_3 = 102$, $k_6/k_5 = 0.25$; (c) for cyclohexene, $k_5/k_3 = 174$, $k_6/k_5 = 0.25$.

It is pertinent to digress at this point and discuss the effects of purity on the hydrogen yield. A typical trace impurity in *n*-hexane would be an olefin boiling in the same range. Taking as a mean value $k_5/k_3 = 150$, and $k_6/k_5 = 0.33$, the decrease in the radiolytic hydrogen due to small amounts of unsaturation in "pure" compounds can be calculated. For example, if it is assumed that the unsaturated impurity is a hexene, 0.5 m*M* hexene (0.006%) reduces $G_{H_2(0)}$ by 0.02 mol./100 e.v., while 5.0 m*M* (0.062%) reduces $G_{H_2(0)}$ to 4.93 mol./100 e.v.

Few commercially-available hydrocarbons have a purity better than 99.9%, although probably only a fraction of the impurity is unsaturated. We have found that prolonged stirring with concentrated sulfuric acid, followed by washing with water, drying over sodium carbonate and distilling will reduce the unsaturated impurity below 0.1 mmole/l.

(13) M. Burton, J. Chang, S. Lipsky and M. P. Reddy, *Rad. Research*, **8**, 203 (1958).

(14) J. D. Strong and J. G. Burr, *J. Am. Chem. Soc.*, **81**, 775 (1959).

(15) B. de B. Darwent and R. Roberts, *Disc. Faraday Soc.*, **14**, 55 (1953).

(16) R. A. Back, *Trans. Faraday Soc.*, **54**, 512 (1958).

Successive fractional distillations of the commercial material is just not good enough.

Troubles of this sort may account for the discrepancies found in the literature for hydrogen gas yields from pure compounds.

The continuous decrease in the hydrogen yield found on irradiating pure *n*-hexane (Section I) undoubtedly results from the buildup of hexene concentration in the system. These hexenes scavenge hydrogen atoms in a reaction which does not produce hydrogen gas (reaction 5). On irradiating hexane to 100 j./g., a hexene production of 31 μmoles/g. is found (Fig. 2). For our "typical" hexene such a concentration would reduce the hydrogen yield to 4.4 mol./100 e.v. Experimentally, a hydrogen yield of 4.4 mol./100 e.v. is found at 100 j./g. (Fig. 1).

This agreement is perhaps fortuitous, for five hexenes are produced simultaneously at different yields, and presumably all react with hydrogen atoms at different rates. However, from the measured relative values of the rate constants, the hydrogen yield for the system hexene + 4% hexene-1 can be calculated to be 3.35 mol./100 e.v. Experimentally, a value of 3.4 ± 0.1 mol./100 e.v. was found (Table I). From these data it is concluded that in the radiolysis of pure *n*-hexane the decrease in hydrogen may be related quantitatively to the buildup of hexene concentration.

Section IV

Miscellaneous Experiments

In this section are reported results of some unrelated experiments which have a bearing on understanding the mechanism of hexane radiolysis.

Determination of the Products—Equation 1.—Using a spot beam as described in Section II, 200-ml. volumes of hexane containing 1, 2 and 3% methyl methacrylate were irradiated to 100 j./g. After radiolysis 10 ml. of nonane was added as a holdup fluid, and the hexane–hexene removed by fractional distillation. Blank experiments showed no methyl methacrylate in the distillate under our conditions. The rationale of this experiment was that the monomer would scavenge all radicals, thus any hexene formed must be formed directly, as defined in reaction 1.

The hexene yield, when corrected for direct energy absorption in methyl methacrylate was within experimental error the same in all three cases, and had a value of 1.47 ± 0.02 mol./100 e.v. The remaining products are therefore produced in a yield equal to 0.65 mol./100 e.v. These latter products must be saturated, for unsaturated products having more than six carbon atoms are not formed initially.

In Table IV comparison is made of the initial yields of the various hexenes from the radiolysis of pure *n*-hexane, and those hexene yields obtained in the presence of methyl methacrylate. The following results should be noted: (1) hexene is formed by processes other than reaction 1; (2) the yields of all three types are affected; (3) the *trans*/*cis* ratio is the same for reaction 1 and for total initial hexene production in the case of both hexene-2 and hexene-3.

TABLE IV

HEXENE PRODUCED IN HEXANE RADIOLYSIS

	Unsaturation yield, mol./100 e.v. Total initially	"Molecular"
Hexene-1	0.73	0.41
Hexene-2	1.82	.77
Hexene-3	0.55	.29
	3.10	1.47
	Ratio *trans*/*cis*	
Hexene-2	2.2 ± 0.3	2.2
Hexene-3	4 ± 1.5	2.9

Although the hexene yield when all radicals are scavenged is 1.47 mol./100 e.v. an initial hexene yield of 3.10 mol./100 e.v. is found on the radiolysis of pure *n*-hexane. This increase in hexene yield is considered to result from the disproportionation of a hexyl radical with some alkyl radical to form hexene. Further evidence for such disproportionation is supplied by Dewhurst[1] who irradiated hexane containing small amounts of cyclohexene. Among his products was cyclohexane. The mechanism of formation of this naphthene was most likely

$$c\text{-}C_6H_{10} + H \longrightarrow c\text{-}C_6H_{11} \quad (7)$$

$$c\text{-}C_6H_{11} + C_6H_{13} \longrightarrow c\text{-}C_6H_{12} + C_6H_{12} \quad (8)$$

Other reactions will, of course, be competing with these reactions but our data show reaction 7 to be the most likely method of hydrogen atom reaction, while reaction 8 is typical of a disproportionation reaction to produce cyclohexane. It has not been found possible from the data available to make quantitative estimates of the degree of disproportionation.

In contrast to alkyl radicals, alkenyl radicals, in this case the hexenyl radical, appear to react by addition only. In Fig. 6 the circles indicate the measured yield of unsaturation in the C_7-C_{12} range when mixtures of hexane and hexene-1 are irradiated (Section II). From the kinetic data obtained from the hydrogen yield in the same system the yield of hexenyl radical can be calculated as a function of hexene-1 concentration. This yield is plotted as the continuous line in Fig. 6.

Within experimental error of the measurement of k_6/k_5, the calculated values of hexenyl radical yield and the yield of unsaturation in heavier products are equal, hence it appears that all hexenyl radicals react by addition. If this conclusion is general, a measure of the total unsaturation in the heavier fraction is a measure of the alkenyl radical production. It might be noted that about 1–2% of the unsaturated product in the C_{12} fraction were dienes.

Formation of High Molecular Weight Products.—Using the technique described in Section II, 200-ml. samples of hexane were irradiated at various doses up to 2000 j./g. To each 100-ml. sample, 5 ml. of benzonitrile was added, and the hexene–hexane fraction removed by distillation. The residue was analyzed in the mass spectrometer using benzonitrile as an internal standard. Particular care was taken to observe any mass above C_{12}. Not until doses above 1500 j./g. were applied was more than 0.2% of the residue found to be of mass greater than C_{12}.

This result indicates that under the conditions of radiolysis (room temperature, non-polar solvent), alkyl radicals do not react with olefins to any significant extent. If a reaction such as

$$C_2H_5 + C_6H_{12} \longrightarrow C_8H_{17} \quad (9)$$

were to occur, a subsequent step would logically be

$$C_8H_{17} + C_6H_{13} \longrightarrow C_{14}H_{30} \quad (10)$$

Experimentally, no products greater than C_{12} are found until the C_7-C_{12} fraction is several per cent. of the irradiated material. At this product concentration, formation of alkyl radicals in the C_7-C_{12} range would be expected, either by direct absorption of radiation by these alkanes, or by hydrogen atom reaction with these products. Products with more than 12 carbon atoms would then arise by the addition of these radicals to other alkyl radicals. It is therefore concluded that reactions such as (9) are not significant in the present system at 25°.

James and Steacie[17] have shown that the relative probabilities of the reactions

$$C_2H_5 + C_7H_{14}\ (\text{heptene-1}) \longrightarrow C_9H_{19} \quad (11)$$

$$C_2H_5 + C_7H_{14}\ (\text{heptene-1}) \longrightarrow C_2H_6 + C_7H_{13} \quad (12)$$

$$C_2H_5 + C_7H_{16} \longrightarrow C_2H_6 + C_7H_{15} \quad (13)$$

are 39:13:1 at 27°. Since we have shown that reactions of the first type do not occur during hexane radiolysis, it is unlikely that reactions analogous to (12) and (13) occur at room temperature in irradiated hexane.

Nature of the Unsaturated Products C_7-C_{12}.—The unsaturated part of the C_7-C_{12} fractions obtained from hexane radiolysis (to 1500 j./g.) were isolated on a silica gel column. These olefins were eluted and the type of unsaturation determined by infrared analysis. Within small limits the same percentage of olefin type was found throughout the series of fractions. Values obtained were: RCH=CHR (I), 56%; R_2C=CHR (II), 20%; R_2C=CH_2 (III), 3%; RCH=CH_2 (IV), 21%.

As it was concluded that hexenyl radicals react only by addition to alkyl radicals, the structure of the olefins gives information on the structure of the parent hexenyl radical. Olefins of type III and IV could arise only from a hexenyl radical having a terminal olefin and this alkenyl radical must

(17) D. G. L. James and E. W. R. Steacie, *Proc. Roy. Soc.* (*London*), *A***244**, 297 (1958).

have been derived from hexene-1. Types I and II most likely arise from hexenyl radicals produced by hydrogen abstraction from hexene-2 or hexene-3. There is also the possibility that a terminal hydrogen was abstracted from the olefin bond in hexene-1, in which case a type I olefin would be produced. It is interesting to note, however, that hydrogen can be extracted from an olefinic carbon atom, for only in this way could types II and III be produced.

Discussion

Two primary processes in hexane radiolysis, reactions 1 and 2 have been described. To these must be added the primary radiolytic reactions

$$C_6H_{14} \longrightarrow \begin{matrix} CH_3 + C_5H_{11} \\ C_2H_5 + C_4H_9 \\ 2C_6H_7 \end{matrix} \qquad (R)$$

The intermediate radicals are formed by the scission of a carbon–carbon bond. The total number of hexane molecules decomposed in this manner is called G_R; the total number of alkyl radicals in the C_1–C_5 range is $2G_R$.

Total Radical Yield.—The sources of free radicals are reactions 2 and (R). The extent of (2) has been measured (G_2 = 3.16 mol./100 e.v.), and gives rise to 6.32 radicals/100 e.v.

Dewhurst has determined the total extent of reaction (R) by measuring the yields of the C_1-C_5 alkyl iodides produced during the radiolysis of hexane–iodine solutions.[1] The total yield of these alkyl iodides was found to be 1.50 mol./100 e.v., and is, of course, equal to the number of free radicals produced in reaction (R).

Combining this value of C_1-C_5 radical yield with our determination of hexyl radical yield, the total radical yield from reactions (R) and (2) is 1.50 + 6.32 = 7.82 radicals/100 e.v.

Schuler[18] has irradiated solutions of hexane containing dissolved iodine and measured the extent of free iodine disappearance. Molecular iodine disappeared with a yield ($G(-I_2)$) = 3.8 mol./100 e.v. We have repeated this work and find $G_{(-I_2)}$ = 4.0 ± 0.2 mol./100 e.v.

Assuming that iodine scavenges all free radicals, and there is ample evidence that this is the case,[19] the total radical yield lies somewhere between 7.6 and 8.0 radicals/100 e.v. Within experimental error, an identical radical yield has been obtained from reactions 2 and (R). We conclude that these reactions are the sole source of scavengeable radicals, and that other modes of hexane decomposition, if present, do not produce scavengeable free radicals as intermediates.

Speculation on the Nature of the Reaction $C_6H_{14} \rightarrow H_2$ + Products.—Hydrogen gas is produced directly in two distinct reaction sequences, neither of which involves scavengeable free radicals. One sequence produces an olefin, found to be hexene, while the other produces a material which is neither a free radical nor an olefin. This product, as will be shown later, is most likely a branched dodecane. In order to explain the probable mechanisms it is necessary first to consider the phenomenon of hydrogen atom genesis in irradiated systems.

(18) E. N. Weber, P. F. Forsyth and R. H. Schuler, *Rad. Research*, **3**, 68 (1955).

(19) P. F. Forsyth, E. N. Weber and R. H. Schuler, *J. Chem. Phys.*, **22**, 66 (1954).

In the processes following absorption of ionizing radiation, some hexane molecules have energy corresponding to highly excited states. One mode of energy degradation is the splitting of a carbon–hydrogen bond, releasing a hydrogen atom. In this cleavage a fraction of the original energy of the molecule will be transferred to the hydrogen atom, mainly as kinetic energy.

$$RH \longrightarrow H^* + R \qquad (1a)$$

There is, of course, a wide spectrum of energies associated with the ejected hydrogen atoms. Many will lose energy by successive collisions and migrate until scavenged by solvent or solute. Such hydrogen atoms are characterized by reaction 2 and are produced in a yield G_2.

It is possible that a certain fraction of the hydrogen atoms, however, possess sufficient energy to react on first collision; *i.e.*, with a molecule adjacent to the parent molecule (nearest neighbor). In pure alkanes this will be another saturated molecule and abstraction of a hydrogen atom will result.

$$H^* + RH \longrightarrow H_2 + R \qquad (1b)$$

In the over-all process two alkyl radicals will be formed from adjacent molecules, in other words, in the same solvent cage. These radicals may react by disproportionation, giving hexane and hexene, or by combination, which in this case will lead to dodecane. The net chemical change when disproportionation occurs may be written

$$C_6H_{14} \longrightarrow H_2 + C_6H_{12} \quad G = 1.47 \qquad (1c)$$

When combination of two hexyl radicals takes place the net reaction is

$$2C_6H_{14} \longrightarrow H_2 + C_{12}H_{26} \quad G = 0.65 \qquad (1c)$$

The ratio of the yields, G_{1c}/G_{1d} = 2.26 would then be a measure of the relative extent of disproportionation to combination of the hexyl radicals. If it is assumed that for normal hexane, in the main, secondary hydrogens are ejected and abstracted, the ratio disproportionation/combination should be typical of the radical R_2CH. Recent work by Kraus and Calvert[20] has shown that in the gas phase the ratio of rates k_{disp}/k_{comb} for the radical $(CH_3)_2CH$ is 2.27, independent of temperature between 0 and 200°.

Following this line of argument, the sum of the yields of reactions 1c and 1d is a measure of the "hot" hydrogen atom reaction (G_{1c} + G_{1d} = 2.12 mole/100 e.v.) and represents 2.12/5.28 or 40% of the total hydrogen atoms produced. If an activation energy of E kcal. is required for abstraction of a secondary hydrogen atom, it follows that 40% of the hydrogen atoms possess an initial energy greater than this value.

Formation of Alkyl Radicals.—Alkyl radicals C_1–C_5 are considered to be formed by C–C bond scission in an excited hexane molecule. By the nature of the process the newly formed radicals should exist together in a solvent cage. They may react, either by combination, in which case no net effect is observed, or by disproportionation, where an alkane and an olefin are formed. If no reaction

(20) J. W. Kraus and J. G. Calvert, *J. Am. Chem. Soc.*, **79**, 5921 (1957).

occurs they may diffuse out of the cage to be scavenged in the bulk of solution.

As reported previously in this paper, the number of radicals produced in the C_1-C_5 range, as measured by the corresponding alkyl iodide yields in irradiated hexane–iodine solutions, is 1.5 radicals/100 e.v. In the present experiment, the sum of yields of products which may arise from these radicals; *viz.*, C_1–C_5 plus C_7–C_{11}, requires an alkyl radical yield of 1.84/100 e.v. to account for all products formed. It is suggested that the difference, about 0.3 mol./100 e.v. is due to immediate disproportionation of the newly formed alkyl radicals within the solvent cage. The summation of the products formed from lower alkyl radicals would include hydrocarbons formed by such a reaction. On the other hand, iodine scavenging techniques would not reveal their presence.

It follows from this mechanism that radiolysis of hexane in the presence of a radical scavenger should produce small amounts of lower hydrocarbons. In the radiolysis of hexane–iodine solutions a gas was produced whose physical properties indicated it to be a mixture of alkanes and olefins in the C_1-C_3 range, and produced in a yield of 0.2 ± 0.1 mol./100 e.v. A more detailed analysis was not made in view of the small quantity involved (0.5 μ moles). In these experiments a yield lower than 0.3 might be expected, for the olefin components of these light gases can react with the hydrogen iodide formed during the radiolysis. Kraus and Calvert[20] found the ratio k_{disp}/k_{comb} for simple primary alkyl radicals to be about 0.13. A low net value for the direct formation of products C_1–C_5 might therefore be expected in hexane radiolysis.

Extending this argument to branched chain alkanes, carbon–carbon bond scission adjacent to the branching will produce secondary or perhaps tertiary radicals. Such radicals are less likely to react by combination than are those arising from *n*-alkane radiolysis. As a result, a higher yield of low molecular weight products would be expected, and the results of Dewhurst[21] indicate this to be true.

Hydrogen Iodide Yield.—Meshitsuka and Burton[22] have studied the production of hydrogen iodide on irradiating dilute solutions of iodine in hexane. The hydrogen iodide formed reacted with some intermediate to give a stable product, both during and after irradiation. The lower limit of hydrogen iodide yield was determined as 1.3 mol./100 e.v.

If our pattern of reactions in hexane radiolysis is correct, a hydrogen iodide yield equal to G_2, or 3.16 mol./100 e.v., would be expected. This value is much greater than that found experimentally by Meshitsuka and Burton. To explain this discrepancy, reactions of hydrogen iodide with hexane radiolysis products must be considered.

In the radiolysis of hexane containing a scavenger, hexenes are produced with a yield of 1.47 mol./100 e.v. In addition, olefins in the C_2–C_5 range are produced by disproportionation of alkyl radicals; the yield has been estimated as 0.3 mol. olefin/100 e.v. The total alkene yield is therefore 1.77 mol./100 e.v.

It is well known that hydrogen halides will add to double bonds, though less is known of the specific rates of reaction. From Burton and Meshitsuka's work, it is apparent that several compounds are reacting with hydrogen iodide, at different rates. Such a complicated reaction pattern is to be expected, considering the variety of olefins present. When all olefins have disappeared and hydrogen iodide remains in excess, the expected decrease in yield is 3.16 − 1.77 = 1.39 mol./100 e.v. This value is in good agreement with the experimental value of 1.3 mol./100 e.v.

Reaction of H Atoms with Olefins.—It appears that hydrogen atoms react more rapidly with terminal olefins than with secondary olefins. In the case of hexene-1 and the isomeric mixtures of hexene-2, relative reactivity at 25° is 2:1. Back and Miller[23] found a similar result in the radiolysis of pentane containing pentene-1 and pentene-2.

Role of Thermal Hydrogen Atoms in Alkane Radiolysis.—Thermal hydrogen atoms appear to react exclusively with either the parent alkane or with the unsaturated products of radiolysis. There appears to be little evidence that they disappear by reaction with another radical. If the rate constant for reaction 3 is of the order of 10^9 cc./mole/sec. (and evidence for this will be presented in a forthcoming paper), it is unlikely that either the hydrogen atom or the alkyl radical concentration would be high enough for the reaction

$$H + R \longrightarrow HR \qquad (14)$$

to occur. As almost any organic material appears to be susceptible to hydrogen atom attack, the presence of small amounts of impurities may lead to a considerable change in reaction patterns.

Effect of Dose Rate.—Some recent publications[3,24,25] on hydrocarbon radiolysis indicate an effect of dose rate, but no effect of linear energy transfer. We have observed no effect of dose rate, for although irradiations with electrons and X-rays differed in dose rate by a factor of more than 10^4, we have been able to relate, quantitatively, results obtained at high dose rate (Sections I and II) to values obtained at low dose rate (Section III).

Comment on Comparison with Previous Work.—It is not possible to make a critical comparison of hydrogen yields with those of other workers, since they have reported constant values, whereas the hydrogen yield in these experiments decreases continuously with dose. Nor is it clear that the significance of trace impurities on the hydrogen yield was fully recognized previously. In view of this difficulty no attempt has been made to reconcile the present results with those previously published on the radiolysis of the pure alkane.

One further point should be made. Since both combination and disproportionation reactions can occur in radical–radical reactions, the use of the

(21) H. A. Dewhurst, *J. Am. Chem. Soc.*, **80**, 5607 (1958).

(22) G. Meshitsuka and M. Burton, *Rad. Research*, **10**, 499 (1959).

(23) R. A. Back and N. Miller, *Trans. Faraday Soc.*, **55**, 911 (1959).

(24) H. A. Dewhurst and E. H. Winslow, *J. Chem. Phys.*, **26**, 969 (1957).

(25) R. H. Schuler and G. A. Muccini, *J. Am. Chem. Soc.*, **81**, 4115 (1959).

methane yield as a measure of methyl radical production is open to question. Undoubtedly, more methyl radicals are formed in branched chain than in straight chain alkane radiolysis. In the former case however, disporportionation in methyl-alkyl radical reactions would be more probable than in the latter.

Summary of Reactions.—The sequence of reactions which is believed to occur on the radiolysis of *n*-hexane is that listed below:

	G (mol./100 e.v.)	
Primary radiolytic reactions		
$C_6H_{14} \rightsquigarrow H^* + C_6H_{13}$	2.12	(1a)
$\rightsquigarrow H + C_6H_{13}$	3.16	(2)
$\rightsquigarrow CH_3 + C_5H_{11}$; $C_2H_5 + C_4H_9$; $2C_3H_7$	0.92	(R)
Hot hydrogen atom reaction		
$H^* + C_6H_{14} \longrightarrow H_2 + C_6H_{13}$	$(=G_{1a})$	(1b)
Caged radical pair reactions		
From (1) $C_6H_{13} + C_6H_{13} \longrightarrow C_6H_{14} + C_6H_{12}$	1.47	(1c)
$C_6H_{13} + C_6H_{13} \longrightarrow C_{12}H_{26}$	0.65	(1d)
From (R) $CH_3 + C_5H_{11} \longrightarrow CH_4 + C_5H_{10}$; $C_2H_5 + C_4H_9 \longrightarrow C_2H_4 + C_4H_{10}$; $\longrightarrow C_2H_6 + C_4H_8$; $C_7H_7 + C_3H_7 \longrightarrow C_3H_6 + C_3H_8$	0.30	(Ra)

Not included—hexane reformation from 2 alkyl radicals (Rb).

Thermal hydrogen atom reactions

$$H + C_6H_{14} \xrightarrow{k_3} H_2 + C_6H_{13} \quad (3)$$

$$H + C_6H_{12} \xrightarrow{k_5} C_6H_{13} \quad (5)$$

$$H + C_6H_{12} \xrightarrow{k_6} H_2 + C_6H_{11} \quad (6)$$

Alkyl radical recombination reactions

$$C_6H_{13} + C_6H_{13} \longrightarrow C_6H_{12} + C_6H_{14} \quad (15)$$

$$\longrightarrow C_{12}H_{26} \quad (16)$$

$$C_2H_5 + C_6H_{13} \longrightarrow C_2H_4 + C_6H_{14} \quad (17)^{26}$$

$$\longrightarrow C_2H_6 + C_6H_{12} \quad (18)$$

$$\longrightarrow C_8H_{18} \quad (19)$$

Alkyl–alkenyl radical reactions

$$C_6H_{11} + C_6H_{13} \longrightarrow C_{12}H_{24} \quad (20)$$

$$C_2H_5 + C_6H_{11} \longrightarrow C_8H_{16} \quad (21)^{26}$$

The primary yields of radicals and molecular products have been obtained by a consideration of the kinetics of hydrogen gas formation, and from other simple experiments described in Sections III and IV, plus reliance on data already published. The reaction scheme proposed should account quantitatively for the products of radiolysis of pure *n*-hexane. There will be some uncertainty in this, for whereas alkyl–alkenyl radicals react by combination only, alkyl–alkyl radical reactions occur by both disporportionation and combination, and the ratio of alkyl/alkenyl radicals will change continuously during radiolysis. However, the comparison may be made

Irradiation to 1500 j./g.

		G, mol./100 e.v.
A.	Total yield of C_{12} hydrocarbons	1.70
B.	21% of A is unsaturated	0.36
C.	Total saturate C_{12} yield (A − B)	1.34
D.	C_{12} saturated formed by reaction (1d)	0.65
E.	C_{12} saturated formed from 2 hexyl radicals (C − D)	0.69
F.	R radicals found in C_7–C_{11} products	0.84
H.	$CH_4 + C_2H_6 + \ldots C_5H_{12}$ (saturated)	0.38
J.	$C_2H_4 + \ldots C_5H_{10}$ (unsaturated)	0.28[27]
K.	Estimated C_{12} formed initially (no hexene present)	0.87
L.	Total hexyl radicals = $2G_2$	6.32
M.	Hexyl radicals reacting with R radicals F + H + J	1.50
N.	Net number of hexyl radicals reacting with one another (L − M)	4.82
P.	Hexyl radicals producing C_{12} saturated = 2 × K	1.74
Q.	Remaining hexyl radicals reacting by disproportionation N-P (initially)	3.08
S.	Hexene produced by hexyl radical disporportionation $^1/_2 \times$ Q	1.54
T.	Hexene produced as a result of hot H atom reaction (1c)	1.47
U.	Hexene produced by reaction (18) = H	0.38
V.	Total hexene yield initially S + T + U	3.39

The measured initial hexene yield is 3.10 mol./100 e.v., which compares reasonably with the calculated value of 3.39 mol./100 e.v. (V). The ratio disproportionation/combination for hexyl radicals is 2.26 as measured by reactions 1c and 1d, and 1.78 as measured by the ratio of S/K. Considering the assumptions made, this agreement is reasonably close. Since a typical value of k_{disp}/k_{comb} for secondary radicals is 2.27 it would appear that most of the hexyl radicals are secondary in nature.

Throughout this discussion no reference has been made to the role of ion–molecule reactions in liquid hexane radiolysis. Recently Futrell[28] has reported results on the gas phase radiolysis of *n*-hexane in which such reactions play a major part. A similar postulate was made for results obtained in the liquid phase. There is no indication from the present work that such reactions play a significant part in liquid phase hexane decomposition, while on the other hand free radical mechanisms appear to supply a quantitative explanation of the method of formation of products. Furthermore values of rate constant ratios, etc., agree well with those obtained in experiments using light or heat as a source of radicals.

Conclusions

In the radiolysis of liquid *n*-hexane: (1) Carbon–carbon or carbon–hydrogen bonds break as a consequence of the molecule absorbing energy; in the later case some hydrogen atoms may have sufficient energy to react in "hot" atom processes; (2) hydrogen atoms reduced to thermal energies react with solute or solvent, apparently not with another radical; (3) alkyl radicals inter-react by addition or disproportionation, alkenyl radicals by addition

(26) The radical C_7H_8 is taken as a typical alkyl radical in the C_1–C_8 range. Other such radicals will undergo corresponding reactions.

(27) Plus 0.30 formed by alkyl radical disproportionation in a solvent cage (reaction Ra).

(28) J. H. Futrell, *ibid.*, **81**, 5921 (1959).

only; (4) alkyl radicals do not react with olefins at room temperature; (5) the so-called "molecular" products arise from caged radical pairs formed by hot hydrogen atom reactions; (6) much radical reaction data obtained in the gas phase is applicable quantitatively to saturated hydrocarbon solvent medium; (7) the decrease in hydrogen yield observed on alkane radiolysis is due to the reaction of hydrogen atoms on the corresponding alkenes produced during radiolysis.

Acknowledgment.—The author wishes to thank Mr. W. S. Guentner for considerable help in obtaining the data in Section I, the Composition & Structure Division for some of the more difficult analyses, and the Nuclear Physics Section for operation of the Van de Graaff accelerator.

THE HEATS AND ENTROPIES OF FORMATION OF THE COPPER(II)–PYRIDINE COMPLEXES[1a]

BY D. L. LEUSSING[1b] AND P. K. GALLAGHER

Department of Chemistry, University of Wisconsin, Madison, Wisconsin

Received April 7, 1960

The heats for the reactions $Cupy_{i-1}(H_2O)_{7-i}^{++} + py_{aq} \rightarrow Cupy_i(H_2O)_{6-i}^{++} + H_2O_{aq}$ were determined. For values of i in the range one to four approximately identical heats averaging −4.4 kcal./mole were obtained. For $i = 5$ the reaction appears to be endothermic. A comparison is made with the properties of the ammonia complexes. By comparing the reactions with the gaseous ligands in order to do away with the effect of solvent on the ligands themselves, it is shown that a relativley high degree of order exists in the pyridine complexes, even in the monocomplex. The heat of reaction of gaseous pyridine to form an aqueous complex is 3 kcal. more negative than the corresponding reaction with gaseous ammonia although with the aqueous ligands the heat of the pyridine reaction is less negative than the heat of the reaction with ammonia. The spectral properties and natures of the pentammines in the ammonia and pyridine systems are discussed.

A previous paper[2] reported on the nature of the copper(II)–pyridine complexes in 1.0 *M* potassium nitrate at 25°. A stepwise series of five complexes was found. Their stabilities and absorption spectra were determined. The present work concerns the calorimetric determination of the heats and the evaluation of the entropies of complex formation in this same system with the goal of elucidating the nature of the complexes. The pyridine complexes are interesting in that steric effects seem to be negligible as far as the stability constants are concerned. Molecular models show that interference can occur between adjacent coordinated pyridine molecules and it is expected that the higher complexes would reflect this by exhibiting appreciably less stability than the lower complexes. However, the course of the step-wise formation constants in the copper(II)–pyridine system does not show very different variation from that of the copper(II)–ammonia system.[3]

Also of interest is the nature of the pentammine. With ammonia the formation of the pentammine is accompanied by a "red-shift" in the absorption spectrum.[4] On the other hand, with pyridine almost no change, or at best a slight "blue-shift," is noted. It was hoped that a study of the heats and entropies would allow further insight into these effects.

Experimental and Results

The reagents were the same as those described in the earlier work.[2] The same experimental conditions were also maintained so that the equilibrium quotients which were found would apply here.

The calorimeter used has been described by Schug and King.[4] In a typical run a solution approximately 0.030 *M* in copper(II) nitrate, 0.010 *M* in nitric acid and 1.0 *M* in potassium nitrate was cooled to 23° and a 300-ml. volume was measured into the Dewar flask of the calorimeter. The concentration of potassium nitrate was adjusted so that it was 1.00 *M* after the pyridine addition. The pyridine was weighed into a glass bulb which then was suspended in the Dewar flask at the end of a glass rod. The glass rod projected through the cover of the flask so that the bulb could be broken at the appropriate time by depressing the rod. The covered Dewar flask was placed in a water-bath at 27° and a slow, approximately linear, increase in the temperature of the contents began. When the temperature reached the range 24 to 24.5° the bulb was broken. The temperature of the final solution was within one-half a degree of 25.0°. The total number of calories liberated, q, was obtained by multiplying the temperature rise brought about on releasing the pyridine by the average of the heat capacities of the system. The heat capacities were determined as described[4] before and after the formation of the complexes.

In the experiment at the highest concentration of pyridine it was found necessary to preform the lower complexes in order to obtain a satisfactory value of q. This was necessary because the addition of a large amount of pyridine to a solution of the aquo copper(II) ions gives rise to a complicating side reaction. Apparently, this is due to the formation of the dimeric dihydroxy complex[2] by a large local excess of pyridine. By preforming the lower complexes, less pyridine was required in the calorimetric measurement and the difficulty was circumvented.

The heats of solution of liquid pyridine were also determined in 1.00 *M* potassium nitrate. The results are given in Table I where it is seen that the heat of solution of pyridine is a function of its final concentration. This effect seems to be due to the absorption of a slight amount of heat on the dilution of the potassium nitrate solution. At least, after a correction is made for the heat of dilution of potassium nitrate,[5] the heats of solution of pyridine agree within ±.05 kcal./mole of the average for those obtained in pure water.[6,7]

(1) (a) Presented before the Division of Inorganic Chemistry, 136th National American Chemical Society Meeting, Atlantic City, 1959. (b) To whom inquiries should be addressed, National Bureau of Standards, Washington 25, D. C.

(2) D. L. Leussing and R. C. Hansen, *J. Am. Chem. Soc.*, **79**, 4270 (1957).

(3) J. Bjerrum, "Metal-Ammine Formation in Aqueous Solution," P. Haase and Son, Copenhagen, 1941.

(4) J. Bjerrum and E. J. Nielsen, *Acta Chem. Scand.*, **2**, 297 (1948).

(4) K. Schug and E. L. King, *J. Am. Chem. Soc.*, **80**, 1089 (1958).

(5) F. R. Pratt, *J. Franklin Inst.*, **185**, 633 (1918); "International Critical Tables," Vol. 5, McGraw-Hill Book Co., New York, N. Y., p. 160.

(6) R. J. Andon, J. D. Cox and E. F. G. Herington, *J. Chem. Soc.*, 3188 (1954).

This correction was not used in the calculations described below, but rather the data of Table I were interpolated to give the heat of solution appropriate to the amount of pyridine added in a given experiment.

TABLE I

THE HEAT OF SOLUTION OF PYRIDINE

$py_l \longrightarrow py_{aq}$; 1.00 M KNO_3, 25°

Final cond., py, moles/l.	$-\Delta H$, kcal./mole
0.100	2.07
.410	2.04
.490	1.96
0	2.00,[a] 2.27[b]

[a] In pure water, ref. 6. [b] Ref. 7.

The heat for the reaction $py_{aq} + H_{aq}^+ \rightarrow pyH_{aq}^+$ in 1.00 M potassium nitrate also was determined. For the neutralization of 3.032 mmoles of nitric acid in 300 ml. of solution, 15.7 cal. was liberated. This heat, after correcting for small differences in the amount of pyridinium ion formed, was subtracted from the heat liberated in each complex ion run. The molar heat of neutralization of pyridine is calculated from the present result to be −5.2 kcal. in 1.00 M potassium nitrate. This value is comparable to the value −4.72 kcal./mole which is reported for solutions at an ionic strength of 0.056 M, 25°.[8]

The values of q which have been obtained in the experiments with copper(II) are given in Table II The uncertainties in the values of q have been estimated from the uncertainties both in the extrapolation of the calorimeter readings to the time of the reaction and in the differences in the calibration factors determined before and after the reaction. Also given are values of ΔH_c, the total heat absorbed in forming the copper(II)–pyridine complexes. The latter quantity was obtained by subtracting the heat of solution of pyridine and the heat of formation of the pyridinium nitrate from the experimentally determined values of q. The uncertainties assigned to q, therefore, all appear in the result for ΔH_c.

The results are not sufficiently accurate to allow the calculation of the individual heats of complex formation from the ΔH_c by solving five simultaneous equations. However, it is possible to obtain meaningful results by dividing the ΔH_c in a given run by $\bar{n}$, the average number of pyridine molecules complexed to each copper(II) ion. This procedure is identical with that which was used successfully to obtain the heats for the copper(II)–ammonia complexes.[9] From the values of $-\Delta H_c/\bar{n}$ which are given in the last column of Table II it is seen that approximately equal amounts of heat are released in binding each of the first four molecules of pyridine. The addition of the fifth pyridine, however, results in much less heat being liberated.

The average heat for the coördination of each of the first four molecules of pyridine is calculated to be −4.4 kcal./mole. The heat for the coördination of the fifth molecule can be obtained using this average and the stepwise equilibrium quotients,[10] the logarithms of which are given in Table III, to calculate the change in the distribution of the complexes when the pyridine is added. An accurate value is not obtained with the present data but it appears that at least the heat for the reaction $Cupy_4(H_2O)_2^{++} + py \rightarrow Cupy_5(H_2O)^{++} + H_2O$ is more positive than +1 kcal./mole.

For the formation of the ith complex from the $(i-1)$th complex the stepwise entropy changes, ΔS_i have been calculated from the stepwise heat and free energy changes and are reported in Table III. Also given are values of ΔS_{chemi} which have been obtained by correcting the observed ΔS_i for the symmetry numbers, σ,[11] of the reactant and product complex. This correction is made using the relationship $\Delta S_{chemi} = \Delta S_i - 2.303R \log (\sigma Cupy_{i-1}/\sigma Cupy_i)$. The model proposed by Bjerrum, Ballhausen and Jörgensen[12] was used to calculate the symmetry numbers of the complexes. In this model the coördination sites of the copper(II) ion are pictured to lie at the vertices of a distorted octahedron. Four of the sites form a square-planar array about the central ion and the other two sites lie on an axis which is perpendicular to the plane and at a slightly greater distance. The electron density is less at the square planar sites and these are occupied first by pyridine molecules. A statistical distribution of *cis-trans* isomers was assumed in calculating the symmetry number of $Cupy_2(H_2O)_2(H_2O)_2^{++}$.

Discussion

The results here, which show that each of the first four sites on the copper(II) ion are occupied by pyridine with a heat of approximately −4.4 kcal./mole, support Bjerrum's postulate[9] that in a normal complex system with a given dipolar ligand, the successive heats are the same. With the bidentate ethylenediamine, for example, the heats of coördination of the first and second molecules to copper (II) are −13.0 and −12.4 kcal./mole while with ammonia the first four molecules are coördinated each with a heat of −5.0 kcal./mole.[9] This latter value is surprisingly close to the average found here for pyridine and therefore, the somewhat larger values of the formation constants for the copper (II)–ammonia system[3] are due primarily to more positive values of ΔS_i, *e.g.*, for i equals one ΔS_i is + 2.1 e.u. with ammonia[9] and −2.7 e.u. with pyridine.

The values of ΔS_i in Table III become increasingly more negative as i increases from one to four. The greater part of this trend is accounted for by the effect of the symmetry numbers of the complexes. This can be seen by the smaller range of the $\Delta S_{chem\ i}$ values. A tendency to become increasingly more negative still exists with the successive values of $\Delta S_{chem\ i}$, however. The average change per step is about −0.8 e.u. With the ammonia complexes, the symmetry number effect also has the largest influence in causing the ΔS_i values to become more negative with increasing i, but the residual changes in the $\Delta S_{chem\ i}$ are slightly greater, averaging about −1.2 e.u. per step. Because of this, less difference exists between the formation constants of the tetrammines in these two systems than exists between the formation constants of the monoammines. Considering the effect of steric hindrance this trend is opposite to that which is expected since molecular models show that neighboring coördinated pyridine molecules can interfere with each other.

The reason for this anomaly can be seen by considering the reactions in which the gaseous ligands take part. The heat of hydration of gaseous pyridine (− 11.65 kcal./mole)[6] is greater than that of gaseous ammonia (− 8.3 kcal./mole).[13] Thus, the heat for the reaction $py_g + Cu(NH_3)(H_2O)_{5aq}^{++} \rightarrow Cupy(H_2O)_{5aq}^{++} + NH_{3g}$, is calculated to be −3 kcal./mole. This heat actually favors the complexing of copper(II) by pyridine rather than by ammonia. The factor which causes the heats with the

(7) E. Baud, *Bull. soc. chim.*, **5**, 1022 (1909).

(8) D. L. Levi, W. S. McEwan and J. H. Wolfenden, *J. Chem. Soc.*, 760 (1949).

(9) J. Poulsen and J. Bjerrum, *Acta Chem. Scand.*, **9**, 1407 (1955).

(10) The equilibrium quotients have been calculated from the data of ref. 2. The difference between the values given here and those given in ref. 2 do not alter the earlier conclusions. Some changes, are, of course, brought about in the extinction coefficients reported for the individual complexes and in the formation constant of $Cu_2(OH)_2py_4^{++}$.

(11) S. W. Benson, *J. Am. Chem. Soc.*, **80**, 5151 (1958).

(12) J. Bjerrum, C. J. Ballhausen and C. K. Jörgensen, *Acta Chem. Scand.*, **8**, 1275 (1954).

(13) F. D. Rossini, D. D. Wagman, W. H. Evans, S. Levine and I. Jaffe, "Selected Values of Chemical Thermodynamic Properties," Natl. Bur. Standards (US) Circ. No. 500, Supt. of Documents, U. S. Govt. Printing Office, Washington, D. C.

TABLE II

THE HEATS OF FORMATION OF THE Cu(II)–PYRIDINE COMPLEXES

1.00 M KNO_3, 25°, 300 ml. of initial solution

Cu(II), mmoles	HNO_3 initial, mmoles	Pyridine added, g.	Q,[a] cal.	$-\Delta H_c$,[b] kcal./mole	$\bar{n}$	$-\Delta H_c/\bar{n}$, kcal./mole
9.53	3.34	1.239	96.5 ± 0.5	5.0 ± 0.5	1.09	4.6 ± 0.4
9.04	3.32	2.332	154.0 ± 1.0	8.6 ± 1.0	2.08	4.1 ± .5
9.09	3.34	4.315	253.3 ± 2.0	13.7 ± 2.0	3.00	4.6 ± .6
9.18	3.36	6.54	318.4 ± 3.7	14.6 ± 3.7	3.50	4.2 ± 1.0
9.36	3.16	6.48	173.7 ± 0.9	1.0 ± 0.9	0.80[c]	(1.2)[d]

[a] The total heat liberated on the addition of pyridine. [b] The heat of reaction of aqueous pyridine with copper(II) ions. [c] $\bar{n}_{initial} = 3.40$, $\bar{n}_{final} = 4.20$. [d] $-\Delta H_c/\Delta n$.

TABLE III

THE STEPWISE FREE ENERGIES, HEATS AND ENTROPIES FOR THE REACTIONS

$Cupy_{i-1}(H_2O)_{7-i}^{++} + py \longrightarrow Cupy_i(H_2O)_{6-i} + H_2O$[a]

1.00 M KNO_3, 0.010 M py·HNO_3, 25°, $\Delta H_i = -4.4$ kcal./mole (i = 1 to 4), $\Delta H_5 > +1.0$ kcal.

i	log Q_i	$-\Delta F_i$, kcal./mole	ΔS_i, cal./mole/deg.	$\Delta S_{i\ chem.}$, cal./mole/deg.
1	2.58	3.52	− 2.7	−5.4
2	1.86	2.53	− 6.0	−6.7
3	1.41	1.93	− 8.0	−7.2
4	0.82	1.12	−10.6	−7.9
5	0.33	0.42	+ 2	...

[a] In concentration units of moles per liter.

aqueous ligands to be smaller for the reactions with pyridine relative to the reactions with ammonia is the greater interaction of pyridine with the solvent.

The entropy change for the displacement of gaseous ammonia by gaseous pyridine is calculated to be −23 e.u. using entropies of hydration equal to −37.6 e.u. for pyridine[6] and −19.7 e.u.[13] for ammonia. This is sufficient at 25° to offset the heat and to favor the reaction from right to left. The large negative entropy is an indication of much more order in the pyridine complexes than exists in the ammonia complexes even in the monoammines. Possibly, this greater order is due to restraint through steric interactions between the pyridine and the water molecules which are coördinated to a copper(II) ion. Since a high degree of order relative to ammonia is required in forming even the first complex, the absence of further effects due to additional steric requirements in the higher pyridine complexes is understandable. Apparently each of the pyridine molecules, beginning with the first, is required to coördinate with such an orientation that interference with the coördination of the other molecules is held to a minimum (with the exception of the fifth pyridine molecule). To satisfy such a requirement the first four pyridine molecules can be coördinated so that their planes are perpendicular, or skewed, to the plane of the sites to which they are coördinated.

The spectral behavior of the pentammines is in line with their thermodynamic properties. With ammonia the fifth molecule is coördinated with a stepwise heat of −3.2 kcal./mole[9] but the corresponding reaction with pyridine is slightly endothermic. Since coördination of the fifth group takes place along the z-axis of the complex in the Bjerrum, Ballhausen and Jorgensen model,[12] the energy difference between the d_{z^2} and the $d_{x^2-y^2}$ orbitals of the copper(II) ion is decreased by an exothermic reaction, as with ammonia, but is increased in an endothermic reaction, as with pyridine. In the first case a "red shift" occurs in the absorption spectrum and in the second case a "blue shift" is brought about. This is in agreement with observation.

The pentammines in the two systems are seen from these comparisons to be fundamentally different. Perhaps the fifth pyridine molecule is not really coördinated in the true sense of the word but merely finds greater freedom in the region of solvent surrounding the tetrammine. It is to be expected that the field of the large complex ion destroys the structure of the solvent in its vicinity, as is the case with large simple ions.[14] This region may provide better solvent properties for an unassociated pyridine molecule than the highly hydrogen bonded region in the bulk of the solvent.

(14) R. W. Gurney, "Ionic Process in Solution," McGraw-Hill Book Co., New York, N. Y., 1953.

GAS PHASE RADIOLYSIS OF *n*-PENTANE

BY JEAN H. FUTRELL

Aeronautical Research Laboratories, Air Force Research Division, Wright-Patterson Air Force Base, Ohio

Received April 7, 1960

Pyrex ampoules of *n*-pentane vapor were exposed to cobalt-60 γ-rays and hundred electron volt yields of the lower molecular weight products were determined. In decreasing order of importance these included hydrogen, propane, ethylene, ethane, methane, propylene, acetylene and butane. The magnitude of the yields and the product distribution are consistent with the assumption that the reaction sequence is ionization of the molecule, fragmentation, reaction of the fragment ions with pentane molecules, and neutralization of the product ions, followed by intercombination of free radicals from these processes. Certain implications of this mechanism are suggested.

Introduction

A recent paper discussed the radiation chemistry of *n*-hexane and demonstrated a remarkably quantitative correlation between the mass spectral fragmentation pattern and the yields from gas phase radiolysis.[1] Shortly after this paper was submitted, Back and Miller reported a detailed investigation of the gas phase irradiation of *n*-pentane with γ-rays from Po^{210} and Cm^{242} and with X-rays.[2] Calculations based on the same reaction scheme proposed for *n*-hexane revealed essential agreement with the yield data of these authors for hydrogen and the C_2 hydrocarbons, but disagreed in that the calculations predicted that propane was a major product, while experimentally a low value was found. The present research was undertaken in an attempt to resolve this discrepancy.

Experimental Procedures

Irradiation Procedures.—Phillips research grade *n*-pentane was degassed by repeated freeze-pump-melt cycles and trap-to-trap distillation under vacuum and was distilled into Pyrex ampoules 21 × 2.5 cm. diameter fitted with seal-off and break-seal tubes. These were sealed under vacuum and subsequently irradiated for periods of one hour to one month in a 1500 curie Co^{60} source of Brookhaven design.[3] Essential agreement between the lowest molecular weight product distribution and that of Back and Miller[2] was obtained, and our results were arbitrarily normalized to the hundred electron volt yield of ethane reported by these authors.

The irradiated samples were sealed into a vacuum system for separation of products in a manner analogous to that described by Newton[4] for liquid phase studies. Fractions volatile at −190° (H_2 and CH_4) and at −125° (predominately *n*-pentane but also containing the C_2–C_4 hydrocarbons) were separated and the number of μmoles in each were determined by means of pressure and volume measurements at a given temperature. These fractions were pumped into bulbs for subsequent analysis by gas chromatography and mass spectrometry. The residual fraction was retained and examined routinely but was found in all cases to contain only pentane in detectable quantities.

Analysis.—The vacuum separation techniques served merely to concentrate the products sufficiently that gas chromatography using thermal conductivity detection could be used for analysis. The total gas samples separated in this fashion were injected into the carrier gas stream of the gas chromatography apparatus by means of a bypass system incorporated into the flow system. The C_2–C_5 products were determined on a 10 meter column packed with a hexadecane adsorbed on 30–60 mesh firebrick using helium carrier, and the methane–hydrogen fraction was determined on a 1.5 meter molecular sieve 5A column using prepurified nitrogen carrier. At the lowest conversion levels the methane–hydrogen fraction was analyzed with a mass spectrometer. Analyses for methane may have been in error for some samples because of non-linearity in response of the detector using nitrogen carrier.[5]

Discussion of Results

The experimental results are presented in Table I as *G*-values, the yield of products expressed as molecules per hundred electron volts of energy dissipated in the system. In the absence of elaborate dosimetry studies for the source employed, the yields have been normalized arbitrarily to the value $G(C_2H_6) = 1.1$, the value determined by Back and Miller[2] for α-radiolysis. Extrapolation of yield data to zero dose required irradiations in which as little as 0.03% of the pentane was decomposed, as this research confirmed recent observations[2,6] that product distributions change markedly at rather low conversions. This point will be the subject of a future publication.

TABLE I

HUNDRED ELECTRON VOLT YIELDS OF PRODUCTS FROM GAS PHASE RADIOLYSIS OF *n*-PENTANE

	Back and Miller[a]	This research[b]
H_2	7.3	>6
CH_4	0.8	0.7
C_2H_2	0.5	0.5
C_2H_4	1.6	1.5
C_2H_6	1.1	1.1[b]
C_3H_6	0.04	0.6
C_3H_8	0.3	2.0
C_4H_{10}	0.04	0.4

[a] Reference 2. Polonium 210 and curium 242 α-sources. [b] Yields normalized to $G(C_2H_6) = 1.1$. See discussion in text.

Factors involved in dosimetry for gas phase irradiations with Co^{60} sources have been discussed recently by Back[6] and by Armstrong and Spinks.[7] Cross sections for interaction of Co^{60} γ-rays are so small that only the order of 0.5% of the dose received by the hydrocarbon is accounted for by primary interaction. The major process is the ejection of secondary electrons from the walls of the container; hence the gas is exposed to a flux of high energy electrons varying from *ca.* 1 Mev. down. Their number per unit dose and actual energy distribution is determined by the Pyrex walls of the irradiation cells and is independent of the gas in the cell.

(1) J. H. Futrell, *J. Am. Chem. Soc.*, **81**, 5921 (1959).

(2) R. A. Back and N. Miller, *Trans. Faraday Soc.*, **55**, 911 (1959).

(3) M. C. Atkins, WADC Technical Note 55-302, "Accessory Equipment and Procedures for Use of a 1500 Curie Cobalt-60 Gamma Ray Source," April 1956, available from Office of Technical Services, U. S. Department of Commerce, Washington 25, D. C.

(4) A. S. Newton, *Anal. Chem.*, **28**, 1214 (1956).

(5) L. J. Schmauch and R. A. Dinerstein, *Anal. Chem.*, **32**, 343 (1960).

(6) R. A. Back, THIS JOURNAL, **64**, 124 (1960).

(7) D. A. Armstrong and J. W. T. Spinks, *Can. J. Chem.*, **37**, 1210 (1959).

These experimental conditions are clearly quite different from those in α-particle irradiations, and the normalization of yield data may be questioned.[8] This is especially true in view of recent mass spectrometer studies which indicate that ionization processes for electron and α-particle impact differ significantly.[9] However, earlier work by de Vries and Allen,[10] Schuler,[11] and Davison[12] shows that, at least for many liquid hydrocarbons, changing radiation quality produces only a minor effect on G values of the ultimate products. The similarity of the product distributions in Table I for products through C_2 support this assumption for *n*-pentane vapor.[8]

The G-values determined in this fashion appear reasonable, and we attribute the differing C_3 and C_4 yields to differing analytical procedures rather than to an effect of radiation quality. In both sets of experiments the significant measurements were performed at conversions of less than 0.1% to avoid secondary reactions, and analytical problems are rather difficult in this regime. Only by combining separation by vacuum techniques with analysis by gas chromatography were we able to measure these products with meaningful accuracy.

Mechanism.—In calculating the G-values for pentane radiolysis the same simple assumptions previously applied to *n*-hexane[1] are made. These assumptions correspond to a logical sequence of events following interaction of a pentane molecule with ionizing radiation: (1) Ionization occurs with fragmentation of the parent molecule-ion, and it is assumed that the extent of fragmentation corresponds to the mass spectrum of *n*-pentane.[13] (2) Ion-molecule reactions occur at every collision for these fragment ions (*ca.* 10^{-10} sec.), and it is assumed that so-called hydride-ion transfer reactions[14] dominate this phase of the reaction. (3) Ions surviving these processes combine with thermalized electrons yielding various neutral species. Details of this step are purely speculative and the calculation is based on the assumption that the highly excited species formed on neutralization decays by fragmentation into a hydrogen atom and the corresponding entity. (4) Free radical fragments formed in these various processes react by coupling and disproportionation. (5) The G-values of the various products from radiolysis are determined by summing the molecules produced in steps 1–4 and relating the totals to the energy absorbed by the system.

It is assumed that the mass spectral fragmentation pattern for *n*-pentane with 70 v. electrons gives the proper distribution of ions for radiolysis also, and that the proper distribution of neutral fragments is given by the ionization mechanisms postulated to correspond to appearance potential processes by Franklin and Field.[15] This assumption may be illustrated by considering the prominent ion of m/e 27, for which the mechanism

$$C_5H_{12} + e \longrightarrow C_2H_3^+ + H_2 + \cdot C_3H_7 \cdot + 2e \quad (1)$$

is given. The endothermicity of this reaction, obtained from the tabulated heats of formation of reactant and product radicals, ions and molecules equals approximately 10.9 e.v., the appearance potential for this reaction. Indeed, this is the primary basis for suggesting this as the ionization mechanism. These authors offer mechanisms for the principal ions produced from *n*-pentane under electron impact.

To the $C_2H_3^+$ ion from reaction 1 is applied the criterion of Field and Lampe[14] that the hydride-ion transfer reaction.

$$R^+ + C_5H_{12} \longrightarrow RH + C_5H_{11}^+ \quad (2)$$

will occur for all ions R^+ for which the reaction is approximately thermoneutral or is exothermic. For $R^+ = C_2H_3^+$ reaction 2 is exothermic by *ca.* 80 kcal./mole, which exceeds the energy of the decomposition reaction

$$C_2H_4 \longrightarrow C_2H_2 + H_2 \quad (3)$$

even when this excess energy is partitioned between the products of reaction 2 by the requirement of conservation of momentum.

From the tabulation of ions, molecules and free radicals initially formed, the ions are considered as possible reactants in reaction 2. It appears likely that CH_3^+, $C_2H_3^+$ ($C_2H_2 + H_2$), $C_2H_4^+$, $C_2H_5^+$ ($C_2H_4 + H_2$), $C_3H_3^+$, $C_3H_5^+$, $C_3H_6^+$, $C_3H_7^+$ and $C_4H_9^+$ will react. Products in parentheses indicate that further decomposition of the product RH is allowed thermodynamically as illustrated above for $R = C_2H_3^+$ and is assumed to occur.

The completion of the calculation requires certain assumptions regarding the neutralization of surviving ions and reactions of free radical species. Essentially the same procedures previously applied to *n*-hexane were followed[1] with appropriate modifications to account for the presence of two ionic species and four types of free radicals in significant quantities. Results of these calculations[16] are summarized in Table II in which the molecules resulting from each process are presented on the basis of 100 ions initially formed. These quantities are converted to G-values by dividing by W, the energy expended in forming an ion pair in the system. Columns 5 and 6 compare the experimentally measured G-values with calculations, based on an estimated $W = 26$ e.v.[17] The agreement is satisfactory.

In the original paper applying this calculation method to gas phase radiation chemistry,[1] certain serious objections were indicated. Briefly these included the statement that the mass spectrum of a

(8) Data obtained recently from 1 Mev. electron irradiations using thin target current measurement dosimetry indicates $G(C_2H_6) = 1.1 \pm 0.2$. These fragmentary results show product distribution and yield-dose relationship very similar to those in the Co^{60} study reported here.

(9) C. E. Melton and P. S. Rudolph, *J. Chem. Phys.*, **30**, 847 (1959); P. S. Rudolph and C. E. Melton, THIS JOURNAL, **63**, 916 (1959).

(10) A. E. de Vries and A. O. Allen, *ibid.*, **63**, 879 (1959).

(11) R. H. Schuler, *ibid.*, **63**, 925 (1959).

(12) W. H. T. Davison, "The Chemical Society (London) Special Publication," No. 9, 151 (1958).

(13) "Catalog of Mass Spectral Data," API Project 44, Carnegie Institute of Technology, Pittsburgh, F. D. Rossini, Editor, Serial 6, Contributed by National Bureau of Standards, October 31, 1947.

(14) F. H. Field and F. W. Lampe, *J. Am. Chem. Soc.*, **80**, 5587 (1958).

(15) J. L. Franklin and F. H. Field, "Electron Impact Phenomena," Academic Press, Inc., New York, N. Y., 1957.

(16) Details of the calculation may be obtained from the author on request.

(17) G. J. Hine and G. L. Brownell, "Radiation Dosimetry," Academic Press, Inc., New York, N. Y., 1956, p. 38.

Table II

Comparison of Calculated and Experimental *G*-Values

	Basis of 100 ions formed: From initial fragmentation	From ion molecule reactions	From radical interactions	Total	*G*-Values: Calcd.[a]	Obsd.
H_2	18.1	19.4	120	157.5	6.1	>6
CH_4		1.5	4.2	5.7	0.2	0.7
C_2H_2		11.4		11.4	0.4	0.5
C_2H_4	8.0	8.0	8.1	24.1	0.9	1.5
C_2H_6	32.4		6.4	38.8	1.5	1.1
C_3H_6	2.0	13.3	6.2	21.5	0.8	0.6
C_3H_8		33.0	9.3	42.3	1.6	2.0
C_4H_{10}		4.1	5.8	9.9	0.4	0.4

[a] Assuming $W = 26$ e.v./ion pair.

compound represents the extent of unimolecular decomposition of the molecule ion in a microsecond, while the time interval appropriate to radiation chemistry is *ca.* 10^{-10} sec.[18]; that only the hydride ion transfer reaction was considered, while diverse types of ion-molecule reactions have been observed; and that non-ionizing excitation events have been ignored.

While the latter point has not been explored further, certain general remarks pertinent to the first two objections can now be made. In a recent paper, Stevenson[18] applied the methods of the quasi-equilibrium theory of mass spectra[19] to the question of the competition between reaction and fragmentation of hydrocarbon molecule ions. He concluded that for the more complex alkanes the rates of dissociation are comparable with the rates of bimolecular ion-molecule reactions, so that reactions of the fragment ions must be considered; for the simpler paraffins reaction presumably will occur before extensive fragmentation results. Hence we may infer that the mass spectrum represents a reasonable first approximation to the distribution of ions which should be considered in *ab initio* calculations.

The best justification for considering only the so-called hydride ion transfer reaction is found in the mass spectrometer study of this reaction.[14] In parallel experiments these workers studied the intensity of the ion product of the transfer reaction as a function of pressure for a series of paraffin hydrocarbons and also studied the ion intensity for constant pressure of hydrocarbon and varying pressure of methane. Cross sections which were calculated from the assumed occurrence of all thermoneutral or exothermic hydride-ion transfers in the pure hydrocarbon experiments agreed with the cross sections for the mixture experiments in which the reactant ions were known with greater certainty. This fact not only supports the basic assumption that all thermodynamically allowed reactions occur but also implies that, for the paraffin hydrocarbons studied, this reaction competes effectively with other possible ion-molecule reactions.

Field and Lampe[14] also noted that, contrary to theoretical expectations, the measured cross section decreased relatively sharply with increasing molecular weight. Accepting this result permits us to suggest that calculations of the type we have employed can be significant for only a limited number of molecules. For large molecules the cross section for the hydride-ion transfer reaction becomes so small that it probably does not dominate the reaction mechanism for the fragment ions. As discussed above, for the simplest paraffin hydrocarbons mass spectra theory indicates that the mass spectrum cannot be used as a measure of the ion distribution. Hence the range of usefulness of this calculation method is sharply bounded, and its principal value may be the demonstration that the radiation chemistry of certain hydrocarbons can be rationalized on the basis of a consistent set of ion-molecule reactions.

(18) D. P. Stevenson, *Rad. Research*, **10**, 610 (1959).

(19) H. M. Rosenstock, M. B. Wallenstein, A. L. Wahrhaftig and H. Eyring, *Proc. Nat. Acad. Sci., U. S.* **38**, 667 (1952).

INHIBITION OF OIL OXIDATION BY 2,6-DI-*t*-BUTYL-4-SUBSTITUTED PHENOLS

By K. U. Ingold

Division of Applied Chemistry, National Research Council, Ottawa, Canada. *Issued as N.R.C. No. 6011*

Received April 11, 1960

A number of 2,6-di-*t*-butyl-4-substituted phenols have been prepared and their efficiencies in inhibiting the autoxidation of a saturated white mineral oil have been compared. Electron releasing 4-substituents increase the efficiency of the inhibitors and, provided the substituents are small, the results can be represented by a Hammett $\rho\sigma$ plot. For bulky alkyl substituents in the 4-position, the relative inhibiting efficiencies can be related to the Taft steric substituent constants E_s. Replacement of the phenolic hydrogen by deuterium does not affect the efficiency of the inhibitors. It is concluded that the rate controlling step of inhibition involves an addition reaction, perhaps by a charge transfer process, in which the attacking peroxy radical becomes conjugated with the aromatic ring of the inhibitor, probably *via* the π electrons on the phenolic oxygen atom.

Introduction

We have shown recently that the inhibition of autoxidation of a saturated white mineral oil by certain very weak inhibitors (such as phenol and aniline) exhibits a kinetic isotope effect,[1] replacement of the active hydrogen by deuterium resulting in a less efficient inhibitor. This result was assumed to favor an inhibition mechanism in which the

(1) K. U. Ingold and I. E. Puddington, *Ind. Eng. Chem.*, **51**, 1319 (1959).

chain breaking step involved hydrogen abstraction from the inhibitor (IH) by the peroxy radical ($RO_2\cdot$)

$$RO_2\cdot + IH \longrightarrow RO_2H + I\cdot$$

During the course of the above work, Walling and Hodgdon[2] showed that there is a small kinetic isotope effect in the reaction of sterically non-hindered phenols with benzoyl peroxide. It was therefore pointed out[1] that the isotope effect we had observed with non-hindered amines and phenols could be due to their reaction with the peroxidic products of autoxidation and that, in order to obtain definite conclusions about the mechanism of reaction of inhibitors with peroxy radicals, it would be necessary to know the relative rates of reaction of the inhibitors with the peroxidic products and peroxy radicals. The results of Walling and Hodgdon suggest a method for completely suppressing the former reaction. Their results show that sterically hindered phenols such as 2,6-di-*t*-butyl-4-methylphenol and 2,4,6-tri-*t*-butylphenol do not react appreciably with benzoyl peroxide, and we have confirmed that the former compound reacts extremely slowly with the peroxidic products of oil oxidation. Furthermore, the rate of reaction of non-hindered phenols with benzoyl peroxide is reduced by electron attracting *para*-substituents[2]; therefore, replacement of the 4-methyl-substituent by such groups will further reduce the rate of reaction with peroxides and, moreover, the efficiency of the inhibitor will be reduced at the same time[3] which will increase the probability of obtaining a measurable isotope effect for the reaction with peroxy radicals.[1]

A series of 2,6-di-*t*-butyl-4-substituted phenols therefore has been prepared with the 4-substituents covering a large range of electron attracting and releasing power and their relative inhibiting efficiencies on a saturated white mineral oil were compared. The compounds with strong electron attracting groups were deuterated at the phenolic hydrogen and were compared with the corresponding undeuterated phenols.

The phenols prepared and the numbering system used to identify them in the text are given in Table I.

Experimental

The apparatus and method of measuring induction periods have been described previously.[1,4]

I, II, III, IV, VI and X were commercial products which were recrystallized from *n*-hexane before use. XII and XIII were prepared from II by the method of Cohen[5]; their melting points were 190–191° and 146.5°, respectively. XIV was prepared by the chlorination of I,[6] m.p. 77–78°. XI was obtained as a minor product by the butylation of *p*-methoxyphenol,[7] m.p. 106–107°. XVII, m.p. 110° dec. was obtained by the oxidation of XI to 2,6-di-*t*-butylbenzoquinone, m.p. 68°, with nitric acid[8] and then reduction with hydrogen over platinum. V, VII, VIII and IX were prepared in good yield by the butylation of the corresponding 4-substituted phenols.[9] Their melting points were 47, 29–30, 75 and 43°, respectively. XV was prepared by the nitration of I. Fifty ml. of acetic anhydride containing 5 ml. of acetic acid and 1.1 ml. of white fuming nitric acid was cooled to −70°, 2.1 g. of I dissolved in 10 ml. of acetic anhydride was added slowly with vigorous stirring. After the addition of I the mixture was poured into 1500 ml. of ice-water and was stirred until the acetic anhydride was completely hydrolyzed. The precipitated XV was filtered, washed with water, 5% sodium bicarbonate and water again, and finally was dried under vacuum. Recrystallizing from *n*-hexane gave white needles, m.p. 156–157° dec.; yield 75%.

Anal. Calcd. for $C_{14}H_{21}O_3N$: C, 67.0; H, 8.4; N, 5.6; mol. wt., 251. Found: C, 67.0; H, 8.7; N, 5.5; mol. wt.[10] (by non-aqueous titration), 251.

This compound is quite unstable, the solid turning yellow at 150° with marked decomposition above the melting point. During the preparation a weak nitrating mixture and a low temperature must be used or one of the *t*-butyl groups will be replaced to give 2,4-dinitro-6-*t*-butylphenol, yellow needles, m.p. 127°, molecular weight[10] 239, theoretical 240. If the nitrated mixture is allowed to warm to room temperature before the acetic anhydride has been completely hydrolyzed, two condensation products also are produced. The major component is 3,3′,5,5′-tetra-*t*-butyldiphenoquinone,[11] reddish brown needles from alcohol, m.p. 243.8°. A small amount of the corresponding diphenol is also formed, pale yellow needles, m.p. 185°.[11]

XV is a *p*H indicator like *p*-nitrophenol. The sodium salt is water soluble and gives a yellow solution. The free phenol is colorless, insoluble in water, but soluble in aqueous alcohol. The color change occurs at a *p*H 4.5–5.1, compared with 5.4–6.6 for *p*-nitrophenol.

Several attempts were made to convert XV to the corresponding anisole, in view of its fairly close structural similarity to Musk Ambrette and other synthetic nitro musks.[12] Refluxing the sodium salt in toluene with dimethyl sulfate produced only 2,6-di-*t*-butylbenzoquinone. The sodium salt therefore was dissolved in diethyleneglycol dimethyl ether and was heated with methyl iodide in a sealed tube at 100° for 24 hours. Chromatography of the product on alumina separated 2,6-di-*t*-butyl-4-nitrosoanisole as the main product; yellow needles, m.p. 80.5–81.5°.

Anal. Calcd. for $C_{15}H_{23}NO_2$: C, 72.3; H, 9.2; N, 5.6; CH_3O, 12.4. Found: C, 72.3; H, 9.1; N, 5.6; CH_3O, 12.4.

The expected nitro anisole was a minor product with no appreciable musk odor, colorless needles, m.p. 72°.

Anal. Calcd. for $C_{15}H_{23}NO_3$: C, 67.9; H, 8.7; N, 5.3; CH_3O, 11.7. Found: C, 67.7; H, 8.4; N, 5.5; CH_3O, 12.1.

A small amount of 2,6-di-*t*-butylbenzoquinone also was produced.

XVI was produced by hydrogenation of XV in alcohol at room temperature over platinum. This compound is more sensitive to oxygen than *p*-aminophenol, even the dry product turning a bright red in a few minutes when exposed to the air. XVI, purified under nitrogen, melts at 112°.

XII, XIII and XV were deuterated by dissolving their sodium salts in heavy water and acidifying with DCl. The precipitated phenols were filtered off in a dry box and dried under vacuum. The degree of deuteration, which was estimated by infrared, was better than 80%.

Results

The rate of decomposition of the peroxides formed in the autoxidized oil was measured at 150° in the absence of oxygen with several inhibitors at different concentrations. The technique has been described previously.[4] The initial concentration of peroxide was 0.06 mole/l. In Fig. 1 reciprocal half-lives for peroxide decomposition ($1/t_{0.5}(P)$) are plotted against inhibitor concentration for II, XII and XV. Figure 1 also includes for comparative purposes the results obtained with three other

(2) C. Walling and R. B. Hodgdon, Jr., *J. Am. Chem. Soc.*, **80**, 228 (1958).
(3) G. S. Hammond, *et al.*, *J. Am. Chem. Soc.*, **77**, 3238 (1955).
(4) K. U. Ingold, *J. Inst. Petrol.*, **45**, 244 (1959).
(5) L. A. Cohen, *J. Org. Chem.*, **22**, 1333 (1957).
(6) K. Ley, *et al.*, *Chem. Ber.*, **91**, 2670 (1958).
(7) K. U. Ingold, *Can. J. Chem.*, **38**, 1092 (1960).
(8) E. Muller and K. Ley, *Chem. Ber.*, **88**, 601 (1955).
(9) G. H. Stillson, *et al.*, *J. Am. Chem. Soc.*, **67**, 303 (1945).
(10) M. Katz and R. A. Glenn, *Anal. Chem.*, **24**, 1157 (1952).
(11) M. S. Kharasch and B. S. Yoshi, *J. Org. Chem.*, **22**, 1439 (1957).
(12) M. S. Carpenter, W. M. Easter and T. F. Wood, *ibid.*, **16**, 586 (1951).

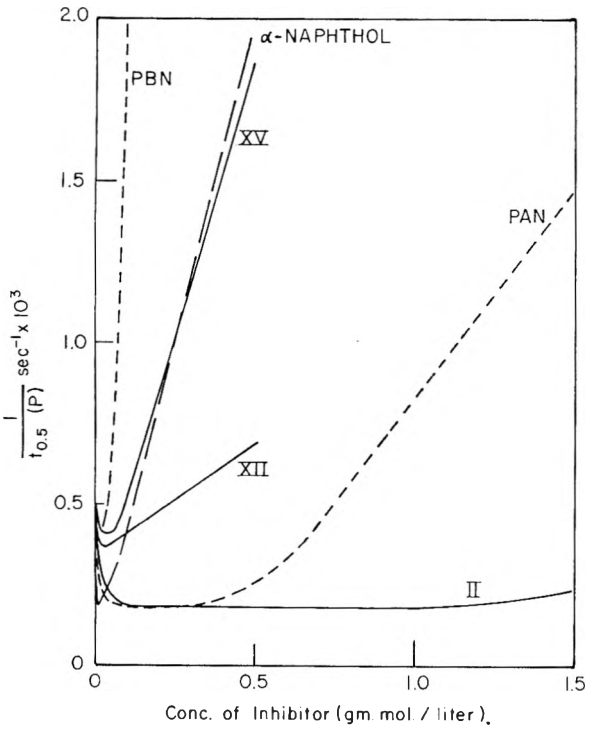

Fig. 1.—Reciprocal half-lives for peroxide decomposition plotted against concentration of inhibitor.

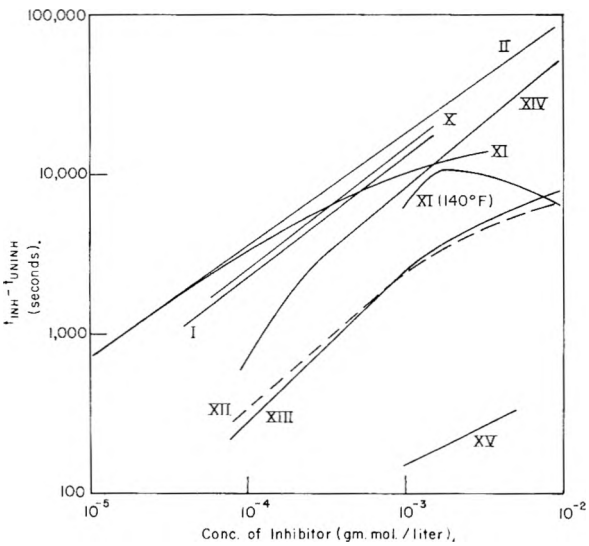

Fig. 2.—Induction period due to the inhibitor plotted against concentration of the inhibitor.

common inhibitors that we have used in previous work (N-phenyl-α-, and N-phenyl-β-naphthylamine (PAN and PBN) and α-naphthol).

Induction period differences between the inhibited and uninhibited oils ($t_{INH} - t_{UNINH}$) were measured over a range of inhibitor concentrations at 160°.[1,4] Reproducibility was generally within 2%. The results are shown in Figs. 2 and 3, the former also includes measurements on XV at 140°. Some measurements were also made at 140° with most of the phenols shown in Fig. 2 at a concentration of 1.0×10^{-3} *M*.

The results obtained with XV were rather scattered and no isotope effect could be observed over a temperature range from 120 to 160° and a concentration range from 10^{-2} to 10^{-3} *M*. Any effect of deuteration on the induction period was therefore less than 10%. No isotope effect could be detected with XII or XIII either, where reproducibility of the results was much better. The effect of isotopic substitution on the induction period was concluded to be less than 2% with these phenols.

Discussion

The results given in Fig. 1 show that II inhibits the radical induced decomposition of the peroxides, the residual reaction presumably corresponding to a molecular decomposition.[4] Although at low concentrations compounds such as PAN and α-naphthol can inhibit completely the radical induced decomposition, at higher concentrations it is obvious that they catalyze the rate of peroxide decomposition. XII and XV should be expected to behave like II in view of their similar structure and, indeed, as was pointed out in the Introduction, their rate of reaction with peroxides should be even slower than II since they contain strong electron attracting groups.[2] Their catalytic activity probably derives from decomposition products, resulting either by thermal decomposition or by free radical attack. The decomposition product responsible for the catalysis may be 3,3′5,5′-tetra-*t*-butyldiphenoquinone which was isolated in good yield from the products of the XV-peroxide reaction.

In previous work[4,13] PAN has been used to inhibit the radical induced decomposition of peroxides. In view of its catalytic activity some errors may have been introduced by its use, in particular, the activation energy measured for unimolecular peroxide decomposition[4,13] may be incorrect. This activation energy is of interest since it is assumed to give the RO–OH bond strength, and since the values usually obtained (28–31 kcal./mole) appear to be low.[4] However, if these values are incorrect, the source of error does not appear to be the choice of inhibitor, since we have obtained a value of 30.5 kcal./mole in the present work using II which is in good agreement with the result obtained previously using PAN in the same system.[4]

The results given in Figs. 2 and 3 show that the induction period due to the inhibitor is proportional to the 2/3 power of the inhibitor concentration over quite a large range of concentration for the majority of the sterically hindered phenols. The kinetics are therefore more complicated than those of some non-hindered inhibitors where the reaction changes from first order at low, to half order at high inhibitor concentrations.[4] The increase in order at low concentrations for XIV is in agreement with theory and suggests that the other inhibitors might also show first-order kinetics at sufficiently low concentrations. The decreasing kinetic order at high inhibitor concentrations of IV, V, XI, XII and XIII, although in agreement with theory,[4] might also be due to thermal instability of the inhibitor or to secondary reactions of the initially formed phenoxy radical. For instance, it has been shown that two 4-cyano-2,6-di-*t*-butylphenoxy radicals can couple through their nitrogen atoms[14] and the same

(13) J. R. Thomas, *J. Am. Chem. Soc.*, **77**, 246 (1955).
(14) K. Ley, *et al.*, *Z. Naturforsch.*, **13B**, [7], 460 (1958).

kind of coupling reaction may occur with the XII radical through the carbonyl oxygen. Two V (or IV) phenoxy radicals can disproportionate to the corresponding quinone methides and parent phenols[15] and the same may be true of III. Both these reactions are second order in phenoxy radical and would therefore increase in importance as the inhibitor concentration is increased. The decrease in kinetic order associated with XI probably is related either to its thermal instability or to a direct reaction of the inhibitor with oxygen.[16] XVII decomposes above its melting point and acts as a catalyst for the oxidation rather than as an inhibitor (at 10^{-3} M $t_{INH} - t_{UNINH} = -800$ sec.). XVI is also a very weak inhibitor (at 10^{-3} M $t_{INH} - t_{UNINH} =$ 3,000 sec.), probably because of its very rapid direct reaction with oxygen. The results with these last three compounds suggest as a general conclusion that, if the 4-substituent is a sufficiently powerful electron donor, the efficiency of phenolic inhibitors may be quite low.

At 160° XV is very unstable, its inhibiting power being much less than would be expected (see below). The fact that it inhibits at all at this temperature may be due to its decomposition to 3,3′,5,5′-tetra-*t*-butyldiphenoquinone which is itself a weak inhibitor (at 160° $t_{INH} - t_{UNINH}$ is 3300 sec. at a concentration of 10^{-3} M). Reproducibility of the results was poor at this temperature, so a number of measurements were made at lower temperatures, but the reproducibility was not much improved even at 120°. The results at 140° are given in Fig. 2 and it is apparent that decomposition predominates over inhibition at concentrations above 2×10^{-3} M, presumably because of a higher kinetic order for decomposition than for inhibition. The inhibiting power at 10^{-3} M concentration at this temperature is in closer agreement with the expected value than at 160° (see Fig. 4).

Hammond, *et al.*,[3] have shown that the efficiency of a large number of inhibitors can be correlated by means of the Hammett equation[17] by plotting the log of the relative efficiency against the Hammett σ constants. The value obtained for ρ, that is, the slope of best straight line through the points, was −3.7. The value appears to be much too large when compared with the ρ values for other similar reactions. For example, $\rho = -0.4$ for the abstraction of hydrogen from thiophenols by 1-cyano-1-cyclohexyl radicals;[18] $\rho = -0.76$ for hydrogen abstraction from toluenes by chlorine atoms;[19] and $\rho = -0.43$ for hydrogen abstraction from cumenes by peroxy radicals.[20] The anomalously large negative value obtained by Hammond, *et al.*, no doubt results from the fact that the majority of the inhibitors studied reacted not only with free radicals but also with the peroxidic products. Although the trend in the latter reaction is such as to suggest a negative value for ρ (*i.e.*, rate increased by electron donating substituents), the results are so scattered that no definite value for ρ could be obtained.[2] This scatter appears to be real and probably accounts in large part for the scatter of the points on Hammond, *et al*'s., $\rho\sigma$ plot.

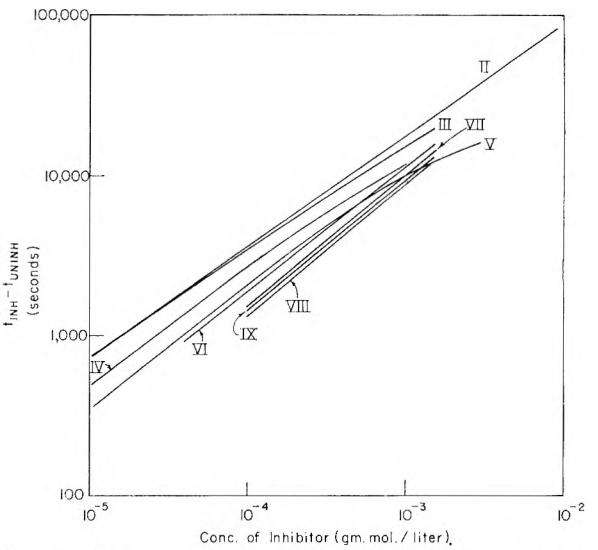

Fig. 3.—Induction period due to the inhibitor plotted against concentration of the inhibitor.

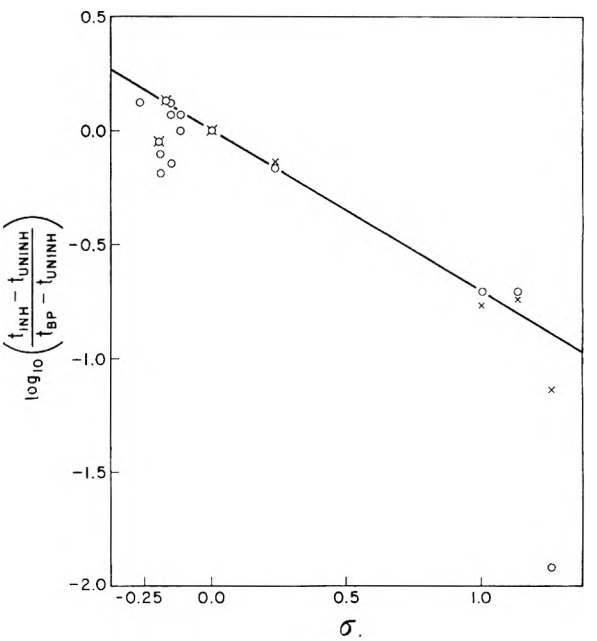

Fig. 4.—Log of inhibiting efficiencies relative to I plotted against σ: ○, values obtained at 160°; X, values obtained at 140°.

In Fig. 4 the log of the inhibiting efficiencies at 160 and 140°, relative to I of the 4-substituted-2,6-di-*t*-butyl-phenols have been plotted against σ-values taken from Jaffé.[21] The σ-values for the 4-dimethylaminomethyl, 4-*t*-*t*-octyl and 4-cumyl groups have been assumed for structural reasons to equal the σ-values of the isobutyl, *t*-amyl and isopropyl groups, respectively. At 160° the relative efficiencies were calculated for those phenols which show curvature in Figs. 2 and 3 at concentrations

(15) C. D. Cook and B. E. Norcross, *J. Am. Chem. Soc.*, **81**, 1176 (1959).

(16) C. J. Pedersen, *Ind. Eng. Chem.*, **48**, 1881 (1956).

(17) L. P. Hammett, "Physical Organic Chemistry," McGraw-Hill Book Co., Inc., New York, N. Y., 1940, Chapt. VII.

(18) Y. Schaafsma, A. F. Bickel and E. C. Kooyman, *Rec. trav. chim.*, **76**, 180 (1957).

(19) C. Walling and B. Miller, *J. Am. Chem. Soc.*, **79**, 4181 (1957).

(20) G. A. Russell, *ibid.*, **78**, 1047 (1956).

(21) H. H. Jaffé, *Chem. Revs.*, **53**, 191 (1953).

in the middle of the concentration range covered where the lines are straight and parallel or nearly parallel to the other phenols. At 140° measurements were made only at 10^{-3} M concentrations (except for XV). The results obtained with XVI and XVII are not included. The relative efficiencies are summarized in Table I.

TABLE I

INHIBITING EFFICIENCIES OF 2,6-DI-*t*-BUTYL-4-SUBSTITUTED PHENOLS RELATIVE TO I AT 160°

4-Substituent	Abbreviation	σ[21]	E_s[25]	Relative efficiency
H	I	0.000		1.00
CH_3	II	− .170	0.00	1.38
C_2H_5	III	− .151	− .07	1.34
$(CH_3)_2CH$	IV	− .151	− .47	1.17
$C_2H_5(CH_3)CH$	V	− .123	−1.13	0.99
$(CH_3)_3C$	VI	− .197	−1.54	.90
$C_2H_5(CH_3)_2C$	VII	− .190	−1.96[a]	.79
$(CH_3)_2CCH_2(CH_3)_2C$	VIII	− .190[a]	−2.57	.65
$C_6H_5(CH_3)_2C$	IX	− .151[a]	−2.06[a]	.72
$(CH_3)_2NCH_2$	X	− .115[a]		1.18
CH_3O	XI	− .268		1.33
CHO	XII	1.126		0.196
CN	XIII	1.000		0.196
Cl	XIV	0.227		0.68
NO_2	XV	1.270		0.012
NH_2	XVI			
OH	XVII			

[a] See text.

With the exception of those phenols which contain bulky alkyl substituents in the 4-position and with the exception of the unstable XV, the points in Fig. 3 lie on an excellent straight line covering a large range of σ-values. The small deviation of the points is not unexpected since no reaction between inhibitor and peroxide occurs. Moreover, the slope of the line at 160° (ρ) is −0.71 which is in the general region expected. Although steric hindrance by the *t*-butyl groups reduces the efficiency of these inhibitors below what might be expected,[22] their steric effect on the phenolic end of the molecule will be constant, so the ρ-value obtained probably is fairly general for the reaction of even non-hindered phenols with peroxy radicals. The large deviation of the XV point at 160° from the $\rho\sigma$ plot is explained by its instability at this temperature, the closer approach to the line at 140° suggests that at sufficiently low temperatures this compound should function as a stable inhibitor with the expected efficiency relative to other phenols. The deviation of XII might be due to oxidation, during the induction period, of the formyl group (σ = 1.126) to a carboxylic acid group (σ = 0.728) with a consequent increase in inhibitor efficiency. Alternatively, infrared results[7] suggest that σ_{para} for the formyl group should be quite close to σ_{para} CN(1.000) in phenols. The low value obtained with XI may not be connected with the curvature exhibited by this phenol in Fig. 2, since it has been suggested that the σ constant for this substituent in phenols is about −0.16[23,24] compared with the value of −0.268 given by Jaffé.[21] Alternatively, the analysis of XI for methoxy shows an increase after the compound has been heated at 100° for a short time, which suggests that the phenolic hydrogen may exchange with a methyl group from the adjacent *t*-butyl group leading to a dimethoxybenzene with low inhibiting power.

The varying deviations of those phenols which contain bulky alkyl substituents in the 4-position can, we have found, be related to Taft E_s values[25] which measure the total steric effect associated with the substituent relative to the steric effect of the methyl group. The log of the inhibiting efficiencies of these phenols at 10^{-3} molar relative to II at 160° is shown in Fig. 5 plotted against E_s. The efficiencies of III, IV and V were obtained by extrapolation from low concentrations where a linear relation holds in Fig. 3. For two of the groups studied (*t*-amyl and cumyl) Taft does not give E_s values, and they were therefore derived from the E_s values of similar groups in the following way. Replacing the H in these various groups by CH_3 decreases the value of E_s by an average of −0.79, $(CH_3)_2CH$–, CH_3(*t*-Bu)CH–, CH_3(neo-pentyl)CH–. Therefore replacement of the H in the structurally similar group $CH_3(C_2H_5)CH$– (E_s = −1.13) by CH_3 should give the *t*-amyl group an E_s value of −1.13 − 0.79 = −1.92. Similarly, the replacement of H by C_2H_5 in the groups $C_2H_5CH_2$–, $(C_2H_5)_2CH$–, $C_6H_5CH_2$– gives an average decrease of E_s of −1.41 which, combined with the E_s value for $(CH_3)_2CH$– (−0.47), gives a value of −1.88 for *t*-amyl. Finally, the decrease in E_s produced by replacement of CH_3 by C_2H_5 in the groups C_2H_5–, $CH_3(C_2H_5)CH$–, $(CH_3)_2CH$– and $CH_3(C_6H_5)CH$ combined with the E_s value for $(CH_3)_3C$– gives E_s (*t*-amyl) = −2.06. The average of these three values (−1.95) for E_s(*t*-amyl) probably is fairly accurate. In the same way, an average E_s value was derived for the cumyl group of −2.06.

The results given in Fig. 5 show that, as the size of the 4-substituent rises above a certain critical point, it starts to interfere with the mechanism of the inhibition reaction. The decrease in efficiency is not associated with a decrease of σ since the σ constant for 4-*t* butyl and 4-*t*-amyl is larger than for 4-CH_3.[21] However, the changes in σ do appear to account for the small deviations in the E_s plot. By using the slope of the line in Fig. 4 we can calculate expected efficiencies relative to II that would be obtained if the σ constants were all equal to σ_{para} CH_3 (−0.17). That is, we can eliminate the effect of changes of σ so that the results show only the relationship between inhibiting efficiency and E_s. The straight line in Fig. 5 is drawn through these calculated efficiencies, its slope (δ) = 0.14.

The over-all efficiency of all the 2,6-di-*t*-butylphenols as inhibitors can therefore be represented by the usual Hammett equation for E_s values more positive than −0.12, *i.e.*

$$\log\left(\frac{t}{t_0}\right) = \rho\sigma = -0.71\sigma$$

and by the Hammett equation as modified by Taft[25] for E_s values more negative than −0.12

(22) D. S. Davies, *et al.*, *J. Chem. Soc.*, 4926 (1956).
(23) R. W. Taft, *et al.*, *J. Am. Chem. Soc.*, **81**, 5352 (1959).
(24) M. M. Fickling, *et al.*, *ibid.*, **81**, 4226 (1959).
(25) R. W. Taft, "Steric Effects in Organic Chemistry," John Wiley and Sons, Inc., New York, N. Y., 1956, Chapt. 13.

$$\log\left(\frac{t}{t_0}\right) = \rho\sigma + \delta E_s = -0.71\sigma + 0.14E_s$$

There appear to be three major possibilities for the mechanism by which these hindered phenols inhibit hydrocarbon autoxidation, since they obviously do not inhibit by peroxide decomposition. The three possible reactions with peroxy radicals are

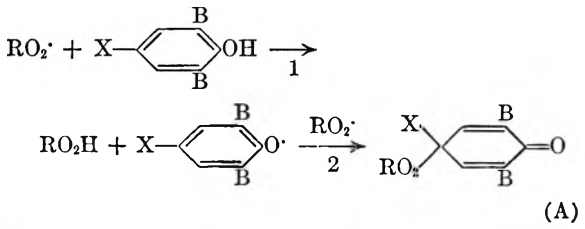

(A)

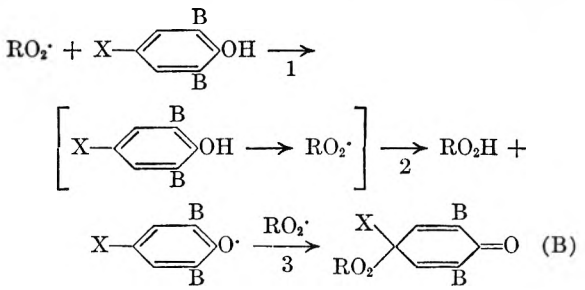

(B)

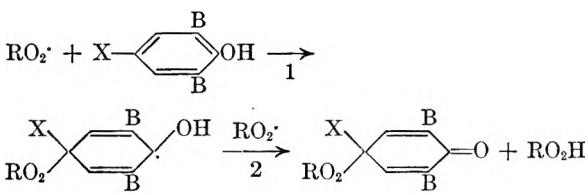

(C)

The products of reaction are the same in each mechanism and are known from the work of Bickel and Kooyman.[26] It should be added that the final addition product also can have the peroxy group attached to the aromatic nucleus in the *ortho* position.

Peroxy radicals, like other free radicals, are electron deficient and therefore will tend to react with the phenols at regions of high electron density. The negative value of ρ in Fig. 4 therefore means that the peroxy radicals react with the phenolic end of the inhibitor, and for this reason mechanism C can be discarded in spite of the fact that bulky X's hinder the inhibition process. The absence of a deuterium isotope effect argues against mechanism A, but as we have pointed out previously[1] the validity of this argument depends on whether the activation energy of reaction A_1 is large enough for an isotope effect to be observed. The inhibiting efficiency of XII and XIII is similar to that of *o*-cresol for which an isotope effect of around 9% was found previously.[1] The absence of an isotope effect with these two hindered phenols therefore suggests that the previously observed isotope effects with non-hindered amines and phenols were due to their reaction with peroxides and not with peroxy radicals. This conclusion receives some support from a very rough estimation of the difference in activation energy for the rate-controlling step of the inhibition

(26) A. F. Bickel and E. C. Kooyman, *J. Chem. Soc.*, 3211 (1953).

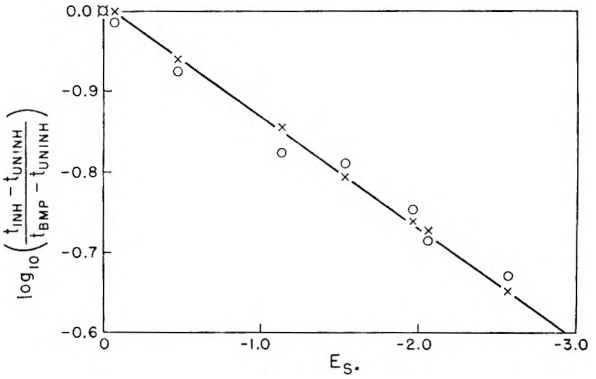

Fig. 5.—Log of inhibiting efficiencies relative to II plotted against E_s: O, measured values; X, values corrected to constant σ.

process between the strongest (II) and weakest stable inhibitors (XII and XIII). The results given in Fig. 2 suggest there is no change of mechanism over this range of inhibitor efficiencies, the Hammett equation therefore can be written

$$\log\left(\frac{t}{t_0}\right) = \rho\sigma = \log\left(\frac{c}{c_0}\right)\log\left(\frac{k}{k_0}\right)^{2/3} = \log\left(\frac{c}{c_0}\right)\left(\log\left(\frac{A}{A_0}\right)^{2/3} + \frac{2}{3}\frac{E_0 - E}{2.3RT}\right)$$

where t is the induction period due to the inhibitor, k is the rate constant, A the pre-exponential factor and E the activation energy for the inhibition reaction. The factor 2/3 is introduced since t is proportional to the 2/3rd power of the inhibitor concentration and k probably is involved in the rate expression to the same order, *i.e.*, $t = ck^{2/3}[\mathrm{IH}]^{2/3}$. Incidentally, the true value of ρ for the inhibition reaction will therefore be $3/2 \times -0.71 = -1.06$.

Since the mechanism is unchanged, the proportionality constant $c = c_0$. The ratio of the induction periods for II to XII or XIII is 7:1 and therefore by assuming the pre-exponential factors are equal, we can write

$$\log 7 = \frac{2}{3}\frac{E_0 - E}{2.3RT}, \quad \therefore E_0 - E = 2.5 \text{ kcal./mole}$$

Although there is no real justification for the last assumption, it may be fairly accurate in the organic reaction medium employed in this work.[27] Moreover, a change of even a factor of 3 between A and A_0 would change $E_0 - E$ by less than 1 kcal. The order of magnitude of $E_0 - E$ should therefore be approximately correct. The activition energy for the reaction of II with peroxy radicals has been roughly estimated to be small,[28] but more recent measurements give a value of about 5.0 kcal./mole.[29] Therefore the activation energy for XII and XIII is almost certainly large enough that a considerable isotope effect should be observed.[30] Russell[31] has compared the observed isotope effect for the abstraction of hydrogen and deuterium from substituted toluenes by a variety of free radicals with the activation energies of the reactions.

(27) E. Tommila, *et al.*, *Suomen Kemistilehti*, **32B**, 115 (1959).
(28) A. F. Bickel and E. C. Kooyman, *J. Chem. Soc.*, 2415 (1957).
(29) J. C. Robb and M. Shahin, *Trans. Faraday Soc.*, **55**, 1753 (1959).
(30) K. Wiberg, *Chem. Revs.*, **55**, 713 (1955).
(31) G. A. Russell, *J. Am. Chem. Soc.*, **79**, 3871 (1957).

Thus, the reaction of peroxy radicals with cumene has an activation energy of 6.7 kcal./mole and $k_H/k_D = 5.5$, even the attack of the very reactive chlorine atom on toluene ($E = 2$–3 kcal.) has an isotope effect $k_H/k_D = 2.0$. The absence of an isotope effect in the present reaction must therefore be taken to rule out mechanism A.

Mechanism B includes a rate-determining step involving radical addition to the inhibitor (B_1) followed by a fast reaction in which the hydrogen atom or perhaps the proton is transferred (B_2). A generally similar mechanism first was proposed by Hammond, *et al.*,[3] and was further developed for amines by Pedersen.[16] Objections to this type of mechanism were based chiefly on the fact that the absence of a deuterium isotope effect with strong inhibitors could be due to the absence of any activation energy for the inhibition process.[1,28] The present work shows that for weak inhibitors this activation energy is almost certainly several kcal./mole and that therefore hydrogen abstraction is not rate determining. The decreasing isotope effect found previously for non-hindered inhibitors as the inhibitor becomes more efficient[1] may be due to the decreasing importance of the reaction between peroxides and inhibitors compared with the increasing importance of the reaction with peroxy radicals.

Reaction B_3 can be written

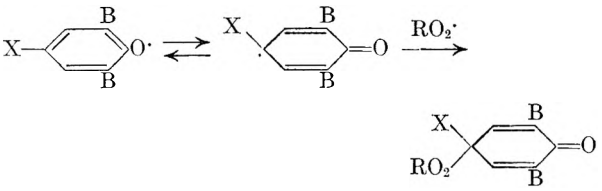

where the equilibrium represents two resonance forms of the free radical. Provided X is small, this reaction will occur rapidly and have virtually no activation energy like most free radical combinations. However, as X is increased beyond a certain critical size, steric factors come into play and the rate of reaction B_3 will decrease (Fig. 5). One can therefore predict that the concentration of free radicals in solution during the induction period will be small when X is small, but will increase rapidly as the E_s value for X decreases. It is therefore not surprising that Harle and Thomas[32] failed to detect free radicals by electron paramagnetic resonance measurements during the oxidation of octadecene in the presence of II and *t*-butylcatechol. Presumably with sufficiently large 4-substituents, the phenoxy radical will no longer take part in the inhibition reaction and further increases in the size of the substituent will not affect its inhibiting efficiency.

The negative value of ρ in Fig. 4 suggests that the peroxy radical attacks the π electrons at the phenolic end of the inhibitor, that is, conjugation of the aromatic ring with the radical perhaps through the oxygen atom. Certain modifications in mechanism B as written cannot be ruled out. For instance, reactions B_2 and B_3 may occur concurrently and not consecutively.[3] Another factor that probably complicates the over-all kinetics is that molecular oxygen will be in competition with peroxy radicals for the phenoxy free radical.[33]

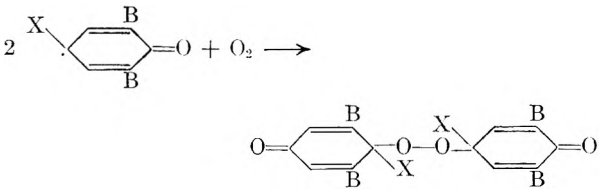

Furthermore, the phenoxy free radical may react with hydroperoxides.[34]

One problem that is not answered by mechanism B is that aromatic ethers either do not inhibit hydrocarbon autoxidations or only inhibit them very weakly. For example, 2-*t*-butyl-1,4-dimethoxybenzene at a concentration of 10^{-3} *M* increased the induction period of the oil by only 160 sec. A possible explanation is that although an inhibition type of reaction occurs, one of the products is not the hydroperoxide RO_2H but is instead a mixed peroxide RO_2CH_3, which will be less stable than the hydroperoxide and will break down rapidly to two alkoxy radicals which can carry on the chain. If this is the case, it might be expected that aryl ethers could inhibit low temperature induced hydrocarbon oxidations although, as far as we are aware, this has not been observed.

The hindered phenols dealt with in this work have a structure in which the hydroxyl group is coplanar with the ring whereby the phenolic hydrogen is tucked into the adjacent *t*-butyl group[7] and is protected from direct attack by a peroxy radical. The transition state may involve a twisting of the O–H bond to a position perpendicular to the plane to meet the approaching peroxy radical, the actual hydrogen transfer being a much faster reaction. The overall inhibition process would therefore have no isotope effect since the rate controlling step would not involve any stretching of the O–H bond. However, it does not necessarily follow that this type of mechanism applies to non-hindered phenols since the results of Davies, *et al.*,[22] and the more recent work of Fueno, Ree and Eyring[35] strongly suggests that the rate controlling step for these phenols involves electron transfer rather than hydrogen atom transfer to the radicals.

Acknowledgment.—The author wishes to thank Dr. I. E. Puddington for his continuing interest and advice throughout the course of this work. Thanks are also due to A. Lafortune for much of the experimental work and to Dr. E. C. Horswill for help and advice on the preparation of many of the compounds.

(32) O. L. Harle and J. R. Thomas, *J. Am. Chem. Soc.*, **79**, 2973 (1957).

(33) C. D. Cook and R. C. Woodworth, *J. Am. Chem. Soc.*, **75**, 6242 (1953).

(34) J. C. McGowan and T. Powell, *J. Chem. Soc.*, 238 (1960).

(35) T. Fueno, T. Ree and H. Eyring, THIS JOURNAL, **63**, 1940 (1959).

THE ENVIRONMENTAL INFLUENCE ON THE BEHAVIOR OF LONG CHAIN MOLECULES[1]

BY R. H. ARANOW AND L. WITTEN

RIAS, 7212 Bellona Ave., Baltimore 12, Md.

Received April 13, 1960

Transition of a molecule upon a change of environment from the state of internal torsional oscillation to the state of hindered internal rotation can account quantitatively for the entropy of fusion per CH_2 group of long chain hydrocarbons, Traube's rule of surface tension, the distribution ratios of long chain hydrocarbons between water and organic solvents immiscible with water, the solubility in water of liquid long chain hydrocarbons, and the effect of chain length and alcohol on critical micelle concentration. The solutions of crystalline long chain molecules in water are predicted to be a special class of non-ideal solution.

I. Introduction

The phenomenon of hindered internal rotation has been the subject of much study.[2] Systems in the temperature region where the hindered internal rotation can still be regarded as a torsional oscillation but where the torsional oscillation can occur around more than one position of potential minimum have interesting properties from the point of view of statistical mechanics. We call such systems pseudo-degenerate torsional oscillators for reasons which shall be described in Section II of this paper. In section II we shall review the relationship between the thermodynamic behavior and the statistical mechanical description of the pseudo-degenerate torsional oscillator. We shall discuss the partition function for two phase systems in order to demonstrate the effect of the pseudo-degenerate oscillator.

In section III the results of the analysis made in section II will be utilized to explain the distribution ratios of long chain molecules between immiscible solvents, solubility of liquid long chain molecules in water, and effect of chain length on critical micelle concentration. In addition the theory of fusion of long chain hydrocarbons[3a] and of Traube's Rule[3b] will be reviewed and restated in order to demonstrate the common physical basis of all the phenomena mentioned. In section IV an example will be given of the biological implications of the pseudo-degenerate oscillator behavior. In addition we will state some predictions with regard to the solubility of crystalline state long chain hydrocarbons.

II. Theory

In the solid state, in condensed surface films, and in aqueous solution the potential energy diagram for torsional oscillation about a single carbon-to-carbon bond is postulated to take the general form shown in Fig. 1a. The effect of interaction with neighboring molecules is to restrict the torsional oscillation to one preferred region of potential minimum. The postulate has been confirmed experimentally for the solid state and condensed films.[4,5] In aqueous solution the water molecules surrounding a given long chain hydrocarbon form a cage where hydrogen bonds between water molecules may be likened to bars. The complete rotation around a carbon-to-carbon bond thus involves not only the relative motion of the parts of the long chain hydrocarbon molecule but also the simultaneous breaking or distortion of many hydrogen bonds of the cage surrounding an individual molecule. Since the total motion requires high energy, the cage of water molecules has the effect of confining a particular bond to the configuration it is in initially. In addition if the shape of the hydrocarbon molecule has a significant effect upon the *number* of hydrogen bonds in the surrounding cage it is reasonable that those shapes which permit maximum hydrogen bonding would correspond to minimum potential energy and hence be preferred. It is a postulate of the theory that there is at room temperature in aqueous solution one or at most a very small number of such over-all molecular shapes.

In the pure liquid state, in organic solutions and in dilute liquid surface films ("gaseous film state"), the potential diagram is postulated to take the form shown in Fig. 1b. In the vapor phase it has been confirmed experimentally for relatively short chain molecules that all configurations around a given carbon-to-carbon bond are *not* equally preferred.[2] Figure 1b is probably not a good representation for the potential energy of rotation about a carbon–carbon bond for long chain molecules in the vapor phase because the relative depths of the three potential minima are considerably different and vary markedly with time due to the interaction with distant atoms and to the many possible configurations of other bonds.

In the organic liquid state and in dilute films, however, interaction of the molecule as a whole with neighboring molecules may tend to average out the effect of the other parts of the molecule associated with a given carbon-to-carbon bond. The contribution to the potential energy of rotation about a given carbon–carbon bond of the more distant CH_2 groups is strongly affected by the interaction of those groups with their environments, *i.e.*, neighboring molecules. When this interaction is strong, the effective moment of inertia of the two groups around a given carbon–carbon bond should be relatively insensitive to the particular configuration

(1) This research was partially supported by the United States Air Force through the Air Force Office of Scientific Research of the Air Research and Development Command, under Contract Number AF 49(638)-735. Reproduction in whole or in part is permitted for any purpose of the United States Government.

(2) See, for example S. Mizushima, "Structure of Molecules and Internal Rotation," Academic Press, Inc., New York, N. Y., 1954.

(3)(a) R. H. Aranow, L. Witten and H. Andrews, THIS JOURNAL, **62**, 812 (1958); (b) R. H. Aranow and L. Witten, *J. Chem. Phys.*, **28**, 405 (1958).

(4) A. Müller, *Proc. Roy. Soc. (London)*, **138**, 514 (1932).

(5) N. K. Adam, "The Physics and Chemistry of Surfaces," Oxford University Press, 1941, Chap. II.

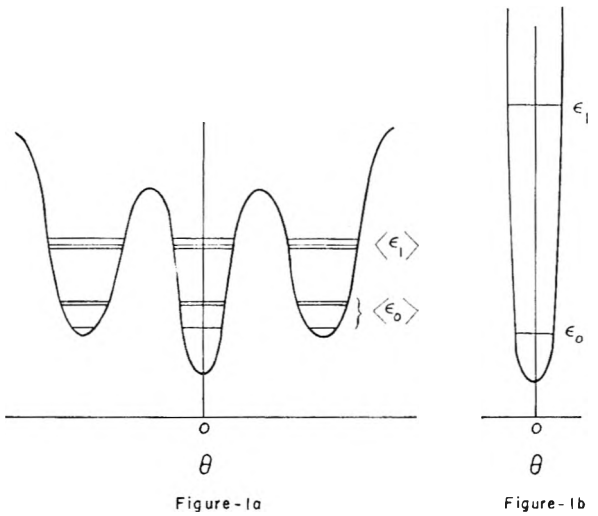

Figure-1a Figure-1b

Fig. 1.—Potential energy curve and energy levels for rotation around a carbon-to-carbon bond: (a) represents conditions in the liquid state, on surfaces, and in organic solutions; (b) represents conditions in the solid state, and in aqueous solution.

of the more distant atoms of the chain. Hence the simplified diagram shown in Fig. 1b may be a valid representation, at least as an average. That such an averaging process is physically reasonable may be inferred from experiments on 1,2-dichloroethane which indicate that the difference in the energy of the succesive minima of the potential curve is of the order of 1 kcal. in the gaseous state while there is no energy difference in the liquid state.[2] The physical concepts presented here are offered as postulates and we will check some consequences of the postulates.

The general characteristics of the energy level diagram for the torsional oscillator (Fig. 1a) are similar to those of the linear harmonic oscillator. The main characteristics of the energy level diagram for the system in Fig. 1b[6] are that the nondegenerate levels of the torsional oscillator (Fig. 1a) have been shifted down and that there are three times as many energy levels available as there would be without the two secondary minima. In the region above the potential barrier the levels become like those of the free internal rotator. But this region is not of interest in the present paper, for the molecules are rarely excited to these levels at room temperature. These general features are preserved even with alteration in the detailed shape of the potential energy curve. In particular, the general features remain even if the depths of the potential minima and the heights of the maxima are varied by different amounts.

Because of the threefold increase in number of energy levels, we can separate the levels into groups of three and call $\langle\epsilon_j\rangle$ the average energy level of the jth group. The partition function Q for the oscillator can be approximated by $Q = \sum_j 3 \exp(-\langle\epsilon_j\rangle/kT)$; k is Boltzmann's constant and T is the temperature. This form is also obtained for a triply degenerate oscillator; we can call the system a pseudo-degenerate torsional oscillator.

(6) See G. Herzberg, "Molecular Spectra and Molecular Structure," Vol. II, D. Van Nostrand Co., Inc., New York, N. Y., 1945, p. 225.

In summary, for the system in Fig 1a, $Q = \sum_i \exp(-\epsilon_i/kT)$; for the system in Fig. 1b $Q = \sum_j 3 \exp(-\langle\epsilon_j\rangle/kT)$. We should point out that these approximate forms can be obtained in many different ways for the problem at hand. The important physical requirement is the impossibility of the molecules performing hindered rotations for the one case and the corresponding possibility for the second case.

Let us look now at the canonical single particle partition function, Z, for a molecule having n carbon to carbon bonds. In an environment such as that of Fig. 1a, the partition function can be represented by

$$Z_n = \psi\left(\sum_i e^{-\epsilon_i/kT}\right)^n \qquad (1)$$

The rotational contribution has been assumed separable from all other contributions, ψ; also the rotational contribution has been assumed to be representable as a product of factors each making the contribution Q. Similarly the partition function in an environment such as that of Fig. 1b can be represented by

$$Z_n = \psi\left(\sum_i 3e^{-\langle\epsilon_i\rangle/kT}\right)^n \qquad (2)$$

The main dependence on the chain length, n, will be in the exponent as explicity shown in these expressions. Actually the factor ψ has a dependence on n as do the energy levels ϵ_i. These dependences can be expected to be small compared with the exponential dependence and will be ignored in the approximation with which we are dealing. We are more interested in demonstrating the physical features and gross predictions of our picture rather than the details.

There are two convenient ways of evaluating the statistical mechanical behavior of two phase systems in order to show the effect of hindered internal rotation. The more rigorous approach for the problem at hand involves the evaluation of μ, the chemical potential, which must have the same value in both phases at equilibrium. Another approach consists of regarding the two phases (which we shall designate as α and β) as being two regions of a single larger system where the energy levels (including the interfacial values) of a molecule depend on the location of the molecule within the system—we can call $\epsilon(\alpha)_j$ the energy levels when the molecule is in the phase α, $\epsilon(\beta)_i$ the energy levels in the phase β, and $\epsilon(\alpha,\beta)_l$ the energy levels at the interface.

$$\frac{n_\alpha}{N_T} = \frac{\sum_j e^{-\epsilon(\alpha)_j/kT}}{\sum_j e^{-\epsilon(\alpha)_j/kT} + \sum_i e^{-\epsilon(\beta)_i/kT} + \sum_l e^{-\epsilon(\alpha\beta)_l/kT}} \qquad (3)$$

where n_α is the number of molecules in phase α, N_T is the total number of molecules, and k is Boltzmann's constant. We use this second approach to describe the effects of internal rotation because, for the problem at hand, it is more direct than the first approach. For the case of a solute distributed

between two phases the effect of the solvent on the energy levels can be included by considering the potential of average forces[7] of the solvent on the solute. The form of equation 3 is then retained but the influence of the solvent is implicit in the evaluation of energy levels. If the contribution of translational motion to the partition function of the single molecule can be regarded as separable and having the form

$$Z_{tr} = \left(\frac{2\pi mkT}{h^2}\right)^{3/2} V \qquad (4)$$

where $V = V_\alpha + V_\beta + V_{\alpha\beta}$, then $Z_{tr} = Z_{tr}(\alpha) + Z_{tr}(\beta) + Z_{tr}(\alpha,\beta)$. This form corresponds mathematically to the situation where $\epsilon_{translation} = \epsilon_{tr}(\alpha)$ or $\epsilon_{tr}(\beta)$ or $\epsilon_{tr}(\alpha,\beta)$ but not all simultaneously. Hence by partitioning the partition function into three classes, α, β and (α,β), one can arrive at the form

$$\frac{n_\alpha}{N_T} = \frac{V_\alpha \sum_j e^{-E_j(\alpha)/kT}}{V_\alpha \sum_j e^{-E_j(\alpha)/kT} + V_\beta \sum_i e^{-E_i(\beta)/kT} + V_{(\alpha,\beta)} \sum_l e^{-E_l(\alpha,\beta)/kT}} \qquad (5)$$

where $E_j(\alpha)$ refers to the jth energy level of all nontranslational motions for a molecule whose translational energy lies anywhere in the set $(\epsilon_{tr}^{(2)})$

$$\frac{n_\alpha}{V_\alpha} = N_T \frac{\sum_j e^{-E_j(\alpha)/kT}}{V_\alpha \sum_j e^{-E_j(\alpha)/kT} + V_\beta \sum_i e^{-E_i(\beta)/kT} + V_{(\alpha,\beta)} \sum_l e^{-E_l(\alpha,\beta)/kT}} \qquad (6)$$

and

$$\frac{\frac{n_\alpha}{V_\alpha}}{\frac{n_\beta}{V_\beta}} = \frac{\sum_j e^{-E_j(\alpha)/kT}}{\sum_i e^{-E_i(\beta)/kT}} \qquad (7)$$

III. Applications to Physical Chemistry

A. The Distribution Ratios of Long Chain Hydrocarbons between Two Immiscible Solvents. —Consider an idealized system of two truly immiscible solvents (water and an organic solvent which is insoluble in water) with a long chain hydrocarbon in dilute solution in the aqueous phase at concentrations much less than the critical micelle concentration. In fact we assume that in both phases the solutions are infinitely dilute.

The definition of the distribution ratio ρ is the ratio of the concentration of solute molecules in the organic phase (α) to that in the water phase (β). From equation 7

$$\rho = \sum_j \exp(-E_j/kT) \Big/ \sum_i \exp(-E_i/kT) \qquad (8)$$

Assuming now that the motions of internal rotation are separable from all other motions and recalling that the internal rotational contribution has been assumed representable as a product of n equivalent factors, and using (1), (2) and (8)

$$\rho_n = \frac{\psi_\alpha}{\psi_\beta} \frac{\left(\sum_j 3e^{-\langle\epsilon_j\rangle/kT}\right)^n}{\left(\sum_i e^{-\epsilon_i/kT}\right)^n}$$

At room temperatures; if kT is much smaller than the spacing between $\langle\epsilon_0\rangle$ and $\langle\epsilon_1\rangle$ or between ϵ_0, and ϵ_1, then

$$\rho_n \cong \frac{\psi_\alpha}{\psi_\beta} 3n \left(e^{-\langle\epsilon_0\rangle - \epsilon_0/kT}\right)^n \qquad (9)$$

If ψ_α/ψ_β is at most only a slowly varying function of n and $\langle\epsilon_0\rangle \sim \epsilon_0$ we get

$$\rho_n/\rho_{n-1} \cong 3$$

This approximation states that the *difference* in all other external internal behavior in the two media is relatively insensitive to chain length although the external and internal rotational behavior in a given medium may exhibit considerable dependence on chain length. The results of the experimental determination of ρ are shown in Table I. The approximate rule of three is followed fairly well for those systems where the two solvents are very immiscible.

The above data has been computed using the data of R. C. Archibald.[8] The assumptions made in the calculations are: 1. Volume of organic solution = sum of volumes of individual components; 2. Moles of water per liter of solution = 55.5.

For those cases where the organic solvent is present to a large extent in the aqueous phase the solute molecule is surrounded by both water and other organic solvent. Hence the solute molecule is expected to have greater freedom for internal rotations than in water alone but less than in organic material alone. Its environment can be represented to be something between Figs. 1a and 1b or to alternate between the two. Hence the contribution to the partition function of a rotational state of such a molecule will be $\left(\sum_i g \exp -\epsilon_i/kT\right)^n$ where g is a parameter greater than one but less than three. Carrying through the analysis in this way, one will get for the ratio of distribution functions

$$\frac{\rho_{n+1}}{\rho_n} = \frac{3}{g}$$

Thus for $\rho_{n+1}/\rho_n = 2$, $g = 1.5$. These considerations may explain why ratios in the table may be less than 3. However, a quantitative evaluation of this effect and of other causes of deviation from the "Rule of Three" are beyond the aims of our general discussion.

The solubility of liquid long chain hydrocarbons in water may be regarded as a special case of distribution ratio where $\rho = d/s$, d is the moles per liter of pure liquid solute, and s in the solubility in water expressed as moles per liter of water. (Note: we have assumed that the volume of solution is approximately the volume of solvent.) The fact that the solubility decreases by a factor of three for every CH_2 group added may thus be expressed as

$$\frac{\rho_{n+1}}{\rho_n} = \frac{d_{(n+1)}/S/3}{d_{(n)}/S} \cong 3$$

Shinoda[9] accounted for the effect of chain length on critical micelle concentration and the effect of alcohol on critical micelle concentration by equating the chemical potential in the aqueous phase to that in the liquid micelle interior (liquid phase of the sol-

(7) W. G. McMillan and J. E. Mayer, *J. Chem. Phys.*, **13**, 276 (1945).

(8) R. C. Archibald, *J. Am. Chem. Soc.*, **54**, 3178 (1932).

(9) K. Shinoda, *Bull. Chem. Soc. Japan*, **26**, 101 (1953).

TABLE I

TYPICAL EXPERIMENTS RESULTS FOR DISTRIBUTION RATIO STUDIES

Solvent	*n*-Amyl alcohol		*n*-Butyl alcohol		*t*-Amyl alcohol		Ethyl methyl ketone	
Solubility of solvent in water, g./100 ml. H_2O	2.7		7.9		12.5		35.3	
Solute	ρ	$\frac{\rho_n}{\rho_{n-1}}$	ρ	$\frac{\rho_n}{\rho_{n-1}}$	ρ	$\frac{\rho_n}{\rho_{n-1}}$	ρ	$\frac{\rho_n}{\rho_{n-1}}$
Acetic acid	5.56		6.28		8.84		5.95	
		3.75		2.63		2.56		2.07
Propionic acid	20.8		16.46		22.6		12.3	
		3.22		2.74		2.79		2.14
Butyric acid	67.0		45.2		63.1		26.3	
		3.28		2.68		2.65		1.95
Valeric acid	219		116.3		167.3		51.3	
		3.08		3.03		2.99		2.24
Caproic acid	675		352		498		115.0	

ute itself). Using the solubility data just discussed to evaluate the contribution of the bond to the change in chemical potential, Shinoda got quantitative agreement between theory and experiment.[10] We refer the reader to the original papers for details of the calculation. The behavior of the alcohol is computed assuming that the alcohol distributes itself between the micelle and the water. For the alcohol with n carbon-to-carbon bonds $\rho_n \propto \exp(n \ln 3)$ is the value Shinoda used. He again got quantitative agreement between theory and experiment.

In summary, the phenomena of solubility, critical micelle concentration as a function of chain length and added alcohol, and distribution ratio studies all exhibit the same approximate "rule of three" which can be explained theoretically by a model which allows pseudo-degenerate torsional oscillation in any liquid organic phase but which only permits torsional oscillation in a single configuration in the aqueous phase.

B. Review of the Application to the Entropy of Fusion of Long Chain Hydrocarbon Compounds.—The carbon–carbon bond in the solid state behaves as a torsional oscillator while in the liquid state it behaves as a pseudo-degenerate torsional oscillator. Thus, using s subscripts for solid and l for liquid

$$Z_s = \psi_s \left(\sum_j e^{-\epsilon_j/kT} \right)^{nN}$$

$$Z_l = \psi_l \left(\sum_i 3e^{-\langle \epsilon_i \rangle/kT} \right)^{nN}$$

Recalling the definition of entropy

$$S = \frac{-\partial}{\partial T}(-kT \ln Z)$$

we get for the entropy of fusion of an n-chain molecule $\Delta S_n = S_l - S_s$, per mole

$$\Delta S_n = \frac{-\partial}{\partial T}\left(-kT \ln \frac{Z_l}{Z_s}\right) \qquad (10)$$

$$\Delta S_n = \frac{\partial}{\partial T}\left(kT \ln \frac{\psi_l}{\psi_s}\right) +$$

$$\frac{\partial}{\partial T}\left(nNkT \ln \frac{\sum_i 3e^{-\langle \epsilon_i \rangle/kT}}{\sum_j e^{-\epsilon_j/kT}} \right) \qquad (11)$$

The first term is assumed to be a constant independent of n. If each bond of two molecules neighboring in the homologous series contributes approximately the same amount to that part of the partition function which is independent of chain length, then $\Delta(\Delta S) = \Delta S_n - \Delta S_{n-1}$ becomes

$$\Delta(\Delta S) \approx \frac{\partial}{\partial T}\left(NkT \ln \frac{\sum_i 3e^{-\langle \epsilon_i \rangle/kT}}{\sum_j e^{-\epsilon_j/kT}} \right) = Nk \ln 3 +$$

$$\frac{\partial}{\partial T} NkT \ln \left(\sum_i e^{-\langle \epsilon_i \rangle/kT} \Big/ \sum_j e^{-\epsilon_j/kT} \right) \qquad (12)$$

The second term which is temperature dependent is comparatively small. It has a value which can be explained in terms of excitation energy levels above the lowest rotational level which can occur at the melting temperatures of these long chain compounds. This theory is in good agreement with observation for even numbered n.[3a] If the entropy of the solid state transition of odd n molecules is included in the analysis these molecules also give good agreement.

C. Review of the Application to the Theoretical Derivation of Traube's Rule.—Traube's Rule is often stated in the following way: The concentration of the members of the homologous series required to achieve equal surface tension lowering of the aqueous solution diminishes about threefold for each CH_2 group added to the chain. Langmuir[11] showed that the rule could be expressed as

$$\lambda_n - \lambda_{n-1} \cong kT \ln 3 \qquad (13)$$

where $\lambda_n - \lambda_{n-1}$ = work required to bring one CH_2 group from the interior to the surface. Calling $F_l(n)$ the free energy of an n-chain molecule in the solution, $F_s(n)$ the free energy on the surface

$$\Delta F(n) = F_s(n) - F_l(n) \text{ and } \Delta(\Delta F) = \Delta F(n) - \Delta F(n-1)$$
$$\Delta(\Delta F) \cong -kT \ln 3 \text{ (per molecule)} \qquad (14)$$

This rule may be statistically derived[3b]

(10) M. L. Corrin and W. D. Harkins, *J. Am. Chem. Soc.*, **69**, 683 (1947).

(11) I. Langmuir, *ibid.*, **38**, 1948 (1917).

$$F_s(n) = -kT\left[\ln\left(\sum_i 3e^{-(\epsilon i)/kT}\right)^n + \ln\psi_s\right]$$

$$F_l(n) = -kT\left[\ln\left(\sum_i e^{-\epsilon i/kT}\right)^n + \ln\psi_l\right] \quad (15)$$

Hence per molecule

$$\Delta(\Delta F) \cong -kT\ln 3 + \delta \quad (16)$$

δ is a small correction term which arises from the ψ_s and ψ_l contributions as well as excitation to higher energy levels. The contribution to $\Delta(\Delta F)$ from these terms is expected to be much smaller than kT ln 3.

Traube's rule may also be considered as a special case of the distribution ratio rule

$$\rho_n = \frac{C_{\text{surface}}(n)}{C_{\text{solution}}(n)}$$

For equal lowering of surace tension, $C_{\text{surface}}(n) = C_{\text{surface}}(n-1)$.

Then

$$\frac{\rho_n}{\rho_{n-1}} = \frac{C_{\text{soln}}(n-1)}{C_{\text{soln}}(n)} = 3 \text{ (experimentally)} = 3\text{(by the ratio rule)} \quad (17)$$

Positive deviations from Traube's rule have been attributed to excitation to higher energy levels. Traube's Rule also applies to perfluoro and ω-hydroperfluorocarboxylic acids in which CH_2 groups are replaced by CF_2 groups.

IV. Application to Biology

An example of the application of our model to biology is a phenomena sometimes known as Ferguson's rule for the effect of narcotics as a function of chain length. An example of this rule is the effect of alcohols on tadpoles.[12] The concentration of alcohol in the aqueous region which just stops tadpole motion is known as, the "limiting concentration." Ferguson's rule states that the limiting concentration decreases threefold with each additional CH_2 group added. We may now interpret this rule as an example of the *distribution ratio rule*. The given limiting concentrations in the aqueous region all correspond according to the rule to just one concentration of the hydroxyl group within an organic region of the tadpole. Since the narcotic effect depends on the hydroxyl group our interpretation is reasonable and consistent. The argument that the effect is one of equal lowering of surface tension is countered when it is demonstrated that straight chain amines have no narcotic action (no inhibitory action dependent on chain length). Since the *surface* effects of amines follow the same behavior as alcohols the narcotic action cannot be a surface effect.

The application of the rule of three resulting from our theory leads to the conclusion that the narcotic action must be taking place in an organic liquid region.

We feel that other examples of the importance of carbon–carbon bond behavior in biological processes will undoubtedly be demonstrated in the future.

(12) Otto Warburg, "Heavy Metal Prosthetic Groups and Enzyme Action," Tr. by Alexander Lawson, Oxford, Clarendon Press 1949, p. 7, F. H. Johnson, H. Eyring and M. J. Polissar, "The Kinetic Basis of Molecular Biology," John Wiley and Sons, New York, N. Y., 1954, p. 429–432.

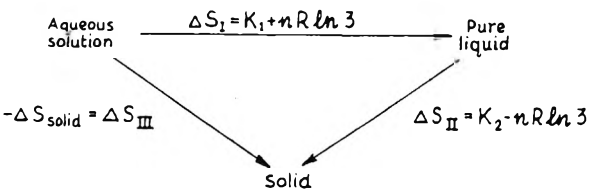

Fig. 2.—Cycle to demonstrate effect of chain length on heat of solution.

V. Further Application to Physico-chemical Behavior

The model of the carbon-to-carbon bond in aqueous solution is roughly the same as that in the solid state. Hence we would expect the homologous series in water (dissolved from the solid state) to act as a special class of non-ideal solution.

For ideal solutions (two components)

$$\frac{\mathrm{d}\ln N_1}{\mathrm{d}T} = \frac{\Delta H_{f_1}}{RT^2} = \frac{\Delta S_{f_1}}{RT} \quad (18)$$

where N_1 = mole fraction of the solute and ΔH_{f_1} molar heat of fusion of the pure solute.

Since the long chain compounds gain internal freedom when they melt but do not gain this freedom when they go into aqueous solution we expect these compounds to follow the equation

$$\frac{\mathrm{d}\ln N_1}{\mathrm{d}T} = \frac{\Delta H_{\text{soln}}}{RT^2} = \frac{\Delta S_{\text{soln}}}{RT} \quad (19)$$

where ΔH_{soln} corresponds to the heat required to bring a mole of the solute from the crystal into aqueous solution without "internal melting." Our prediction based on our model is that ΔH_{soln} will be almost independent of chain length. A direct test of this prediction has not yet been made. But a special test can be applied. Consider the following system at equilibrium at the melting point of the solute system: pure crystalline molecules, pure liquid molecules and aqueous solution of the molecules.

For this system the entropy of fusion study shows that the entropy per bond gained upon bringing a mole from the crystal to the pure liquid is approximately R ln 3. From the distribution ratio rule this entropy per bond is lost when the liquid molecule goes into aqueous solution. Hence when a mole of material is brought from the aqueous region into the crystalline state the entropy change should be approximately independent of chain length.

The cycle is illustrated in Fig. 2. Since the different molecules are compared at different temperatures a small temperature dependence for ΔS_{III} should be observed. This temperature dependence will be indirectly a function of n through the relationship between the melting point and n. (Note $\Delta S_{III} = -\Delta S_{\text{soln}}$ as the process of solution is considered a reverse of the process in the diagram; *i.e.*, $\Delta S_{III} = \Delta S$ of crystallization from aqueous solution.) Careful freezing point studies should confirm our predictions and illustrate that the homologous series form a special class of nonideal solutions.

VI. Summary

The diverse phenomena of entropy of fusion, Traube's Rule of surface tension, solubility of liquid hydrocarbons, distribution ratio of long chain hy-

drocarbons and critical micelle concentration as a function of chain length and of added alcohol can all be unified by a model of CH_2 group behavior which permits pseudo-degenerate torsional oscillation in organic media and on aqueous surfaces but which requires one preferred configuration for torsional oscillation in the solid and in aqueous media.

It may be argued that the factor 3 is a coincidence and could be caused primarily by changes in the behavior of water associated with the introduction of CH_2 groups; however the phenomena of entropy of fusion is independent of the presence of water. Against the argument that the factor 3 is probably inherent in the energetic behavior (internal and external) of the CH_2 group only and not a result of the effect of the geometry of the molecule on torsional oscillation is the fact that Traube's rule is obeyed by the CF_2 group. This group has a geometry similar to the CH_2 group but has very different internal and external interaction energy. The Traube rule behavior indicates that the geometry is the determining factor. If future experiments demonstrate that the "rule of three" also holds for entropy of fusion of long chain fluorocarbons and that the solubility of liquid long chain fluorocarbons in water goes down by a factor of three for each CF_2 added, we will have much stronger evidence for believing that the geometry is the deciding factor. We hope that this article will be useful in demonstrating the unity underlying various seemingly unrelated examples of the physical behavior of hydrocarbons and that the mechanism proposed to explain this unity will be subjected to further analysis and experimental test.

Basic in our interpretation of the various physical effects correlated in this paper is that the free energy changes involved have an origin in entropy considerations and do not arise from changes in potential energy. Many of our colleagues have argued that even if the effects are primarily entropy effects, the origin of the entropy effects lies not in the changing behavior of the hydrocarbon molecules but rather in the changed behavior of water molecules in the presence of a hydrocarbon molecule. Namely, it is argued, that immediately near a hydrocarbon chain water acquires an ordered ice-like structure.[13] When the hydrocarbon chain is removed water loses this ordered arrangement and becomes a randomly arranged liquid with a corresponding increase in entropy. Since all of the effects we mention except the entropy of fusion involve water, they can all be explained in this alternate fashion. The entropy of fusion, it is generally agreed, does have the origin we ascribe to it; it is according to this second view, a pure coincidence that the entropy increase per CH_2 group which is approximately R ln 3 for fusion is also approximately R ln 3 for the aqueous cases. It seems to us crucial to resolve experimentally the issue regarding the two alternate explanations.

(13) H. S. Frank and M. W. Evans, *J. Chem. Phys.*, **13**, 276 (1945).

FLASH PHOTOLYSIS OF CARBON DISULFIDE AND ITS PHOTOCHEMICALLY INITIATED OXIDATION[1]

BY FRANKLIN J. WRIGHT

Central Basic Research Laboratory, Esso Research and Engineering Company, Linden, New Jersey

Received April 13, 1960

The absorption spectrum taken a few milliseconds after flash photolysis of gaseous CS_2 under isothermal conditions at 20° shows characteristic bands due to CS and S_2. The disappearance of S_2 is rapid and follows second-order kinetics. The rate constant of this reaction has been measured in terms of the unknown extinction coefficients of S_2 at 2712 and 2662 Å. It was found to be independent of inert gas pressure over a 350-fold range and to be unaffected by the presence of oxygen. The removal of CS has been shown to be a heterogeneous process occurring at the walls of the reaction vessel. A slowly growing continuous absorption was also observed. The waxing and waning of this continuum as well as its wave length dependence was studied as a function of time at three inert gas pressures in the range 50 to 400 mm. The origin of this continuous absorption is to be found in the sulfur sol formed through the condensation of sulfur to solid particles. The usual coagulation equation for homogeneous aerosols has been shown to apply to this condensation process. Flash photolysis of CS_2 under isothermal conditions in the presence of oxygen results in the appearance of the spectrum of SO_2 and of that now ascribed to S_2O. The addition of oxygen was found to decrease the amount of S_2 formed but to have no appreciable effect on its rate of disappearance.

The absorption spectrum taken a few milliseconds after illumination of gaseous carbon disulfide by a high intensity flash shows the characteristic bands of S_2 and CS.[2] The lifetimes of these two species are greatly different; whereas S_2 disappears in a matter of a few milliseconds, the spectrum of CS remains visible for several minutes.[2b] Flash photolysis of CS_2 under isothermal conditions offers, therefore, a convenient way of obtaining sulfur radicals in a relatively simple environment.

This paper describes a preliminary study of sulfur radicals both in the presence and in the absence of oxygen. The work was carried out several years ago but only recently has the identity of one of the principal intermediate spectra—that now assigned to S_2O—been established.

Experimental

The apparatus used for this work was essentially the same as that used in previous investigations.[3-6] The absorption spectra were recorded photographically using a Hilger E 1 spectrograph.

(1) This work was carried out at the Physical Chemistry Department, University of Cambridge.

(2) (a) R. G. W. Norrish and G. Porter, *Proc. Roy. Soc.* (*London*) **A200**, 284 (1950); (b) G. Porter, *Disc. Faraday Soc.*, **9**, 60 (1950).

The deposition of solid sulfur on the walls of the reaction vessel caused clouding of the windows and reduced the effective intensity of the photolyzing light. Since each point on a decay curve represents a separate experiment, such variation in light intensity could not be tolerated. In order to obtain reproducible results, it was necessary to clean the quartz reaction tube between each run by burning away the sulfur and the CS polymer. Also, the amount of deposit was kept to a minimum by using small quantities of carbon disulfide usually *ca.* 0.2 mm.

Intensity Measurements.—The spectrum of S_2 shows diffuse bands attributed by Henri[7] to predissociation and microdensitometer readings can therefore be related to concentrations in the same way as for a continuous spectrum. In order to be able to compare intensities of spectra obtained on different photographic plates, each plate was calibrated separately using the continuous absorption of methyl ethyl ketone as a standard.

This technique could not be used for CS which has a discrete spectrum imperfectly resolved by the spectrograph used. The disappearance of the CS radical had therefore to be studied by comparing the times taken for the CS bands to decrease from one standard intensity to another as observed by visual examination. In spite of interference by a continuous absorption superimposed on the CS spectrum, such matching of intensities could be done with satisfactory accuracy using a comparator which balanced the background intensities. A relationship between the concentration of CS and apparent intensity was also obtained by the two-path method.[8]

Results and Discussion

Identification of the Spectra and their Occurrence as a Function of Time. 1. CS.—The radical CS is readily identified by the band heads at 2576 Å. (0,0), 2507 Å. (1,0) and 2445 Å. (2,0). Under our experimental conditions, using a reaction vessel 2 cm. in diameter, CS has a lifetime of the order of 2 minutes. It can readily be calculated that such a rate of disappearance is too slow to be rate determined by diffusion of a molecular species to the walls. Further confirmation of this was obtained from the effect of inert gas pressure on CS disappearance. This was studied by measuring the times t_1 and t_2 taken for the strong (0,0) band at 2576 Å. to decrease from one standard intensity I_1 to another I_2 and also from intensity I_2 to intensity I_3. These intensities were matched visually using an optical comparator. The significance of any errors in the measurements was largely eliminated by covering a wide range of pressures. Table I clearly shows the rate of removal to be constant to within a factor of 2, whilst the pressure was varied over a 300-fold range. The accuracy of the measurements was not sufficient, however, to enable the order of the reaction with respect to [CS] to be determined.

Since the rate of CS disappearance is independent of inert gas pressure, it is evident that the controlling rate is not the rate of diffusion to the walls but that it must be the rate of the reaction occurring at the walls. Additional evidence in support of this view was obtained from the observation that the rate of CS decay is independent of the amount of sulfur formed and, as shown below, is unaffected by oxygen. The conclusion that the removal of CS is a heterogeneous process and that no condensation or reaction with sulfur occurs in the gas phase is in agreement with the findings of Jakovleva and Kondratiev[9] and of Dyne and Ramsay.[10]

TABLE I

EFFECT OF INERT GAS PRESSURE ON THE DISAPPEARANCE OF CS

$P(CO_2)$, mm.	t_1, sec.	t_2, sec.
1	40	40
10	40	40
50	45	35
150	20	40
300	30	50

2. S_2.—S_2 has a well-known spectrum in the region 2530–3100 Å., consisting of a very extensive system of regularly spaced bands with heads degraded to the red. Measurement of the S_2 concentrations was not very accurate owing to the uncertainty of the correction for the continuous absorption which also appeared in the S_2 spectral region. Yet in spite of this difficulty, it was established that the formation of S_2 took place completely during the photolysis flash and that the disappearance of S_2 could be best described by second-order kinetics. Thus

$$-\mathrm{d}[S_2]/\mathrm{d}t = k[S_2]^2$$

If k_1 and k_2 are defined by the equations

$$-\mathrm{d}([S_2]\epsilon_{2712})/\mathrm{d}t = k_1([S_2]\epsilon_{2712})^2$$

and

$$-\mathrm{d}[(S_2]\epsilon_{2662})/\mathrm{d}t = k_2([S_2]\epsilon_{2662})^2$$

where ϵ_{2712} and ϵ_{2662} are the molar decadic extinction coefficients for S_2 at 2712 and 2662 Å., respectively, then the value of k_1 and k_2 can be obtained from the gradient of plots of $1/[S_2]\epsilon_{2712}$ and $1/[S_2]\epsilon_{2662}$ against time.

The absolute rate constant is given by

$$k = k_1\epsilon_{2712}\ \mathrm{mm.^{-1}\ sec.^{-1}} = k_2\epsilon_{2662}\ \mathrm{mm.^{-1}\ sec.^{-1}}$$

or

$$k = 1.70 \times 10^4\, k_1\epsilon_{2712}\ \mathrm{l.\ mole^{-1}\ sec.^{-1}} = 1.70 \times 10^4\, k_2\epsilon_{2662}\ \mathrm{l.\ mole^{-1}\ sec.^{-1}}$$

Since, however, the extinction coefficients ϵ_{2712} and ϵ_{2662} are unknown, it is not possible to express the rate k in absolute units.

Table II shows that over a 300-fold range, the rate of S_2 disappearance is independent of the total inert gas pressure. The slightly higher values at 1 mm. of CO_2 may be a result of the fact that at such a low inert gas pressure conditions probably are no longer isothermal.

3. Continuous Absorption.—The spectrum of sulfur is well-known at high temperatures where the absorption is almost entirely due to S_2. Little information is, however, available about the sulfur vapor spectrum at temperatures below 300°. Henri[7] described it as being continuous and Bass[11] found that in the range of 150° to 250°, the absorption spectrum of sulfur evidenced unresolved maxima at 2100, 2550 and 2850 Å. These were

(3) G. Porter and F. J. Wright, *ibid.*, **14**, 23 (1953).

(4) G. Porter and F. J. Wright, *Z. Elektrochem.*, **56**, 782 (1952).

(5) G. Porter and F. J. Wright, *Trans. Faraday Soc.*, **10**, 1205 (1955).

(6) G. Porter and F. J. Wright, *ibid.*, **11**, 1469 (1955).

(7) V. Henri, "Structure des Molecules." Hoffman, Paris, 1928.

(8) R. G. W. Norrish, G. Porter and B. A. Thrush, *Proc. Roy. Soc.* (*London*), **A216**, 165 (1953).

(9) A. Jakovleva and V. Kondratiev, *Acta Physicochim., U.R.S.S.* **13**, 241 (1940).

(10) P. J. Dyne and D. A. Ramsay, *J. Chem. Phys.*, **20**, 1055 (1952).

(11) A. M. Bass, *ibid.*, **21**, 80 (1953).

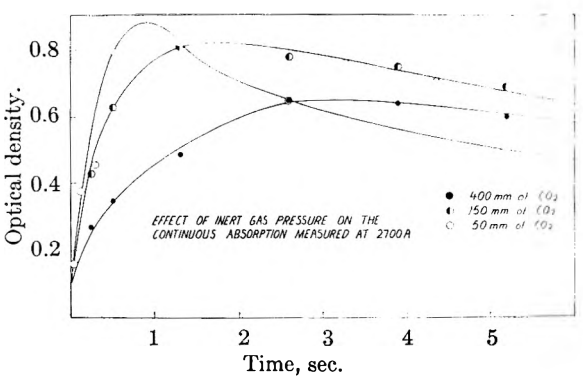

Fig. 1.—Effect of inert gas pressure on the continuous absorption measured at 2700 Å.

TABLE II

EFFECT OF INERT GAS PRESSURE ON THE RATE OF DISAPPEARANCE OF S_2

$P(CO_2)$, mm.	$k_1 \times \epsilon_{2712}$, Å.[a]	$k_2 \times \epsilon_{2662}$, Å.[a]
1	9.0	6.8
10	4.0	3.9
40	5.7	5.0
150	6.4	4.6
350	4.7	4.6

[a] k_1 and k_2 are measured in mm.$^{-1}$ sec.$^{-1}$ ϵ_{2712} units^{-1} and m.$^{-1}$ sec.$^{-1}$ ϵ_{2662} units^{-1}, respectively, where ϵ_{2712} and ϵ_{2662} are the extinction coefficients of S_2 at 2712 and 2662 Å.

assumed to be due to the presence of S_8 rings. Vapor density measurements indicated that besides S_2 and S_8, another species—possibly S_6—may also be present in the vapor phase.

The continuous absorption which could be observed in our system was, therefore, studied with some care in an attempt to obtain evidence for the existence of these various species.

Origin of the Continuum.—The observed continuum may result from many causes. On closer analysis, however, several of these can be ruled out. A consideration of the persistence of the continuum precludes hot CS_2 as being responsible for it. Polymers of CS can also be disregarded, since the continuum reaches its peak intensity in a time during which no decrease in CS concentration is observed. Only sulfur therefore needs to be considered as the progenitor of the continuum and from the evidence which will be presented later, it seems likely that it is in fact solid sulfur particles which are responsible for it.

Effect of Inert Gas Pressure on the Continuum.—The growth and decay of the continuous absorption measured at 2700 Å. was studied as a function of inert gas pressure and are represented graphically in Fig. 1.

The coagulation equation for a homogeneous aerosol may be written as

$$-dn/dt = kn^2$$

or

$$kt = 1/n - 1/n_0$$

where n and n_0 are the number of particles per cm.^{3} at time t and zero time and k is a constant.[12] This equation has been shown to apply to a large number of coagulating smokes. It was also found to apply to our system at the three pressures studied. (See Appendix.)

As evidenced in Fig. 1, both the rate and the decay increase as the inert gas pressure is decreased. This might be expected since both the growth and the removal of the sulfur particles through settling on the walls of the reaction vessel are diffusion controlled processes which are inversely proportional to the pressure. There is, however, another possible explanation for the change of appearance of the three curves in Fig. 1.

It has been shown[13] that a change in the size distribution can produce a characteristic change in the shape of the optical density/time relationship if the rate of coagulation is not appreciably altered by a change in size distribution. When the particle size range is small, the optical density/time curve is peaked and sharply defined. When the size range is large, the curve tends to be flat-topped with long periods in which there is little or no change in the optical density. It would appear, therefore, that the changes in the shape of the curves reproduced in Fig. 1 lie in the homogeneity of the sol. The higher the inert gas pressure, the less homogeneous is the sol produced. Electron microscope photographs of the solid sulfur particles taken from the walls of the reaction vessel showed them to be 0.5 to 0.6 μ in size but did not enable any conclusions to be reached about the homogeneity of the sol.

Wave Length Dependence of the Continuum.—The wave length dependence of the continuous absorption as a function of time has also been studied and is illustrated in Fig. 2. These curves show a general absorption which decreases with time. Superimposed on this is a maximum which takes approximately 10 seconds to reach its peak value and then slowly decreases.

For a system of uniformly distributed isotropic spherical particles which have a diameter less than one tenth of the wave length of the incident light, the intensity of the scattered light is proportional to the inverse fourth power of the wave length. When the system consists of steadily growing particles, the observed scattering is however more complex especially if the particles also absorb light as is the case for sulfur sol. This problem has been fully treated by LaMer and his colleagues.[14,15] Curves they have reported for mono-dispersed sulfur sols in water exhibit the same general structure as the ones shown in Fig. 2.

They showed that the complexity of such transmittance curves and their rapid change with time resulted from several causes, *inter alia*, the general scattering by the sulfur particles, molecular absorption when the sol had a radius less than 0.3 μ, the size and homogeneity of the sol.

The change with time in the nature of the transmittance curves shown in Fig. 2 can thus be visualized to result from a sequence of events such as the following.

In the early stages, small particles are present

(12) R. Whytlaw-Gray and H. S. Patterson, "Smoke," Arnold and Company, London, 1932, pp. 57–72.

(13) D. W. E. Axford, K. F. Sawyer and T. M. Sugden, *Proc. Roy. Soc.* (*London*), *A***195**, 13 (1948).

(14) M. D. Barnes and V. K. LaMer, *J. Colloid Sci.*, **1**, 79 (1946).

(15) M. D. Barnes, A. S. Kenyon, E. M. Zaiser and V. K. LaMer, *ibid.*, **2**, 349 (1947).

in the system, and these give rise to a general scattering on which the weak absorption due to S_8 may well be superimposed. As the particles grow in size, a maximum appears on the transmittance curve. Simultaneously with this process of coagulation, diffusion and gravitational settling of the particles on the walls of the reaction vessel also occur. Since the largest and heaviest particles might well be expected to be removed from the gas phase preferentially, the maximum on the absorption curve would tend to disappear with time. This is in fact which is observed.

Photolysis of Carbon Disulfide in the Presence of Oxygen.—When CS_2 is flash photolyzed in the presence of oxygen, a strong system of absorption bands is observed between 2500 and 3400 Å. This spectrum resembles in all respects the one reported by Jones[16] and attributed by him and others[17-19] to Schenck's sulfur monoxide S_2O_2. This interpretation, however, has often been questioned.[20-22] Recently on the basis of mass spectroscopic evidence, Meschi and Myers[23] concluded that disulfur monoxide S_2O was in fact the major constituent of Schenck's compound. In view of these findings, the system that we observed is therefore assigned to S_2O. Table III shows the effect of adding increasing amounts of O_2 to a mixture of CS_2 and CO_2 on the appearance of the S_2O and SO_2 spectra.

TABLE III

$P(CS_2)$, mm.	$P(O_2)$, mm.	$P(CO_2)$, mm.	
0.2	0.1	150	S_2O
.2	5.0	145	S_2O
.2	25.0	125	$S_2O + SO_2$
.2	50.0	100	SO_2
.2	150.0	0	SO_2

The striking fact to be observed from the above table is that a very large excess of oxygen is required before SO_2 becomes the only observable product.

Effect of Oxygen on the Formation and Disappearance of CS.—The amount of CS observable 1 msec. after the photolysis flash was found to decrease as the pressure of oxygen is increased. This was confirmed by recording on the same photographic plate the CS spectrum obtained by flashing mixtures containing 0.2 mm. and 5 mm. of oxygen. Using the two-path technique, it was also determined that the presence of oxygen reduces the amount of CS formed to less than half.

The rate of removal of CS is constant within a factor of two over a 25-fold range of oxygen pressure. This indicates that CS does not react with molecular oxygen in the gaseous phase. Whether CS or its polymer slowly oxidizes heterogeneously on the walls on the reaction vessel, it has not been possible to ascertain.

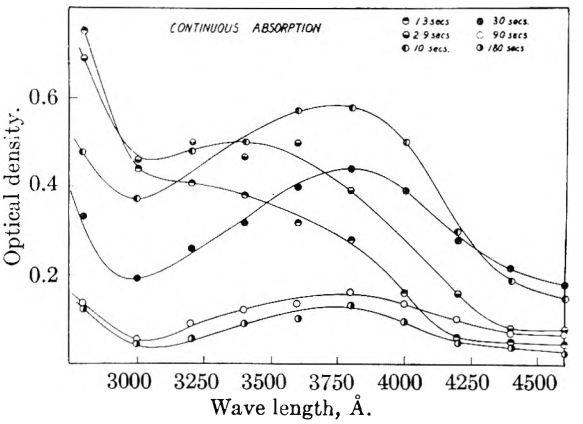

Fig. 2.—Effect of time on the wave length dependence of the continuous absorption.

Effect of Oxygen on the Formation and Disappearance of S_2.—The addition of oxygen greatly affects the formation of S_2. The presence of approximately 1 mm. of oxygen in a mixture containing 0.2 mm. of CS_2 diluted with 150 mm. of carbon dioxide, completely eliminates the S_2 spectrum even at the shortest time. It is consequently difficult to determine the effect of oxygen on the rate of disappearance of S_2 as only a very limited range of concentrations is available. However, using a mixture of 0.2 mm. of CS_2, 0.2 mm. of O_2 and 150 mm. of CO_2, the bimolecular rate constant of disappearance of S_2 was found to be the same, within experimental error, as that obtained in the absence of oxygen.

Photolysis of Carbon Disulfide in the Presence of Sulfur Dioxide.—When carbon disulfide is flash photolyzed in the presence of sulfur dioxide, S_2O is formed. This suggests that the S_2O obtained in the photolysis of carbon disulfide in the presence of oxygen might be formed *via* SO_2. Whilst it is true that in these experiments no SO_2 is observed unless a very large excess of oxygen is present, this fact does not eliminate the possibility that a small amount of it might nevertheless be formed since the absorption coefficient of S_2O is between 10 and 100 times greater than that of SO_2. The possibility that SO_2 might be the intermediate was therefore further tested. To a mixture of 0.2 mm. of CS_2 diluted with 150 mm. of CO_2, 0.05 mm. of SO_2 was added. The concentration of SO_2 was such that its spectrum was only just visible. On photolysis, this mixture yielded S_2O but the amount was considerably less than that obtained with an identical mixture containing an amount of oxygen equivalent to the oxygen in the SO_2. This clearly shows that in order to produce S_2O in the concentrations usually encountered in experiments with large amounts of oxygen, SO_2 would be visible if it were the intermediate.

The Role of Oxygen.—The experimental data indicate that neither S_2 nor CS react to any appreciable extent with molecular oxygen or with S_2O. It must perforce be concluded that S_2O is formed *via* S atoms. This view is fully supported by the observation that the presence of oxygen reduces

(16) A. Vallance Jones, *J. Chem. Phys.*, **18**, 1263 (1950).
(17) P. W. Schenk, *Z. anorg. allgem. Chem.*, **211**, 150 (1933).
(18) H. Cordes, *Z. Physik*, **105**, 251 (1937).
(19) E. Maxted, "Modern Advances in Inorganic Chemistry," Oxford Press, London, 1947.
(20) A. L. Myerson, F. R. Taylor and P. L. Hanst, *J. Chem. Phys.*, **26**, 1309 (1957).
(21) R. G. W. Norrish and G. A. Oldershaw, *Proc. Roy. Soc. (London)*, **A249**, 498 (1959).
(22) E. Evans, A. Scott and J. Huston, *J. Am. Chem. Soc.*, **74**, 5525 (1952).
(23) D. J. Meschi and R. J. Meyers, *ibid.*, **78**, 6220 (1956).

the concentration of CS observed at the end of the flash. Since CS is formed both in the primary act

$$CS_2 \xrightarrow[h\nu]{} CS + S \qquad (1)$$

and in the secondary act

$$CS_2 + S \longrightarrow CS + S_2 \qquad (2)$$

removal of S atoms by oxygen would result in less CS being formed. The most likely reaction by which this could occur is

$$S + O_2 \longrightarrow SO + O + 6.5 \text{ kcal.}^{24} \qquad (3)$$

The fact that spectral evidence for SO was never obtained is not too surprising since all our observations were made at least 1 msec. after the end of the photolysis flash when the SO concentration might be expected to be low.

Even the complete suppression of reaction 2 by the successful competition of reaction 3 would account for no more than a 50% reduction in the CS concentration. The presence of oxygen, however, reduces the CS concentration by more than this amount. It is therefore clear that some of the CS formed must also be removed directly. Moreover, this must occur *via* a reaction with a species which is present only during the photolysis flash since no removal of CS is observed afterwards. Reactions 4 and 5 would fulfill these requirements.

$$CS + SO \longrightarrow CO + S_2 \qquad (4)$$
$$CS + O \longrightarrow COS \qquad (5)$$

It is possible for S_2O to be formed from SO in a number of ways

$$SO + CS_2 \longrightarrow CS + S_2O \qquad (6)$$
$$SO + S_2 \longrightarrow S + S_2O \qquad (7)$$
$$SO + S \longrightarrow S_2O \qquad (8)$$
$$SO + SO \longrightarrow S_2O + O \qquad (9)$$

On a statistical basis, reaction 6 is to be favored.

In order to account for the replacement of S_2O by SO_2 at the higher oxygen pressures it must be presumed that reaction 10 successfully competes

$$SO + O_2 \longrightarrow CS + O \qquad (10)$$

with reaction 6 when the oxygen partial pressure is sufficiently high.

The oxygen atoms resulting from reactions 6, 9 or 10 are also capable of reacting with CS_2

$$CS_2 + O \longrightarrow CO + S_2 + 70 \text{ kcal.} \qquad (11)$$
$$CS_2 + O \longrightarrow COS + S + 47 \text{ kcal.} \qquad (12)$$
$$CS_2 + O \longrightarrow CS + SO + 19 \text{ kcal.} \qquad (13)$$

Of these, 12 is probably to be favored. It is unlikely that 11 will occur to any great extent since it involves the breaking of two CS bonds, whereas only one is involved in the other two reactions. Also since the strength of the CO bond in COS is greater than that of the SO bond (148 and 123.5 kcal., respectively), the activation energy of 12 might be expected to be lower than that of 13.

In its turn COS can further react with O.

$$COS + O \longrightarrow CO + SO + 47.5 \text{ kcal.} \qquad (14)$$
$$COS + O \longrightarrow CO_2 + S + 51 \text{ kcal.} \qquad (15)$$

(24) Based on a dissociation energy for SO of 123.5 kcal.

Acknowledgment.—The work reported in the present communication was supported by a grant from the Department of Scientific and Industrial Research. The author would like to offer his sincere thanks to Professor G. Porter F.R.S. for his continuous help and encouragement and for many suggestions.

Appendix

Using LaMer's data, Axford, Sawyer and Sugden[13] have constructed curves showing the relative scattering as a function of the diameter and refractive index m of the scattering particles. For sulfur m can be taken as 2. By combining this optical density/particle size curve with the experimentally obtained optical density/time curves (Fig. 1), it is possible to construct particle diameter/time curves. Moreover the number of particles per cc. n, having a diameter d can be calculated from the relationship

$$n = 6W/\pi\rho d^3$$

where W is the concentration of sulfur in g./cc. and ρ the density of the sulfur particle (taken as 2 g./cc.).

The concentration W was obtained in the following way. A mixture of 0.2 mm. of CS_2 and 150 mm. of CO_2 was photolyzed by means of a 2100 J flash. After the mixture had been allowed to stand for several hours in order to allow complete settling of the solid sulfur and CS on the walls of the reaction vessel, the CO_2 and unreacted CS_2 were slowly pumped out of the system and replaced by O_2. The whole of the reaction vessel was then thoroughly heated by means of a hand torch in order to burn all the sulfur to SO_2. When the vessel had cooled down to room temperature, the absorption spectrum of the SO_2 so formed was recorded and the photographic plate calibrated with known amounts of SO_2. Two independent measurements which agreed to within 10% showed that 20% of the CS_2 had been decomposed resulting in a concentration of elemental sulfur of 0.75×10^{-7} g./cc. In the calculation, it was assumed that the CS (or CS polymer) had also been completely burnt to SO_2.

Plots of $1/n$ against time were thus obtained at 50, 150 and 400 mm. of CO_2. In each case a straight line was obtained, demonstrating the applicability of the coagulation equation to our system.

THE BASICITY OF AMINO ACIDS IN D_2O[1]

BY H. H. HYMAN, ARLENE KAGANOVE AND J. J. KATZ

Argonne National Laboratory, Argonne, Illinois

Received April 14, 1960

The basicity of a number of amino acids in D_2O has been measured by a spectrophotometric method. For simple amino acids, the apparent ionization constant is approximately 0.5 pK unit higher in D_2O than in H_2O.

One by-product of the nuclear energy program has been the availability of heavy water in essentially unlimited quantities at moderate cost. This has stimulated a good deal of research, particularly in biological systems where there are important qualitative differences between ordinary and heavy water.[2] The striking differences which show up in these biological experiments are believed to be the cumulative effects of many quantitative differences which may be unraveled *in vitro*. The general problem of acid–base interaction is of major importance in studying biological systems. The changes in equilibrium constants that occur when deuterium ion transfer is substituted for proton transfer may be measured in relatively simple experiments and seem to be important in understanding more complicated phenomena.

A simple case of interest is the ionization constant of an amino acid. The acid ionization is usually representated as an equilibrium involving a cation and a dipolar ion.

$$^+H_3NRCOOH + H_2O \rightleftharpoons {}^+H_3NRCOO^- + H_3O^+$$

While data have been tabulated for many amino acids in H_2O,[3] measurements in D_2O are very limited.

Schwarzenbach, Epprecht and Erlenmeyer[4] studied the ionization constants of a number of weak acids in D_2O, and included glycine (H_2NCH_2COOH). They used a deuterium gas electrode, a light-water saturated calomel electrode, and obtained 2.752 for the pK of glycine in 99.6% D_2O as compared with 2.350 for an analogous measurement in H_2O.

The ionization of weak acids in D_2O was discussed by Schwarzenbach[5] and Rule and LaMer[6] who objected to liquid junctions in the cells chosen by Schwarzenbach. There appears to have been no study of amino acid basicity constants since larger quantities of D_2O became available, and macro techniques could be employed. While electrode measurements have been most frequently employed for determination of basicity constants, indicator methods using modern spectrophotometry are capable of comparable precision. While there are uncertainties in the interpretation of any acid strength measurement in both H_2O and D_2O, it was decided to investigate a few amino acid systems by an indicator method.

Experimental

The experimental procedure employed followed the classical procedure described by Sorensen.[7] The pH of an amino acid–mineral acid mixture is measured by means of an indicator. The concentration of hydrogen ions corresponding to the indicator color is assumed to be the concentration of strong acid which would produce the same indicator spectrum. The difference between the stoichiometric concentration of strong acid in the system and the measured concentration of hydrogen ion is the concentration of amino acid in the cationic form.

In the H_2O system, pH is probably best defined as $-\log C_{H_3O^+} - \log \gamma_{\pm}$, where $\gamma_{\pm}$ is the activity coefficient appropriate to the solution. The value of the activity coefficient may be either calculated, usually from a modified Debye–Hückel equation using a reasonable estimate of ionic size, or measured for similar solutions. For measurements made at a total ionic strength of 0.11 M, $-\log \gamma_{\pm} \leqq 0.10$ and this value is used for all solutions discussed in this paper.[8] All the solutions studied were prepared by mixing stock solutions of amino acid and perchloric acid in sodium perchlorate. The sodium perchlorate concentration was 0.1 M and the perchloric acid or amino acid concentration 0.01 M, so that for all mixtures, the amino acid plus perchloric acid concentration totaled 0.01 M and the ionic strength 0.11 M.

A number of indicators were investigated. For the pH region of interest, thymol blue was found most satisfactory and the data reported were obtained with this indicator. Eastman Kodak thymol blue indicator was used without purification.

pH measurements were also made using a conventional glass electrode in both H_2O and D_2O systems. In D_2O systems, glass electrodes were conditioned by immersion for periods up to one week in D_2O buffer solutions with no change in the observed potentials. In general, the glass electrode determinations of pH agreed with the indicator values within experimental uncertainties.

The sodium perchlorate and perchloric acid were reagent grade chemicals. The amino acids were the best readily available commercial grades. All were used without additional purification. The D_2O was redistilled water available in this Laboratory containing more than 99.6 atom % deuterium. All spectrophotometric measurements reported were made using a Perkin–Elmer Spectracord in a temperature controlled room at 25°.

Observations

The apparent pH measurements for a series of mixtures of glycine and perchloric acid in a constant ionic strength solution containing sodium perchlorate are given for both H_2O and D_2O systems in Table I. As mentioned above, these data were obtained by spectrophotometric observations using thymol blue indicator. Thymol blue has an absorption maximum at 560 mμ in acid solution with a molar absorption (A_m) of 4.04×10^4 and an absorption maximum at 440 mμ in basic solutions with $A_m = 1.51 \times 10^4$. At 440 mμ, the A_m is about 6×10^3 in acid solution,

(1) Based on work performed under the auspices of the U. S. Atomic Energy Commission.

(2) J. J. Katz, H. L. Crespi, A. J. Finkel, R. J. Hasterlik, J. F. Thomson, W. Lester, Jr., W. Chorney, N. Scully, R. L. Shaffer and Sung Hwang Sun, Proceedings of Second International Conference on Peaceful Uses of Atomic Energy, Vol. 25, p. 173, 1958; J. J. Katz, H. L. Crespi, R. J. Hasterlik, J. F. Thomson and A. J. Finkel, *J. Nat. Cancer Inst.*, **18**, 641 (Mar. 1957).

(3) E. J. Cohn and J. T. Edsall, "Proteins, Amino Acids and Peptides," A. C. S. Monograph Series No. 90, Reinhold Publ. Corp., New York, N. Y., 1943.

(4) G. Schwarzenbach, A. Epprecht and H. Erlenmeyer, *Helv. chim. acta*, **19**, 1292 (1936).

(5) G. Schwarzenbach, *Z. Elektrochem.*, **44**, 46 (1938).

(6) C. K. Rule and V. K. LaMer, *J. Am. Chem. Soc.*, **60**, 1974 (1938).

(7) S. P. L. Sorensen, *Z. Biochem.*, **21**, 131 (1909).

(8) Symposium on pH Measurement, ASTM Special Technical Publication No. 190, 1956.

while the A_m for absorption at 560 mμ is well under 10^3 in basic solution. The extinction coefficients are the same in H_2O and D_2O within the precision of the measurements. For a given solution, the fraction of indicator found in the acid form based on the molar absorption at 560 mμ yields the most accurate measure of the pH.

TABLE I

APPARENT pH OF GLYCINE–PERCHLORIC ACID MIXTURE IN 0.1 M $NaClO_4$

Ratio G/A	Concn. (mole/l.) Glyc.	Acid	Apparent pH H_2O	D_2O	pD in D_2O
0	0	0.01	2.10	1.70	2.10[a]
.25	.002	.008	2.28	1.90	2.30
.667	.004	.006	2.46	2.16	2.56
1.00	.005	.005	2.57	2.33	2.73
1.667	.006	.004	2.70	2.49	2.89
2.57	.0072	.0028	3.00	2.81	3.21
4.0	.008	.002	3.16	3.07	3.47
	.01		5.6	5.6	6.0

[a] In D_2O the pD of a 0.01 M $DClO_4$ solution is assumed to equal the pH of a 0.01 M $HClO_4$ solution in H_2O.

For indicator measurements $pH \cong pK - \log C_{IH^+}/C_I$.

If the pH of a 0.1 M $NaClO_4$–0.01 M $HClO_4$ solution in H_2O is taken as 2.10, the pK for thymol blue is 1.65 and the apparent pH of a 0.1 M $NaClO_4$–0.01 M $DClO_4$ solution in D_2O is 1.70. The apparent pH of a perchloric acid solution in D_2O is 0.4 unit less than a similar solution in H_2O.

As shown in Table I, this difference decreases as the amino acid replaces perchloric acid. For a glycine–sodium perchlorate solution, with no added perchloric acid, the apparent pH is the same in H_2O and D_2O.

In solutions containing only dilute perchloric acid and sodium perchlorate, the concentration of H_3O^+ in H_2O solutions cannot differ substantially from the concentration of D_3O^+ in D_2O. In both cases the equilibrium must favor essentially complete hydrogen ion transfer to the solvent from perchloric acid. Therefore, in the pH region where this indicator is useful, the pK of thymol blue is 0.4 unit higher in D_2O than in H_2O; *i.e.*, 2.05. The pD of a D_2O solution in the acid strength region where thymol blue is useful may be taken therefore as $2.05 - \log C_{IH^+}/C_I$.

In fact, the glass electrode gives a quantitatively similar measurement. A number of other indicators show a comparable though not always identical difference between the apparent pH when comparing H_2O and D_2O solutions containing an equal concentration of strong acid.[9] To calculate the ionization constant in D_2O, therefore, the pD of any solution is taken as the apparent pH + 0.4.

Sorensen[6] used an ionization constant for the amino acids defined by the equation

$$pK_A' = pH - \log (C/(A - H^+) - 1)$$

For the experiments reported here

C is the concn. of amino acid (moles/l.)
A is the concn. of added perchloric acid (moles/l.)
H^+ is the concn. of H_3O^+ defined as 1/antilog (pH − 0.10)

It is recognized that this ionization constant will differ from the true thermodynamic ionization constant for the amino acid by a term depending on the ratio of the activity coefficients of the dipolar and cationic forms of the amino acid. In H_2O the difference between pK_A and the pK_A' determined by the Sorensen method appears to be about 0.1 unit at 0.1 M and the difference between this correction term in H_2O and D_2O must be very small indeed. Therefore no attempt was made to obtain the thermodynamic ionization constant as might be done by measurement at lower concentrations and extrapolation to infinite dilution.

Table II shows the pD of equimolar mixtures of five amino acids with perchloric acid in D_2O and the pK_A' values for these acids. The pK_A's are calculated by the method described above from measurements at a number of acid/amino acid ratios as shown in Table I for glycine.

TABLE II

IONIZATION OF SOME AMINO ACIDS IN H_2O AND D_2O AT 25°

Amino acid	pH[a] H_2O	pD[b] D_2O	pK_A'[c] H_2O	D_2O	Δ[d]
Glycine	2.57	2.73	2.24	2.78	0.54
Alanine	2.57	2.73	2.24	2.73	.49
Phenylalanine	2.53	2.65	2.02	2.56	.54
Threonine	2.55	2.66	2.10	2.59	.49
Glutamic acid	2.52	2.68	1.96	2.59	.63

[a] Concn. amino acid 0.05 M = C; Concn. $HClO_4$ 0.05 M = A; Concn. $NaClO_4$ 0.1 M; Thymol blue indicator pK = 1.65. [b] Concn. amino acid 0.05 M; Concn. $DClO_4$ 0.05 M; Concn. $NaClO_4$ 0.1 M; Thymol blue indicator pK = 2.05. [c] $pK_A' = pH - \log (C/(A - H^+) - 1)$; $H^+ = 1/\text{antilog}\ (pH - 0.10)$. [d] $\Delta = pK_A$ in $D_2O - pK_A'$ in H_2O.

Conclusions

A number of indicators commonly used for pH measurements, as well as the glass electrode, will show a lower apparent pH in D_2O solutions containing a given D_3O^+ content than in H_2O solutions containing the equivalent H_3O^+ concentration. This has been previously reported by Fischer and Potter[10] and with improved accuracy by Hart.[11] Quantitatively, the glass electrode and thymol blue indicator can be used in D_2O in the pD region near 2 by adding 0.40 to the apparent pH to determine the pD. Högfeldt and Bigeleisen[9] have extended the use of indicators in D_2O to the Hammett type used in very strong acids, *i.e.*, neutral molecules which are relatively weak proton acceptors. While they note a slight trend in favor of increasing ΔpK with decreasing acid strength of the protonated species, as predicted by Lewis and Schutz[12] and Halpern,[13] the effect is very much less than Rule and LaMer[6] believed.

Högfeldt and Bigeleisen[9] conclude that the type of acid is more important than the acid strength in so far as the difference of ionization constants between H_2O and D_2O is concerned.

For simple amino acids, the apparent ionization constant is approximately 0.5 pK unit higher in

(9) E. Högfeldt and J. Bigeleisen, *J. Am. Chem. Soc.*, **82**, 15 (1960).

(10) R. B. Fischer and R. A. Potter, MDDC-715, Sept. 1945.

(11) R. G. Hart, CRE 423, Natl. Res. Council of Canada, June 1949.

(12) G. N. Lewis and P. W. Schutz, *J. Am. Chem. Soc.*, **56**, 1913 (1934).

(13) O. Halpern, *J. Chem. Phys.*, **3**, 456 (1935).

D_2O than in H_2O. Glutamic acid has a second ionization and the slightly greater difference between pK in H_2O and D_2O may be due to a contribution from this second ionization. The difference of 0.5 pK unit is equal to the difference in pK for the ionization of acetic acid in light and heavy water. Although the pK_A for the acetic acid ionization is 4.7 rather than ~2, the proton transfer mechanism is the same for each of the amino acids as for the carboxylic acid. This is in agreement with the conclusion mentioned above that the most important single criterion in determining the difference in pK in H_2O and D_2O systems is the nature of the group to which the proton is attached.

Unfortunately, this ΔpK is so close to 0.5 for all equilibria where valid measurements exist, that a systematic study of the differences which can be attributed to the specific bonds affected seems remote.

When deuterium is substituted for hydrogen in an acid base interaction, the change in equilibrium constant measures a difference in the relative binding power of two bases for hydrogen and deuterium. There appears to be no simple way to determine how much of this difference between the two bases should be attributed to either base.

INFRARED STUDIES OF SOME COMPLEXES BETWEEN KETONES AND CALCIUM MONTMORILLONITE. CLAY-ORGANIC STUDIES. PART III[1]

BY LOWELL G. TENSMEYER,[2] REINHARD W. HOFFMANN AND G. W. BRINDLEY

Contribution No. 59-87 from the College of Mineral Industries, Dept. of Ceramic Technology, The Pennsylvania State University, University Park, Pennsylvania

Received April 20, 1960

Infrared spectra of one- and two-layer complexes of 2,5-hexanedione and 2,5,8-nonanetrione with calcium montmorillonite have been obtained by differential techniques. The samples were prepared by evaporation of clay suspensions with and without ketones on AgCl-windows and glass plates. Infrared absorption spectra and X-ray diffraction patterns were taken of the resulting films. Infrared spectra were obtained also of solutions of the ketones of CCl_4 and CS_2, of liquid 2,5-hexanedione and of solid 2,5,8-nonanetrione, the latter presented to the beam by several techniques. The following vibrational assignments are made for the unadsorbed ketones: 3005 cm.$^{-1}$ CH_3 stretching α to C=O; 2959 cm.$^{-1}$ CH_2 asymmetric stretching; 2912 cm.$^{-1}$ CH_2 symmetric stretching; 1724 cm.$^{-1}$ C=O stretching; 1412 cm.$^{-1}$ CH_2 deformation α to C=O; 1401 cm.$^{-1}$ CH_2 deformation coupled to C–C; 1365 cm.$^{-1}$ CH_3 deformation α to C=O; 1360 cm.$^{-1}$ CH_2 and CH_3 deformation α to C=O. Upon adsorption, significant changes occur in the carbonyl stretching frequency and the methyl and methylene deformation frequencies. Spectra of the one-layer complexes of 2,5-hexanedione and 2,5,8-nonanetrione are quite similar to that of solid 2,5,8-nonanetrione, whereas the two-layer complexes show less similarity. These data are interpreted in terms of a highly ordered one-layer complex and a decrease in order upon introduction of a second layer.

1. Introduction

This investigation forms part of a program for studying the adsorption of organic molecules on clay minerals. A previous paper[1] gave results for the adsorption of neutral organic molecules from aqueous solutions on calcium montmorillonite. With a view to obtaining more detailed information on the state of the adsorbed molecules this study has been made of the infrared absorption spectra of two organic–clay complexes, chosen from among the organic materials examined in the previous work.

The compounds selected were 2,5-hexanedione and 2,5,8-nonanetrione. Structurally similar to each other, they are adsorbed to differing extents on montmorillonite from aqueous solutions. The most interesting parts of their spectra, the C=O and C–H vibrations, have frequencies not obscured by the vibrations of the montmorillonite lattice.

The interaction between clay mineral surface and adsorbed organic molecules would be expected to produce frequency and intensity changes in the spectrum of the adsorbed molecule. Intensity changes may also arise from different orientations of the organic molecules on the clay surface and from different orientations of the clay particles with respect to the infrared beam. To interpret the spectra of the adsorbed molecules profitably and also to detect unadsorbed ketone in a clay–organic complex, one must have available the frequencies, frequency assignments and the extinction coefficients for the unadsorbed compound, at least for the spectral regions not obscured by infrared absorption of the clay.

Strictly considered, only the frequencies of a gas at low pressure can be considered unperturbed, especially for molecules containing highly polar bonds. The spectrum of a dilute solution of a compound in a non-polar solvent approaches that of the gas, and dilute solution spectra are used as references in the present work, as well as the spectra of liquid 2,5-hexanedione and of solid 2,5,8-nonanetrione.

2. Experimental

I. **Materials.**—(a) 2,5-Hexanedione was obtained from Aldrich Chemicals Co. and was redistilled before use; b.p. 82.2–82.7° (17 mm.).

(b) 2,5,8-Nonanetrione was prepared in this laboratory as white plate-like and prismatic crystals, m.p. 55°. (5-Methylfurfuryl)-acetone was prepared according to Alder and Schmidt.[3] The reaction was by no means spontaneous

(1) Part II. R. W. Hoffmann and G. W. Brindley, "Adsorption of Non-ionic Aliphatic Molecules from Aqueous Solutions on Montmorillonite," submitted to *Geochim. Cosmochim. Acta.*

(2) Temporary Research Fellow at the Pennsylvania State University during Summer 1959, now at Linde Company, Indianapolis, Ind.

(3) K. Alder and C. H. Schmidt, *Ber. deut. chem. Ges.*, **76B**, 183 (1943).

and the yield obtained (38%) was less than that quoted (65%). Both effects may be due to the higher hydroquinone content of the methyl vinyl ketone starting material. Attempts to saponify (5-methylfurfuryl)-acetone with HCl/CH_3OH according to Alder resulted in black tars which gave only poor yields of 2,5,8-nonanetrione. Saponification similar to that described by Benson[4] for 2,5-dimethylfurane gave satisfactory results. Forty-seven and one-half g. of (5-methylfurfuryl)-acetone, 30 ml. of H_2O, 25 ml. of acetic acid, and 1.5 ml. of 10% H_2SO_4 were refluxed for 36 hours. After adding 1.65 g. of CH_3COONa the solvent was distilled off *in vacuo*. The dried residue was digested with 200 ml. of ether and subsequently extracted in a Soxhlet apparatus with ether. From the combined ether solutions the product was precipitated by the same volume of petroleum ether and filtered off after standing overnight in a refrigerator. Including a second fraction from the mother liquor the yield of crude product was 29.5 g. (55%). Two recrystallizations from ether–petroleum ether with Norite produced 18.5 g.

(c) The preparation of the clay suspension containing 30 mg. of Ca montmorillonite per ml. has been described elsewhere.[1]

(d) All solvents used were spectral grade.

II. Spectra.—All spectra reported were obtained on a Perkin–Elmer Model 21 Infrared Spectrophotometer, using a resolution setting of 925. Mechanical and spectral slit widths for this setting at absorbed frequencies are presented in Table I. The wave length scale was expanded to 50 cm./μ when necessary for accurate wave length determinations. The instrument, using a NaCl prism, was calibrated with polystyrene film and gaseous H_2O, NH_3 and CO_2 using frequencies listed in the Perkin–Elmer Instruction Manual. Calibration wave lengths were reproducible to within 0.004 μ. The wave length drive was run very slowly, often in the range 1–2 μ/hr.

(a) **Spectra of Solutions.**—Spectra were measured using a 0.103 mm. NaCl cell against a solvent-filled 0.106 mm. NaCl cell. The solutions had the concentrations: 2,5-hexanedione: 1.305 *M* in CS_2, 0.2898, 0.1967, 0.1179 and 0.0143 *M* in CCl_4; 2,5,8-nonanetrione: 0.440 *M* in CS_2, 0.3366, 0.1757 and 0.0780 *M* in CCl_4.

(b) **Spectrum of Liquid 2,5-Hexanedione.**—The optical absorption of the carbonyl group is so intense that, for the pure liquid, a cell of 2 μ or less would be required to determine extinction coefficients. As this is impracticable, a qualitative spectrum was obtained by pressing the liquid between two NaCl-plates.

(c) **Spectra of Solid 2,5,8-nonanetrione.**—The spectra of solid 2,5,8-nonanetrione were obtained by three methods:

2,5,8-Nonanetrione was mixed with Harshaw KBr and "ground" for a definite period of 15, 25 or 120 seconds on a Wig-L-Bug amalgamator, then evacuated and pressed to 24 tons/cm.^{2} into a stainless steel disk having an oval opening of 1.18 cm.^{2}. The disc was notched for positioning in the spectrometer.[5]

In the second method, flat flakes of 2,5,8-nonanetrione were placed on a pure KBr pellet, then covered with KBr powder and pressed again in the die, leaving the "layered" 2,5,8-nonanetrione firmly fixed between KBr pellets, but perhaps with some crystal distortions.

In the third method, CCl_4 solutions were allowed to evaporate on KBr discs, presenting a "precipitated" group of small crystals to the infrared beam.

(d) **Spectra of the Clay-Organic Complexes.**—One- and two-layer complexes of the ketones with calcium montmorillonite were prepared by mixing 2 ml. of Ca montmorillonite suspension (30 mg./ml.) and 0.5 ml. of an appropriate concentrated ketone solution in water. One ml. each of the resulting suspension was dried on a glass slide (for X-ray measurement) and on a silver chloride infrared window. Teflon washers each having an open area of 3.75 cm.^{2} held the evaporating suspension and fixed the shape of the resultant film. Both samples were dried together over P_2O_5 at temperatures below 20°. To protect the sample from atmospheric moisture, the film was covered by a NaCl window separated from the AgCl plate by a Teflon spacer. The whole system was held tightly in a lucite sample holder.

For the reference beam a similar assembly was prepared containing a film of the same amount of pure Ca montmorillonite without any organic material.

(4) G. Benson, *Org. Synthesis*, **XVI**, 26 (1936).

(5) H. T. Grendon and H. L. Lovell, *Anal. Chem.*, **32**, 300 (1960).

III. Calculations of Extinction Coefficients. (a) Dissolved Ketones.—Following Jones and Sandorfy,[6] apparent molecular extinction coefficients $\epsilon_\nu^{(a)}$ were obtained from the relationship

$$A_\nu = \log\left(\frac{T_0}{T}\right)_\nu = \epsilon_\nu^{(a)}\, Cl$$

where A_ν is the observed absorbance, T_0 and T the intensity of incident and transmitted light, respectively, at frequency ν, C the concentration of solute in moles per liter, and l the cell length in cm. The dimensions of $\epsilon_\nu^{(a)}$ are therefore 10^3 cm.^{2} per mole. In the calculation of $\epsilon_\nu^{(a)}$ only absorbance values between 0.15 and 0.80 were used. When several values in this range were obtained for a particular frequency, the average deviation in ϵ_ν was less than 2%, with the exception of the carbonyl peak at 1721 cm.$^{-1}$ (5.809 μ) which is discussed below.

The apparent molar extinction coefficient is a function of the spectral slit width, and therefore of the resolution setting. The resolution program used in this research, 925, gives slit widths narrower than are usually used in solid and liquid studies, but still not so narrow that the $\epsilon^{(a)}$ values can be taken as $\epsilon_{max}^{(a)}$ values.[7] Quantitative reproducibility suffers, however, with narrower slit spacings, and the setting 925 was chosen as a compromise between reproducibility and an approach to $\epsilon_{max}^{(a)}$.

(b) **Solid 2,5,8-Nonanetrione.**—It has been shown[8] that under certain conditions the infrared absorption of a finely divided (<0.1 μ) compound mixed thoroughly in KBr follows the Bouguer–Beer law. When 2,5,8-nonanetrione was ground in KBr neither adsorption nor reaction with the matrix, nor crystal distortion and polymorphism, occurred during the process of pelletting, since the infrared absorbance of 2,5,8-nonanetrione was found to be proportional only to the total amount of the compound in the pellet. For a compound following the Bouguer–Beer law this proportionality follows directly. One can write

$$A_\nu = \epsilon_\nu^{(a)\prime} \times C' \times b = \epsilon_\nu^{(a)\prime} \times \frac{m}{Sb} \times b = \frac{\epsilon_\nu^{(a)\prime}}{S} \times m$$

where the primes refer to a thorough dispersion of the compound in KBr rather than in a non-polar solvent as previously. A is the absorbance, S the measured area of the pressed disk facing the infrared beam, b its thickness and m the number of moles of compound contained in the disk. The extinction coefficients $\epsilon_G^{(a)\prime}$ for "ground" and $\epsilon^{(a)}$ for dissolved 2,5,8-nonanetrione having the same dimension area/mole can be compared directly, provided the same units are used in calculation.

Duykaerts[8] has shown that extinction coefficients in the "ground" samples (also randomly oriented) tend to be lower than in liquid samples, especially for the intense bands, if the particle size is greater than 0.1 μ. The general reduction of light transmission in the range 1–2.5 μ by 2,5,8-nonanetrione demonstrated that a fair fraction of the particles were in this size range. Extinction coefficients $\epsilon_G^{(a)\prime}$ for the "ground" samples were calculated directly from the absorbance of two weighed mixtures ground for 120 seconds. The reported values are 0–20% higher than values obtained from three similar samples ground for only 30 seconds. Values of each set agree within 2%. Our $\epsilon_G^{(a)\prime}$ values for ground 2,5,8-nonanetrione are not maximum values, such as might be obtained by freeze-drying techniques or longer grinding time.

Calculated extinction coefficients for the second and third methods of sample preparation (see Section IIc) showed considerable variation for a given frequency, due to orientation and light scattering effects. Frequencies of solid nonanetrione were independent of the method of preparation. No additional information appropriate to this discussion was obtained from the latter two methods.

(c) **Adsorbed Ketones.**—Extinction coefficients for adsorbed 2,5,8-nonanetrione were calculated as for "ground" 2,5,8-nonanetrione under the assumption that the total amount of organic material present in the suspension before drying was incorporated uniformly into the clay–organic

(6) R. N. Jones and C. Sandorfy, The application of infrared and raman spectrometry to the elucidation of molecular structure, "Technique of Organic Chemistry," (Ed. A. Weissberger) Vol. IX, Interscience, New York, N. Y., 1956.

(7) R. N. Jones, *Spectrochim. Acta*, **9**, 235 (1957).

(8) G. Duykaerts, *Analyst*, **84**, 201 (1959).

TABLE I

SPECTRA OF KETONES IN CS_2 AND CCl_4 SOLUTION

2,5-Hexanedione			2,5,8-Nonanetrione			Both compounds		
Wave length λ, μ	Frequency ν, cm.$^{-1}$	ϵ_ν(a)	Wave length λ, μ	Frequency ν, cm.$^{-1}$	ϵ_ν(a)	Vibration assignment	Mechanical slit width, μ	Spectral slit width, cm.$^{-1}$
3.328	3005	16.1	3.327	3006	21	CH_3 stretching, α to C=O	42	14
3.379	2959	16.9	3.379	2959	27	CH_2 stretching (asymmetric)	43	14
3.443	2904	27.6	3.433	2912	54	CH_2 stretching (symmetric)	43	13
5.809	1721	525	5.799	1724	765	C=O stretching	67	4.5
7.079	1412	89.9	7.081	1412	141	CH_2 deformation ? α to C=O	81	2.9
7.142	1401	98.0	7.138	1401	156	CH_2 deformation coupled to C-C ?	82	2.8
7.333	1363	163	7.326	1365	213	CH_3 deformation α to C=O	84	2.7
7.357	1359	174	7.353	1360	223	CH_2, CH_3 deformation α to C=O	84	2.7
7.675	1303	25.4	....	..	...		88	2.5
....	..	...	7.72	1295	52			
7.88	1269	16.1	....	..	...		90	2.3
....	..	...	7.91	1264	35			
8.159	1225	27.0	8.09	1236	41		93	2.2
8.352	1198	48.6	8.32	1202	40		95	2.1
8.522	1174	50.0	8.548	1170	163		97	2.0
							99	
8.631	1159	205	....	..	...		108	
....	..	...	9.074	1102	118		109	1.9
9.35	1070	13.0	9.30	1075	29.8		113	
9.67	1034	23.7	9.58	1044	22.1		119	1.8
....	..	...	9.74	1027	29.8		121	
9.95	1005	10.5	9.88	1012	34.0			
10.37	974	20.9	10.26	975	30.2		134	
....	..	...	10.66	948	26.5		140	1.6
....	..	...	11.08	903	9.9			
12.0	833	2	....	..	...		175	1.5
....	..	...	12.40	806	8.4			
12.67	789	6.6	....	..	...		203	1.5
....	..	...	13.15	761	30.0			
13.44	744	10.1	....	..	...		250	1.4
13.50	741	9.8	....	..	...			

Skeletal Frequencies

film after drying. This calculation was not applicable to hexanedione which evaporated partially during the drying process.

IV. X-Ray Measurements.—From the clay film on a glass slide, an X-ray diffraction pattern was obtained with a Philips Norelco diffractometer with filtered Cu Kα radiation at 40 kv., 15 ma. During the X-ray measurement the sample was kept under an atmosphere dried over P_2O_5 at 0°.

3. Spectra of the Unadsorbed Ketones

I. Spectra of Solutions and of Liquid 2,5-Hexanedione.—The spectra are presented in Table I and illustrated by Fig. 1.

As would be predicted, the infrared spectra of 2,5-hexanedione and 2,5,8-nonanetrione are very similar. In the high frequency range, 3300–1700 cm.$^{-1}$, where absorptions are due to small molecular groupings, the spectra can be distinguished only by differences in relative absorption among the peaks; the absorption frequencies are the same within the accuracy limits of the instrument. In the lower frequency ranges, differences in the carbon skeletons of the molecules give rise to significant frequency differences. The spectrum of liquid 2,5-hexanedione differs from that in solution only in the broadening of carbonyl and methylene group frequencies.

The peak at 1721 cm.$^{-1}$ is readily assigned to the carbonyl stretching frequency.[9] In dilute solutions of the compounds only one sharp peak occurs. The molar extinction coefficient for 2,5,8-nonanetrione is 765, very nearly 1.5 times that for 2,5-hexanedione, 525. The extinction coefficient per carbonyl group is therefore near 260 in each compound at spectral slit width of 4.5 cm.$^{-1}$. In more concentrated solutions the $\epsilon_\nu^{(a)}$ at 1721 cm.$^{-1}$ decreases, as a new sharp peak appears at 1714 cm.$^{-1}$, probably due to intermolecular carbonyl association. In the liquid spectrum the dominant peak is that at 1714 cm.$^{-1}$.

Absorptions at 2904 and 2959 cm.$^{-1}$ arise from stretching vibrations of a methylene group adjacent to a carbonyl group, demonstrated in studies of partially and completely deuterated diethyl ketone.[10] Two similar peaks (2912 and 2967 cm.$^{-1}$) appear in 1,4-cyclohexanedione where C–H bonds occur only in methylene groups adjacent to one carbonyl group.[11] For the more intense peak at 2904 cm.$^{-1}$ extinction coefficients per methylene group at spectral slit width 13 cm.$^{-1}$ were calculated to be 13.8 for 2,5-hexanedione and 13.5 for 2,5,8-nonanetrione. Such excellent agreement gives further evidence for the assignment. At the resolution used, the peak at 2959 cm.$^{-1}$ receives intensity contributions from peaks at 2904 cm.$^{-1}$ (methylene) and 3005, 2963 cm.$^{-1}$ (methyl, data of Francis, discussed below) and it is therefore not surprising

(9) L. J. Bellamy, "The Infrared Spectra of Complex Molecules," John Wiley and Sons, New York, N. Y., 1958.

(10) B. Nolin and R. N. Jones, *J. Am. Chem. Soc.*, **75**, 5626 (1953).

(11) M. Fétizon, unpublished spectra.

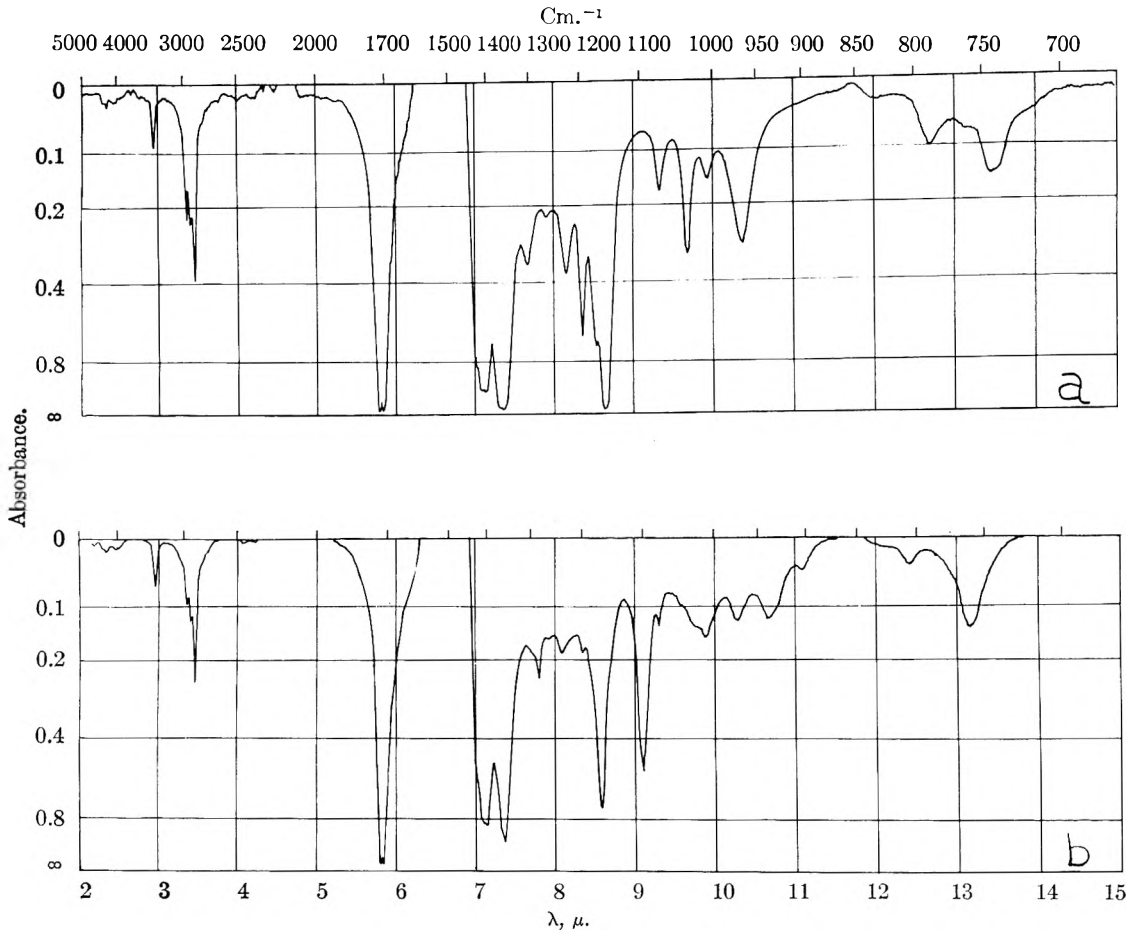

Fig. 1.—Differential spectra of the ketones in CS_2 solution: (a) 2,5-hexanedione; (b) 2,5,8-nonanetrione.

that a simple calculation of the extinction coefficient per methylene group gives poorer agreement for the 2959 cm.$^{-1}$ vibration. The peaks at 2904 and 2959 cm.$^{-1}$ can be tentatively assigned, respectively, as symmetrical and non-symmetrical stretching vibrations of the methylene groups. These frequencies reflect perturbations by the adjacent carbonyl from the usual methylene frequencies in saturated hydrocarbons.

The assignment of the weak 3005 cm.$^{-1}$ absorption to a methyl group stretching frequency adjacent to a carbonyl group is almost as certain. Of the methyl ketones whose spectra are tabulated in the 3030–2800 cm.$^{-1}$ region by Pozefsky and Coggeshall,[12] only acetone has a peak listed at 3007 ± 20 cm.$^{-1}$. However, reproduced grating spectra of butanone and 2-pentanone by Francis[13] show a definite shoulder near 3000 cm.$^{-1}$ as well as the low intensity maximum at 3008 cm.$^{-1}$ for acetone. Francis suggests 3008, 2963 and 2922 cm.$^{-1}$, the latter two of very low intensity, as CH stretching modes in acetone. Prism spectra reproduced by the A.P.I. project[14] also show clearly a maximum near 3010 cm.$^{-1}$ for methyl vinyl ketone. Aside from overtones of lower frequencies a fundamental vibration of a methyl group adjacent to carbonyl is the only unaccounted vibration capable of producing the 3005–3008 cm.$^{-1}$ peak in 2,5-hexanedione, 2,5,8-nonanetrione and acetone. If this assignment be correct, the difference between ϵ_{3005}[a] for the 2,5-hexanedione and 2,5,8-nonanetrione, 16 and 21, respectively, suggests contributions other than from the two methyl groups per molecule. Because of their small extinction coefficients these stretching vibrations are less important to the present adsorption studies than the C–H deformation frequencies in the range 1420–1300 cm.$^{-1}$.

From integrated intensity measurements Francis[13] has shown that methylene groups α to C=O groups absorb between 1430–1410 and 1370–1355 cm.$^{-1}$. The deuteration studies of Nolin and Jones[10] have shown conclusively that vibrations at 1414 and 1355 cm.$^{-1}$ in diethyl ketone are associated with the CH_2 group between C=O and CH_3 groups. In this region 1,4-cyclohexanedione exhibits only a peak near 1420 cm.$^{-1}$. All CH_2 groups in 2,5-hexanedione and 2,5,8-nonanetrione are found between C=O and other CH_2 groups. The peaks at 1412 and 1359–1360 cm.$^{-1}$ in these compounds are probably due at least in part to methylene deformations. Methyl groups adjacent to a carbonyl group produce a peak at 1356 cm.$^{-1}$ in steroids[15] and near 1370 cm.$^{-1}$ in smaller methyl ketones, [13,16] perturbed

(12) A. Pozefsky and N. D. Coggeshall, *Anal. Chem.*, **23**, 1611 (1951).

(13) S. A. Francis, *J. Chem. Phys.*, **19**, 942 (1951).

(14) American Petroleum Institute Research Project 44, Carnegie Institute of Technology, Catalog of Infrared Spectra, Serial No. 760, contributed by National Bureau of Standards.

(15) R. N. Jones and A. R. H. Cole, *J. Am. Chem. Soc.*, **74**, 5648 (1952).

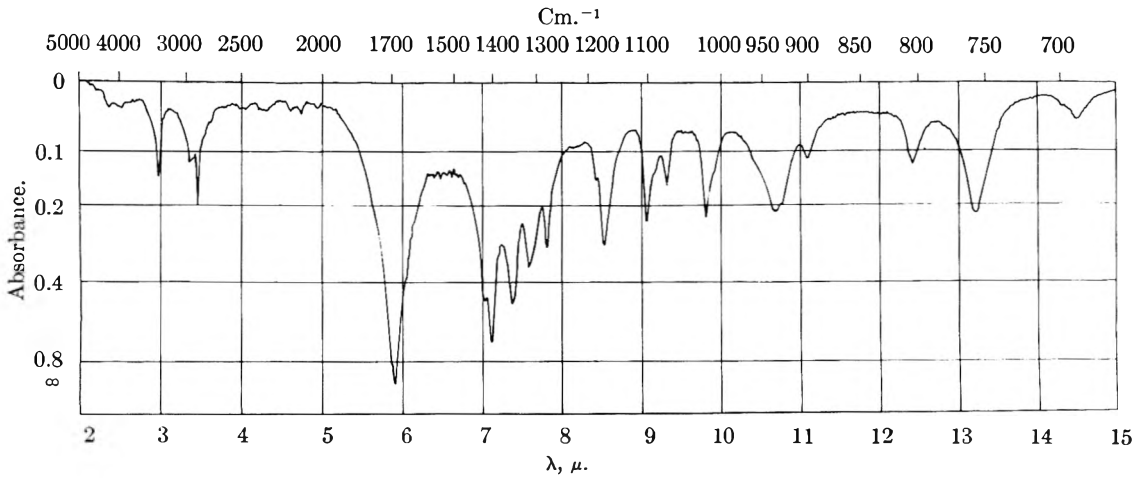

Fig. 2.—Spectrum of solid 2,5,8-nonanetrione, "ground" in KBr.

from the usual symmetrical vibration mode near 1375 cm.$^{-1}$ in hydrocarbons. The partially resolved doublet at 1359–1360, 1363–1365 cm.$^{-1}$ in 2,5-hexanedione and 2,5,8-nonanetrione is, therefore, assigned to methylene and methyl groups deformations, respectively. The extinction coefficients for this doublet in 2,5,8-nonanetrione are 1.28–1.31 times the corresponding coefficients in 2,5-hexanedione. This value lies between unity, the ratio of methyl groups present, and two, the ratio of methylene groups.

Perhaps the 1401 cm.$^{-1}$ absorption is assignable to the asymmetrical CH_3 deformation mode, perturbed from 1450 cm.$^{-1}$ in hydrocarbons in a manner similar to the CH_2 deformation which has been shown to be perturbed from 1465 to 1412 cm.$^{-1}$. However, the 1401 cm.$^{-1}$ peak, a strong one in 2,5-hexanedione and 2,5,8-nonanetrione, does not appear in other methyl ketones. The doublet 1412, 1401 cm.$^{-1}$ may be a complex absorption from the coupling of perturbed CH_2 with C–C bonds (whose normal frequency and symmetry would permit coupling) and the superimposed CH_3 absorption. The ratios of extinction coefficients in 2,5,8-nonanetrione to corresponding ones in 2,5-hexanedione 1.57–1.59 argue for a complex absorption.

The vibrations between 1300–800 cm.$^{-1}$ of the adsorbed molecules are completely obscured by Si–O–Si and Al–O–Al vibrations in the clay–organic system, and those from 800–650 cm.$^{-1}$ are too weak to be significant in the complexed state. The "finger-print region" 1300–650 cm.$^{-1}$ involves skeletal rather than functional group vibrations, and marked differences occur here in the spectra of 2,5-hexanedione and 2,5,8-nonanetrione. Vibrational assignments in this range will not be attempted, but extinction coefficients and frequencies are included in Table I for reference purposes. This region may later provide valuable steric information in studies of clay–organic complexes.

II. Spectra of Solid 2,5,8-Nonanetrione.—Spectra of solid 2,5,8-nonanetrione are of particular interest because the spectra of adsorbed 2,5-hexanedione and 2,5,8-nonanetrione have features in common with both their solution spectra and that of solid 2,5,8-nonanetrione, where the liquid and solid spectra differ. The spectra of solid 2,5,8-nonanetrione are presented in Table II and illustrated in Fig. 2. They are taken from three "ground," two "layered" and two "precipitated" samples.

Comparison of the different spectra of solid 2,5,8-nonanetrione shows that the frequencies appearing in ground, layered and precipitated nonanetrione, while differing in many respects from the solution spectra, do not differ from each other. They are presented in column 3 of Table II. Possible frequency differences appear in the several shoulders and peaks 1750–1650 cm.$^{-1}$ due to perturbed carbonyl peaks in the solid; the frequencies of such shoulders are difficult to determine precisely. Intensity differences at these and other frequencies are marked, and are caused largely by different orientation of the crystals to the infrared beam.

The change from solution to solid phase alters the frequencies of C–H stretching and skeletal motions by less than ± 15 cm.$^{-1}$. Important changes occur in the CH_3 and CH_2 deformation region (1450-1250 cm.$^{-1}$) and are illustrated in Fig. 3. One of the close doublets of the dissolved 2,5,8-nonanetrione is completely split to 1356 and 1319 cm.$^{-1}$ and a new intense peak at 1282 cm.$^{-1}$ also appears. This splitting of CH_2 deformation frequencies also occurs in crystalline *n*-paraffins, and is due to intermolecular methylene coupling,[17] when the molecules lie essentially straight alongside each other, the methylene groups bonded zig-zag to their nearest intermolecular neighbors, and the carbon atoms of each molecule lying in one plane.

The crystal structure of 2,5,8-nonanetrione has not yet been elucidated, but inspection of molecular models shows the possibility of hydrogen bonding between partially active methylene groups and carbonyl groups in the solid state if the molecules lie more or less parallel to each other.

4. Spectra and Character of the Adsorbed Ketones.—The preparation of the clay–organic complexes in the form of films resulted in a well ordered state in which the clay plates lay parallel

(16) H. W. Thompson and P. Torkington, *J. Chem. Soc. (London)*, **A184**, 640 (1945).

(17) J. K. Brown, N. Sheppard and D. M. Simpson, *Phil. Trans.*, **A247**, 35 (1954).

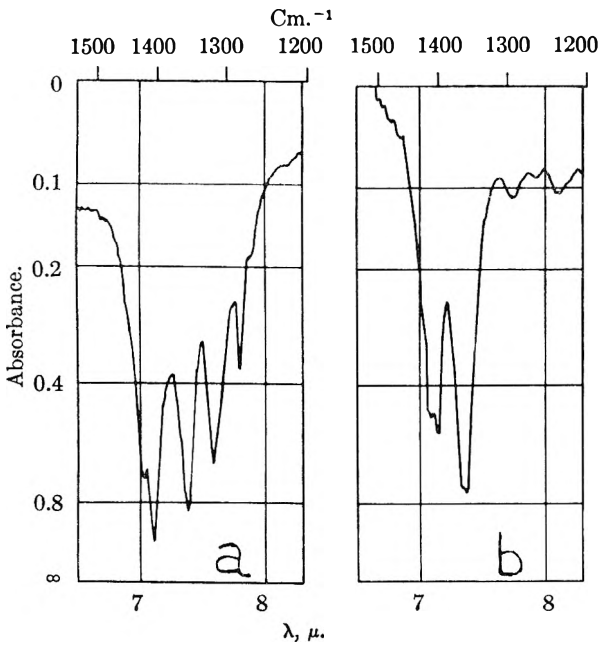

Fig. 3.—Comparison of the spectra of 2,5,8-nonanetrione in the region 1450–1200 cm.$^{-1}$: (a) "ground"; (b) dissolved.

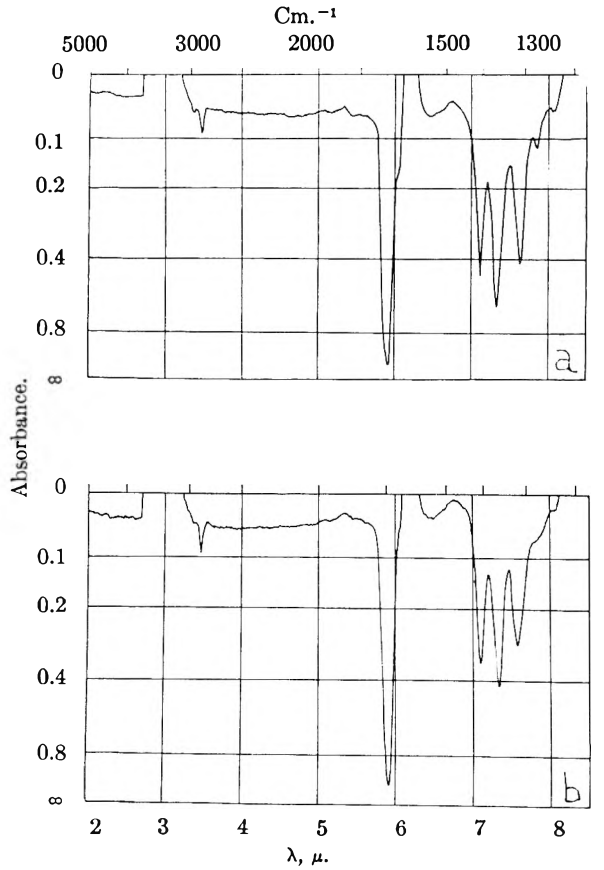

Fig. 4 —Differential spectra of the one-layer complexes of the ketones: (a) 2,5-hexanedione; (b) nonanetrione.

to the supporting surface. The X-ray diffraction pattern showed only 00l reflections with (001) spacings of 9.5 Å. for dry Ca montmorillonite. Dry complexes with 2,5-hexanedione exhibited a 13.05 Å. spacing for the one-layer complex and a 16.85 Å. spacing for the two-layer complex. The

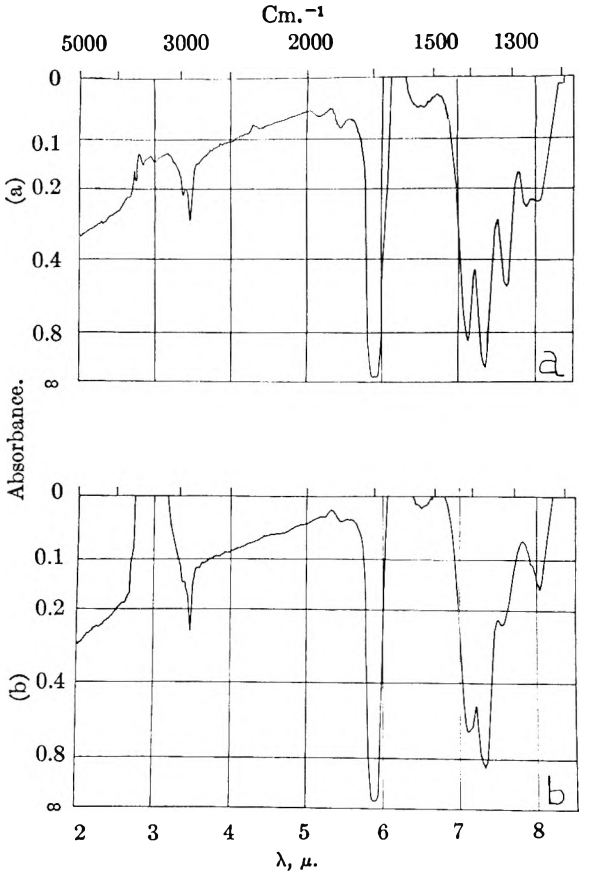

Fig. 5.—Differential spectra of the two-layer complexes of the ketones: (a) 2,5-hexanedione; (b) 2,5,8-nonanetrione.

corresponding values for 2,5,8-nonanetrione complexes were 12.95 and 17.30 Å., respectively. A detailed discussion of the X-ray diffraction pattern and the orientation of the organic molecules in the clay–organic complexes was given in a previous paper.[1]

The infrared spectrum of the Ca montmorillonite itself is not changed discernably upon adsorption of the ketones. However the spectrum of the adsorbed water is altered appreciably, as seen in spectra taken without clay in the reference beam. Water adsorbed on pure Ca montmorillonite absorbs at 1632 cm.$^{-1}$; after adsorption of the ketones the absorption is shifted to 1653 cm.$^{-1}$. Adsorption of the ketones leads to a more pronounced appearance of the shoulders at 3406 and 3242 cm.$^{-1}$, in the region of the bonded hydroxyl vibrations.

The spectra of the adsorbed ketones are presented in Table II and Fig. 4 and 5. The C–H stretching, the C=O stretching vibrations and several peaks in the 7.0–8.3 μ region are prominent. The spectra are very similar to each other in general appearance and have features in common with both the corresponding spectra of the solutions and the solid.

I. The One-layer Complexes.—The frequencies of the adsorbed ketones are very similar to each other. Slight differences occur only in the methylene-stretching vibration and in the peaks at 1311 and 1320 cm.$^{-1}$, respectively. Both spectra show a tiny shoulder at 1424 cm.$^{-1}$. The carbonyl peak of the adsorbed 2,5-hexanedione has a shoulder

TABLE II

SPECTRA OF ADSORBED AND UNADSORBED KETONES

2,5-Hexanedione In CCl_4		2,5,8-Nonanetrione In CCl_4		2,5,8-Nonanetrione Ground in KBr		One layer complex: 2,5-Hexanedione		2,5,8-Nonanetrione			Two layer complex: 2,5-Hexanedione		2,5,8-Nonanetrione		
							Rel.		Rel.			Rel.		Rel.	
ν	ϵ	ν	ϵ	ν	ϵ	ν	int.[a]	ν	int.[a]	ϵ	ν	int.[a]	ν	int.[a]	ϵ
2959	16.9	2959	27	2959	7.71	2981	0.028				2999	0.065			
2904	27.6	2912	54	2912	17.4	2903	0.104	2916	0.148	16.7	2914	0.146	2913	0.193	16.4
1721	525	1724	765	1710	107	1703	Shoulder				1707	≈2.2	1699	3.69	>228
				1694	>121	1689	3.00	1692	3.47	400	1690	≈2.2			
1412	90	1412	141	1422	51.5	1424	[b]	1424	[b]						
1401	98	1401	156	1405	84.4	1404	1.00	1407	1.00	115	1404	1.00	1406	1.00	84.6
													1399	Shoulder	
1363	163	1365	213			1365	1.36	1364	1.23	141	1364	1.57	1367	1.44	122
1359	174	1360	223	1356	64.4										
				1319	45.0	1311	0.903	1320	0.83	95	1313	0.576	1329	0.382	32.4
1303	55	1295	52	1282	27.7										
						1277	0.218	≈1270	≈0.18	≈21	1274	0.274	1267	≈0.16	≈13.9
1269	16.1	1264	35		[c]										
						1242	0.062	1240	≈0.04	≈ 5	1244	0.263	1247	0.253	21.4
		1236	41												
1225	27.0														
1198	48.6	1202	40								1202	≈0.012			

[a] The intensity of the 1406 cm.$^{-1}$ peak taken as unity. [b] Very weak shoulder. [c] Additional absorptions occur at 1189, 1176, 1106, 1090, 1075, 1019, 936, 928, 909, 806 and 757 cm.$^{-1}$.

at 1703 cm.$^{-1}$, whereas in adsorbed 2,5,8-nonanetrione the peak is only asymmetric.

The relative absorption intensities of the adsorbed ketones in the one-layer complexes are startlingly alike (within 10%) in spite of the different ratios of functional groups in the two ketones. The only exception is the methylene-stretching vibration. In 2,5-hexanedione the two methylene groups produce a relative intensity 70% that of 2,5,8-nonanetrione which contains four methylene groups.

A comparison of the spectra of the one-layer complexes with those of the unadsorbed ketones in solutions shows a similar sharpness of the peaks (especially the carbonyl stretching vibration). The CH_2 stretching frequencies at 2903 and 2916 cm.$^{-1}$ for 2,5-hexanedione and 2,5,8-nonanetrione, respectively, are the same in solution as in the adsorbed state. The same holds for the CH_3 deformation frequency α to C=O at 1365 cm.$^{-1}$.

Much more pronounced are the general similarities between the spectra of the one-layer complexes and those of solid 2,5,8-nonanetrione. Upon adsorption from solution the carbonyl frequency is shifted to the same value as upon crystallization. The same strength of bonding to the carbonyl group must be involved in the adsorbed state as in the crystalline state of 2,5,8-nonanetrione. The second peak in the solid at 1710 cm.$^{-1}$ appears as a shoulder at 1703 cm.$^{-1}$ in the adsorbed state.

For the range 1450–1200 cm.$^{-1}$, the shapes of the spectra of solid and adsorbed 2,5,8-nonanetrione are compared in Fig. 6. Upon adsorption the doublet at 1422, 1405 cm.$^{-1}$ in the solid state loses the 1422 cm.$^{-1}$ peak almost completely and the 1405 cm.$^{-1}$ peak increases in relative intensity. After adsorption the 1365 cm.$^{-1}$ peak becomes the strongest peak in this region. For 2,5,8-nonanetrione the 1320 cm.$^{-1}$ peak has the same frequency in the solid as in the adsorbed state. Adsorbed 2,5-hexanedione gives a corresponding peak at 1311 cm.$^{-1}$. It cannot be decided whether the sharp peak at 1282 cm.$^{-1}$ in solid 2,5,8-nonanetrione has something in common with the unpronounced absorption around 1275 cm.$^{-1}$ in the adsorbed

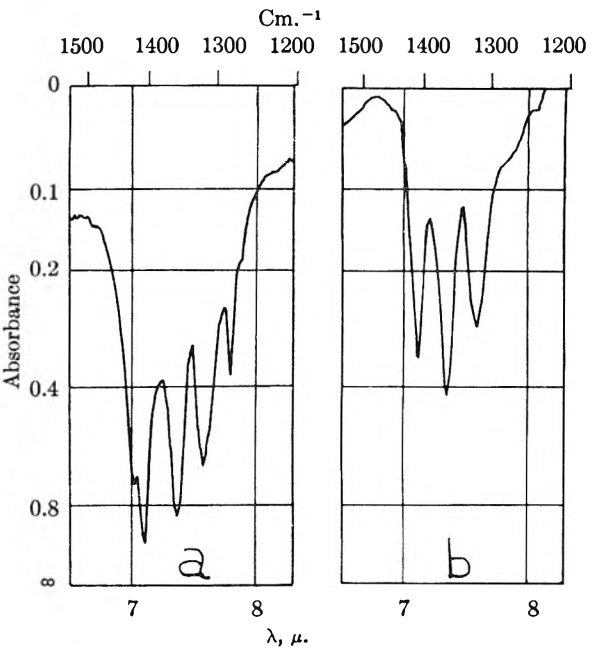

Fig. 6.—Comparison of the spectra of 2,5,8-nonanetrione in the region 1450–1200 cm.$^{-1}$: (a) "ground"; (b) one-layer complex.

ketones. Identification of these vibrations awaits studies carried out with deuterated ketones.

Although differences do occur, the similarities of the spectra of the one-layer complexes to that of bulk solid 2,5,8-nonanetrione permit some inferences as to the state of the adsorbed molecules. A type of molecular packing and a high degree of order must be postulated for the one-layer complexes similar to, or even higher, with regard to the sharpness of the peaks, than that of the solid state. Thus we may picture a one-layer complex of 2,5-hexanedione or 2,5,8-nonanetrione with the ketone molecules lying flat between the clay plates, the carbonyl groups providing bonding to adjacent molecules. In a sense the clay particles have induced the 2,5-hexanedione to "solidify" at a temperature above its normal melting point. Hydrogen bonding by the partially active methylene and

methyl groups to the oxygen atoms of the silicate layer, and ion dipole interaction with the Ca^{++} ions of the clay mineral probably cannot account for more than 2–3 kcal. per molar group. However, several such groups are available in each ketone molecule, and the forces involved appear sufficient to form weak complexes between hydrocarbons and clay minerals.

II. The Two-layer Complexes.—The spectra are characterized by the scattering effects in the high frequency region and general broadness of the peaks. In the two-layer complex of 2,5,8-nonanetrione the 1406 cm.$^{-1}$ peak is broadened on the lower frequency side giving rise to a second maximum at 1399 cm.$^{-1}$. Compared with the corresponding spectrum of 2,5-hexanedione, the carbonyl peaks of the two-layer complex of 2,5,8-nonanetrione has so high an intensity that the two maxima can no longer be recognized.

In addition to the peaks discussed for the one-layer complexes, the relative intensities do not agree well for the 1320 and 1270 cm.$^{-1}$ absorptions, which also show appreciable frequency differences between the two ketones. For both peaks, 2,5-hexanedione has the higher relative intensity.

Comparison of the two-layer complexes with the corresponding one-layer complexes shows only small changes in relative intensities for the 1405 and 1365 cm.$^{-1}$ peaks but striking intensity changes of the 1320 and 1245 cm.$^{-1}$ absorptions: the first peak diminishes and the latter increases in the two-layer complex. Both effects are more pronounced in the case of adsorbed 2,5,8-nonanetrione. There are no marked frequency shifts upon change of complex type except for adsorbed 2,5-hexanedione in C–H stretching frequency. In the one-layer complex the frequency is the same as in the unperturbed molecule whereas in the two-layer complex it is shifted to the position of the same vibration in 2,5,8-nonanetrione. It should be noted that the second maximum of the carbonyl absorption around 1708 cm.$^{-1}$ appears more pronounced in the two-layer complexes. In the discussion of the dissolved ketones this peak occurring only at high concentrations was attributed to the carbonyl–carbonyl interaction. The same explanation would be meaningful for the preferential appearance of this peak in the two-layer complex which gives a further dimension for organic–organic interaction compared with the one-layer complex.

Going from a one-layer complex to a two-layer complex results in replacement of a clay–organic contact by an additional organic–organic contact for the adsorbed molecules, and perhaps also in a change in molecular orientation with regard to the beam. Precise information on the organic molecular arrangement in a two-layer complex is still not available. However, it seems reasonable to consider that the adsorbed molecules are less strictly confined in space than in a one-layer complex. A variety of contact distances and interaction possibilities leads to the observed broadening of the spectra.

Conclusions

The sharp spectra of the one-layer complexes of 2,5-hexanedione and 2,5,8-nonanetrione are very similar to each other and point to a similar highly ordered molecular arrangement. The close similarity of the spectra of 2,5,8-nonanetrione in a one-layer complex and in the solid state suggests that the type of molecular arrangement and bonding must be similar in the two cases. This means that organic–organic interaction predominates and that the adsorption is of physical rather than chemical nature. The conclusion is drawn that the formation of a clay–organic complex does not proceed through random adsorption, but that once a few molecules are adsorbed as nuclei succeeding molecules are adsorbed in a manner similar to a crystallization process. This is supported by previous X-ray studies[1] which show that, under the same working conditions as used in this study, sequences of one-layer complexes are formed while unexpanded clay is still present, or two-layer complexes with one-layer complexes still present. This concept involves the organic–organic interaction as the main factor, and the clay–organic interaction as the inducing factor. That the latter is not negligible can be seen by the spectral differences between liquid and adsorbed 2,5-hexanedione. The liquid substance is not merely occluded between the clay plates, but the interaction with the clay surface has caused the liquid to "solidify."

The two-layer complexes offer the adsorbed molecules more possibilities of interaction and arrangement. The spectra show that the kind of arrangement is similar to that in the one-layer complex but somewhat less ordered.

Acknowledgment.—Grateful acknowledgment is made to the donors of The Petroleum Research Fund, administered by the American Chemical Society, for support of this research. Dr. M. Fétizon, École Polytechnique, Paris, France, very kindly supplied us with spectra of 1,4-diketones made in his laboratory. One of us (L.G.T.) also desires to thank the Research Committee of Utah State University, Logan, Utah; infrared techniques for clays were developed with its support.

THE KINETICS OF THE HYDROLYSIS OF CHLORINE. I. REINVESTIGATION OF THE HYDROLYSIS IN PURE WATER

BY ASSA LIFSHITZ AND B. PERLMUTTER-HAYMAN

Department of Physical Chemistry, Hebrew University, Jerusalem, Israel

Received April 25, 1960

In a reinvestigation of the kinetics of the hydrolysis of chlorine in pure water, using the thermal method, the experimental results of previous authors are confirmed. The two possible reaction mechanisms are discussed, and it is shown that OH^- cannot take part in the rate-determining step.

Introduction

In a recent investigation of the hydrolysis of bromine in phosphate buffer solution[1] we found that the observed rate was compatible with the assumption that the buffer anion takes part in the rate-determining step. However the reaction was too fast for measurement by the flow method and therefore this assumption could not be quantitatively verified.

The question of the mechanism according to which the homonuclear halogen molecule reacts to yield ionic products seemed however sufficiently interesting to warrant further research. Instead of trying to find the conditions under which the hydrolysis of bromine *can* be investigated, we thought it more promising to turn our attention to the hydrolysis of chlorine, firstly because in the case of chlorine the equilibrium

$$X_2 + H_2O \underset{k_1'}{\overset{k_1}{\rightleftharpoons}} HOX + H^+ + X^- \qquad (1)$$

(where X represents the halogen) lies much more to the right than in the case of bromine, and secondly, because the rate of hydrolysis of chlorine in pure water has been investigated[2] and found to be in a range which is accessible to measurement by the flow method.

Shilov and Solodushenkov[2] assumed reaction 1 to represent the actual mechanism, although in their first paper[2a] the rate constants corresponding to this scheme showed a downward trend as the reaction proceeded. On reinvestigation,[2b] this trend did not recur, and was ascribed to some systematic error.

On the other hand, Morris[3] pointed out that the decrease of the rate constant corresponding to mechanism 1 can be explained if we assume the rate-determining step to involve the hydroxyl ion, whose concentration decreases as the reaction proceeds. He therefore suggested the mechanism

$$Cl_2 + OH^- \underset{k_2'}{\overset{k_2}{\rightleftharpoons}} HOCl + Cl^- \qquad (2)$$

Recalculating the results in Shilov and Solodushenkov's first paper on this basis, Morris indeed found much better constancy for the rate constants. Morris' argument does not apply,[4] however, to Shilov and Solodushenkov's second paper.[2b] Furthermore, the value of k_2 calculated by Morris is extremely high. In spite of this, his mechanism has been accepted, for instance, by Sidgwick.[5] As a first step in our program of investigating the kinetics of the hydrolysis of chlorine we decided to reinvestigate the reaction in pure water with the aim of clarifying its mechanism.

Experimental

The rate of reaction was measured by the continuous flow method, utilizing the temperature effect. The apparatus used was essentially as described previously.[1,6] An observation tube was employed which accommodated 12 thermistors. Temperature differences could be measured with a precision of $\pm 0.001°$.

The chlorine solution was prepared by bubbling gaseous chlorine (Matheson) under atmospheric pressure into one of the reaction-vessels while it was isolated from the rest of the apparatus by suitable stopcocks.

The concentration of the chlorine water and of the reaction mixture was determined by measuring iodometrically the concentration of the liquid as it ran out of the observation tube.

When the undiluted chlorine solution was passed through the observation tube, a slight temperature drop was noticed along the tube. This is probably due to the fact that we employed a chlorine solution which was almost saturated at atmospheric pressure: owing to the pressure gradient along the observation tube the solution becomes supersaturated and endothermal de-solution of chlorine may take place. This difficulty does not arise in the case of the more dilute and therefore more strongly hydrolyzed reaction *mixture*. The changes of temperature due to the reaction, ΔT, at each thermistor were therefore calculated by comparing the temperature of the reaction mixture with that of the pure water. The temperature of the chlorine solution relative to that of the pure water was determined from measurements at the first three thermistors only. There was usually a slight temperature difference between the two solutions and the values of ΔT were corrected by adding this difference, multiplied by the dilution ratio.

A reaction temperature of 9.5° was chosen on the basis of the following considerations: the temperature should be *low* in order to (a) keep the reaction rate within a range accessible to measurement in our apparatus (even in buffer solution where the reaction may be expected to proceed faster[1]) and (b) increase the solubility of chlorine. On the other hand, there exists a chlorine hydrate which dissociates according to

$$Cl_2 \cdot 8H_2O(s) \rightleftharpoons 8H_2O + Cl_2(gas)$$

As soon as the partial pressure of chlorine over the solution becomes equal to the dissociation pressure, any further addition of chlorine causes the hydrate to precipitate in the form of small crystals. The formation of this hydrate must obviously be avoided, *i.e.*, the temperature must be *high* enough for its dissociation pressure to lie above atmospheric pressure. The pressure *vs.* temperature curve is very steep[7]

(1) A. Lifshitz and B. Perlmutter-Hayman, *Bull. Research Council Israel*, **A8**, 166 (1959).

(2) (a) E. A. Shilov and S. M. Solodushenkov, *Compt. rend. acad. sci. U.R.S.S.*, **1**, 96 (1936); (b) *J. Phys. Chem.* (*U.S.S.R.*), **19**, 404 (1945); *Acta Physicochim. U.R.S.S.*, **20**, 667 (1945).

(3) J. C. Morris, *J. Am. Chem. Soc.*, **68**, 1692 (1946).

(4) M. Anbar and H. Taube, *ibid.*, **80**, 1073 (1958).

(5) N. Sidgwick, "Chemical Elements and their Compounds," Vol. II, Oxford University Press, Oxford, 1950, p. 1213.

(6) E. Giladi, A. Lifshitz and B. Perlmutter-Hayman, *Bull. Research Council Israel*, **A8**, 75 (1959).

(7) "International Critical Tables," Vol. VII, McGraw-Hill Book Co., Inc., New York, N. Y., 1930, p. 253.

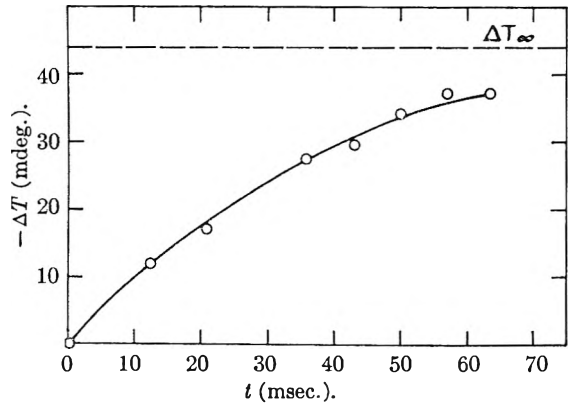

Fig. 1.—The dependence of the change of temperature on time, for a typical experiment (run III; $a = 6.03 \times 10^{-2}$ M).

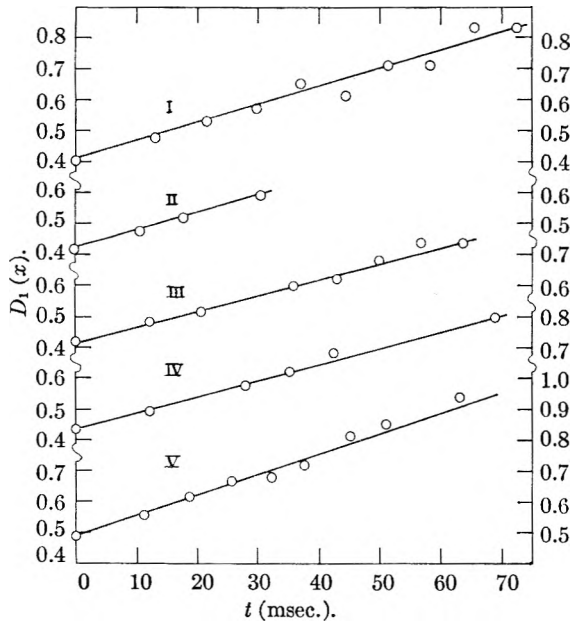

Fig. 2.—The dependence of $D_1(x)$ on time, for 5 experiments, presented in the order of decreasing stoichiometric chlorine concentration. (Straight lines correspond to mechanism 1.)

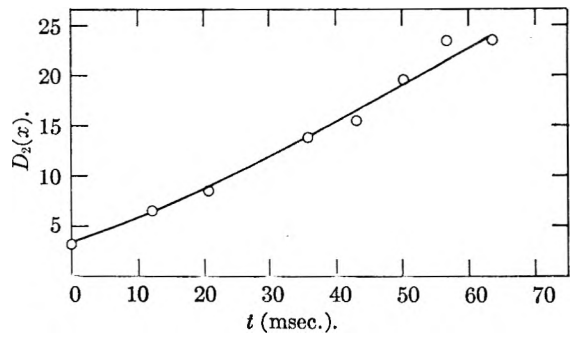

Fig. 3.—The dependence of $D_2(x)$ on time, for a typical experiment (run III). (A straight line would correspond to mechanism 2.)

and cuts the point of our atmospheric pressure (690 mm.) at 9.0°.

A driving pressure of about 400 mm. Hg was used, and the flow velocity was between 5.35 and 6.52 cc. sec.$^{-1}$.

The pressure was again[1,6] applied over *both* vessels from a nitrogen cylinder. Thus, while the mixture of the two reagents is being run through the observation tube, the two vessels are in contact *via* the gas-phase, and there exists the danger of chlorine from one vessel entering into the other and dissolving. This indeed occurred, but to a very small extent, and was corrected for. Furthermore, the partial pressure of chlorine over the chlorine solution decreases during the experiment, and the solution may become more dilute. The chlorine concentration was determined before and immediately after the reaction had been carried out. A very small change was noticed, and the mean value was applied for calculating the kinetic results. The fortunate lack of equilibration between the chlorine solution and the gas-phase may be ascribed to the short duration of the experiment (~15 min.). (The position is different from that of previous work[2] where the gas bubbled *through* the solution and special precautions had to be taken.)[8]

Results

The rate equation corresponding to mechanism 1 is

$$dx/dt = k_1(a - x_t) - k_1' x_t^3 \qquad (I)$$

where a is the total stoichiometric concentration of chlorine in the reaction mixture, and x_t the molarity of the reaction products at time t. This yields on integration[2]

$$k_1 t = \frac{K_1}{3x_e^2 + K_1}\left[\frac{1}{2}\ln(x_t^2 + x_t x_e + K_1 a/x_e) - \ln(x_e - x_t) + \frac{3x_e}{\sqrt{3x_e^2 + 4K_1}}\tan^{-1}\frac{2x_t + x_e}{\sqrt{3x_e^2 + 4K_1}}\right] + \text{const.} \equiv D_1(x) + \text{const.} \qquad (II)$$

where K_1 is the equilibrium constant of reaction 1 and x_e the value of x when equilibrium is reached. The value of x_0, the amount hydrolyzed at zero time, is equal to the equilibrium value of x in the chlorine water *before* dilution, times the dilution factor. We used[9] $K_1 = 2.23 \times 10^{-4}$, which was corrected[9] for the influence of ionic strength by dividing by the appropriate value of the square of the mean activity coefficient[10] of HCl. (The values of x_0 and x_e were calculated from K_1 corresponding to the ionic strength *before* dilution, and at the *end* of the reaction, respectively. In expression II the mean of the values of K_1 corresponding to the ionic strength immediately *after* dilution, and at the *end* of the reaction was used.[11]) The values of a lay between (5.1 to 6.9) $\times 10^{-2} M$, those of x_0 between (1.43 to 1.68) $\times 10^{-2}$ M and those of x_e between (2.07 to 2.38) $\times 10^{-2}$ M.[12] The values of x_t were calculated from the expression

(8) Nevertheless, it would have been more desirable to apply a driving-force of *chlorine* over the chlorine solution and a driving-force of nitrogen over the bottle containing pure water. However, the slightest fluctuation in one of the pressures would then cause a considerable change in the ratio of the amounts of liquid flowing from the two bottles. This effect can be greatly decreased by inserting between the vessels and the mixing chamber capillary tubes whose hydrodynamic resistance is at least equal to that of the mixing chamber and observation tube. This device, however, cannot be applied. Apart from the fact that it necessitates the use of inconveniently high pressures to achieve the desired flow velocity, it entails a large pressure drop between the reagent vessels and the mixing chamber which would cause part of the chlorine to de-solve.

(9) R. E. Connick and Yuan-tsan Chia, *J. Am. Chem. Soc.*, **81**, 1280 (1959).

(10) H. S. Harned and B. B. Owen, "The Physical Chemistry of Electrolyte Solutions," Reinhold Publ. Corp., New York, N. Y., third ed., 1958, p. 716.

(11) If the change of K_1 during the reaction were taken into account the integration of equation I would become very difficult. However, K_1 changes during the reaction only by about 4%; furthermore, expression II is not very sensitive to small changes in K_1. The error introduced by neglecting the change in K_1 is therefore small in comparison with our experimental inaccuracy.

$$x_t = x_0 + (x_e - x_0)\Delta T_t/\Delta T_\infty \qquad \text{(III)}$$

where ΔT_t is the temperature effect at a given thermistor, and ΔT_∞ is the total temperature effect. The measured values of ΔT_∞ lay between $-(44$ to $50) \times 10^{-3}$ degrees, and were in good agreement with those calculated from $(x_e - x_0)$ and[9] $\Delta H_1 = 6.55$ kcal. mole^{-1}.

Figure 1 shows a plot of ΔT *vs.* time for a typical experiment (run III), and Fig. 2 shows the dependence of $D_1(x)$ on time for 5 experiments. Straight lines are seen to be obtained *which show no trend as the reaction proceeds.* The values of k_1 can be calculated from the slope of these lines. We find

$$k_1 = 5.60 \text{ sec.}^{-1}$$

with a standard deviation of $\pm$ 0.45. The comparatively high scatter is probably due to the small value of $(x_e - x_0)$ and therefore of the total heat effect. A small error in ΔT will therefore cause a considerable error in $D(x)$. (This is especially true for the last few points of each experiment, where x_t approaches x_e.)

In addition we plotted the expression (see also Morris,[3] eq. 6)

$$\frac{x_e}{3x_e^2 + K_1}\left[\frac{1}{2}\ln(x_t^2 + x_t x_e + K_1 a/x_e) - \ln(x_e - x_t) - \frac{2K_1/x_e + 3x_e}{\sqrt{3x_e^2 + 4K_1}}\tan^{-1}\frac{2x_t + x_e}{\sqrt{3x_e^2 + 4K_1}}\right] \equiv D_2(x)$$

against time. If mechanism 2 were operative, this would yield straight lines. Concave curves were obtained. An example (run III) is shown in Fig. 3.

Discussion

The fact that the plots of $D_1(x)$ *vs.* time exhibit no downward trend as the reaction proceeds, whereas the plots of $D_2(x)$ exhibit an upward trend shows mechanism 1 to be compatible with the experimental results. Apart from this experimental confirmation of mechanism 1, mechanism 2 can be ruled out on theoretical grounds, which have been stressed in recent years.[13] Firstly, according to Morris,[3] it leads to a rate constant of 5×10^{14} mole^{-1} l. sec.$^{-1}$, and zero activation energy (the increase of the rate of hydrolysis with increasing temperature is ascribed to the change in the dissociation constant of water). However, the highest possible value for a second-order rate constant has been shown[13] to be much lower than this, whereas a value of zero for the apparent activation energy seems incompatible with the mechanism of diffusion-controlled reactions. An even stronger argument against mechanism 2 is obtained when we consider the question whether OH^- — which at a *p*H of about 2 is present in the solution at a concentration very much lower than chlorine—can be regenerated at a sufficient rate. According to Morris' estimate,[3] this may indeed be the case, but in the meantime, both theoretical considerations[13] and direct measurement,[14] have shown that at 25° the rate of formation of OH^- in water is only about 1.4×10^{-3} mole l.$^{-1}$ sec.$^{-1}$, *i.e.*, much slower than the rate of hydrolysis of chlorine (about 0.1 mole l.$^{-1}$ sec.$^{-1}$ at our concentration). This excludes the possibility of the hydroxyl ion playing any important role in the hydrolysis of chlorine in pure water. (Experimental results so far obtained by us show that the situation may well be different in buffer solution, where OH^- can be supplied faster than in pure water.[1,14])

The reaction thus proceeds according to the reaction scheme represented by equation 1. This does not answer the question of the actual *mechanism*, namely whether we have to consider the reaction as a monomolecular one in which a hydrated chlorine molecule dissociates with a rate constant of 5.6 sec.$^{-1}$ or as a bimolecular one involving collision between chlorine and water, and proceeding at a specific rate of 10^{-1} mole^{-1} l. sec.$^{-1}$. At the moment, there seems to be no possibility of deciding this point on theoretical grounds, but an investigation of the rate of hydrolysis in buffer solutions may be expected to throw some light on the question.

The authors wish to thank Prof. G. Stein for making valuable comments.

(12) Unfortunately, we cannot employ any drastic changes in a, and hence in x_0 and x_e, since we are limited by the decreasing heat effect at low concentration, and the solubility of chlorine at high concentration.

(13) See *e.g.* M. Eigen, *Disc. Faraday Soc.*, **17**, 194 (1954), where the relevant literature is quoted.

(14) M. Eigen and L. de Maeyer, *Z. Elektrochem.*, **59**, 986 (1955).

SPECTROPHOTOMETRIC DETERMINATION OF FAST XANTHATE DECOMPOSITION KINETICS

BY ELIAS KLEIN, J. KEITH BOSARGE AND IRWIN NORMAN

Research Department, Courtaulds, Inc., Mobile, Alabama

Received April 28, 1960

The decomposition kinetics of potassium ethyl xanthate in 0.02 to 4.0 *N* hydrochloric acid solutions have been determined at 0 and 10°. The concentrations of the xanthate ion and xanthic acid species were determined simultaneously by monitoring their respective absorbancies at 302 and 270 mμ. From the resulting data, the rate constants, thermodynamic ionization constant, molar extinction coefficients, and the Hammett *h*-function were determined. This is the first report of the aqueous xanthic acid extinction coefficients known to us. From the temperature dependence of the equilibrium and rate constants, an estimate has been made of the heat of ionization of xanthic acid, and of the activation energy of the reaction. The kinetics are shown to be pseudo-first order under the conditions employed, the rate constant showing a maximum at 0.4 *N* HCl. It is shown that alternate mechanisms can be postulated to account for this maximum. The resolution of these explanations lies in the interpretation of activity coefficients appearing in the rate expression. Several experiments at constant ionic strength are presented, and the mechanisms are discussed.

Introduction

Since the discovery of cellulose xanthate in 1892 by Cross and Bevan, and the commercial application of this compound in 1900 in the viscose rayon process, the acid-catalyzed decomposition of the substituted dithiocarbonic acid ester has been of practical and theoretical interest. Studies of its model compounds, such as potassium ethyl xanthate, date back to the work of von Halban and Kirsch.[1,2] A more modern approach to the mechanism of the reaction was utilized by Lewis[3] who studied the non-aqueous kinetics of ethylxanthic acid decomposition. He demonstrated that in the absence of a base, the acid was stable, and postulated an ion-pair as the transition state intermediate. A spectrophotometric experimental approach to the problem, using acid normalities approaching 1.0, was first reported by Iwasaki and Cooke.[4] A more comprehensive study in both dilute and strong acid solutions was carried out by Ballard, Bamford, Gray and Totman[5] who showed that the rate constant passed through a maximum as the (H^+) increased, and postulated that in strong acid solutions, a new equilibrium involving a protonated xanthic acid species became dominant.

Experimental

Four samples of potassium ethyl xanthate were used: two were Eastman White Label, repeatedly recrystallized and stored in a vacuum desiccator. The other two were laboratory preparations also recrystallized four times. The agreement in molar extinction coefficient was considered a better measure of purity than the standard iodine titration.

The method suggested by Lewis[3] was employed in the preparation of stable solutions of ethylxanthic acid. The choice of the solvent was dictated by the type of experiment to be performed. Spectral grade isooctane was used for analysis in the ultraviolet and CS_2 for infrared analysis.

A Cary Model 14 automatic recording spectrophotometer, with the cell carriage replaced by a metal block through which constant temperature water circulated, was employed for the kinetic measurements.

The xanthate solution, generally 6.2×10^{-3} *M*, was introduced first by micropipet (0.100 ml.) into the standard cell, and allowed to equilibrate thermally. The reaction was initiated by injecting 3.0 ml. of the acid solution as a jet into the cell, using an all-glass jacketed syringe capped with a polyethylene needle to avoid metallic contamination.

The diverse problems of maintaining isothermal conditions were overcome in the following manner. The cell mount was cooled by circulating constant temperature water from a reservoir. The acid solution, together with the jacketed syringe, was pre-cooled in this reservoir. To minimize heat transfer due to condensation on the cell faces, compartment was dried with desiccants and a flow of dry nitrogen.

To avoid fogging of the cell window from residual moisture, the cell was coated initially with an alcoholic solution of an anionic detergent.

The mode of operation was as follows: After the xanthate solution had reached thermal equilibrium (20 minutes after loading, as determined by a small thermistor bridge circuit) 3.00 ml. of the acid solution was injected from the syringe. At the same time, the recorder of the spectrophotometer was started. As soon as the compartment cover was closed, the pen and wave length sweep of the instrument were activated, and the absorption was scanned from 310 to 260 mμ. At the lower wave length the scan direction was reversed, and this cycling procedure continued until the major absorption peak had an absorbance lower than 0.1. After a suitable waiting period, the entire spectrum again was scanned, and the base line values determined for correcting the instrumental zero.

From a knowledge of the molar extinction coefficients of the undissociated acid and anion species, it is then possible to convert the absorbances at 270 and 302 mμ into molar concentrations. The sum of these concentrations suitably extrapolated to zero time should then yield the original xanthate concentration, unless some undetected species were also present.

Results

The ultraviolet spectrum of xanthate ion (X^-) has been reported for some time, but no information is available which characterizes the ultraviolet spectrum of the undissociated acid (HX). During the course of preparation of various samples of ethylxanthic acid and its thioesters for infrared analysis, for a related problem in this Laboratory, it was established that the undissociated acid had an ultraviolet absorption band at 270 mμ (the position of the maximum and extinction coefficient being slightly affected by solvent effects). The assignment of the ultraviolet band was facilitated by comparison of a parallel examination in the infrared region. In Fig. 1 are shown the infrared spectra of potassium ethyl xanthate and of ethylxanthic acid—the latter isolated as previously mentioned, as well as the S-ethyl ester of the latter.

In the spectra of the xanthic acid the intense

(1) H. von Halban and A. Kirsch, *Z. physik. Chem.*, **82**, 325 (1913).

(2) C. V. King and A. Chatenever, *J. Am. Chem. Soc.*, **71**, 3587 (1949).

(3) G. M. Lewis' Dissertation, New York University, 1947.

(4) Iwasaki and Cooke, *J. Am. Chem. Soc.*, **80**, 285 (1958).

(5) D. G. H. Ballard, C. H. Bamford, K. L. Gray and E. D. Totman, Courtauds Limited, Maidenhead, England; Viscose Research Laboratory, Coventry—private communication.

absorption region (8–10 μ) shows distinctive bands at 8.08, 8.96 and 9.37–9.44 μ compared to the xanthate salt (*cf.* 8.79, 8.91–9.09 and 9.51 μ). If one assumes that the vibrations in this region arise from the R–O–C part of the molecule, then the frequency shift can be attributed to the effect of interaction of the SH group on the O–C bond.[6]

Figure 2 shows the molar extinction coefficients of ethyl xanthic acid, its anion and its S-ethyl ester in the ultraviolet region. The ionic form has a maximum at 302 mμ and the undissociated acid at 268 mμ in isoöctane. The magnitude of the extinction coefficients is great enough to indicate that these bands are of the "K" type[7] arising from the C=S chromophore and enhanced by either an S^- or SH terminal auxochrome. This is supported by the bathochromic shift in the maximum due to the electron donating S^- group, compared to the SH group, and by the bathochromic shift encountered with increasing dielectric constant of the solvent. A summary of relevent spectral data is shown in Table I, supporting the conclusion that the 270 mμ band is indeed due to the undissociated acid form.

TABLE I

SUMMARY OF ULTRAVIOLET ABSORPTION DATA OF ETHYLXANTHIC ACID AND RELATED COMPOUNDS

Species	Solvent	λ, mμ	ϵ, l. mole^{-1} cm.$^{-1}$
$C_2H_5OCS_2K$	Water	302	17,420
	Water	270	660
$C_2H_5OCS_2H$	Isoöctane	268	9,772
	Isoöctane	302	117
$C_2H_5OCS_2C_2H_5$	Isoöctane	278	11,200
$C_2H_5OCS_2H$	Water	270	10,670
	Water	302	117[b]
R–OCS_2CH_2CO–OC_2H_5[a]	2-Chloroethanol	278	8,600[c]
R–OCS_2CH_2CO–$N(C_2H_5)_2$[a]	2-Chloroethanol	280	960[d]
$C_2H_5OCS_2C_2H_5$	Ligroin	280	....[e]
$C_2H_5OCS_2H$	Ligroin	267 approx.	....[e]

[a] R = cellulose. [b] Taken from isoöctane data. [c] J. Schurtz, *Microchim. Acta*, 589 (1955). [d] J. Schurtz, *Das Papier*, 9, 333 (1955). [e] A. Hantzsch and C. Scharb, *Ber.*, 3570 (1913).

Utilizing the extinction coefficients of Table I, it is possible to determine molar concentrations of both the acid and anion species by the standard analyses of two-component mixtures. The resulting equations are

$$L_x(HX) \times 10^{-4} = 0.937A_{270\,m\mu} - 0.0356A_{302\,m\mu} \quad (1a)$$

$$L_x(X^-) \times 10^{-4} = 0.570A_{320m\mu} - 0.063A_{270\,m\mu} \quad (1b)$$

(L = cell length in cm.) (A = absorbance)

By the addition of the values obtained from equations 1a and 1b, we obtain the total xanthate concentration (X_T), and from the ratio of (1b) to (1a), a function which is related to the ionization constant of xanthic acid.

A semi-logarithmic plot of (X^-), (HX) or (X_T) as a function of time is found to be linear for over 50% of the reaction. As is to be expected, the slopes of the plots of each species are identical for any given acid concentration, indicating that the acid/anion equilibrium is fast in comparison to the speed of the decomposition reaction. From the extrapolated value of (X_T) to zero time, it is also shown that the stoichiometry of the system is established in terms of only the anion and acid concentrations.

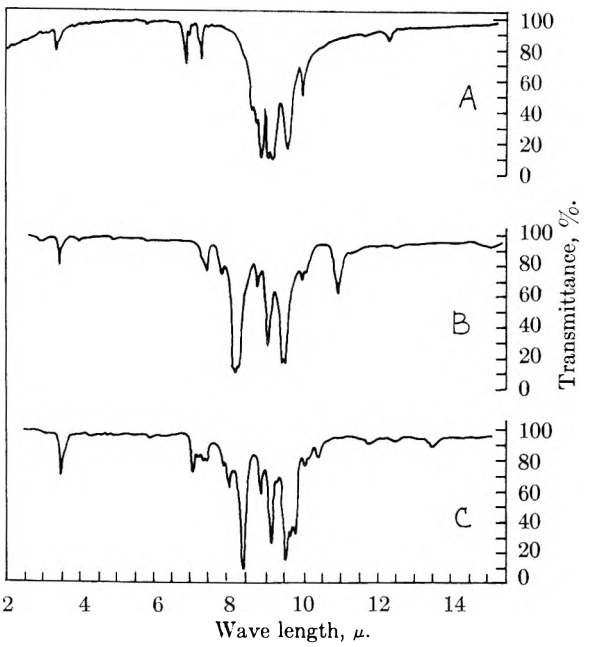

Fig. 1.—Infrared absorption spectra of: (a) potassium ethylxanthate; (b) ethylxanthic acid; (c) ethylxanthic S-ethyl ester.

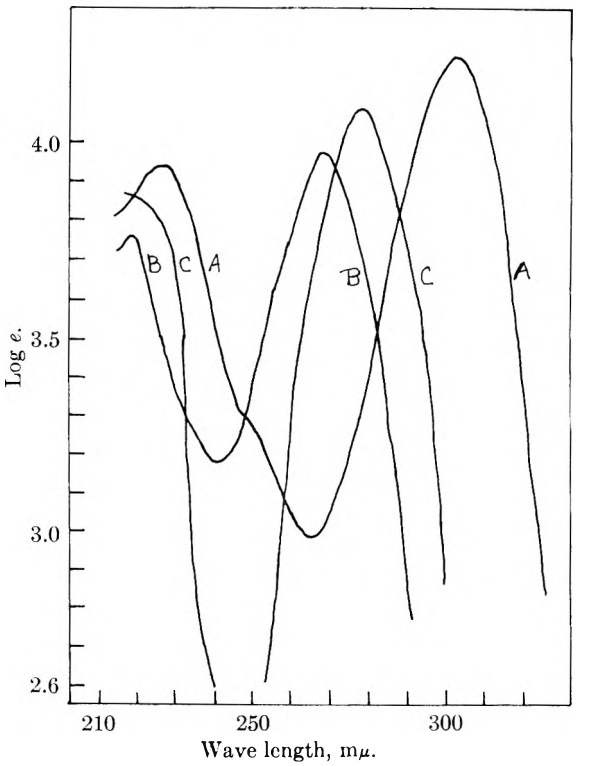

Fig. 2.—Log extinction *vs.* wave length: (A) potassium ethylxanthate; (B) ethylxanthic acid; (C) ethyl ester of ethylxanthic acid.

(6) F. G. Pearson and R. B. Stasiak, *J. Applied Spectroscopy*, **12**, 116 (1958).

(7) A. E. Gillam and E. S. Stern, "Electronic Absorption Spectroscopy," E. Arnold Publishing Ltd., London, 1954, Chap. 8.

TABLE II

CALCULATED IONIZATION CONSTANTS AND HAMMETT h-FUNCTIONS FOR ETHYLXANTHIC ACID AS A FUNCTION OF HYDROCHLORIC ACID CONCENTRATION

HCl, N	10°: X^-/HX	$f_{\pm}^2$	K_i	$K_C f_{\pm}^2$	h_-	10° with $[Cl^-] = 0.9\ M$: X^-/HX	$f_{\pm}^2$	K_i	h_-	0°: X^-/HX	$f_{\pm}^2$	K_i	h_-
0.0199	1.695 ± 0.014	0.769	0.0259	0.0152	2.13 ± 0.02	0.672	0.0285	0.0121	1.537 ± 0.007	0.877	0.0235	0.0154
.0995	.401 ± .002	.645	.0257	.0643	.433 ± .003	.672	.0290	.0596	.366 ± .003	.803	.0235	.0642
.298	.1435 ± .0018	.585	.0250	.180	.142 ± .005	.672	.0284	.182	.130 ± .004	.765	.0227	.181
.496	.0861 ± .0003	.596	.0254	.300	.0815 ± .0004	.672	.0271	.317	.0717 ± .0011	.776	.0215	.328
.696	.0561 ± .0006	.626	.0245	.460					.0478 ± .0020	.798	.0212	.492
.884	.0426 ± .0060	.669	.0252	.586	.0110 ± .0005	.672	.0243	.632	.0331 ± .0006	.824	.0199	.710
1.19	.0293 ± .0002	.758	.0266	.880					.0193 ± .0016	.877	.0177	1.218

TABLE III

PSEUDO-FIRST ORDER RATE CONSTANTS AND ACTIVATION ENERGIES FOR THE DECOMPOSITION OF ETHYLXANTHIC ACID AS A FUNCTION OF ACID STRENGTH

HCl, N	k_{exp} 10°, sec.$^{-1}$ $(Cl^-) = 0.9M$	k_{exp} 10°, sec.$^{-1}$	k_{exp} 0°, sec.$^{-1}$	$(X_T)_0$, 0° extrapd.[a]	k_{exp} 10° / k_{exp} 0°	Ea (cal./mole)
0.0199	0.00755	0.00962	0.00348	2.00×10^{04}	2.76	15,500
.0995	.0171	.0181	.00627	2.02	2.88	16,200
.298	.0196	.0208	.00700	2.00	2.97	16,700
.496	.0203	.0213	.00720	2.03	2.96	16,700
.696		.0211	.00688	2.00	3.04	17,200
.884	.0204	.0205	.00653	2.00	3.13	17,500
1.19		.0190	.00585	1.95	3.24	18,000
1.59		.0176	.00603	1.99	2.91	16,400
1.99		.0160	.00502	2.05	3.20	17,900
4.00		.00907	.00295	2.09	3.07	17,200
					3.02 Av.	16,900 Av.

[a] Total xanthate added: $2.00 \times 10^{-4}\ M$.

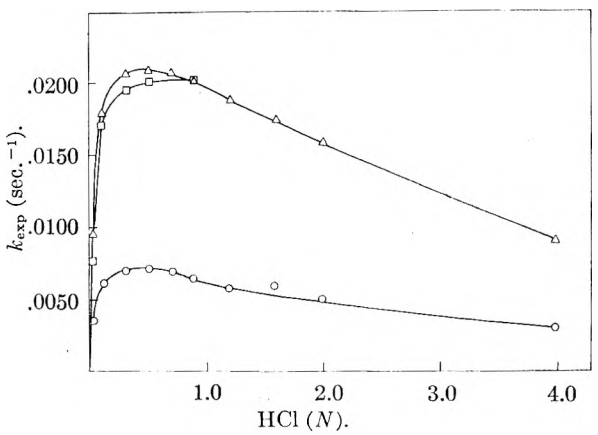

Fig. 3.—Experimental pseudo-first order rate constant for the decomposition of ethylxanthic acid as a function of HCl normality: △, 10°; □, 10°, $[Cl^-] = 0.9\ M$; ○, 0°.

The evaluation of the "pseudo" first-order rate constants was carried out from the slope of log X_T *vs.* time graphs. The X_T values were used once it had been established that $-dX_T/dt = -d(HX)/dt = -d(X^-)/dt$, and $-dX_T/dt \propto X_T$. A summary of the calculated experimental rate constants is given in Table III and Fig. 3 for the two temperatures employed. In addition, data are shown at 10° for experiments at a constant (Cl^-) of 0.9 M, obtained by adding appropriate quantities of NaCl to aqueous hydrochloric acid solution of 0.02 to 0.90 N. Because of the small salt effect on the rate (less than 10%), an additional experiment at 0.1 N HCl and 2.0 M NaCl was performed. The decrease in rate again was less than 10%.

In Table III are also shown the ratio of the rate constants for the two temperatures, and an estimate of the activation energy derived therefrom. The average of the ratio is seen to be 3.02, leading to an estimate of 16.9 kcal./mole.

The experimental ratio $(X^-)/(HX)$ can be treated in several ways. We have preferred to use a combination of classical thermodynamics, and the Hammett acidity function[8] h_-. The equations

$$K_i = \frac{(H^+)(X^-)f_{X^-}f_{H^+}}{(HX)f_{HX}} = \frac{(X^-)h_-}{(HX)}$$

where

$$h_- = \frac{(H^+)f_{X^-}f_{H^+}}{f_{HX}}$$

define the relationship between the Hammett function and the classical ionization constant, K_i. Since the experimental data are at 0.02 and higher ionic strengths, the preliminary assumption was made that the mean activity coefficient of the HCl solutions, $f_{\pm}$, was equal to the mean activity coefficient of HX, *i.e.*, $(f_{\pm})^2HCl = f_{H^+}f_{X^-}$, and that $f_{HX} = 1$.

Using Harned and Owen[9] data for $(f_{\pm})^2_{HCl}$, the K_i values of ethylxanthic acid were calculated, and plotted against acid normality. The data are shown in Table II. Extrapolation of the 0 and 10° data to zero acid normality gave K_i values of 0.0235 and 0.0258, respectively. The extrapolations show that the original assumptions were in error by a second-order term, the latter being

(8) L. P. Hammett, "Physical Organic Chemistry," McGraw-Hill Book Co., New York, N. Y., 1940.

(9) Harned and Owen, "The Physical Chemistry of Electrolytic Solutions," Reinhold Publ. Corp., New York, N. Y., Chap. 11, 1950.

inversely related to temperature. The K_i values for a constant ionic strength of 0.9, arising from mixed NaCl/HCl solute concentrations show an activity coefficient non-linearity typical of mixed salt solutions.[10]

Having extrapolated a value for K_i at the two temperatures, we can then calculate h_- as a function of (H^+); these data are shown in Table II. The temperature dependence of K_i also leads to an estimate of the thermodynamic values for the reaction

$$(HX) \rightleftharpoons (H^+) + (X^-) \quad \Delta H = 1400 \text{ cal. mole}^{-1}, \quad \Delta S = -2.2 \text{ e.u.}$$

Discussion

Any explanation of the mechanism of potassium ethylxanthate decomposition in HCl solution must explain both the observed pseudo-first order dependence on total xanthate concentration, and the maximum in the rate constant *vs.* acid concentration curve. The explanations postulated in the literature involve direct decomposition *via* ethylxanthic acid[1,2,4] in equilibrium with the xanthate ion. However, rate equations derived from this postulate cannot explain the maximum in the experimental rate constant curve.

Two basic alternate mechanisms can be devised which are consistent with present knowledge.

In 1954, Ballard, Bamford, Gray and Totman[5] postulated equilibria and reaction schemes, based in part on their own experiments and in part on the work of Lewis.[3]

$$\begin{array}{l} (X^-) + (H^+) \overset{K_1}{\rightleftharpoons} (HX) \qquad (2) \\ \quad K_2 \uparrow\downarrow \\ (HX^{\pm}) \overset{(H^+)}{\underset{K_3}{\rightleftharpoons}} (H_2X)^+ \\ \quad k \downarrow \\ \quad ROH + CS_2 \end{array}$$

where

(X^-) = concn. of $C_2H_5OCS_2^-$, xanthate anion

(HX) = concn. of $C_2H_5OCS_2H$, xanthic acid

$(HX^{\pm})$ = concn. of $C_2H_5\overset{+}{O}HCS_2^-$, ion-pair activated complex

$(H_2X)^+$ = concn. of $C_2H_5OCS_2H_{H^+}$, protonated xanthic acid

and K_1, K_2 and K_3 the appropriate equilibrium constants. The protonated xanthic acid was introduced to account for the maximum in the rate curve.

The relationship between k_{exp} and k is given by

$$k_{exp} = \frac{kK_2(H^+)}{1 + (K_1 + K_2)(H^+) + K_2K_3(H^+)^2} \qquad (3)$$

and differentiation of this equation with respect to (H^+) indicates that the maximum should occur when $(H^+)^2 = 1/K_2K_3$. Since neither of these constants is tractable experimentally, they must be calculated. A good fit to the experimental data is obtained from a solution having these values for the constants.

$$kK_2 = 0.3845; \; K_1 + K_2 = 45.06; \; K_2K_3 = 16.26$$
$$K_2 = 2.51; \; K_3 = 6.48 \qquad (4)$$

(10) Ref. 9, Chapter 14.

For comparison, the experimental and calculated values, based on the above solution, are shown in Table IV. While the agreement is excellent, the numerical values lead to improbable predictions. For example, combining the values of (4) with the material balance of (2), one arrives at an expression relating the total xanthate concentration to xanthic acid concentration, all measured at zero time

$$(X_T) = (HX)[1.059 + 6.48(H^+) + 0.0235/(H^+)] \qquad (5)$$

For acid normalities of 1.0, this would predict that only a fraction (13%) of the total xanthate exists in the xanthic acid form. Yet experimentally, the extrapolation data (Table III) show that the xanthate concentration is accounted for on the basis of the sum of equation 1a and 1b. The material balance could only be reconciled if the rather tenuous assumption were made that the ion-pair, the protonated acid, and the undissociated xanthic acid all had identical spectra. However, even if this assumption were accepted, the magnitude of the equilibrium constant, K_2, (2.51) would predict that the majority of the xanthate in dilute to intermediate acid levels were in the form of a stable ion-pair, which again leads to an improbability.

TABLE IV

COMPARISON OF CALCULATED AND EXPERIMENTAL SOLUTIONS TO EQUATION 6

HCl, N	k_{exp}, sec.$^{-1}$	k_{exp} (calcd.), sec.$^{-1}$
0.0199	0.00348	0.00348
.0995	.00627	.00623
.2985	.00700	.00717
.4975	.00720	.00720
.6965	.00688	.00698
.8840	.00653	.00662
1.194	.00585	.00585

It should be noted that, assuming that the protonated acid is in equilibrium with the undissociated acid rather than the ion-pair as shown the derivation results in an expression mathematically equivalent to equation 3.

The second mechanism to be considered is based on a generalized reaction scheme using the basic postulates of the transition state theory. One assumes here that, in addition to the experimentally verified equilibrium involving the xanthic acid and its anion, there is another equilibrium between the reactants (X^-) and (H^+), and some activated complex of indeterminate nature (M), the latter decomposing to form the products, C_2H_5OH and CS_2. The system is described by

$$\begin{array}{l} (X^-) + (H^+) \overset{K_1}{\rightleftharpoons} (HX) \\ \quad K^{\ddagger} \uparrow\downarrow \\ \quad (M) \longrightarrow \text{Products} \end{array}$$

where

$$K^{\ddagger} = \frac{(M)f_M}{(X^-)(H^+)f_{H^+}f_{X^-}} \text{ and } K_i = \frac{(X^-)h_-}{(HX)}$$

The rate expression is given by

$$\text{rate} = -d(X_T)/dt = \frac{RT}{Nh}(M) = k'(X^-)(H^+)\frac{f_{X^-}f_{H^+}}{f_M} \qquad (6)$$

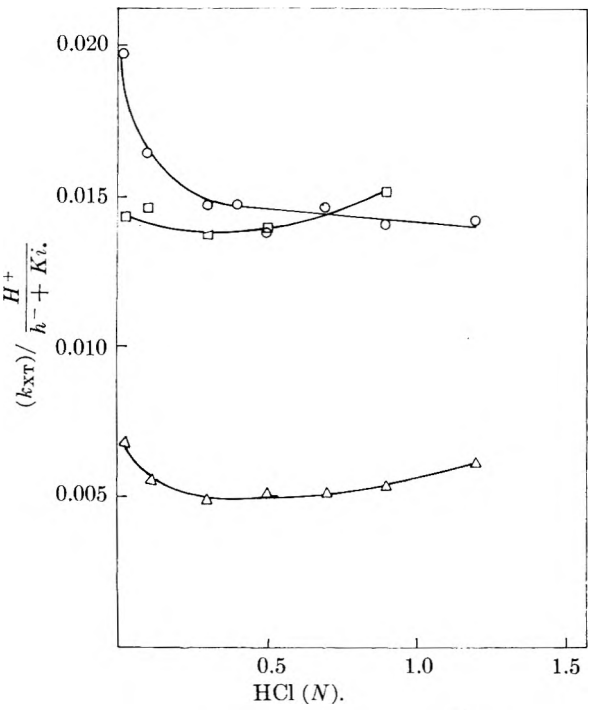

Fig. 4.—Plot of $\frac{k_{XT}}{H^+/(h^- + Ki)} \equiv k'Ki\,\frac{f_{X^-}f_{H^+}}{f_M}$ *vs.* HCl normality: ○, 10°; □, 10°, $[Cl^-] = 0.9\ M$; △, 0°.

Introduction of the material balance $(X_T) = (X^-) + (HX)$, integration, and equating with the experimental rate constant, k_{exp}, leads to

$$k_{exp} = \frac{k'K_i(H^+)f_{X^-}f_{H^+}}{(K_i + h_-)f_M} \qquad (7)$$

The right side of equation 7 shows a maximum when plotted against (H^+), without requiring the postulate of a protonated acid species; it results from the divergence of (H^+) and h_- values at high acid concentration.

In Fig. 4, the ratio $k_{exp}/(H^+)/h_- + K_i$ is plotted against N_{HCl}; the linearity is found to be good at $N_{HCl} > 0.1$ and remarkably independent of the acid strength. One concludes that the neglect of the activity coefficient ratio does not lead to gross error at the higher ionic strength and, consequently, this ratio is not highly sensitive to the latter (*cf.* $\log f_M = \log f_{X^-} + \log f_{H^+}$). The criteria for the mechanism on this basis therefore reduce to the question of what must the structure of (M) be to predict that the activity ratio coefficient should be independent of ionic strength.

One can begin by assuming that (M) is identical to (HX). There are several objections to this position, beginning with the observation that the ΔH value for ionization and the activation energy, E_a, differs by an order of magnitude in contrast to the expectation that they would be closely related if the initial hypothesis were valid. If, however, it is further assumed that (M) is a collision energized form of (HX), the contrary argument must take the following rationale: the activation of (HX) to (M) would not be expected to result in a change in electrolyte character and, consequently, $f_{HX} = f_M$, which when combined with equation 7, leads to

$$k_{exp} = \frac{k'K_ih_-}{K_i + h_-} \qquad (8)$$

The right side of equation 8 does not show a maximum as a function of (H^+), and thereby contradicts the experimental facts.

Considerations of several other mechanistic possibilities using the criteria of pseudo-first order kinetics, and maximum in the rate constant curve, have led to the tentative conclusion that the most probable form of (M) is that postulated by Lewis,[3] the ion-pair complex

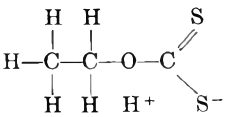

This hypothesis demands that the equation

$$\log f \text{ ion pair} = \log f_{X^-} + \log f_{H^+} \qquad (9)$$

be substantiated by theory, as it is in experimental fact.

A more obvious proof of the mechanism must await isotope studies to elucidate the exact nature of the transition complex.

Acknowledgment.—We wish to express our appreciation to Drs. Bamford, Ballard, Gray and Totman for making their work available to us, and for informative discussions and correspondence. We also wish to thank Mr. John Wharton, Director of Research, and members of the Board of Courtaulds, Inc., for permission to publish.

KINETIC ISOTOPE EFFECTS IN THE REACTION OF METHYL RADICALS WITH ETHANE, ETHANE-d_6 AND ETHANE-1,1,1-d_3

BY J. R. MCNESBY

National Bureau of Standards, Washington, D. C.

Received May 2, 1960

Photolyses of acetone-d_6 in the presence of a mixture of C_2H_6 and C_2D_6 and in the presence of CH_3CD_3 were carried out to measure kinetic isotope effects for the reactions: (1) $CD_3 + C_2H_6 \rightarrow CD_3H + C_2H_5$; (2) $CD_3 + CH_3CD_3 \rightarrow CD_3H + CH_2CD_3$; (3) $CD_3 + CH_3CD_3 \rightarrow CD_4 + CH_3CD_2$; (4) $CD_3 + C_2D_6 \rightarrow CD_4 + C_2D_5$. The conclusions drawn from the results is that the relative rate constants are within experimental error: $k_1/k_4 = \exp(1500/RT)$; $k_2/k_3 = 0.73 \exp(1900/RT)$; $k_1/k_2 = 1.95 \exp(100/RT)$.

The objective of the present study was to evaluate with precision the kinetic parameters of the reactions

$$CD_3 + C_2H_6 \longrightarrow CD_3H + C_2H_5 \quad (1)$$
$$CD_3 + CH_3CD_3 \longrightarrow CD_3H + CH_2CD_3 \quad (2)$$
$$CD_3 + CH_3CD_3 \longrightarrow CD_4 + CH_3CD_2 \quad (3)$$
$$CD_3 + C_2D_6 \longrightarrow CD_4 + C_2D_5 \quad (4)$$

The kinetics of the above reactions were obtained relative to those for the reaction

$$CD_3 + CD_3COCD_3 \longrightarrow CD_4 + CD_2COCD_3 \quad (5)$$

whose kinetics are known.[1,2] Reaction 1 has been studied[3,4] as well as the CH_3 analogs of (2), (3)[5] and (4).[3,6] However, no comparative study has appeared in which the kinetics of (1) through (4) could be intercompared. The work was divided into two parts; the photolysis of acetone-d_6 in the presence of mixtures of C_2H_6 and C_2D_6 and the photolysis of acetone-d_6 in the presence of CH_3CD_3.

For the photolysis of acetone-d_6 in the presence of ethane + ethane-d_6

$$[CD_4]/[CD_3H] = (k_5[Ad_6])/(k_1[E]) + (k_4[Ed_6])/(k_1[E]) \quad (1)$$

Since the quantity $(k_5[Ad_6])/(k_1[E])$ is known very accurately,[3,4] evaluation of k_4/k_1 is obtained by measurement of $[CD_4]/[CD_3H]$. Evaluation of k_4/k_1 at a number of temperatures permits A_4/A_1, and E_4-E_1 to be calculated from the expression

$$\frac{k_4}{k_1} = \frac{A_4}{A_1} \exp\left(\frac{E_1 - E_4}{RT}\right) \quad (2)$$

The photolysis of acetone-d_6 in the presence of CH_3CD_3 produces methane so that

$$[CD_4]/[CD_3H] = (k_5[Ad_6])/(k_2[Ed_3]) + k_3/k_2 \quad (3)$$

A plot of $[CD_4]/[CD_3H]$ *vs.* $[Ad_6]/[Ed_3]$ gives k_5/k_2 and k_3/k_2 from the slope and intercept, respectively.

Experimental

The light source was the full arc of a Hanovia medium pressure mercury lamp. A cylindrical fused silica reaction vessel 4 × 4 cm. was placed in the center of a hollowed five inch aluminum cylinder. The latter was fitted with two quartz windows on one end and was heated electrically. Temperature gradients across the reaction vessel varied from about two degrees at the lowest to five degrees at the highest temperature. The average temperature was used in all calculations.

The entire system was fitted with brass bellows valves and contained no stopcocks or grease. The acetone-d_6, ethane-d_6 and ethane-d_3 were obtained from Merck, Ltd., Montreal and were specified 98% [D/(D + H)] in the $-CD_3$ positions. Ethane was Phillips research grade material and contained 0.05% ethylene.

Purity of C_2D_6.—The C_2D_6 contained 6.5% C_2D_5H and $[C_2D_6]$ is considered to mean $[C_2D_6] + [C_2D_5H]$. No correction was applied for the CD_3H arising from abstraction of H from C_2D_5H by CD_3. There was no CD_4 or CD_3H present in the C_2D_6. Ethylene was present to the extent of 0.05%.

Purity of CH_3CD_3.—The CH_3CD_3 contained about 1% CD_4 + CD_3H. Since the reactions which produced CD_4 and CD_3H were to be carried out to only a few hundredths per cent. destruction of ethane, this impurity was prohibitively high. In order to remove the last traces of CD_3H and CD_4 from CH_3CD_3, it was necessary to add CH_4, freeze, pump, melt, freeze, pump, melt, etc. for several days. Finally nitrogen was added and the procedure repeated to remove as much CH_4 as possible. The final ethane-d_3 was found by gas chromatography to contain 1.4% CH_4 and 0.5% N_2. No CD_4 or CD_3H was detectable on the mass spectrometer. In addition an ethylene impurity of 1% was found and was considered to have no effect on the results.

Mixtures were made up in reservoirs by adding an appropriate amount of CD_3COCD_3 to the $C_2H_3D_3$ or C_2H_6 + C_2D_6 mixture and allowing to mix overnight. After the required number of photolyses and analyses had been made on representative samples of this mixture, at different temperatures, more CD_3COCD_3 was added to the reservoir and a second series of photolyses and analyses were run on the new mixture. A third mixture was prepared similarly in the reservoir and photolyses carried out as before. In this way the $[C_2H_6]/[C_2D_6]$ ratio was kept constant while [acetone-d_6]/$[C_2H_6]$ was varied. After terminating a reaction, the whole reaction mixture was Toepler-pumped through a double-U trap at 77°K. and into a sample flask for mass spectrometric analysis. The sample flask thus contained only carbon monoxide, methane and very small amounts of hydrogen. The mass ratio 20/19 gave directly $[CD_4]/[CD_3H]$. Masses 19 and 20 were rescanned 6 times and average ratios were used.

A small amount of the CD_3H came from the acetone-d_5 impurity. Acetone-d_6 was photolyzed alone at 280 and 420°. The $[CD_3H]/[CD_4]$ ratio was, in both cases, 0.04 and is a measure of the acetone-d_5 contained in the acetone-d_6. Corrections of CD_3H formed from mixtures of CD_3COCD_3, C_2D_6 and C_2H_6 were made on the basis that to a first approximation all CD_3H came from reaction 1 and the CD_4 from 5 could be calculated, since $(k_5[Ad_6])/(k_1[C_2H_6])$ is known. Now, 4% of the CD_4 from reaction 5 was subtracted from the total CD_3H as the contribution of the acetone-d_5 impurity. The quantity $[CD_3COCD_3]$ here means $[CD_3COCD_3] + [CD_2HCOCD_3]$. A similar correction was made to CD_3H in the acetone-d_6–ethane-d_3 system except that k_1/k_2 was assumed to be equal to 2.0 and independent of temperature. That this correction is justified is borne out by the results to be described.

Results

A. The CD_3COCD_3–C_2H_6–C_2D_6 System.—The quantity $(k_5[Ad_6])/(k_1[E])$, having been precisely measured over a temperature range,[3,4] can be subtracted from $[CD_4]/[CD_3H]$ and k_4/k_1 evaluated.

(1) J. R. McNesby, T. W. Davis and A. S. Gordon, *J. Am. Chem. Soc.*, **76**, 823 (1954).

(2) J. R. McNesby and A. S. Gordon, *ibid.*, **76**, 1416 (1954).

(3) J. R. McNesby and A. S. Gordon, *ibid.*, **77**, 4719 (1955).

(4) M. H. J. Wijnen, *J. Chem. Phys.*, **23**, 1357 (1955).

(5) F. O. Rice and T. A. Vanderslice, *J. Am. Chem. Soc.*, **80**, 291 (1958).

(6) F. O. Rice and R. E. Varnerin, *ibid.*, **77**, 221 (1955).

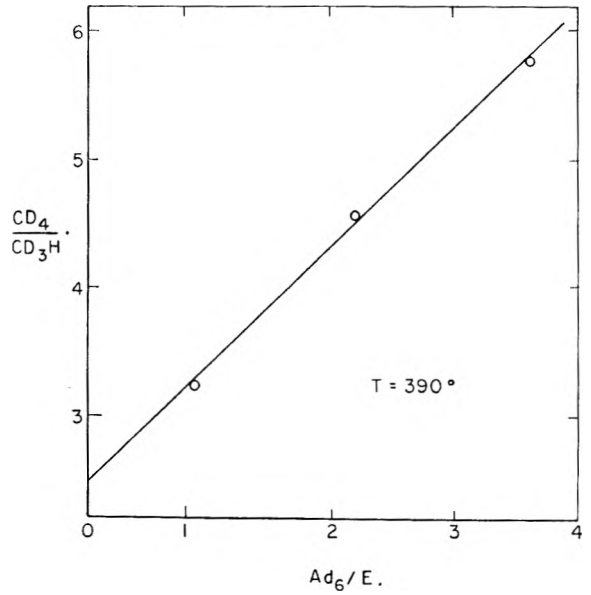

Fig. 1.—Demonstration of linearity of CD_4/CD_3H *vs.* Ad_6/E for the system acetone-d_6–ethane–ethane-d_6; ethane/ethane-d_6 = 0.137.

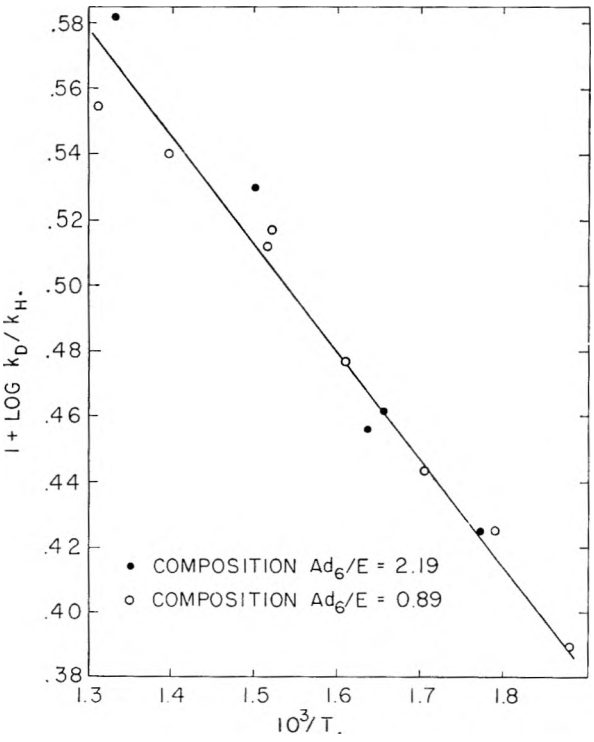

Fig. 2.—Arrhenius plot for isotope effect in reaction of methyl-d_3 radical with C_2H_6 and C_2D_6.

The product ratio $[CD_4]/[CD_3H]$ was measured at a constant $[C_2H_6]/[C_2D_6]$ ratio and at three different $[Ad_6]/[E]$ ratios. Other methanes CH_2D_2, CH_3D and CH_4 were looked for and found to be absent over the entire temperature range.

The most meaningful measurements are those at low $[Ad_6]/[E]$, since here the CD_4 comes mainly from abstraction from C_2D_6. At the highest of the three ratios the precision of k_4/k_1 is poor and experiments on this mixture were only used to demonstrate the linearity of the $[CD_4]/[CD_3H]$ *vs.* $[Ad_6]/[E]$ plot (Fig. 1). The thirteen measurements made on mixtures I and II (Table I) were used in the evaluation of k_1 and k_4 and are shown in the Arrhenius plot in Fig. 2 where the drawn line is for the $C_2H_6 + C_2D_6$ system. The slope and intercept were measured by a least mean squares calculation and the values obtained are $E_4 - E_1 = 1.47 \pm 0.05$ kcal. and $A_4/A_1 = 1.0 \pm 0.2$.

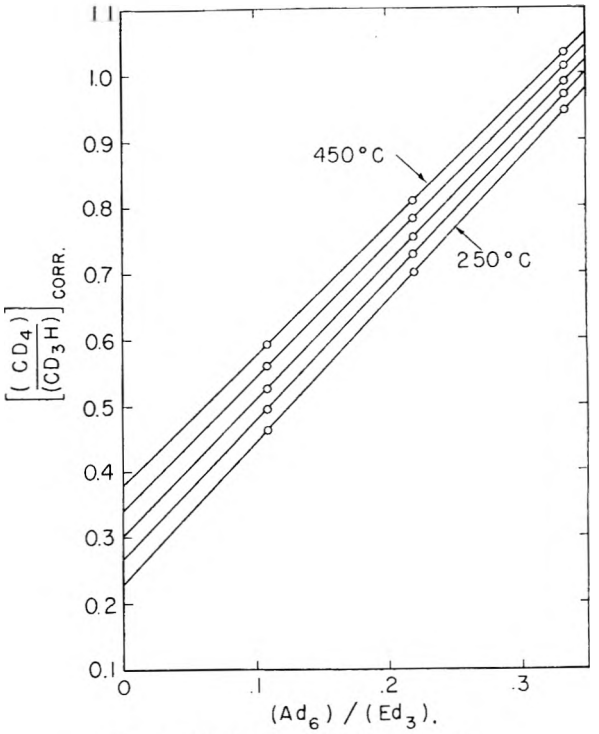

Fig. 3.—Evaluation of k_5/k_2 and k_3/k_2.

B. The $CD_3COCD_3 + CD_3CH_3$ System.—Since none of the rate constants in the CD_3CH_3 experiments were known relative to k_5, direct application of equation 3 was required for the evaluation of all relative rate constants.

In order to know the ratios $[CD_4]/[CD_3H]$ at the same temperature but at three compositions it is necessary to interpolate in the experimental data. For this reason, plots were made for each of the three mixtures of $[CD_4]/[CD_3H]$ *vs.* T. For the purposes of interpolation the best smooth curves were drawn through the data and all subsequent data used for analysis were taken directly from these curves. Experimental precision is such that a maximum error of 1% in any of the sixteen $[CD_4]/[CD_3H]$ ratios would place it directly on the appropriate curve. The data are presented in Table II and obedience to equation 3 is shown in Fig. 3. The plot of $1 + \log k_3/k_2$ *vs.* $1/T$ included in Fig. 4 gives $E_3 - E_2 = 1.87 \pm 0.05$ kcal. and $A_3/A_2 = 1.4 \pm 0.2$. Analysis of the slopes of the plots of equation 3 gives $A_5/A_2 = 1.6$ and $E_2 - E_5 = 0.3$.

Discussion

While least mean squares calculation of the probable errors in the ratio of A factors and Δ (activation energy) produces the illusion of great precision, the fact is that a systematic error of $\pm 2\%$ in the measurement of k_3/k_2 can give an error of $\pm 40\%$ in A_3/A_5 and $\pm 25\%$ in Δ(activation energy). It is, therefore, questionable to attach significance to differences of the indicated magnitudes. It is perhaps more instructive to weigh the sum of the evidence. For the reaction of CD_3 with acetone,[1,2] *s*-*n*-butane,[7] $C_2H_6 + C_2D_6$ and CH_3CD_3 the values of A_D/A_H are 1.25, 1.65, 1.00 and 1.38. It is possible that A_D/A_H generally exceeds unity. If departure from unity is real, quantum mechanical tunnelling may provide an explanation. Tunnelling would be expected to give departures of A_D/A_H from unity

(7) J. McNesby and A. Ceider, *J. Am. Chem. Soc.*, 78, 1170 (1956).

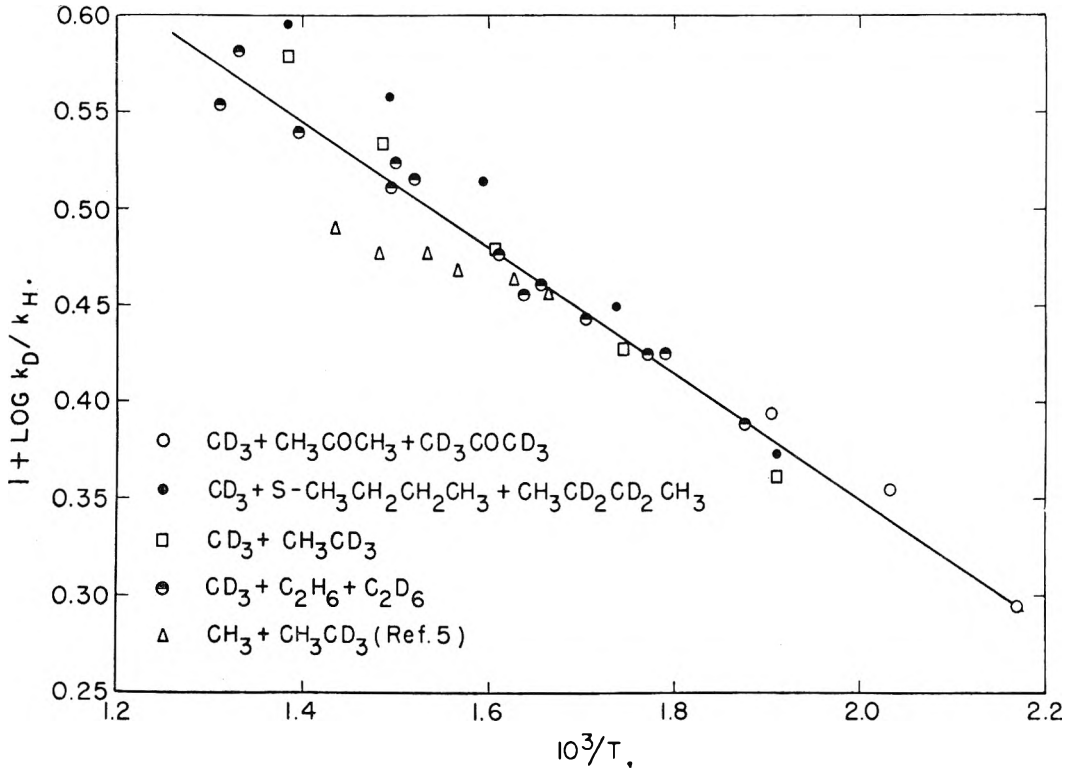

Fig. 4.—Isotope effect for reaction of methyl-d_3 radicals.

TABLE I

PHOTOLYSIS OF ACETONE-d_6 IN THE PRESENCE OF ETHANE AND ETHANE-d_6 (E/E_d = 0.137)

T, °C.	$\frac{[CD_4]}{[CD_3H]}$ obs.	k_6/k_1	$\frac{k_5[Ad_6]}{k_1[E]}$	$\frac{[CD_4]}{[CD_3H]}$ corr.
	Mix I: Ad_6/E = 0.89			
260	2.56	1.01	0.90	2.66
286	2.65	1.00	.89	2.75
314	2.75	0.99	.88	2.85
349	2.90	.99	.88	3.00
385	3.07	.97	.86	3.18
396	3.03	.96	.85	3.14
444	3.17	.95	.85	3.28
490	3.24	.94	.84	3.35
	Mix II: Ad_6/E = 2.19			
290	3.72	1.00	2.19	4.08
331	3.85	0.99	2.17	4.22
338	3.81	.99	2.17	4.17
393	4.07	.96	2.10	4.44
487	4.30	.94	2.06	4.68
	Mix III: Ad_6/E = 3.62			
277	4.33	1.00	3.62	5.06
294	4.33	1.00	3.62	5.06
310	4.59	0.99	3.58	5.36
339	4.59	.99	3.58	5.36
387	4.89	.97	3.51	5.69
392	4.90	.96	3.48	5.69
422	4.92	.95	3.44	5.71
428	4.92	.95	3.44	5.71
482	5.09	.94	3.40	5.89

in the observed direction and also give anomalously large values for E_D–E_H. However, the temperature of the present experiments seems too high to permit tunnelling to be important.

TABLE II

PHOTOLYSIS OF ACETONE-d_6 IN THE PRESENCE OF CH_3CD_3

T, °C.	$[CD_4]/[CD_3H]$ obsd.	$[Ad_6]/[Ed_3]$	$[CD_4]/[CD_3H]$ corr.
290	0.485	0.109	0.489
328	.511	.109	.515
344	.527	.109	.531
396	.550	.109	.554
462	.595	.109	.600
266	.700	.221	.712
270	.704	.221	.716
337	.736	.221	.749
393	.760	.221	.773
433	.787	.221	.800
464	.810	.221	.824
270	.926	.334	.950
307	.954	.334	.979
347	.960	.334	.985
403	.981	.334	1.007
459	1.014	.334	1.040

The view can also be taken that departures of A_D/A_H from unity merely reflect experimental error. If it is assumed that $A_D/A_H = 1$, an additional point at $1/T = 0$ is available for the Arrhenius plot. If a straight line is drawn through this point and the experimental points, the slope gives Δ (activation energy). It is interesting that when the data for the attack of CD_3 radicals upon C_2H_6 + C_2D_6, CH_3CD_3, CD_3COCD_3 + CH_3COCH_3, CH_3-$CH_2CH_2CH_3$ + $CH_3CD_2CD_2CH_3$ (secondary attack) are plotted, a single line can be drawn which may be within experimental error for all of these systems. This is shown in Fig. 4. The slope of the line corresponds to 1.50 kcal. for $E_D - E_H$. It is thus possible to predict k_D/k_H for any of the above systems at any temperature by the expression

Table III

Summary of Isotope Effects

Reaction	Experimental E, kcal.	Experimental A, mole^{-1} cc. sec.$^{-1}$	Assumption: $A_D/A_H = 1$ E, kcal.	Assumption: $A_D/A_H = 1$ A, mole^{-1} cc. sec.$^{-1}$
$CD_3 + C_2H_6 \rightarrow CD_3H + C_2H_5$	11.5	$4.3 \times 10^{10}T^{1/2}$	11.5	$4.3 \times 10^{10}T^{1/2}$
$CD_3 + C_2D_6 \rightarrow CD_4 + C_2D_5$	13.0	$4.3 \times 10^{10}T^{1/2}$	13.0	$4.3 \times 10^{10}T^{1/2}$
$CD_3 + CH_3CD_3 \rightarrow CD_3H + CH_2CD_3$	11.6	$2.2 \times 10^{10}T^{1/2}$	11.5	$2.2 \times 10^{10}T^{1/2}$
$CD_3 + CH_3CD_3 \rightarrow CD_4 + CH_3CD_2$	13.5	$3.0 \times 10^{10}T^{1/2}$	13.0	$2.2 \times 10^{10}T^{1/2}$

$$k_D/k_H = \exp[-1500/(RT)] \quad (4)^a$$

The experimental values obtained in this work, together with values obtained on the basis of the above argument are given in Table III.

It is appropriate to comment on the paper of Rice and Vanderslice[5] in which a study was made of the isotope effect for the reactions.

$$CH_3 + CH_3CD_3 \longrightarrow CH_3D + CH_3CD_2 \quad (7)$$

$$CH_3 + CH_3CD_3 \longrightarrow CH_4 + CH_2CD_3 \quad (8)$$

The quantity E_7–E_8 was found to be 0.6 kcal. Since this value is in very poor agreement with the present work, possible sources of the disagreement must be sought. In the work of Rice and Vanderslice, one part of $CH_3N_2CH_3$ was decomposed in the presence of 100 parts of CH_3CD_3 and, under these conditions, k_7/k_8 is given directly by $[CH_3D]/[CH_4]$ in the products. The important assumption was that the reaction

$$CH_3 + CH_3N_2CH_3 \longrightarrow CH_4 + CH_2C_2CH_3 \quad (9)$$

is negligibly slow. Evidence cited in support of this assumption consists of the observation that changing the concentration of aomethane from 1–5% produced an error of only 0.3 kcal. in E_7–E_8. However, certain other evidence indicates that it might have been occurring to an important degree. First, only minor deviations from $A_D/A_H = 1$ are to be expected, while the extrapolated value of Rice and Vanderslice gives $A_D/A_H = 0.48$. The ratio of rates of reactions 9 and 8 can be calculated from known rate constants[8] and the assumption that k_8 has the same kinetics as reaction 2. This calculation reveals that reaction 9 must have been proceeding from 13 to 22% as fast as (8) under the conditions of the experiments. Further objection to the values obtained by Rice and Vanderslice is seen by extrapolation of k_D/k_H for attack of CH_3 on CH_3CD_3, $CH_3CD_2CH_3$ and $(CH_3)_3CD$ which gives $A_D/A_H = 0.48$, 0.22 and 0.31, respectively, on a per atom basis. These deviations from unity are uniformly in the direction of too much H abstraction and can be understood if an extraneous source of CH_4 is present.

Two investigations of the reaction

$$CH_3 + C_2D_6 \longrightarrow CH_3D + C_2D_5 \quad (10)$$

have been reported with widely differing results.[3,6]

It is possible to compare (10) with (1)

$$CD_3 + C_2H_6 \longrightarrow CD_3H + C_2H_5 \quad (1)$$

for each of the reported studies. According to the results of Rice and Varnerin[6]

$$k_{10}/k_1 = 0.46e^{+300/RT}$$

while according to McNesby and Gordon

$$k_{10}/k_1 = 3.6e^{-3300/RT}$$

Although these two results are in very poor agreement, the high temperature measurement of k_{10}/k_1, in each case, is probably within experimental error of the value predicted by

$$k_D/k_H = \exp[-1500/(RT)]$$

Judging by the large deviations of A_{10}/A_1 from unity it is probable that both studies were subject to systematic errors of unknown origin. While it is possible that CH_3 and CD_3 exhibit very different kinetic behavior, this seems unlikely in view of evidence obtained in other systems. A comparison has been made for the reactions[2]

$$CH_3 + CH_3COCH_3 \longrightarrow CH_4 + CH_2COCH_3 \quad (11)$$

$$CD_3 + CH_3COCH_3 \longrightarrow CD_3H + CH_2COCH_3 \quad (12)$$

and for

$$CD_3 + CH_4 \longrightarrow CD_3H + CH_3^9 \quad (13)$$

$$CH_3 + CH_4 \longrightarrow CH_4 + CH_3^{10} \quad (14)$$

No difference could be detected in the kinetics of (11) and (12) while at 625°K., $k_{14}/k_{13} = 0.6$.

[a] Herck and Szwarc, *J. Am. Chem. Soc.*, **82**, 3558 (1960), have obtained for abstraction of H and D from $C_6H_5CHDCH_3$, $k_H/d_D = 1.28 \exp(-1560/RT)$. This agrees with equation 4 within their experimental error.

(8) P. Ausloos and E. W. R. Steacie, *Can. J. Chem.*, **33**, 31 (1955).

(9) J. R. McNesby and A. S. Gordon, *J. Am. Chem. Soc.*, **76**, 4196 (1954).

(10) F. S. Dainton, K. J. Ivin and F. Wilkinson, *Trans. Faraday Soc.*, **55**, 929 (1959).

THE SOLUBILITY OF QUARTZ

BY J. A. VAN LIER, P. L. DE BRUYN[1] AND J. TH. G. OVERBEEK[2]

Department of Metallurgy, Massachusetts Institute of Technology, Cambridge 39, Mass.

Received May 2, 1960

The surface structure of finely ground quartz particles, ranging in size from 1 to 50 μ, was studied by dissolution measurements in NaOH solutions. The results indicate the presence of a disturbed surface layer. The thickness of this layer is estimated to be approximately 300 Å., a result agreeing with values reported by other workers. After removal of this disturbance, the solubilities of quartz in H_2O, 10^{-2} *N* NaCl solutions and 10^{-2} *M* borax solutions were measured at temperatures ranging from 60 to 100°. The solubility of quartz in H_2O at these temperatures is shown to be in good agreement with the solubilities above 180° as measured by Kennedy.[3] The solubility of quartz in H_2O follows the empirical equation, $\log c = 0.151 - 1162/T$ (*c* expressed in moles of SiO_2 per kg.) from 25 up to 473°. The extrapolated solubility at 25° is 1.8×10^{-4} mole/kg. The standard heat, the standard entropy and the standard free energy of the dissolution reaction were calculated The rate constant of the dissolution reaction at 25° is of the order of 10^{-18} g. of SiO_2 per cm.^{2} surface per second. The rate of dissolution is not controlled by diffusion. The reaction is strongly accelerated by the presence of NaCl in concentrations below 10^{-1} *N*, without any measurable effect on the position of the equilibrium. If 10^{-1} *N* NaCl is used, the solubility increases in addition to the increase in reaction velocity.

Introduction

Only a few measurements of the solubility of quartz at room temperature are reported in the literature. Gardner[4] mentions a value of 1×10^{-4} mole/kg. without specification of method and particle size. Lenher[5] gives a value of 5×10^{-3} mole/kg. for particles of 4 μ in diameter. Paterson and Wheatly[6] found a constant concentration of 1.8×10^{-4} mole/kg. for an HF-treated quartz sample (0.5–2 μ in diameter) after successive leachings with Ringer's solution[7] at 37°. They expected this value to be close to the solubility of quartz. Kennedy[3] concluded from his measurements in the hydrothermal temperature range that quartz is essentially insoluble at room temperature. Stöber[8] and Baumann[9] consider the dissolution of quartz in water at room temperature as an irreversible process. In the opinion of these authors, the only species participating in the equilibrium is silica gel. For this hypothesis to be true, quartz would have to be less stable thermodynamically than silica gel. No experimental evidence is found in the literature supporting this hypothesis.

Several authors in the field of silicosis research have worked with fine quartz dust. Gibb[10] and co-workers presented evidence for the existence of a layer of highly disordered structure on the surface of finely ground quartz particles. Their estimate of the thickness of this layer is about 300 Å. The presence of a disturbance of considerable depth on the ground quartz particles was also concluded by others.[11–18]

Experimental

Materials.—Large colorless crystals of Brazilian quartz were crushed. Material finer than 3 mm. in diameter was screened out and discarded. Further reduction was carried out in a roll crusher. The fraction containing particles between 3 and 0.5 mm. was collected and kept for fine grinding. This fraction was cleaned repeatedly in hot 1 *N* HCl solution and washed free from HCl with distilled water. The final grinding was carried out between two fused silica discs of optical quality. The ground quartz was sized by sedimentation in distilled water. The sized material was dried at 110°.

For the preliminary studies at room temperature three size ranges of quartz were used; 1–5, 5–25 and 25–50 μ with respective specific surfaces of 21,500, 3400 and 1150 cm.^{2}/gram. The studies at elevated temperatures were made with narrower size ranges; 3–5, 5–10 and 10–15 μ with respective surfaces of 10,000, 5000 and 3200 cm.^{2}/gram. The surface area measurements[19] were obtained by the B.E.T. method with krypton gas as adsorbate. The determinations were made at −195° and a value of 19.5 Å.^{2} was used for the cross-sectional area of the krypton molecule.

In the initial phase of this work the quartz was used without any further treatment. In later stages of this investigation some additional treatments were necessary. These additional treatments will be referred to as Methods I and II. Method I consisted of washing the quartz with an HF solution. The strength of the solution (9–15% HF by weight) and the amount of quartz (up to 10 g. per 50 ml. of HF solution) were chosen such that approximately 25% of the quartz was dissolved within 5 minutes. The HF was removed by successive washings with NaOH solutions of decreasing strength (0.1, 0.01 and 0.001 *N*). The NaOH was removed by repeated washings with conductivity water and then the quartz was dried in a vacuum desiccator over P_2O_5. Method II included the HF treatment of Method I followed by agitation of the quartz in 0.1 *N* NaOH at 90° for 20 to 30 days until a constant SiO_2 concentration independent of particle size and amount of quartz was reached. The NaOH was removed by washing the quartz with conductivity water. The specific surface of the quartz decreased as a result of this further treatment, values of 7500, 3600 and 2300 cm.^{2}/g. were obtained for the 3–5, 5–10 and 10–15 μ size ranges, respectively.

All chemicals used were of reagent grade and with the exception of NaCl were not further purified. The NaCl used in the dissolution rate experiments was further purified by precipitating it from a near-saturated solution in conductivity water by the addition of absolute alcohol. Double

(1) Associate Professor of Metallurgy, M.I.T., Cambridge 39, Mass.

(2) Visiting Professor of Chemistry, University of Southern California, Los Angeles.

(3) G. C. Kennedy, *Econ. Geol.*, **45**, 629 (1950).

(4) L. U. Gardner, *Mining Technology*, **2**, A.I.M.E. Techn. Publ. 929.

(5) V. Lenher, *J. Am. Chem Soc.*, **43**, 391 (1921).

(6) M. S. Paterson and K. H. Wheatly, Safety in Mines Research Establishment, Research Report Number 124 (Dec. 1955).

(7) Ringer's solution is made up of a solution of chlorides of potassium, sodium, calcium and magnesium in concentrations comparable to those in blood. Paterson and Wheatly added dimethylglyoxaline to keep the *p*H at 7.4.

(8) W. Stöber, *Kolloid-Z.*, **147**, 131 (1956).

(9) H. Baumann, "Beiträge zur Silikose-Forschung," Heft 37 (Bochum 1955).

(10) J. Gibb, P. D. Ritchie and J. W. Sharpe, *J. Appl. Chem. (London)*, **3**, 182 (1953).

(11) A. F. Boyer, *Bull. soc. franc. mineral. et cryst*, **77**, 116 (1954).

(12) R. L. Gordon and G. W. Harris, *Nature*, **175**, 1135 (1955).

(13) A. J. Beal and A. L. Godbert, Safety in Mines Research Establishment, Research Report Number 115 (1955).

(14) R. Tregan, *Compt. rend.*, **241**, 219 (1955).

(15) O. S. Heavens, *Acta Cryst.*, **6**, 571 (1953).

(16) G. S. Khodakow and E. R. Plutsis, *Dokl. Akad. Nauk. S.S.S.R.* **123**, 725 (1958).

(17) M. Cignitti and A. Uva, *Ricerca Sci.*, **28**, 1915 (1958).

(18) J. A. Waddams, *Research (London)*, **11**, 370 (1958).

(19) These measurements were made by Mr. S. Mitchell of the Metallurgy Department at MIT.

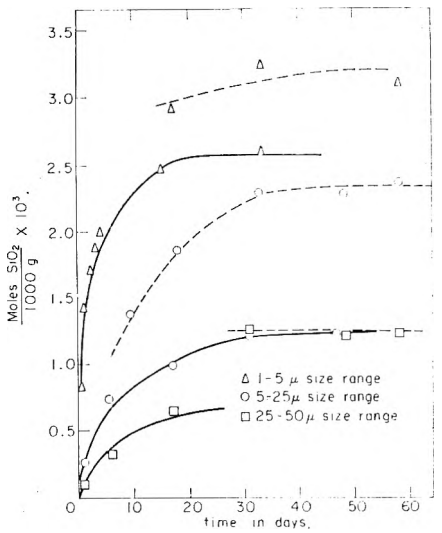

Fig. 1.—Dissolution rate of quartz in 10^{-3} N NaOH at 25°.

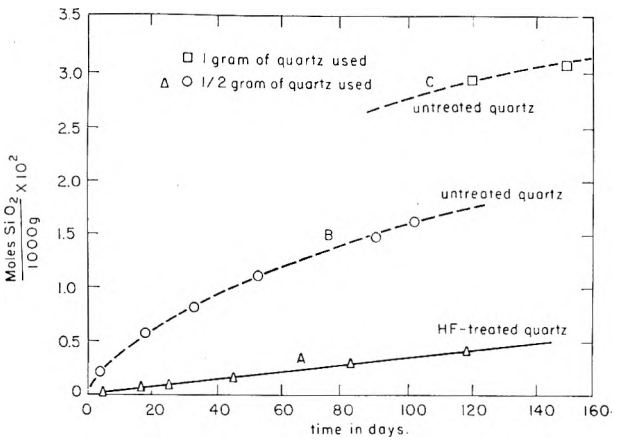

Fig. 2.—Dissolution rate of 1–5 μ quartz particles in 10^{-1} N NaOH at 25°.

distilled water of a specific conductance lower than 5×10^{-7} ohm^{-1}cm.$^{-1}$ was used throughout the work.

Polyethylene bottles of 35-ml. capacity were used for the measurements at room temperature. At higher temperatures a stainless steel tube, 80 mm. long, 25 mm. in diameter and 3.75 mm. thick was used. These cylinders were fitted with Pt tubes of 0.125 mm. thickness A vapor-tight seal on these containers was obtained as follows: the Pt-liner had a flange resting on the wall of the stainless steel container, a thin Pt–Ruthenium ring (diameter 0.125 mm.; 5% Ru) was soldered onto this flange with pure gold, then the top of the container was covered with a thin disc of pure gold (thickness 0.0075 cm.) and a Teflon disc was placed on top of the gold disc. Thus upon tightening the stainless steel screw cap the ring pressed the gold into the Teflon and a perfect seal was obtained. The reaction vessels were attached to stainless steel racks which were placed on the bottom of the constant temperature water or oil-baths. The assemblage was rotated at a constant speed of 30 r.p.m.

The *p*H-measuring Cell.—The cell consisted of a 1-liter Pyrex beaker filled with saturated (at 25°) KCl solution, containing the calomel reference electrode. A small wide-mouthed polyethylene bottle (Ziegler-type) was suspended in the KCl solution. This bottle served as compartment for two platinized Pt electrodes. Thus the solution of which the *p*H had to be measured did not come in contact with glass. The two solutions were in electrical contact through a small hole (0.015 cm.) in the bottom of the polyethylene bottle. To ensure a flow of KCl into the solution to be measured, the level of the KCl solution was always kept approximately 0.5 cm. higher than the level of the solution inside the hydrogen electrode compartment. The hydrogen was purified by bubbling it through two wash bottles filled with alkaline pyrogallol, one wash bottle containing chromous chloride dissolved in 1.5 N HCl in contact with Zn-amalgam, one wash bottle containing 37% KOH solution and finally through two wash bottles filled with conductivity water. From here the H_2 was led into the measuring cell *via* a copper spiral 3 meters in length, immersed in the constant temperature bath.

The cell was calibrated by using a $10^{-2}M$ borax solution for which the *p*H was determined by Bates[20] from 0 to 95°.

Experimental Techniques.—The procedure used in making solubility measurements was straight-forward. The amounts of quartz used in the experiments were varied but approximately 30 g. of solvent was used in most experiments except in those tests with large amounts of quartz when the quantity of solution was slightly reduced. It should be mentioned that at elevated temperatures more than one sample was taken from the same Pt-lined steel container for analysis. Some time before a sample was to be taken, the container was removed from the agitator and placed on the bottom of the constant temperature bath to allow the quartz to settle at the measuring temperature. Then the container was removed from the bath, a sample (0.5–1.5 g.) was taken and the container was returned to the bath.

Analytical Method.—The amount of silica in solution was determined colorimetrically by the molybdenum blue method. For the formation of the yellow silica–molybdate complex the recommendations of Strickland[21] were followed. The yellow complex was reduced by an acidic-metol-sulfite solution. This method of reduction was developed by Mullin and Riley.[22] The advantage of this method over other reduction methods is the stability of both the reducing solution as well as the reduced blue complex. The extinction of the blue solution does not change over a period of up to 5 days. The extinction was measured in a Beckman D. U. spectrophotometer using a one cm. cell at 810 mμ and a slit width of 0.03 mm. Conductivity water to which the same reagents were added, was used as a blank. The calibration was carried out with solutions containing accurately known amounts of $Na_2SiO_3 \cdot 9H_2O$. Duplicate SiO_2-determinations did not differ by more than 0.2%.

Results

Nature of the Quartz Surface.—Figure 1 shows the results of a series of experiments at room temperature in $10^{-3}N$ NaOH solutions. The dotted curves in Fig. 1 indicate experiments in which twice as much quartz was used as in the experiments represented by the solid curves. For both the 5–25 and 25–50 μ size ranges the concentration of SiO_2 in solution after about 20 days is proportional to the amount of quartz in suspension. This is not the case in the experiments with quartz of the 1–5 μ size range. The solid curve for the 1–5 μ size range shows a final concentration of 2.5×10^{-3} mole/kg., the dotted curve for the same size range approaches a concentration of approximately 3.3×10^{-3} mole/kg. This is perhaps not surprising because the solubility of amorphous silica at the final *p*H in these experiments (9.4–9.5) is also approximately 3.3×10^{-3} mole/kg.[23]

The picture suggested by Fig. 1 agrees with the presence of a superficial amorphous layer on the quartz particles. Estimates of the layer thickness in the literature vary from 300–1000 Å. To check on these estimates, a few experiments were carried out in a 0.12 N NaOH solution because the more alkaline solution would dissolve cracked structures

(20) R. G. Bates, "Electrometric *p*H Determinations," John Wiley and Sons, Inc., New York, N. Y., 1954, p. 74.

(21) J. D. Strickland, *J. Am. Chem. Soc.*, **74**, 862 (1952).

(22) J. B. Mullin and J. P. Riley, *Anal. Chim. Acta*, **12**, 162 (1955).

(23) G. B. Alexander, W. H. Heston and R. K. Iler, THIS JOURNAL, **58**, 453 (1954).

and small fragments in addition to any amorphous silica. The results of some of these experiments are shown in Fig. 2. It is clear that the "layer effect" is considerably stronger than would be concluded from the experiments at lower *p*H (Fig. 1). The thickness of the disturbed layer as estimated from the experiments at high *p*H is approximately 300 Å. To check whether any amorphous silica was present in suspension a series of experiments were run in which the silica concentration was determined both gravimetrically and colorimetrically. The results are given in Table I.

TABLE I

COMPARISON OF THE RESULTS OF GRAVIMETRIC AND COLORIMETRIC ANALYSIS

1–5 μ size range; solvent 0.12 *N* NaOH soln.

Agitation time, days	Amt. of quartz, g.	Concn. SiO_2, mole/kg. $\times 10^2$ Colorimetric	Gravimetric	Final *p*H
3	0.5464	1.8	..	12.40
10	.5737	3.1	3.1	12.46
17	.7023	4.7	4.9	12.20
31	.5293	4.8	5.3	12.20
52	.4088	4.8	5.1	12.34
74	.3854	4.8	5.3	12.30

This table shows no significant differences in concentration between the results of both methods, indicating the absence of amorphous silica in the suspensions.

After the results reported above had been obtained it was clear that a "clean" quartz surface was necessary for solubility measurements. This was accomplished by washing the quartz with HF solution according to treatment Method I. The result of this treatment is shown in Fig. 2. The low rate of dissolution (about 7×10^{-15} mole SiO_2/cm.^{2} sec.) and the fact that there is a straight-line variation between concentration and time suggest the dissolution of one species only. Quartz treated in this way was also used for the experiments at elevated temperatures.

Figure 3 shows the results of a series of experiments at 90° in 10^{-3} *N* NaOH solution. The amount of quartz was varied from 1 to 4 g. The final *p*H in the horizontal part of the curve was 8.95 ± 0.05 (at 90°), whereas the *p*H was 0.1 to 0.2 unit lower along the hump in the curve. The occurrence of the hump is probably the result of damage done to the particle surfaces by the HF treatment. Small fragments broken off from the quartz particles will have a higher solubility and thus tend to supersaturate the solution with respect to the larger particles. To prevent the occurrence of supersaturation in subsequent experiments, the quartz was given an additional treatment according to Method II.

Solubility Studies at Elevated Temperatures.—Measurements in water and 10^{-2} *N* NaCl solutions were carried out at 5 different temperatures. The results at 100, 90, 80 and 70° are shown in Figs. 4 to 7 and those at 60° in Table II. Shaded symbols in these figures indicate experiments in 10^{-2} *N* NaCl, open symbols indicate experiments in H_2O and crosses indicate experiments in 10^{-4} *N* NaOH solutions. These figures illustrate the approach to equilibrium from above and below.

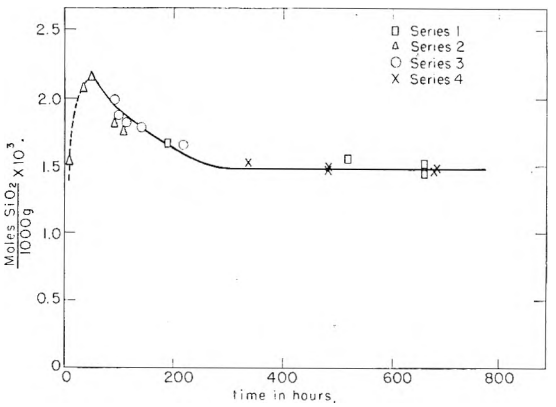

Fig. 3.—Solubility of quartz in 10^{-3} *N* NaOH at 90°; size ranges 2–5 μ and 5–10 μ.

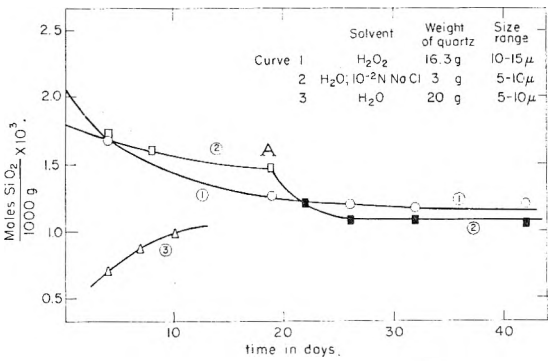

Fig. 4.—Solubility of quartz in H_2O and 10^{-2} *N* NaCl at 100°.

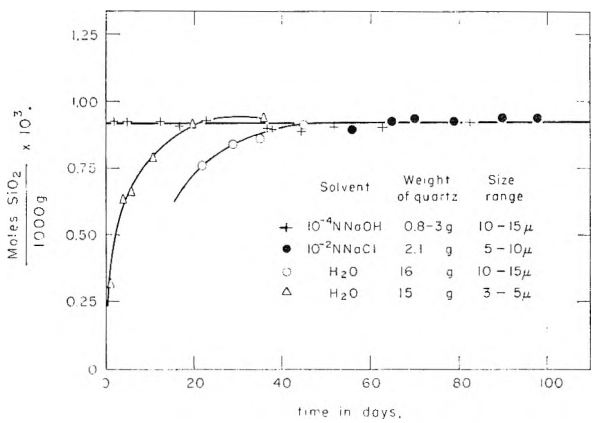

Fig. 5.—Solubility of quartz in H_2O, 10^{-2} *N* NaCl and 10^{-4} *N* NaOH solutions at 90°.

At 100°, samples were taken after quenching the containers in ice-water. The high starting concentrations (Fig. 4 and Table II) were obtained by heating container and contents in a drying oven at 135° for 24 hours prior to the start of an experiment. Curve 2 in Fig. 4 is the result of an experiment in water, to which at point A (after a sample had been taken) a small amount of 10^{-1} *N* NaCl solution was added to yield an NaCl concentration of approximately 10^{-2} *N*. The second part of curve 2 shows a strong acceleration of the recrystallization of quartz by NaCl. The total surface area of quartz used to determine curve 1 was roughly four times that of the quartz used in establishing curve 2.

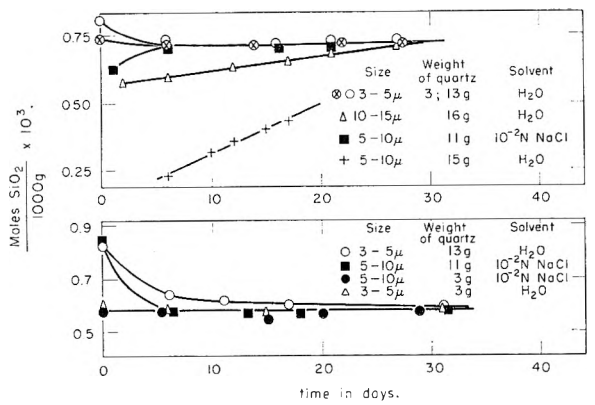

Fig. 6.—(Top) rate of dissolution of quartz at 80°.

Fig. 7.—(Bottom) rate of dissolution of quartz at 70°.

TABLE II

DATA OBTAINED AT 60° IN 10^{-2} *N* NaCl SOLUTION

Amt. of quartz, g.	Amt. of solvent, g.	Size range of quartz, μ	Reaction time, days	Concn. SiO_2 moles/kg. × 10^4 Final	Initial
10.4	30	10–15	1	5.2	19.4
			3	4.7	
			7	5.2	
			12	4.9	
			16	5.1	
			19	5.1	
11	25	5–10	3	4.5	5.8
			6	4.7	(equilibrium
			9	4.8	concn. at 70°)
			14	4.6	
			21	4.5	

From Fig. 7, it becomes evident, that 70° represents the practical lower limit for the solubility measurements in pure water. In the experiment indicated by open circles, a total surface of 90,000 cm.^{2} was used per 32 g. of water. Even with this large surface area it took one month to reach equilibrium from a starting concentration only 2.4×10^{-4} mole/kg. higher than the equilibrium concentration.

No attempt was made to measure the solubility in H_2O below 70°. As previous experiments had shown an accelerating effect of NaCl, two experiments in 10^{-2} *N* NaCl solution were run at 60°. The results of these experiments are given in Table II. Of interest is the decrease of concentration by 1.4×10^{-3} mole/kg. within one day in the first experiment. Both experiments indicate that it should be possible to obtain results at 50° or even lower, when 10^{-2} *N* NaCl is used as a solvent.

Because of the difficulties in measuring *p*H at elevated temperatures, the solubility of quartz was also determined in alkaline solutions of known *p*H. A 10^{-2} *M* borax solution was chosen because its *p*H is known over the desired temperature range.[20] Table III summarizes the results of the measurements in these solutions.

The observed solubilities of quartz in neutral and alkaline solutions at different temperatures are summarized in Table IV.

Rate Studies.—The dissolution rates of quartz in pure water and in the presence of 10^{-1}, 10^{-2} and 10^{-3} *N* NaCl solutions were studied at 90, 80 and 70°. The quartz was pretreated in the same way as described before except that after the treatment with 10^{-1} *N* NaOH, the washed quartz was again agitated in conductivity water at 90° for 14 days and then filtered and washed with fresh conductivity water and dried over P_2O_5 *in vacuo*. The results of the experiments are given in Figs. 8, 9 and 10. The dotted curves indicate experiments in which 0.96 g. of quartz was used. All other tests were made with 3 g. of quartz. A strong accelerating effect of NaCl is evident. The influence of 10^{-1} *N* NaCl is very remarkable. With reference to the upper curve in Figs. 9 and 10 the quartz is seen to keep on dissolving, even though the concentration in solution is higher than the equilibrium concentration found in previous experiments in 10^{-2} *N* NaCl solution and in H_2O as indicated by the arrows. A similar behavior in 10^{-1} *N* NaCl solution at 90° (upper curve, Fig. 8) is not evident. Perhaps this may be related to the fact that the starting silica concentration in the 10^{-1} *N* NaCl experiment at 90° was zero whereas in the 10^{-1} *N* NaCl experiment at 70° (Fig. 10) the initial SiO_2 concentration in solution was 4.9 $\times 10^{-4}$ mole/kg. The reason for the difference in results, when using 10^{-1} *N* NaCl solution as compared to 10^{-2} *N* NaCl solution as solvent is not clear. It may indicate a higher solubility of quartz in NaCl solutions. Sadek[24] reports the formation of a complex between SiO_2 (in solution) and HCl in a ratio of 1:1. He reports, however, a decrease in the formation of this complex with decreasing SiO_2 concentration. His lowest SiO_2 concentration was 1.5×10^{-1} mole/kg. whereas the highest SiO_2 concentration in our NaCl experiments was about 1.2×10^{-3} mole/kg. On the other hand, Wyart and Sabatier[25] report the same solubility for quartz in H_2O and in 10^{-1} *N* NaCl at 500° and 500 atmospheres of pressure. Piryutko[26] found that high salt concentrations, especially chloride and nitrates lower the solubility of silicic acid. Greenberg and Price[27] report that NaCl and Na_2SO_4 in concentrations below 1 *N* do not change the solubility of colloidal silica. In 1 *N* solutions of these salts they found a slight decrease in solubility. More measurements are needed to explain this effect.

Discussion

The presence of a disturbance of considerable thickness on the surface of finely ground quartz has been verified in this investigation (see Figs. 1 and 2). If this layer were amorphous silica, enough material would be present to saturate the solution with respect to amorphous silica at the lower *p*H (Fig. 1). The dissolution rate of amorphous silica at room temperature is sufficiently high, even in pure water, to cause saturation within the time of the experiments.[23] Thus the disturbance certainly consists of a material closer to quartz in structure. A combination of cracks, dislocations and protruding edges seems to disturb

(24) H. Sadek, *J. Indian Chem. Soc.*, **29**, 507 (1952).

(25) J. Wyart and G. Sabatier, *Compt. rend.*, **240**, 2157 (1955).

(26) M. M. Piryutko, *Izvest. Akad. Nauk, S.S.S.R. Otdel, Khim. Nauk*, 379 (1959).

(27) S. A. Greenberg and E. Price, THIS JOURNAL, **61**, 1539 (1957).

TABLE III

EXPERIMENTS IN 10^{-2} M BORAX SOLUTION

Temp., °C.	Amt. of quartz, g.	Amt. of solvent, g.	Size range of quartz, μ	Reaction time, days	Concn. of SiO_2, moles/kg. Final	Initial	pH
60	10	30	5–10	24	6.9×10^{-4}	0	8.96
70	7.5	30	10–15	35	1.0×10^{-3}	1.1×10^{-3}	8.92
80	7.5	34	10–15	27	1.2×10^{-3}	0	8.88
90	7.5	34	10–15	29	1.5×10^{-3}	0	8.85
100	3	35	3–5	23	1.6×10^{-3}	0	8.83[a]

[a] This value is not given by Bates[20] but was obtained by extrapolation from his data.

TABLE IV

SOLUBILITIES OF QUARTZ IN WATER AND 10^{-2} M BORAX SOLUTIONS

Temp., °C.	Solubility, moles/kg. Water	Borax soln.	pH^{20} of borax soln.	pK
60	4.42×10^{-4}	6.87×10^{-4}	8.96	9.3
70	5.79×10^{-4}	1.01×10^{-3}	8.92	9.1
80	7.15×10^{-4}	1.18×10^{-3}	8.88	9.1
90	9.06×10^{-4}	1.48×10^{-3}	8.85	9.1
100	10.89×10^{-4}	1.64×10^{-3}	8.83	9.1

the original quartz structure in such a way that abnormal solubilities[10,13,14,16] are obtained and that the results of X-ray diffraction,[12,28] differential thermal analysis[11] and infrared absorption[17] deviate from the results on a pure quartz specimen. After removal of the disturbed layer it was shown that a true measure of the solubility of quartz could be obtained.

Solubility of Quartz in H_2O and 10^{-2} N NaCl Solution.—The dissolution of quartz in H_2O may be represented by the reaction

$$SiO_2\,(s) + 2H_2O \rightleftarrows H_4SiO_4 \qquad (1)$$

In writing this reaction the assumption is made that H_4SiO_4 is the chemical species in solution. Evidence for this can be found in the work of Weitz,[29] Alexander[23] and Wood.[30] The equilibrium constant (K) for reaction 1 may be written

$$K = c_{H_4SiO_4} \qquad (2)$$

and the variation of K with temperature will be given by the well-known relation

$$\frac{d\,(\ln K)}{dT} = \frac{\Delta H^\theta}{RT^2} \qquad (3)$$

where ΔH^θ is the differential standard heat of the dissolution reaction 1. On combining equations 2 and 3 and integrating we obtain

$$\log c_{H_4SiO_4} = -\frac{\Delta H^\theta}{4.5767T} + \text{constant} \qquad (4)$$

This relation was plotted for the five different temperatures used in this investigation. By extrapolation of the straight line obtained to 25°, a solubility of quartz in water of 1.8×10^{-4} mole/kg. was found. The temperature variation of the solubility of crystalline quartz as based on our measurements assumes the form

$$\log c_{H_4SiO_4} = 0.151 - 1162/T \qquad (5)$$

With the help of equation 5 the standard heat (ΔH^θ), standard free energy (ΔG^θ) and standard entropy (ΔS^θ) of dissolution may be calculated. The following values for these thermodynamic quantities are found at 25°.[31]

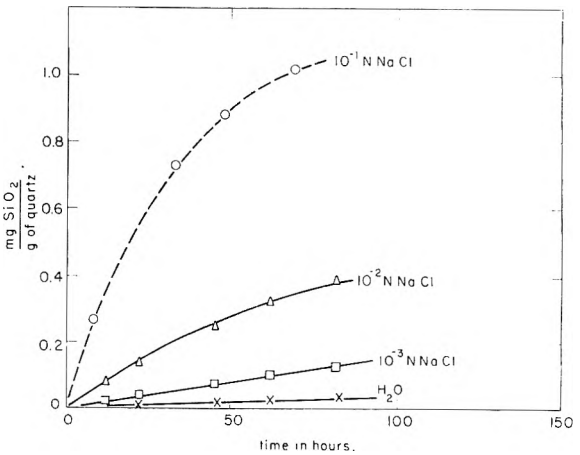

Fig. 8.—Dissolution rate of quartz in H_2O and NaCl solutions at 90°.

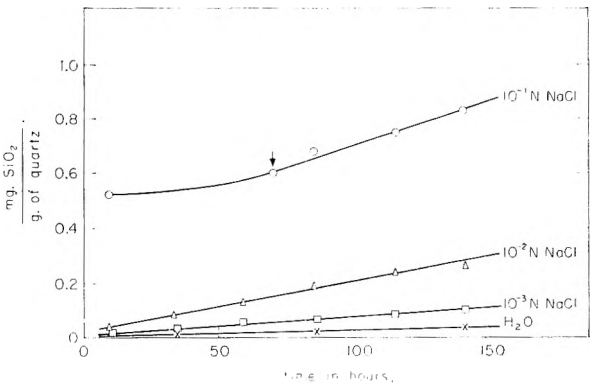

Fig. 9.—Dissolution rate of quartz in H_2O and NaCl solutions at 80°.

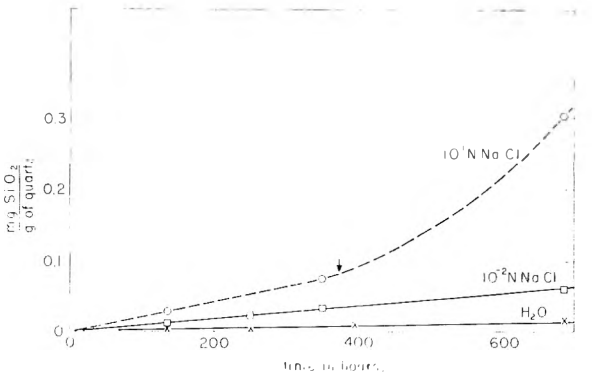

Fig. 10.—Dissolution rate of quartz in H_2O and NaCl solutions at 70°.

(28) G. Sabatier, *Compt. rend.*, **237**, 77 (1953).

(29) E. Weitz, H. Franck and M. Schuchard, *Chem. Z.*, **74**, 256 (1950).

(30) J. A. Wood, *Am. J. Sci.*, **256**, 40 (1958).

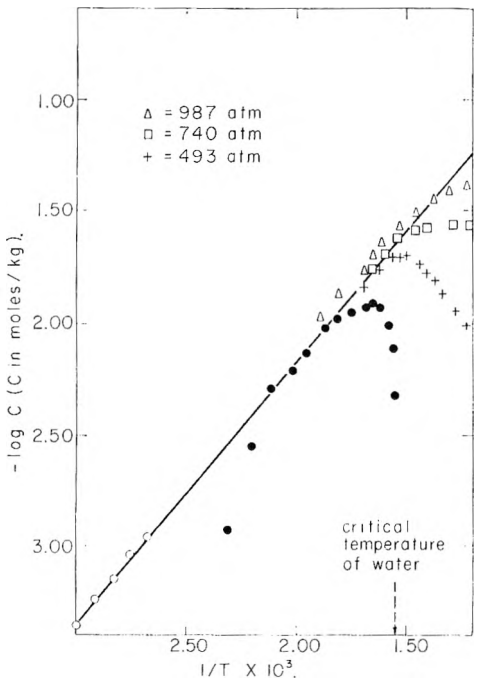

Fig. 11.—Comparison of solubility data of quartz as obtained by Kennedy[3] with data obtained in this investigation.

ΔH^θ = 5.32 kcal./mole; ΔG^θ (25°) = 5.11 kcal./mole; ΔS^θ (25°) = 0.7 cal. deg.$^{-1}$ mole^{-1} ≷ 0

The standard heat of dissolution was also calculated by Greenberg[32] who used Kennedy's[3] data, which he extrapolated to 200°. Greenberg reports a value of 7.34 kcal./mole for ΔH^θ. Unfortunately, it is not clear from Greenberg's paper, what part of Kennedy's data he has used. Two factors are important in this respect, Kennedy's mea urements at the lowest temperatures are according to himself the least reliable and secondly the assumption of a constant ΔH^θ is unjustified at temperatures around the critical temperature of water. Both factors are evident from Fig. 11 where the results of Kennedy's[3] work are compared with the results of the authors. The line in Fig. 11 is described by equation 5. The solid points indicate Kennedy's measurements in the three-phase region, *i.e.*, quartz in H_2O with a vapor pressure present. The open circles represent our data at lower temperatures and the other symbols indicate several series of experiments (Kennedy) at constant high pressures. The decrease in solubility along the constant pressure curves may be due to the decreasing density along these curves. This has been discussed by Kennedy[3] and by Iler.[33] It is clear, however, that the agreement between Kennedy's data above 200° and our data is excellent as long as the density of the solutions does not change too much. The two lower values of Kennedy at 160 and 182° could be explained by assuming that insufficient time was allowed for equilibrium to be reached. This becomes more obvious when it is realized that in Kennedy's measurements only 12 cm.^{2} of quartz surface were exposed to probably 150 cc. of water. Not all of Kennedy's data are included in Fig. 11, as this would cause too much crowding, but the data not shown do not deviate any more from the straight line than the data that are shown.

The Solubility of Quartz in Alkaline Solutions.—The following assumptions will be made with regard to the dissolution of quartz in alkaline solutions: (a) The concentration of the species H_4SiO_4 is independent of *p*H; (b) $H_3SiO_4^-$ is the only ionic species present in solution.

In alkaline solution the equilibrium constant for the dissolution of quartz may then be written

$$K = \frac{[H^+][H_3SiO_4^-]}{[H_4SiO_4]} \qquad (6)$$

or because of assumption (a)

$$K' = [H^+][H_3SiO_4^-] \qquad (6a)$$

Alexander and co-workers[23] have shown that this relation is reasonable at room temperature and a value of $10^{-9.8}$ for K at room temperature is given by Roller and Ervin.[34]

In Table IV the calculated *pK* values based on measurements in the borax solutions are shown. The *pK* values were calculated with the aid of the two assumptions previously mentioned and compare reasonably well with the value of 9.8 reported by Roller and Ervin.[34]

Some further results of solubility measurements in unbuffered alkaline solutions at 90° are given in Table V. This table also includes calculated quantities needed to obtain an estimate of the *pK*.

Table V

Solubilities in Alkaline Solutions at 90°

Solubility, moles SiO_2/kg.	—[OH^-], moles/kg.— Initial	Final	[$H_3SiO_4^-$], moles/kg.	*pK*
9.2×10^{-4}	10^{-4}	1.3×10^{-5}	3.1×10^{-5}	9.1
1.5×10^{-3}	10^{-3}	2.5×10^{-4}	6.2×10^{-4}	9.1
6.7×10^{-3}	10^{-2}	4.2×10^{-3}	5.8×10^{-3}	9.3
6.7×10^{-2}	10^{-1}	3.4×10^{-2}	6.6×10^{-2}	9.2

The first three columns in this table give the experimental data with the exception of the last two values in the third column. The final *p*H was not measured in these two tests, but was calculated by assuming that the final OH^- concentration equals the difference in concentration between the starting OH^- concentration and the amount required for the formation of $H_3SiO_4^-$. The $H_3SiO_4^-$ concentration was calculated with the aid of equation 6a. It may be shown that if ions of the type $H_2SiO_4^=$ or $H_3Si_2O_7^=$ were present, the final *p*H would be so low that the experimentally observed SiO_2 concentrations would be much too high. Furthermore the presence of polymeric ions at concentrations of SiO_2 far below the saturation concentration of amorphous silica is very unlikely. The *pK* values shown in Table V agree well with those calculated in borax solutions (Table IV) and one may conclude that the assumptions on which these calculations are based are thus validated.

In Table VI, the solubility of quartz in H_2O and 10^{-4} *N* NaOH as determined in this investiga-

(31) ΔH^θ is assumed to be independent of temperature.

(32) S. A. Greenberg, This Journal, **61**, 196 (1957).

(33) R. K. Iler, "The Colloid Chemistry of Silica and Silicates," Cornell University Press, Ithaca, N. Y., 1955.

(34) P. S. Roller and G. E. Ervin, *J. Am. Chem. Soc.*, **62**, 461 (1940).

tion is compared with data on the solubility of amorphous silica from the literature.

TABLE VI

COMPARISON OF THE SOLUBILITY OF QUARTZ AND AMORPHOUS SILICA

	Solubility (moles/kg.)			
	H_2O		NaOH 10^{-4} N	
T, °C.	Quartz	Amorphous silica	Quartz	Amorphous silica
90	9.0×10^{-4}	7.5×10^{-3} [35]	9.2×10^{-4}	1.3×10^{-2} [35]
25	1.8×10^{-4}	2×10^{-3} [23]	$\sim 1.8 \times 10^{-4}$	$\sim 6.7 \times 10^{-3}$ [35]

Reaction Velocity in Water.—Very little is known about the rate of dissolution of quartz in aqueous solutions. Recently Laudise[36] discussed the kinetics of crystallization of quartz under hydrothermal alkaline conditions.

Removal of the disturbed layer at the quartz surface before any kinetic measurements can be made has been shown to be essential in the present investigation. O'Connor and Greenberg[37] and Brown, Paap and Ritchie[38] also came to the same conclusion.

In the present investigation it was observed that the rate of dissolution of quartz in water at a fixed temperature is constant (see for example Figs. 8 to 10). From this observation a rate constant (k_1) may be evaluated as

$$\frac{dc}{dt} = \text{constant} = k_1 \frac{S}{V} \qquad (7)$$

where c is the concentration of soluble silica at time t, V is the volume of solution and S the total quartz surface. The dependence of the rate of dissolution on the total surface area is a reasonable assumption although this relationship could not be well established because of limited experimental data. In Table VII the calculated rate constants for the dissolution of quartz in pure water at several temperatures are shown. These values were obtained from measurements in which extreme care was taken to remove any disturbance from the surface of the quartz. The values marked by an asterisk are considered to be the most accurate and reliable as they were obtained from experiments specifically designed to give kinetic information.

TABLE VII

RATE CONSTANTS FOR THE DISSOLUTION OF QUARTZ IN WATER AT 70, 80 AND 90°

T, °C.	Total surface area, cm.^{2}	k_1, g. SiO_2 cm.$^{-2}$ sec.$^{-1}$	Reaction time, hr.	Boundary layer thickness (δ), cm.
90	10,000	3.3×10^{-14}	813	
90	10,000	5×10^{-14}	1000	
90	43,000	1.2×10^{-14}	500	
90	10,000	3.6×10^{-14}*	83	30,000
80	10,000	1.8×10^{-14}*	140	38,000
70	10,000	3.6×10^{-15}*	680	130,000

In view of the proposed dissolution reaction (equation 1) for quartz in water, the above kinetic relation 7 suggests that the dissolution rate is controlled by the chemical reaction. To rule out the possibility that the kinetics may be diffusion-controlled, the following analysis will be helpful. If the dissolution rate were controlled by diffusion of soluble silica from the quartz surface through a boundary layer of effective thickness δ then it follows that

$$V \frac{dc}{dt} = DS \frac{(c_s - c)}{\delta} \qquad (8)$$

where D is the diffusivity of the soluble species (H_4SiO_4) and c_s the saturation concentration. A value for δ, the effective diffusion boundary layer thickness, may be determined from equation 8 if the diffusivity of H_4SiO_4 in water is known. According to Jander and Jahr[39] the diffusivity at room temperature is 6.15×10^{-6} cm.^{2}/sec.[40] The calculated values for δ are also shown in Table VII and are unreasonably large to be in agreement with a diffusion controlled kinetic process. It may be concluded that the rate of dissolution of quartz in pure water at temperatures below 100° is controlled by the dissolution reaction 1 for which the rate constants are given in Table VII.

A value of about 10^{-18} g. of SiO_2 cm.$^{-2}$ sec.$^{-1}$ is found for the rate constant at 25° by a rough extrapolation from k_1 values at higher temperatures. This should be compared with a dissolution rate of 4×10^{-13} g. of SiO_2 cm.$^{-2}$ sec.$^{-1}$ in a 0.1 N NaOH solution at 25°.

The presence of NaOH or NaCl results in a considerable increase in the reaction velocity but the absolute rate is still very small.

The rate constant for the crystallization of quartz from solutions supersaturated with H_4SiO_4 may be estimated from the available data. According to equations 1 and 7 the rate of crystallization of quartz may be written

$$-\frac{V}{S}\frac{dc}{dt} = k_2[H_4SiO_4] \qquad (9)$$

The rate constant k_2 at 90° may be obtained from the solubility of quartz in pure water (9×10^{-4} moles/kg.) and the rate constant for the dissolution reaction (3.6×10^{-14} g. cm.$^{-2}$ sec.$^{-1}$)

$$k_2 = \frac{k_1}{K} = 6.67 \times 10^{-10} \text{ g. (soln.) cm.}^{-2} \text{ sec.}^{-1}$$

Assuming the density of quartz to be 2.65 g./cc. it is seen from equation 9 that a thousandfold supersaturation; that is, a concentration of 0.9 mole/kg. would give only a linear rate of crystallization of 1.4×10^{-11} cm./sec. or 4.3 μ per year. Even the accelerating effects of alkaline pH and NaCl very probably will not be sufficient to grow quartz crystals normally at these temperatures.

Conclusions

1. Quartz has a well-defined solubility at temperatures below 100°.

2. The solubility of quartz in NaCl solutions below a concentration of 10^{-1} N NaCl is the same as the solubility in H_2O.

(35) Go Okamoto, T. Okura and K. Goto, *Geochim. et Cosmochim. Acta*, **12**, 123 (1957).

(36) R. A. Laudise, *J. Am. Chem. Soc.*, **81**, 562 (1959).

(37) T. L. O'Connor and S. A. Greenberg, THIS JOURNAL, **62**, 1195 (1958).

(38) J. Brown, W. J. Paap and P. D. Ritchie, *J. Appl. Chem.* (*London*), **9**, 153 (1959).

(39) G. Jander and K. F. Jahr, *Kolloid-Beihefte*, **41**, 48 (1934).

(40) The relation $D_{T_1}/D_{T_2} = T_1\eta_2/T_2\eta_1$ where η is the viscosity of the solution, was used to obtain the diffusivity at temperatures above 25°.

3. Quartz has a definite solubility in alkaline solutions of OH^- concentrations up to at least 10^{-1} N.

4. The solubilities of quartz in H_2O and NaOH solutions are approximately ten times lower than the corresponding solubilities of amorphous silica at the same temperature.

5. The rate of dissolution of quartz in H_2O is extremely slow at temperatures below 100°. The dissolution rate is not controlled by diffusion. NaCl in solution has a strong accelerating effect on the dissolution reaction as well as on the crystallization reaction.

6. The surface of finely ground quartz particles is disturbed in such a way as to cause abnormally high dissolution rates of the quartz in water and alkaline solutions.

Acknowledgments.—This work was supported by the United States Atomic Energy Commission under Contract No. AT(30-1)-956. The helpful suggestions made by Dr. G. Scatchard and Prof. A. M. Gaudin and their interest shown in this research study are gratefully acknowledged.

MASS SPECTRA OF DEUTERATED DIBORANES[1]

BY J. F. DITTER,[2a] E. B. KLUSMANN,[2a] J. C. PERRINE[2a] AND I. SHAPIRO[2b]

Research Laboratory, Olin Mathieson Chemical Corporation, Pasadena, California

Received May 3, 1960

The mass spectrum of completely deuterated diborane and approximate spectra of the five partially deuterated diboranes have been determined by an extrapolation technique based on a series of spectra of diborane of varying protium/deuterium ratios. For the partially deuterated compounds it was possible to obtain the spectra of formula groups only; the spectra of compounds labelled at specific positions were not resolvable. From the ion intensities of peaks for which there were no overlapping contributions, it was observed that the relative fragmentation of H *versus* D is substantially lower than is reported for deuterated hydrocarbons.

Mass spectra have been published,[3,4] for isotopically normal diborane and for slightly protiated deuterodiboranes, but not for completely deuterated diborane nor any of the partially deuterated species. Determination of these latter spectra is rendered particularly difficult by two factors, *viz.*, the existence of an equilibrium between the diborane molecule and the borane species ($B_2H_6 \rightleftarrows 2BH_3$),[5] and the negligibly small parent ion intensity of diborane at the usual ionizing voltages. Because of the diborane–borane equilibrium, a sample that is subjected to deuteration undergoes transition to a mixture of all the various species, B_2H_6, B_2H_5D, $B_2H_4D_2$, ... B_2D_6, both bridge and terminally substituted, in equilibrium with one another through their respective borane radicals. The half-life of the protium–deuterium exchange in diborane is of the order of minutes at room temperature,[5] so it is impossible to isolate a particular deuterated species and analyze it separately in the mass spectrometer. The concentrations of the various formula groups in an equilibrium mixture can be calculated from the expression

$$[B_2H_xD_{6-x}] = W[H]^x[D]^{6-x} \qquad (1)$$

where W is the statistical weight, numerically given by the binomial coefficients for six entities. A discussion of this relationship as well as a graph showing the changes in distribution with changing deuterium concentration has been published previously.[6]

The second complication, that of the negligibly small parent ion intensity, renders conventional stripping techniques useless even if any or all of the spectra might be known, since none of the species have unique peaks available for stripping. For example, a sample composed of B_2D_6 and B_2D_5H (plus small amounts of less deuterated species) would have a mass spectral cut-off at m/e 32, corresponding to $B_2{}^{11}D_5{}^+$, but since this ion comes from both B_2D_6 and B_2D_5H there is no way to determine relative contributions. Since the spectra also overlap on all other peaks, it would not be possible to strip known spectra from a composite spectra unless one could determine concentrations independently. The technique of determining relative concentrations by lowering the ionizing potential in the instrument to the point where only the parent ions are observed cannot be employed because the appearance potentials of several of the lower mass ions of diborane are essentially equal to that of the parent ion.[4,7] Consequently, one cannot produce the parent ions without simultaneously producing lower mass ions. Since the ion currents due to the parent ions are not equivalent if lower mass ions are produced (because of differences in zero point energies of the fragment ions),[8] the relative amounts of the parent compounds cannot be determined from the parent ion intensities.

To circumvent the difficulty we utilized a dilution technique to obtain the spectra and to measure the concentrations of all species. The general method involved mass spectral analysis of a series of samples

(1) Presented at Seventh Annual Meeting, ASTM Committee E-14 on Mass Spectrometry, Los Angeles, May, 1959.

(2) (a) National Engineering Science Co., Pasadena, California; (b) Hughes Tool Company—Aircraft Division, Culver City, California.

(3) (a) V. H. Dibeler and F. L. Mohler, *J. Am. Chem. Soc.*, **70**, 987 (1948); (b) V. H. Dibeler, F. L. Mohler and L. Williamson, *J. Research Natl. Bur. Standards*, **44**, 489 (1950).

(4) W. S. Koski, J. Kaufman, C. F. Pachucki and F. J. Shipko, *J. Am. Chem. Soc.*, **80**, 3202 (1958).

(5) P. C. Maybury and W. S. Koski, *J. Chem. Phys.*, **21**, 742 (1953).

(6) W. J. Lehmann, J. F. Ditter and I. Shapiro, *ibid.*, **29**, 1248 (1958).

(7) J. L. Margrave, THIS JOURNAL, **61**, 38 (1957).

(8) D. P. Stevenson and C. D. Wagner, *J. Chem. Phys.*, **19**, 11 (1951).

made up of isotopically-normal diborane diluted with known amounts of a highly deuterated sample, the deuterium content of the deuterated specimen being about 99% (precise value initially unknown). The spectrum of completely deuterated diborane was determined by an extrapolation technique similar to that used to determine the spectrum of B_5D_9,[9] namely, the plotting of peak heights *vs.* protium content of samples containing successively smaller amounts of protium, then extrapolating to zero per cent. protium. The deuterium content in the original (99%) sample was determined by extrapolating the dilution factors to 100% B_2D_6, as will be explained later, and hence the concentrations of all the various species could be calculated. The mass spectra of the five partially deuterated groups were obtained by a similar extrapolation technique involving the residual spectra from which known spectra had been stripped.

Experimental

Diborane was prepared by conventional reaction of boron trifluoride etherate with lithium aluminum hydride.[10] To eliminate impurities such as carbon dioxide and ethane, which are very difficult to remove by vacuum fractionation, the diborane was first converted to tetraborane by electrical discharge.[11] The tetraborane was freed of the more volatile impurities by fractionation at −130°, then converted back to diborane by decomposition under four atmospheres of hydrogen at 100° for 30 minutes.[12] Fractionation of the resultant diborane through a −155° bath then removed less volatile impurities, including tetraborane. Deuterated diborane (*ca.* 99% D) was prepared by successive exchanges of B_2H_6 with D_2 at 80°.[5]

Seventeen samples for mass spectral analyses were prepared by adding measured amounts of deuterated diborane to measured amounts of B_2H_6, covering the entire range from 0 to 99% D. Total sample volumes were about 0.5 cc. STP. The individual components were measured in a 1-cc. thermostated system equipped with two differential manometers, one for measuring B_2D_6 and the other for B_2H_6. To avoid cross-contamination, all sample vessels were first filled with the requisite amounts of B_2H_6, then later with B_2D_6. The samples were sealed in tubes equipped with break-off devices and were allowed to stand overnight at room temperature to ensure equilibrium. (Decomposition of pure diborane under these conditions is negligible.) To avoid introduction of air into the sampling system between spectral recordings, samples were introduced into the mass spectrometer inlet from a common manifold. B_2H_6, containing only the natural isotopic abundance of deuterium, 0.15%, was run first, followed by samples with successively larger percentages of deuterium.

The mass spectrometer was a Consolidated Model 21-103 operating at an ionizing potential of 70 volts.

B_2D_6 Spectrum.—The mass spectra of the various samples, not tabulated here because they are extremely bulky, were first normalized on the basis of total ion currents to make them suitable for graphical plotting. It was observed that the sums of the ion intensities of the B_2^+ groups displayed a linear decrease with increasing deuterium content, while those of the B_1^+ groups were linear in the reverse direction. The total sums (both groups combined) were essentially constant for all samples, the deviations in linearity as well as in total ion sums being less than 1% in all cases. Consequently, the spectra were adjusted so that the two respective ion groups fitted linear plots of opposite slope, which in turn provided normalization on the basis of a constant total ion sum.

Fairly smooth gradations with changing deuterium content were uniformly apparent for all mass numbers except for minor discrepancies in samples of very low deuterium content. These samples had been run first, and the discrepancies probably reflect a conditioning of the filament in the instrument, despite the fact that the instrument had been flushed with B_2H_6 prior to the first run.

Extrapolation of data to obtain the spectrum of B_2D_6 was based on the following conditions. In any given experimental spectrum, the peak height (ion intensity) for each m/e can be represented as a function of the deuterium content; more specifically, it can be written as the sum of the contributions from B_2D_6, B_2D_5H, $B_2D_4H_2$, etc., which in turn are functions of the deuterium concentration according to eq. 1, *viz.*,

$$P_{m/e} = a[B_2D_6] + b[B_2D_5H] + c[B_2D_4H_2] + \ldots\ldots\ldots + g[B_2H_6] \quad (2)$$

The expressions in brackets are formula group concentrations; a represents the peak height for pure B_2D_6, b represents the peak height for pure B_2D_5H, etc. When all mass numbers are considered, a, b, c, . . . , represent the spectra of B_2D_6, B_2D_5H, $B_2D_4H_2$, . . . , respectively.

According to eq. 2 we can obtain the spectrum of B_2D_6 if we extrapolate the data to the point where $P_{m/e} = a[B_2D_6]$. If we know the protium content or some function of the protium content, $F(h)$, for each experimental spectrum, we can plot $P_{m/e}$ *vs.* $F(h)$ and extrapolate to $F(h) = 0$, and the intercept will correspond to $P_{m/e} = a[B_2D_6]$. Since $[B_2D_6]$ is necessarily unity at this point, $P_{m/e} = a$, which is the peak height for pure B_2D_6 for that particular m/e. A convenient value for $F(h)$ is the ion intensity of $B_2{}^{11}D_4H^+$, which is determined for each spectrum as follows, based on $B^{11}/B^{10} = 4.0$ and $B_2{}^{11}/B^{10}B^{11} = 2.0$[13]

$$P_{32} = B_2{}^{11}D_5{}^+ \text{ and } P_{31} = B^{10}B^{11}D_5{}^+ + B_2{}^{11}D_4H^+$$

Therefore

$$B_2{}^{11}D_4H^+ = P_{31} - 0.5P_{32}$$

The B_2D_6 spectrum was obtained by plotting, for each m/e, the ion intensities of samples of high deuterium content (greater than 80%) *vs.* their $B_2{}^{11}D_4H^+$ ion intensities, as shown in Fig. 1. In this plot we were able to utilize two checks on the plotting accuracy and thus minimize plotting errors. The first check required the sums of the ion intensities to be in line with experimental spectra, while the second required the B_2D_6 spectrum to strip down with negligibly small residues for a B^{11}/B^{10} ratio of 4.0. Conveniently, every other peak in the spectrum of B_2D_6 is zero and thus serves as a check point. Hence, the plotting could be regulated somewhat to conform to these parameters. The actual plotting, particularly for lower intensity ions, was carried out on a considerably expanded scale, and the intercept values obtained from the expanded plots are those shown in parentheses in Fig. 1.

Determination of Deuterium Concentrations.—To obtain the deuterium content of our original deuterated sample (approximately 99% deuterium content), and hence the deuterium content and the concentrations of all molecular species in every sample, the ion intensities for the 80 through 99% samples were plotted again (not shown), but this time against the fraction (or partial pressure) of 99%-deuterated material in the various samples. That is, if in sample n we represent the deuterium content by d_n and the experimentally measured partial pressures by p_{99} and p_0, then

$$d_n = \frac{p_{99}}{p_{99} + p_0} \times d_{99} = A_n \times d_{99}$$

The ion intensities were plotted *vs.* A_n, and on these plots were then superimposed the ion intensities for the B_2D_6 spectrum from Fig. 1. The value of A_n corresponding to the point where the B_2D_6 values were superimposed represented 100% deuteration, and this was determined to be 1.011 (estimated error of ± 0.0005). Hence, since $d_{100} = 1.0$, the concentration of deuterium in the 99% sample was simply $d_{99} = d_n/A_n = 1.0/1.011 = 0.989$. The deuterium concentrations in the remaining samples are then equal to

(9) I. Shapiro and J. F. Ditter, *J. Chem. Phys.*, **26**, 798 (1957).

(10) I. Shapiro, Weiss, Schmieh, Skolnik and Smith, *J. Am. Chem. Soc.*, **74**, 901 (1952).

(11) A. Stock and W. Mathing, *Ber.*, **69B**, 1469 (1936).

(12) A. Burg and H. I. Schlesinger, *J. Am. Chem. Soc.*, **55**, 4009 (1933).

(13) There is increasing evidence that the correct B^{11}/B^{10} ratio is very close to 4.0 rather than the "official" value of 4.31. At least it appears to be the best choice for the stripping ratio of boron hydrides and their derivatives. For a discussion and list of references on this subject see W. J. Lehmann and I. Shapiro (to be published) and footnote 10 of ref. 9.

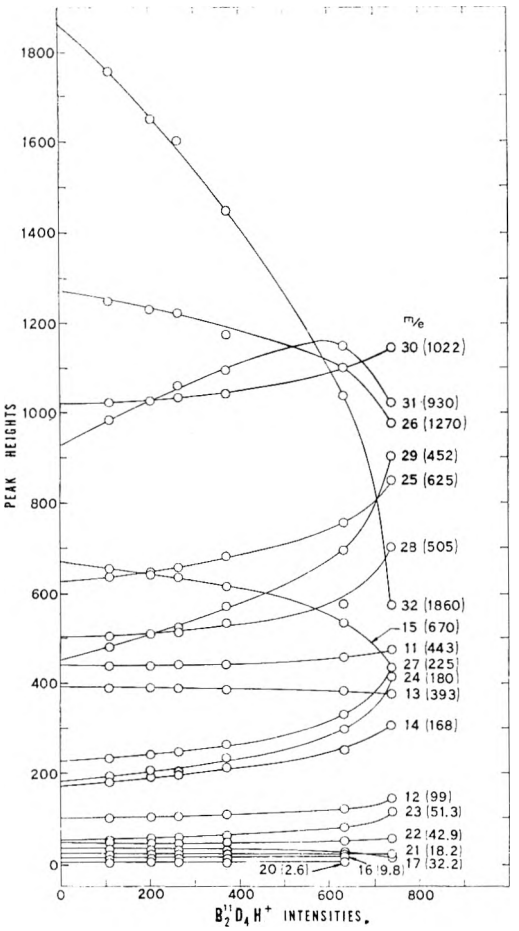

Fig. 1.—Extrapolation of data for determination of B_2D_6 spectrum.

0.989 times A_n, and the concentration of any given species in any given sample could be calculated from substitution of the appropriate value of the deuterium content in eq. 1. It must be remembered that concentrations calculated in this way are based on simple statistics, which undoubtedly do not hold precisely in an actual sample, but since infrared measurements have indicated the concentrations of the deuterated species to be within a per cent. or so of the statistical values,[6] any error introduced by statistical assumptions should be fairly small.

Spectra of the Partially Deuterated Diboranes.—As the deuterium content is varied from one sample to another, the concentration ratios between the various formula groups, B_2D_6, B_2D_5H, etc., undergo corresponding changes, as determined by eq. 1, while those between the various terminal and bridge substituted isomers within each formula group remain constant. Hence, the only effects discernible in the mass spectra are due to the over-all formula groups. Group spectra were therefore resolvable, but the spectra of individual isomeric species within each group were not. Further mention of "partially deuterated" spectra in this paper, therefore, will refer to formula groups only.

When the spectra of B_2D_6 and B_2H_6 are stripped from the experimental spectra, only the contributions of the partially deuterated compounds remain. That is

$$P'_{m/e} = b[B_2D_6H] + c[B_2D_4H_2] + \ldots f[B_2DH_5]$$

Residual spectra with high deuterium contents will be primarily B_2D_5H, while those of high protium content will be primarily B_2DH_5. Hence, the possibility of extrapolating to 100% B_2D_5H and 100% B_2DH_5 again presents itself, as with B_2D_6. Unfortunately, however, the residuals become smaller and smaller as they approach 100% values, until at 100% deuterium and 100% protium content they become zero. Furthermore, the smaller the residual spectra become, the more susceptible they are to errors, since they were obtained from the differences of large numbers, *e.g.*, $P_{m/e}$ minus $a[B_2D_6]$. However, the ion intensities can be made to intercept b on extrapolation to 100% B_2D_5H by dividing the residual spectra by their respective values of $[B_2D_5H]$. Since all species are functions of one another through the deuterium content, we can write

$$P'_{m/e}/[B_2D_5H] = P''_{m/e} = b + F([B_2D_6H])$$

Plotting P'' *vs.* $[B_2D_5H]$, for example, will produce b at 100% concentration of B_2D_5H since at this point the contributions from all other species equal zero. It is better to plot P'' *vs.* the concentration of B_2D_5H in the various residual spectra than its concentration in the original spectra. The reason is that in the original spectra the fraction of B_2D_6H in the optimum spectrum (about 17% D) attains a maximum of only *ca.* 40%, which would require an unduly long extrapolation to 100%; in the residual spectra, on the other hand, it is the principal constituent and runs as high as 95%.

Because the small residual spectra near 100% B_2D_5H were susceptible to large errors and fluctuated considerably in some instances, it was found advantageous to extrapolate from spectra having somewhat lower concentrations. In order to guide some of the uncertain extrapolations, advantage was taken of the known ion sum ($^1/_6$ of the way between B_2D_6 and B_2D_5H).

To reduce the intervals between points, additional ion intensities were obtained by plotting the original data for each m/e *vs.* the deuterium content, then reading ion intensities at intermediate percentages from the curves. These were added to the experimental values in all extrapolation curves.

The procedure for determination of the remaining partially deuterated spectra was identical to that of B_2D_5H. All spectra from B_2D_6 through B_2H_6 are listed in Table I, based on a value of 100 for the m/e 32 peak of $B_2^{11}D_6$. Because of the uncertainties discussed above the partially deuterated spectra can be regarded only as approximate, although composite spectra synthesized from these spectra were found to fit the original experimental data reasonably well. The synthesized spectra of the same composition as the experimental ones were compared with their experimental counterparts by taking the root-mean-square differences and dividing them by the total ion sums. The samples containing large quantities of both hydrogen and deuterium, *i.e.*, around 50% of each, gave the poorest fit, as expected, while the highly deuterated samples were the best. In general, the seven spectra listed in Table I represent the original data within 1 or 2% although any given value may be susceptible to greater errors.

TABLE I

B^{11} SPECTRA OF THE DIBORANES

m/e	B_2D_6	B_2D_5H	$B_2D_4H_2$	$B_2D_3H_3$	$B_2D_2H_4$	B_2DH_5	B_2H_6
32	100	20.8					
31		83.0	38.5				
30	48.7	17.0	64.5	50.0			
29		31.0	27.0	65.5	65.5		
28	24.1	14.5	22.8	30.7	50.0	81.3	0.40
27		8.0	13.0	19.0	34.5	46.7	94.4
26	66.8	44.7	36.5	33.0	23.7	32.7	50.2
25		20.3	35.0	40.2	44.0	39.3	25.5
24	5.49	5.0	9.0	9.2	30.1	44.5	73.8
23		0.5	0.8	2.4	2.9	5.3	7.93
22	1.96	2.0	2.5	1.4	2.1	3.1	3.31
17	1.73	0.6	0.4	0.2			
16		1.3	0.4	.5	0.4		
15	36.0	24.0	18.2	7.2	4.0	1.2	
14		12.6	11.7	26.5	17.5	14.7	1.84
13	21.1	15.7	19.0	12.5	18.5	21.4	28.9
12		2.7	5.2	5.8	11.5	12.7	16.1
11	23.8	24.0	24.5	25.5	25.7	26.2	27.3
ΣB_2^+	247.05	246.8	249.6	251.4	252.8	252.9	255.54
ΣB_1^+	82.63	80.9	79.4	78.2	77.6	76.2	74.14
Total	329.68	327.7	329.0	329.6	330.4	329.1	329.68

Discussion

Our mass spectra of B_2H_6 and B_2D_6 agree only qualitatively with previously published spectra,[3,4] the differences being due undoubtedly to different

types of instruments. We have run numerous spectra of these compounds over the past seven years, and all are in close agreement with the ones presented here.

A number of papers have been published[14] on the relative ease of abstraction of H *vs.* D atoms from partially deuterated hydrocarbons. The ratios are generally obtained by comparing corresponding ion intensities, after due allowance for *a priori* probabilities, and the general observation has been that abstraction of H occurs with about 1.2 and D about 0.6 times the probability of abstraction of H from the corresponding protiated compound. H *vs.* D in the same compound, then, is about 2 to 1, with some observations reported as high as 3 to 1. With the diboranes, however, these ratios are somewhat lower. Disregarding for the time being the approximate nature of the partially deuterated spectra in Table I, abstraction of an H from the parent ions of the series B_2D_5H . . . . . B_2DH_5 occurs with the following probability ratios, compared with B_2H_6: 1.32, 1.22, 1.06, 1.04 and 1.04. Abstraction of a D atom can only be determined for B_2D_5H, which has a probability value of 1.05 compared with abstraction of an H from B_2H_6. H *vs.* D in B_2D_5H calculated to 1.26, considerably less than comparable fragmentation in hydrocarbons. Such calculations, however, have little real significance because they are based only on observed ion intensities, which depend on the ground state energies of the ions (which determine the magnitude of fragmentation into smaller components) as well as on the relative abstraction of H and D. Hence, the fragmentation probabilities of the diboranes should be compared only in a very general way with other compounds.

(14) See V. H. Dibeler, F. L. Mohler and M. de Hemptinne, *J. Research Natl. Bur. Standards*, **53**, 107 (1954) for further references.

HEATS OF ISOMERIZATION OF THE SEVENTEEN ISOMERIC HEXENES[1]

By Henry F. Bartolo[2a] and Frederick D. Rossini[2b]

Chemical and Petroleum Research Laboratory, Carnegie Institute of Technology, Pittsburgh 13, Pennsylvania

Received May 6, 1960

Measurements were made of the relative heats of combustion of the seventeen isomeric hexenes in the liquid state at 25°. With these and related data on the heats of vaporization, values were calculated for the heats of isomerization, and the differences in heat of hydrogenation, in both the liquid and gaseous states, at 25°, for each of the isomeric hexenes. The relation between energy content and structure is discussed.

I. Introduction

One of the aims of the work of this Laboratory has been to build a framework of experimental data from which one may study the relation between energy content and molecular structure and calculate values for the heats of formation of many hundreds of compounds without need of further experimental measurements.[3-5] Among the important groups of compounds for which are needed experimental data suitable for a basic framework of this kind are the monoölefin hydrocarbons. With experimental data already available for the monoölefins through the butenes and most of the pentenes, it appeared desirable to have for this purpose experimental data on the seventeen isomeric hexenes, for only three of which were any data available, and these only by reference to the corresponding paraffins. Accordingly, the present investigation reports experimental data on the relative heats of combustion of the seventeen hexenes, and presents results of the calculations made from these and related data on heats of vaporization, leading to values of the heats of isomerization, and differences in the heats of hydrogenation, of the isomeric hexenes in both the liquid and gaseous states at 25°.

II. Apparatus and Experimental Procedure

The experimental values of this investigation are based on the absolute joule as the unit of energy. Conversion to the defined thermochemical calorie is made using the relations 1 calorie = 4.184 (exactly) joules. For internal consistency with other investigations from this Laboratory, the molecular weight of carbon dioxide was taken as 44.010 g./mole.

In this investigation, the chemical and calorimetric apparatus and procedures were the same as described by Browne and Rossini.[3] The bomb had an internal volume of 380 ml. One ml. of water was placed in the bomb prior to each combustion experiment. The pressure of the oxygen for combustion was made 30 atmospheres (calculated to 25°). The rise of temperature in each calorimetric experiment was near 2°, with the final temperature being near 30°, the temperature of the jacket of the calorimeter. The amount of reaction in each hydrocarbon combustion experiment was determined from the mass of carbon dioxide formed in the combustion as previously described.[3]

The compounds measured in the present investigation were API Research hydrocarbons, made available through the API Research Project 44 from materials purified by the API Research Project 6. The samples had the values of purity given in Table I. Description of the purification and determination of purity of these samples has already been given.[6-9] As a result of the methods of purification, the impurities in these samples are substantially all isomeric,

(1) This investigation was supported in part by a grant from the National Science Foundation. Submitted in partial fulfillment of the requirements for the degree of Doctor of Philosophy in Chemistry at the Carnegie Institute of Technology.

(2) (a) Allied Chemical Corporation Fellow in Chemistry, 1955–1956; (b) Department of Chemistry University of Notre Dame, Notre Dame, Indiana.

(3) C. C. Browne and F. D. Rossini, This Journal, **64**, 927 (1960).

(4) Sr. M. C. Loeffler and F. D. Rossini, *ibid.*, **64**, 1530 (1960).

(5) D. M. Speros and F. D. Rossini, *ibid.*, **64**, 1723 (1960).

(6) A. J. Streiff, E. T. Murphy, J. C. Zimmerman, L. F. Soule, V. A. Sedlak, C. B. Willingham and F. D. Rossini, *J. Research Natl. Bur. Standards*, **39**, 321 (1947).

(7) A. J. Streiff, J. C. Zimmerman, L. F. Soule, M. T. Butt, V. A. Sedlak, C. B. Willingham and F. D. Rossini, *ibid.*, **41**, 323 (1948).

(8) A. J. Streiff, L. F. Soule, C. M. Kennedy, M. E. Janes, V. A. Sedlak, C. B. Willingham and F. D. Rossini, *ibid.*, **45**, 173 (1950).

(9) A. J. Streiff, A. R. Hulme, P. A. Cowie, N. C. Krouskop and F. D. Rossini, *Anal. Chem.*, **27**, 511 (1955).

and the amounts are such as to have an insignificant effect on the results.

TABLE I

PURITY OF THE COMPOUNDS MEASURED

Compound	Purity, mole %
1-Hexene	99.87 ± 0.08
cis-2-Hexene	99.94 ± .05
trans-2-Hexene	99.94 ± .11
cis-3-Hexene	99.90 ± .08
trans-3-Hexene	99.95 ± .03
2-Methyl-1-pentene	99.92 ± .07
3-Methyl-1-pentene	99.75 ± .20
4-Methyl-1-pentene	99.85 ± .12
2-Methyl-2-pentene	99.96 ± .03
3-Methyl-*cis*-2-pentene[a]	99.89 ± .09
3-Methyl-*trans*-2-pentene[b]	99.89 ± .08
4-Methyl-*cis*-2-pentene	99.93 ± .07
4-Methyl-*trans*-2-pentene	99.92 ± .07
2-Ethyl-1-butene	99.95 ± .04
2,3-Dimethyl-1-butene	99.86 ± .13
3,3-Dimethyl-1-butene	99.91 ± .06
2,3-Dimethyl-2-butene	99.94 ± .05

[a] This isomer, formerly labeled "*trans*", has the following properties: boiling point at 1 atm., 67.70°; refractive index, n_D, at 25°, 1.3988; density at 25°, 0.6886 g./ml. [b] This isomer, formerly labeled "*cis*", has the following properties: boiling point at 1 atm., 70.44°; refractive index, n_D, at 25°, 1.4017; density at 25°, 0.6930 g./ml.

The method of determining heats of isomerization from data on the relative heats of combustion has been described in detail.[4,10] Briefly, the method applied here consists of determining the ratio of the heat of combustion of each isomer to that of 1-hexene. The difference between unity and the value of the ratio, multiplied by a given value for the heat of combustion of 1-hexene, gives the energy of isomerization

$$\Delta E_B(\text{isomerization}) = (-\Delta E_B)_n - (-\Delta E_B)_i = (-\Delta E_B)_n (1 - B_i/B_n) \quad (1)$$

In equation 1, the subscripts B, n and i refer to the bomb process, 1-hexene, and a given isomer, respectively, and B is the quantity evaluated experimentally as the corrected rise of temperature, expressed in ohms, divided by the true mass of carbon dioxide formed in the combustion. The value of the Washburn correction[9] was calculated to be −0.0316%, the same for all seventeen isomers. Since this is the same for all isomers, it follows the value of the energy of isomerization under the conditions of the bomb process, pressure of 30 atmospheres, will be the same as the standard energy of isomerization, within the limits of measurement

$$\Delta E_B(\text{isomerization}) = \Delta E^0(\text{isomerization}) \quad (2)$$

Since the value of the energy of isomerization is less than 10 kcal./mole, and since the heat of combustion is near 1000 kcal./mole, it follows that one does not need an accurate value of the heat of combustion of 1-hexene for the present calculations. The accuracy of the energy of isomerization depends upon the accuracy and precision of the ratio of the given heats of combustion, B_i/B_n. Furthermore, the ratio B_i/B_n may be taken the same at 25 as at 30°, far within the uncertainty, because the temperature coefficient of the heat of combustion in the bomb process is not significantly different for any two of the hexenes. Also, since Δ(PV) is not significantly different for the several isomers

$$\Delta E^0(\text{isomerization}) = \Delta H^0(\text{isomerization}) \quad (3)$$

For these combustions in the liquid state, the hydrocarbons were sealed in thin-walled soft glass ampoules, prepared as previously described.[3-5]

III. Data of the Present Investigation

The results of experiments to determine the energy of the ignition process, including the combustion of 6.4 cm. of No. 34 B and S gage Parr iron wire, having a mass of 0.0973 g., are given in Table II.

TABLE II

EXPERIMENTS TO DETERMINE THE CHANGE IN TEMPERATURE OF THE STANDARD CALORIMETER SYSTEM BY THE STANDARD IGNITION PROCESS (6.4 CM. OF NO. 34 B AND S GAGE PARR IRON WIRE, OF MASS 0.00973 G.)

No. of experiments	Range of mass of iron wire burned, g.	Range of Δr, ohm	Range of cor. for excess of iron wire burned, ohm	Range of Δri, ohm	Mean value and stand. dev. of the mean, ohm
4	0.00969 to .00976	0.000348 to .000353	−0.000001 to + .000001	0.000349 to .000352	0.000350 ± .000001

The results of the combustion experiments for each of the seventeen hexenes are given in Table III. The symbols in this table are as previously defined.[3]

IV. Data of Other Investigations

There appear to be reported in the literature no experimental values for the heats of combustion of any of the hexenes. However, Kistiakowsky and co-workers[11-13] reported data on the heats of hydrogenation in the gas phase at 82° for the three dimethylbutenes. Converting their data to 25°, taking the standard heat of hydrogenation of 1-hexene as given in the tables of the API Research Project 44,[14] and calculating the value of the heat of hydrogenation of 1-hexene less than that of the given isomer, in the gas phase at 25°, one obtains for the difference in the resulting values from the two investigations the following in kcal./mole: 2,3-dimethyl-1-butene, −1.06 ± 0.63; 3,3-dimethyl-1-butene, −0.45 ± 0.63; and 2,3-dimethyl-1-butene, 0.23 ± 0.59. It is seen that for the last two compounds the differences in the values from the investigations are within the respective limits of uncertainty. For the first-named compound however the difference is a little larger than the sum of the respective uncertainties.

V. Heats of Isomerization and Differences in the Heats of Hydrogenation

Table IV gives the following values: the ratio of the standard heat of combustion of the given isomer to that of 1-hexene, for the liquid state at 25°, taken the same as the corresponding ratio for the bomb process at 25°, which is not significantly different from the corresponding ratio for the bomb process at 30°, which was determined experimentally in the present investigation; the standard heat of isomerization of 1-hexene to the given isomer, for the liquid state at 25°, calculated from the foregoing data and equation 1, with the value for 1-hexene recommended by Loeffler and Rossini,[4] and

(10) E. J. Prosen and F. D. Rossini, *J. Research Natl. Bur. Standards*, **27**, 289 (1941).

(11) G. B. Kistiakowsky, J. R. Ruhoff, H. A. Smith and W. E. Vaughan, *J. Am. Chem. Soc.*, **57**, 876 (1935).

(12) G. B. Kistiakowsky, J. R. Ruhoff, H. A. Smith and W. E. Vaughan, *ibid.*, **58**, 137 (1936).

(13) M. A. Dolliver, T. L. Gresham, G. B. Kistiakowsky and W. E. Vaughan, *ibid.*, **59**, 831 (1937).

(14) F. D. Rossini, K. S. Pitzer, R. L. Arnett, R. M. Braun and G. C. Pimental, "Selected Values of Physical and Thermodynamic Properties of Hydrocarbons and Related Compounds," API Research Project 44, Carnegie Press, Pittsburgh, Pennsylvania, 1953.

TABLE III

RESULTS OF THE COMBUSTION EXPERIMENTS ON THE SEVENTEEN HEXENES IN THE LIQUID STATE AT 30°

No. of experiments	Range of mass of CO_2 formed, g.	Range of k, min.$^{-1}$	Range of K, ohm	Range of U, ohm	Range of ΔR_c, ohm	Range of Δr_i, ohm	Range of Δr_n, ohm	Range of B, ohms/g. CO_2	Mean value and stand. dev. of the mean B, ohms/g. CO_2
					1-Hexene				
8	2.70946 to 2.78281	0.001562 to .001621	0.000548 to .000623	0.000621 to .001310	0.199699 to .204975	0.000334 to .000352	0.000019 to .000042	0.0735214 to .0735716	0.0735548 ± .0000059
					cis-2-Hexene				
5	2.74361 to 2.94506	.001567 to .001595	.000463 to .000732	.000594 to .000717	.201635 to .216363	.000350 to .000352	.000032 to .000087	.0733252 to .0733583	.0733429 ± .0000072
					trans-2-Hexene				
8	2.57615 to 2.74392	.001563 to .001646	.000627 to .000933	.000578 to .001245	.189194 to .201640	.000340 to .000352	.000038 to .000068	.0732761 to .0733530	.0733128 ± .0000082
					cis-3-Hexene				
4	2.67993 to 2.73872	.001599 to .001616	.000635 to .000785	.000693 to .001131	.197145 to .201484	.000346 to .000350	.000038 to .000073	.0734224 to .0734465	.0734338 ± .0000065
					trans-3-Hexene				
4	2.61078 to 2.80407	.001548 to .001589	.000620 to .000833	.000646 to .001195	.193970 to .205921	.000343 to .000352	.000016 to .000085	.0732845 to .0733157	.0733029 ± .0000065
					2-Methyl-1-pentene				
4	2.93702 to 2.95908	.001583 to .001590	.000420 to .000613	.000635 to .000774	.217071 to .215451	.000350 to .000351	.000047 to .000075	.0732463 to .0732215	.0732315 ± .0000060
					3-Methyl-1-pentene				
4	2.51227 to 2.58879	.001581 to .001610	.001024 to .001110	.000294 to .000672	.184843 to .190496	.000328 to .000353	.000041 to .000055	.0734272 to .0734650	.0734488 ± .0000095
					4-Methyl-1-pentene				
3	2.74952 to 2.84085	.001588 to .001611	.000520 to .000667	.000654 to .001027	.202233 to .209018	.000349 to .000352	.000044 to .000066	.0733911 to .0734358	.0734143 ± .0000129
					2-Methyl-2-pentene				
4	2.46403 to 2.63509	.001570 to .001628	.000933 to .001203	.000315 to .000710	.180425 to .192954	.000339 to .000351	.000023 to .000056	.0730488 to .0730879	.0730736 ± .0000085
					3-Methyl-*cis*-2-pentene[a]				
4	2.55918 to 2.59244	.001591 to .001599	.001000 to .001066	.000334 to .000406	.187614 to .189998	.000351 to .000352	.000019 to .000068	.0731332 to .0731604	.0731467 ± .0000057
					3-Methyl-*trans*-2-pentene[a]				
4	2.49700 to 2.53476	.001583 to .001594	.001001 to .001152	.000275 to .000362	.183019 to .185731	.000349 to .000351	.000016 to .000092	.0731348 to .0731752	.0731497 + .0000092
					4-Methyl-*cis*-2-pentene				
5	2.50892 to 2.53568	.001563 to .001606	.001072 to .001103	.000413 to .000752	.184257 to .186187	.000350 to .000352	.000032 to .000041	.0732786 to .0732940	.0732855 ± .0000034
					4-Methyl-*trans*-2-pentene				
4	2.55575 to 2.57553	.001561 to .001607	.001044 to .001060	.000347 to .000605	.187433 to .188938	.000350 to .000353	.000034 to .000053	.0731865 to .0732191	.0732024 ± .0000073

TABLE III (*Continued*)

No. of experiments	Range of mass of CO_2 formed, g.	Range of k, min.$^{-1}$	Range of K, ohm	Range of U, ohm	Range of ΔR_c, ohm	Range of Δr_i, ohm	Range of Δr_n, ohm	Range of B, ohms/g. CO_2	Mean value and stand. dev. of the mean B, ohms/g. CO_2
				2-Ethyl-1-butene					
	2.52558	.001586	.001051	.000330	.185513	.000349	.000047	.0732594	.0732841
4	to	to	to	to	to	to	to	to	± .0000088
	2.56280	.001615	.001127	.000813	.188227	.000352	.000074	.0733017	
				2,3-Dimethyl-1-butene					
	2.49574	.001559	.001041	.000594	.182852	.000350	.000020	.0731088	.0731275
4	to	to	to	to	to	to	to	to	± .0000116
	2.56871	.001607	.001174	.000781	.184915	.000353	.000102	.0731589	
				3,3-Dimethyl-1-butene					
	2.72758	.001572	.000724	.000656	.200147	.000350	.000020	.0732496	.0732626
4	to	to	to	to	to	to	to	to	± .0000099
	2.75623	.001672	.000789	.000768	.202402	.000352	.000080	.0732919	
				2,3-Dimethyl-2-butene					
	2.61958	.001596	.000726	.000662	.191545	.000350	.000028	.0729819	.0730023
4	to	to	to	to	to	to	to	to	± .0000088
	2.77025	.001699	.000980	.000872	.202617	.000354	.000063	.0730210	

[a] See footnotes *a* and *b* of Table I.

TABLE IV

HEATS[a] OF ISOMERIZATION, AND THE DIFFERENCE IN THE HEATS OF HYDROGENATION, FOR BOTH THE LIQUID AND GASEOUS STATES AT 25°

Compound	Ratio of the heats of combustion at 25°	Heat of isomerization for the liquid at 25°, kcal./mole	ΔHv^0 (isomer) $-\Delta Hv^0$ (1-hexene) at 25°, kcal./mole	Heat of isomerization for the gas at 25°, kcal./mole	Standard heat of hydrogenation, ΔHh^0, of 1-hexene less that of the isomer,[c] at 25°, kcal./mole: Liquid	Gas
1-Hexene	1.00000	0.00	0.00	0.00	0.00	0.00
cis-2-Hexene	0.99712 ± 0.00025	−2.75 ± 0.24	.20 ± 0.04	−2.55 ± 0.24	−2.75 ± 0.32	−2.55 ± 0.32
trans-2-Hexene	.99671 ± .00032	−3.14 ± .31	.22 ± .04	−2.92 ± .31	−3.14 ± .36	−2.92 ± .36
cis-3-Hexene	.99836 ± .00024	−1.57 ± .23	.15 ± .04	−1.42 ± .23	−1.57 ± .31	−1.42 ± .31
trans-3-Hexene	.99658 ± .00024	−3.27 ± .23	.22 ± .04	−3.05 ± .23	−3.27 ± .31	−3.05 ± .31
2-Methyl-1-pentene	.99561 ± .00023	−4.20 ± .22	− .03 ± .04	−4.23 ± .22	−2.90 ± .34	−2.53 ± .34
3-Methyl-1-pentene	.99856 ± .00030	−1.38 ± .29	− .48 ± .04	−1.86 ± .29	−0.62 ± .38	−0.80 ± .38
4-Methyl-1-pentene	.99809 ± .00039	−1.83 ± .37	− .45 ± .04	−2.28 ± .37	−0.53 ± .45	−0.58 ± .45
2-Methyl-2-pentene	.99346 ± .00028	−6.25 ± .27	.23 ± .04	−6.02 ± .27	−4.95 ± .37	−4.32 ± .37
3-Methyl-*cis*-2-pentene[b]	.99449 ± .00029	−5.26 ± .28	.36 ± .04	−4.90 ± .28	−4.50 ± .32	−3.84 ± .32
3-Methyl-*trans*-2-pentene[b]	.99445 ± .00022	−5.30 ± .21	.18 ± .04	−5.12 ± .21	−4.54 ± .37	−4.06 ± .37
4-Methyl-*cis*-2-pentene	.99634 ± .00018	−3.50 ± .18	− .27 ± .04	−3.77 ± .18	−2.20 ± .31	−2.07 ± .31
4-Methyl-*trans*-2-pentene	.99521 ± .00025	−4.58 ± .26	− .15 ± .04	−4.73 ± .24	−3.28 ± .35	−3.03 ± .35
2-Ethyl-1-butene	.99632 ± .00029	−3.52 ± .28	.10 ± .04	−3.42 ± .28	−2.76 ± .37	−2.36 ± .37
2,3-Dimethyl-1-butene	.99419 ± .00035	−5.55 ± .34	− .34 ± .04	−5.89 ± .34	−3.59 ± .42	−3.36 ± .42
3,3-Dimethyl-1-butene	.99603 ± .00031	−3.80 ± .30	− .94 ± .04	−4.74 ± .30	−0.32 ± .38	−0.35 ± .38
2,3-Dimethyl-2-butene	.99249 ± .00029	−7.18 ± .27	.46 ± .04	−6.72 ± .27	−5.22 ± .37	−4.19 ± .37

[a] The uncertainties in this table are twice the standard deviation. [b] See footnotes *a* and *b* of Table I. [c] The uncertainties given for the heats of hydrogenation are taken to be those for the isomer.

taking the difference between ΔH and ΔE to be the same for all isomers; the standard heat of vaporization of 1-hexene less that of the given isomer, at 25°, from the data of Camin and Rossini,[15] with 0.02 kcal./mole being added to the heat of vaporization at saturation pressure; the standard heat of isomerization of 1-hexene to the given isomer, for the gaseous state at 25°, calculated from the corresponding values for the liquid state and the differences in the heats of vaporization; and the standard heat of hydrogenation of 1-hexene less that of the given isomer, for both the liquid and gaseous states at 25°.

To obtain values for the heats of formation (and combustion) of the isomeric hexenes from these data, for both liquid and gaseous states, the reader may use the following values for the standard heat of formation, ΔHf^0, at 25°, in kcal./mole: 1-hexene (liq),[4] −17.30; 1-hexene (g),[14] −9.96.

VI. Discussion

Taylor, Pignocco and Rossini[16] and Prosen and Rossini[17] presented a simple correlation of the properties of monoölefin hydrocarbons involving classification into six types, as had Boord.[18] For the purpose of this work, we wish to identify seven simple types of monoölefins. The first and second columns of Table V identify the structures in question. The third column gives the number of hexenes having the given structure. The last two

(15) D. L. Camin and F. D. Rossini, THIS JOURNAL, **60**, 1446 (1956).

(16) W. J. Taylor, J. M. Pignocco and F. D. Rossini, *J. Research Natl. Bur. Standards*, **34**, 313 (1945).

(17) E. J. Prosen and F. D. Rossini, *ibid.*, **36**, 269 (1946).

(18) C. E. Boord, *Petroleum Refiner*, **21**, 372 (1942).

columns give, for the liquid and gaseous states, respectively, the mean value of the differences from

TABLE V

HEATS OF HYDROGENATION CORRELATED WITH MOLECULAR STRUCTURE OF THE HEXENES

Type	Structure	No. of isomers	Standard heat[c] of hydrogenation, ΔH_h^0, of 1-hexene less that of the given isomer, at 25°: Liquid	Gas
I[a]	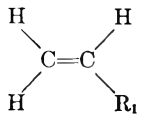	1	0.00	0.00
II[b]	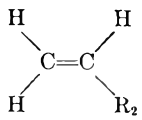	3	−0.49 ± 0.11	−0.58 ± 0.15
III	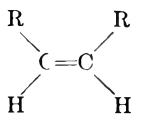	3	−2.17 ± .40	−2.01 ± .40
IV	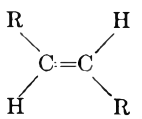	3	−3.23 ± .06	−3.00 ± .05
V	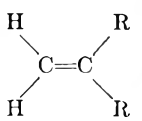	3	−3.08 ± .34	−2.75 ± .41
VI	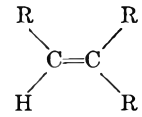	3	−4.66 ± .19	−4.07 ± .16
VII	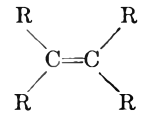	1	−5.22	−4.19

[a] In Type I, R_1 represents the normal alkyl radical. [b] In Type II, R_2 represents an alkyl radical with branching on the carbon atoms once or twice removed from the doubly bonded carbon. [c] The uncertainties given here are average deviations.

1-hexene of the heats of hydrogenation of the hexenes of the given type. It is seen that the average deviations of the several values from the mean is less than 0.5 kcal./mole. However, it is expected that as the substituents on the doubly-bonded carbon atoms become larger and introduce significant effects between non-bonded atoms, significant departures from these values will occur. In particular, this would be true of the isomers of 2,2,5,5-tetramethyl-2-hexene, as has now been determined experimentally.[19] In order to develop a suitable correlation between energy and molecular structure for the monoölefins, some additional selected monoölefin hydrocarbons, C_7 and higher, need to be measured.[19]

(19) J. D. Rockenfeller and F. D. Rossini, THIS JOURNAL, **64**, in press (1960).

SECOND VIRIAL COEFFICIENTS OF NEON, ARGON, KRYPTON AND XENON WITH A GRAPHITIZED CARBON BLACK[1]

BY J. R. SAMS, JR.,[2] G. CONSTABARIS AND G. D. HALSEY, JR.

Department of Chemistry, University of Washington, Seattle 5, Washington

Received May 9, 1960

Precise measurements of the adsorption of neon, argon, krypton and xenon on the highly graphitized carbon black P33 (2700°) at coverages of less than 10% of the monolayer are reported. These data have been analyzed in terms of a virial coefficients treatment to yield interaction energies and apparent areas. Several models for the interaction potential have been investigated, but no definite choice of a model can be made on the basis of these data. Various theories for obtaining the area from the data are discussed and compared with the usual BET method for determining the area of the black. Values for the isosteric heats of adsorption at zero coverage are also discussed.

Introduction

The interaction of rare gas atoms with the highly graphitized carbon black P33(2700°) has been studied in the temperature range where the gas atoms are interacting with the surface without interacting with each other.[3,4] This black is particularly well suited for such a study because of its well-defined, nearly homogeneous surface.[5]

The experiments consist of determinations of the apparent volume, V_a, of the sample bulb containing the solid. These data, extrapolated to zero pressure, can be analyzed in terms of various potential models by the method of Steele and Halsey,[3] to give an apparent area and interaction energy.

One does not obtain an area directly from such an analysis, but rather a product of area and an apparent distance of closest approach. This latter parameter can be evaluated from the observed energy of interaction through one of the formulas which have been derived for the constant in the London formulation of dispersion forces.[6] Those theories which have been employed here are due to Slater and Kirkwood,[7] Kirkwood and Müller,[8,9] and London.[7]

(1) This research was supported in part by the United States Air Force through the Air Force Office of Scientific Research of the Air Research and Development Command under contract No. AF 49 (638)-723.

(2) Thesis presented in partial fulfillment of the requirements for the degree of Doctor of Philosophy.

(3) W. A. Steele and G. D. Halsey, Jr., *J. Chem. Phys.*, **22**, 979 (1954).

(4) W. A. Steele and G. D. Halsey, Jr., THIS JOURNAL, **59**, 57 (1955).

(5) M. H. Polley, W. D. Schaeffer and W. R. Smith, *ibid.*, **57**, 469 (1953).

(6) M. Polanyi, *Trans. Faraday Soc.*, **28**, 316 (1932).

(7) H. Margenau, *Rev. Modern Phys.*, **11**, 1 (1939).

(8) J. G. Kirkwood, *Z. Physik*, **33**, 57 (1932).

(9) A. Müller, *Proc. Roy. Soc.* (*London*), **A154**, 624 (1936).

In addition, we have considered the metallic interaction theories of Bardeen[10] and Margenau and Pollard.[11] Although graphitic carbon is highly anisotropic, there is considerable conduction within the basal plane, and it is of interest to see how the areas determined by these latter theories compare with those calculated from non-metallic interaction theories.

The experimental results can also be converted to conventional adsorption isotherms and the isosteric heats may be calculated at essentially zero coverage.

Experimental

The apparatus employed in these investigations has previously been described.[12] The only modification which has been made is an improved mercury injector which allows easier zeroing of the manometer. Clamps C_1 and C_2 shown in Fig. 4 of ref. 10 have been replaced by two Teflon packed, stainless steel valves, one for fixing the quantity of mercury in the manometer, and the other for adjusting the zero. These valves are connected to the glass tubing by means of standard tapers sealed with a ring of wax which is not in contact with the mercury.

The gases used were assayed reagent grade He, Ne, A, Kr and Xe obtained from Air Reduction Sales Company.

As all but one temperature for the neon data are below the oxygen point, it was necessary to determine these temperatures gas thermometrically. The bulb containing the carbon black was removed, and an empty sample bulb of about 90-cc. volume was substituted. Reagent grade helium was loaded into the bulb at the oxygen point to ensure agreement of the gas thermometer results and the resistance thermometer calibration at this point. The cryostat was set in turn on each of the temperatures for the neon runs, as determined by resistance readings, and the temperatures measured with the gas thermometer. Two determinations of each temperature were made with different gas doses and the worst disagreement between any two corresponding values was 0.01°. The gas thermometer result for the one neon temperature above the oxygen point (94°K.) agreed with the resistance thermometer calibration to within 0.002°. The effect of this uncertainty in temperature on the neon results is discussed below.

Reduction of the experimental data and further analysis of the results were carried out on an IBM 650 computer. In addition to those corrections mentioned in ref. 12 which must be applied to the raw data, two others have been incorporated into the present results.

The first of these is the effect of the differential thermal contraction of the carbon black on the volume of the sample bulb, which was taken into account through an equation given by Walker, *et al.*[13] This correction is negligible at the higher temperatures, but is of considerable importance for the neon data. At 90°K. the effect from this source on the excess volume is about 4 parts in 10,000.

The second correction is the effect of the hydrostatic head on the reduced pressures. The correction is different for the pressure in the sample bulb and for that in the pipets, and these two pressures were corrected independently. For xenon at room temperature and at a pressure of 40 cm., the correction to the excess volume is about 3 parts in 10,000.

Theoretical

The results to be presented have been analyzed in terms of the apparent volume at zero pressure[3]

$$V_0 = V_{geo} + B_{AS} \qquad (1)$$

The value for V_{geo} is obtained from the helium dead space volume at the ice point, and B_{AS} is defined by the equation

$$B_{AS} = \int V_{geo} [\exp(-\epsilon_{is}/kT) - 1]\, dV \qquad (2)$$

where ϵ_{is} is the interaction energy of a single gas atom with the surface in a given volume element dV.

We have analyzed the data by four models for ϵ_{is}. The first of these is the original Steele–Halsey model[3] which employs an inverse cube attraction coupled with a hard sphere repulsion to give

$$B_{AS} = As_0 \sum_{\tau=1}^{\infty} [1/\tau!(3\tau - 1)](\epsilon^*/kT)^\tau \qquad (3)$$

where A is the surface area and ϵ^* is the interaction energy at the apparent distance of closest approach, s_0.

The three other models employ a Lennard-Jones type potential function

$$\epsilon_{ij} = \nu r^{-n} - \mu r^{-m} \qquad (4)$$

where ϵ_{ij} is the energy of interaction between one gas atom and one atom in the solid. This can be expressed in terms of only one constant

$$\epsilon_{ij} = (n/(m - n))(n/m)^{m/(n-m)}\, \epsilon_{ij}^* [(r_0/r)^n - (r_0/r)^m] \qquad (5)$$

where r_0 is the distance between a gas atom and a surface atom when the net energy of interaction is zero. Note that in this paper we have adopted the convention that positive energies denote attraction.

Assuming a semi-infinite solid bounded by a plane, eq. 5 can be integrated over the three dimensions of the solid to yield

$$\epsilon_{is} = (\beta/(\beta - \alpha))(\beta/\alpha)^{\alpha/(\beta-\alpha)}\, \epsilon_{is}^* [(s_0/s)^\alpha - (s_0/s)^\beta] \qquad (6)$$

Here ϵ_{is}^* is the maximum energy of gas–surface interaction, s_0 is the distance between a gas atom and the plane surface at zero net interaction energy, and α and β are equal to $n - 3$ and $m - 3$, respectively.

Substitution of this expression for ϵ_{is} in eq. 2 and evaluation of the integral gives

$$B_{AS} = AS_0 \sum_{\tau=0}^{\infty} (1/\beta\tau!)(1/T_{is}^*)^{[\tau(\beta-\alpha)+1]/\beta} \times \Gamma(\tau\alpha - 1/\beta) \qquad (7)$$

where we have adopted the reduced notation

$$1/T_{\epsilon_{is}^*} = (\beta/(\beta - \alpha))(\beta/\alpha)^{\alpha/(\beta-\alpha)}\, (\epsilon_{is}^*/kT)$$

The large distance between basal planes in graphite, compared to the short in-plane distance between carbon atoms suggests that a useful model might be obtained by integrating over the atoms in the surface plane only. At short distances from the surface, the contributions from the first layer of atoms are of much the greatest importance, while the contributions from the underlying planes become relatively important only when the total interaction energy is small anyway. In this case one obtains equations identical in form with (6) and (7) with α and β now given by $n - 2$ and $m - 2$, respectively.

The three potential models we have used employing such equations are a 6–12 which is integrated (1) over a semi-infinite solid to yield a 3–9 and (2) over a single infinite plane, resulting in a 4–10 potential law, and a 3–12 law which corresponds to integration over the attractive part of the potential alone.

(10) J. Bardeen, *Phys. Rev.*, **58**, 727 (1940).

(11) H. Margenau and W. G. Pollard, *ibid.*, **60**, 128 (1941).

(12) G. Constabaris, J. H. Singleton and G. D. Halsey, Jr., This Journal, **63**, 1350 (1959).

(13) P. L. Walker, Jr., H. A. McKinstry and C. C. Wright, *Ind. Eng. Chem.*, **45**, 1711 (1953).

Discussion

Error Analysis.—The neon data were treated twice, once with each of the two sets of temperatures obtained gas thermometrically, in order to assess the effect of such discrepancies in temperature on the final results. The two sets of curve fit results gave the same value for the interaction energy with all the models, but slightly different values for As_0. The corresponding As_0 values for the 3–9, 3–12 and 4–10 models all differed by about 0.1% between the two sets, but for the 3-∞ case, the difference was nearly 1%. The second set of temperatures gave slightly lower standard deviations (*e.g.*, 1.35×10^{-3} *vs.* 1.68×10^{-3} for the 3–9 model) and are the ones reported here.

A more complete error analysis was carried out with the krypton data, to determine more accurately what effect errors in the experimental data have on the final curve fit results. There are several individual readings which must be taken for each experimental point. In addition to the temperature of the sample bulb, one must also read the temperature of the ice mantle and of the manometer housing, and the temperature distribution along the gas inlet tube must be determined through a series of thermocouple readings. In each determination of the pressure there are four readings which must be taken, one on the short leg, one on the free leg, and two on the meter bar. Errors may also occur in the determination of the meniscus height and of the mis-set of the mercury levels in the pipets from the calibration marks. The magnitudes of these errors have been discussed previously.[12]

There are two distinct types of readings which one makes. The first type, which we shall speak of as "head" readings, are made before admitting the gas into the sample bulb, in order to determine the total quantity of gas in the system. The second type, or "tail" readings, are made after gas has been admitted to the bulb. The number of moles in the sample bulb, which must be known to compute the apparent volume, is obtained for each tail reading as the difference in the total number of moles in the system and in the number of moles outside the bulb. In general, a fairly large number of tail readings are made for each head reading. It is for this reason that a large error in a tail reading is not very serious, while a correspondingly large error in a head reading is. Such an error in a tail reading will merely give an experimental point which is out of line with the other points determined at that temperature, but if, on the other hand, it occurs in a head reading it will affect all the tail readings based on it. Moreover, it will affect them to a different extent, depending upon the difference in pressure between the head reading and a given tail reading. Thus, the slope of the isotherm is altered and the error in the value of V_a extrapolated to zero pressure is magnified.

In any given case one expects that the errors in the individual readings which together determine the experimental point will tend to cancel each other to a large degree, but there is always the possibility that a preponderance of the errors will be acting in the same direction. We have therefore assumed the maximum probable error in each of the individual readings to be acting all in the same direction, and have calculated krypton results based on head readings incorporating these maximum errors. We did not change any of the original tail readings in making these calculations. The new values of V_x at zero pressure obtained from this analysis were fitted to each of the four models. A comparison of these results with the original ones gave the following approximate limits of error: $\pm 0.7\%$ in ϵ_{is}^*/R and a corresponding $\mp 4\%$ in As_0. This will cause an error of about $\pm 3\%$ in the areas. It must be remembered, however, that these calculations assume the simultaneous occurrence of the maximum probable error in a number of readings, with no cancellation of errors, and that consequently the limits quoted are considerably larger than the probable values of the error. They do, however, serve to give an indication of the minimum accuracy to be expected.

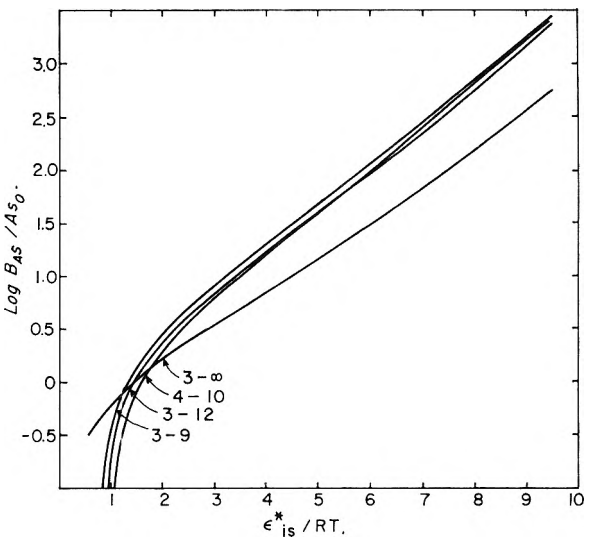

Fig. 1.—Curves of log B_{AS}/As_0 *vs.* ϵ_{is}^+/RT for the four potential models considered (see eqs. 3 and 7).

Curve Fit Results.—The experimental values of the excess volume at zero pressure (Table I) have been fitted as a function of reduced temperature to each of the four models discussed above, to determine the values of the parameters ϵ_{is}^* and As_0 which give the best fit. The theoretical curves for the models are shown in Fig. 1. The fitting is done on the computer by a scanning process. A range of values of ϵ_{is}^*/R is chosen; the scanning proceeds from the low to the high end of the range in any desired increment, and the value of ϵ_{is}^*/R is found which gives the smallest standard deviation from the theoretical curve for the experimental log B_{AS}/As_0. All fitting has been done to the nearest one degree in ϵ_{is}^*/R. The parameters of best fit, along with the standard deviation of the fit (in log As_0) are presented in Table II. The fitted values for the 3–12 and 3–∞ models are plotted in Figs. 2 and 3, in which the solid line represents the theoretical values.

The data for neon and argon give a significantly worse fit to the 3–∞ model than they do to the softer Lennard–Jones type potential models, but there is

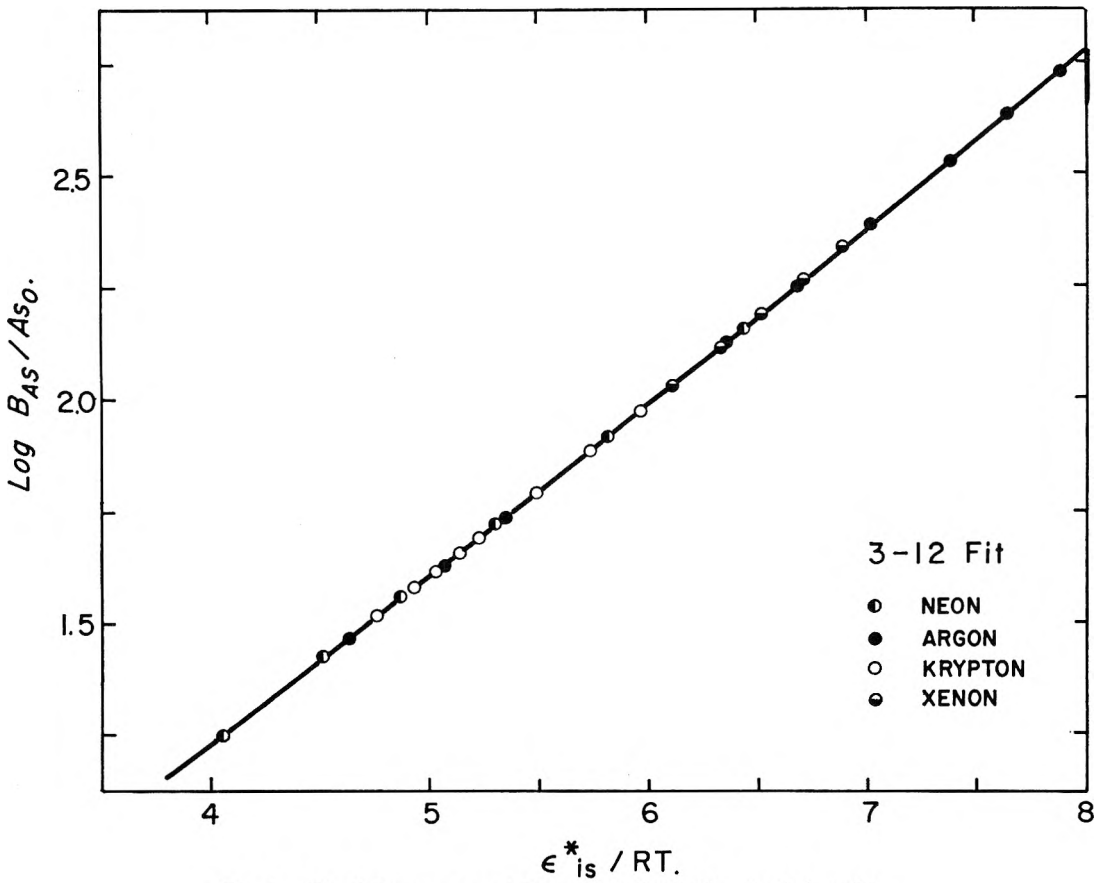

Fig. 2 —Fit of the experimental results to the 3-12 potential model.

Table I

Excess Volume at Zero Pressure—Ne, A, Kr, Xe

Neon		Argon	
V_x, ml./g.	Temp., °K.	V_x, ml./g.	Temp., °K.
0.3637	59.519	1.4811	140.607
.2098	65.949	1.1861	145.115
.1347	72.293	0.9422	150.140
.0928	78.611	.6725	158.077
.0679	84.814	.4937	166.135
.0455	94.337	.3655	175.082
		.1512	207.773
		.1160	220.393
		.0813	240.019

Krypton		Xenon	
V_x, ml./g.	Temp., °K.	V_x, ml./g.	Temp., °K.
0.2645	245.173		
.2147	255.401		
.1736	266.901		
.1383	279.472	0.6549	279.197
.1266	285.119	.5558	287.046
.1160	291.173	.4717	295.052
.1065	297.159	.4003	303.222
.0925	307.171	.3269	315.033

little room for choice among the models when one considers the krypton and xenon data. This latter fact is due partly to the limited ϵ_{is}^*/RT range into which both the krypton and xenon data fall, and partly to the fact that in these (nearly linear) portions of the curves the fit is not very sensitive to the model anyway. The most critical region for testing the models is ϵ_{is}^*/RT less than about 3, but unfortunately, with a low area powder such as P33 the present apparatus will not give sensible results in this region. The higher end of this region should be attainable with helium, but even at room temperature the quantum mechanical correction for this gas is probably substantial.

Table II

Parameters of Best Fit for Various Models—Ne, A, Kr, Xe

Model	ϵ_{is}^*/R, °K.	$A_{s0} \times 10^3$, ml./g.	St. dev. $\times 10^3$
	Neon		
3–9	382	2.199	1.35
3–12	383	2.541	1.31
3–∞	435	4.240	5.69
4–10	367	3.117	0.47
	Argon		
3–9	1107	2.393	0.72
3–12	1110	2.762	0.72
3–∞	1229	5.149	4.60
4–10	1071	3.278	1.45
	Krypton		
3–9	1460	2.406	1.57
3–12	1463	2.797	1.57
3–∞	1651	4.782	1.61
4–10	1403	3.399	1.66
	Xenon		
3–9	1919	2.625	1.48
3–12	1923	3.042	1.44
3–∞	2117	5.942	1.42
4–10	1860	3.549	1.46

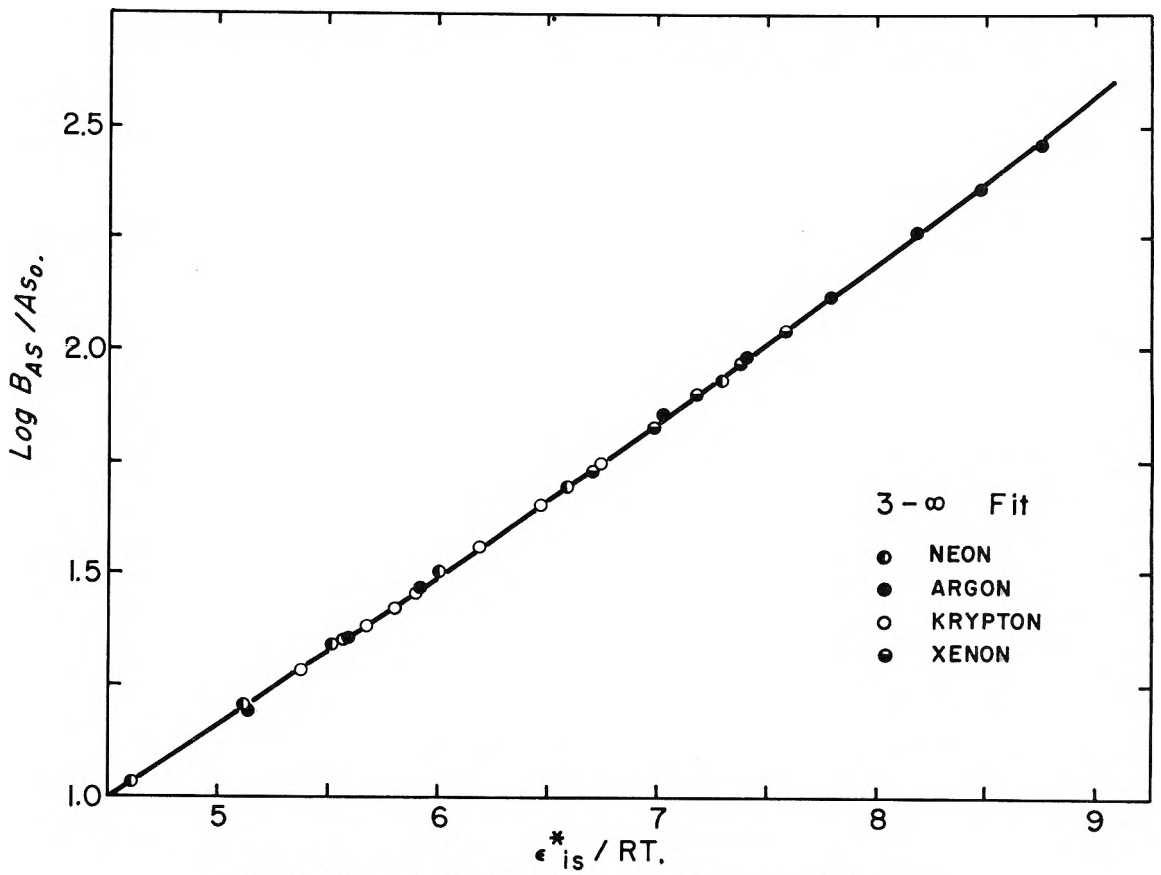

Fig. 3.—Experimental results fitted to the crude 3–∞ potential model.

It is significant that the argon results, which cover a wide range of values encompassing the Xe, Kr and about two-thirds of the Ne results, show such a (relatively) poor fit for the 3–∞ model. One does not expect to find a clear-cut preference for either the 3–9 or the 3–12, since a fit of this type, especially in the present range of values, is quite insensitive to the exact nature of the repulsive potential employed. Moreover, the 3–9 and 3–12 curves are very nearly parallel even in the range of low ϵ_{is}^*/RT, so that only extremely accurate data in this region would enable one to make a definite choice as to which is the better model. In fact, it is unlikely that such a choice can be made on the basis of second-order interactions only.

The neon data show a preference for the 4–10 model, which is possibly due to the fact that the neon atoms approach the surface more closely than do those of the other gases, and hence feel contributions from the underlying planes to a lesser extent. Thus, neon effectively appears to be interacting with a single plane.

The values for the interaction energies given in Table II may be compared with those calculated by Crowell[14] for the interactions of rare gases with graphite by his approximation to a direct lattice sum, assuming a 6–12 potential between gas atoms and carbon atoms in the lattice. Crowell's results apply to systems where lateral interactions are negligible, and thus should be comparable to the present values obtained by the 3–9 and 3–12 models. His calculated values of ϵ_{is}^*/R are: Ne, 375°K.; A, 906°K.; Kr, 1369°K.; Xe, 1696°K. The agreement is fairly good in light of the approximations inherent in both sets of values, except in the case of argon, where Crowell's value appears to be unreasonably low.

The data for the apparent volumes can be converted into the usual terms of volume adsorbed at STP, V_{STP}, through the equation

$$V_{STP} = (273.15P)(V_a - V_{DS})/(76.000T) \quad (8)$$

where V_{DS} is the internal dead space volume. The isotherms in these low coverage regions are all straight lines, so that isosteres taken from the data all have the same slope. Thus, one is in effect computing the isosteric heat of adsorption, q_{st}, at zero coverage. Values for this quantity are given in Table III. From the definition of the isosteric heat of adsorption one can show by a thermodynamical argument[15] that q_{st} is $1/2RT$ greater than ϵ_{is}^* for non-localized adsorption, and $1/2RT$ smaller for localized adsorption. Our results clearly indicate adsorption which is non-localized. Values for $q_{st} - 1/2RT$ are included in Table III, where the temperature taken is the middle of the range of experimental temperatures for the given gas. The use of this as a criterion for choosing a model requires values for q_{st} which are accurate to within two or three calories per mole. This accuracy is about an order of magnitude greater than that of the present values, and no choice can be

(14) A. D. Crowell, *J. Chem. Phys.*, **26**, 1407 (1957).

(15) *E.g.*, D. H. Everett, *Trans. Faraday Soc.*, **46**, 453 (1950).

made among the three Lennard–Jones type potential models. However, the 3–∞ model gives values for ϵ_{is}* which are much too high.

Table III

Isosteric Heats of Adsorption at Zero Coverage

Gas	q_{st}, cal./mole	$(q_{st} - \frac{1}{2}RT)/R$, °K.
Ne	849	389
Ar	2355	1083
Kr	2999	1370
Xe	4059	1892

Estimation of the Area.—In the present method there is no way that one can obtain an area without recourse to assumptions which are external to the model. The curve fit gives an experimental value for the product As_0, but there is no provision for calculating s_0. In the past, the gas–surface attractive potential has been identified with the London forces attraction of two isolated systems

$$\epsilon_{ij}^* = C/r^6_{ij} \qquad (9)$$

and the constant of proportionality C evaluated by means of the Kirkwood–Müller formula[8,9]

$$C_{KM} = (6mc^2\alpha_1\alpha_2)/(\alpha_1/\chi_1 + \alpha_2/\chi_2) \qquad (10)$$

where the α's and χ's are the atomic polarizabilities and diamagnetic susceptibilities, respectively, of the atoms. We have also followed this procedure here, but in addition have employed two other equations which have been proposed for the constant C, those due to Slater and Kirkwood[7]

$$C_{SK} = (3eh/4\pi m^{1/2})\{(\alpha_1\alpha_2)/[(\alpha_1/n_1)^{1/2} + (\alpha_2/n_2)^{1/2}]\} \qquad (11)$$

and to London[7]

$$C_L = (3\alpha_1\alpha_2 I_1 I_2)/2(I_1 + I_2) \qquad (12)$$

In these equations e is the charge and m the mass of an electron, h is Planck's constant, the I's are the ionization potentials and the n's the numbers of electrons in the outer shells of the atoms.

Comparison of one of these C values with the experimental value of ϵ_{is}* then gives s_0. For the 3–∞ model, integration of eq. 9 over a semi-infinite solid gives

$$\epsilon_{is}^* = -N_0 C/6s_0^3 \qquad (13)$$

where N_0 is the number of atoms per cc. in the solid. For the 3–9 and 3–12 models, in order to make eq. 5 and 9 consistent at large separations, one must identify

$$C = (n/(m - n))(n/m)^{m/(n-m)}\,\epsilon_{ij}^*\, r_0^n \qquad (14)$$

so that in these cases the right-hand side of eq. 13 must be multiplied by the factor

$$1/(\beta(\beta - \alpha))(\beta/\alpha)^{\alpha/(\beta-\alpha)} \qquad (15)$$

Integration of eq. 9 over a single infinite plane results in the expression

$$\epsilon_{is}^* = -N_0' C/2s_0^4 \qquad (16)$$

where N_0' is the number of atoms per cm.^{2} of the surface. For the 4–10 model, the right-hand side of eq. 16 must be multiplied by the factor (15) with α and β now given by $n - 2$ and $m - 2$, respectively.

We have also used two metallic interaction theories for the calculation of s_0 for the 3–9, 3–12 and 3–∞ models. Bardeen's expression for the interaction of a rare gas atom with a metal surface is[10]

$$\epsilon_B^* = (\alpha_0 I/8s_0^3)(Ke^2/2rI)/(1 + Ke^2/2rI) \qquad (17)$$

where α_0 and I refer to the gas, K is a numerical constant approximately equal to 2.6, and r is the radius of a sphere in the solid containing one conduction electron. Margenau and Pollard derived the equation[11]

$$\epsilon_{MP}^* = (e^2\alpha_0/16s_0^3)[(K/r) - (hn_0/\pi m\nu_0)] \qquad (18)$$

where n_0 is the number of conduction electrons per cc. of the solid and ν_0 is the resonant frequency of the gas.

Values used for the polarizabilities, susceptibilities and ionization potentials are given in Table IV and the areas computed by the various formulas appear in Table V. For the models considered, the Kirkwood–Müller formula consistently gives the lowest areas, and the London formula the highest. The differences among the various formulas indicate that it is impossible to attach much quantitative significance to areas determined in this way, but in general the values are in fairly good agreement with the BET area of about 12.5 m.^{2}/g. Preliminary results for argon obtained with this apparatus[16] gave a Kirkwood–Müller area of 15.9 m.^{2}/g. when analyzed in terms of the 3–∞ model, and the values ϵ_{is}* = 2410 cal./mole and q_{st} = 2330

Table IV

Physical Properties of Substances

Molecule	Polarizability, × 10^{24} cc.	Susceptibility, × 10^{29} cc.	Ionization potential, e.v.
Ne	0.39[a]	1.17[b]	25.7[a]
Ar	1.63[a]	3.24[c]	17.5[a]
Kr	2.46[a]	4.65[c]	14.7[a]
Xe	4.00[a]	7.04[c]	12.2[a]
C	1.02[d]	13.5[f]	11.2[e]

[a] H. Margenau, *Rev. Modern Phys.*, 11, 1 (1939). [b] E. C. Stoner, "Magnetism," Methuen and Co., Ltd., London, 1948, p. 38. [c] K. E. Mann, *Z. Physik*, 98, 548 (1936). [d] "International Critical Tables," Vol. I and IV, McGraw–Hill Book Co., Inc., New York, N.Y., 1926–1928. [e] "Handbook of Chemistry and Physics," Chemical Rubber Publishing Co., Cleveland, Ohio, 1953. [f] H. T. Pinnick, *Phys. Rev.*, 94, 319 (1954).

Table V

Areas Determined by Various Formulae

Potential model	Gas	A_{KM}	A_{SK}	A_L	A_B	A_{MP}
3–9	Ne	8.00	12.09	14.87	12.65	11.77
	Ar	8.64	12.80	14.96	12.80	11.81
	Kr	8.44	12.73	14.76	12.66	11.68
	Xe	8.75	13.53	15.44	13.26	12.38
3–12	Ne	8.64	13.11	16.10	13.68	12.72
	Ar	9.33	13.81	16.15	13.81	12.73
	Kr	9.17	13.81	15.98	13.78	12.71
	Xe	9.48	14.63	16.71	14.42	13.40
3–∞	Ne	11.71	17.57	21.54	18.34	17.07
	Ar	14.03	20.76	24.29	20.76	19.14
	Kr	12.72	19.13	22.14	19.05	17.58
	Xe	14.89	23.03	26.18	22.59	21.00
4–10	Ne	8.45	10.91	13.45		
	Ar	8.86	11.38	13.38		
	Kr	8.97	11.76	13.65		
	Xe	9.05	12.11	13.81		

(16) G. Constabaris and G. D. Halsey, Jr., *J. Chem. Phys.*, **27**, 1433 (1957).

cal./mole. The present results extend and revise these values.

With the exception of the Kirkwood–Müller and Slater–Kirkwood areas for the 4–10 model, no definite drift in area with molecular size is observed, although in every instance xenon gives the highest area. This could be explained by the size of the xenon atom, which makes it more highly polarizable, thus allowing of stronger interaction with the surface. On the basis of this argument, however, one would expect krypton to show a larger area than argon, which is apparently not the case.

The fact that neon gives smaller areas than the other gases is of interest as regards surface homogeneity. Even if the crystallites in P33 are arranged in a more or less perfect surface of basal planes, one might still expect high energy sites in the form of boundaries between adjacent planes. As Beebe[17] has pointed out, an adsorbate capable of closer approach would be expected to be more sensitive to such irregularities in the surface. Since neon does not show a larger area than the other gases, however, it appears that it is not "seeing" such defects as undoubtedly do exist, and that the surface remains essentially homogeneous even as regards such a small molecule.

The Kirkwood–Müller formula shows much smaller changes in area than do either the London or Slater–Kirkwood formulas upon going from either a 3–9 or 3–12 to a 4–10 model. Why this should be so is not readily apparent, but the fact remains that the Kirkwood–Müller areas are not as sensitive to the potential model.

The values for the areas given by the metallic interaction theories of Bardeen and of Margenau and Pollard serve to indicate that for our purposes highly graphitized carbon black can be treated reasonably well as a metal. It is not possible here to make any estimate as to which of these two is the better formula for area determinations, however.

It would be highly desirable if the area could be determined without resorting to any of these formulas. Now s_0 is the sum of some value for the radius of a carbon atom in the solid and an effective radius of the adsorbed gas atom. If the former quantity can be assumed to remain constant when the gas is changed, then the slope of a plot of As_0 against, say, the second virial radii of the gas atoms should give a value for the area. Such a plot is shown in Fig. 4. The As_0 values are from the 3–12 curve fit. The second virial radii are based on the Lennard–Jones 6–12 potential and were taken from the tabulation of Hirschfelder, Curtiss and Bird.[18] The straight line was constructed by a least squares treatment of the data, and the slope gives a value for the area of 7.41 m.^{2}/g. This value is somewhat lower than the lowest value obtained through the use of the various formulas above. If one makes the same treatment using crystal radii[19] rather

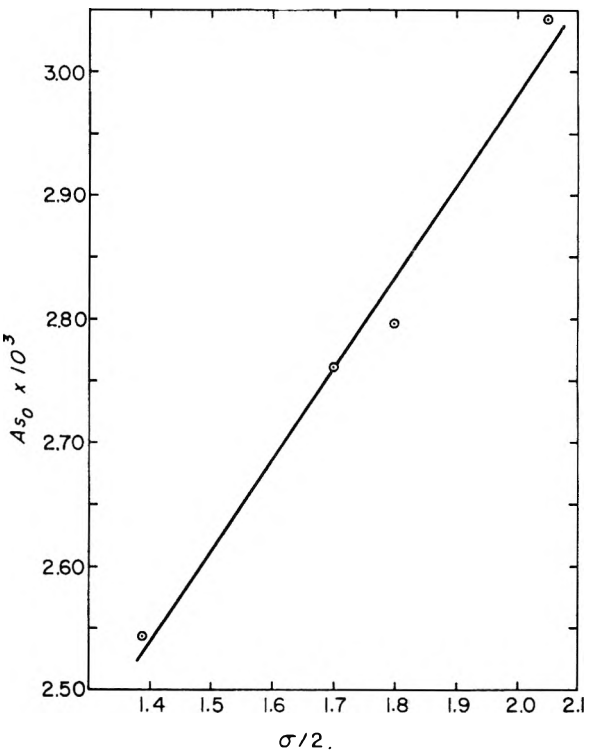

Fig. 4.—Plot of As_0 *vs.* second virial radius of the rare gas atoms. As_0 values are those obtained by fitting the experimental results to the 3–12 potential model.

than the second virial radii for the gas atoms, a value of 8.38 m.^{2}/g. emerges, in more substantial agreement at least with the Kirkwood–Müller estimate of the area. This points up a difficulty inherent in the present method of obtaining the area, namely the problem of what "radius" to use for the gas atom. A possible argument for using crystal radii rather than gas–gas radii is that the larger and more polarizable krypton and xenon atoms might well show a greater diminution in radius in the presence of the force field of the solid than the smaller, more compact, neon and argon atoms, and that the use of crystal radii might thus be more nearly correct. There is no assurance, however, that the force field acting upon a rare gas atom in the crystalline state is comparable to the field of the carbon surface, which is acting in one direction only. Hence, there seems to be only slight justification for choosing any one set of radii rather than another, and the best that one can do is to be consistent in one's choice of values.

Conclusions

The results have not enabled as clear-cut a choice of potential model as had been hoped for, due to the experimental difficulties of obtaining data in the range of low ϵ_{1S}^*/RT with the present low area carbon black. A solid with approximately the same degree of surface homogeneity as P33, but having a surface area an order of magnitude greater should provide more sensitive results. It may prove necessary in this connection to employ something other than a carbon surface in order to obtain the desired properties. We are also investigating the possibility of performing a direct lattice summa-

(17) C. H. Amberg, W. B. Spencer and R. A. Beebe, *Can. J. Chem.*, **33**, 305 (1955).

(18) J. O. Hirschfelder, C. F. Curtiss and R. B. Bird, "Molecular Theory of Gases and Liquids," John Wiley and Sons, Inc., New York, N. Y., 1954, p. 1110.

(19) R. W. G. Wyckoff, "The Structure of Crystals," 2nd ed., Reinhold Publ. Co., New York, N. Y., 1931, pp. 192–193.

tion, which we hope will give a clearer picture of the correct form of the second-order interaction potential.

The argon measurements have been extended into the region of third-order interactions, and it is hoped that these results will settle some of the questions left unanswered here. Of course, a choice of a suitable potential model is rather more difficult for third order than for second-order interactions, and moreover, as has recently been shown,[20,21] the assumption of pairwise additivity of potentials results in very large errors, which further complicates the problem. With a suitable correction for a three-body potential, however, tractable results should be obtainable.

Acknowledgment.—We wish to express our appreciation to Dr. B. E. F. Fender for his assistance in making the gas thermometer measurements.

(20) M. P. Freeman, THIS JOURNAL, **62**, 729 (1958).
(21) O. Sinanoğlu and K. S. Pitzer, *J. Chem. Phys.*, **32**, 1279 (1960).

ETHERATES OF LITHIUM BOROHYDRIDE. IV. THE SYSTEM LITHIUM BOROHYDRIDE–TETRAHYDROFURAN[1]

BY THADDEUS L. KOLSKI[2] AND GEORGE W. SCHAEFFER

Contribution from the Department of Chemistry, Saint Louis University, St. Louis, Missouri

Received May 9, 1960

Pressure–composition isotherms at 35.0, 0.0 and −22.9° for the system lithium borohydride–tetrahydrofuran show the existence of a solid tetrahydrofuranate, $LiBH_4 \cdot (CH_2)_4O$ (I). The heat, free energy and entropy of dissociation of I per mole of tetrahydrofuran evolved at 25° are ΔH_d = 10.1 kcal., ΔF_d = 3.3 kcal. and ΔS_d = 23 e.u. Approximate heats of solution of lithium borohydride (II) and I in tetrahydrofuran at 25° are (II) −10.8 kcal./mole and (I) −8.9 kcal./mole. The solubility of II in tetrahydrofuran is 15.5 g./100 g. solvent at −22.9° and 24.3 g./100 g. solvent at 35.0°. Inflection points in the isotherms at mole fraction II 0.33 are interpreted as indicating existence of a liquid lithium borohydride bis(tetrahydrofuranate), $LiBH_4 \cdot 2(CH_2)_4O$. Stabilities of the solid etherates of lithium borohydride with dimethyl ether, diethyl ether, diisopropyl ether and tetrahydrofuran are compared and discussed.

A phase study of the system lithium borohydride–tetrahydrofuran demonstrates the existence of the solid addition compound lithium borohydride tetrahydrofuranate, $LiBH_4 \cdot (CH_2)_4O$. Pressure–composition isotherms for the system at 35.0, 0.0 and −22.9° are shown in Fig. 1; Table I gives representative data for these and for a partial isotherm at 25.0° in the saturated solution region from which the solubility of lithium borohydride at this temperature may be calculated.

One of the more striking features of the phase diagrams is the marked vapor pressure depression of solutions of lithium borohydride in tetrahydrofuran with increase in lithium borohydride mole fraction (N_2). The high solubility is also clearly indicated. The single plateau in each isotherm corresponds to the constant vapor pressure of a saturated solution in equilibrium with solid phase; visual observation corroborated the stable coexistence of solid and liquid phases at all points on the plateaus. No liquid phase was observed at compositions richer in lithium borohydride than N_2 = 0.500 at temperatures below 35.0°. The region from N_2 = 0.500 to N_2 = 1.000 appears to be one of solid solution. Compositions richer in lithium borohydride than N_2 = 0.500 begin to liquefy at temperatures not far above 35°.

The apparent non-existence of an abrupt pressure change at N_2 = 0.667 distinguishes the lithium borohydride–tetrahydrofuran system from the lithium borohydride–dimethyl ether[3] and lithium borohydride–diethyl ether[4] systems, in which the existence of lithium borohydride hemi-(etherates) is sharply defined. However, the lithium borohydride–diisopropyl ether[5] system, which is not complicated by solid solution formation, clearly forms no hemi-(etherate). The difficulty of attaining equilibrium and measuring the small pressures between N_2 = 0.500 and N_2 = 1.000 in

TABLE I

DATA FOR PRESSURE–COMPOSITION ISOTHERMS AT VARIOUS TEMPERATURES FOR THE SYSTEM LITHIUM BOROHYDRIDE–TETRAHYDROFURAN

−22.9°		0.0°		25.0°		35.0°	
Comp., N_2	Press., mm.	Comp., N_2	Press., mm.	Comp., N_2	Press., mm.	Comp., N_2	Press., mm.
0.000	11.7	0.000	48.4	0.000	167.9	0.000	264.8
.0729	10.8[a]	.0731	45.8[a]	.333	35.4[a]	.237	160.8[a]
.1144	10.1[a]	.1146	43.9[a]	.355	24.5[a]	.269	125.0[a]
.183	9.2[a]	.152	41.2[a]	.371	18.0[a]	.312	79.3[a]
.230	7.5[a]	.183	38.0[a]	.392	13.4[a]	.334	57.7[a]
.281	5.1[a]	.231	31.1[a]	.418	8.7[a]	.356	42.2[a]
.307	3.2[a]	.282	21.3[a]	.446	7.8	.380	29.6[a]
.330	1.6[a]	.308	13.1[a]	.470	7.8	.393	23.5[a]
.359	1.0	.331	7.6[a]	.491	7.8	.419	14.6[a]
.420	1.1	.359	4.4[a]			.446	9.1[a]
.445	1.0	.391	3.5			.470	9.0
.490	1.0	.445	3.3			.491	9.1
.516	0.4	.490	3.2			.518	3.6
.556	.4	.516	1.1			.556	3.0
.600	.3	.556	1.0			.599	2.5
.648	.2	.600	0.7			.648	2.3
.704	.1	.648	.5			.682	2.1
		.681	.3			.705	1.9
		.704	.2			.752	1.6
		.835	.2			.836	1.4
		.974	.1			.974	1.1

[a] No solid phase present.

(1) Presented at the 132nd meeting of the American Chemical Society, New York, N. Y., September, 1957. Taken in part from a thesis presented by T. L. Kolski to the Graduate School of Saint Louis University in partial fulfillment of the requirements for the degree of Doctor of Philosophy, June, 1957.

(2) Pigments Department, Experimental Station, E. I. du Pont de Nemours and Co., Inc., Wilmington, Delaware.

(3) G. W. Schaeffer, T. L. Kolski and D. L. Ekstedt, *J. Am. Chem. Soc.*, **79**, 5912 (1957).

(4) T. L. Kolski, H. B. Moore, L. E. Roth, K. J. Martin and G. W. Schaeffer, *ibid.*, **80**, 549 (1958).

(5) J. J. Burns and G. W. Schaeffer, THIS JOURNAL, **62**, 380 (1958).

the present system prevents its precise description in this region. There may be a wide range of mutual solubility between lithium borohydride and lithium borohydride tetrahydrofuranate, or a definite compound lithium borohydride hemi-(tetrahydrofuranate) may be formed which enters into solid solution with both lithium borohydride and lithium borohydride tetrahydrofuranate.

Approximate values for the heats of solution in tetrahydrofuran at 25° of lithium borohydride, lithium borohydride tetrahydrofuranate and a sample of composition 67 mole % lithium borohydride and 33 mole % tetrahydrofuran, were determined calorimetrically. Sample sizes were such that the final solution had a concentration of 0.1–0.15 weight % lithium borohydride in tetrahydrofuran. The heats of solution of lithium borohydride, −10.8 kcal./mole, and lithium borohydride tetrahydrofuranate, −8.9 kcal./mole, allow calculation of the heat of dissociation of lithium borohydride tetrahydrofuranate to lithium borohydride

$$LiBH_4\cdot(CH_2)_4O(s) + X(CH_2)_4O(l) = 0.1\%\ \text{soln.} \quad (1)$$
$$\Delta H = -8.88 \pm 0.44\ \text{kcal.}$$
$$LiBH_4(s) + (X+1)(CH_2)_4O(l) = 0.1\%\ \text{soln.} \quad (2)$$
$$\Delta H = -10.83 \pm 0.15\ \text{kcal.}$$
$$(CH_2)_4O(l) = (CH_2)_4O(g) \quad \Delta H = +8.17 \pm 0.10\ \text{kcal.}$$
$$LiBH_4\cdot(CH_2)_4O(s) = LiBH_4(s) + (CH_2)_4O(g) \quad (3)$$
$$\Delta H = +10.12 \pm 0.69\ \text{kcal.}$$

The heat of solution of material whose composition may be described as $(LiBH_4)_2\cdot(CH_2)_4O$, −18.1 kcal./g. formula weight, sheds little light on its nature, for while this value is slightly less than the sum of heats of solution of lithium borohydride and lithium borohydride tetrahydrofuranate, the difference of 1.6 ± 1.1 kcal. is not a positive indication of compound formation. It may be the heat effect accompanying mutual solution of lithium borohydride and lithium borohydride tetrahydrofuranate.

Extrapolation of the vapor pressure curves back to $N_2 = 0.500$ from higher lithium borohydride mole fractions gives an estimate of the dissociation pressure of lithium borohydride tetrahydrofuranate; this value is about 2.8 mm. at 25°. Using this value and the calorimetrically obtained heat of dissociation (ΔH_d = 10.1 kcal./mole), the free energy (ΔF_d = 3.3 kcal./mole) and entropy (ΔS_d = 23 e.u.) of the dissociation process described by equation 3 may be estimated. Because of uncertainty as to the actual product of dissociation and lack of precise pressure data, ΔF_d may seem questionable, but the limited range of pressures in the region above $N_2 = 0.500$ justifies that it is very close to the exact free energy change for the process described by equation 3. Since the heat of dissociation was obtained from heat of solution measurements, its validity is not dependent on the presence or absence of lower etherates.

The solubility of lithium borohydride in tetrahydrofuran may be estimated from the isotherms by the points of intersection of vapor pressure curves of unsaturated solutions with plateaus corresponding to vapor pressures of saturated solutions. Solubility data are given in Table II.

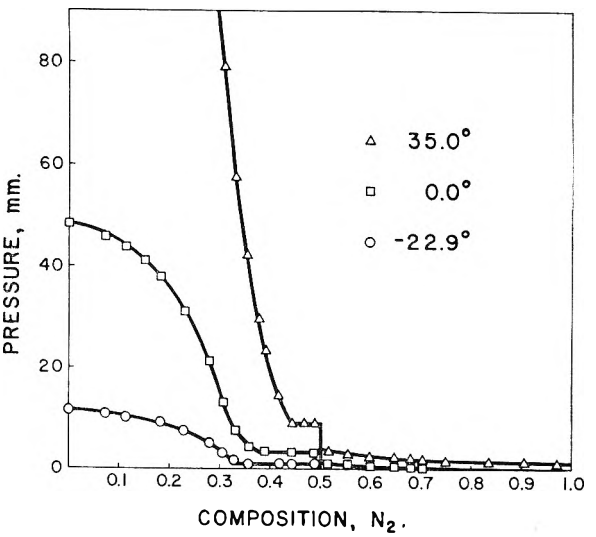

Fig. 1.—Pressure–composition isotherms for the system lithium borohydride–tetrahydrofuran.

TABLE II

SOLUBILITY OF LITHIUM BOROHYDRIDE IN TETRAHYDROFURAN

Temp., °C.	Solubility, g./100 g. solvent
35.0	24.3
25.0	22.2[a,b]
0.0	17.8
−22.9	15.5

[a] Metal Hydrides, Inc., reports a solubility of *ca.* 21 g./100 g. solvent.[6] [b] J. R. Elliott, *et al.*,[7] report a solubility of 28 g./100 g. solvent at 25°.

Since the isotherms in Fig. 1 all refer to temperatures above −22.9° where compositions near N_2 = 0.333 are liquid, the system's bivariance does not allow clear demonstration of the existence of a bis-(tetrahydrofuranate). However, the steepness of vapor pressure curves for liquid phases is indicative of a solute–solvent interaction much stronger than that usually associated with simple solution. Further, presence of inflection points in the vapor pressure curves at $N_2 = 0.333$ may be interpreted as resulting from lithium borohydride bis-(tetrahydrofuranate) formation in the liquid phase. The vapor pressure curves rising from saturated solution plateaus thus may be ascribed to vapor pressures of lithium borohydride tetrahydrofuranat solutions in lithium borohydride bis-(tetrahydrofuranate). At $N_2 = 0.333$, where the change in slope of the curves reverses direction, the condensed phase consists principally of liquid lithium borohydride bis-(tetrahydrofuranate). Högfeldt[8] has shown how change in degree of solvation of solute species with concentration change may be estimated from van't Hoff i values. Application of this concept to the lithium perchlorate–diethyl ether system has been described in some detail.[9] A similar treatment of the present system gives added evidence for the existence of liquid lithium borohydride bis-(tetrahydrofuranate). While

(6) Technical Bulletin 402-C.

(7) J. R. Elliatt, W. L. Roth, G. F. Roedel and E. M. Boldebuck, *J. Am. Chem. Soc.*, **74**, 5211 (1952).

(8) E. Högfeldt, *Acta Chem. Scand.*, **5**, 1400 (1951).

(9) K. Ekelin and L. G. Sillen, *ibid.*, **7**, 987 (1953).

these arguments do not prove the existence of this compound above −22.9°, they are powerfully corroborated by its isolation at lower temperatures by Wiberg and co-workers,[10] who showed it to melt at −35°. The high viscosity of solutions in all but the very dilute concentrations strongly suggests that the solvate aggregates are highly ordered, and in the most concentrated solutions may approach a lattice array.

It was observed that lithium borohydride tetrahydrofuranate, although very deliquescent, is far more stable when exposed to the atmosphere than is lithium borohydride itself. Small amounts of the tetrahydrofuranate can be handled in the open with reasonable safety under conditions which cause lithium borohydride to burst spontaneously into flame. Small quantities of the tetrahydrofuranate have been dissolved in water with only very slow evolution of hydrogen, in contrast to the violently hydrolytic reaction which is observed with lithium borohydride.

Experimental

The experimental apparatus and techniques employed in determining the isotherms have been described previously.[5]

Purification of Tetrahydrofuran.—Tetrahydrofuran was purified by fractionation in a column after standing over lithium hydride for two days and refluxing with lithium hydride for about two hours prior to fractionation. A cut was taken from a fraction boiling at 64.8° (uncor.) at 738.9 mm. This distilled sample was introduced into the vacuum system and condensed into a bulb containing lithium borohydride. On warming and standing overnight at room temperature, then freezing down again with liquid nitrogen, a small amount of non-condensable gas was observed. This residual gas was removed by pumping, after which the warming and freezing procedure was repeated. After 5 or 6 such cycles, no appreciable amount of additional non-condensable gas was observed. The tetrahydrofuran sample was transferred to the fractionation train and allowed to vaporize slowly from a U-tube at −45° through another U-tube at −45° into a third U-tube held at −196°. The fraction collecting in the −196° trap was found to be tensiometrically homogeneous and exhibited vapor pressures summarized by the expression $\log P_{mm.} = 8.203 - 1785.9/T$

Temp., °C.	20.0	0.0	−22.9	−35.3	−45.2
Press., mm. (obsd.)	129.3	48.4	11.7	5.0	2.5
Press., mm. (calcd.)	129.4	46.3	11.7	5.0	2.3

The boiling point extrapolated from these data is 62.4°, slightly lower than that reported in the literature.[11] From these data, the heat of vaporization is 8.17 ± 0.10 kcal./mole and Trouton's constant 24.4.

Determination of Heats of Solution.—The type of calorimeter employed has been described in a previous publication.[6] For the calorimetric measurements, tetrahydrofuran was dried by refluxing with lithium hydride for about two hours, then distilled.

1. **Lithium Borohydride.**—The heat effect accompanying solution of 165–210 mg. samples of purified lithium borohydride[5] in 150 ml. of tetrahydrofuran at 25° was measured. Five determinations gave the results

ΔH, kcal./mole	Final concn. of $LiBH_4$, g./100 g. solvent
−10.97	0.158
−10.67	.136
−10.71	.150
−10.73	.137
−11.05	.125
Av. −10.83 ± 0.15	

2. **Lithium Borohydride Tetrahydrofuranate.**—A slight excess of tetrahydrofuran was condensed on a sample of purified lithium borohydride. After several days, the product remained a mixture of viscous liquid with undissolved solid. On being heated in a stream of warm air, the mass formed a homogeneous solution of greatly increased fluidity. Cooled to room temperature, the solution easily transformed into a solid crystalline mass. Following the pressure above the sample with a specially constructed mercury manometer requiring only a small vapor space, tetrahydrofuran was removed in small portions until the equilibrium pressure indicated that no more solution phase was present. Analysis of this material showed 23.1% lithium borohydride (theory 23.21%). Samples of 580–690 mg. were dissolved in 150 ml. of tetrahydrofuran at 25°. Five runs gave the results

ΔH, kcal./mole	Final concn. of $LiBH_4$, g./100 g. solvent
−8.52	0.113
−8.48	.120
−9.41	.102
−8.55	.121
−9.45	.107
Av. −8.88 ± 0.44	

3. **Material of Composition** $(LiBH_4)_2 \cdot (CH_2)_4O$.—The requisite amount of tetrahydrofuran was absorbed by purified lithium borohydride, with the evolution of considerable heat, to produce a solid material of apparent homogeneity. The reactor was attached to the vacuum apparatus through a short length of Teflon tubing which allowed the solid to be shaken during the absorption. Analysis of the product showed the lithium borohydride content to be 38.3% (theoretically 37.67% for $(LiBH_4)_2 \cdot (CH_2)_4O$). Five samples of 285–400 mg., each dissolved in 150 ml. of tetrahydrofuran at 25°, gave the heats of solution

ΔH, kcal./mole	Final concn. of $LiBH_4$, g./100 g. solvent
−17.81	0.095
−17.98	.093
−19.04	.082
−18.07	.105
−17.48	.113
Av. −18.08 ± 0.52	

Comparison of the Etherates of Lithium Borohydride

The relative stabilities of lithium borohydride adducts with dimethyl ether,[5] diethyl ether,[6] diisopropyl ether[7] and tetrahydrofuran, in terms of dissociation pressures and heats, free energies, and entropies of dissociation at 25°, are summarized in Table III. The data shown in the upper part of the table refer to processes which yield the next lower etherate as the product of dissociation (lithium borohydride if no lower etherates are shown) and the thermodynamic values are per mole of evolved ether. Although the comparison is somewhat obscured because the four ether systems form different numbers and types of etherates, a meaningful comparison of the one-to-one adducts may be made. For this reason, the lower part of Table III lists thermodynamic data associated with the process

(10) E. Wiberg, H. Nöth and R. Uson, *Z. Naturforsch.*, **11b**, 490 (1956).

(11) F. Klages and F. Möhler, *Chem. Ber.*, **81**, 411 (1948), report 63.9°.

TABLE III

STABILITIES OF THE ETHERATES OF LITHIUM BOROHYDRIDE AT 25°

Dissociation to lower etherate	P_d, mm.	ΔH_d, kcal.	ΔF_d, kcal.	ΔS_d, e.u.
$LiBH_4 \cdot 2(CH_3)_2O$	971	10.42 ± 0.04	−0.145 ± 0.01	35.4 ± 0.17
$LiBH_4 \cdot (CH_3)_2O$	45.8	11.13 ± .04	1.66 ± .01	31.7 ± .17
$(LiBH_4)_2 \cdot (CH_3)_2O$	18.4	12.25 ± .04	2.21 ± .01	33.7 ± .17
$LiBH_4 \cdot (C_2H_5)_2O$	90.4	13.36 ± .04	1.26 ± .01	40.6 ± .17
$(LiBH_4)_2 \cdot (C_2H_5)_2O$	45.6	11.90 ± .04	1.67 ± .01	34.3 ± .17
$LiBH_4 \cdot [(CH_3)_2CH]_2O$	94.8	12.68 ± .04	1.24 ± .01	38.4 ± .17
$LiBH_4 \cdot 2(CH_2)_4O$[a]	35.4			
$LiBH_4 \cdot (CH_2)_4O$[b]	2.8	10.12 ± .69	3.32 ± .04	22.8 ± 2.4
Dissociation to $LiBH_4$		**ΔH_d, kcal.**	**ΔF_d, kcal.**	**ΔS_d, e.u.**
$LiBH_4 \cdot (CH_3)_2O$		11.69 ± 0.08	1.94 ± 0.02	32.7 ± 0.34
$LiBH_4 \cdot (C_2H_5)_2O$		12.63 ± .08	1.46 ± .02	37.4 ± .34
$LiBH_4 \cdot [(CH_3)_2CH]_2O$		12.68 ± .04	1.24 ± .01	38.4 ± .17
$LiBH_4 \cdot (CH_2)_4O$		10.12 ± .69	3.32 ± .04	22.8 ± 2.4

[a] Existence postulated in the liquid phase. [b] Error limits for thermodynamic data ascribed to the tetrahydrofuranate are large because these data are derived from heats of solution and a very small dissociation pressure. Data for the other three ether systems are based entirely on manometric measurements, which could be carried out with much greater precision.

$$LiBH_4 \cdot \text{ether(s)} = LiBH_4\text{(s)} + \text{ether(g)} \qquad (4)$$

for each of the monoetherates.

It is clear from free energies of dissociation that of the four ethers, tetrahydrofuran forms the most stable etherate. Stabilities of the four ether addition compounds decrease in the order

$$(CH_2)_4O >> (CH_3)_2O > (C_2H_5)_2O \geq [(CH_3)_2CH]_2O$$

This order is that which would be predicted if, as shown by Brown and Adams[12] in a study of the boron trifluoride etherates, the relative base strengths of these ethers are determined largely by steric effects.

Examination of the entropies of dissociation for the processes described by equation 4 bears out the importance of steric factors in these adducts. Etherates of the acyclic ethers give rise to larger entropies of dissociation than does the tetrahydrofuranate. Compared to the relatively free rotation about all bonds in the uncomplexed acyclic ether,[13] the complexed ether is "strained" by virtue of an orientation of carbon chains necessary to bring the oxygen atom into an appropriate position relative to the electron-attracting group. Dissociation of the complex relieves this restriction and restores higher randomness of orientation to the carbon chains. As expected, the entropy change is greater with increasing complexity of the carbon chains. Comparison of the diethyl ether and tetrahydrofuran complexes of lithium borohydride is particularly informative in this respect, for the structures of the two ethers are such that on purely polar grounds they would be expected to possess approximately the same base strength. But it is found that in the case of tetrahydrofuran, where except for oscillatory motion about mean point loci the carbon chains maintain the same relative orientation in both the free and complexed state, dissociation of the adduct is not accompanied by an appreciably increased degree of randomness within the ether group; this is clearly reflected in the substantially lower entropy of dissociation for the tetrahydrofuran adduct.

Although the base strengths of ethers as measured by the free energies of dissociation of lithium borohydride etherates parallel those determined from dissociation of boron trifluoride etherates,[12] it does follow that the entropies of dissociation need be parallel. The boron trifluoride etherate studies were carried out in the gas phase; the steric requirements are therefore probably less stringent than in the case of solid–gas equilibria. One might expect that accommodation of an ether molecule into the lattice of a crystalline complex would require considerably more constraint than formation of a molecular one-to-one addition compound in the vapor phase. The unexpectedly low value for the heat of dissociation of lithium borohydride tetrahydrofuranate is partially responsible for the low entropy change evidenced on dissociation of the adduct; however, even if the heats of dissociation for the tetrahydrofuranate and the diethyl etherate were the same, dissociation of the tetrahydrofuran complex would involve a significantly lower entropy gain than that of the diethyl etherate.

Searles and Tamres,[14] in a study of hydrogen bond formation between saturated ethers and methanol-*d* or chloroform, have concluded that steric factors are not the primary reason for the high base strength of 4, 5 and 6-membered cyclic ethers. They prefer to ascribe the effect to an alteration of electron density about the oxygen atom with ring formation. That electron distribution in cyclic ethers does indeed vary with ring size has been clearly demonstrated in a study of chemical shifts in the proton magnetic resonance of a series of saturated cyclic ethers.[15] While this ring effect appears well established, it remains true that acid–base relationships between electron donors and bulk-free acceptors like the proton can be quite different from those involving larger acceptors. This is demonstrated by the difference in order of base strengths of the following three ethers

(12) H. C. Brown and R. M. Adams, *J. Am. Chem. Soc.*, **64**, 2557 (1942).

(13) This is not meant to suggest that all atomic positions are equally feasible energetically.

(14) S. Searles and M. Tamres, *J. Am. Chem. Soc.*, **73**, 3704 (1951).

(15) H. S. Gutowsky, R. L. Rutledge, M. Tamres and S. Searles, *ibid.*, **76**, 4242 (1954).

toward lithium borohydride

$$(CH_2)_4O >> (C_2H_5)_2O \geq [(CH_3)_2CH]_2O$$

and toward methanol-*d* or chloroform[14]

$$(CH_2)_4O \geq [(CH_3)_2CH]_2O > (C_2H_5)_2O$$

In the present study, then, although the Tamres–Searles ring effect is undoubtedly a contributing factor, the over-all base strength of the ethers appears to be determined predominantly by a more gross interaction; there seems insufficient reason to seek factors other than steric.

The number of complexes formed in each of the ether systems similarly appears determined by steric requirements. While two dimethyl ether molecules have no difficulty in approaching a lithium borohydride unit sufficiently closely to form a stable bis-(etherate), one diethyl ether or diisopropyl ether molecule satisfies the attraction of the lithium borohydride group to the extent that another ether molecule cannot be accommodated. In the case of a borohydride with a larger cation, however, there is enough space for two diethyl ether molecules. This has been demonstrated by the isolation at 0° of thorium borohydride bis-(diethyl etherate).[16] The formation of a bis-(tetrahydrofuranate) of lithium borohydride may be rationalized on a steric basis, for while the tetrahydrofuran molecule is somewhat larger than the dimethyl ether molecule, the frontal approach requirements which it exhibits toward a lithium borohydride group are approximately equivalent to (or slightly less than) those associated with dimethyl ether. It is interesting to note here that stable solid bis-(tetrahydrofuranates) of alkaline earth borohydrides are formed readily.[17] The greater stability of these compounds stems from the larger size of the central cations.

(16) H. R. Hoekstra and J. J. Katz, *J. Am. Chem. Soc.*, **71**, 2488 (1949).

(17) E. Wiberg, H. Nöth and R. Hartwimmer, *Z. Naturforsch.*, **10b** 292, 294, 295 (1955).

The very striking stabilization of lithium borohydride toward hydrolysis by formation of the tetrahydrofuran or dioxane[18] complex suggests that formation of a short-lived lithium borohydride hydrate, $LiBH_4 \cdot H_2O$, is a necessary initial step in the hydrolytic process, and implies that the structure of this hydrate is much like that of the etherates which apparently can block its formation. It is reasonable to think of the etherates of lithium borohydride as being structurally similar to hydrates on the basis of ionic size; lithium halides, the anions of which are comparable in radius (Cl^- 1.81 Å., Br^- 1.95 Å., I^- 2.16 Å.)[19] to the borohydride ion (2.03 Å.),[20] form both hydrates and dioxanates. The following hydrates have been described: $LiCl \cdot H_2O$, $LiCl \cdot 2H_2O$ and $LiCl \cdot 3H_2O$; $LiBr \cdot H_2O$, $LiBr \cdot 2H_2O$ and $LiBr \cdot 3H_2O$; $(LiI)_2 \cdot H_2O$, $LiI \cdot H_2O$, $LiI \cdot 2H_2O$ and $LiI \cdot 3H_2O$.[21] The existence of tris-(hydrates) is entirely consistent with the steric concept discussed above. The following dioxanates are known: $LiCl \cdot (CH_2)_4O_2$, $LiBr \cdot (CH_2)_4O_2$ and $LiI \cdot 2(CH_2)_4O_2$.[22] The existence of a mixed dioxanate–hydrate of lithium chloride, $LiCl \cdot (CH_2)_4O_2 \cdot H_2O$,[23] emphasizes the functional similarity of ether or water molecules about the central cation of a lithium halide.

Acknowledgment.—This work was supported in part by funds from the Olin Mathieson Chemical Corporation through the Bureau of Aeronautics Contract NOa 52-1023-C, Subcontract 3181-14.

(18) R. Paul and N. Joseph, *Bull. soc. chim. France*, 758 (1953).

(19) L. Pauling, "The Nature of the Chemical Bond," 2nd Ed., Cornell Univ. Press, Ithaca, N. Y., 1948, p. 346.

(20) S. C. Abrahams and J. Kalnajs, *J. Chem. Phys.*, **22**, 434 (1954).

(21) G. F. Hüttig, F. Reuscher and F. Pohle, *Z. anorg. allgem. Chem.*, **137**, 155; **138**, 1 (1924).

(22) H. Rheinboldt, A. Luyken and H. Schmittmann, *J. prakt. Chem.*, **148**, 81 (1937).

(23) C. C. Lynch, THIS JOURNAL, **46**, 366 (1942).

STERIC ORDER AND DIELECTRIC BEHAVIOR IN POLYMETHYLMETHACRYLATES

By Herbert A. Pohl, Robert Bacskai and William P. Purcell

Princeton University Plastics Laboratory, Princeton, N. J.

Received May 11, 1960

The effects of steric order along the chain of polymethyl methacrylate upon the molar polarization, the infrared absorption spectrum, and the X-ray diffraction were compared. Steric order was seen to affect all these parameters. This is in accord with known data for diastereomers. Solution measurements of the dielectric properties showed the isotactic material to have the highest molar polarization, the shortest mean relaxation time, and the narrowest spread of relaxation times. The bulk isotactic material showed the fewest infrared absorption peaks, and as judged by X-ray analysis, the greatest ease of crystallization. The syndiotactic material in dilute solution showed the lowest molar polarization, the longest mean relaxation time, and the greatest spread of relaxation times. The bulk syndiotactic material showed the most infrared absorption peaks and an intermediate ease of crystallizability. The atactic material exhibited dielectric and infrared absorption behaviors intermediate to the other polymer species, and exhibited the lowest ease of crystallizability. The study of the structure of the various stereospecific form of polymethyl methacrylate indicates that there are 18 most probable conformations possible. By taking account of the effect of steric hindrance and the resultant moment of each conformation, the root mean square dipole moment per monomer was calculated for the several species. Reasonable agreement of calculated and observed moments was found.

Introduction

Since the early demonstrations of marked effects on the crystallizability of polymers by control of the catalytic conditions during polymerization, numerous attempts have been made to additionally characterize stereospecificity in high polymers. Natta and co-workers[1] have investigated polymers of varied tacticity with the aid of X-ray crystallography and melting point studies on the solid material. They showed that solution viscosities were of little help. Danusso and Moraglio[2] found that solution viscosity–molecular weight relations were relatively insensitive to tacticity, but that noticeable differences existed in the second virial coefficients. Their results were corroborated by Ang.[3] Kinsinger and Wessling[4] recently indicated that differences in the "Flory (θ) temperature" and the entropy parameter existed for stereoisomeric polystyrenes. Hydrolysis rate studies have also been made in an attempt to find distinguishing characteristics of stereospecificity.[5,6] Krigbaum, Carpenter and Newman[7] studied isotactic and atactic polystyrene, and from observed differences in intrinsic viscosity and virial coefficient data suggested that the isotactic molecule occupied a larger volume in dilute solution.

In the present work, use has been made of dielectric behavior in dilute solution. The method has been used in the past[8-10] on small organic molecules, particularly on diastereomers, molecules which contain pairs of asymmetric carbon atoms. Debye and Bueche[11] have emphasized the significance of polymer configuration on the dipole moment. Stereostructural differences should thus be detectable by polarization measurements of high polymers which are polar.[12] Polymethyl methacrylate polymers were chosen because they are polar and are synthesizable in isotactic, atactic and syndiotactic forms.

Experimental

Results on dilute solution dielectric measurements of the several polymer species were obtained over a wide frequency range. These results were correlated with measurements on films using infrared spectra and X-ray diffraction.

Dielectric Polarization Measurements at 1000 Cycles Per Second.—The dielectric capacitance cell used for the 1000 c.p.s. measurements was described earlier.[13,14] It has a volume of 400 ml., and a capacitance of 380 mmf. It is made mainly of monel and quartz. Capacitance measurements were made with it using a General Radio Type 716-BS3 Capacitance Bridge. After appropriate amplification, an oscilloscope was used to determine balance on the bridge. The measuring cell was maintained at 30 ± 0.05° during the runs. A Robertson pycnometer[15] was used to assist in the determination of the solution densities. Calculations of the molar polarization in these dilute solution measurements were made using a modified form of the Debye molar polarization equation.[13] The value of 24.55 ml./mole for the molar refractivity, R, per monomer unit of the PMMA was calculated from atomic refractivities The molar orientation polarization per monomer unit, p_0, was calculated (neglecting "atomic refractivity") for these relative measurement purposes as

$$P_0 = P_2 - R$$

where P_2 is the molar polarization per monomer unit observed for the PMMA in the solution measurements. The reproducibility of the P_2 values was ± 0.5 ml./mole. The apparent dipole moment per monomer unit, μ_{app}, was calculated from the P_0 values as

$$\mu_{app} = 0.01281 \times 10^{-18} (P_0 \times T)^{1/2}$$

where T is the absolute temperature, degrees Kelvin.

Dielectric Measurements at High Frequencies.—The real (ϵ') and imaginary (ϵ'') parts of the dielectric constant were measured at 10, 25 and 50 cm. wave lengths. Dilute benzene solutions (0.4–1.0 wt. %) were measured at 30°.

A resonant cavity apparatus which has a cell coupled to a signal generator and a detector by magnetic loops was employed. A moveable plunger changed the effective length of the cavity and resonant lengths, corresponding

(1) G. Natta, *Angew. Chem.*, **68**, 393 (1956); *J. Polymer Sci.*, **16**, 143 (1955).

(2) F. Danusso and Moraglio, *ibid.*, **24**, 161 (1957).

(3) F. Ang, *ibid.*, **25**, 126 (1957).

(4) J. B. Kinsinger and R. A. Wessling, *J. Am. Chem. Soc.*, **81**, 2908 (1959).

(5) H. Moravetz and E. Gaetjens, *J. Polymer Sci.*, **32**, 526 (1958).

(6) B. Boteler Y T.G. Fox, Mellon Institute Tech. Report No. 1, Office of Naval Research Contract No. 2693(00) 1959.

(7) W. R. Krigbaum, D. K. Carpenter and S. Newman, This Journal, **62**, 1586 (1958).

(8) A. Weissberger, *J. Org. Chem.*, **2**, 245 (1937–38).

(9) S. Winstein and R. E. Wood, *J. Am. Chem. Soc.*, **62**, 548 (1940).

(10) V. Ramakrishman, *Kolloid Z.*, **132**, 30 (1953).

(11) P. Debye and F. Bueche, *J. Chem. Phys.*, **19**, 589 (1951).

(12) R. Bacskai and H. A. Pohl, "Stereospecificity and Electric Polarization in High Polymers," Plastics Laboratory Technical Report 55A, October 1, 1959; *J. Polymer Sci.*, **42**, 151 (1960).

(13) H. A. Pohl, M. E. Hobbs and P. M. Gross, *Ann. N. Y. Acad. Sci.*, **40**, 389 (1940).

(14) H. A. Pohl, M. E. Hobbs and P. M. Gross, *J. Chem. Phys.*, **9**, 408 (1941).

(15) G. R. Robertson, *Ind. Eng. Chem., Anal. Ed.*, **11**, 464 (1939).

to values of one-half wave lengths, were observed at power peaks. The real part of the dielectric constant was calculated from the wave length in the dielectric while the loss was obtained by measuring the widths of the resonant peaks at one-half the maximum power. The apparatus and measuring techniques have been thoroughly described elsewhere.[16]

Calculations.—The complex dielectric constant is defined as[17]

$$\epsilon^* = \epsilon' - i\epsilon''$$

where

ϵ^* is the complex dielectric constant
ϵ' is the real part of the dielectric constant
ϵ'' is the loss factor
i is the $\sqrt{-1}$

Debye derived[17a]

$$\epsilon^* = \epsilon_\infty + \frac{\epsilon_0 - \epsilon_\infty}{1 + i\omega\tau}$$

where

ϵ_∞ is the optical dielectric constant
ϵ_0 is the static dielectric constant
ω is the angular frequency
τ is the dielectric relaxation time

Cole and Cole developed the useful empirical relationship[18]

$$\epsilon^* = \epsilon_\infty + \frac{\epsilon_0 - \epsilon_\infty}{1 + (i\omega\tau)^{1-\alpha}}$$

where

τ is the most probable relaxation time
α is the distribution parameter with values between 0 and 1

To calculate τ_0, one plots ϵ'' *vs.* ϵ'. Generally a semicircle intersecting the abscissa at the values of ϵ_∞ and ϵ_0 is obtained. The radius of the circle drawn through the center from the ϵ_∞ point makes an angle of $\alpha\pi/2$ with the abscissa. The relaxation time can then be calculated from the relation

$$\frac{v}{u} = (\omega\tau_0)^{1-\alpha}$$

where v is the distance on the Cole and Cole plot between ϵ_0 and the experimental point, and u is the distance between the point and ϵ_∞.

In the present paper in which dilute solutions were employed, slopes ($a' = \partial\epsilon'/\partial c$, $a'' = \partial\epsilon''/\partial c$ where c = concentration) were used in place of absolute values as in studying pure substances, and the differential method, as indicated below, was employed.

$$\epsilon_{12}' \cong \epsilon_1'(\lambda_1/\lambda_{12})^2$$
$$\epsilon_{12}'' \cong 2\epsilon_{12}'K_{12}$$

where

λ is the wave length in the cavity
K is the absorption index
subscript 1 corresponds to the pure solvent
subscript 12 corresponds to the solution

A full description of the method is given in detail in the paper by Pitt and Smyth.[16]

Higasi, Bergmann and Smyth have recently developed a method[19] for determining the upper and lower limits of the relaxation time distribution from values of τ_0 and α.

$$\tau_1 = \tau_0 e^{-A/2}$$
$$\tau_2 = \tau_0 e^{A/2}$$

where A is related to α in the following way

$$\tan\left[(1 - \alpha)\frac{\pi}{4}\right] = \frac{2}{A}\tan^{-1}\sinh(A/2)$$

(16) D. A. Pitt and C. P. Smyth, *J. Am. Chem. Soc.*, **63**, 582 (1959).
(17) C. P. Smyth, "Dielectric Behavior and Structure," McGraw-Hill Book Co., New York, N. Y., 1955, p. 54.
(18) K. S. Cole and R. H. Cole, *J. Chem. Phys.*, **9**, 341 (1941).
(19) K. Higasi, K. Bergmann and C. P. Smyth, THIS JOURNAL, **64**, 880 (1960).

Results

The polarization measurements made at low frequency are summarized in Table I.

TABLE I

THE AVERAGE MOLAR POLARIZATIONS AND MOMENTS PER MONOMER UNIT OF PMM STEREOISOMERS IN DILUTE SOLUTIONS IN BENZENE AT 30.0°[12]

Polymer	Initiator	P_2, cc./mole	P_0, cc./mole	$\mu_{app} \times 10^{18}$
2007, isotactic	C_6H_5MgBr	65.33	40.8	1.425
2007, isotactic	C_6H_5MgBr	65.48	41.0	1.428
2008, atactic	Bz_2O_2	57.69	33.2	1.285
2008, atactic	Bz_2O_2	57.69	33.2	1.285
2011, syndiotactic	UV + benzoin	56.51	32.0	1.261
2011, syndiotactic	UV + benzoin	56.95	32.4	1.269
2006, atactic	Bz_2O_2	60.92	36.4	1.346
2006, atactic	Bz_2O_2	60.92	36.4	1.346

Isotactic material was observed to have the highest molar polarization and average dipole moment. The syndiotactic material was observed to have the lowest molar polarization and moment, while the atactic material (a copolymer of isotactic and syndiotactic chain segments) exhibited intermediate values.

The polarization data obtained at higher frequencies are shown in Fig. 1 as graphs of the specific dielectric loss *vs.* the specific dielectric constant, in the manner of Cole–Cole plots. The geometric constructions for estimating the relaxation times is indicated. Table II gives the observed data, Table III contains the results of the theoretical analysis of that data in terms of the critical wave length λ_m, the most probable relaxation time, τ_0, the relaxation constant, α, and the lower and upper relaxation times of the systems as calculated from Higasi's theory[19] as discussed earlier.

TABLE II

RESULTS OF MICROWAVE MEASUREMENTS OF PMMA POLYMERS

Polymer	10 cm. a'	10 cm. a''	25 cm. a'	25 cm. a''	50 cm. a'	50 cm. a''	Static a_0
2007, isotactic	0.48	0.33	0.75	0.62	1.12	0.96	2.88
2008, atactic			.64	.26	0.72	.36	2.35
2011, syndiotactic	.60	.17	.69	.26	.88	.34	2.28

TABLE III

DERIVED RELAXATION TIMES FOR PMMA POLYMERS

	λ_m, cm.	$\tau_0 \times 10^{10}$, sec.	α	$\tau_1 \times 10^{10}$, sec.	$\tau_2 \times 10^{10}$, sec.
2007, isotactic	88.7	4.7	0.09	1.8	12.7
2008, atactic	270	14.3	.21	2.7	76.0
2011, syndiotactic	323	17.1	.47	0.6	512

The infrared spectra of the polymers used in the dielectric measurements showed considerable differences. They are mentioned here mainly for identification purposes and to demonstrate the change of some physical properties other than dielectric properties with changing stereoregularity.

A Perkin–Elmer Model 21 double beam recording

infrared spectrophotometer with NaCl optics was used to obtain infrared spectra. Samples were prepared by casting benzene solutions of the polymer onto a NaCl disc, whereupon the solvent was completely evaporated *in vacuo*.

Our results generally confirm the data of Miller, *et al.*,[20] in the case of the atactic and isotactic polymers. In addition, we were able to detect several other small relative intensity differences between absorption peaks of the syndiotactic and atactic polymer which had not yet been described.[12]

Examination of the ease of crystallizability, as judged by X-ray spectra of films which had been treated with a semi-solvent (methanol) to promote crystallization, showed the isotactic material to be the most readily crystallizable, the syndiotactic to be less readily crystallizable, and the atactic material to be very little crystallized under the experimental conditions used.

X-Ray spectrograms were made using thin films of the samples which had been treated with boiling methanol (a semi-solvent) for 20 min. to promote crystallization, dried as a thin film in air at 50° for 15 hours, and annealed for 24 hours at 50° between ferrotype plates under mild pressure. A recording Norelco Geiger Counter X-ray Spectrometer, Type No. 12021, having an Fe α-source with a thin Mn Filter was used.

Discussion

We may briefly summarize the experimental results as showing serial order in properties as one goes from isotactic through atactic to syndiotactic as: (1) decreasing average molar polarization per monomer unit, or, equivalently, decreasing average dipole moment per monomer unit; (2) increasing mean relaxation times (τ_0 values); (3) increasing spread of relaxation times (α values, and τ_1 vs. τ_2 values). As judged from the ease of crystallizability, the isotactic material appears to be more easily crystallizable than the syndiotactic, and it in turn more easily crystallizable than the atactic material.

It is possible to talk about interpreting these observed differences among the three polymer species in terms of hindrance. There are two types of hindrance to be distinguished here; hindrance to rotation about main chain bonds, and hindrance to positioning of chain-attached groups. It is possible, for example, to suggest that the above results arise from a differing degree of freedom of rotation about the main chain bonds. Study of the molecular structure of the isotactic and of the syndiotactic forms of PMMA, particularly on using models, indicates that the isotactic form possesses the greater degree of free rotation about the CH_2 group joining the assymmetric carbons of successive monomer units.[21] Greater freedom of rotation in the isotactic PMMA material would lead to a shorter relaxation time than in the case of the syndiotactic, as observed. It would also explain that a narrower range of relaxation times occurs in the isotactic PMMA material, for the average length of field oriented segments would be shorter and the spread in size of detectable relaxing units would be narrower than in the syndiotactic material with its relatively stiffer bonds. Greater freedom of rotation in the isotactic arrangement would also be expected to permit greater ease of crystallizability, despite the similarity of perfection along the chains of either isotactic or syndiotactic forms. This is consonant with the observed X-ray data.

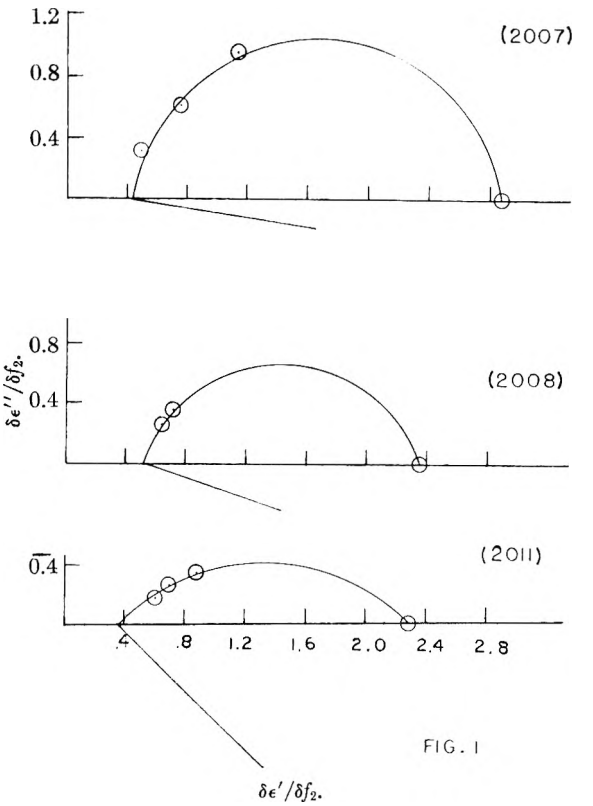

Fig. 1.—Diagram of the relation of the partial molar quantities, $\delta\epsilon''/\delta f_2$ and $\delta\epsilon'/\delta f_2$ for isotactic (sample 2007), atactic (sample 2008) and syndiotactic (sample 2011) polymethyl methacrylates, from determinations made in dilute solutions of the polymers in benzene at various frequencies.

It is not logically adequate to speak, however, as though almost completely free rotation existed in the C–C bonds of organic polymer chains. There is abundant evidence to show that considerable restricted rotation is the general rule as ably reviewed and demonstrated by Mizushima,[22] and by Debye and Bueche.[11] The energy barrier height for rotation is in the order of 3 kcal./mole, much higher than room temperature average energy. It must be concluded that rotation about C–C bonds is normally highly restricted even in such simple molecules as ethane, and that it is too much of an oversimplification to say that, for example, the polarization differences observed between isotactic and syndiotactic PMMA arise because one species has more free rotation about the C–C bonds while

(20) R. G. J. Miller, B. Mills, P. A. Small, A. Turner-Jones and D. G. M. Wood, *Chemistry & Industry*, 1323 (1958).

(21) It is interesting to note in this connection that Krigbaum, Carpenter and Newman, using intrinsic viscosity and virial coefficient data, concluded that their fractions of isotactic polystyrene occupy a volume some 25–30% larger than that occupied by an atactic chain of equivalent molecular weight when either is in dilute solution. This can be interpreted as meaning that the main chain bonds are more hindered in rotation in the isotactic form than in the atactic form.

(22) S. Mizushima, "Structure of Molecules and Internal Rotation," Acad. Press, Inc., New York, N. Y., 1954.

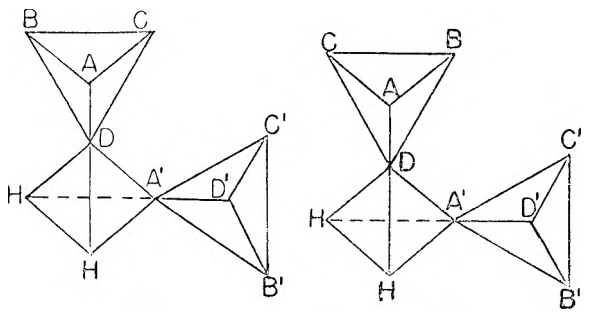

Fig. 2.—Selected steric conformations of the repeating units in isotactic and syndiotactic polymethacrylates: (a) a conformation showing two monomeric units, (*d-d*), isotactic arrangement; (b) a conformation showing two monomeric units, (*l-d*), syndiotactic arrangement. Key. A,A′ = $-CH_2-$ of first and second monomer units, respectively. B,B′ = $-CH_3$ of first and second monomer units, respectively. C,C′ = –COOR of first and second monomer units, respectively.

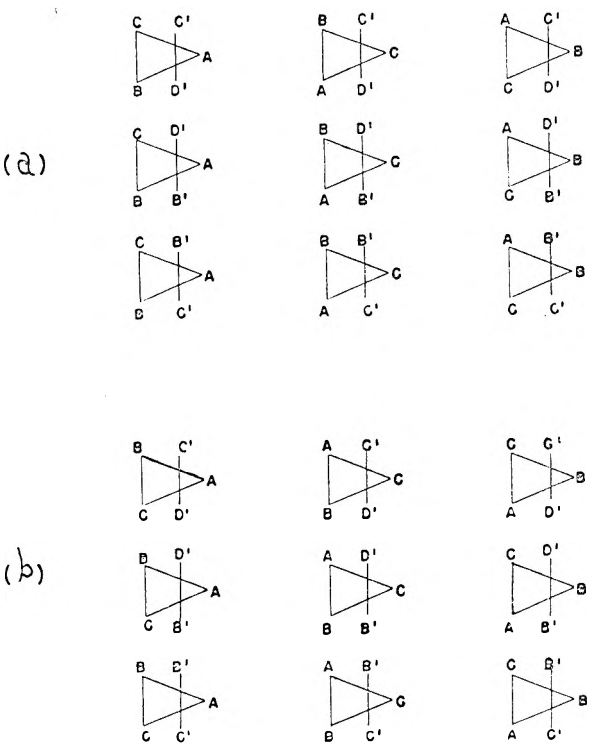

Fig. 3.—Diagram of the 18 more probable conformations of pairs of monomer units of polymethacrylates: (a) diagrams of pairs of monomer units, in isotactic arrangements; (b) diagrams of pairs of monomer units in syndiotactic arrangements. The identity of the attached groups is that shown in Fig. 2.

the other has less. Accordingly the preceding explanation, strictly in terms of free rotation about C–C bonds, while helpful perhaps, is to be regarded as inadequate. An additional factor, such as that of hindrance to positioning of chain-attached groups appears to be required.

Weissberger studied the dipole moments of optically active and inactive diastereomers.[8] Le Fevre[23] considered the differing moments between the optically active and *meso* forms of several diastereomers to arise from a hindrance of free rotation.

(23) R. J. W. LeFevre, "Dipole Moments," Methuen & Co., Ltd., London, 1948, p. 98.

He predicted the optically active forms to have high moments and the *meso* forms to have low moments because of the inability of the dipoles in *trans* conformations to compensate completely in the optically active form, whereas the *trans* conformation of the *meso* form could compensate. The argument appeared to apply to the then available data except for diethyl tartrate, but since then other diastereomeric compounds measured show contrarily sized moments of the two forms,[9] negating his conclusions. Mizushima[22] suggested that the exception shown by diethyl tartrate to Le Fevre's hypothesis might be due to the presence of hydrogen bonding in that molecule. It occurred to us that the existence of differing specific steric repulsions arising among the various steric forms might more satisfactorily account for the observed differences in the average moments. In view of the formidable difficulties in assigning degrees of steric repulsion factors for the various conformations the following analysis is presented as a suggestive method. Fortunately, there are many conformations in which the isotactic and syndiotactic forms may lie, so that the individual preciseness of assignment of degree of steric hindrance to each conformation can be somewhat masked in the statistics of handling many in the final calculation of the average resulting moment.

The Estimation of Average Moment in Stereospecific Vinyl Polymers.—The following simple and approximate method has been used here to obtain a prediction of the relative polarizations and average dipole moments of stereospecific vinyl polymers. It consists in essence of considering the successive monomer units pair by pair as they may lie in space, with the aid of molecular models. Each pair can be shown to exist in 18 most probable conformations. Among these 18 conformations the probability of each conformation was examined with the aid of molecular models and the moment of the paired monomers calculated. The relative average polarization of the chain was calculated from a weighted average of the pair moments.

For the specific case of polymethyl methacrylate the configurations of the isotactic and syndiotactic forms may be written

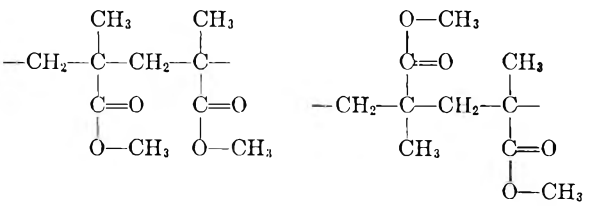

dd-configuration *ld*-configuration

In more fully spatial representation, we may represent the essential differences in the configuration as with the aid of Fig. 2. As a shorthand method of representing the 18 different interlapping conformations of the two asymmetric carbon tetrahedral assemblies, the system shown in Fig. 3 may be used. Conformations other than the gauche, in which the direct overlapping of attached groups is present, are regarded for the present as too improbable to include in the calculation.

The moment of a monomer pair, μ_p, is

$$\mu_p = 2\mu_0 \cos(\delta/2) \quad (1)$$

where μ_0 is the moment of the monomer molecule, and δ is the angle between the average moments of the monomer units as directed along the asymmetric carbon–carboxyl carbon bond.

To evaluate the average polarization of the whole polymer, we assume as a first approximation that the average moment μ_{ave} per monomer unit of the ensemble of monomer pairs in the polymer chain is the root mean square of the weighted moments of the pairs

$$(\mu_{ave})^2 = \frac{\sum_1^n f_i \mu_i^2}{4\Sigma f_i} = \frac{\mu^2 \sum_1^n f_i \cos^2(^2\delta_i/2)}{\sum_1^n f_i}$$

where "n" is the number of different conformations possible to the given polymer species (*e.g.*, 9 for the isotactic or the syndiotactic species), μ_i is the moment of the ith pair and the f_i's are the probabilities of the individual pair conformations of moment μ_i as shown in shorthand form in Fig. 3 above. The values of f_i were $0 \leqq f_i \leqq 1$.

Inspection of the molecular models in the form of pentamers (*e.g.*, Fisher–Taylor–Hirschfelder models) permitted an estimate of the relative probability of the various conformations and the dipole–dipole angles of the monomer pairs. The results of this analysis are recorded in Table IV.

The values of $\Sigma f_i \cos^2(\delta/2)/\Sigma f_i$ for the two species, calculated from the above data are: 0.767 and 0.570. for the isotactic and syndiotactic, respectively. The values for the polymer average moments, $\mu_{ave} = \mu_0 (\Sigma f_i \cos^2/(\delta/2))^{1/2}/\Sigma f_i$, using the value $\mu_0 = 1.69$ Debyes, as for a similar simple ester, methyl propionate.[17b] are 1.48 and 1.27 Debyes, respectively. The observed moments for the isotactic and syndiotactic species, expressed as the apparent moment per monomer unit were 1.43 and 1.265 Debyes, respectively. This is in the order and magnitude expected for such molecules when calculation of the average moment is made as above using consideration of the steric repulsions and basic moment for the ester units. The closeness of the calculated to the observed values of the average unit moments is regarded as rather fortuitous, but the calculation is expected to show the relative sizes of the two species' moments to a fair approximation.

$$\left(\text{estimated precision, } \pm 5\% \text{ in the ratio } \frac{\mu_{ave}\,(d-d)}{\mu_{ave}\,(l-d)}\right)$$

The method of calculation given has had a measure of success in predicting the relative moments for the isotactic and syndiotactic forms of several other related polymers. It is planned to describe this more fully in a forthcoming discussion of those polymers.

TABLE IV

STERIC FACTORS IN THE CONFORMATIONS OF ISOTACTIC AND SYNDIOTACTIC POLYMETHYL METHACRYLATE

Conformation symbol	Isotactic species, *d-d* f_i	Isotactic species, *d-d* Dipole–dipole angle, degrees	Syndiotactic species, *l-d* f_i	Syndiotactic species, *l-d* dipole–dipole angle, degrees
I	0	50	0	140
II	1/2	45	1/2	50
III	0	160	0	60
IV	0	120	0	100
V	1/4	120	1/2	115
VI	0	105	0	120
VII	0	160	0	55
VIII	3/4	60	3/4	55
IX	1/2	20	1/4	175

Acknowledgment.—The authors wish to acknowledge with appreciation the helpful discussions with Dr. Keniti Higasi.

INFRARED STUDIES OF AMINE–HALOGEN INTERACTIONS[1]

BY RALPH A. ZINGARO AND W. B. WITMER

Department of Chemistry of the Agricultural and Mechanical College of Texas, College Station, Texas

Received May 11, 1960

The marked changes which are brought about in the 1000 cm.$^{-1}$ region of the infrared spectrum of pyridine upon the addition of iodine have been found to be generally characteristic for amine–halogen solutions. Infrared studies on a series of solutions made up from five different halogens and inter-halogens in pyridine and various pyridine derivatives, all reveal corresponding infrared shifts. Several new solid amine–halogen complexes have been isolated, and, in every case, the frequency shifts observed in the solutions can be correlated with infrared bands characteristic of the solids. Comparison of the spectra with those of substituted benzenes gives a reasonable interpretation of the data.

Introduction

It has been recently demonstrated[2] that the marked changes which are observed in the infrared spectrum of pyridine upon the addition of iodine[3] can be correlated with the spectra of solid compleves of the type (PyI)X and (Py_2I)X. These solids possess infrared bands which have the same location, and which are of the same intensity as the new bands which are found in the infrared spectrum of pyridine following the addition of iodine. The present investigation represents an extension of these studies and includes a variety of solutions made up of different halogens and interhalogens in a number of pyridine derivatives. The amines were chosen so that both steric and electronic effects could be observed. The fundamental purpose of this study was to determine whether the rather profound infrared shifts which are observed in iodine–pyridine solution could be observed as a phenom-

(1) Presented at the Southwest Regional Meeting of the American Chemical Society, Baton Rouge, Louisiana, December 4, 1959.

(2) R. A. Zingaro and W. E. Tolberg, *J. Am. Chem. Soc.*, **81**, 1353 (1959).

(3) D. L. Glusker and H. W. Thompson, *J. Chem. Soc.*, 471 (1955).

enon generally characteristic of halogen–amine systems. Such a generalization, if established, should contribute substantially to a better understanding of the nature of amine halogen interactions.

Experimental

Amines.—The pyridine was of the same quality as described previously[2] and was purified in the same manner. The other starting materials were Eastman white label grade in the case of 2-chloropyridine, 2-bromopyridine and quinoline. The starting materials in the case of the amyl- and benzylpyridines were either Eastman yellow label or Matheson technical grade products. All were dried over sodium hydroxide for several days and distilled from calcium oxide under reduced pressure. Middle fractions, only, were used. The four amyl- and benzylpyridine middle fractions were subjected to at least one, or more, additional fractionations. Because of the limited amount of data available on the physical constants of these compounds, the boiling points and refractive indices of the amines used are listed in Table I.

TABLE I

PHYSICAL PROPERTIES OF SOME SUBSTITUTED PYRIDINES

Pyridine substituent	B.p., °C.	Refractive index Found	Reported
2-Benzyl	98.5 (4.0)[a]	1.5771 (26)[b]	[c]
4-Benzyl	110.0 (6.0)	1.5814 (25)	[c]
2-*n*-Amyl	63.0 (2.0)	1.4861 (26)	[c]
4-*n*-Amyl	78.0 (2.5)	1.4892 (25.4)	1.4908 (20)[4]
2-Chloro	49.0 (7.0)	1.5322 (20)	1.5322 (20)[5]
2-Bromo	49.0 (2.7)	1.5713 (20)	1.5713 (20)[5]

[a] Figure in parentheses gives the pressure in mm. [b] Figure in parentheses gives the temperature. [c] No literature values were found.

Halogens and Interhalogens.—The bromine and iodine were Mallinckrodt "Analytical Reagent" grade and were used without further purification. Iodine monochloride and iodine monobromide were prepared according to published directions.[6] Their purification was accomplished by cooling and separation of the crystalline interhalogen from the liquid. The solids were subjected to this crystallization process several times.

Bromine monochloride was used in the form of a mixture. To liquid chlorine, at −70°, was added an equimolecular quantity of bromine. The container was then warmed to −10 to −15° and complete mixing accomplished by rapid stirring of the mixture.

Samples for Infrared Study.—The chloroform used was "Analytical Reagent" grade. Standard solutions of the halogen, interhalogen or of the amine in chloroform, were prepared separately by weighing out the appropriate amount of solute and diluting to volume. The solutions were prepared as near to the time of measurement as possible, and mixing of the two solutions to achieve the desired relative concentrations was done just preceding the measurement. In no case was any change in the spectrum noticed during the first several hours, thus precluding any complications which may have arisen as a result of any extensive chemical reaction taking place during the actual time of measurement of the spectrum.[7] Potassium bromide discs were prepared in the usual manner.[2]

Instrumentation.—A Beckman IR-4 was used for all measurements. The instrument was calibrated regularly by means of a standard polystyrene sample.

Amine–Halogen Complexes.—Several solid 1:1 addition compounds, previously unreported in the literature, were prepared.

In the case of the 4-*n*-amylpyridine derivatives, equimolecular quantities of 4-*n*-amylpyridine and the halogen, or interhalogen, were combined in chloroform at Dry Ice temperature. The major portion of the chloroform was evaporated at reduced pressure and the solid, after removal by filtration in a dry atmosphere, was washed with anhydrous carbon tetrachloride and sodium dried ethyl ether.

The quinoline–bromine complex was prepared by direct combination of solutions containing equimolecular quantities of bromine and quinoline in carbon tetrachloride. The solid, which separated out immediately, was separated and washed as described in the paragraph immediately preceding.

Analysis of the compounds for "free" halogen was performed by titrating the iodine liberated upon treatment of the complex with potassium iodide solution.

The compounds showed an analogous solubility pattern. They were only very slightly soluble in carbon tetrachloride, ether or ligroin, but soluble in chloroform and alcohol. The relevant data is summarized in Table II.

TABLE II

AMINE-HALOGEN ADDITION COMPOUNDS

Coördinating base	Halogen	Color	Total halogen, % Found	Calcd.	M.p., °C.
4-*n*-Amylpyridine	Br_2	Orange	51.0	51.7	85–87.5, sl. d
4-n-Amylpyridine	BrCl	Pale yellow	43.3	43.6	105–105.5
4-*n*-Amylpyridine	IBr	Yellow	57.5	58.1	100.5–101
Quinoline	Br_2	Orange	55.7	55.3	79–79.5

Positive Bromine and Iodine Salts.—The compounds, $(BrPy_2)NO_3$ and $(BrPy_2)ClO_4$, were prepared according to methods described in the literature.[8,9]

Dipyridinebromine(I) acetate, $(BrPy_2)C_2H_3O_2$, was prepared as a new compound in the following way. In a dry, glass stoppered ehrlenmeyer flask, 0.055 mole of pyridine and 0.02 mole of silver acetate were combined with about 50 ml. of chloroform. In a second flask, 0.026 mole of bromine was mixed with 30 ml. of chloroform. Both solutions were cooled in Dry Ice after which the cold bromine solution was added in small portions to the pyridine–silver acetate solution. Silver bromide was removed by filtration and the clear filtrate was poured into cold, dry ether. A precipitate did not form at once so the solution was stored in a stoppered flask in a Dry Ice chest. The pale yellow solid which formed overnight changed in color to a light orange on separation from the solution. The material was washed with cold, dry ether and further dried by pulling dry air through it. This compound decomposes very rapidly in presence of water. The complex melts at 45–50° with decomposition. Calcd. for $C_{12}H_{13}O_2N_2Br$: Br, 26.9. Found: Br, 26.7. The yield was 20%.

Mono-2-bromopyridineiodine(I) benzoate was prepared in very small quantities. Into 100 ml. of anhydrous chloroform, 11.5 g. (0.05 mole) of silver benzoate, 9 g. of 2-bromopyridine (1.5 g. in excess of 0.05 mole) and 12.7 g. (0.1 mole) of iodine crystals were combined. The suspension was vigorously stirred for 20 minutes in an anhydrous atmosphere. The dissolved iodine gave a violet solution and only a very small quantity of the iodine was consumed. The solution was filtered and to the filtrate was added 250 ml. of petroleum ether. After storage for 48 hours at Dry Ice temperature, the very small quantity, *ca.* 1 g., of orange-brown crystals was removed and washed with cold petroleum ether and dried *in vacuo* over sulfuric acid. Analysis for iodine gave 31.6%. For the indicated complex, the calculated value is 31.3%. The compound decomposed over a wide range from 55–90°, with liquefaction occurring over the range 79–90°.

Results

The characteristic infrared absorption system in the 1000 $cm.^{-1}$ region for the eight amines investi-

(4) J. P. Wibaut and J. W. Hey, *Rec. trav. chim.*, **72**, 513 (1953).

(5) H. C. Brown and X. R. Mihm, *J. Am. Chem. Soc.*, **77**, 1723 (1955).

(6) "Inorganic Syntheses," Vol. I, McGraw-Hill Book Co., Inc., New York, N. Y., 1939, p. 165.

(7) The possibility that there may occur a rapid chemical reaction between the halogen and the amine is very real, but unavoidable. However, the concentration of reaction products, if formed, is so small that they are not detectable by infrared methods. The formation of small amounts of reaction products may be of much greater importance when methods such as ultraviolet spectroscopy or conductivity are used. Not only are such methods more sensitive to the presence of impurities, but may themselves be causative. For instance, ultraviolet radiation is known to catalyze free radical halogenations, and the electrode surfaces may also function similarly.

(8) H. Carlsohn, *Ber.*, **68**, 2209 (1935).

(9) M. Ushakov, X. Chistov and N. Zelinskii, *ibid.*, **68**, 824 (1934)

TABLE III

INFRARED ABSORPTION OF VARIOUS PYRIDINES AND SOME OF THEIR HALOGEN COMPLEXES

	Compound	Physical state	Location of band, cm.$^{-1}$						
1	Pyridine[a] (1.0 *F*)	$CHCl_3$ soln.	989		1027				1070
2	Iodine[b]	Satd. soln. in Py		1005		1031[c]		1060	
3	Bromine (1.0 *F*)	+1.0 *F* Py in $CHCl_3$		1010	1029[e]	1039[e]		1065	
4	BrCl (1.0 *F*)[i]	+1.0 *F* Py in $CHCl_3$		1013	1032[e]	1040[c]		1065	
5	(IPy)Br[a]	Solid		1011		1031[c]		1057	
6	(IPy)Cl[a]	Solid		1012		1033[c]		1054	
7	(IPy)F[a]	Solid		1014	1027[c]	1032[c]		1056	
8	$(PyH^+)I^-$[a]	Solid	995		1030			1051	
9	(BrPy)Br	Solid		1008		1035	1044[e]	1058	
10	$(BrPy_2)NO_3$	Solid		1015		1034		1058	
11	$(BrPy_2)$acetate	Solid		1009		1039[e]		1059	
12	$(BrPy_2)ClO_4$	Solid		1016		Obscured by perchlorate			
13	2-*n*-Amylpyridine (2-AP), 1.0 *F*	$CHCl_3$ soln.	996					1051	
14	Iodine	+1.0 *F* 2-AP in $CHCl_3$		1006	1017[c]			1051	
15	Bromine (1.0 *F*)	+1.0 *F* 2-AP in $CHCl_3$		1010			1044[e]	1056	
16	IBr (1.0 *F*)	+1.0 *F* 2-AP in $CHCl_3$		1010				1057	
17	ICl (1.0 *F*)	+1.0 *F* 2-AP in $CHCl_3$		1013				1058	1075[e]
18	BrCl (1.0 *F*)	+1.0 *F* 2-AP in $CHCl_3$		1016				1057	1080[e]
19	4-*n*-Amylpyridine (4-AP), 1.0 *F*	$CHCl_3$ soln.	995					1050[e]	1068
20	Iodine, satd.	+1.0 *F* 4-AP in $CHCl_3$		1011	1023[e]				1065
21	Bromine, 1.0 *F*	+1.0 *F* 4-AP in $CHCl_3$		1018					1065
22	IBr, 1.0 *F*	+1.0 *F* 4-AP in $CHCl_3$		1018					1065
23	ICl, 1.0 *F*	+1.0 *F* 4-AP in $CHCl_3$		1021					1066
24	BrCl, 1.0 *F*	+1.0 *F* 4-AP in $CHCl_3$		1026					1066
25	[Br(4-AP)]Br	Solid		1026					1066
26	[I(4-AP)]Br	Solid		1015					1062
27	[Br(4-AP)]Cl	Solid		1024					1057
28	2-Benzylpyridine (2-BzP), 1.0 *F*	$CHCl_3$ soln.	997		1029[d]			1050	
29	Iodine, satd.	+1.0 *F* 2-BzP in $CHCl_3$	997[e]	1005	1028[d]			1052	
30	Bromine, 1.0 *F*	+1.0 *F* 2-BzP in $CHCl_3$	1003[e]	1013	1029[d]		1043[e]	1055	
31	IBr, 1.0 *F*	+1.0 *F* 2-BzP in $CHCl_3$		1009	1028[d]			1055	
32	ICl, 1.0 *F*	+1.0 *F* 2-BzP in $CHCl_3$		1014	1024[d]			1058	
33	BrCl, 1.0 *F*	+1.0 *F* 2-BzP in $CHCl_3$		1013	1029[d]			1058	
34	4-Benzylpyridine (4-BzP), 1.0 *F*	$CHCl_3$	995	1001[c,d]		1028[d]		1048[e]	1069
35	Iodine, satd.	+1.0 *F* 4-BzP in $CHCl_3$	995[e]	1002[e,d]	1011	1028[d]		1049[e]	1064
36	Bromine, 0.4 *F*	+1.0 *F* 4-BzP in $CHCl_3$	995[e]	1001[e,d]	1015	1028[d]		1048[e]	1064
37	Bromine, 1.0 *F*	+1.0 *F* 4-BzP in $CHCl_3$		1002[e,d]	1019	1029[d]			1064
38	IBr, 1.0 *F*	+1.0 *F* 4-BzP in $CHCl_3$		1002[e,d]	1018	1024[d]			1064
39	ICl, 1.0 *F*	+1.0 *F* 4-BzP in $CHCl_3$		1002[e,d]	1020	1028[d]			1065
40	BrCl, 1.0 *F*	+1.0 *F* 4-BzP in $CHCl_3$		1002[e,d]	1018	1028[d]			1065
41	Quinoline (Q) 1.0 *F*	$CHCl_3$ soln.	939	952[e]					
42	Iodine, satd.	+1.0 *F* Q in $CHCl_3$	939[e]	943					
43	Bromine, 1.0 *F*	+1.0 *F* Q in $CHCl_3$	939[e]	947					
44	[Br(Q)]Br	Solid		952					
45	2-Chloropyridine (CP), 1.0 *F*	$CHCl_3$ soln.	991					1043	
46	Bromine, 0.4 *F*	+1.0 *F* CP in $CHCl_3$	991[e]	1002[e]	1012			1043	
47	Bromine, 1.0 *F*	+1.0 *F* CP in $CHCl_3$	991[e]	1002[e]	1012			1043	
48	Bromine, 2.0 *F*	+1.0 *F* CP in $CHCl_3$	991[e]	1001[f]	1009[e]			1043	
49	2-Bromopyridine (BP), 1.0 *F*	$CHCl_3$ soln.	988		1015[e]			1041	
50	Bromine, 0.3 *F*	+1.0 *F* BP in $CHCl_3$	988[e]	999[e]	1015[e]			1041	
51	Bromine, 2.0 *F*	+1.0 *F* BP in $CHCl_3$	988[e]	999[f]	1007[g]			1043	
52	Bromine, 3.0 *F*	+1.0 *F* BP in $CHCl_3$	988[e]	999[f]	1007[g]			1043	
53	Bromine, 4.0 *F*	+1.0 *F* BP in $CHCl_3$	988[g]	999[f]				1043	
54	[I(BP)]benzoate	Solid			1006	1025[h]		1043	

[a] From data of Zingaro and Tolberg.[2] [b] From data of Glusker and Thompson.[3] [c] Band of weak intensity; all other bands are strong to very strong in intensity. [d] Probably ring vibrational frequency associated with benzyl group. [e] Large decrease in band intensity. [f] Increase in band intensity. [g] Shoulder. [h] Benzoate absorption band. [i] One of the referees questioned the meaning of a 1.0 F BrCl solution since BrCl is an equilibrium mixture of bromine and chlorine. Experimentally, such a solution is 0.5 F with respect to bromine and chlorine and the total halogen concentration is 1.0 F. In the presence of the amine donor the equlibrium mixture is assumed to exist almost quantitatively in the form of the complex B:BrCl, where B is the donor molecule. This assumption is supported by the existence of stable solids such as Py:BrCl and physical properties of the solution, *e.g.*, the non-volatility of the halogens, which differ radically from the properties of the free equilibrium mixture.

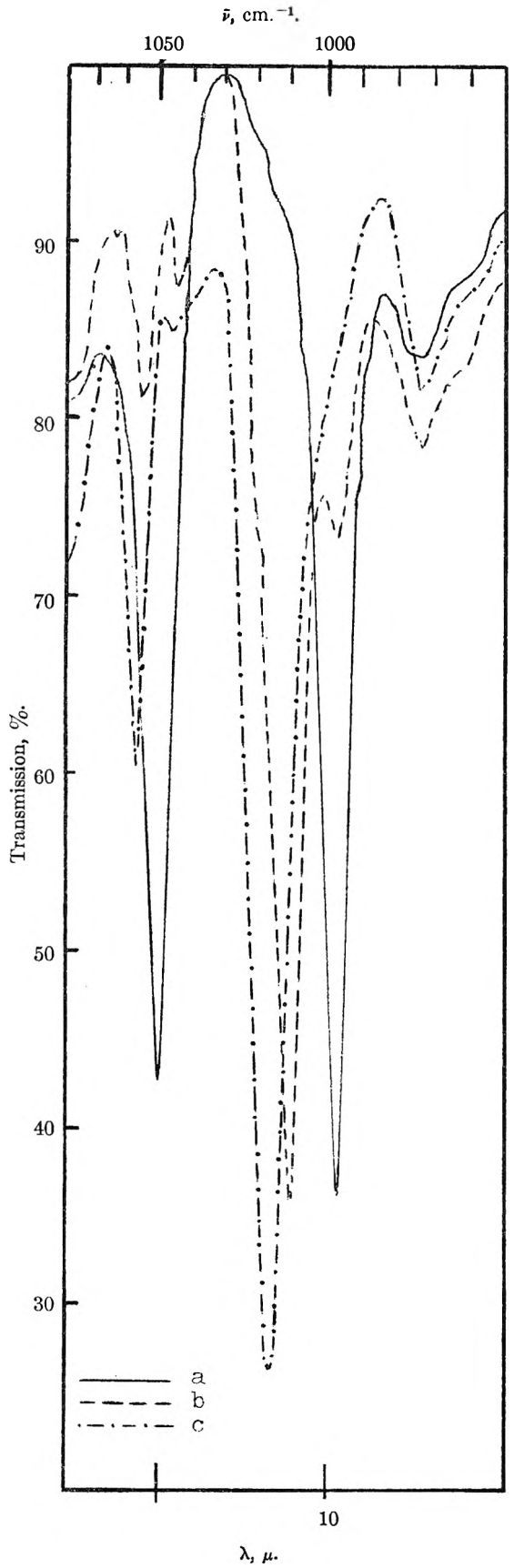

Fig. 1.—Infrared absorption in 1000 cm.$^{-1}$ region: a, 2-*n*-amylpyridine (1.0 *M*) in $CHCl_3$; b, same as a + Br_2 (1.0 *M*); c, same as a + BrCl (1.0 *M*).

gated are listed in Table III. The highly characteristic band (quinoline excluded) and one of considerable interest in this study is the very sharp and intense absorption near 1000 cm.$^{-1}$ which is found at a low frequency of 988 cm.$^{-1}$ for 2-bromopyridine and at a high frequency of 997 cm.$^{-1}$ in the case of the 2-benzyl derivative. The pair of intense bands at 1027 and 1070 cm.$^{-1}$ characteristic of pyridine does not persist through the series. With the exception of 2-bromopyridine and 4-*n*-amylpyridine in which the two bands remain, but with the band of lower frequency greatly diminished in intensity, this pair of bands is replaced in the substituted compounds by a single intense absorption at 1060 ± 15 cm.$^{-1}$. These observations are in excellent agreement with those of other investigators.[10,11] The change from a three to a two band system in this region appears to be characteristic of monosubstitution in the pyridine ring.

Both benzyl derivatives show strong absorption at 1029 cm.$^{-1}$, which undoubtedly is due to aromatic ring vibrations in the benzyl group. The 4-benzylpyridine also possesses a weak absorption at 1002 cm.$^{-1}$ probably due also to the benzyl group. Neither of these bands is affected by the addition of halogen.

Examination of Table III shows that the disappearance of the 1000 cm.$^{-1}$ band and the simultaneous appearance of a new, intense band at a frequency of up to 31 cm.$^{-1}$ higher (Table III, 24, 25) is characteristic not only of solutions of halogens and interhalogens with pyridines, but also of the crystalline, solid derivatives (Table III, 5–12, 25–27, 44). It has been noted[2] that the 990 cm.$^{-1}$ band of pyridine is replaced by a band at successively higher frequencies in the series PyI_2 (solution), (IPy)Br, (IPy)Cl and (IPy)F. Similar trends were observed in the present investigation for the series BI_2, BIBr and BICl, where B represents the coördinating pyridine base. Also, as shown in Fig. 1, and in Table III, the addition of BrCl invariably results in the 1000 cm.$^{-1}$ band being located at a higher frequency than is observed on the addition of bromine alone.

The effect of changing the basic strength of the coördinating amine can be seen by examining the data in Table III (45–54) and Fig. 2. Although numerous attempts were made to prepare solid derivatives of 2-chloropyridine and 2-bromopyridine, only one solid was obtained, the mono-(2-bromopyridine)-iodine(I) benzoate, characterized in the 1000 cm.$^{-1}$ region by a pair of bands at 1006 cm.$^{-1}$ and at 1043 cm.$^{-1}$. Examination of Fig. 2 shows that the 988 cm.$^{-1}$ band of 2-bromopyridine diminishes gradually in intensity as the bromine concentration is increased. It persists as a shoulder even when the bromine is present in a molar ratio of four to one. The 988 cm.$^{-1}$ band of the free base is eventually replaced by a new band at 999 cm.$^{-1}$. Also, comparison of Figs. 1 and 2 shows that the new band at 999 cm.$^{-1}$ in the case of the 2-bromopyridine solution, is broader and less intense than that of the free donor, whereas the new band is as

(10) G. L. Cook and F. M. Church, THIS JOURNAL, 61, 458 (1957).
(11) A. R. Katritzky, J. N. Gardner and A. R. Hands, *J. Chem. Soc.*, 2198 (1958).

sharp and as intense, if not more so, in the case of the halogen complexes formed with the strong donor.

It would be desirable to be able to compare solution spectra with those of solids in the case of every amine studied. This was done wherever possible.

Considerable effort was devoted to the preparation of coördinated halogen(I) salts using silver salt metathesis reactions, and to the preparation of crystalline molecular addition compounds, but it was possible to isolate only very viscous oils in many cases. For example, both iodine and bromine reacted rapidly and quantitatively with silver salts in the presence of 2-amyl-, 2-benzyl- or 4-benzylpyridines, but crystalline derivatives were not obtained. The highly viscous, non-crystallizable products that were isolated possessed the chemical properties characteristic of halogen(I) salts, *e.g.*, rapid oxidation of iodide. Also, their infrared spectra were examined and they showed bands typical of the solids, *i.e.*, the lower frequency absorption at 1000 cm.$^{-1}$ region replaced by a band at a frequency of 15–35 cm.$^{-1}$ higher than that found for the free base. These data are not tabulated since these oils could not be characterized as definite compounds. Their formation and properties, however, do corroborate the conclusions which will be drawn concerning the nature of the amine–halogen interactions.

It is to be noted also that in every case, the characteristic absorption at 1060 ± 15 cm.$^{-1}$ is retained, even following halogen, or interhalogen interaction.

Discussion

In the first paper of this series[2] the interpretation of the data was based on the assumption that the 990 cm.$^{-1}$ absorption of pyridine was an in-plane hydrogen deformation mode. The new band observed on halogen complexing was interpreted as a shift in this band due to the influence of the large, polarized iodine atom on the adjacent ring hydrogens. A similar argument can be made for the effects presently observed. Such an interpretation, while plausible, requires that the bromine interaction be stronger than that of iodine since bromine has been found consistently to bring about a larger shift in the 990 cm.$^{-1}$ band of the various amines investigated than does iodine. It is difficult to conceive of the bromine molecule being more highly polarized than iodine. This argument is also inconsistent with the effects that would be expected when the relative electronegativities and the sizes of bromine and iodine are compared.

Part of the difficulty in the interpretation was due to the lack of agreement in the assignment of the 990 cm.$^{-1}$ band which is highly characteristic of pyridine and monosubstituted pyridines. For instance, Bellamy[12] reports that this band is due to either a ring vibration or a hydrogen deformation mode. In independent studies this band has been assigned to a γ-CH mode[11] and to a symmetrical ring vibration.[10] In earlier studies on deuterated pyridines,[13,14] this absorption was assigned to an A_1

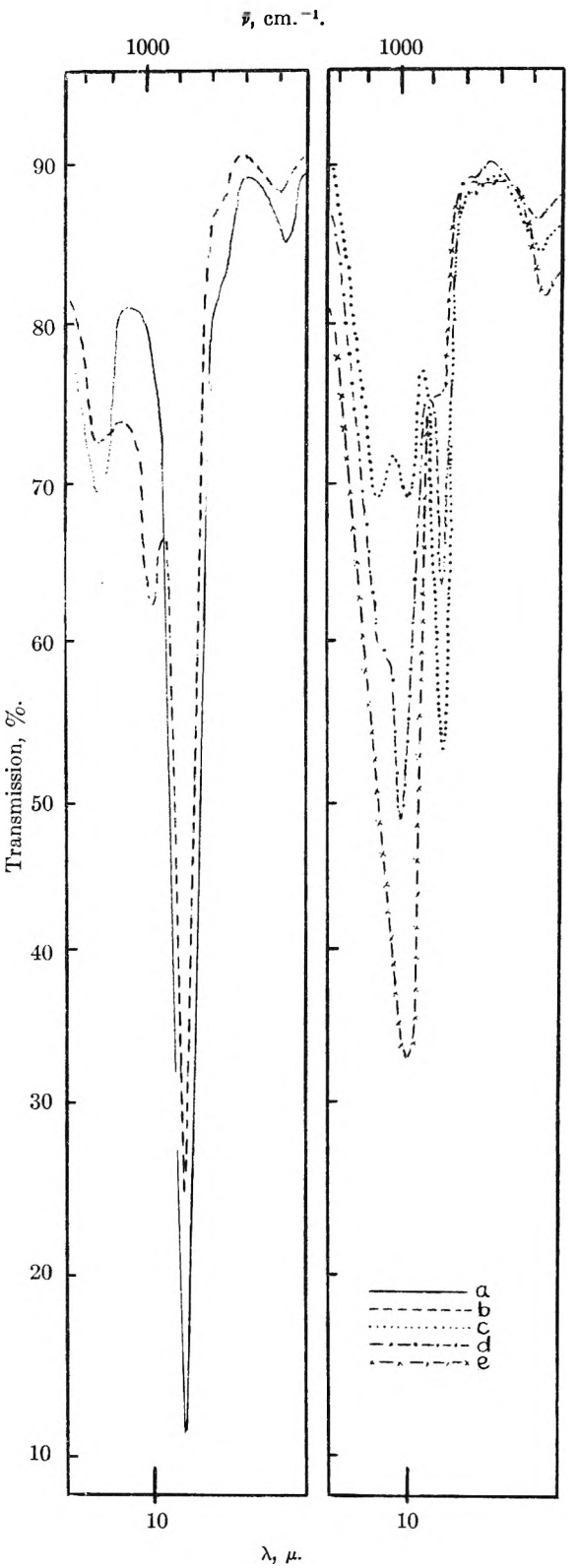

Fig. 2.—Infrared absorption in 1000 cm.$^{-1}$ region: a, 2-bromopyridine (1.0 *M*) in $CHCl_3$; b, same as a + Br_2 (0.3 *M*); c, same as a + Br_2 (1.0 *M*); d, same as a + Br_2 (2.0 *M*); e, same as a + Br_2 (4.0 *M*).

(12) L. J. Bellamy, "The Infrared Spectra of Complex Molecules," John Wiley and Sons, Inc., New York, N. Y., second edition, 1958, p. 277.

(13) L. Corrsin, B. J. Fox and R. C. Lord, *J. Chem. Phys.*, **21**, 1170 (1953).

(14) F. A. Anderson, B. Bak, S. Brodersen and J. R. Anderson, *ibid.*, **23**, 1047 (1955).

symmetrical ring vibration. Recently, Katritzky[15] has also changed his original assignment[12] from a hydrogen deformation to a ring breathing mode. There now appears to be general agreement on this assignment. For purposes of clarity and simplification, the presently accepted vibrational modes associated with the observed active infrared frequencies of pyridine in the 1000 cm.$^{-1}$ region are illustrated.

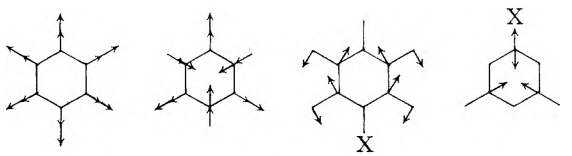

I	II	III	IV
Mode no.			
A_1	A_1	B_1	B_1
Species			
989 cm.$^{-1}$	1029	1068	
Band location a. for C_6H_6N			
	1004 ± 6	1020 ± 5	1070 ± 15
b. for C_6H_5X			

Randle and Whiffen[16] have discussed the absorption of mono- and *para*-substituted benzene derivatives in the 1000 cm.$^{-1}$ region. There exists a striking similarity in the infrared absorption in this region between the pyridine–halogen complexes and the monosubstituted benzenes as well as between the 4-substituted-pyridine–halogen complexes and *para*-substituted benzenes.

The monohalobenzenes are characterized in the 1000 cm.$^{-1}$ region by a 3-band system. The 1004 ± 6 cm.$^{-1}$ band is a symmetrical ring breathing (mode no. II),[17] that at 1020 ± 5 cm.$^{-1}$, an in-plane hydrogen deformation (mode no. III), and the 1070 ± 15 cm.$^{-1}$ band is a trigonal A_1 breathing (mode no. IV) which is highly sensitive to the C–X stretching vibration. The strong similarity which exists in infrared absorption in this region between the monohalobenzenes and the pyridine–halogen complexes becomes apparent when the frequencies listed for the monosubstituted benzenes are compared with those observed for the iodine–pyridine complexes[2] and the data herein reported (Table II, 1–12). A most reasonable interpretation is that the lowest frequency band *does not* represent a shift in the totally symmetric ring vibration, (I), of pyridine, but is due, after halogen coördination, to a trigonal ring breathing (mode no. II). The middle band at about 1030 cm.$^{-1}$ no longer corresponds to a ring breathing mode, but is attributable to inplane hydrogen deformation (mode no. III). The highest frequency absorption at 1060 ± 5 cm.$^{-1}$ no longer corresponds to the in-plane hydrogen deformation found at 1070 cm.$^{-1}$ for free pyridine (mode no. III), but represents a mixing of the trigonal ring breathing frequency of pyridine with the N–X stretching vibration. Since this is a function of the substituent mass, a larger effect should be observed for iodine than for bromine. However, this effect is strongly dependent on the nature of the N–X bond, the strength of which is by no means comparable to that of a C–X bond. A careful study of the absolute intensities of these bands would be more useful in understanding these mass effects.

The effect of halogen complexing on the absorption of the 4-substituted pyridines is reasonably interpreted by comparison with *para*-substituted benzenes. The band system of the 4-substituted pyridines in this region consists of a ring-breathing mode at 993 ± 3 cm.$^{-1}$ (mode II)[15] and an in-plane hydrogen deformation (mode III) at 1067 ± 3 cm.$^{-1}$. It is to be noted that on halogen complexing (Table III, 19–27 and 34–40), the two band system (ignoring, of course, the benzyl frequencies which also appear in this region) is retained, and is made up of bands at 1020 ± 10 cm.$^{-1}$ and at 1065 ± 1 cm.$^{-1}$. Comparison of the higher frequency band with the 1070 ± 20 cm.$^{-1}$ band of the *para*-substituted benzenes as discussed by R and W[16] suggests that this is derived from a combination of C–X and N–X stretching modes with ring breathing frequencies. The lower frequency band, as before, does not simply represent a shift in the trigonal breathing mode at 993 cm.$^{-1}$, but is due instead to a mixing of the C–X and N–X stretching with the in-plane hydrogen deformation.

In the case of the changes brought about in the 2-substituted pyridines, a comparison with the *ortho* - substituted benzenes seems reasonable. Qualitatively, the spectra of the halogen complexed 2-substituted pyridines is very similar to that of the *ortho*-substituted benzenes. However, the nature of the 2-substituted groups in this work (except for the 2-halopyridines) was such as to make it sterically impossible for the complexed halogen molecules to possess a linear orientation with respect to the nitrogen and the 4-carbon atom. Also, the C_{2v} symmetry characteristic of all the previous cases is no longer retained in the 2-substituted species. Hence, a meaningful discussion must be deferred pending an interpretation of the absorption of the *ortho*-substituted benzenes in this region.

The results clearly corroborate the highly localized nature of the forces which stabilize the amine–halogen type of complexes. The geometry of these complexes has been well established,[18] heats of formation of the order of 8 kcal./mol and greater[19–21] have been reported and a large number of stable salts containing the IPy grouping are known. Both the amine–halogen and hydrocarbon–halogen type of interactions are analogous if defined according to the broad donor–acceptor sense of Mulliken's charge-transfer theory.[22] The experimental differences between the two types are great, however, and an experimental classification, based perhaps on a limiting minimum heat of formation of the complex, may be much more useful from a purely chemical point of view.

(15) A. R. Katritzky, *Quart. Revs.*, **13**, 353 (1959), and personal communication.

(16) R. R. Randle and D. H. Whiffen, *Trans. Faraday Soc.*, **52**, 9 (1956).

(17) These assignments are due to D. H. Whiffen, *J. Chem. Soc.*, 1350 (1956).

(18) G. Eia and O. Hassel, *Acta Chem. Scand.*, **10**, 139 (1956); O. Hassel, *J. Mol. Phys.*, **1**, 241 (1958); O. Hassel and C. Rømming, *Acta Chem. Scand.*, **10**, 696 (1956).

(19) K. Hartley and H. A. Skinner, *Trans. Faraday Soc.*, **26**, 621 (1950).

(20) S. Nagakura, *J. Am. Chem. Soc.*, **80**, 520 (1958).

(21) H. Tsubomura, *ibid.*, **82**, 40 (1960).

(22) R. S. Mulliken, *ibid.*, **72**, 600 (1950); **74**, 811 (1952).

Acknowledgment.—We should like to express our appreciation to Dr. F. A. Matsen and Dr. E. E. Ferguson of the University of Texas for interesting and useful discussions and to Dr. A. R. Katritzky of the University Chemical Laboratory, Cambridge, for helpful correspondence.

THE DIFFERENTIAL THERMAL ANALYSIS OF PERCHLORATES. IV. A SPURIOUS HEAT EFFECT

BY MEYER M. MARKOWITZ AND DANIEL A. BORYTA

Foote Mineral Company, Research and Development Laboratories, Chemicals Division, Berwyn, Penna.

Received May 18, 1960

A serious source of error has been found in DTA studies of highly turbulent condensed phase-gas reactions (*viz.*, the thermal decompositions of the alkali metal perchlorates) when carried out in an open furnace exposed to the ambient atmosphere. Recession of the sample from the thermocouple is shown to occur, giving rise to endothermal breaks which have been incorrectly attributed to part of the decomposition mechanism of the material under study. This spurious thermal behavior appears to be eliminated when a closed furnace is used. The thermal decompositions of lithium and potassium perchlorates are discussed in some detail.

Introduction

During the course of a continuing program of study concerned with the thermal behavior of perchlorate salts,[1-3] an equipment-dependent effect was found in the differential thermal analysis (DTA) of lithium, potassium and rubidium perchlorates. In order to distinguish between DTA breaks due to the samples and those introduced by the equipment, the origin of the anomalous effects was sought.

In a frequently applied DTA apparatus (set-up A),[4] the sample and inert reference material (alumina), each contained in a separate test-tube, are set symmetrically into a steel block which fills the cylindrical cavity of a crucible furnace. Since the entire arrangement is open to the atmosphere, a sharp temperature gradient exists between the surface of the steel block and its environment. Many DTA studies on alkali metal perchlorates using this equipment gave results in good agreement with those previously reported.[2,4-8] Subsequently, a new furnace arrangement employing an enclosed cavity within a muffle furnace (K. H. Huppert Co., 6830 Cottage Grove Ave., Chicago, Ill., Model 434 Deluxe Furnace without pyrometer and controller) was adopted. The only contact between the heated chamber and the atmosphere is by way of a narrow slit in the top of the heavily insulated furnace through which the differential thermocouples enter. Surprisingly, the DTA curves obtained with this equipment (set-up B) were significantly different from those using the open furnace. The reasons for these differences and their importance in the proper application of DTA comprise the subject matter of this paper.

(1) M. M. Markowitz, THIS JOURNAL, **61**, 505 (1957).
(2) M. M. Markowitz, *ibid.*, **62**, 827 (1958).
(3) M. M. Markowitz and R. F. Harris, *ibid.*, **63**, 1519 (1959).
(4) S. Gordon and C. Campbell, *Anal. Chem.*, **27**, 1102 (1955).
(5) V. D. Hogan and S. Gordon, THIS JOURNAL, **62**, 1433 (1958).
(6) S. Gordon and C. Campbell, *Bull. Am. Ceram. Soc.*, **34**, 372 (1955).
(7) V. D. Hogan, S. Gordon and C. Campbell, *Anal. Chem.*, **29**, 306 (1957).
(8) S. Gordon and C. Campbell, "Proceedings of the Fifth Symposium on Combustion," Reinhold Publ. Corp., New York, N. Y., 1955, pp. 277-284.

Experimental Procedures

DTA runs on the purified anhydrous perchlorates of lithium, potassium and rubidium were performed both in set-up A and in set-up B. Five-gram samples were heated at 10° per minute using a motorized variable transformer to program the current to the furnace. The recording equipment consisted of a 5.5 mv. span strip-chart potentiometric recorder (Fisher Scientific Co., 717 Forbes Street, Pittsburgh 19, Penna., "Recordall"), the inputs to which were alternated through an automatic stepping switch (Fisher Scientific Co., "Auto-Step Switch").

The sample temperature signal was attenuated with a 10 turn, 1000 ohm linear precision potentiometer held at a setting of 0.15. The range for the differential input was −2.75–0–2.75 mv. on the recorder, achieved by addition of a bias voltage. Thus, T and ΔT were recorded on the same time basis. The T value corresponding to any point on the ΔT curve is readily found by drawing a horizontal line between the two curves.

The curves given represent differential temperature–time plots with the areas indicative of thermal effects designated by Roman numerals. The temperature values for these areas are given where appropriate.

Experimental Results

The DTA curves for anhydrous lithium perchlorate, obtained with both set-ups, are depicted in Fig. 1. Curves A and B differ markedly in the decomposition regions (III-IV-V in A and III in B). The small endothermal breaks IA and IB correspond to the dissociation reaction: $LiClO_4 \cdot H_2O \rightarrow LiClO_4 + H_2O$ at about 150°[2,9]; water may be absorbed by anhydrous lithium perchlorate during handling and exposure to the air.[10] Endotherms IIA and IIB correspond to the fusion of anhydrous lithium perchlorate at about 247°.[2] The sequence IIIA (exotherm)–IVA (endotherm)–VA (exotherm) extends from approximately 480 to 555°, whereas the sole decomposition break IIIB (exotherm) extends from about 480 to about 560°. Endotherms VIA and IVB coincide with the melting point of the reaction product, lithium chloride, at about 615°.

Figure 2 shows the corresponding DTA curves for potassium perchlorate. Endothermal breaks IA and IB are attributable to a reversible crystallographic transition in the solid potassium perchlorate at 300°.[4,11] The decomposition sequence IIA (fusion endotherm)–IIIA (exotherm)–IVA (endotherm)–IV′A (exotherm) extends from about 595 to about 685°, and the sequence IIB (fusion endotherm)–IIIB (exotherm) covers approximately the same tempera-

(9) J. P. Simmons and C. D. L. Ropp, *J. Am. Chem. Soc.*, **50**, 1650 (1928).
(10) R. F. Muraca and L. L. Taylor, Progress Report No. 20-347, Jet Propulsion Laboratory, California Institute of Technology, Pasadena, Jan. 17, 1958.
(11) D. Vorlaender and E. Kaascht, *Ber.*, **56**, 1157 (1923).

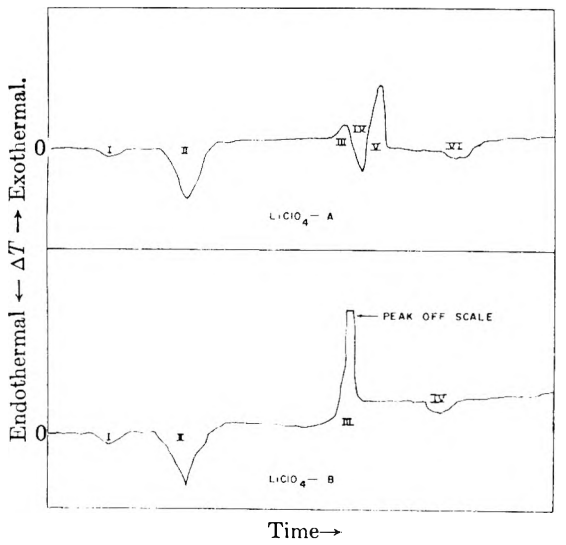

Fig. 1.—Thermograms of anhydrous lithium perchlorate: A, open furnace; B, closed furnace.

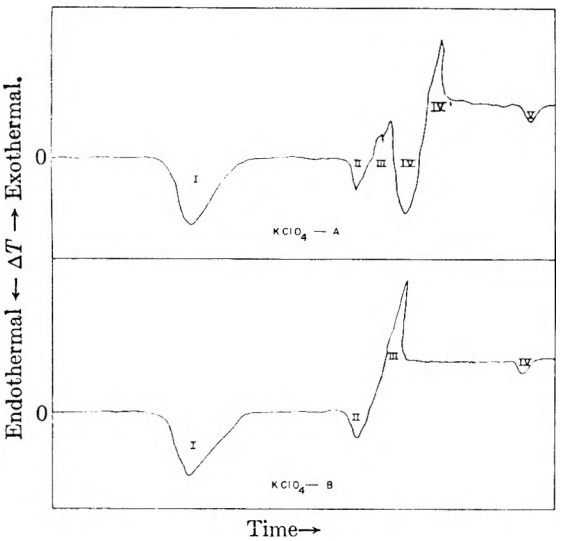

Fig. 2.—Thermograms of potassium perchlorate: A, open furnace; B, closed furnace.

ture span. The endotherms VA and IVB correspond to fusion of potassium chloride at about 776°.

The DTA patterns for rubidium perchlorate are quite similar to those obtained for potassium perchlorate under like furnace conditions and will not be discussed at length here. Again, the important difference between traces A and B in the case of rubidium perchlorate is the extension of the initial exotherm (see IIIA, $KClO_4$ in the decomposition region with the exclusion of the endotherm (see IVA, $KClO_4$) so that the decomposition sequence as in the instance of potassium perchlorate in set-up B is given by IIB (fusion endotherm)–IIIB (exotherm). It is to be anticipated that similar sets of results will be obtained for sodium and cesium perchlorates.

Discussion

The primary difference in the thermograms obtained from set-up B as compared to those from set-up A is in the absence of the endotherm preceding the steep exotherm in the decomposition region. In the cases of potassium and rubidium perchlorates, a small endotherm corresponding to the fusion of a mixture of the perchlorate salt and the decomposition products appears. Thus, for these salts fusion and decomposition are concomitant processes. Lithium perchlorate, however, melts at 247°, a temperature appreciably below the onset of rapid decomposition.[2,3]

Visual observation of the events occurring in the open furnace correlated with the movement of the recorder pen, afforded an explanation for the divergence in results with those from the closed furnace. As the perchlorate salt decomposes in the open furnace, the melt boils vigorously and bubbles up the side of the test-tube. This brings about recession of the sample from the thermocouple resulting in a cooling of the bead, and an endothermal break. This break may be erroneously attributed to the decomposition of the salt.[4] The final exotherm occurs when the metal chloride crystallizes from the melt and solidifies along the length of the glass thermocouple enclosure. The effect is seen in Fig. 3 which is a photograph of sample test-tubes after a DTA run. The decomposition product is seen to be distributed along the length of the test-tube with only a small amount remaining in contact with the thermocouple junction. It is evident that there are large temperature gradients along the length of the test-tube inasmuch as each run was conducted beyond the melting point of the chloride end product. This would also account for the variable appearance of the chloride fusion endotherm,[1,4] as well as for the small size of the DTA break.

In the closed furnace, however, no appreciable cooling of the thermocouple bead can occur because recession of the sample from the bead brings about contact of the hot furnace atmosphere with the thermocouple junction. This essentially results in a regime under which there is little or no cooling effect by the atmosphere on the thermocouple. Thus, the exotherm for lithium perchlorate (Fig. 1, IIIA) which is so seriously distorted appears to be the only thermal effect accompanying decomposition of this salt (see Fig. 1, IIIB).

Quantitative studies have shown molten lithium perchlorate to decompose to lithium chloride and oxygen with the formation of minor amounts of lithium chlorate (about 1 weight %) as a reaction intermediate.[12] Depending on the extent of decomposition and the temperature, the decomposing melt may be a homogeneous solution of perchlorate and chloride or a mixture of molten lithium perchlorate–lithium chloride saturated solution and suspended lithium chloride solid. There are thus two reactions to be considered, *viz.*, (a) $LiClO_4$ (solution) → LiCl (solution) + $2O_2$ (gas), and (b) $LiClO_4$ (solution) → LiCl (solid) + $2O_2$ (gas). Neglecting heat capacity effects, approximate values for the enthalpy changes for reactions (a) and (b) were calculated. The heat of formation of anhydrous lithium perchlorate was taken as −91.7 kcal./mole,[13] the heat of fusion of anhydrous lithium perchlorate of 3.8 kcal./mole was computed by application of the Clapeyron–Clausius equation[14] to the melting point data for the systems $LiClO_4$–$LiNO_3$,[2] $LiClO_4$–$KClO_4$[15] and $LiClO_4$–$NaClO_4$,[15]

(12) M. M. Markowitz and D. A. Boryta, unpublished results.

(13) M. M. Markowitz, R. F. Harris and H. Stewart, Jr., THIS JOURNAL, **63**, 1325 (1959).

(14) W. C. McCrone, Jr., "Fusion Methods in Chemical Microscopy," Interscience Publishers, Inc., New York, N. Y., 1957, pp. 156–157.

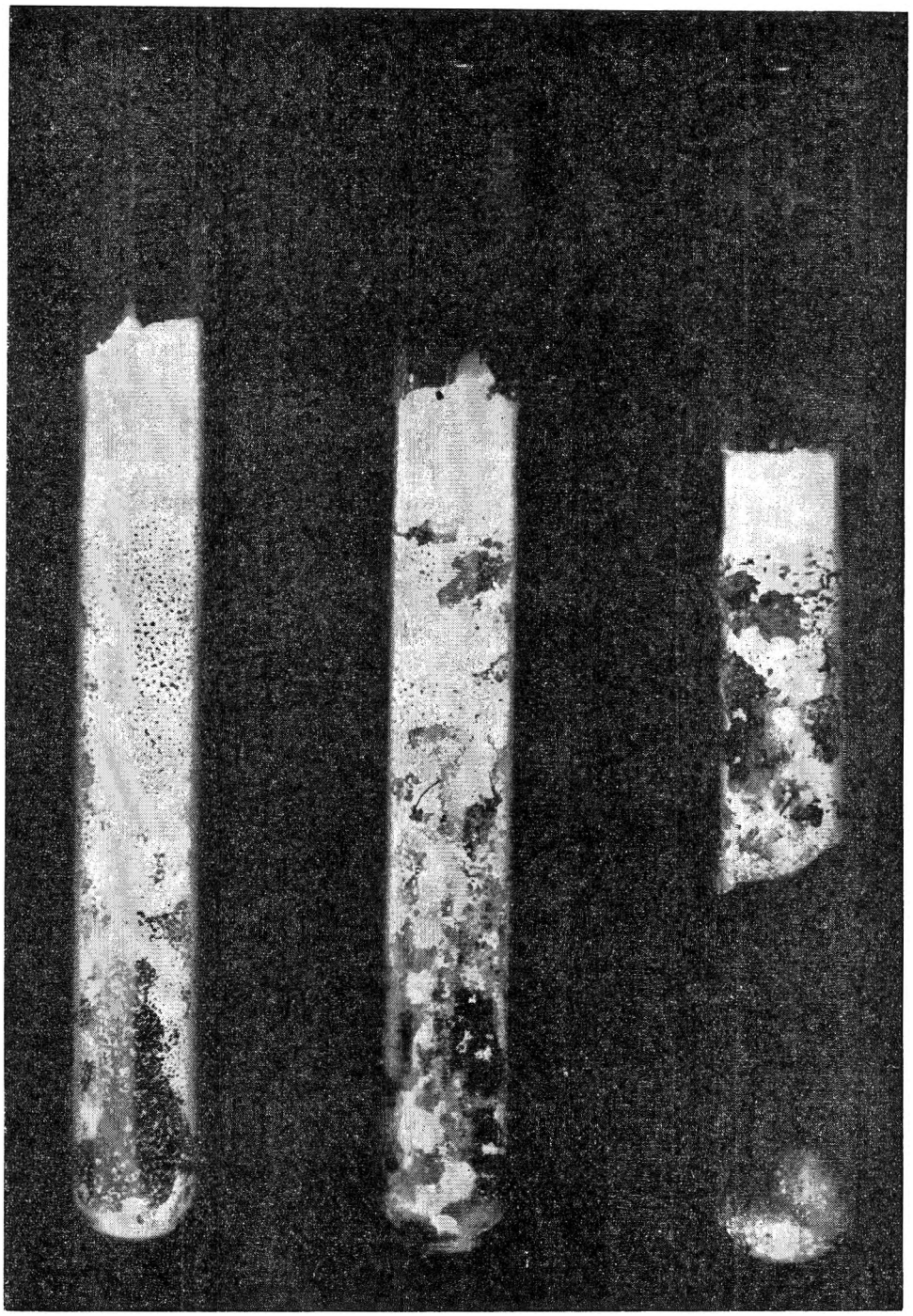

Fig. 3.—Sample test-tube after a DTA run in the open furnace assembly from left to right: LiCl, KCl, RbCl decomposition residues.

and the heats of fusion and of formation of lithium chloride were taken as 4.7 and −97.7 kcal./mole, respectively.[17] Reactions (a) and (b) were thus found to be exothermic to the extent of about 5.1 and 9.8 kcal./mole, respectively. These enthalpy values are consistent with the appearance during DTA of a single large exothermic break for the decomposition of lithium perchlorate (Fig. 1, IIIB).

A DTA constant temperature experiment performed in the open furnace indicated the cause of endotherm IVA in Fig. 1 for lithium perchlorate. The block of set-up A, the empty sample tube, the alumina reference, and the thermocouples were all put in place and kept at 480° prior to addition of the lithium perchlorate. The salt was then added to the sample tube and a differential trace was taken. Preliminary studies had indicated that the thermal decomposition of lithium perchlorate is

(15) M. M. Markowitz, R. F. Harris and D. A. Boryta, unpublished results.

(16) M. M. Markowitz and R. F. Harris, unpublished results.

(17) National Bureau of Standards Report No. 6297, U. S. Department of Commerce, Washington, D. C., Jan. 1, 1959, pp. 31, 72.

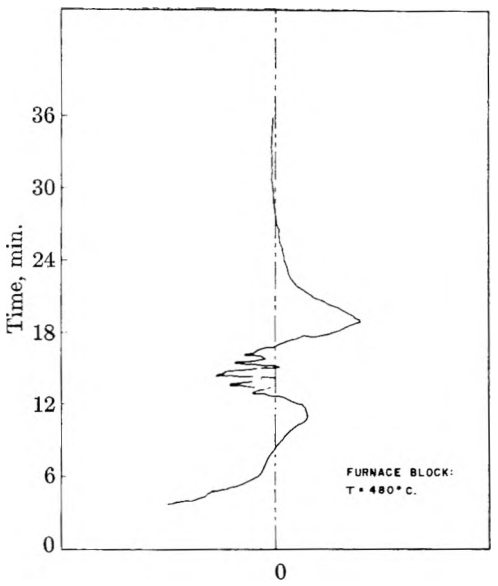

Fig. 4.—Constant temperature thermogram (480°) of anhydrous lithium perchlorate in the open furnace

autocatalyzed by the lithium chloride product. Thus, it was possible to secure a complete rapid decomposition of the perchlorate salt once the initially slow decomposition produced sufficient lithium chloride. The resulting trace is shown in Fig. 4. All the features of the dynamic DTA curve in the decomposition region (see Fig. 1, A) obtained in the open furnace are seen except that the endotherm in Fig. 4, which would correspond to the area IVA in Fig. 1, A has a saw-tooth appearance. Visual observations showed that as the bubbling melt rose in the tube, the initial exotherm (Fig. 4) reversed in direction and turned into an endotherm. The periodic rise and fall of the decomposing melt coincided with the periodic oscillations of the pen. The large exotherm occurred after the lithium chloride precipitation had become appreciable and decreased the turbulence in the partially solidified melt.

The thermal decomposition of potassium perchlorate becomes rapid only after fusion of the material.[1,18] As in the case of lithium perchlorate, two decomposition reactions are applicable, *viz.*, (a) $KClO_4$ (solution) → KCl (solution) + $2O_2$ (gas), and (b) $KClO_4$ (solution) → KCl (solid) + $2O_2$ (gas). The nature of the thermal effect accompanying reaction (a) is very difficult to determine by DTA. This is probably due to the relatively small heat effect involved in the decomposition which has been computed to be about 0.8 to 1.7 kcal./mole endothermic.[1] Reaction (a) may be masked by the concomitant occurrence of the exothermic reaction (b) for which an enthalpy change of −(4.4 to 5.3) kcal./mole was calculated. The net result of the DTA run is a single, large exothermic break attributable to over-all decomposition.

As a result of this study, it appears that the following points are worthy of consideration: (a) the use of an open furnace in DTA studies of highly turbulent condensed phase-gas reactions gives spurious results because of sample recession from the thermocouple sensor leading to thermocouple-atmosphere interactions, (b) use of an open furnace is permissible for the study of completely condensed phase reactions, *e.g.*, crystalline transitions, melting phenomena, solid phase reactions, etc., (c) quantitative information may not be obtainable from highly turbulent condensed phase-gas reactions using the open furnace technique, and probably in the closed furnace as well, because of the heat transients due to sample–thermocouple–atmosphere interactions, and (d) open furnace decomposition studies reported in the literature should be reviewed in the light of the present investigation.

(18) A. E. Harvey, Jr., M. T. Edmison, E. D. Jones, R. A. Seybert and K. A. Catto, *J. Am. Chem. Soc.*, **76**, 3270 (1954).

ELECTRONIC SPECTRA OF ADSORBED MOLECULES: STABLE CARBONIUM IONS ON SILICA ALUMINA

BY HARRY P. LEFTIN[1]

Mellon Institute, Pittsburgh 13, Pennsylvania

Received May 13, 1960

A novel method for the measurement of the electronic absorption spectra of adsorbed molecules is described. The electronic spectra of triphenylmethane and of 1,1-diphenylethylene adsorbed on silica gel and on a silica–alumina catalyst are presented. While on silica gel the spectra are identical to those of the parent hydrocarbons (indicating physical adsorption), on silica–alumina the spectra are those of the corresponding carbonium ions formed by reaction of the hydrocarbons with the active (acidic) centers of the catalyst, (chemisorption). It is shown that on these acid sites carbonium ions can be formed either by addition to an olefinic bond or by the rupture of a tertiary aliphatic carbon hydrogen bond.

Introduction

The demonstration of surface acidity of cracking catalysts[2] in conjunction with product distribution[3] and isotope exchange studies[4] has led workers[3,2a,5] to suggest reaction mechanisms which differ in detail but most of which assume an initial chemisorption

(1) The M. W. Kellogg Company, Jersey City, New Jersey.

(2) (a) C. L. Thomas, *Ind. Eng. Chem.*, **41**, 2564 (1949); (b) M. W. Tamele, *Disc. Faraday Soc.*, **8**, 2701 (1950); (c) A. G. Oblad, T. H. Milliken, Jr., and G. A. Mills, in "Advances in Catalysis," W. G. Frankenburg, Ed., Academic Press, Inc., New York, N. Y., 1951, Vol. 3, pp. 199–247.

(3) B. S. Greensfelder, H. H. Voge and G. M. Good, *Ind. Eng. Chem.*, **41**, 2573 (1949).

(4) (a) G. Parravano, E. F. Hammel and H. S. Taylor, *J. Am. Chem. Soc.*, **70**, 2269 (1948); (b) For a recent review, see H. H. Voge, in "Catalysis," P. H. Emmett, Ed., Reinhold Publ. Corp., New York, N. Y., 1958, Vol. 6, pp. 435–439.

process leading to the formation of adsorbed carbonium ions. Although, carbonium ion formation has been demonstrated for the chemisorption of an olefin,[6] there is no direct evidence for this process in the case of paraffin chemisorption. Moreover, while the uncertainty concerning the chemisorption of paraffins on silica–alumina[7] has very recently been resolved in favor of a small amount of chemisorption[8] in the case of isobutane, the identity of the chemisorbed species remains unknown. Since chemisorption is generally considered to be a necessary prerequisite for heterogeneous catalysis,[9] it is of interest to inquire into the structure and properties of chemisorbed molecules. Detailed knowledge within this area would be of prime importance to any discussion of catalytic reaction mechanisms.

Studies of the infrared spectra of adsorbed molecules have already provided insight into the molecular transformations associated with adsorption.[10] In the visible and ultraviolet regions, however, owing to the difficulty in preparing suitably transparent samples, few results of catalytic significance have been reported. Early work in this field, which employed either slurry, reflection or evaporated film techniques, has been summarized.[11]

The purpose of the present paper is to describe a simple and practical technique for the measurement of the electronic spectra of adsorbed molecules and to show from the data obtained, that carbonium ions are formed by the chemisorption of paraffinic and olefinic hydrocarbons on an active silica–alumina catalyst.

Experimental

Catalysts.—Silica–alumina catalyst (DSA-1) was prepared by the neutral hydrolysis of an alcoholic solution of aluminum isopropoxide (Eastman, Technical grade, twice redistilled) and ethylorthosilicate (Carbide and Carbon Co., pure grade). The hydrolysis was carried out in a sealed container at 100°. Large pieces of the resultant gel were heated in air to 600° over an 8 hour period and then calcined at this temperature for an additional 22 hours. The finished catalyst (88% SiO_2 and 12% Al_2O_3) which was in the form of large semi-transparent chunks had a B.E.T. surface area of 278 m.²/g. Emission analysis indicated only the following impurities, in p.p.m.

Ba, <1; Fe, 10–20; Ca, 4; Mg, 3; Na, 4; Ti, 4; and V, 9

The catalytic activity per unit surface area of DSA-1 was found to be 30% greater than that of a commercial silica–alumina catalyst for the cracking of 2,3-dimethylbutane at 525°.[12]

A pure silica gel sample was prepared by the hydrolysis of ethylorthosilicate. After calcination at 600° the adsorbent was in the form of glassy chunks and had a B.E.T. surface area of 550 m²/g.

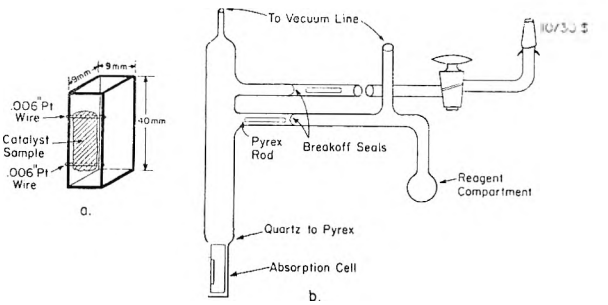

Fig. 1.—Apparatus for spectral measurements of adsorbed molecules: a, sample holder; b, vacuum cell.

Reagents.—The reagents used in this work were commercial samples which were further purified by conventional methods until constant infrared, ultraviolet and proton n.m.r. spectra were obtained. These spectra showed no bands due to impurities and, wherever comparison was possible, were in good agreement with reported data.

Eastman White Label triphenylmethane after 4 recrystallizations from 95% ethanol had m.p. 93.2–94.2°, lit. 91–93°.[13]

Aldrich Chemical Co., 1,1-diphenylethylene was redistilled under reduced pressure and dried over calcium hydride; $n^{20}D$ 1.6088, lit.[14] $n^{20}D$ 1.6087.

Procedure.—All spectra were measured with a Beckmann recording spectrophotometer, model DK-1. A light tight box was fitted over the detector and cell compartment in order to accommodate the cells used in this work. Catalyst samples for optical measurements were prepared in the form of thin platelets (0.5 ± 0.2 mm. thick) by grinding on emery cloth. These platelets were mounted on the vertical uprights of rectangular quartz cages with 6 mil platinum wire as shown in Fig. 1a. The cages fit snugly into commercial fused silica absorption cells having a 1 cm. path length. Mounted samples were cleaned and regenerated between runs by calcination in a stream of dried oxygen at 500° for 16 to 24 hours. They were then placed in the optical cells, (Fig. 1b), sealed directly to a vacuum system, evacuated for 1 hour at 500°, and further calcined *in situ* with oxygen at 500° for 24 hours. After final evacuation for 24 hours at 500° (to $\sim 10^{-6}$ mm.) the cells were sealed-off under vacuum.

For each catalyst sample studied, a closely matched sample was identically pretreated in a separate cell. This was used as a blank in the reference beam in order to compensate for the light scattering of the catalyst samples so that the full absorbance range of the spectrophotometer could be utilized. By selecting pairs of closely matched samples, it was possible to make adequate corrections for background absorbance. Since, however, exact compensation would require tedious matching of fragile samples, it was more convenient to measure background curves prior to chemisorption. These curves were used to correct the observed spectra so that the resulting curves represent the absorbance due only to the adsorbed species.

Weighed samples of the adsorbates were introduced into the reagent compartment of the optical cell which was then sealed to the vacuum system, evacuated for at least 4 hours, and sealed under vacuum. After recording the background curve, the catalyst sample was exposed to the hydrocarbon vapors by rupturing a break-off membrane. Due to the low vapor pressures of these hydrocarbons, it was often advantageous to thermostat the entire cell at 100°. Therefore, in order to avoid contamination of the catalyst by constituents of the stopcock lubricant, the stopcock shown in Fig. 1a was not joined to the second side arm of the cell until the chemisorption process was completed and an initial spectrum measured. This stopcock could be used to admit more volatile gases such as H_2O and NH_3 into the system.

As a precaution against contamination of the catalyst samples by residual hydrocarbons from previous experiments the optical cells were cleaned between runs in a heated sulfuric acid–nitric acid bath.

(5) (a) T. H. Milliken, Jr., G. A. Mills and A. G. Oblad, *Disc. Faraday Soc.*, **8**, 279 (1950); (b) J. D. Danforth, Preprints of General Papers, *Div. of Pet. Chem.*, ACS September 1956, Vol. 1, p. 15; (c) For a recent review of this subject, see ref. 4b.

(6) A. G. Evans, *Disc. Faraday Soc.*, **8**, 302 (1950).

(7) R. C. Zabor and P. H. Emmett, *J. Am. Chem. Soc.*, **73**, 5639, (1951).

(8) D. S. MacIver, P. H. Emmett and H. S. Frank, THIS JOURNAL, **62**, 935 (1958).

(9) K. J. Laidler, in "Catalysis," P. H. Emmett, Ed., Reinhold Publ. Corp., New York, 1954, Vol. 1, Ch. 3.

(10) R. P. Eischens and W. A. Pliskin, in "Advances in Catalysis," W. G. Frankenburg, ed., Academic Press, Inc., New York, N. Y., Vol. 10, pp. 1–56.

(11) M. Robin and K. N. Trueblood, *J. Am. Chem. Soc.*, **79**, 5138 (1957).

(12) W. K. Hall, H. P. Weber and D. S. MacIver, *Ind. Eng. Chem.*, **52**, 421 (1960).

(13) A. G. Brook and H. Gilman, *J. Org. Chem.*, **18**, 447 (1953).

(14) K. T. Serijan and P. H. Wise, *J. Am. Chem. Soc.*, **74**, 4766 (1951).

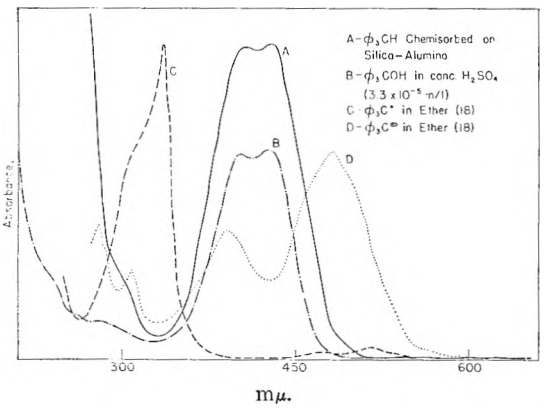

Fig. 2.—Absorption spectra.

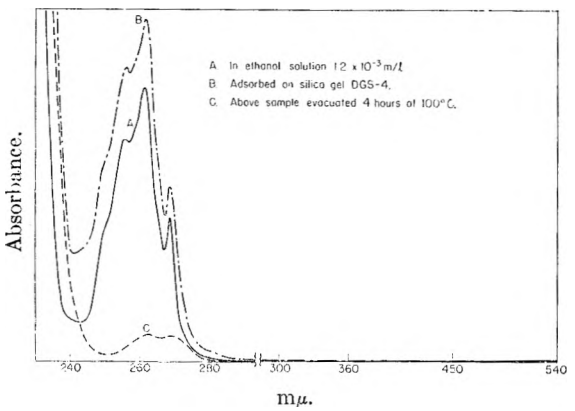

Fig. 3.—Absorption spectra of triphenylmethane.

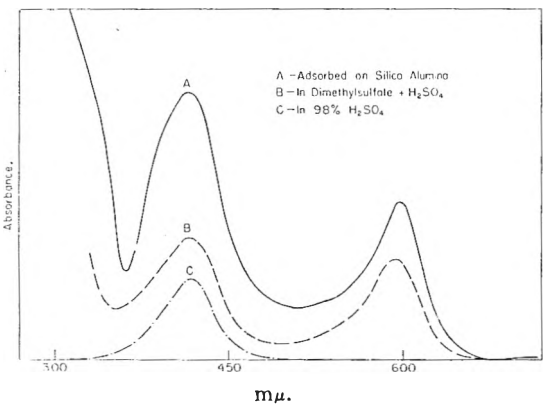

Fig. 4.—Absorption spectra of 1,1-diphenylethylene.

Results

Chemisorption of Paraffins.—Alkyl carbonium ions formed on the surface during a catalytic reaction rapidly decompose according to the usual Whitmore[15] type transformations which are permitted by their structural features. Once these transformations have occurred, the products are desorbed and, hence, it is not surprising that alkyl carbonium ions have never been isolated or identified on catalyst surfaces. Since the structural features of the triphenylcarbonium ion prohibit rapid decomposition, it is sufficiently stable to permit its identification under suitable circumstances. Thus, the triphenylcarbonium ion in solution is well known. Its existence as a stable species has been amply demonstrated by cryoscopic measurements in sulfuric acid solutions of triphenylcarbinol[16] and by conductivity measurements in liquid sulfur dioxide solutions of the corresponding halides.[17] The spectrum of the ion is also well established[18] and is characterized by a double peaked absorption band in the 404 to 432 mμ region. Curve B of Fig. 2 is a redetermination of this spectrum obtained from a solution of triphenylcarbinol in concentrated sulfuric acid. Curve A is the spectrum obtained when triphenylmethane is adsorbed on DSA-1 at 50°. Comparison of these two curves provides convincing evidence for the existence of the triphenylcarbonium ion on the surface. Also shown in Fig. 2 are the curves for the triphenylmethyl radical (curve C) as observed by Anderson[19] in an ether solution of hexaphenylethane and for the triphenylmethide ion[19] (curve D). Comparison with these curves demonstrates that neither the carbanion nor the free radical are formed in the process of chemisorption.

That the observed spectrum was the result of a chemical reaction between the hydrocarbon and the catalytically active acidic centers of the silica-alumina surface (chemisorption), and not due to a spectral shift caused by perturbations of the electronic states of the parent hydrocarbon molecule upon adsorption, can be demonstrated from the data given in Fig. 3. Here it is evident that the spectrum of silica gel exposed to triphenylmethane vapor for 1000 hours at 100° (curve B) is identical with the spectrum (curve A) of an alcoholic solution of this hydrocarbon. Thus, on the non-acidic or weakly acidic surface of silica gel, the triphenylcarbonium ion is not formed. The close agreement of these spectra suggests that on silica gel the triphenylmethane is physically adsorbed. This is further evidenced by the marked loss of spectral intensity after evacuation at 100° for 4 hours (curve C). In contrast, in the case of silica alumina where the hydrocarbon is chemisorbed as the carbonium ion, no decrease in absorbance was noted even after evacuation at 275° for 48 hours. These data are believed to constitute the first direct demonstration of the formation of carbonium ions as a consequence of the chemisorption of a "tertiary" hydrocarbon on the surface of a silica-alumina catalyst by a reaction involving the rupture of an aliphatic C-H bond.

Chemisorption of Olefins.—Carbonium ion formation by the addition of a proton or Lewis acid to an olefinic bond is well known. It is expected, therefore, that carbonium ions should be formed as a result of the chemisorption of olefins on acid catalysts such as silica-alumina, and if the olefin employed is conjugated with one or more phenyl substituents, the surface carbonium ion should easily be detected from its characteristic spectrum.

(15) (a) F. C. Whitmore, *J. Am. Chem. Soc.*, **54**, 3274 (1932); (b) *Chem. Eng. News*, **26**, 668 (1948).

(16) L. P. Hammett and A. Deyrup, *J. Am. Chem. Soc.*, **55**, 1900 (1933).

(17) (a) P. Walden, *Ber.*, **35**, 2018 (1902); (b) M. Gomberg, *ibid.*, **35**, 2403 (1902); (c) N. N. Lichtin and H. P. Leftin, THIS JOURNAL, **60**, 164 (1956).

(18) (a) A. Hantzsch, *Z. physik. Chem.*, **61**, 257 (1908); (b) G. Branch and H. Walba, *J. Am. Chem. Soc.*, **76**, 1564 (1954).

(19) L. C. Anderson, *ibid.*, **57**, 1673 (1935).

When 1,1-diphenylethylene is chemisorbed on the surface of a silica–alumina catalyst, an absorption spectrum (Fig. 4) composed of two principal bands in the visible region is obtained. One of these, the band at 423 mμ ($\epsilon = 3 \times 10^4$), can be assigned to the methyldiphenylcarbonium ion, formed by proton addition to the double bond. The existence of this species has been adequately demonstrated by cryoscopic measurements on solutions of the olefin and the corresponding carbinol in concentrated sulfuric acid.[20] The spectrum of this ion has been determined[21] and its structure has recently been verified from the proton n.m.r. spectrum of a solution of the olefin in concentrated sulfuric acid.[22] The other absorption band occurs at 600 mμ and is of uncertain origin.

In Fig. 4, it is demonstrated that these same two bands can be developed in solutions of this olefin in dimethyl sulfate +5% concentrated H_2SO_4, but that only the band corresponding to the carbonium ion (423 mμ) appears in concentrated H_2SO_4 solutions. It has previously been noted[23,24] that both bands appear in sulfuric acid–acetic acid mixtures.

Discussion

On the basis of these results, the over-all course of the reaction involved in the chemisorption of triphenylmethane must be

$$(C_6H_5)_3CH \xrightarrow{\text{silica–alumina}} (C_6H_5)_3C^+ + H^-$$

where clearly the hydrocarbon molecule has lost a hydride ion to form the observed tertiary carbonium ion. The fate of the hydride ion and the role of the catalyst in this process is discussed elsewhere.[25] That the carbonium ion does not form a covalent carbon-to-surface bond, as had been suggested previously,[4a] is indicated by the fact that such bonding would destroy the resonance system responsible for the stability and characteristic spectrum of this ion. The carbonium ions must, therefore, be held in the vicinity of the surface by coulombic forces and may be considered to constitute the positively charged half of an electrical double layer. In this state, they may be free to rotate and may also be free to migrate over limited regions of the surface. Recent n.m.r data,[26] tend to support this view.

In the case of olefin chemisorption, the mode of carbonium ion formation cannot be defined on the basis of the present spectral data. This is due to the fact that closely similar spectra would be expected from the addition of either a Lewis acid or a proton to the double bond of 1,1-diphenylethylene, since the spectrum of the resulting carbonium ion, namely, $(C_6H_5)_2\overset{+}{C}-CH_2Y$, would be only slightly influenced by the nature of the substituent on the β carbon atom. In accord with this reasoning is the observation[27] that the spectra of the protonated forms of 1,1-diphenylethylene, triphenylethylene and anthracene are closely similar.

It is of interest to note, however, that while a carbonium ion formed by proton transfer from a Bronsted acid site would be free of the surface (as in the case of the triphenylcarbonium ion), an ion formed by interaction with a catalyst Lewis acid would be bonded to the surface.

Evans[6] reported that a broad absorption band in the 430 mμ region appeared when a solution of 1,1-diphenylethylene was added to a suspension of activated floridin clay. This result is in agreement with the present work insofar as formation of the methyldiphenylcarbonium ion is concerned. The long wave length absorption[28] (λ 600 mμ) was not observed by Evans; however, it has been independently reported by Webb.[29] On the basis of a suggestion of Evans, *et al.*,[23] Webb has attributed this absorption band to a π-complex formed between the olefin and a hydrated Lewis acid center on the catalyst surface. The nature of the species responsible for the 600 mμ band will be discussed elsewhere; however, it may be stated, our recent data[30] suggest a quite different interpretation.

The results presented in this paper are in agreement with the hypothesis that a carbonium ion mechanism is involved in catalytic cracking and related processes.

Acknowledgment.—This work was sponsored by the Gulf Research & Development Company as a part of the research program of the Multiple Fellowship on Petroleum.

(20) V. Gold, B. W. V. Hawes and F. L. Tye, *J. Chem. Soc.*, 2167 (1952).

(21) A. G. Evans, *J. Appl. Chem.*, **1**, 240 (1951).

(22) D. E. O'Reilly and H. P. Leftin, unpublished results.

(23) A. G. Evans, P. M. S. Jones and J. H. Thomas, *J. Chem. Soc.*, 104 (1957).

(24) Lavrushin, *Zhur. Obshchei Khim.*, **26**, 2697 (1954).

(25) H. P. Leftin and W. K. Hall, Proceedings of 2nd International Congress on Catalysis, Paris, France, July 1960.

(26) D. E. O'Reilly, H. P. Leftin and W. K. Hall, to be published.

(27) V. Gold and F. L. Tye, *J. Chem. Soc.*, 2172 (1952).

(28) H. P. Leftin and W. K. Hall, Abstracts of Papers, 134th National Meeting, ACS, Chicago, Illinois, September 1958, p. 94-P.

(29) A. N. Webb, 135th National Meeting ACS, Boston, Massachusetts, April 1959, Petroleum Preprints, p. C-171.

(30) H. P. Leftin and W. K. Hall, THIS JOURNAL, **64**, 382 (1960).

THE TORTUOSITY FACTOR OF A WATER-SWOLLEN MEMBRANE

BY D. MACKAY

The Chemistry Department, Old Aberdeen, Scotland

Received May 13, 1960

In order to diffuse through a membrane swollen with water any water-soluble molecular or ionic species must follow a tortuous path of length greater than the membrane thickness. The ratio of the average path length to the geometrical membrane thickness is the tortuosity factor k. The ratio of the diffusion coefficient of a species in water to its value in the membrane can give a measure of the tortuosity factor for that particular ion or molecule. In addition to the increased path length two other important factors which may affect the diffusion of a species in the membrane are: (a) steric or sieve effects, if the diffusing particle is comparable in size with the resin mesh; and (b) electrostatic drag between charged species diffusing through the membrane and fixed charges, of opposite sign, on the membrane matrix.

Therefore if the tortuosity factor determination is to take into account all pathways across the membrane the molecular species used should be small and uncharged, and should distribute itself uniformly throughout the membrane. A suitable substance is heavy water.

An earlier attempt by Mackie and Meares[1] to use ethyl alcohol as test substance was unsuccessful, because the alcohol was concentrated close to the membrane matrix. A more recent attempt by Schlogl and Stein[2,3] to determine the tortuosity factor of a cation exchange membrane by measuring self diffusion of ions in steady and non-steady states was invalid. These authors pointed out that tortuosity factors for uncharged molecules, gegenions and nebenions may all differ appreciably if the membrane is heterogeneous on the submicroscopic scale, and suggested that such differences might be used as a rough measure of microheterogeneity.

In diffusion studies with heavy water it is advisable to use only small concentration differences, since it has been shown by Adamson and Irani[4] that the apparent diffusion coefficient of heavy water in water varies markedly with the heavy water content. If the experiments are performed under steady-state conditions the method is further simplified. Denoting the concentrations of heavy water in the external solutions, in moles cm.$^{-3}$, by C^i and C^0, the total flux of heavy water through 1 cm.^{2} of membrane in moles sec.$^{-1}$, is

$$J = \frac{(1 - v_R)D_R (C^i - C^0)}{\delta} \qquad (1)$$

Here v_R is the volume fraction of matrix and D_R the apparent diffusion coefficient of heavy water in the water in the membrane, while δ is the thickness of the water-swollen membrane in cm.

(1) J. S. Mackie and P. Meares, *Disc. Faraday Soc.*, **21**, 111 (1956).
(2) R. Schlogl and B. Stein, *Z. Electrochem.*, **62**, 340 (1958).
(3) R. Schlogl and B. Stein, *ibid.*, **63**, 341 (1959).
(4) A. W. Adamson and I. Irani, *J. chim. phys.*, **55**, 107 (1958).

Apparatus and Technique.—The diffusion apparatus and experimental technique were similar to those described by Mackie and Meares,[5] as modified by Mackay and Meares.[6] The Zeo-Karb 315 (phenolsulfonic acid–formaldehyde) membrane was supplied by Permutit Ltd. Experiments were carried out with the membrane in the sodium and in the hydrogen form. Distilled water was flowed through one half-cell while through the other flowed distilled water containing an accurately known concentration (3–5%) of heavy water. In a third experiment 0.1 N hydrochloric acid and 0.1 N hydrochloric acid containing a known amount of heavy water were used as influents.

The experiments were performed at 16° and were continued for 6–8 hr. at low flow rates (50–80 ml. hr.$^{-1}$). The difference in heavy water content between the solutions entering and leaving the half cells was determined by measuring the infrared absorption in a calcium fluoride cell at 3.98 μ, according to the method of Gaunt.[7] The absorption of the unknown solution was always compared and bracketed with that of solutions of known composition. The maximum error in these analyses was ±5%.

Results and Discussion

The results of the experiments are recorded in Table I. Using the value 1.93×10^{-5} cm.^{2} sec.$^{-1}$ for the diffusion coefficient of heavy water in dilute aqueous solution at 16°, obtained from the data of Wang and co-workers,[8] the tortuosity factors obtained are close to 1.8.

TABLE I

TORTUOSITY FACTORS FROM DIFFUSION OF HEAVY WATER ACROSS A ZEO-KARB 315 MEMBRANE, AT 16°

Solvent	Membrane form	$D_R \times 10^{-5}$, cm.^{2} sec.$^{-1}$	k
H_2O	Na	1.08	1.79
H_2O	H	1.06	1.82
0.1 N HCl	H	1.12	1.72

The agreement between the tortuosity factors for heavy water in the sodium and hydrogen forms of the membrane was unexpected. With the membrane in the sodium form there is little tendency for D^+ ions to be formed in the membrane or solution, so that diffusion of heavy water across the membrane is by migration of HDO and D_2O molecules, as in aqueous solution. With the resin in the hydrogen form, however, a portion of the deuterium may be present as D^+ ions and could presumably diffuse across the membrane as such. The apparently lower value of k for heavy water in 0.1 N hydrochloric acid may be due to migration of D^+ ions. It would therefore seem inadvisable to measure the tortuosity factor of an ion-exchange membrane in the hydrogen form by this method.

The values of k obtained may be compared with that calculated from the theoretical equation of Mackie and Meares,[9] which relates the tortuosity

(5) J. S. Mackie and P. Meares, *Proc. Roy. Soc.* (*London*), **A232**, 510 (1955).
(6) D. Mackay and P. Meares, *Kolloid Z.*, **161**, 31 (1959).
(7) J. Gaunt, *Analyst*, **79**, 580 (1954).
(8) J. H. Wang, C. V. Robinson and I. S. Edelman, *J. Am. Chem. Soc.*, **75**, 466 (1953).
(9) J. S. Mackie and P. Meares, *Proc. Roy. Soc.* (*London*), **A232**, 498 (1955).

factor to the volume fraction of matrix in the resin

$$k_{\text{theor}} = \left(\frac{1 + v_R}{1 - v_R}\right)^2 \qquad (2)$$

For the membrane used here v_R was 0.168, so that k_{theor} was 1.96, in fair agreement with that observed.

The self-diffusion of sodium and chloride ions in a Zeo-Karb 315 membrane has been studied by Meares,[10] who compared his observed diffusion coefficients with those calculated using equation 2. Interpreting his results in terms of tortuosity factors, the observed value of k was 7% less than calculated for chloride ions, and also for sodium ions when the membrane was in contact with concentrated solutions. Under such conditions sorption of electrolyte by the membrane was probably sufficient to screen the electrostatic drag between gegen and fixed ions.

In the derivation of equation 2 the diffusing particles were assumed to be of dimensions equal to the resin monomer units, whereas heavy water molecules and the hydrated ions discussed here are considerably smaller. It has been suggested by Kitchener and Lagos[11] that the tortuosity factor for small diffusing species may be less than for larger molecules. This might account for the fact that the observed k values are about 8% less than those calculated.

Acknowledgment.—The author wishes to thank Dr. D. C. McKean, The Chemistry Dept., Old Aberdeen, for his advice on the infrared absorption measurements, and Dr. P. Meares of the same department for advice and encouragement.

(10) P. Meares, *J. chim. phys.*, **55**, 276 (1958).

(11) J. A. Kitchener and Lagos, *Trans. Faraday Soc.*, **56**, 1245 (1960).

KINETICS OF THE REACTIONS OF SODIUM CYANIDE WITH SOME ALKYL IODIDES

BY K. R. LYNN AND PETER E. YANKWICH

Noyes Laboratory of Chemistry, University of Illinois, Urbana, Illinois

Received May 14, 1960

The kinetics of the reactions between cyanide ions and methyl, ethyl and *n*-propyl iodides were studied between 11 and 43° in 50% aqueous ethanol; with methyl iodide the measurements were repeated for water solvent in the temperature range 11–58°. The reactions are kinetically of the first order with respect to either reagent. Observed differences in entropies of activation agree with the explanations for medium effects proposed by Hughes and Ingold and with the symmetry change arguments of Crowell and Hammett.

Introduction

Kinetic studies on the reactions in solution of simple alkyl iodides with cyanide ions are numerous but fragmentary,[1-3] except for an investigation of the cyanization of methyl iodide in water.[4] Such reactions as these, now well recognized as bimolecular nucleophilic substitutions,[5] seemed to us to be suitable for the study of carbon isotope fractionation in the formation of carbon–carbon bonds. As a desirable preliminary to such investigations, we have studied the kinetics of reactions between cyanide ions and methyl iodide (in water and aqueous ethanol), and ethyl and *n*-propyl iodides (in aqueous ethanol only), over 30 to 40° ranges of temperature.

Experimental

Reagents.—The alkyl iodide samples used were center cuts distilled from Eastman "White Label Grade" reagents the sodium cyanide was Fisher "Certified" reagent, and was used without further purification. Solvent water was deionized by passage through a mixed-bed resin ion exchanger. The solvent referred to below as "50% ethanol" was prepared by diluting with an equal volume of purified water U. S. Industrial Chemical Co.'s absolute ethanol. Reagents of analytical grade were employed in the analyses of reaction mixtures.

Kinetic Runs.—The solutions of cyanide and iodides ranged in concentration from 0.05 to 0.15 *M*. Five-ml. aliquots of freshly prepared reagent solutions were pipetted into Pyrex tubes which were sealed rapidly (flame sealing for water runs, tubes with ground glass stoppers being employed for aqueous ethanol runs) and immersed in the constant (±0.1°) temperature bath.[6] At pre-selected times reaction tubes were removed from the bath, the reaction quenched by their immersion in ice–water mixture, and samples prepared for analysis.

Analyses.—Both iodide ion production and cyanide ion consumption were measured, the former by titration with iodate,[7] the latter by titration with silver ion.

Results

In Table I are collected the results for the reaction of cyanide ion with methyl iodide in the two solvents. Four to ten kinetics runs were made at various concentration ratios at each temperature. The rate of reaction is strictly first order with respect to each reagent, and no deviation from overall second-order kinetics could be detected in runs which were allowed to proceed to as much as 70% reaction. It is important to note that the specific rate constants based on iodide ion production and cyanide ion disappearance are the same within the

(1) A. Lieben and A. Rossi, *Ann. Chim.*, **159**, 58 (1871).

(2) R. A. Ogg, *Trans. Faraday Soc.*, **31**, 1385 (1935).

(3) M. F. Hawthorne, G. S. Hammond and B. M. Graybill, *J. Am. Chem. Soc.*, **77**, 486 (1955).

(4) B. W. Marshall and E. A. Moelwyn-Hughes, *J. Chem. Soc.*, 2640 (1959).

(5) See, for example, C. K. Ingold, "Structure and Mechanism in Organic Chemistry," Cornell University Press, Ithaca, N. Y., 1953.

(6) At the final concentrations used and over the temperature ranges of the experiments, no appreciable error attributable to reaction during warm-up of the vessels and their contents was expected nor was any observed.

(7) Cyanide does not interfere nor is there during the analysis detectable hydrolysis of either the alkyl iodide or the cyanide ion.

experimental scatter of replicate determinations of either kind; the same conclusion obtains for the experiments on ethyl iodide and *n*-propyl iodide (*vide infra*).

TABLE I

SPECIFIC RATE CONSTANTS FOR THE REACTION BETWEEN CYANIDE ION AND METHYL IODIDE

t, °C.	(k_2 ± av. devn., l. mole^{-1} sec.$^{-1}$) × 10^4 from estimation of CN^-	from estimation of I^-	Av.
	A. Solvent: water		
11.4	1.08 ± 0.11		
19.5	3.04 ± 0.26		
31.0		10.5 ± 0.3	
45.8	40.3 ± 0.8		
58.3	137.1 ± 6.9		
	B. Solvent: 50% aqueous ethanol		
11.4	4.95 ± 0.05	4.89 ± 0.14	4.91 ± 0.14
31.0	38.4 ± 0.3	37.1 ± 0.4	37.8 ± 0.3
43.0	129.2 ± 5.6	125.5 ± 5.5	127.4 ± 5.7

The results obtained for the reaction of cyanide ion with ethyl and *n*-propyl iodides are summarized in Table II. The Arrhenius and Eyring equation parameters are collected in Table III.

TABLE II

SPECIFIC RATE CONSTANTS FOR THE REACTION BETWEEN CYANIDE ION AND ETHYL AND *n*-PROPYL IODIDES IN 50% AQUEOUS ETHANOL

t, °C.	(k_2 ± av. devn. l. mole^{-1} sec.$^{-1}$) × 10^4 from estimation of CN^-	from estimation of I^-	Av.
	A. Ethyl iodide		
11.4	1.12 ± 0.09	1.22 ± 0.09	1.17 ± 0.09
31.0	8.62 ± 0.28	9.13 ± .15	8.94 ± 0.26
43.2	50.4 ± 6.2	48.4 ± .8	49.2 ± 3.3
	B. *n*-Propyl iodide		
11.4	0.91 ± 0.06	0.91 ± 0.06	0.91 ± 0.06
31.0	7.10 ± 0.48	6.70 ± 0.35	6.90 ± 0.42
43.2	27.9 ± 2.4	27.9 ± 2.4	27.9 ± 2.4

TABLE III

PARAMETERS OF THE ARRHENIUS AND EYRING EQUATIONS FOR REACTION OF CYANIDE ION WITH ALKYL IODIDES

Iodide	Solvent	log A[8]	E_{exp}, kcal. mole^{-1}	$\Delta H^{\pm}$, kcal. mole^{-1}	$\Delta S^{\pm}_{298}$, e.u.
CH_3	W	10.8	19.2	18.6	−11.1
CH_3	Aq. EtOH	11.5	19.4	18.8	−7.5
C_2H_5	Aq. EtOH	11.7	20.4	19.8	−6.9
n-C_3H_7	Aq. EtOH	11.2	19.9	19.3	−9.3

Discussion

The values recorded in Table III are in general correspondence with activation parameters reported for similar ion–molecule reactions,[9−11] and in good agreement with the Arrhenius parameters reported recently by Marshall and Moelwyn-Hughes[12] for the methyl iodide cyanization in aqueous solution.

For methyl iodide cyanization the difference of about 3.5 e.u. in the entropies of activation in the two solvent systems is in the direction and of the magnitude which would be expected for a simple dielectric effect.[13,14] For a cyanide ion radius of 1.05 Å.,[15,16] and using values for the dielectric constants of water–ethanol mixtures interpolated from the data of Akerlof,[17] the effects of solvent on k_2, attributed solely to variation in the entropy of activation, correspond to a radius for the activated complex of approximately 4 Å., which seems quite reasonable.

Acknowledgment.—This research was supported by the U. S. Atomic Energy Commission.

(8) Estimates of imprecision: log A, ±0.3; E_{exp} and $\Delta H^{\pm}$, ± 0.3 kcal. mole^{-1}; $\Delta S^{\pm}_{298}$, ±0.8 e.u.

(9) T. I. Crowell and L. P. Hammett, *J. Am. Chem. Soc.*, **70**, 3444 (1948).

(10) P. M. Dunbar and L. P. Hammett, *ibid.*, **72**, 109 (1950).

(11) J. Hine and W. H. Brader, Jr., *ibid.*, **75**, 3964 (1953).

(12) R. W. Marshall and E. A. Moelwyn-Hughes, *J. Chem. Soc.*, 2640 (1959).

(13) K. J. Laidler and H. Eyring, *Ann. N. Y. Acad. Sci.*, **39**, 303 (1940).

(14) E. D. Hughes and C. K. Ingold, *J. Chem. Soc.*, 244 (1935).

(15) J. M. Bijvoet and J. A. Lely, *Rec. trav. chim.*, **59**, 908 (1940).

(16) G. J. Verweel and J. M. Bijvoet, *Z. Krist.*, **100**, 201 (1938).

(17) G. Akerlof, *J. Am. Chem. Soc.*, 54, 4125 (1932).

THE PREPARATION OF FINE POWDER HEXAGONAL Fe_2C AND ITS COERCIVE FORCE

BY W. D. JOHNSTON, R. R. HEIKES AND J. PETROLO

Westinghouse Research Laboratories, Pittsburgh 35, Pennsylvania

Received May 16, 1960

The relatively rare hexagonal form of Fe_2C has been prepared in fine powder form by the reaction of a gaseous mixture of H_2 and CO with Raney iron at 240°. The occurrence of the hexagonal form appears to require the exclusion of Fe_3O_4. If Fe_3O_4 is present, the carbide is found in the more common Hägg form. The coercive force of the fine powder hexagonal Fe_2C prepared by this method is approximately 800 oe.

Introduction

The compound Fe_2C is known to exist in two crystalline forms. The more common form is referred to as the Hägg carbide which may be indexed on either hexagonal or orthorhombic axes. The formula for this carbide has been given as both Fe_2C and $Fe_{20}C_9$.[1] The other form is relatively rare and is a distinctly different hexagonal structure in which the iron atoms are believed to be arranged in hexagonal close packing.[2] This form is referred to as the hexagonal carbide. The conditions for

(1) K. H. Jack, *Proc. Roy. Soc. (London)*, **A195**, 56 (1948).

(2) L. J. E. Hofer, E. M. Cohn and W. C. Peebles, *J. Am. Chem. Soc.*, **71**, 189 (1949).

formation of the hexagonal carbide are quite obscure. It has been suggested that iron catalysts containing copper,[2] or iron catalysts promoted by a mixture of K_2O and Al_2O_3[3] or partial carbiding[3] result in the hexagonal form. It has also been shown that the hexagonal form transforms appreciably to the Hägg form at temperatures in excess of 300°.[3,4]

Little magnetic data are available for these materials. Hofer *et al.*[2,4,5] have given 247 and 350–380° as the Curie points for the Hägg and hexagonal forms respectively. Hofer[5] also gives data from which the average values of the saturation magnetization per gram of compound, σ, may be calculated. These values are 145 for hexagonal Fe_2C 130 for Hägg Fe_2C and 139 for cementite Fe_3C. Since both forms of Fe_2C are crystallographically uniaxial, it is probable that they have high values of the magnetocrystalline anisotropy constant K. Since coercive force is directly proportional to K by the relationship ${}_IH_c = 0.96\ K/\sigma d$ where ${}_IH_c$ is the coercive force and d is the density, a large value of coercive force might be expected for single domain spherical particles. Although the values of K for these materials are unknown, it is possible to get some feeling for the magnitude of coercive force that might be expected if one uses the reported value K_{ac} for Fe_3C (1.18×10^6 ergs/cm.^{3})[6]. The value obtained for ${}_IH_c$ using this approximation is of the order of 1000 to 1200 oe for the various iron carbides.

Since the iron carbides are thermally unstable materials they cannot be prepared by methods which involve elevated temperatures. Further, for the production of the fine particle materials (~200 Å. diameter) which might yield high values of coercive force, temperature must be kept to a minimum.

Hofer, Cohn and Peebles[2] have studied Fe_2C in connection with catalysis in the Fisher Tropsch synthesis. In this work they developed a method for preparing both Fe_2C and Fe_3C. Their preparations can be described in terms of the reactions.[2,4,5,7]

$$2Fe + 2CO \xrightarrow{240^\circ} Fe_2C + CO_2$$
$$Fe_2C + Fe \longrightarrow Fe_3C$$

In preparing Fe_3C Cohn and Hofer interrupted the first reaction at 2/3 completion where Fe and Fe_2C were present in equal amounts. They then annealed this mixture *in vacuo* and allowed the second reaction to take place.

The preparation of Fe_2C has also been described by Emmett[3] whose interest was also in catalysis. Emmett preferred to carburize iron-containing catalysts with a hydrocarbon such as propane. He states that with a hydrocarbon there is no oxidation of the product, no exotherm in the carburization reaction (as has been noted for a CO carburization) and no free carbon precipitated.

Preparation Techniques.—At the outset of this work attempts were made to obtain Fe_2C in ultrafine particles by applying the methods of either Hofer and Cohn or Emmett. In order that ultrafine Fe_2C would result, the iron starting material necessarily had to be ultrafine, ~200 A. Fine iron prepared by the Raney process was used in this work. The preparation and magnetic properties of this material have been described previously.[8]

Initial carburization experiments involved the handling of the pyrophoric iron powder in a nitrogen-filled dry box. This procedure was subsequently abandoned since it was difficult to ensure that the dry box remained free of traces of oxygen. Instead of using a glove box it was possible to transfer Raney Fe to the Pyrex carburization vessel through a ground joint by pipetting the iron powder under pyridine. This transfer technique prevents oxidation of the pyrophoric iron powder by the air. The use of pyridine as a protective agent for Raney iron has been previously described.[8] The pyridine could be quantitatively removed from the iron by continuous evacuation first at room temperature and finally at 100°. (The grease used in the two stopcocks and the ground joint of this apparatus was Dow Corning high vacuum silicone grease which interacted only slightly with pyridine vapor.) By this technique the carburization vessel could be brought to constant weight in order to determine the weight of the iron sample (generally 2–4 g.). At the end of the carburization run a second weighing permitted the carbon uptake to be calculated. Carbiding gases were passed over the iron sample contained in an enlarged part of the vessel which was contained in a well-regulated furnace. A thermocouple placed in the well of the carburization vessel permitted the sample temperature to be measured during the course of a run. Products could be removed from the carburization vessel at the end of a run by evacuating the vessel and then introducing a protective cover of pyridine by way of a separatory funnel which was connected to the vessel by one of the stopcocks. In this way, contact with the air was completely eliminated and the sample could be easily transferred by pipetting as previously described. Before carburization all gas lines were evacuated and then flushed with the appropriate gases to prevent any possibility of oxidation of the sample.

Instrument-grade propane gas purified over hot copper gave little or no carbide formation at temperatures of 240–275° and for times as long as 9 hours in contrast to the findings of Emmett[3] which suggests that an oxide supported iron catalyst may be considerably more reactive than bulk Raney iron. Purified CO gave carbide formation but the products were always contaminated with Fe_3O_4. (Both tank CO and CO formed from CO_2 and graphite at 1200° were used. These gases were purified by passing through Ascarite and magnesium perchlorate.) Finally, pure samples of Fe_2C were prepared by carbiding at 240° with a stream of CO and hydrogen in which the ratio CO/H_2 varied from 1/3 to 6/1. (A mixture of H_2 and CO has previously been used by Trillat and Oketoni[9] and Michel and Bernier[10] for the preparation of cementite from iron at temperatures in excess of 500°.) Little or no oxide was found in the X-ray patterns of the Fe_2C products. In addition more carbon was taken up by the iron when hydrogen was used in addition to CO. In this case however a side reaction also occurred yielding small amounts of a yellow liquid. This liquid has not been investigated but it is probably either a mixture of hydrocarbons or iron carbonyl.

Results

In Fig. 1 are graphed data obtained by carbiding with $CO + H_2$. The carbon uptake indicated as x in Fe_2C_x, was determined from the weight gain of the sample. Values of 1.0 and 0.9 in the x parameter correspond to the two formulas proposed, Fe_2C and $Fe_{20}C_9$.[1] Invariably the carbiding reaction proceeded rapidly at first accompanied by a 40–60° exotherm and then proceeded more slowly to complete carburization in about 6 hours as indicated on the graph. X-Ray diffraction patterns obtained on these materials provided qualitative confirmation of the weight gain data. In samples no. 15 and 16

(3) H. H. Podgurski, J. T. Kummer, T. W. DeWitt and P. H. Emmett, *J. Am. Chem. Soc.*, **72**, 5382 (1950).
(4) E. M. Cohn and L. J. E. Hofer, *ibid.*, **72**, 4662 (1950).
(5) L. J. E. Hofer and E. M. Cohn, *ibid.*, **81**, 1576 (1959).
(6) P. Blum and R. Pauthenet, *Compt. rend.*, **237**, 1501 (1953).
(7) L. J. E. Hofer and E. M. Cohn, *J. Chem. Phys.*, **18**, 766 (1950).
(8) W. D. Johnston, R. R. Heikes and J. Petrolo, *J. Am. Chem. Soc.* **79**, 5388 (1957).
(9) J. J. Trillat and S. Oketoni, *Comp. rend.*, **233**, 51 (1951).
(10) A. Michel and R. Bernier, *Rev. Met.*, **46**, 821 (1949).

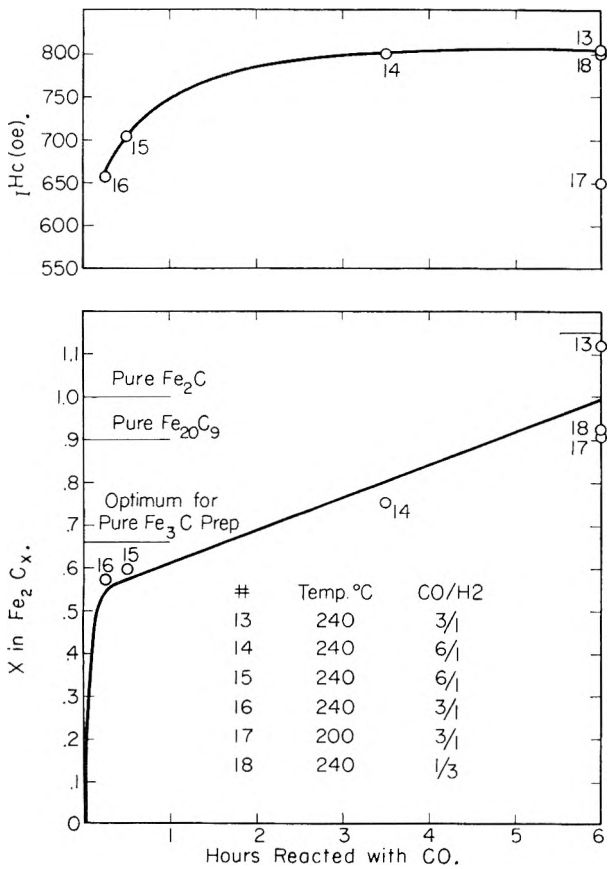

Fig. 1.—Carburization time *vs.* $_I$H$_c$ and carbon uptake.

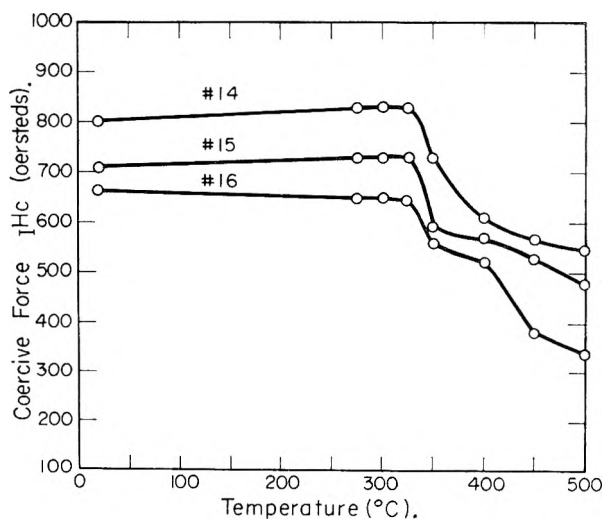

Fig. 2.—Temperature *vs.* coercive force; samples 14, 15, 16, of Fe + Fe_2 C. Each sample annealed for 0.5 hr. at each temperature indicated from 275 to 500°.

weak iron lines were visible in accord with the partial carbon uptake due to insufficient reaction time. In samples no. 13, 14 and 18 where the weight gains approached that for a complete reaction, only iron carbide lines appeared. Sample no. 18 is of particular interest since the CO/H_2 ratio used was $^1/_3$ instead of the usual $^6/_1$ or $^3/_1$. The satisfactory agreement of the data indicated that the CO/H_2 ratio was not critical. Sample No. 17 provided the only discrepancy between the weight gain data and the X-ray observations. This sample was carburized at 200° instead of the usual 240°. The weight uptake was high in this case but according to the X-ray pattern only partial carbide formation occurred. Thus we conclude that at 200° part of the weight gain of the sample was due to the deposition of gross amounts of either iron carbonyl or the formation of high molecular weight hydrocarbons and that a higher temperature is required for the formation of pure iron carbide.

It was surprising to find that the carbide was formed almost entirely in the relatively rare hexagonal form in the experiments where hydrogen was used with the carbon monoxide. In reactions where hydrogen was not added to prevent oxide contamination, the amount of the hexagonal form decreased and the more common Hägg form increased in amount. It thus appears that the predominant effect in the stabilization of the hexagonal carbide is the absence of Fe_3O_4, and it is conceivable that there may be little or no connection with the presence of copper or $Al_2O_3 + K_2O$.

The saturation magnetization of sample no. 13 was measured and found to be 127.5 c.g.s./g. at −78.5° and 122.4 c.g.s./g. at −18° which are somewhat lower than the 145 c.g.s./g. measured by Hofer[5] at 50°.

Figure 1 shows that the coercive force of these samples is relatively high indicating that fine particles have been obtained. The graph also shows that $_IH_c$ increases rapidly with carbide formation. The sample prepared at 200° has a relatively low value of $_IH_c$ as would be expected since as mentioned above the X-ray pattern indicates that only partial carbide formation occurred.

It should be pointed out that the values of $_IH_c$ for earlier samples, in which oxide contamination occurred, are much lower than those shown here. For eight earlier samples the values for $_IH_c$ range from 450–635. These data emphasize that for high purity samples hydrogen is required in the carbiding gas.

Vacuum annealing of partially carburized mixtures of Fe and Fe_2C successfully gave Fe_3C at 400°. This reaction has been observed to start at temperatures as low as 260°.[2,4,5,7] In order to note the change in $_IH_c$ as this reaction progressed, annealing experiments were performed on samples no. 14, 15 and 16 by measuring the coercive force of the specimens as a function of annealing time and temperature. These three samples were used since they spanned the optimum composition for the preparation of Fe_3C. In all cases the value of $_IH_c$ remained essentially constant to 325° and then dropped gradually as shown in Fig. 2. This may be due to a number of effects among which are particle growth or an unfavorable difference in either critical particle size or magnetocrystalline anisotropy between the two materials.

HEATS OF COMBUSTION AND FORMATION OF NAPHTHALENE, THE TWO METHYLNAPHTHALENES, *cis* AND *trans*-DECAHYDRONAPHTHALENE, AND RELATED COMPOUNDS[1]

BY DIMITRIOS M. SPEROS AND FREDERICK D. ROSSINI*

Chemical and Petroleum Research Laboratory, Carnegie Institute of Technology, Pittsburgh 13, Pennsylvania

Received May 18, 1960

Measurements were made of the heats of combustion of naphthalene (c), 1-methylnaphthalene (liq), 2-methylnaphthalene (c), *cis*-decahydronaphthalene (liq), and *trans*-decahydronaphthalene (liq), at 25°. With these and related other data, values were calculated for the standard heats of formation at 25° for naphthalene and 2-methylnaphthalene in the solid, liquid and gaseous states, for 1-methylnaphthalene and the *cis* and *trans* isomers of decahydronaphthalene in the liquid and gaseous states, and for the higher members of the series of 1-*n*-alkyl naphthalenes and 2-*n*-alkyl naphthalenes in both the liquid and gaseous states. Equations are also given for the standard heats of vaporization at 25° for the last two series of compounds. The relation between energy content and molecular structure is discussed.

I. Introduction

Lack of reliable data on the heats of formation of naphthalene, the two methylnaphthalenes, and the *cis*- and *trans*-decahydronaphthalenes has greatly hampered the making of reliable calculations of the thermodynamic properties of the important reactions in which these hydrocarbons take part. To evaluate the heats of formation, isomerization and hydrogenation, as appropriate, of these compounds, precise and accurate measurements of the heats of combustion are required. With such data available, the relation of energy content with structure can be studied for these molecules. The present investigation reports experimental data on the heats of combustion of naphthalene, 1-methylnaphthalene, 2-methylnaphthalene, *cis*-decahydronaphthalene and *trans*-decahydronaphthalene, and presents the results of the calculations made therefrom. In particular, it was possible to calculate values for the heats of combustion and formation of all the higher members of the normal alkyl series of 1-naphthalene and of 2-naphthalene,[2,3] in both the liquid and gaseous states.

II. Apparatus and Experimental Procedures

The experimental values of this investigation are based on the absolute joule as the unit of energy. Conversion to the defined thermochemical calorie is made using the relation 1 calorie = 4.184 (exactly) joules. For internal consistency with other investigations from this Laboratory, the molecular weight of carbon dioxide was taken as 44.010 g./mole.

In this investigation, the chemical and calorimetric apparatus and procedures were the same as described by Browne and Rossini.[4] The rise of temperature in each calorimetric experiment was near 2°, with the final temperature being near 30°, the temperature of the jacket of the calorimeter. The amount of reaction in each hydrocarbon combustion experiment was determined from the mass of carbon dioxide formed in the combustion as previously described.[4] The bomb had an internal volume of 380 ml. One ml. of water was placed in the bomb prior to each combustion experiment. The pressure of the oxygen for combustion was made 30 atmospheres (calculated to 25°).

The compounds measured in the present investigation were API Research hydrocarbons, made available through the API Research Project 44 from materials purified by the API Research Project 6. The samples had the following values of purity, in mole per cent.: naphthalene, 99.97 ± 0.03; 1-methylnaphthalene, 99.97 ± 0.03; 2-methylnaphthalene, 99.92 ± 0.06; *cis*-decahydronaphthalene, 99.93 ± 0.05; *trans*-decahydronaphthalene, 99.97 ± 0.03. Description of the purification and determination of the purity of these samples has already been given.[5,6] The impurities in these samples are similar to the parent substances, as a result of the methods of purification, and are believed to have an insignificant effect on the results.

The three hydrocarbons that were liquid at room temperature were enclosed in sealed thin-walled glass ampoules of appropriate volume, as previously described.[3,4] The 2-methylnaphthalene, with melting point near 34.6°, was similarly sealed in thin-walled glass ampoules using a special procedure of introducing the melted material in portions and letting the material in the ampoule solidify each time. The naphthalene, with melting point near 80.3°, was burned in the form of a solid, pressed pellet, unsealed. It was determined from measurements made in the balance case that the loss in weight of the unsealed naphthalene was small enough to be insignificant. In the latter case, the error arising from vaporization of the naphthalene in the bomb would be that due to the heat of sublimation of the vaporized naphthalene, the determination of the amount of reaction being unaffected.

III. Data of the Present Investigation

Table I gives the results on the determination of the energy of ignition. In these experiments, only the standard amount of fuse wire was burned in oxygen, using the same procedure and ignition apparatus as in regular combustion experiments.

The energy equivalent of the standard initial calorimeter system was determined from a series of six combustion experiments with NBS Standard benzoic acid, No. 39g, using the value 26,433.8 joules/g. mass for the heat of combustion of this sample under the conditions of the standard bomb process at 25°, with appropriate corrections for the differences between the actual and standard bomb processes. The results of these calibration experiments are given in Table II. The symbols are as previously defined.[4]

The results of the calorimetric combustion experiments for naphthalene, 1-methylnaphthalene, 2-methylnaphthalene, *cis*-decahydronaphthalene and *trans*-decahydronaphthalene are given in

* Department of Chemistry, University of Notre Dame, Notre Dame, Indiana.

(1) This investigation was supported in part by a grant from the National Science Foundation. Submitted in partial fulfillment of the requirements for the degree of Doctor of Philosophy in Chemistry at the Carnegie Institute of Technology.

(2) E. J. Prosen and F. D. Rossini, *J. Research Natl. Bur. Standards*, **34**, 263 (1945).

(3) Sr. M. C. Loeffler and F. D. Rossini, THIS JOURNAL, **64**, 1530 (1960).

(4) C. C. Browne and F. D. Rossini, *ibid.*, **64**, 927 (1960).

(5) A. J. Streiff, L. F. Soule, C. M. Kennedy, M. E. Janes, V. A. Sedlak, C. B. Willingham and F. D. Rossini, *J. Research Natl. Bur. Standards*, **45**, 173 (1950).

(6) A. J. Streiff, A. R. Hulme, P. A. Cowie, N. C. Krouskop and F. D. Rossini, *Anal. Chem.*, **27**, 44 (1955).

TABLE I

RESULTS ON THE DETERMINATION OF THE ENERGY OF IGNITION

Expt.	Mass of iron wire, g.	ΔR, ohm	Total energy of ignition, j.	Energy due to combustion of iron wire, j.	Energy due to electric current, j.	Dev. from the mean, j.
1	0.008190	0.000440	90.6	54.3	36.3	+0.63
2	.008080	.000429	88.4	53.6	34.8	−0.87
3	.008000	.000432	88.9	53.0	35.9	+0.24
				Mean value	35.7	
				Av. deviation		±0.6

TABLE II

RESULTS OF THE CALIBRATION EXPERIMENTS WITH BENZOIC ACID

No. of expt.	Range of mass of benzoic acid, g.	Range of k, min.$^{-1}$	Range of K, ohm	Range of U, ohm	Range of ΔR_c, ohm	Range of q_n, j.	Range of q_i, j.	Range of E_i, j./ohm	Mean and stand. dev. of the mean, j./ohm
6	1.52015 to 1.55320	0.001544 to 0.001610	0.000780 to 0.000913	0.000067 to 0.000266	0.195401 to 0.199643	13.9 to 17.3	89.0 to 90.2	206,127 to 206,160	206,142 ± 6

TABLE III

RESULTS OF THE COMBUSTION EXPERIMENTS

No. of expt.	Range of Mass of CO_2 formed, g.	Range of k, min.$^{-1}$	Range of K, ohm	Range of U, ohm	Range of ΔR_c, ohm	Range of Δr_i, ohm	Range of Δr_n, ohm	Range of B, ohm/g. CO_2	Mean and stand. dev. of the mean ohm/g. CO_2
					Naphthalene (c)				
6	3.31467 to 3.55938	0.001575 to 0.001607	0.000771 to 0.001083	0.000048 to 0.000176	0.188660 to 0.202686	0.000437 to 0.000141	0.000015 to 0.000024	0.0567830 to 0.0568398	0.0568155 ± 0.0000086
					1-Methylnaphthalene (liq)				
6	3.39429 to 3.48652	0.001562 to 0.001630	0.000734 to 0.001071	0.000048 to 0.000144	0.198129 to 0.203484	0.000439 to 0.000443	0.000020 to 0.000027	0.0581990 to 0.0582528	0.0582352 ± 0.0000082
					2-Methylnaphthalene (c)				
5	3.33895 to 3.57303	0.001577 to 0.001610	0.000626 to 0.000947	0.000080 to 0.000203	0.194489 to 0.200811	0.000437 to 0.000441	0.000023 to 0.000033	0.0580821 to 0.0581193	0.0581078 ± 0.0000068
					cis-Decahydronaphthalene (liq)				
6	2.85643 to 2.96221	0.001580 to 0.001608	0.000896 to 0.001588	0.000048 to 0.000112	0.198124 to 0.205475	0.000425 to 0.000443	0.000018 to 0.000044	0.0691824 to 0.0692173	0.0691993 ± 0.0000045
					trans-Decahydronaphthalene (liq)				
5	2.81739 to 2.97173	0.001580 to 0.001629	0.000674 to 0.001126	0.000016 to 0.000129	0.195091 to 0.205760	0.000437 to 0.000447	0.000006 to 0.000049	0.0690644 to 0.0690859	0.0690753 ± 0.0000045

TABLE IV

VALUES[a] OF THE STANDARD HEATS OF COMBUSTION FOR NAPHTHALENE, 1-METHYLNAPHTHALENE, 2-METHYLNAPHTHALENE, *cis*-DECAHYDRONAPHTHALENE AND *trans*-DECAHYDRONAPHTHALENE

Compound			B at 30°, ohms/g. CO_2	$-\Delta E_n$ at 30°, kj./mole	$-\Delta E^0$ at 30°, kj./mole	$-\Delta H^0$ at 30°, kj./mole	$-\Delta H^0$ at 25°	
Name	Formula	State					kj./mole	kcal./mole
Naphthalene	$C_{10}H_8$	c	0.0568155 ± 0.0000172	5154.00 ± 1.60	5151.13 ± 1.60	5156.17 ± 1.60	5156.95 ± 1.60	1232.54 ± 0.38
1-Methylnaphthalene	$C_{11}H_{10}$	liq.	0.0582352 ± 0.0000164	5811.07 ± 1.68	5808.11 ± 1.68	5814.42 ± 1.68	5815.42 ± 1.68	1389.59 ± 0.40
2-Methylnaphthalene	$C_{11}H_{10}$	c	0.0581078 ± 0.0000136	5798.36 ± 1.45	5795.40 ± 1.45	5801.71 ± 1.45	5802.71 ± 1.45	1386.88 ± 0.35
cis-Decahydronaphthalene	$C_{10}H_{18}$	liq.	0.0691993 ± 0.0000090	6277.40 ± 0.94	6275.14 ± 0.94	6286.48 ± 0.94	6288.23 ± 0.94	1502.92 ± 0.22
trans-Decahydronaphthalene	$C_{10}H_{18}$	liq.	0.0690753 ± 0.0000090	6266.25 ± 0.94	6263.89 ± 0.94	6275.23 ± 0.94	6276.98 ± 0.94	1500.23 ± 0.22

[a] The uncertainties given in this table are twice the standard deviation.

Table III. The symbols are as previously defined.[4]

The magnitude of the Washburn correction, to convert the value of ΔE for the bomb process of the present investigation to the value of ΔE^0 for the standard states, was calculated[3,4] to be as follows, in per cent.: naphthalene, −0.056; 1-methylnaphthalene or 2-methylnaphthalene, −0.051; *cis*-decahydronaphthalene or *trans*-decahydronaphthalene, −0.036.

In Table IV are presented the resulting values of the standard heats of combustion of the five compounds measured in the present investigation. The symbols have the same meaning as previously given.[3,4]

The values of the standard heats of combustion given in Table IV apply to the following reactions, respectively, with each substance in its standard state

$$C_{10}H_8\text{(c, naphthalene)} + 12O_2(g) = 10CO_2(g) + 4H_2O(liq) \quad (1)$$

$$C_{11}H_{10}\text{(liq, 1-methylnaphthalene)} + 13\tfrac{1}{2}O_2(g) = 11CO_2(g) + 5H_2O(liq) \quad (2)$$

$$C_{11}H_{10}\text{(c, 2-methylnaphthalene)} + 13\tfrac{1}{2}O_2(g) = 11CO_2(g) + 5H_2O(liq) \quad (3)$$

$$C_{10}H_{18}\text{(liq, \textit{cis}-decahydronaphthalene)} + 14\tfrac{1}{2}O_2(g) = 10CO_2(g) + 9H_2O(liq) \quad (4)$$

$C_{10}H_{18}$(liq, *trans*-decahydronaphthalene) + $14\frac{1}{2}O_2$(g) = $10CO_2$(g) + $9H_2O$(liq) (5)

IV. Results of Other Investigations

Relatively few data on heats of combustion are available for comparison with the data of the present investigation. Most of the uncertainty in the earlier investigations usually lies in the chemical part of the work, that is, in the purity of the compounds and in the accurate measurement of the amount of chemical reaction occurring in the experiment in which the heat is being measured.

Measurements made by investigators who used naphthalene as a calibrating substance, the value for which was certified for heat of combustion but *not* for purity, cannot be compared with the present measurements because it is known that the naphthalene so used was not only not certified as to purity but actually contained an appreciable amount of impurity. This impurity, however, did not affect significantly the usefulness of the sample as a calibrating substance.

Measurements on naphthalene were reported by Beckers,[7] Keffler,[8] and Matsui and Abe.[9] In each case, these investigators determined the amount of reaction from the mass of sample placed in the bomb. Their results, converted as well as can be done to the basis used in the present investigation, were as follows, for the standard heat of combustion of the solid at 25°, in kcal./mole: Beckers,[7] 1230.9; Keffler,[8] 1229.5; Matsui and Abe,[9] 1233.4. These are to be compared with the value from the present investigation, 1232.54 ± 0.38 kcal./mole.

No previous data on 1-methylnaphthalene are available.

Data on 2-methylnaphthalene were reported by Richardson and Parks,[10] who determined the amount of reaction from the mass of sample placed in the bomb, and reported for the standard heat of combustion of the solid at 25°, 1384.0 kcal./mole. This value is to be compared with the value 1386.88 ± 0.35 kcal./mole from the present investigation.

Measurements of the heats of combustion of the *cis* and *trans* isomers of decahydronaphthalene were reported by Roth and Lasse,[11] and Davies and Gilbert.[12] In each case, the amount of reaction was determined from the mass of sample placed in the bomb. Calculating from the values of freezing points reported,[5,12] the samples used by Davies and Gilbert had the following purity in mole %: *cis*-decahydronaphthalene, 99.68; *trans*-decahydronaphthalene, 97.88. Converting to the basis of the present investigation, the values of these earlier investigators for the standard heats of combustion at 25° of the *cis* and *trans* isomers of decahydronaphthalene in the liquid state are as follows, in kcal./mole: Roth and Lasse,[11] *cis*-isomer, 1501.4, *trans* isomer, 1499.8; Davies and Gilbert,[12] *cis* isomer, 1502.4, *trans* isomer, 1500.3. These values are to be compared with the following values from the present investigation: *cis* isomer, 1502.92 ± 0.22, *trans* isomer, 1500.23 ± 0.23. The heat of isomerization from the data of Davies and Gilbert[12] is 2.1 kcal./mole, which is to be compared with the value 2.69 kcal./mole from the present investigation.

V. Values of Heats of Formation

By appropriate combination with the values for the standard heats of formation of gaseous carbon dioxide and of liquid water at 25°,[13] the values of the standard heats of combustion for the five compounds measured in the present investigation, as given in the last column of Table IV, can be used to calculate the values of the standard heats of formation of the corresponding compounds in the same physical state, liquid or solid, as measured.

In the case of the two compounds which are solid at 25°, namely, naphthalene and 2-methylnaphthalene, values of the heats of fusion to the undercooled liquid at 25° were used to calculate values for the heat of formation of the undercooled liquid. The values of the heats of fusion at 25° used for this purpose were 4.27 ± 0.02 kcal./mole for naphthalene and 2.83 ± 0.01 kcal./mole for 2-methylnaphthalene. These values were calculated from the data of McCullough, *et al.*[14]

For the study of energy as related to the molecular structure of molecules, the values of heats of formation most useful are those for the gaseous state. To obtain the heat of formation of naphthalene in the gaseous state, there was combined with the heat of formation of solid naphthalene a value for its heat of sublimation at 25°. This latter was taken as 17.50 ± 0.25 kcal./mole.[15-17] For *cis*-decahydronaphthalene and *trans*-decahydronaphthalene, calculated values for the heats of vaporization at 25° were also available and were taken as 12.00 ± 0.50 and 11.60 ± 0.50 kcal./mole, respectively.[15-17] Similarly, calculated values for the heats of vaporization at 25° for 1-methylnaphthalene and 2-methylnaphthalene were available, being taken as 14.50 ± 0.50 and 14.20 ± 0.50 kcal./mole, respectively.[15-17]

Values for the standard heats of formation of the five compounds, in the different physical states as appropriate, are given in Table V.

From the values given in Table V, the following heats of isomerization at 25° may be readily calculated

1-methylnaphthalene (liq) = 2-methylnaphthylene (liq)
$\Delta H^0_{298.16} = 0.12 \pm 0.53$ kcal./mole (6)

1-methylnaphthalene (g) = 2-methylnaphthalene (g)
$\Delta H^0_{298.16} = -0.18 \pm 0.88$ kcal./mole (7)

(7) M. Beckers, *Bull. soc. chim. Belg.*, **40**, 518 (1931).

(8) L. Keffler, *J. chim. phys.*, **28**, 457 (1931).

(9) M. Matsui and T. Abe, *Bull. Tokyo Univ. Eng.*, **8**, 339 (1939); *Chem. Zentr.*, **I**, 804 (1941).

(10) J. W. Richardson and G. S. Parks, *J. Am. Chem. Soc.*, **61**, 3543 (1939).

(11) W. A. Roth and R. Lasse, *Ann.*, **441**, 52 (1925).

(12) G. F. Davies and E. C. Gilbert, *J. Am. Chem. Soc.*, **63**, 1585 (1941).

(13) F. D. Rossini, K. S. Pitzer, R. L. Arnett, R. M. Braun and G. C. Pimentel, "Selected Values of Physical and Thermodynamic Properties of Hydrocarbons and Related Compounds," API Research Project 44. Carnegie Press, Pittsburgh, Pennsylvania, 1953.

(14) J. P. McCullough H. L. Finke, J. F. Messerly, S. S. Todd, T. C. Kincheloe and G. Waddington, THIS JOURNAL, **61**, 1105 (1957).

(15) American Petroleum Institute Research Projects 6 and 44. Chemical and Petroleum Research Laboratory, Carnegie Institute of Technology, Pittsburgh, Pennsylvania. Private communication. Calculated values.

(16) T. Miyazawa and K. S. Pitzer, *J. Am. Chem. Soc.*, **80**, 60 (1958).

(17) D. L. Camin and F. D. Rossini, THIS JOURNAL, **60**, 1446 (1956).

TABLE V

VALUES OF THE STANDARD HEATS OF FORMATION

Compound			$\Delta Hf^0_{298.16}$
Name	Formula	State	kcal./mole
Naphthalene	$C_{10}H_8$	c	18.75 ± 0.38
		liq	23.02 ± .38
		g	36.25 ± .45
1-Methylnaphthalene	$C_{11}H_{10}$	liq	13.43 ± .40
		g	27.93 ± .64
2-Methylnaphthalene	$C_{11}H_{10}$	c	10.72 ± .35
		liq	13.55 ± .35
		g	27.75 ± .62
cis-Decahydronaphthalene	$C_{10}H_{18}$	liq	−52.45 ± .22
		g	−40.45 ± .55
trans-Decahydronaphthalene	$C_{10}H_{18}$	liq	−55.14 ± .22
		g	−43.54 ± .55

cis-decahydronaphthalene (liq) = *trans*-decahydronaphthalene(liq)

$$\Delta H^0_{298.16} = -2.69 \pm 0.31 \text{ kcal./mole} \quad (8)$$

cis-decahydronaphthalene (g) = *trans*-dehydronaphthalene (g)

$$\Delta H^0_{298.16} = -3.09 \pm 0.77 \text{ kcal./mole} \quad (9)$$

Similarly the following heats of hydrogenation at 25° may be calculated

naphthalene(g) = *cis*-decahydronaphthalene(g)

$$\Delta H^0_{298.16} = -76.70 \pm 0.71 \text{ kcal./mole} \quad (10)$$

naphthalene(g) = *trans*-decahydronaphthalene(g)

$$\Delta H^0_{298.16} = -79.79 \pm 0.71 \text{ kcal./mole} \quad (11)$$

naphthalene(liq) = *cis*-decahydronaphthalene(liq)

$$\Delta H^0_{298.16} = -75.47 \pm 0.44 \text{ kcal./mole} \quad (12)$$

naphthalene(liq) = *trans*-decahydronaphthalene(liq)

$$\Delta H^0_{298.16} = -78.16 \pm 0.44 \text{ kcal./mole} \quad (13)$$

With the values for the heats of formation at 25° given above for 1-methylnaphthalene and 2-methylnaphthalene, together with previously reported data, it is possible to calculate reliable values for the heats of formation for the entire series of the 1-*n*-alkyl naphthalenes and the 2-*n*-alkyl naphthalenes, in both the liquid and gaseous states. It has been shown that, within the limits of present-day measurements, there is a constant increment per CH_2 group in the standard heat of formation of the members of any normal alkyl series of hydrocarbons, beyond the first several members, for both the gaseous and liquid states.[2,3] At 25°, the increment per CH_2 group in the standard heat of formation is −6.106 kcal./mole for the liquid state and −4.926 kcal./mole for the gaseous state.[2]

It has been shown[18] that the increment per CH_2 group changes most markedly from constancy for the introduction of the first CH_2 group on the end group Y to start the normal alkyl chain, with the deviation from constancy being much less for the next substitution to make an ethyl group, and approaching constancy from then on. The proper increment to be added to 1-methylnaphthalene to form 1-ethylnaphthalene may be taken the same as between 1,2-dimethylbenzene and 1-methyl-2-ethylbenzene. Similarly, the proper increment to be added to 2-methylnaphthalene to form 2-ethylnaphthalene may be taken the same as between 1,3-dimethylbenzene and 1-methyl-3-ethylbenzene. The values for the dimethylbenzenes and the methylethylbenzenes are given in the tables of the API Research Project 44,[13] the values being based on the work of Johnson, Prosen and Rossini.[19] Proceeding in this way, one may obtain values for the standard heat of formation at 25° for both the liquid and gaseous states for 1-ethylnaphthalene and 2-ethylnaphthalene. For the values of the standard heat of formation at 25°, ΔHf^0, one obtains the following values for the liquid and gaseous states, respectively, in kcal./mole: 1-ethylnaphthalene, 8.17, 23.72; 2-ethylnaphthalene, 7.96, 23.17.

With the values for 1-ethylnaphthalene and 2-ethylnaphthalene thus obtained for both the liquid and gaseous states, the values for the standard heats of formation at 25° for the higher members of these series may be obtained by using the constant increments per CH_2 group,[2,3] −6.106 kcal./mole for the liquid state and −4.926 kcal./mole for the gaseous state. The following equations give the values for the standard heats of formation at 25° for the ethyl and higher *n*-alkyl members of these series

1-*n*-alkyl naphthalenes(liq):

$$\Delta Hf^0 = 20.38 - 6.106m \text{ kcal./mole } (m > 1) \quad (14)$$

1-*n*-naphthalenes(g):

$$\Delta Hf^0 = 33.57 - 4.926m \text{ kcal./mole } (m > 1) \quad (15)$$

2-*n*-alkyl naphthalenes(liq):

$$\Delta Hf^0 = 20.17 - 6.106m \text{ kcal./mole } (m > 1) \quad (16)$$

2-*n*-alkyl naphthalenes(g):

$$\Delta Hf^0 = 33.02 - 4.926m \text{ kcal./mole } (m > 1) \quad (17)$$

In the foregoing equations (and also following), m is the number of carbon atoms in the normal alkyl chain attached to the end group Y, as $Y-(CH_2)_m-H$, with Y being here naphthalene (less one hydrogen atom) and the point of attachment of the radical being in the 1- or 2-positions as indicated.

From the foregoing, one may write the following equations for the standard heat of vaporization, from the liquid to the gaseous state, at 25°, for the members of these series beginning with the ethyl members

1-*n*-alkyl naphthalenes:

$$\Delta Hv^0 = 13.19 + 1.18m \text{ kcal./mole } (m > 1) \quad (18)$$

2-*n*-alkyl naphthalenes:

$$\Delta Hv^0 = 12.85 + 1.18m \text{ kcal./mole } (m > 1) \quad (19)$$

VI. Discussion

In addition to providing base lines from which one may calculate the heats of formation, for both the liquid and gaseous states, for a great number of compounds that have not been, and may never be, measured experimentally, the data of the present investigation give quantitative information on the relation between energy content and molecular structure for these substances.

For the two isomers of methylnaphthalene, the present data indicate that, within the limits of uncertainty of the measurements, the two isomers have substantially the same energy, in both the liquid and the gaseous states, —the actual dif-

(18) E. J. Prosen, W. H. Johnson and F. D. Rossini, *J. Research Natl. Bur. Standards*, **37**, 51 (1946).

(19) W. H. Johnson, E. J. Prosen and F. D. Rossini, *ibid.*, **35**, 141 (1945).

ferences being, respectively, 0.12 ± 0.53, and −0.18 ± 0.88 kcal./mole at 25°.

With regard to the *cis* and *trans* isomers of decahydronaphthalene, the data indicate that, for the liquid state at 25°, the *trans* isomer is more stable (lesser energy content) with respect to energy than the *cis* isomer by 2.69 ± 0.31 kcal./mole. For the gaseous state, the difference increases slightly to 3.09 ± 0.77 kcal./mole. This value is in substantial accord with the theoretical calculations which have been made, involving the non-bonded skew interactions in these molecules, considering that the *cis* isomer is largely comprised of two "chair" forms of cyclohexane joined together (with loss of two carbon and four hydrogen atoms) in "*cis*" fashion and that the *trans* isomer is largely comprised of two "chair" forms of cyclohexane joined together in "*trans*" fashion.[19-25]

(20) K. S. Pitzer and C. W. Beckett, *J. Am. Chem. Soc.*, **69**, 977 (1947).

(21) C. W. Beckett, K. S. Pitzer and R. Spitzer, *ibid.*, **69**, 2488 (1947).

(22) R. B. Turner, *ibid.*, **74**, 2118 (1952).

(23) W. S. Johnson, *ibid.*, **75**, 1498 (1953).

(24) H. D. Orloff, *Chem. Revs.*, **54**, 347 (1954).

(25) W. G. Dauben, O. Rohr, A. Labbauf and F. D. Rossini, THIS JOURNAL, **64**, 283 (1960).

THE EFFECTS OF X-RAY AND GAMMA RAY IRRADIATION ON THE THERMAL[1] DECOMPOSITION OF AMMONIUM PERCHLORATE IN THE SOLID STATE

BY ELI S. FREEMAN, DAVID A. ANDERSON AND JOSEPH J. CAMPISI[2]

Pyrotechnics Chemical Research Laboratory, Picatinny Arsenal, Dover, New Jersey

Received May 18, 1960

The effect of exposure of ammonium perchlorate to X-ray and γ-ray radiation on its chemical reactivity with respect to thermal decomposition was investigated. The course of the reaction was followed by differential thermal analysis and by thermogravimetric experiments conducted under ambient and reduced pressures. Decomposition was also studied by microscopic observations. The data show that several stages of reaction are involved in the decomposition of ammonium perchlorate and that the low temperature stages are appreciably enhanced as a result of pre-irradiation. The relative importance of the various stages of reaction were found to be a function of the exposure dose. Although direct evidence is lacking it is suggested that the increased reactivity of the irradiated substance may be due to the presence of positive holes which would favor an electron transfer mechanism of decomposition. The effect of impurities such as Ag^+, Cu^{++} and I^- ions on decomposition seem to support the suggested mechanism. The decomposition pattern of samples exposed to γ-rays is similar to that of the X-ray irradiated ammonium perchlorate.

Introduction

Research concerning the effects of high energy radiation on ionic crystals has been principally concerned with physical changes and chemical reactions induced by radiation. There is little in the literature, however, concerned with the effects of pre-irradiation on the chemical reactivity of inorganic solids. This important aspect of the problem of radiation effects is considered in this paper with respect to the solid state thermal decomposition of ammonium perchlorate.

An indication that radiation affected the isothermal decomposition of NH_4ClO_4 was reported by Bircumshaw and Phillips,[3] who found that the induction period for reaction was reduced after exposure to ultraviolet light. Further preliminary evidence for increased chemical reactivity was reported by Freeman and Anderson,[4] who showed that the differential thermal analysis reaction spectrum of NH_4ClO_4 was altered after being irradiated with X-ray radiation. In the present work the effects of X-rays on the thermal decomposition of NH_4ClO_4 were more fully investigated and the effects of γ-ray irradiation were also probed.

(1) This paper was presented in part before the Division of Physical Chemistry at the Boston National Meeting of the ACS, April 1959.

(2) Explosives and Propellants Laboratory.

(3) L. L. Bircumshaw and R. R. Phillips, *J. Chem. Soc.*, **956**, 4741 (1957).

(4) E. F. Freeman and D. A. Anderson, THIS JOURNAL, **63**, 1344 (1959).

Decomposition was investigated at atmospheric and reduced pressures by differential thermal analysis (d.t.a.) and by recording changes in sample weight as temperature was continuously increased. By increasing sample temperature at a pre-determined rate, the transition from one stage of reaction to another may be observed continuously over the complete temperature range of reaction resulting in unique reaction spectra.

Experimental

Samples of ammonium perchlorate (Fisher Scientific Co., certified reagent grade) were irradiated with X-rays under a vacuum of 2 mm. in Pyrex tubes, 1.8 cm. diameter and 5 cm. long. The analysis given on the label is, Cl^-, 0.000%, $SO_4^=$, 0.003%; ClO_3, 0.000%, Fe, 0.0004% and heavy metals, 0.0002%. The principal radiation source was an OEG-50 X-ray tube with a molybdenum target, which was operated to give a dose rate of 2.1×10^5 roentgens/hour. Samples were also irradiated at the Brookhaven National Laboratory at a rate of 1.0×10^6 r./h. for $^1/_2$ and 24 hours using a cobalt-60 source. The exposure doses were determined by ferrous sulfate dosimetry.[5] The ferrous sulfate doses were converted to ammonium perchlorate doses by multiplying the dosimeter values by the ratio of electron densities of NH_4ClO_4 and the dosimeter. The radiation units are reported in e.v. absorbed/molec. D.t.a. experiments were conducted on 250-mg. samples heated at the nominal rate of 5°/min. in air and under a pressure of 1 mm. An equivalent amount of powdered alumina was used as the reference material. The apparatus was the same as that previously described[6] with the excep-

(5) H. G. Swope, "Dosimetry in the Argonne High-Level Gamma Irradiation Facility, ANL,"—5819, Jan. 1958.

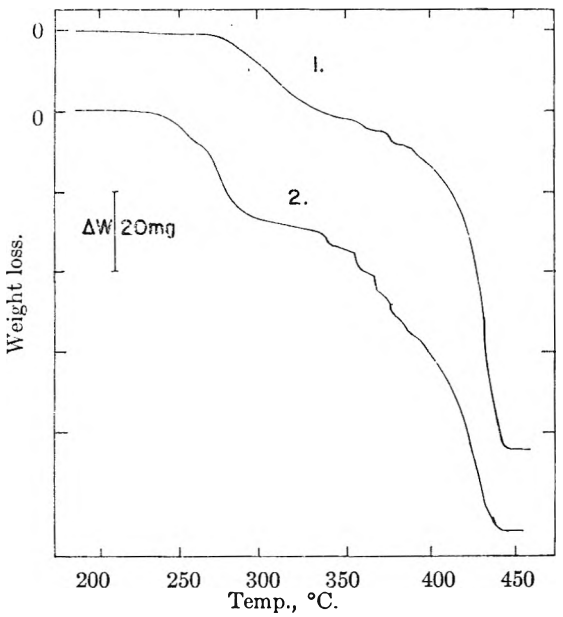

Fig. 1.—The decomposition of X-ray irradiated and non-irradiated ammonium perchlorate. Heating rate 5°/min., dose rate 1.4×10^{-3} e.v. absorbed molec.$^{-1}$ hr.$^{-1}$, total dose 0.14 e.v. absorbed/molec., reaction carried out in air at atm. pressure, sample wt. 100 mg. Weight change *vs.* temperature: 1, non-irradiated NH_4ClO_4; 2, X-ray irradiated NH_4ClO_4.

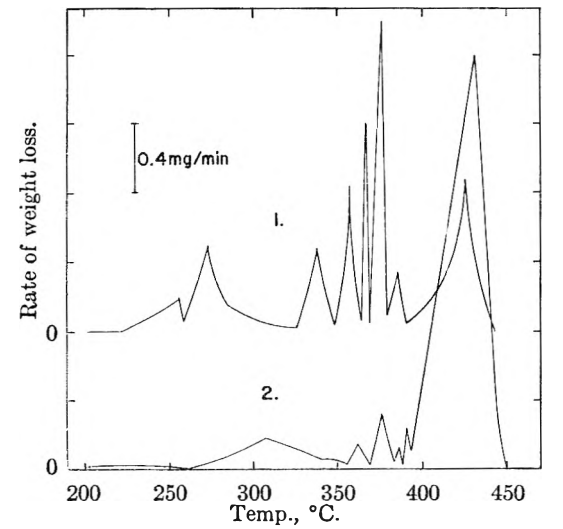

Fig. 2.—The rate of weight loss as a function of temperature. Heating rate 5°/min., data determined from Fig. 1: 1, X-ray irradiated NH_4ClO_4; 2, non-irradiated NH_4ClO_4.

tion that a two-pen Leeds and Northrup Speedomax potentiometric strip chart recorder was used in place of the Moseley Autograph X-Y and Brown Electronic recorders. Sample and differential temperatures were recorded as a function of time. For vacuum differential thermal analysis the furnace and block containing the samples were placed under a bell jar which was evacuated. Chromel–alumel, 28 gage, thermocouples were used.

The thermal degradation of irradiated and non-irradiated ammonium perchlorate was also investigated in air and under vacuum by continuously recording changes in weight as the sample was heated at the nominal rate of 5°/min. to complete decomposition. In addition the crystals were observed microscopically during decomposition at 220°. A Chevenard thermobalance modified for electronic recording[7] was used in conjunction with a Moseley Autograph X-Y recorder for recording sample weight loss as a function of furnace temperature.

The vacuum thermobalance consisted of a helically wound precision spring from which an armature is suspended in the field of a linear variable differential transformer.[7] One hundred-mg. samples were contained in Coors No. 0000 glazed porcelain crucibles which were suspended from the armature by chromel wire into a non-inductively wound furnace obtained from the Marshall Products Co., Columbus, Ohio. The spring and sample are housed in Pyrex tubing which may be evacuated. A chromel–alumel thermocouple was located approximately 1/4 inches beneath the sample. The nominal heating rate of 5°/min. was maintained by a Gardsman Pyrometric proportioning controller purchased from West Instrument Co., Chicago, Illinois.

Ammonium perchlorate samples containing chloride, nitrate and nitrite ions were prepared by recrystallization from aqueous solutions containing NH_4Cl, NH_4NO_3 and KNO_2. Chloride was determined quantitatively by precipitation with $AgNO_3$: nitrate by the Duboscq Colorimeter using Greiss Reagent and the combined nitrate and nitrite were determined polarographically. The quantity of nitrate was obtained by difference. The analyses showed that the maximum impurities in the form of Cl^-, NO_2^- and NO_3^- in the reagent grade sample was 0.0001% each. The particle size of the samples was determined microscopically.

Samples of ammonium perchlorate, each containing either iodide, cupric or silver ions, were prepared by adding one mole per cent. of ammonium iodide silver or cupric perchlorates to a solution of ammonium perchlorate. The samples containing silver were protected from exposure to light. The solutions were evaporated to dryness and then oven-dried at 100° for 15 hours. These samples were exposed to doses of 6.0×10^{-4} e.v. absorbed/molec. The density of the crystals were determined by the flotation method using bromoform and benzene. Unless otherwise specifically stated reagent grade samples are used in the experimental work. Replicate runs of each experiment were conducted and the typical curves are given in this paper.

Results and Discussion

Figure 1 shows graphs of the loss in weight as a function of temperature of X-ray irradiated (0.14 e.v. absorbed/molec.) and non-irradiated ammonium perchlorate heated from room temperature to elevated temperatures at the nominal rate of 5°/min. These experiments were conducted in air under ambient conditions in crucibles wrapped in perforated aluminum foil to prevent the decrepitative loss of irradiated ammonium perchlorate crystals. The crucibles containing the non-irradiated samples, which did not undergo decrepitation, were also wrapped so that the experimental conditions of reaction would be similar.

It is apparent from the curves that the decomposition of ammonium perchlorate involves a complex multi-stage reaction and that exposure to X-rays has profoundly affected its chemical reactivity. The primary effect of pre-irradiation appears to be enhancement of the low temperature stages of decomposition. This is more clearly seen in Fig. 2, which shows plots of the rate of weight loss *vs.* temperature. Although the number of stages of decomposition appear to be the same for the irradiated and non-irradiated samples, the initial phases of reaction have been appreciably enhanced as a result of irradiation. The extent of reaction and maximum rates of reaction were markedly greater for irradiated ammonium perchlorate in both the first and second stages of decomposition which occur over the temperature

(6) V. D. Hogan, S. Gordon and C. Campbell, *Anal. Chem.*, **29**, 306 (1957).

(7) S. Gordon and C. Campbell, *ibid.*, **28**, 124 (1956).

ranges of 200 to 260° and 260 to approximately 300°, respectively. The ensuing five stages of decomposition, which appear in the form of step-like weight losses in Fig. 1 and as bands in Fig. 2, are also more extensive and occur at lower temperatures for the irradiated sample. A considerably smaller quantity of irradiated material undergoes the final stage of decomposition due to more extensive reaction below 385°.

A comparison between the d.t.a. curves in Figs. 3 and 2 shows that the temperature ranges over which the exothermal changes occur correspond to the various stages of weight loss observed during decomposition. Most notable among these are the exotherms at 236° and at approximately 270°. The endotherm at 244° represents the crystalline transition from the orthorhombic to cubic lattice. It may be noted that near completion of the endotherm at 260° an inflection appears in the thermogravimetric curve and a minimum in the corresponding derivative curve in Fig. 2. This may be attributed to the difference in the kinetics of decomposition of orthorhombic and cubic NH_4ClO_4.[8] The broad exotherm between 310 and 385 corresponds to the step-like loss regions over the same temperature range. The resolution of this region into the series of discrete stages shown in Fig. 2 is not apparent in the d.t.a. curves, undoubtedly because of overlap giving the appearance of a single broad band.

It is clear from the experimental results that the four principal changes in the details of the decomposition of ammonium perchlorate due to pre-irradiation are: (1) more extensive reaction prior to and during crystalline transition, (2) highly exothermal decomposition immediately following crystalline transition, (3) more extensive reaction over the temperature range of 310 to 385° and (4) a decrease in the extent of the final stage of decomposition at temperatures greater than 385°.

A comparison of the curves in Fig. 3 reveals that as the dose of radiation is increased there is a sharp rise in the exotherm at 270° which reaches a maximum and then decreases. For samples receiving doses greater than 3.4×10^{-4} e.v. absorbed/molec. an exotherm at 236° occurs which increases with increasing dose. Similarly the exotherm between 310 and 385° increases with increases in dose. The decrease in exothermicity at 270° accompanied by the simultaneous increase in exothermicity at 236° is probably due to a higher rate of decomposition prior to crystalline transition. The appearance of the sample was colorless up to doses of approximately 0.1 e.v. absorbed/molec. Samples exposed to greater doses exhibit a tannish coloration.[4]

The dependency of the parameters of the d.t.a. bands on radiation dose suggests that further research may be worthwhile to evaluate the potential application of the solid state thermal decomposition of ammonium perchlorate to dosimetry. The exotherm at 270° is sensitive to low doses up to 4.3×10^{-4} e.v. absorbed/molec., and the parameters of the exotherm at 236° may be useful for higher doses. The quantity of sample required is conveniently small, approximately 200 to 300 mg. Furthermore the changes caused by radia-

(8) L. L. Bircumshaw and B. H. Newman, *Proc. Roy. Soc.* (*London*), **A227**, 228 (1955).

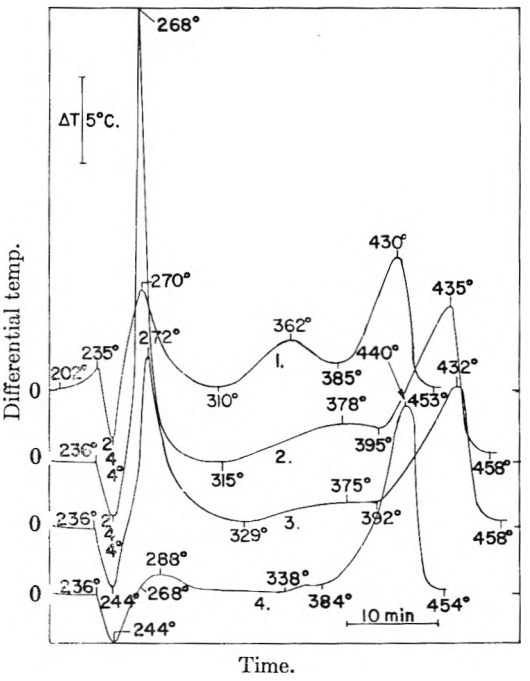

Fig. 3.—The effect of X-ray radiation on the thermal decomposition of ammonium perchlorate as indicated by Differential Thermal Analysis. Heated in air at 5°/min. X-Ray dose rate 1.4×10^{-3} e.v. absorbed molec.$^{-1}$ hr.$^{-1}$. Downward direction endothermal, upward direction exothermal.

Curve	Dosage, ev. absorbed/molec.
1	0.27
2	3.5×10^{-4}
3	5.4×10^{-5}
4	Non-irradiated

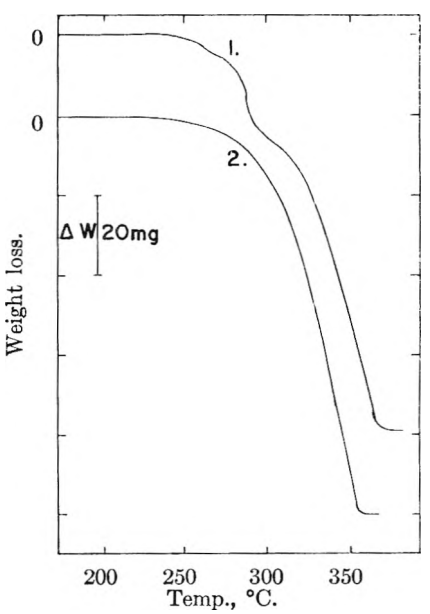

Fig. 4.—The decomposition of X-ray irradiated and non-irradiated ammonium perchlorate under vacuum 2 mm. Heating rate 5°/min., dose rate 2.3×10^{-3} e.v. absorbed molec.$^{-1}$ hr.$^{-1}$, dosage 5.4×10^{-2} e.v. absorbed/molec., 100-mg. samples. Weight change *vs.* temperature: 1, irradiated NH_4ClO_4; 2, non-irradiated NH_4ClO_4.

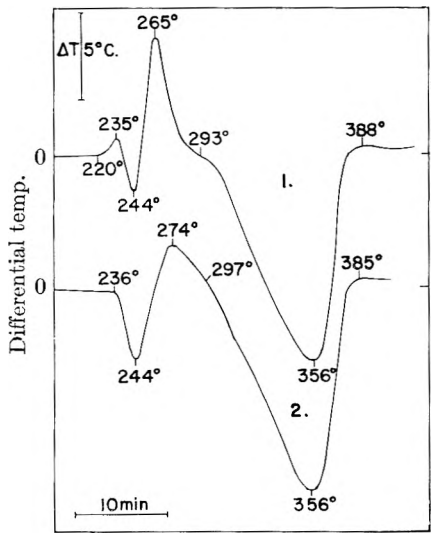

Fig. 5.—Differential thermal analysis of X-ray irradiated and non-irradiated ammonium perchlorate under vacuum (2 mm.), dosage 5.4 × 10^{-2} e.v. absorbed molec., sample weight 250 mg., heating rate 5°/min. Downward direction endothermal, upward direction exothermal: 1, irradiated NH_4ClO_4; 2, non-irradiated NH_4ClO_4.

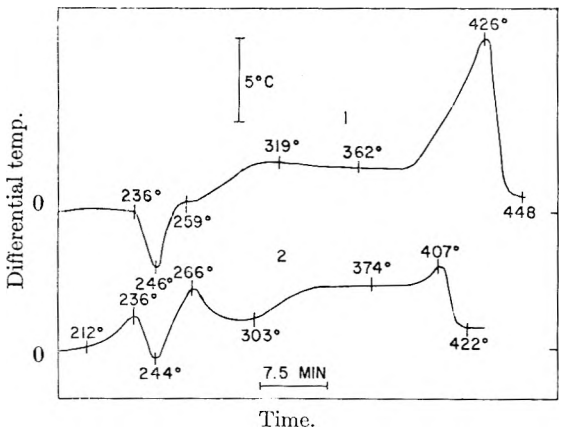

Fig. 6.—Differential thermal analysis curves for irradiated and non-irradiated NH_4ClO_4 containing 1 mole % Ag ion; 250-mg. samples, curves obtained in air at a heating rate of 5°/min. Absorbed dose 7.0 × 10^{-4} e.v./mole. Downward direction endothermal, upward direction exothermal: curve 1, non-irradiated NH_4ClO_4 containing 1 mole % Ag^+; curve 2, irradiated NH_4ClO_4 containing 1 mole% Ag^+.

tion appear to be stable since heating the samples for more than 200 hours at 100° did not significantly alter the d.t.a. parameters.

Ammonium perchlorate irradiated with 4.9 × 10^{-3} and 2.6 × 10^{-1} e.v. absorbed/molec. of γ-radiation (dose rate 1.1 × 10^{-2} e.v. absorbed molec.$^{-1}$ hr.$^{-1}$) show d.t.a. spectra similar to those of samples exposed to approximately the same dose of X-ray radiation.

Under vacuum the decomposition patterns of irradiated and unirradiated ammonium perchlorate are similar to those observed under atmospheric conditions with the exception that at temperatures greater than 290° the samples sublime. In both cases sublimation is complete at 385°. The thermogravimetric and corresponding d.t.a. curves are shown in Fig. 4 and 5.

Considering the interpretation of the above results it appears that there may be several possible causes for the enhanced reactivity of irradiated ammonium perchlorate. Prominent among these are: (1) the presence of new chemical species formed during radiation induced decomposition, (2) lattice defects which act as reaction nuclei caused by radiation induced decomposition and (3) the presence of electronic lattice defects.

Chloride, nitrate and nitrite as well as other products reported to be formed by thermal decomposition[4,9] are formed to a small extent during irradiation. Samples of ammonium perchlorate were therefore prepared containing 0.001% Cl^-, 0.27% NO_3^- and 0.080% NO_2^-, present to no more than 0.0001% each in the irradiated samples, and subjected to d.t.a. Likewise differential thermal analyses were carried out on samples of 20% partially decomposed ammonium perchlorate. In both cases the resulting curves were not analogous to the d.t.a. patterns of the irradiated material. On this basis it does not appear that reason (1) could account for the changes in reactivity due to radiation. An indication that exposure to X-rays did not result in the appreciable disorganization of the lattice by the displacement of ions to interstitial positions and by migration was obtained from X-ray powder diagrams. While the unirradiated portion of the sample which was partially decomposed showed line broadening the X-ray irradiated sample did not exhibit this effect. In addition, since decomposition also results in a disorganization of the lattice ions[8] it is doubtful that this factor is important in the decomposition of irradiated ammonium perchlorate. By elimination therefore it appears that (3), namely, the presence of electronic defects may account for the observed results. More specifically the formation of positive holes in the electronic structure of perchlorate ions equivalent to the formation of free radicals may be expected to enhance the electron transfer properties of the solid and thus the low temperature stages of decomposition below 300°. The transfer of electrons from ClO_4^- ions to interstitial NH_4^+ ions forming radicals was postulated in the work of Bircumshaw and Newman[8] as the rate-determining step of the low temperature stages of decomposition of non-irradiated NH_4ClO_4. This seems reasonable since the energy required to rupture a Cl–O bond in the ClO_4^- ion is too high to explain decomposition below 300°. On the other hand the less stable ClO_4 radicals may be expected to decompose at these low temperatures.

It therefore appears that the evidence points to an explanation for the increased reactivity in terms of positive hole formation. If this is valid then the presence of an impurity which may act as an electron trap such as Ag^+ ion may be expected to enhance the effect of radiation. This is confirmed by the d.t.a. curves in Fig. 6 of irradiated, and unirradiated ammonium perchlorate both containing 1 mole % Ag^+ ion. The increase in the exotherm at 236°, which was previously demonstrated to increase with increases in dose, is greater

(9) L. L. Bircumshaw and B. H. Newman, *Proc. Roy. Soc. (London)*, **A227**, 115 (1954).

than for samples of pure NH_4ClO_4, not containing Ag^+, exposed to more than 0.1 e.v. absorbed/molec. The silver doped sample received a dose of 7.0×10^{-4} e.v. absorbed/molec. This indicates that the susceptibility to radiation damage was increased over 100 times by the presence of Ag^+ ions which may act as electron traps. The d.t.a. curves for the non-irradiated samples doped with Ag^+ ion, which were kept out of direct light do not exhibit exotherms at 236 and 270°.

The d.t.a. curves of samples containing one mole % of Cu^{++} ion, irradiated and unirradiated are shown in Fig. 7. The thermograms exhibit sharp exotherms immediately following crystalline transition at 270°, the same band found to be enhanced as a result of exposure to X-rays and γ-radiation. For samples containing Cu^{++} ion which have been irradiated, the exotherm at 236° is also observed. The above results may be explained in terms of the electron transfer as

$$Cu^{++} + ClO_4^- = Cu^+ + ClO_4$$
$$Cu^+ + NH_4^+ = Cu^{++} + NH_4$$

The role of the cupric ion may be thought of as a bridge in the electron transfer process. A similar mechanism was previously suggested[8] for the catalytic effect of MnO_2 on the decomposition of ammonium perchlorate.

The presence of iodide ion also enhances the low temperature decomposition of ammonium perchlorate. This is apparent from the d.t.a. curves in Fig. 8. In this case less energy is required for removal of an electron from iodide than from the perchlorate ion. It may be noted that whereas the exotherm immediately following crystalline transition for the X-ray irradiated and Cu^{++} ion containing samples appears to begin during the latter phase of the crystalline transition just after the minimum of the endotherm at 244°, the exotherm for the I^- ion containing sample occurs after the transition is completed at 262°. Again the catalytic effect may be accounted for in terms of the iodide acting as a bridge in the electron transfer process as

$$I^- + NH_4^+ = I + NH_4$$
$$I + ClO_4^- = I^- + ClO_4$$

The d.t.a. curve for the irradiated sample containing iodide is similar to that of ammonium perchlorate not containing this impurity. This may be accounted for by the loss of iodine while heating the sample, leaving a residue of purified ammonium perchlorate. This was confirmed by the starch test for iodine performed on the vapors above the irradiated sample heated at 150°. The sample, which prior to heating had a tannish coloration, turned colorless after the loss of the iodine. It is apparent, therefore, that iodine probably in the form of free radicals and subsequently I_2 was formed during irradiation.

The apparently catalytic effect of the impurities discussed above lend support to the electron transfer hypothesis and to the suggestion that the catalytic effect of pre-irradiation is related to an increase in the electron transfer properties of the solid caused by pair formation.

The most active reaction sites may be expected

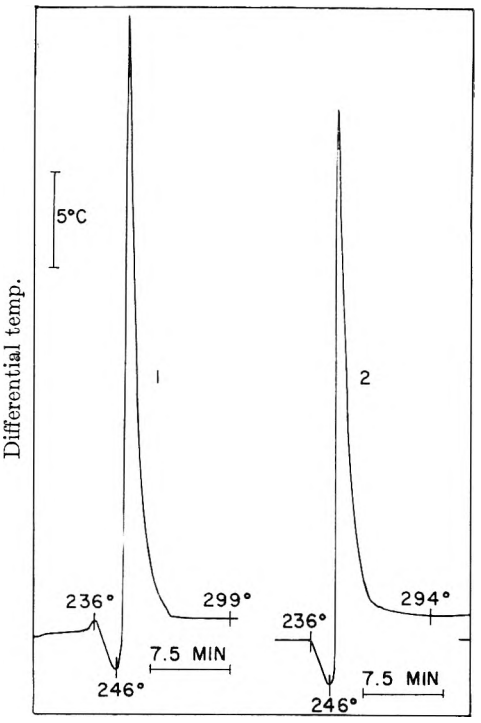

Fig. 7.—Differential thermal analysis curves for ammonium perchlorate containing 1 mole % cupric ion heated in air at atmospheric pressure, heating rate 5°/min., 250-mg. samples. Differential temperature *vs.* reference temperature. Exposure dose 7.0×10^{-4} e.v. absorbed/molec. Downward direction endothermal, upward direction exothermal: curve 1, irradiated sample; curve 2, non-irradiated sample.

to be located at the points of radiation damage on the surface and within the crystals. This appears to be confirmed by microscopic observation of the decomposing crystals at 200°. The crystals exposed to radiation appeared to have points of opaqueness throughout the solid. These are probably areas where radiation induced reaction and damage occurred. Some of the irradiated crystals also appear clear as was the case for the unirradiated samples. During decomposition the opaque areas in the irradiated solid grew in size or are observed to form and grow throughout the entire crystal. The irradiated samples also undergo repeated decrepitation and the crystals are for the most part in vigorous translational and rotational motion during decomposition. The formation and presence of occluded gases and their subsequent escape from the interior of the solid can explain these observations. The exposure of new surfaces during reaction resulting from decrepitation will also accelerate decomposition. In contrast, the unirradiated samples were observed initially to undergo reaction at the surface of the particles and progress into the interior of the crystals in agreement with previously reported findings.[8] The unirradiated samples neither underwent appreciable decrepitation nor were the particles in motion during reaction.

Interestingly, ammonium perchlorate sublimate exhibits the same pattern of decomposition as the irradiated samples as demonstrated in Fig. 9.

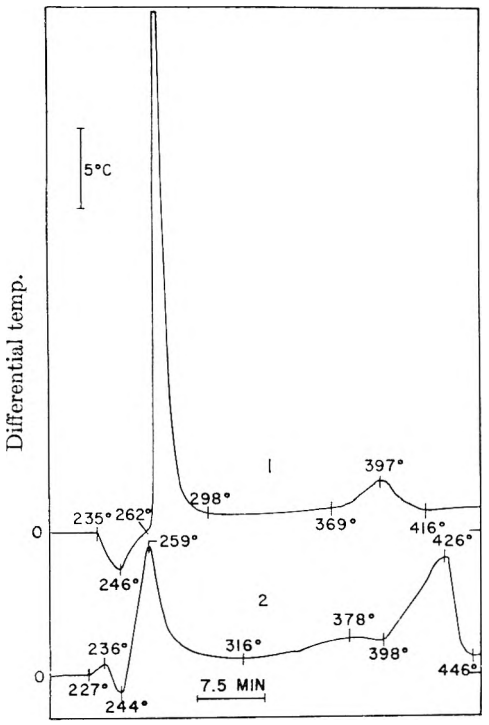

Fig. 8.—Differential thermal analysis curves for ammonium perchlorate containing 1 mole % iodide ion heated in air at atmospheric pressure, heating rate 5°/min., 250-mg. samples. Differential temperature *vs.* reference temperature. Absorbed dose 7.0×10^{-4} e.v./molec. Downward direction endothermal upward direction exothermal: curve 1, non-irradiated; curve 2, irradiated.

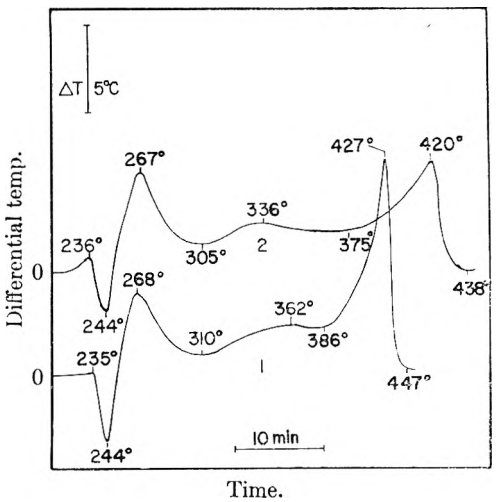

Fig. 9.—A comparison between the differential thermal analysis curves of non-irradiated sublimed NH_4ClO_4 and irradiated NH_4ClO_4 carried out in air at atmospheric pressure. Total absorbed dose 5.4×10^{-2} e.v./molec. Heating rate 5°/min., 250-mg. samples. Downward direction endothermal, upward direction exothermal: 1, non-irradiated sublimed NH_4ClO_4; 2, irradiated NH_4ClO_4.

The reason for this is not clear. It would seem, however, that whatever factors affect reactivity caused by exposure to radiation are operating for the sublimate. The sublimate appears to consist of agglomerates of spherical particles of about 5 μ in diameter. Samples of unirradiated ammonium perchlorate ground gently to approximately the same average particle size did not exhibit a decomposition spectrum similar to that of the sublimate. Spheroidal shape may indicate poorly ordered crystals, as was confirmed by appreciable X-ray line broadening.

Acknowledgment.—The authors wish to acknowledge the partial financial support of this research by the Office of Ordnance Research under Project TB1-0004.

THE EXCHANGE OF Li^+, Na^+ AND K^+ WITH H^+ ON ZIRCONIUM PHOSPHATE[1]

BY EDWIN M. LARSEN AND DONALD R. VISSERS

The Department of Chemistry, the University of Wisconsin, Madison, Wisconsin

Received May 18, 1960

The equilibrium exchange of Li^+, Na^+, K^+ with the hydrogen form of zirconium phosphate in 0.1005 *N* HCl was studied over the temperature range 1.17 to 44.5°. The following data were obtained for Li^+, Na^+ and K^+, respectively: ΔF^0 +2.0, +1.1, +0.56 kcal./mole; ΔH^0 0.0, −2.7, −5.7 kcal./mole and ΔS^0, −6.7, −13, −21 e.u.

The use of zirconium phosphate as an ion-exchange material has been reported by Kraus[2-6] and Amphlett.[7-9] Since no systematic quantitative studies of the equilibria have been reported, an examination of the exchange of Li^+, Na^+ and K^+, with hydrogen ion was undertaken.

Experimental

Preparation of Zirconium Phosphate.—In general, the phosphates were prepared by the slow addition of 0.015 to 0.2 *M* sodium dihydrogen phosphate solution or phosphoric acid to a 0.01 to 0.1 *M* zirconium oxychloride solution with rapid stirring, both solutions being 0.1 *M* in hydrochloric

(1) Based on a thesis submitted by Donald R. Vissers in partial fulfillment of the requirements of the degree of Doctor of Philosophy.

(2) K. A. Kraus, *Chem. Eng. News*, **34**, 4760 (1956).

(3) K. A. Kraus, *J. Am. Chem. Soc.*, **78**, 694 (1956).

(4) K. A. Kraus and F. Nelson, "Proc. Intern. Conf. on Peaceful Uses of Atomic Energy," Vol. 7, 113, 131 United Nations (1956).

(5) K. A. Kraus, T. A. Carlson and J. S. Johnson, *Nature (London)* **177**, 1128 (1956).

(6) K. A. Kraus, H. O. Philips, T. A. Carlson and J. S. Johnson, Abstracts, Boston Meeting, Am. Chem. Soc., 1959.

(7) C. B. Amphlett, L. A. McDonald and M. J. Redman, *Chemistry and Industry*, 1314 (1956).

(8) C. B. Amphlett, L. A. McDonald and M. J. Redman, *ibid.*, **6**, 220 (1958).

(9) C. B. Amphlett, L. A. McDonald, J. S. Burgess and J. C. Maynard, *ibid.*, **10**, 69 (1959).

acid. The gelatinous precipitate was washed by decantation with distilled water to a *p*H of about 3.4, filtered and air dried. The glassy material, when replaced in water, broke up into particles about 10 mesh in size. The properties and compositions of the products are given in Table I.

Hydrolysis Studies.—Samples of the five preparations were studied with respect to their stability toward hydrolysis. An apparatus was assembled in which the agitated sample was washed continuously with conductivity water (*p*H 7.0 to 6.85). The system was under slight pressure of nitrogen, and protected from the carbon dioxide of the atmosphere by drying tubes containing Ascarite. The *p*H of the effluent was recorded and the washing was continued until the *p*H approached the value of the pure water. The effluent was collected in a large storage bottle and the phosphate and hydrogen-ion concentrations determined.

Determination of the Capacity and Equilibrium Data.—Two-tenths gram samples of 10 mesh zirconium phosphate in the hydrogen form were packaged in Visking tubing (1/8th inch) to prevent loss during handling. A pre-soaked 2.0 inch section of Visking tubing was tied off at one end, the sample introduced by means of a small long-stemmed funnel, rinsed down with a few drops of water and the remaining end tied off. The sample occupied about one-fifth of the total volume of the sack. Blank runs with 0.1 *M* $KMnO_4$ in the Visking sack showed that the electrolyte equilibrated with the external solution within 15 minutes. The same batch of phosphate (D) was used throughout, and a new portion was used for each equilibration. In one set of experiments, the sodium form of the phosphate was prepared by equilibration in sodium acetate solution at *p*H 5. This sample was used to approach equilibrium from the other direction. The samples for the equilibrium constant data were equilibrated with 200 ml. of lithium, sodium and potassium chloride solutions ranging from 0.1 to 0.8 molal all in 0.1005 *N* HCl. The ion-exchange studies were carried out over the temperature range 1.17 to 44.5 ± 0.1°. Equilibration time varied from a month at 0° to four days at 44°. To determine the cation capacity, samples were equilibrated at 25° for one week with 200 ml. of 1 *M* lithium, sodium and potassium acetate–acetic acid mixtures. At least two samples were run for each system and the average taken. In all cases, the sample was removed from the mother liquor, washed to remove absorbed ions (negative chloride test), and then the alkali metal in the solid phase was completely displaced by the addition of a copper(II) salt solution. The copper form of the zirconium phosphate was separated, washed, and the combined filtrate and washings, which now contained the alkali metal, were prepared for analysis by electrodeposition of the copper.

Analytical Methods.—The alkali metals were determined flame-photometrically using a Perkin–Elmer Flame Photometer. Standard solutions using the same amounts of nitric acid and sulfuric acid as contained in the unknown solutions were used as references. The readings were checked with standard solutions just below and above that of the unknown. The errors in the metal ion analyses were judged to be Li, ±3%; Na, ±4%; K, ±4%.

The analysis of zirconium phosphate was based on the fact[10] that zirconium compounds dissolve completely in an alkaline hydrogen peroxide mixture, which upon digestion at an elevated temperature, yields an acid-soluble peroxyzirconium precipitate. In the case of the zirconium phosphate, the phosphate is in solution, and may be quantitatively separated from the zirconium-containing precipitate. The zirconium and phosphate may then both be determined by standard methods. The determination of phosphate at very low concentrations was accomplished using the photometric method based on the absorption at 315 mμ of a molybdovanadophosphoric acid complex.[11]

Results and Discussion

Stumper and Metlock[12] studied the composition of zirconium phosphate as a function of the composition of the reagents used. When an excess of phosphate relative to that required for the normal phosphate, (ZrO_2/P_2O_5 mole ratio = 1) was used, the product was the normal phosphate. When 100% or greater excess of zirconium(IV) was used, the product had a ZrO_2/P_2O_5 ratio of 2.0. Products of intermediate composition could be obtained by varying the initial solution compositions. Amphlett prepared the phosphates from solutions which had initial ZrO_2/P_2O_5 mole ratios in the range 0.8 to 4 in an accompanying 1 *N* acid. The products were not analyzed. Kraus,[6] on the assumption that an excess of the phosphoric acid anhydride was necessary for the product to exhibit cation-exchange properties, precipitated zirconium phosphate from solutions containing an excess of phosphoric acid. The products were not analyzed. We have observed (Table I) that the ZrO_2/P_2O_5 mole ratio of the product is higher than the ZrO_2/P_2O_5 mole ratio of the solutions from which the product is precipitated. We have also observed that cation-exchange properties are exhibited by products with a ZrO_2:P_2O_5 ratio of more than one.

TABLE I

Sample	Mole ratio ZrO_2/P_2O_5 Soln.	Product	Lowest equil. *p*H	Total Cu^{++} capacity meq. cation per Meq. P_2O_5	G. air dried	Mm. ZrO_2
A	0.50	0.98	3.7	..	..	..
B	1.00	1.35	5.85	1.35	6.98	2.32
C	1.16	1.30	5.40	1.36	6.02	2.10
D	1.16	1.28	6.3	..	..	..
E	1.33	1.55	6.55	1.37	5.46	1.98

Zirconium phosphate precipitation can be used for the quantitative determination of phosphate; therefore a product of known and reproducible composition can be produced. However, it is a well known fact[13] that the freshly precipitated material is subject to loss of phosphate by hydrolysis and this must be repressed. The dry, normal phosphate also shows a tendency toward hydrolysis and therefore is undesirable for the quantitative study of its ion-exchange properties. It was thus necessary for our purpose to produce a phosphate of a composition which was at least kinetically stable with respect to hydrolysis. The normal phosphate (A, Table I) hydrolyzed to give a product of a ZrO_2/P_2O_5 mole ratio of 1.16. A mass balance was made to substantiate the phosphate loss. From the eleven liters of wash water of *p*H 4.8, the calculated total phosphate associated with this hydrogen-ion concentration was 1.59×10^{-5} mole. The experimentally determined phosphate content of the wash water was 2.08×10^{-5} mole which agreed with the calculated value within experimental error. From the original composition of product A, and the phosphate loss, the residue should have had the ZrO_2/P_2O_5 mole ratio of 1.16. The experimentally determined mole ratio was identical with this. This hydrolysis explains the low *p*H of 3.7 recorded for sample A. Amphlett,[7] who made a similar observation, remarks that "the hydrogen form of the zirconium phosphate imparts an acid reaction to distilled water when equilibrated with it due to the ionization of the more acid groups." However, this idea is not reasonable for it would require a charged solid

(10) P. Hurst, Doctoral Thesis, University of Wisconsin, 1956.

(11) O. B. Michelson, *Anal. Chem.*, **29**, 633 (1957).

(12) R. Stumper and P. Metlock, *Bull. soc. chim.*, **1**, 674 (1947).

(13) I. M. Kolthoff and E. B. Sandell, "Textbook of Quantitative Inorganic Analysis," The Macmillan Co., New York, N. Y., 1953.

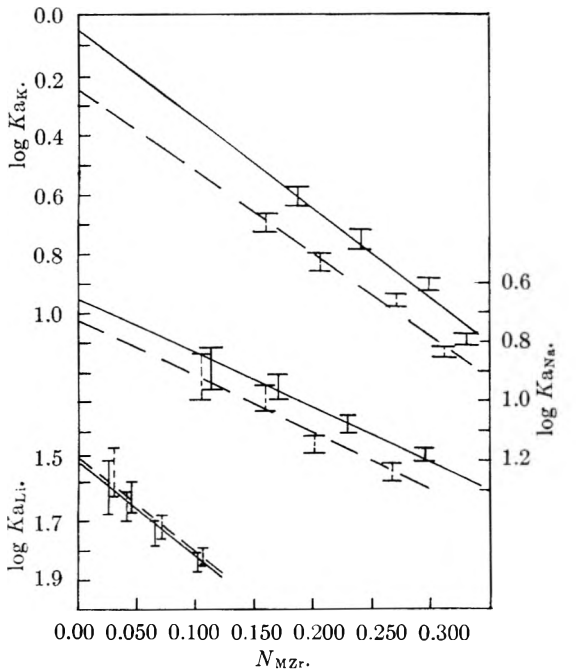

Fig. 1.—Solid line, data 1.17°; dashed line, data 14.5°.

residue at the bottom of the beaker. Samples of composition B, C, D and E were subjected to the same hydrolysis experiment (Table I). Only a small drop in *p*H was noted and the test for phosphate in the wash water was negative. It was concluded that for our purposes preparations of ZrO_2/P_2O_5 mole ratio 1.16 and higher were kinetically stable with respect to hydrolysis. However, when samples were equilibrated in conductivity water for a period (Table II) of a week rather than hours, some slight phosphate loss was observed for sample D even at low *p*H's, but this was not considered significant. At higher *p*H's however, the sample was largely decomposed, and it is clear that zirconium phosphate is not stable in basic solution.

TABLE II

PHOSPHATE LOSS AS A FUNCTION OF *p*H

*p*H of soln.	1.0	3.0	5.0	6.0	8.0	9.0	10.0	11.0	13.0
% P_2O_5 lost in 1 wk. at 25°	0.2	0.3	0.6	0.8	3.95	7.9	15.8	19.3	43.0

From titration data it would appear that the zirconium phosphate exchange sites are multifunctional.[7] In view of the degradation of the phosphate at *p*H's above 6 one might question the interpretation of Amphlett's curves, nevertheless it is reasonable to expect multifunctional cation-exchange sites. To make possible the interpretation of the equilibrium data it was necessary to study the exchanger in a *p*H range in which it was behaving unifunctionally. It was also necessary to choose a *p*H at which the phosphate loss was negligible. For this reason *p*H 1 was chosen. The choice of solution volume and sample size was such that the absorption of solvent by the solid sample had a negligible effect on the solution concentration, and so that the hydrogen-ion and metal-ion concentrations of the solution remained essentially constant during equilibration. The combined effects resulted in a maximum change of one per cent.

Owing to the unfavorable equilibrium constant for this reaction, it was impossible to saturate the phosphate with univalent metal ion at *p*H 1 to determine the capacity. Since the titration curves show a straight portion up to *p*H 6, it was assumed that the exchanger was unifunctional up to *p*H 5, and the capacity was determined in a buffer solution of the alkali-metal ion acetates at this *p*H (Table III). It should be pointed out

TABLE III

CAPACITY OF ZIRCONIUM PHOSPHATE D

Meq. M^+/meq. P_2O_5		
Li^+	Na^+	K^+
0.315	0.316	0.313
.316	.315	.310
.313	.320	.316

that the actual metal-ion concentration on the phosphate was determined, rather than measuring the difference in the alkali-metal concentration of the solution. The strong affinity of the zirconium phosphate for copper ion provided an excellent means of removing the exchanged sodium, lithium and potassium from the sample. In this way the average capacity of 0.315 ± 0.002 meq. H^+/meq. of P_2O_5 was determined. The capacity was determined with the alkali-metal ions rather than by exchange of copper. The total capacity by copper exchange was much greater than that determined by the alkali-metal ions which was interpreted to mean that the copper exchanged with the less-acid sites as well as the strong acid sites. The copper data, however, did originally provide evidence of the fact that the exchange sites are related to the phosphate content of the sample, for the only correlation of capacity was with the phosphate content (Table I).

For the exchange of a univalent ion with the hydrogen form of the zirconium phosphate the following equation and associated equilibrium constant expression may be written

$$M_{aq}^+ + HZr_{(s)} \rightleftharpoons MZr_{(s)} + H_{aq}^+$$

$$K_a = \frac{(N_{MZr})}{(N_{HZr})} \times \frac{(m_{H^+})}{(m_{M^+})} \cdot \frac{(\gamma_{\pm HCl})^2}{(\gamma_{\pm MCl})^2}$$

The concentrations of the species in the solid phase are expressed in terms of their respective mole fractions (Table IV). The solution species are expressed in molalities corrected by the mean activity coefficient for the solute in a binary solution. The mean activity coefficients were calculated by the method and from data given by Harned and Owen.[14] The assumption has been made that the activity coefficient ratio is little changed with temperature and the data at 25° were used at all temperatures.

It was necessary also to consider the activity of the ions in the solid phase. Our calculations of equilibrium constant showed, that like the organic exchangers, the activities of the ions in the solid phase were changing appreciably with changes in

(14) H. S. Harned and B. B. Owen, "The Physical Chemistry of Electrolyte Solutions," Reinhold Publ. Corp., New York, N. Y., 1958, p. 593 ff.

TABLE IV
EQUILIBRIUM DATA

Li^+				
$M_{aq}{}^+(m)$	0.1005	0.2010	0.4040	0.8160
$(\gamma_{\pm a})^2/(\gamma_{\pm s})^2$	1.008	1.032	1.023	1.044
$N_{MZr} \times 10^2$				
1.17°	2.54	4.45	6.67	10.2
14.5°	2.86	4.13	6.98	10.5
25.0°	2.54	4.45	6.98	10.5
44.5°	2.54	4.13	6.66	10.2
Na^+				
$M_{aq}{}^+(m)$	0.1010	0.2015	0.4050	0.8160[a]
$(\gamma_{\pm a})^2/(\gamma_{\pm s})^2$	1.039	1.085	1.122	1.263
$N_{MZr} \times 10^2$				
1.17°	11.1	17.1	22.9	29.5
14.5°	10.5	15.9	20.1	26.7
25.0°[b]	9.43	14.0	19.4	24.8
44.5°	7.30	10.8	15.9	20.6
K^+				
$M_{aq}{}^+(m)$	0.1005	0.2020	0.4060[a]	0.8230[a]
$(\gamma_{\pm a})^2/(\gamma_{\pm s})^2$	1.068	1.143	1.173	1.328
$N_{MZr} \times 10^2$				
1.17°	18.7	23.8	29.8	33.0
14.5°	15.9	20.6	27.0	31.1
25.0°	13.3	19.4	24.4	28.9
44.5°	11.4	14.0	20.0	25.4

[a] HCl 0.1015 rather than 0.1005 N. [b] Sodium form of zirconium phosphate used.

concentration. With organic exchangers the problem of the activities of the ions in the solid phase has been studied by Argersinger[15] and Sillén,[16] both of whom arrived at the expression for the true equilibrium constant as $\ln K = \int_0^1 \ln K_a \, dN_m$ where K_a is the apparent equilibrium constant, and N_m is the mole fraction of the ion exchanger in the metal form. The evaluation requires graphical integration over the mole fraction of the metal form from zero to 1. In this treatment the standard state of each ion in the solid phase is the corresponding pure form of the exchanger. In the present work we do not make any observations on systems in which the fraction of the sites occupied by the metal ion exceeds the mole fraction 0.35, thus it is not possible to use this procedure to obtain a thermodynamic equilibrium constant for the exchange reaction. However, by extrapolating the apparent equilibrium constants to the pure hydrogen form, (Figs. 1 and 2), we obtain an equilibrium constant based on one state for the hydrogen ion in the solid phase, the pure hydrogen-ion form of the solid phase, and a different standard state for the alkali-metal ions in the solid phase. This state is the hypothetical pure alkali-metal form of the solid phase which has the properties extrapolated from the hydrogen ion containing solid phase in which the alkali-metal ion is infinitely dilute.

(15) W. J. Argersinger, A. W. Davidson and O. D. Bonner, *Trans. Kans. Acad. Sci.*, **53**, 404 (1950).

(16) E. Hogfeldt, E. Ekedahl and L. G. Sillén, *Acta Chem. Scand.*, **4**, 556 (1950).

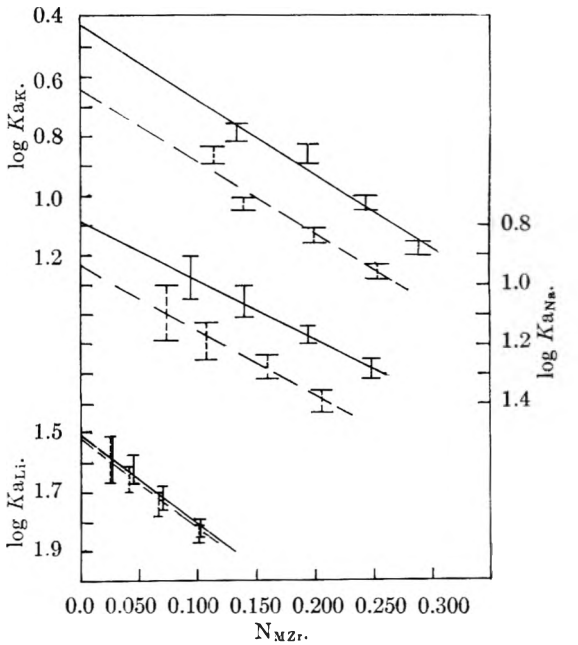

Fig. 2.—Solid line, data 25.0°; dashed line data, 44.5°.

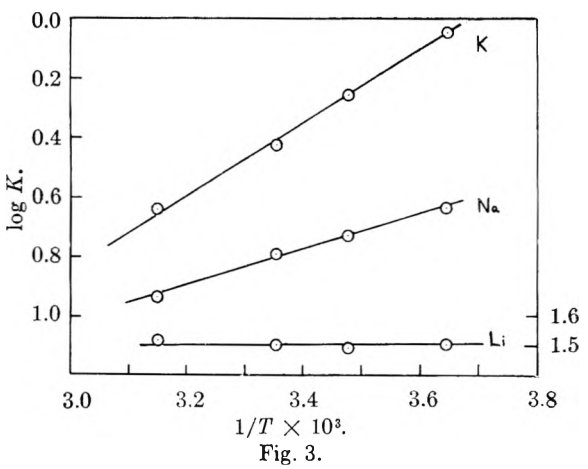

Fig. 3.

From the equilibrium constants thus determined, ΔF^0 was calculated and along with the ΔH^0 from the $1/T$ plots of the equilibrium constants (Fig. 3), ΔS^0 was calculated. The entropy changes are strikingly close to the relative entropies for the aqueous ions tabulated by Latimer,[17] which are Li^+, 4.7; Na^+, 14 and K^+, 24.2. One can conclude that upon exchange of cations the entropy change of the solid phase is small. The trend in ΔF^0 with ion size is in agreement with the elution experiments of Kraus and Amphlett. The organic, strong-acid, cation exchangers have equilibrium constants greater than one for the alkali metals.

TABLE V

Ion	ΔF^0, kcal./mole	ΔH^0, kcal./mole	ΔS^0, e.u.
Li	+2.0	0.0	−6.7
Na	+1.1	−2.7	−13
K	+0.56	−5.7	−21

(17) W. M. Latimer, "Oxidation Potentials," Prentice-Hall, Inc., New York, N. Y., 1952.

Acknowledgment.—The authors wish to thank Professor E. L. King for helpful discussions concerning this work. This work was supported in part by the Research Committee of the Graduate School from funds supplied by the Wisconsin Alumni Research Foundation.

THERMODYNAMICS OF THE LEAD–ANTIMONY SYSTEM[1]

By Linda Warner Diller, Raymond L. Orr and Ralph Hultgren

Department of Mineral Technology, University of California, Berkeley, California

Received May 21, 1960

Heats of formation of solid α-phase Pb–Sb alloys have been measured by solution calorimetry. These data have been combined with previously known data in the liquid state and the phase diagram to complete the thermodynamic description of the α-phase. The thermodynamic data for both solid and liquid alloys and the phase diagram have been critically evaluated and discussed, and selected thermodynamic properties have been tabulated. An attempt is made to interpret the unusually large positive values found for the excess partial molar entropy of Sb in the α-phase.

Introduction

Although a considerable number of thermodynamic measurements have been made on liquid Pb–Sb alloys, there exist none at all on the alloys in the solid state. Thermodynamic properties of the Pb-rich solid phase are calculable from the phase diagram and the liquid data, but entropies of formation so derived seem implausibly high (*e.g.*, $\Delta\bar{S}^{xs}_{Sb}$ = 10.8 e.u. at x_{Sb} = 0.058 and 525°K.).

In order to establish better the thermodynamic properties of the solid phases, it was decided to measure directly heats of formation within the Pb-rich (α) solid solution. These data, together with a critical analysis of the liquid data and the phase diagram, are presented in this paper.

Experimental

Materials.—Antimony in the form of rods was obtained from Johnson-Matthey and Co., Ltd., Toronto, Canada, who stated it to be 99.9+% pure. Lead rods specified to be 99.998% pure were obtained from the American Smelting and Refining Co.

Preparation of Alloys.—Four 10-g. ingots, containing 2.00, 3.00, 4.00 and 5.00 at. % Sb, all in the α-solid solution range, were prepared by melting together at 500° the weighed components in evacuated, sealed Vycor tubes. The tubes were shaken briskly for five minutes while in the furnace, then quenched rapidly in ice-water to minimize segregation. Weight losses on fusion were less than 0.03%; the weighed compositions of the alloys were therefore taken to be correct. The ingots were cold worked, re-sealed in evacuated Pyrex tubes, and homogenized for seven weeks at 252°, the eutectic temperature. They were again quenched in ice-water and stored in a refrigerator until used.

Filings taken from both ends of each ingot were strain annealed at 250° and quenched in ice-water. The sharp X-ray diffraction lines obtained from the filings indicated the alloys to be homogeneous. Measured lattice constants were in excellent agreement with the measurements of Tyzack and Raynor,[2] while disagreeing with the older measurements of Ageev and Krotov.[3]

Apparatus and Methods.—Heats of solution in liquid Pb of pure Sb and the alloys were measured using the calorimetric apparatus and methods described previously.[4] Samples were dropped from an initial temperature, T_i, near 520°K., into the lead-bath at temperature T_f, near 677°K. The heat capacity of the calorimeter was determined by dropping specimens of pure Pb from room temperature, using the heat content values of Kelley.[5] From these data heats of formation at temperature T_i were calculated in the usual way.[4] During the runs the concentration of Sb in the liquid Pb-bath never exceeded 0.4 at. %. Within this dilute range the heat of solution of Sb was independent of Sb concentration within the experimental uncertainty.

Results

The experimental results are given in Table I. The heats of formation have been referred to a common temperature, 525° K., assuming Kopp's law of additivity of heat capacities in correcting the results for the small deviations of T_i from that temperature. The heats of formation (Fig. 1) appear to be best represented by the straight line, $\Delta H = 6300x_{Sb}$, with an average deviation of 14 cal./g.-atom. The relative partial molar heat contents thus obtained are $\Delta\bar{H}_{Pb} = 0$ and $\Delta\bar{H}_{Sb} = 6300$ cal./g.-atom.

Table I

Experimental Results

Sample comp., at. % Sb	Run no.	T_i, °K.	T_f, °K.	$\Delta H_{soln.}$, cal./g.-atom	$\Delta H_{form.}$, 525°K., cal./g.-atom
100.00	64-3	523.7	676.6	5652	
	64-15	519.1	677.3	5713	
	65-3	523.5	676.5	5729	
	65-15	514.9	677.2	5692	
2.00	64-5	523.6	677.5	2190	138
	65-13	515.6	677.5	2264	124
3.00	64-7	526.5	677.6	2130	220
	65-11	519.7	677.3	2203	188
4.00	64-11	522.3	677.8	2195	211
	65-7	526.0	677.3	2151	234
5.00	64-13	522.5	677.8	2130	310
	65-5	522.4	677.3	2117	321

Selecting from published data the value ($H_{667°K} - H_{525°K}$) = 1000 cal./g.-atom for Sb, the relative partial molar heat of solution of $Sb_{(s)}$ at infinite dilution in $Pb_{(l)}$ at 677°K. may also be evaluated from the data yielding

$$\Delta\bar{H}_{Sb,\ 677°K,\ x_{Pb}=1} = 4670 \text{ cal./g.-atom}$$

(1) Based on a thesis by Linda Warner submitted in partial satisfaction of the requirements for the degree of Master of Science in Engineering Science to the University of California, 1959. This work was supported in part by grants from the Office of Ordnance Research, U. S. Army, and the U. S. Atomic Energy Commission.

(2) C. Tyzack and G. V. Raynor, *Acta Cryst.*, **7**, 505 (1954).

(3) N. V. Ageev and I. V. Krotov, *J. Inst. Metals*, **59**, 301 (1936).

(4) R. L. Orr, A. Goldberg and R. Hultgren, *Rev. Sci. Instr.*, **28**, 767 (1957).

(5) K. K. Kelley, U. S. Bur. Mines Bull. 584, 1960.

Evaluation of Thermodynamic Data

Phase Diagram.—The selected diagram of Hansen[6] is shown in Fig. 2. The liquidus is estimated to be accurate to ±2° from 0 to 25 at. % Sb, and there is good agreement in published measurements of the liquidus from 87 to 100 at. % Sb. However, in the intermediate ranges there is wide divergence in reported liquidus temperatures, due, probably, to strong tendencies to supercooling. The Pb-rich solidus and solvus seem to be reasonably well established. For the Sb-rich solidus and solvus no accurate data exist. Hansen concludes that the solubility of Pb in Sb at the eutectic temperature lies between 1.5 and 2.7 at. %. The eutectic temperature seems to have been well established at 251.5 ± 0.5°.

Liquid Alloys.—The e.m.f. measurements of Seltz and DeWitt[7] and Elliott and Chipman[8] are in excellent agreement, not only in free energies derived from them, but also in entropies calculated from their temperature coefficients. These data have been used in evaluating the thermodynamic properties of liquid alloys given in Table II. Later e.m.f. measurements of Eremenko and Eremenko,[9] while showing more scatter, check well with the free energies of the former investigators. Their entropies agree well at high Sb contents ($x_{Sb} = 0.7 - 1.0$) but diverge to values lower by as much as 0.15 e.u. at lower Sb contents.

TABLE II

LIQUID ALLOYS AT 900°K.

$$(1 - x)Pb_{(l)} + xSb_{(l)} = [Pb_{1-x}Sn_x]_{(l)}$$

x_{Sb}	ΔF, cal./g.-atom	ΔH, cal./g.-atom	ΔS, e.u.	a_{Pb}	a_{Sb}
0.1	− 625	10	0.70	0.899	0.080
.2	− 970	0	1.08	.794	.166
.3	−1195	−20	1.31	.685	.259
.4	−1325	−40	1.43	.575	.360
.5	−1365	−60	1.45	.466	.465
	(±30)	(±100)	(±0.11)	(±0.008)	(±.008)
.6	−1325	−70	1.39	.361	.573
.7	−1200	−80	1.24	.261	.682
.8	− 975	−70	1.00	.167	.791
.9	− 625	−50	0.64	.079	.897

Calorimetric determinations by Kawakami[10] of heats of formation by direct reaction agree in general with the selected values with a maximum deviation of −70 cal./g.-atom. Oelsen, Johannsen and Podgornik[11] calculated integral heats of formation from measurements of heat contents of solid and liquid alloys, obtaining results as much as 125 cal./g.-atom more exothermic. Wüst and Durrer[12] by a similar method checked the selected values better but with wider scatter. In this case it was felt that the values obtained from the temperature coefficients of e.m.f. measurements were more reliable than the calorimetric.

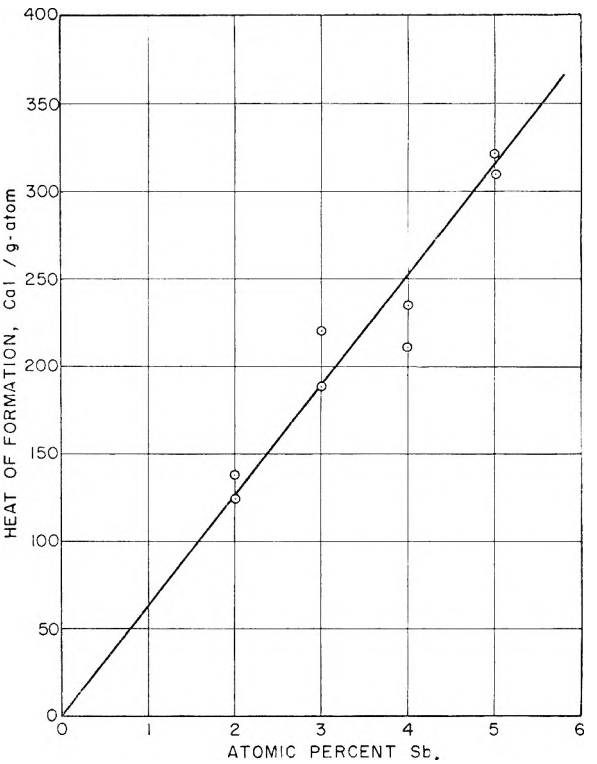

Fig. 1.—Integral heats of formation of α-phase lead-antimony alloys at 525°K.

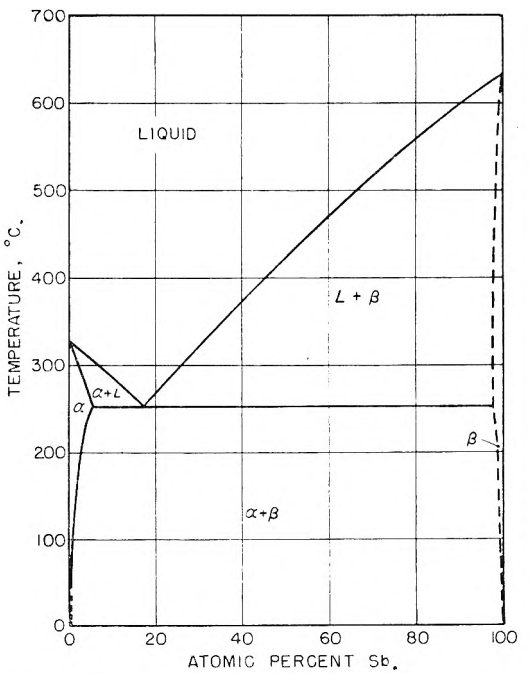

Fig. 2.—Phase diagram of the lead-antimony system.

Solid Alloys.—The only thermodynamic measurements on solid alloys are the heats of formation reported in this paper. However, since the α-phase liquidus and solidus are reasonably well established, free energies along the solidus can be calculated from the liquid data and the principle that partial molar free energies (or activities) of

(6) M. Hansen and K. Anderko, "Constitution of Binary Alloys," 2nd Edition, McGraw-Hill Book Co., Inc., New York, N. Y., 1958.

(7) H. Seltz and B. J. DeWitt, *J. Am. Chem. Soc.*, **61**, 2594 (1939).

(8) J. F. Elliott and J. Chipman, *ibid.*, **73**, 2682 (1951).

(9) V. N. Eremenko and O. M. Eremenko, *Ukrain. Khim. Zhur.*, **18**, 232 (1952).

(10) M. Kawakami, *Sci. Repts., Tohoku Imp. Univ.*, **19**, 521 (1930).

(11) W. Oelsen, F. Johannsen and A. Podgornik, *Z. Erzbergbau Metallhuttenw.*, **9**, 459 (1956).

(12) F. Wüst and R. Durrer, *Forsch. Gebiete Ingenieurw.*, **241**, 3 (1921).

each component are equal across the two-phase region when referred to the same standard state.

The change in reference state requires an evaluation of the free energies of melting of the pure components at the temperatures concerned. This may be done with fair certainty in the case of Pb as its entropy of fusion (1.89 e.u.) is accurately known and the liquidus temperatures lie within 0 to 75° of its melting point. The change of reference state involves some problems in the case of Sb, however, as its entropy of fusion is not well established. However, the liquid alloy at the eutectic temperature and composition is in equilibrium with nearly pure Sb. Taking the concentration of Sb in the Sb-rich solid phase to be 98 at. % and assuming Raoult's law, $\Delta\bar{F}_{Sb} = -22$ cal./g.-atom in the coexisting liquid phase referred to solid Sb. If the average entropy of fusion of Sb between 525°K. and the melting point, 903°K., is assumed to be 5.39 e.u., this value of $\Delta\bar{F}_{Sb}$ at 525°K. will be in accord with the tabulated values of $\Delta\bar{F}_{Sb}$ and $\Delta\bar{S}_{Sb}$ for the liquid state, assuming $\Delta\bar{C}p_{Sb} = 0$. Since this entropy of fusion is in reasonably good agreement with the scattered experimental values, it was adopted in referring liquid free energies to the solid components as standard states.

Hence, partial molar free energies for Pb and Sb in the α-phase can be calculated along the solidus. By assuming Kopp's law of additivity of heat capacities, it is now possible to calculate the thermodynamic functions for all temperatures and compositions. The $\Delta\bar{H}$ values experimentally determined at 525°K. also apply at the solidus temperatures; hence values of $\Delta\bar{S}$ along the solidus may be calculated from $\Delta\bar{F}$ and $\Delta\bar{H}$ for each component. These $\Delta\bar{S}$ values are valid at all temperatures. Slight adjustments are necessary to fulfill the Gibbs–Duhem conditions; Raoult's law applies to Pb and Henry's law to Sb well within experimental error. Results calculated for 525°K. are summarized in Table III.

Along the α-phase solvus line, where there is equilibrium with nearly pure Sb, $\Delta\bar{F}_{Sb}$ should lie between 0 and −22 cal./g.-atom. For the tabulated values and Hansen's phase diagram, this is not quite the case. Agreement is obtained only if slightly larger solubilities of Sb in Pb are assumed (the maximum increase being about 0.5 at. % Sb at 220°). The solvus curve given by Hansen[6] is based solely on the solubility measurements of Obinata and Schmid[13] except at the eutectic temperature where the value (5.8 at. % Sb) of Pellini and Rhines,[14] derived from solidus measurements, is accepted. Since a straightforward extrapolation of Obinata and Schmid's solubilities to the eutectic would lead to a smaller value (5.0 at. % Sb), it seems possible that all their solubilities may be low, in agreement with these calculations, due perhaps to precipitation in their quenched samples before X-raying.

Table III

Solid α-Phase Alloys at 525°K.

$(1-x)\ Pb_{(s)} + xSb_{(s)} = [Pb_{1-x}\ Sb_x]_{(s)}$

x_{Sb}	ΔF, cal./g.-atom	ΔH, cal./g.-atom	ΔS, e.u.	a_{Pb}	a_{Sb}
0.01	−30	65	0.18	0.990	0.169
.02	−45	125	.32	.980	.338
.03	−50	190	.46	.970	.507
	(±10)	(±20)	(± .04)	(± .010)	(± .024)
.04	−60	250	.59	.960	.676
.05	−60	315	.71	.950	.845
.058	−60	365	.81	.942	.980

Discussion

The excess partial molar entropy found here for Sb in the α-phase, independent of composition, is $\Delta\bar{S}^{xs}_{Sb} = 6.38 \pm 0.21$ e.u. While this value is less than that obtained previously from the liquid data and phase diagram alone, it is still much larger than those usually encountered (0-1 e.u.) in similar eutectic systems. It seems likely that the large positive contribution to $\Delta\bar{S}^{xs}_{Sb}$ is at least partly due to an increase in the vibrational entropy of Sb in the lattice of the Pb-rich solution over that in the pure metal. The "looser" nature of the Pb lattice is suggested by the high entropy of pure Pb at 525°K. which is about 4.8 e.u. higher than that of Sb at the same temperature. That the vibrational entropy of pure solid Sb is abnormally low is indicated by its large entropy of fusion, 5.39 e.u., which is about 3 e.u. larger than for most other metals. The relatively high value of $\Delta\bar{H}_{Sb}$, 6300 cal./g.-atom, may also partly result from the absorption of increased vibrational energy.

(13) I. Obinata and E. Schmid, *Metallwirtschaft*, **12**, 101 (1933).

(14) W. S. Pellini and F. N. Rhines, *Trans. AIME*, **152**, 65 (1943).

DISSOCIATION CONSTANTS OF TARTARIC ACID WITH THE AID OF POLARIMETRY[1]

BY LEONARD I. KATZIN AND ELSIE GULYAS

Chemistry Division, Argonne National Laboratory, Argonne, Illinois

Received May 26, 1960

With the aid of optical rotation determinations at 5461 Å., the dissociation constants of tartaric acid (0.2 M) are shown to be $K_1 = 1.8 \times 10^{-3}$ and $K_2 = 1.0_3 \times 10^{-4}$, respectively, with systems containing 0.4 N Na^+. The specific rotations $[\alpha]$, based on the weight of tartrate ion, T^{--}, for tartaric acid, bitartrate ion and tartrate ion are, respectively, 12.7, 35.3 and 48.1° at 5461 Å. The contribution of salting-out of the undissociated acid to the activity coefficients of the component ions is pointed out. Grounds are given for considering the possibility that the dissociation constant itself is a function of solution composition, particularly the cation composition.

In the course of other studies, it became necessary to observe the effect of pH on the optical rotation of tartrate over the pH range, 0 to 11. Inasmuch as the rotations of undissociated tartaric acid and of tartrate ion, at the wave length investigated, differed by almost a factor of 4, and were determined in general to better than 1% precision, it was realized that it should be possible to extract from the data both the rotation of the intermediate bitartrate ion and a verification of the dissociation constants of tartaric acid. This work is being published because on closer investigation of the data the procedure proved not only to be a sensitive way of determining these dissociation constants, but the values found to fit our data, namely, $K_1 = 1.8 \times 10^{-3}$ and $K_2 = 1.0_3 \times 10^{-4}$ (0.4 N in Na^+), differ considerably from values encountered in the literature. The cation concentration is specified in this way because it is well known that the optical rotation of tartrate is a marked function not only of concentration but of the cation accompanying it. It is also possible, as will be discussed below, that the same factors which affect the optical rotation may also affect the acid strength (dissociation constant).

Experimental

A stock solution was made containing 0.2000 formula weight of chemically pure sodium tartrate per liter. Portions of this were adjusted in pH by the addition of concentrated nitric acid (or NaOH, when required), and the necessary corrections were made for the small volume change. The pH of the solution was measured with the Beckman Model G pH meter to a precision estimated at ±0.02 unit. For measurements in the acid range the pH meter was adjusted with pH 4.00 buffer, and in the alkaline range with pH 7.00 buffer. The electrodes were repeatedly rinsed with the sample solution until constant readings were obtained. The optical rotation at 5461 Å. was measured with the Rudolph Photoelectric Spectropolarimeter, using a 10.0 cm. jacketed polarimeter tube through which water at 25 ± 0.1° was circulated. Some 5–10 readings on each solution were averaged. The reproducibility of the rotation readings was about ±0.002° for both experimental and blank solutions, which amounts to about ±0.1° in the specific rotations, $[\alpha]$, derived.

Results

The results are shown in Fig. 1. For comparison with the experimental values of $[\alpha]$, the curve gives the specific rotations calculated using $K_1 = 1.80 \times 10^{-3}$, $K_2 = 1.03 \times 10^{-4}$, $[\alpha]_{H_2T} = 12.7°$, $[\alpha]_{T^-} = 48.1°$ and $[\alpha]_{HT^-} = 35.3°$. The specific rotations were calculated on the basis of the weight of tartrate *ion*, $T^=$, in the species indicated. The contribution of each species to the total rotation at a given pH was the product of the corresponding specific rotation and the fraction of the total tartrate present in that form. The last was given by the equations

$$(T^=)/C = K_1K_2/F \quad (1a)$$

$$(HT^-)/C = K_1(H^+)/F \quad (1b)$$

$$(H_2T)/C = (H^+)^2/F \quad (1c)$$

where C is the sum of the concentrations of the undissociated acid, bitartrate and tartrate ions, and

$$F = K_1K_2 + K_1(H^+) + (H^+)^2 \quad (2)$$

These relations were derived algebraically from the usual expressions for the dissociation constants, and the definition of C. In the calculations the difference between the hydrogen ion concentration used in the equations and the hydrogen ion activities as obtained from pH measurement is ignored.

The quantities $[\alpha]_{H_2T}$ and $[\alpha]_{T^-}$ were determined by the necessity of matching the experimental rotations in the regions of complete association and complete dissociation, respectively, and were therefore approximately fixed by the data. Values for K_1 and K_2 were chosen, and the three quantities of equations 1 computed. For those pH values for which $(HT^-)/C$ was equal to or greater than 0.2, the difference between the experimental rotation and that ascribable to $H_2T + T^=$, when divided by $(HT^-)/C$, gave a tentative value for $[\alpha]_{HT^-}$. The average was taken of the 25–30 such $[\alpha]_{HT^-}$ values. From the three $[\alpha]$ values and the fraction of total tartrate present as each species, the total expected rotation for each pH was computed, and compared with the experimental value. The magnitude and direction of systematic deviations dictated the choice of dissociation constant values for the next approximation, and these in turn gave the corresponding value of $[\alpha]_{HT^-}$. Two fairly sensitive criteria were available by which goodness-of-fit could be judged: the absence of systematic deviations from the experimental rotations, and the absence of systematic deviations in the series of $[\alpha]_{HT^-}$ values, which should be constant within experimental error if the dissociation constants were correctly chosen. With respect to the uncertainties in the values chosen for computing the curve in Fig. 1, it can be said that a K_1 of 1.8×10^{-3} gave a detectably better numerical match to the data than 1.7×10^{-3}; that it was not clearly certain whether 1.00×10^{-4} gave a worse numerical fit than 1.03×10^{-4} for K_2; and that with these values of K_1 and K_2, 17 out of 31 $[\alpha]_{HT^-}$ values fell

(1) Based on work performed under the auspices of the U. S. Atomic Energy Commission.

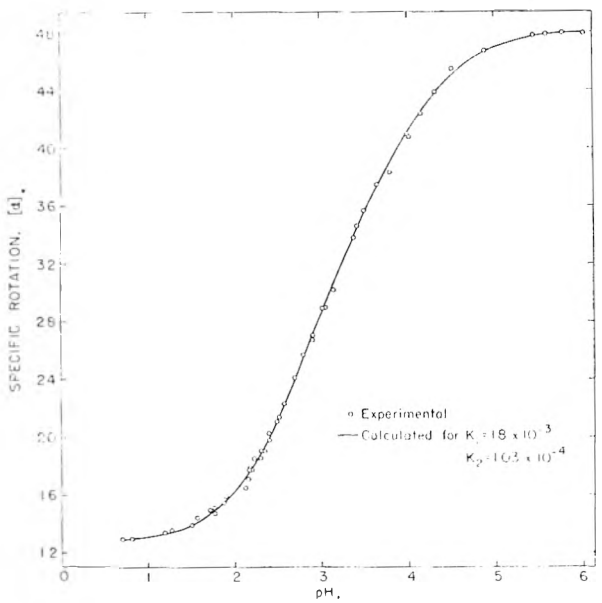

Fig. 1.—The variation of the specific rotation of 0.2000 *M* sodium tartrate solution with *p*H.

within ± 0.4° of the mean value, 35.3°. (With $K_2 = 1.00 \times 10^{-4}$, 15 out of 31 $[\alpha]_{HT}$ - values were within ±0.4° of the mean.) Of some 50 points for which experimental and calculated rotations are compared in Fig. 1, some three-quarters agreed within ±0.1° (the reproducibility expected of the rotation readings) or within the ± 0.02 unit reliability of the *p*H readings, which in the *p*H 3 region might mean ± 0.3°. The remaining quarter, with gross deviations (equally negative and positive), dated from a period in the measurements, which had been accumulated over a considerable period of time, when the *p*H meter was behaving erratically. These points were not so obviously "off" that they could be discarded out of hand.

Discussion

There is a considerable number of papers in the literature which contain values for one or another of the dissociation constants of tartaric acid. Reference to a number of them can be found in the papers of Jones and Soper,[2] and Bates and Canham.[3] Values closest to those fitting our data are given by Britton[4] and Britton and Jackson,[5] with $K_1 = 1.2 \times 10^{-3}$ and $K_2 = 1.0 \times 10^{-4}$. Most other values for K_1 are in the range $0.9–1.0 \times 10^{-3}$ while the K_2 values scatter from 1 to 10×10^{-5}.

Many of the literature values are admittedly approximate. A number of the determinations differ from ours in being aimed to give dissociation constants at infinite dilution, and therefore may be expected to yield different values. An important difference must be noted between the usual salt effects on strong electrolytes, which is assumed in these papers and the situation when a weak electrolyte is involved.

If one has, say, an HCl solution of *p*H 2.0, and adds to this NaCl to, say, 0.4 *M*, the *p*H will be expected to *increase* slightly. This is because activity coefficients tend to decrease with concentration for these salt systems, until concentrations became greater than 0.5 molal. We have found the *p*H of 0.2 *M* tartaric acid to be 1.90; the inclusion of $NaNO_3$ or NaCl to 0.4 *M lowers* the *p*H to 1.74. This difference from the behavior of the HCl solution cited is to be ascribed to the salting-out of the undissociated organic acid molecule, a well-known effect. The activity of the undissociated acid is raised, and therefore the value of the ion activity product in equilibrium with it is also increased. The decrease in *p*H is evidence of this effect. This behavior of tartaric acid with salt has been known for a long time (*e.g.*, Britton and Jackson,[5] Kolthoff and Busch[6]) and in fact the corresponding explanation was given[6] in 1928. This explanation does not, however, face the question of a possible change in dissociation constant of the acid, a question which will be returned to later.

As was pointed out in connection with the iodine–iodide–triiodide equilibrium,[7] whenever a neutral component is involved which is subject to salting-out, the activities and the activity coefficients of the ions in equilibrium with it are elevated somewhat in parallel. This can be such as to override normal ionic strength relations of activity coefficients and to invalidate calculations in which these "normal" relations are assumed. This may well be one of the factors in the discrepancies between different determinations of the second dissociation constant for tartaric acid, even when apparently done by the same sensitive techniques insofar as *p*H determination goes. In all instances, extrapolations to zero ionic strength are involved in which activity coefficient relations are assumed (*e.g.*, Bates and Canham,[3] Sartori, Costa and Camus[8]). The details of the assumed activity coefficient relations may well determine the differences in extrapolation.

The value for K_1 calculated from the *p*H data given above for 0.2 *M* solution is 0.91×10^{-3} in the absence of salt, and 1.82×10^{-3} with 0.4 *M* sodium salt added. ($K_1 = (H^+)^2/(0.20 - (H^+))$). Bates and Canham[3] give a K_1 value of 0.92×10^{-3}. Therefore the salt effect alone will account for the difference in the K_1 value obtained by us and that of the Bureau of Standards determination for infinite dilution. Our value for K_2 differs from theirs by a factor of about 2.4. The difference in the K_2 values may be due additionally to their extrapolations involving the tartrate ion activities. More direct comparisons with the earlier data[3] are impossible since they do not contain determinations at two or more *p*H values for the same salt (cation) concentration. Such data would permit explicit evaluation of both dissociation constants for a fixed salt concentration by use of the equation[9]

(2) I. Jones and G. G. Soper, *J. Chem. Soc.*, 1836 (1934).

(3) R. G. Bates and R. G. Canham, *J. Research Natl. Bur. Standards*, **47**, 343 (1951).

(4) H. T. S. Britton, *J. Chem. Soc.*, 1896 (1925).

(5) H. T. S. Britton and P. Jackson, *ibid.*, 998 (1934).

(6) I. M. Kolthoff and W. Busch, *Rec. trav. chim.*, **47**, 861 (1928).

(7) L. I. Katzin and E. Gebert, *J. Am. Chem. Soc.*, **77**, 5814 (1955).

(8) G. Sartori, G. Costa and A. Camus, *Ann. chim. (Rome)*, **42**, 205 (1952).

(9) Activity coefficient terms aside, Bates and Canham's equations 2 and 3, or 4 and 3, reduce to our relation above (the sign of m_{H_2Tar}, as it appears in their equation 3, is incorrect); Sartori, Costa and Camus[8] also use an equivalent equation.

$$K_1K_2 = K_1a_{H^+}\left[\frac{C - B + a_{H^+}/f^{\pm}}{B - a_{H^+}/f^{+}}\right]f^{-}/f^{-} + a^2_{H^+}\left[\frac{2C - B + a_{H^+}/f^{\pm}}{B - a_{H^+}/f^{+}}\right]f^{=}/f^{0}$$

The symbols f^0, f^-, $f^=$ represent the activity coefficients of the undissociated acid, bitartrate and tartrate ions respectively, f^+ that of the proton. The symbol C is the sum of tartrate species as before and

$$B = (H^+) + (HT^-) + 2(H_2T) = (HT^-)_{initial} + 2(H_2T)_{initial}$$

Such a set of determinations would be valuable in tracing the actual course of the activity coefficients of the several species with concentration and with salt cation.

As pointed out by Kolthoff and Busch,[6] the salt effect on tartaric acid dissociation may be due to activity effects alone, but there also exists the possibility of some real alteration of the dissociation constant itself. Though these workers chose to attribute the whole effect to activity change, the second alternative cannot be ruled out. As is now well-known[10-12] optical rotation is related to the existence of absorption peaks in the far ultraviolet. Alterations in rotation are to be related to changes in the wave length and relative intensity of these absorptions. Such changes infer alterations in the energy levels of the molecule, and therefore possibly in the binding of the acidic protons to the carboxylate oxygens in the case of tartrate. It is therefore possible that there may in fact be changes in the dissociation of the acid under the influence of salts, and in a manner specific to the cations, as is true of the optical rotatory effects themselves. Extension of this to other weak acids with electron-donor groups is obvious.

(10) E. U. Condon, *Rev. Mod. Phys.*, **9**, 432 (1937).
(11) W. Kuhn and E. Braun, *Z. physik. Chem.*, [B] **8**, 445 (1930).
(12) W. Moffitt and A. Moscowitz, *J. Chem. Phys.*, **30**, 648 (1959).

METAL COMPLEXING BY PHOSPHORUS COMPOUNDS. II. SOLUBILITIES OF CALCIUM SOAPS OF LINEAR CARBOXYLIC ACIDS[1]

BY R. R. IRANI AND C. F. CALLIS

Monsanto Chemical Company, Research Department, Inorganic Chemicals Division, St. Louis 66, Mo.

Received May 31, 1960

Solubility products of calcium soaps of linear carboxylic acids from C_8 to C_{18} are reported from measurements of the competition for the calcium between the insoluble soap and the soluble calcium tripolyphosphate complex. Data are given for various temperatures and ionic strengths. For the saturated soaps, the negative logarithm of the thermodynamic solubility product at 25°, $p[K_{sp}]_\infty$, is related to the number of carbons in the soap chain by the equation $p[K_{sp}]_\infty = -2.63 + 1.24$ (No. of Carbons). The unsaturated linear calcium soaps, oleate and linoleate, were significantly more soluble than calculated from the expression for the saturated soaps.

Introduction

One of the techniques for measuring complexity constants is to use a nephelometric end-point for determining the competition for the metal ion between complexing and precipitating anions. In a previous paper,[2] this procedure was utilized to measure the complexity constants of calcium with linear polyphosphates, using measured values of the solubility product of calcium oxalate.

In the present study, the reverse is done; linear carboxylate anions are made to compete with the tripolyphosphate anion in tying up calcium, in order to measure the solubility product of these calcium soaps.

Experimental

Chemicals.—Sodium tripolyphosphate hexahydrate was used as the source of tripolyphosphate anions. It was prepared by four repeated fractional crystallizations of commercial sodium tripolyphosphate from aqueous solutions of ethyl alcohol. The final sample analyzed to better than 99.7% $Na_5P_3O_{10}$. Tetramethylammonium tripolyphosphate was prepared by ion exchanging the sodium salt with the hydrogen form of 100–200 mesh Dowex 50W-X2 and neutralizing the resulting acid immediately with tetramethylammonium hydroxide, as previously described.[3] The stock solution was maintained at 25° and a *p*H of 12 to avoid hydrolytic degradation.

The C.P. grade hexanoic, octanoic, decanoic, lauric, myristic, palmitic, stearic and oleic acids were obtained from Eastman Kodak. The C.P. grade heptanoic, undecylic and linoleic acids were purchased from Matheson, Coleman and Bell. The nonanoic acid was technical grade from Matheson, Coleman and Bell. The tridecylic acid was obtained from the K and K Labs., Jamaica, New York. The acids were converted to tetramethylammonium derivatives by neutralization with Eastman Kodak reagent grade tetramethylammonium hydroxide.

Other chemicals were C.P. grade.

Procedure.—The nephelometric titrations were carried out at a *p*H of 12 using the same procedure previously described[2] except for temperature control and precipitating anions. In the present experiments, temperature was controlled to ± 0.1° using a heater in combination with a heat-sensing Thermotrol unit, manufactured by Hallikainen Instruments, Berkeley, California. The concentrations of the calcium-precipitating anions, the linear carboxylates, were chosen below the critical micelle concentration, and such that the competition for calcium with tripolyphosphate was favorable. In addition, no P_2O_5 was detected in the precipitates formed upon addition of a slight excess of Ca^{++} to the solution containing $P_3O_{10}^{-5}$ and linear carboxylate anions.

The ionic strengths were adjusted to the desired values using tetramethylammonium bromide.

Results and Discussion

The raw data showing the number of cc. of a calcium solution that must be added to a solution containing tripolyphosphate and linear carboxylate

(1) Presented before the Division of Inorganic Chemistry, 138th Meeting of the American Chemical Society, New York, September 1960.
(2) R. R. Irani and C. F. Callis, THIS JOURNAL, **64**, 1398 (1960).
(3) J. R. Van Wazer, E. J. Griffith and J. F. McCullough, *J. Am. Chem. Soc.*, **77**, 287 (1955).

anions to reach a point of incipient precipitation, are given in Table I.

TABLE I

SUMMARY OF DATA FOR THE Ca^{++}–$P_3O_{10}^{-5}$–LINEAR CARBOXYLATE SYSTEMS[a]

Temp., °C.	Tripolyphosphate, M ($C_1 \times 10^3$)	Linear carboxylate, M (C_2)	Cc. of 8.86×10^{-2} M Ca^{++} soln. (y) to nephelometric end-point at ionic strengths of 0.1	1.0
		Heptanoate (7)		
25	2.23	0.416	3.92[b]	..
		0.498	4.15[b]	..
		Octanoate (8)		
25	2.23	0.208	5.98[c]	5.87[d]
		0.277	5.65[c]	5.28[d]
		Nonanoate (9)		
25	2.23	3.16×10^{-2}	5.2	..
		3.79×10^{-2}	4.8	..
	1.94	3.79×10^{-2}	..	4.6
37	1.94	2.53×10^{-2}	4.79	..
		3.79×10^{-2}	4.00	..
50	1.94	2.53×10^{-2}	4.82	..
		3.79×10^{-2}	4.43	..
		Decanoate (10)		
25	2.33	1.16×10^{-2}	6.20	5.75
		1.74×10^{-2}		
		Undecylate (11)		
25	2.23	1.21×10^{-3}	6.11	..
		2.42×10^{-3}	..	5.75
		3.63×10^{-3}	..	4.85
		2.16×10^{-3}	..	5.90
	2.90	3.23×10^{-3}	..	7.37
37	1.94	6.44×10^{-3}	4.49	..
		8.04×10^{-3}	4.30	..
50	1.94	5.36×10^{-3}	5.24	..
		6.44×10^{-3}	5.20	..
		8.04×10^{-3}	5.04	..
		Laurate (12)		
25	2.33	5.0×10^{-4}	6.03	5.50
		1.0×10^{-3}	4.96	3.56
37	1.94	2.0×10^{-3}	3.73	..
		3.0×10^{-3}	2.58	..
50	1.94	2.0×10^{-3}	5.11	..
		3.0×10^{-3}	4.51	..
		Tridecylate (13)		
25	2.23	1.86×10^{-4}	5.29	..
		2.33×10^{-4}	4.86	..
		3.27×10^{-4}	4.40	..
	2.90	2.33×10^{-4}	5.89	4.04
		3.27×10^{-4}	..	2.40
		Myristate (14)		
25	2.33	4.37×10^{-5}	5.36	4.30
		8.74×10^{-5}	3.40	1.92
		1.31×10^{-4}	2.27	0.95
37	1.94	0.84×10^{-4}	3.98	..
		1.67×10^{-4}	2.45	..
50	1.94	0.84×10^{-4}	4.91	..
		1.67×10^{-4}	3.68	..
		Palmitate (16)		
25	2.33	7.62×10^{-6}	1.57	1.56
		1.15×10^{-5}	0.86	0.55
		Oleate (unsat. 18)		
25	2.33	3.53×10^{-5}	4.61	..
		7.06×10^{-5}	2.53	3.37
		1.06×10^{-4}	1.17	2.92
		Linoleate (double unsat. 18)		
25	2.33	3.57×10^{-4}	0.69	..
		1.43×10^{-4}	2.69	3.74
		2.14×10^{-4}	1.58	3.18
		2.86×10^{-4}	..	2.92

[a] Total volume of solution was always 250 cc. [b] Ionic strength = 0.56. [c] Ionic strength = 0.35. [d] Ionic strength = 1.25.

For any ionic strength and temperature at a pH of 12 and a nephelometric end-point[2]

$$\frac{K_{sp}}{\beta_{CaP_3O_{10}^{-3}}} = \frac{C_2^2}{(C_A/yz - 1)} \quad (1)$$

where K_{sp} is the solubility product of the calcium soap

$$K_{sp} = (Ca^{++})(CH_3(CH_2)_nCOO^-)^2 \quad (2)$$

and $\beta_{CaP_3O_{10}^{3-}}$ is the complexity constant, A is the

$$\beta_{CaP_3O_{10}^{3-}} = \frac{(Ca^{++})(P_3O_{10}^{5-})}{(CaP_3O_{10}^{3-})} \quad (3)$$

volume of the solution in cc., C_2 and C_1 are the molar concentrations of the linear carboxylate and tripolyphosphate anions, respectively, and z and y are the molar concentration and cc. of calcium to the nephelometric end-point, respectively.

Using the known[2,4] values of $\beta_{CaP_3O_{10}^{3-}}$ the data in Table I were interpreted with equation 1 to give the apparent solubility products given in Table II. The uncertainties shown as ± are statistical 95% confidence limits.

TABLE II

SOLUBILITY PRODUCTS OF CALCIUM SOAPS

Calcium soap	Temp., °C.	Neg. log solubility product at ionic strength of 0.1	1.0	0.0[a]
Heptanoate	25	6.12 ± 0.05[b]	.....	6.3 ± 0.2
Octanoate	25	6.16 ± .03[c]	5.50 ± 0.07[d]	6.40 ± .06
Nonanoate	25	8.79 ± .04	.....	9.10 ± .06
	37	8.69 ± .04	.....	9.00 ± .06
	50	8.53 ± .04	.....	8.84 ± .06
Decanoate	25	9.10 ± .1	8.47 ± .02	9.32 ± .15
Undecanoate	25	10.64 ± .13	9.90 ± .03	10.90 ± .18
	37	10.00 ± .04	.....	10.31 ± .06
	50	9.38 ± .04	.....	9.69 ± .06
Laurate	25	11.93 ± .02	11.27 ± .02	12.16 ± .04
	37	11.49 ± .02	.....	11.80 ± .04
	50	10.74 ± .08	.....	11.05 ± .10
Tridecylate	25	13.14 ± .10	12.68 ± .03	13.30 ± .15
Myristate	25	14.46 ± .03	13.88 ± .06	14.66 ± .15
	37	14.01 ± .05	.....	14.32 ± .08
	50	13.49 ± .02	.....	13.80 ± .04
Palmitate	25	17.10 ± .02	16.18 ± .07	17.42 ± .04
Oleate	25	14.94 ± .06	13.54 ± .1	15.42 ± .08
Linoleate	25	14.20 ± .01	12.75 ± .09	14.69 ± .03

[a] Extrapolated. [b] Ionic strength = 0.56. [c] Ionic strength = 0.35. [d] Ionic strength = 1.25.

The solubility products at infinite dilution, $[K_{sp}]_\infty$, were estimated using the relation

$$pK_{sp} = p[K_{sp}]_\infty + a\sqrt{\mu} \quad (4)$$

where μ is the ionic strength. It was found that the ratio of the solubility products at ionic strengths of 0.1 and 1.0 was fairly independent of the specific soap. This justified extrapolation for calcium

(4) J. I. Watters and S. M. Lambert, *J. Am. Chem. Soc.*, **81**, 3201 (1959).

soaps, *e.g.*, nonanoate, for which no data at $\mu = 1$ were collected. In all cases, the activity coefficient correction factors were much smaller than the actual values, so that no serious errors were introduced by using equation 4 rather than the extended Debye–Hückel relation.[5]

The thermodynamic solubility products for the saturated soaps, $Ca[CH_3(CH_2)_nCOO]_2$, at 25°, shown in Fig. 1, were found to fit the semiempirical equation proposed by Skau and Boucher.[6] Specifically, it was found that

$$p[K_{sp}]_\infty = \text{neg. log. of thermodynamic } K_{sp} = -2.63 + 1.24 \times (\text{No. of Carbons}) \quad (5)$$

The solubility data for the saturated linear soaps at 25°, fit equation 5 with a standard deviation of ± 0.34 pK_{sp} unit, immaterial of whether the chain length of the soap was even or odd. The solubility product values at 25° for calcium oleate and calcium linoleate, also shown in Fig. 1, lay significantly below those for the saturated calcium soaps, presumably due to unsaturation in the chain.

The solubility products from this work are more precise than those obtained by Yoke[7] on calcium palmitate, laurate and oleate using radio-tracer techniques. However, the two sets of data agree within experimental error.

Solubility product measurements for calcium soaps of saturated linear carboxylic acids having chain lengths of 6 or lower, or 18 or higher, were not possible with the technique used in this work due to unfavorable competition with the tripolyphosphate anion; the former gave too weak, and the latter too strong a competition. Nevertheless, the estimated values at 25° would lie very close to the line shown in Fig. 1. This implies that under experimental conditions in the presence of Ca^{++} and immaterial of the relative concentrations of all species, presence of $P_3O_{10}^{-5}$ would prohibit $Ca[CH_3(CH_2)_4COO]_2$ precipitation, but cannot solubilize $Ca[CH_3(CH_2)_{16}COO]_2$.

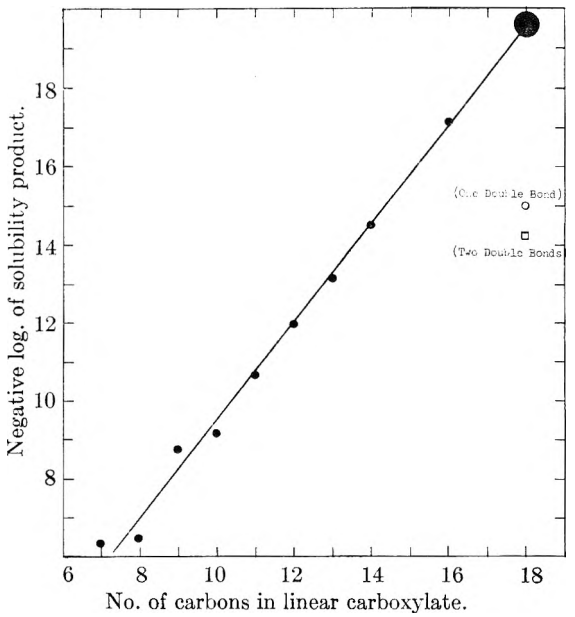

Fig. 1.—Thermodynamic solubility products of calcium soaps at 25°: ●, $Ca[CH_3(CH_2)_nCOO]_2$; ○, calcium oleate (one double bond); □, calcium linoleate (two double bonds).

The solubility product data at various temperatures fit the equation

$$\frac{d \ln K_{sp}}{dT} = -\frac{\Delta H}{RT^2} \quad (6)$$

where ΔH is the heat of solution of the precipitate in water at infinite dilution. The values of ΔH for calcium undecanoate, laurate and myristate were calculated to be − 22.2 ± 0.8, − 19.8 ± 5 and −15.8 ± 3.6 kcal./mole, respectively. For precipitation of calcium nonanoate, the value of ΔH was found to be − 4.7 ± 1.2 kcal./mole, significantly lower than that determined for the other calcium soaps. Since the nonanoic acid was the only technical grade material, no valid arguments for the discrepancy can be presented.

(5) H. S. Harned and B. B. Owen, "The Physical Chemistry of Electrolytic Solutions," Reinhold Publ. Corp., New York, N. Y., 1950, 2nd ed., p. 121.

(6) E. L. Skau and R. E. Boucher, THIS JOURNAL, **58**, 460 (1954).

(7) J. T. Yoke, *ibid.*, **62**, 753 (1958).

NUCLEAR MAGNETIC RESONANCE STUDIES OF HYDROGEN BONDING. II. ALCOHOLS

BY JEFF C. DAVIS, JR.,[1] KENNETH S. PITZER[2] AND C. N. R. RAO

Department of Chemistry and Lawrence Radiation Laboratory, University of California, Berkeley, California

Received June 3, 1960

The proton magnetic resonance spectra of solutions of methanol, ethanol, 2-propanol and *t*-butyl alcohol in carbon tetrachloride and of ethanol in benzene have been measured over the temperature range 20–60°. The shifts δ in very dilute solutions yield values of δ_M for the monomeric alcohols. Finite values of $(\partial\delta/\partial x)$ at zero mole fraction are obtained which clearly indicate the presence of a dimeric species. The relationships between these data and the equilibrium constants and enthalpies of dimerization are discussed, but the probable presence of both cyclic and open dimers complicates the interpretation. For ethanol in benzene, where open dimers are believed to predominate, the enthalpy of dimerization is found to be 5.1 ± 1 kcal./mole of dimer. Only qualitative comments are made concerning the results in concentrated solution where many polymeric species are present.

Many physical methods have been used to investigate association of alcohols by hydrogen bonding. A complete review of the very extensive literature is both impractical and unnecessary in view of the recent monograph by Pimentel and McClellan.[3] Although a number of n.m.r. investigations have concerned the alcohols, it is desirable to cover a wider temperature range in order to yield information about the various species present. The present investigation was undertaken as a systematic study of the chemical shifts at different concentrations and temperatures with the purpose of broadening the application of n.m.r. techniques to these systems and with the aim of elucidating the nature of the various species and the characteristics of the equilibria.

Experimental

The purification and handling of the reagents have been reviewed previously.[4] All of the alcohols were distilled twice from calcium hydride to remove traces of water. All of the solutions were made by dilution of gravimetrically prepared stock solutions.

Shifts were measured at 60 Mcps. on a Varian V4300B High Resolution NMR Spectrometer utilizing special apparatus constructed for maintaining the desired sample temperatures as previously described.[4] Shifts were measured by the side-band technique.[5] Some shifts were measured by means of known fine splittings of adjacent or superimposed peaks as, for example, when the ethanol OH peak was located inside the CH_3 triplet. Shifts were measured to an accuracy of ± 0.5 c.p.s. and each reported shift is the result of at least six separate measurements.

Experimental Results

The chemical shifts of the hydroxyl protons of methanol, ethanol, isopropanol and *t*-butyl alcohol in CCl_4 and of ethanol in benzene are listed in Tables I–V. The symbol x designates the total apparent mole fraction of alcohol in the solution assuming no association. Shifts are reported in cps measured at 60 Mcps. A positive shift indicates that the hydroxyl resonance occurs at a higher applied magnetic field than that of the reference peak. In all cases the centers of the methyl group resonance were used as references. These peaks were found to be independent of concentration by measurements with both external and internal standards.

TABLE I

CHEMICAL SHIFTS OF METHANOL IN CARBON TETRACHLORIDE SOLUTIONS

x	δ (c.p.s. at 60 Mc. from methyl peak) 23°	35°	53.5°
1.00	−92.5	−88.0	−76.1
0.742	−87.5	−79.6	−66.0
.502	−74.5	−62.9	−40.1
.249	−48.0	−28.7	8.7
.099	44.8	72.0	133.7
.077	79.1	106.1	147.0
.052	115.4	135.6	158.9
.027	145.5	145.2	167.6
.020	152.8	160.4	168.0
.016	157.0	163.0	168.9
.010	163.4	166.8	170.0
.0082	165.2	167.8	170.5
.0077	165.8	168.1	170.5
.0066	166.7	168.5	170.9
.0052	168.1	169.5	171.0
.0040	169.2	170.0	171.3
δ_M	172.9	172.2	172.1
$(\partial\delta/\partial x)_0$	950	540	200

TABLE II

CHEMICAL SHIFTS OF ETHANOL IN CARBON TETRACHLORIDE SOLUTIONS

x	δ (c.p.s. at 60 Mc. from methyl peak) 22°	39°	56°
1.00	−250.0	−241.5 (37)	−228.1 (54)
0.505	−219.8	−201.5	−176.0
.250	−200.3	−167.8	−134.0
.100	−169.0	−124.2	− 83.1
.0775	−160.1	−118.1	− 76.6
.0525	−120.0	− 77.8	− 36.3
.0270	− 32.3	4.2	6.0
.0206	− 19.0	12.1	21.0
.0165	− 9.0	16.9	23.1
.0104	4.0	23.9	27.0
.0083	7.1	25.3	28.1
.0067	13.0	27.5	29.0
.0052	16.7	29.4	29.9
.0042	18.9	30.4	30.1
δ_M	28.2	34.9	32.4
$(\partial\delta/\partial x)_0$	2250	1070	500

Monomer–Dimer Equilibrium.—There is considerable evidence that in dilute solutions of alcohols

(1) Based in part on the Ph.D. thesis of J. C. D. whose present address is Department of Chemistry, University of Texas, Austin, Texas.

(2) To whom correspondence should be directed at the above address.

(3) G. C. Pimentel and A. L. McClellan, "The Hydrogen Bond," W. H. Freeman and Co., San Francisco, Cal., 1960.

(4) J. C. Davis, Jr., and K. S. Pitzer, THIS JOURNAL, **64**, 886 (1960).

(5) J. T. Arnold and M. E. Packard, *J. Chem. Phys.*, **19**, 1608 (1951).

TABLE III

CHEMICAL SHIFTS OF ISOPROPANOL IN CARBON TETRACHLORIDE SOLUTIONS

x	δ (c.p.s. at 60 Mc. from methyl peak) 25°	36°	53.5°
1.00	−237.6	−227.0	−211.6
0.746	−235.1	−223.5	−210.0
.507	−203.9	−185.9	−161.5
.254	−166.0	−140.5	−105.8
.101	−113.8	− 82.0	− 37.6
.078	− 95.6	− 56.4	− 12.2
.053	− 86.2	− 35.0	3.1
.027	− 36.2	3.1	15.3
.021	− 10.8	12.1	18.8
.017	− 3.0	14.9	19.4
.011	11.8	17.6	20.2
.0084	13.0	19.0	20.8
.0078	13.7	19.0	20.9
.0067	14.2	19.2	21.0
.0053	15.0	19.7	21.1
δ_M	18	21.0	21.9
$(\partial\delta/\partial x)_0$	400	220	130

TABLE IV

CHEMICAL SHIFTS OF *t*-BUTYL ALCOHOL IN CARBON TETRACHLORIDE SOLUTIONS

x	δ (c.p.s. at 60 Mc. from methyl peak) 21°	37°	53°
1.00	−210.1	−190.1	−170.0
0.745	−198.0	−178.3	−156.8
.505	−168.8	−143.0	−113.1
.252	−130.0	− 96.1	− 60.0
.100	− 70.1	− 27.5	− 1.0
.078	− 34.3	− 2.0	9.2
.053	− 9.0	10.2	17.3
.027	10.0	17.1	20.0
.0206	15.1	18.9	20.9
.0165	17.5	20.1	21.6
.0104	20.0	21.3	23.0
.0083	21.0	22.2	23.2
.0078	21.4	22.4	23.5
.0067	21.9	22.6	23.6
.0053	22.6	23.1	24.0
δ_M	24.8	24.5	25.0
$(\partial\delta/\partial x)_0$	430	270	200

TABLE V

CHEMICAL SHIFTS OF ETHANOL IN BENZENE SOLUTIONS

x	δ (c.p.s. at 60 Mc. from methyl peak) 22°	37°	54°
1.00	−250.5	−242.0	−229.5
0.504	−229.0	−208.8	−185.0
.276	−201.4	−174.7	−142.2
.145	−156.7	−129.0	− 90.1
.0742	− 87.0	− 58.2	− 27.2
.0373	− 4.8	8.1	16.0
.0189	9.8	18.0	20.0
.0151	15.3	21.0	24.1
.0076	23.9	25.9	26.0
.0064	24.2	26.9	28.5
.0057	25.0	27.2	28.8
.0047	26.4	28.2	29.1
δ_M	31.0	31.2	31.3
$(\partial\delta/\partial x)_0$	1020	680	440

in non-hydrogen-bonding solvents the monomer–dimer equilibrium is of importance.[3] Huggins,

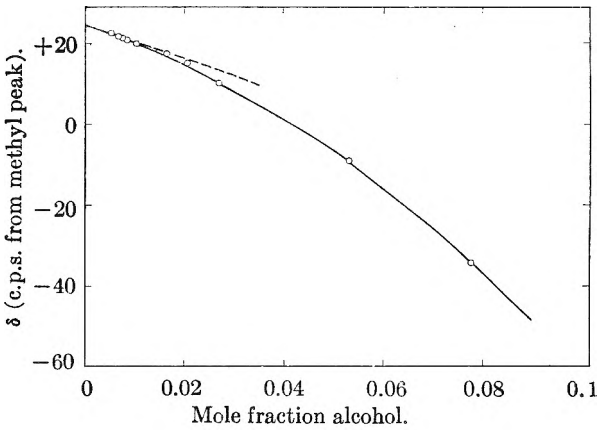

Fig. 1.

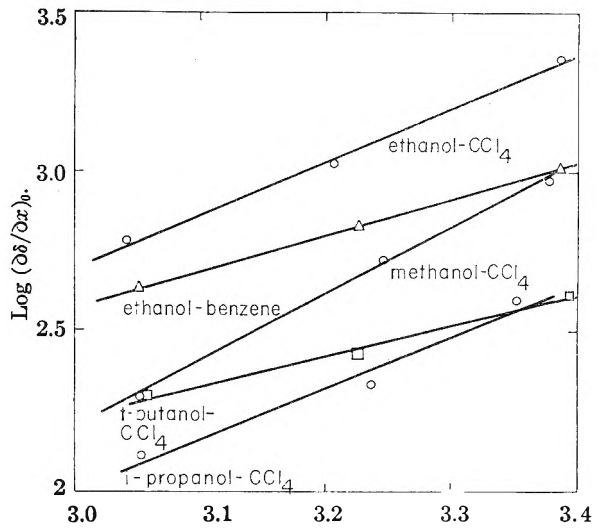

Fig. 2.

Pimentel and Shoolery[6] have shown that for a system containing only monomer and dimer in equilibrium the observed chemical shift is given by the relation

$$\delta = \frac{m}{a}\delta_M + \frac{a-m}{a}\delta_D = \delta_M + \left(1 - \frac{m}{a}\right)\Delta_D \quad (1)$$

where m is the number of moles of monomer in the solution, a is the total number of moles of alcohol used to make up the solution, δ_M and δ_D are the shifts characteristic of the monomer and dimer species, and $\Delta_D = \delta_D - \delta_M$. If the equilibrium constant for the system is expressed in mole fraction units

$$K_2 = \frac{x_D}{x_M^2} \quad (2)$$

then it can be shown that an infinite dilution

$$\left(\frac{\partial\delta}{\partial x}\right)_{x=0} = 2K_2\Delta_D \quad (3)$$

Figure 1 shows a typical set of data in the low concentration region. It is clear that a satisfactory extrapolation can be made to yield both δ_M and the slope $(\partial\delta/\partial x)_0$. Values of these quantities are given in Tables I–V. Unfortunately the pres-

(6) C. M. Huggins, G. C. Pimentel and J. N. Shoolery, THIS JOURNAL, **60**, 1311 (1956).

ence of higher polymers makes it impossible to obtain δ_D, and thereby K_2, from the n.m.r. data.

The assumption that the value of δ_D is independent of temperature, as it seems to be for certain carboxylic acids,[4] makes possible a calculation of an apparent ΔH dimerization. From equation 3 we see that, if Δ_D is constant

$$-\Delta H = R \frac{\partial}{\partial(1/T)} \ln \left(\frac{\partial \delta}{\partial x}\right)_0 \qquad (4)$$

Figure 2 shows the appropriate plot of log $(\partial\delta/\partial x)_0$ *vs.* $1/T$ and Table VI collects the apparent ΔH values. Liddel and Becker[7] measured the infrared spectra of methanol, ethanol and *t*-butyl alcohol in carbon tetrachloride at several temperatures. They assumed that the decrease in the intensity of the characteristic non-bonded O–H stretching band near 3630 cm.$^{-1}$ could be taken as a measure of dimerization in the dilute solutions, and from the temperature coefficient of this effect they obtained the apparent ΔH values which are also listed in Table VI. The agreement between the two sets of values is excellent. But we shall indicate later that these treatments are probably oversimplified and that the true ΔH of dimerization is somewhat smaller in some cases.

Table VI

Dimerization of Alcohols in Solution

	Apparent[a] ΔH, kcal./mole	
	This research	L.B.[7]
CH_3OH in CCl_4	-9.4 ± 2	-9.2 ± 2.5
C_2H_5OH in CCl_4	-7.6 ± 2	-7.2 ± 1.6
C_2H_5OH in C_6H_6	-5.1 ± 1	.....
i-C_3H_7OH in CCl_4	-7.3 ± 3[b]	.....
t-C_4H_9OH in CCl_4	-4.4 ± 2	-4.8 ± 1.1

[a] See section on Discussion for relationship to true ΔH of dimerization. [b] The effect of higher polymers so interferes that this value is particularly uncertain.

Higher Polymers.—It is clear that higher polymers are formed in even moderately concentrated solution. Saunders and Hyne[8] have treated their n.m.r. data for several alcohols on the basis of only a single type of polymer in addition to the monomer. They obtained rough agreement for a cyclic tetramer with methanol and ethanol and a cyclic trimer for *t*-butyl alcohol. However, the evidence from various sources for the presence of some dimer is incontrovertible. We tried extensions of the Saunders and Hyne treatment which considered the monomer, dimer and a single higher polymer. The inclusion of the dimer changed substantially the size of polymer yielding best agreement. But no case showed agreement within experimental error nor was this result surprising in view of the simplified assumptions.

The dielectric constant data[9] on these systems clearly show that much of the polymeric alcohol must be open ended chains rather than rings, and in that case it is unreasonable to assume a single dominant species. Consequently, we believe any realistic treatment of concentrated solutions must consider an extensive array of associated species such as Coburn and Grunwald[10] assumed in treating their infrared data on ethanol–CCl_4 solutions. Since n.m.r. data alone do not suffice to show the various species present, a proper interpretation must combine data from additional sources. It is beyond the scope of this paper to attempt such an interpretation for the higher polymers, but the present n.m.r. data should be useful in such a project.

Discussion

The shift between δ_M for the monomer and the δ-value for fully hydrogen bonded polymer appears to be roughly 280 c.p.s. for each alcohol if we assume some dissociation in the pure liquids and that this dissociation increases with temperature. There appears to be most dissociation in *t*-butyl alcohol and successively less for the smaller molecules. The reference frequency for the CH_3 protons is, of course, much lower in the case of methanol, and this increases the relative values of δ for that substance as compared to the other alcohols.

The values of δ_M show no significant change with temperature, and this result throws some additional doubt upon the large temperature change of the apparent δ_M values for certain carboxylic acids that we reported previously.[4] The very much smaller dissociation made the δ_M values of the acids much less certain than the present values for the alcohols, but the acids may associate more strongly with the solvent and hence behave differently.

There has been much discussion and speculation about the linear or cyclic nature of polymeric species of alcohols. For example, the dimer species may be either a symmetrical ring, A, with two nonlinear hydrogen bonds, or an unsymmetrical open chain, B, with a single linear hydrogen bond.

While there is good reason to believe that the linear hydrogen bond in B is stronger than one bent bond, it is not obvious whether one linear bond gives lower energy than the two bent bonds in A or not. The cyclic form would be expected to have no infrared absorption at the monomeric O–H frequency whereas the open dimer (B) would have one O–H vibration which would still absorb at approximately the monomer frequency. Likewise the n.m.r. chemical shift for the non-bonded proton in the open form would be expected to be about that of the monomer while in the cyclic form both alcohol protons would have shifts affected by the hydrogen bonding. However, only the average shift is observed for the alcoholic protons of all species and there is no independent evidence for this average value in either the open or cyclic form.

In the vapor phase the entropy and enthalpy of formation[11] of the dimer indicate the open struc-

(7) U. Liddel and E. D. Becker, *Spectrochim. Acta*, **10**, 70 (1957).

(8) M. Saunders and J. B. Hyne, *J. Chem. Phys.*, **29**, 1319 (1958), **31**, 270 (1959); see also E. D. Becker, *ibid.*, **31**, 269 (1959).

(9) K. L. Wolf, H. Frahm and H. Harms, *Z. physik. Chem.*, **B36**, 237 (1937), gives a summary of such data and references to earlier papers and to theses.

(10) W. C. Coburn and E. Grunwald, *J. Am. Chem. Soc.*, **80**, 1318 (1958).

(11) W. Weltner and K. S. Pitzer, *ibid.*, **73**, 2606 (1951); C. B. Kretschmer and R. Wiebe, *ibid.*, **76**, 2579 (1954); G. M. Barrow, *J. Chem. Phys.*, **20**, 1739 (1952).

ture, whereas at very low temperatures in inert matrices, the spectral data[12] favor cyclic structures.

There seems no doubt that cyclic tetramers and possibly pentamers, hexamers, etc., have special stability. Such a molecule can have linear hydrogen bonds and still close the ring. Coburn and Grunwald[10] fit their infrared data on dilute ethanol–CCl_4 solutions to a model of open dimers and trimers together with ring structures for higher polymers.

Nevertheless, the dielectric constant data[9] for alcohol solutions show that open chain polymers of high dipole moment dominate in moderately concentrated solutions. There is a deep minimum in the molar polarization curve for systems such as methanol or ethanol in cyclohexane at approximately 0.03 mole fraction. For ethanol in CCl_4 the minimum is less deep and lies at approximately 0.05 mole fraction. The results of Coburn and Grunwald indicate that at this concentration the cyclic polymers have become very important species, and they have, of course, small or zero dipole moments. The rise in molar polarization indicates, however, that the still larger polymer species formed at higher concentration must have large dipole moments and are presumably of open structure.

(12) M. Van Thiel, E. D. Becker and G. C. Pimentel, *J. Chem. Phys.*, **27**, 95 (1957).

It will require dielectric constant values of extreme precision for very dilute solutions to give a clear decision between open and cyclic dimers. We have not found such data in the literature. It seems to us entirely plausible that the dimeric species may be partly cyclic and partly open chain at room temperature but with the proportion of the cyclic form decreasing with rise in temperature. In this case the assumption of a constant Δ_D in the calculation of the ΔH values in Table VI is subject to question. The ΔH values calculated from the infrared data of Liddel and Becker[7] are also based upon the assumption of a single type of dimer and are likewise subject to some question. In either case, however, the difference between the true and apparent ΔH values is not likely to be very large.

In the case of ethanol–benzene solutions the molar polarization data[9] show no minimum corresponding to cyclic polymers, hence, it seems safe to assume that the dimer is predominantly open chain and the apparent ΔH value may be adopted as reliable.

Acknowledgments.—We thank Dr. George C. Pimentel for interesting discussion and many helpful suggestions. This work was performed under the auspices of the Atomic Energy Commission.

COPPER CHELATE POLYMERS DERIVED FROM TETRAACETYLETHANE[1]

BY ROBERT G. CHARLES

Westinghouse Research Laboratories, Pittsburgh 35, Pennsylvania

Received June 8, 1960

Chelate polymers have been prepared by the reaction of tetraacetylethane with copper(II) acetate in aqueous tetrahydrofuran solution. The products are crystalline and are of relatively low molecular weight with an average chain length of about five units. The polymers decompose rapidly in the temperature range 250 to 350°. They have about the same thermal stability as the structurally analogous cupric acetylacetonate. Part of the copper is reduced to the metal during the pyrolysis with the concurrent formation of tetraacetylethane. In addition to metal, the non-volatile portion of the degradation products appears to consist of highly conjugated polymeric organic materials in which some of the metal chelate ring systems are retained.

Previously reported work from this Laboratory has concerned the heat stabilities of metal acetylacetone chelates.[2,3] Because of current interest in metal chelate polymers as possible heat stable materials[4–8] it has seemed worthwhile to extend these studies to metal chelates derived from tetraacetylethane (I).

Tetraacetylethane (TAE) is capable, in its dienolic form, of reacting with divalent metal ions to form polymeric materials with the recurring unit shown in II. The recurring unit is closely similar in structure to the (non-polymeric) divalent metal acetylacetonates III. Metal-containing polymers derived from TAE, as well as from other bis-β-diketones, have been reported previously,[4a,6,9] but there has been very little information published regarding the properties of these materials.

In the present work we have prepared copper chelate polymers derived from TAE and have studied their composition and some of their properties, with particular attention to their thermal stabilities.

Results and Discussion

Preparation and Characterization.—Copper-containing polymeric materials are formed as finely

(1) Presented, in part, at the Inorganic Polymer Symposium, 136th National A.C.S. Meeting, Atlantic City, N. J., Sept. 1959.

(2) R. G. Charles and M. A. Pawlikowski, THIS JOURNAL, **62**, 440 (1958).

(3) J. von Hoene, R. G. Charles and W. M. Hickam, *ibid.*, **62**, 1098 (1958).

(4) W. C. Fernelius, Wright Air Development Center Report WADC 56-203, Part I (Oct. 1956); b., Part II (Sept. 1957); c., Part III (Feb. 1958).

(5) K. V. Martin, *J. Am. Chem. Soc.*, **80**, 233 (1958).

(6) J. C. Bailar, Jr., W. C. Drinkard, Jr., and M. L. Judd, Wright Air Development Center Report WADC 57-391 (Sept. 1957).

(7) C. S. Marvel and J. H. Rassweiler, *J. Am. Chem. Soc.*, **80**, 1197 (1958).

(8) C. S. Marvel and M. M. Martin, *ibid.*, **80**, 6600 (1958).

(9) J. P. Wilkins and E. L. Wittbecker, U. S. Patent 2,659,711 (Nov. 17, 1953).

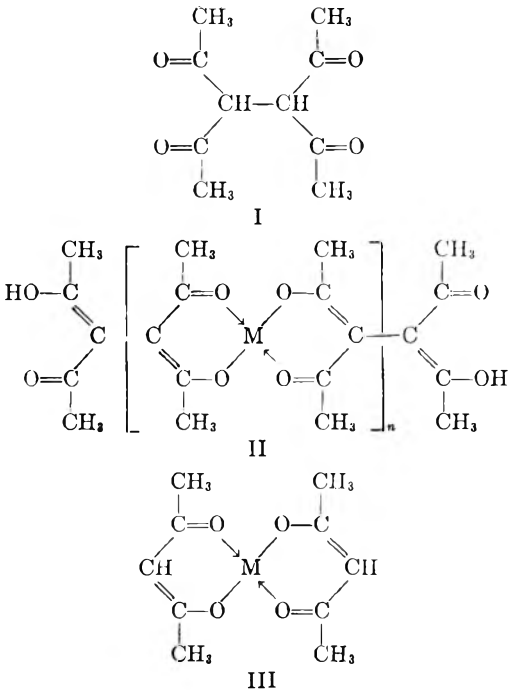

divided green precipitates when aqueous copper acetate solutions are added, at room temperature, to dilute solutions of TAE in tetrahydrofuran. The reaction can be represented by (1). With equimolar quantities of copper acetate and TAE

$$(n + 1)\mathrm{I} + n\mathrm{Cu(OCOCH_3)_2} \longrightarrow \mathrm{II(M = Cu)} + 2n\mathrm{CH_3COOH} \quad (1)$$

it was found that a significant part of the copper remained in solution while the TAE was precipitated quantitatively. It is evident from this that polymers of very high molecular weight are not formed by the procedure used since this would require equimolar quantities of copper and TAE in the precipitate.

Table I lists the yields and elemental analyses for four separate preparations, as well as the theoretical values for $n = 1$, 5 and ∞ in formula II. The experimental results are not in agreement with the values for either of the two extremes, $n = 1$ or $n = \infty$, but do agree moderately well with the calculated value for $n = 5$. It is probable that the products consist of mixtures of polymers of various chain lengths with an average value of n near 5. The molecular weight is very likely determined by the chain length necessary to produce an insoluble product under the experimental conditions used. Once precipitated, a given polymeric species would not be expected to grow further or, at least, its reactivity should be greatly reduced. With the preparative procedure used here, the average molecular weight achieved appears to be quite reproducible.

Direct measurement of molecular weight of the polymers obtained is ruled out by their insolubility. The materials were found to be insoluble in water and in all the common organic solvents. The products did not melt when heated on a melting point block to 300° but gradually decomposed at the higher temperatures.

The copper TAE polymers apparently do not form stable hydrates although two coördination positions are available for bonding water to each copper atom in II. The lack of hydrate formation is not unusual since a coördination number of four is frequently preferred by copper in the divalent state. That stable hydrates are not formed in the present case is evident from the analytical results (Table I) and from the fact that no significant weight loss occurred when the materials, airdried at room temperature, were heated at 100° and 10 mm. The presence of water was also not detectable from infrared absorption spectra.

Principal infrared absorption bands for the copper polymers occur at 1570 (*sym.* C–O stretching), 1416 (CH_3 deg. def.), 1368 (CH_3 *sym.* def.), 1337, 1268 (*sym.* C–C stretching), 1017 (CH_3 rock.), 950 and 920 cm.$^{-1}$. Assignments are based on the interpretation of the spectrum of copper acetylacetonate given by Nakamoto and Martell.[10] The assignments of these authors differ in some respects from those of earlier workers.[11,12] The frequencies of the assigned bands above do not differ significantly from the corresponding frequencies for copper acetylacetonate.[10] The presence of these bands in the spectra of the polymers is good supporting evidence for the structure of the recurring unit in II. Copper acetylacetonate gives an additional band at 1534 cm.$^{-1}$ which is stated[10] to be due to *asym.* C–O stretching vibrations coupled with C–H bending modes. A corresponding band is not present in the spectra of the polymers. This is evidently due to the fact that the polymer ring systems(II) do not have hydrogens bonded to the ring at the C_3 position. Other metal chelates related to the acetylacetonates, but substituted in the C_3 position, also do not have absorption bands in this region.[13]

Additional bands which are present in the spectrum of copper acetylacetonate[10] but absent from the polymer spectra occur at 1580 cm.$^{-1}$ (*asym.* C–C stretching) and 1190 cm.$^{-1}$ (C–H bending).

TABLE I

YIELDS AND ANALYSES FOR COPPER TETRAACETYLETHANE POLYMERS

	Calculated[a]			Preparations			
Yield, mg.	$n = 1$ 458	$n = 5$ 499	$n = \infty$ 519	1 507	2 506	3 508	4 504
Cu, %	13.87	21.22	24.44	21.0	21.2	20.4	20.4
C, %	52.45	48.14	46.25	47.2	47.8	..	..
H, %	5.72	4.98	4.66	4.6	5.4	..	..
$C_{16}H_{14}O_4$, %	86.6	79.4	76.3	..	..	78.0	78.6

[a] Theoretical values for the structure II given in the text. The quantity n is the number of recurring units in II.

The polymers are paramagnetic as would be expected for copper(II) containing materials. The gram susceptibility was found to be 5.7×10^{-6}. The polymers give well-defined X-ray diffraction powder patterns and must therefore be crystalline. The crystalline character of the materials is not, however, obvious from visual inspection of the finely powdered chelates themselves.

(10) K. Nakamoto and A. E. Martell, *J. Chem. Phys.*, **32**, 588 (1960).

(11) H. F. Holtzclaw, Jr., and J. P. Collman, *J. Am. Chem. Soc.*, **79**, 3318 (1957).

(12) R. West and R. Riley, *J. Inorg. Nucl. Chem.*, **5**, 295 (1958).

(13) R. P. Dryden and A. Winston, THIS JOURNAL, **62**, 635 (1958).

Sealed Tube Experiments.—Weighed samples of the polymers were heated for 4 hours at constant temperatures in sealed glass tubes. The volatile products of decomposition were identified, and their amounts determined, with a mass spectrometer, after cooling to room temperature. For comparison, parallel experiments were carried out with tetraacetylethane. Similar studies have already been reported for a number of metal acetylacetonates[3] and for acetylacetone.[14]

In Fig. 1 is plotted the quantity of each major volatile decomposition product as a function of pyrolysis temperature. The products observed for TAE in Fig. 1 are the same as those found previously for acetylacetone[14] except that water is produced by the TAE while no significant water resulted from the pyrolysis of acetylacetone. It seems likely that the water is formed through the dehydration of TAE to form 3,4-diacetyl-2,5-dimethylfuran (III). In support of this hypothesis

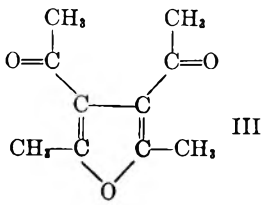

III

is the fact that III forms readily from TAE through dehydration in sulfuric acid.[15] Part, or all, of the other products in Fig. 1 may then result from the pyrolysis of III or from reactions involving water and III. Compound III is not observable directly by the mass spectrometer because of its low volatility. It is interesting that TAE pyrolyzes at a very much lower temperature than does the structurally similar acetylacetone, which cannot undergo dehydration to III.[14]

From Fig. 1 it is seen that the copper TAE polymers are somewhat less heat stable than is TAE. The former materials show measurable decomposition even at 150°. The products from the copper polymers are essentially the same as those from TAE except that H_2, CO and CH_4 are produced in addition. The results suggest that TAE is produced as a decomposition product from the polymers. TAE may then decompose to III and the products derived from III. Such a course would be completely analogous to the pyrolysis of copper acetylacetonate which gives acetylacetone as a principal decomposition product.[3] In support of this mechanism is the fact that compound III has been identified as a pyrolysis product from the copper TAE polymers. (See below.) The production of H_2, CO and CH_4 by the copper polymers shows, however, that reactions other than the production of TAE also occur.

In Fig. 2 the heat stability of a copper TAE polymer is compared with that of copper acetylacetonate. On the basis of the volatile products formed, the two materials are seen to have very similar stabilities. The polymers begin to decompose at slightly lower temperature than does copper acetylacetonate. The latter compound,

(14) R. G. Charles, W. M. Hickam and J. von Hoene, THIS JOURNAL, **63**, 2084 (1959).

(15) S. Mulliken, *Am. Chem. J.*, **15**, 523 (1893).

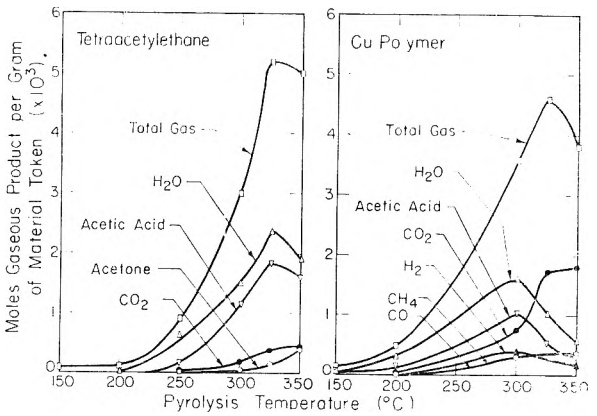

Fig. 1.—Gaseous decomposition products from the pyrolyses of tetraacetylethane and its copper chelate polymer.

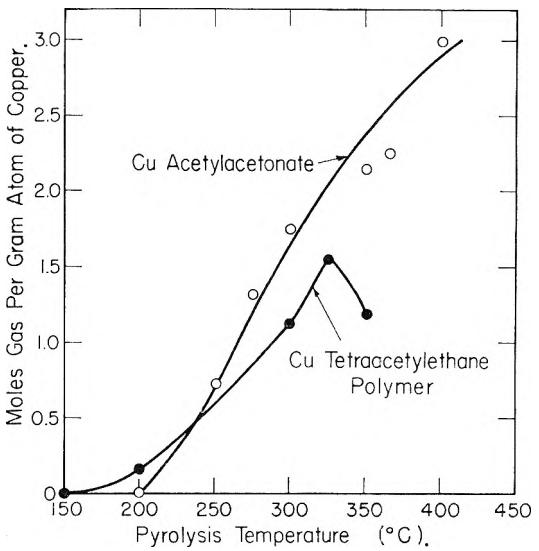

Fig. 2.—Total gaseous decomposition products as a function of pyrolysis temperature.

however, gives the larger quantity of volatile decomposition products at the higher temperatures.

Thermogravimetric Experiments.—Thermogravimetric methods are applicable to a study of the pyrolysis of the copper TAE polymers since these materials are themselves completely non-volatile under the conditions used.[16] Any weight loss observed upon heating these materials in an open container must therefore be ascribed to pyrolysis.

Weight loss–temperature curves resulting from raising the temperature of a copper TAE polymer at a constant rate, in argon, are plotted in Fig. 3 for two different heating rates.[17] Curves obtained at the same heating rate for separately synthesized samples were essentially superimposable. It will be observed from Fig. 3 that while the curve is shifted to higher temperatures with increasing rate of heating, this effect is relatively small.

(16) Thermogravimetry is less suitable for the study of the pyrolysis of non-polymeric metal chelate compounds since these often possess significant volatility at elevated temperatures (ref. 22). Observed weight losses can then be difficult to interpret since they may be due to evaporation of unchanged compound, to pyrolysis, or to some combination of these two effects.

(17) A third curve obtained at 2.1°/min. was superimposable with the 1.6°/min. curve.

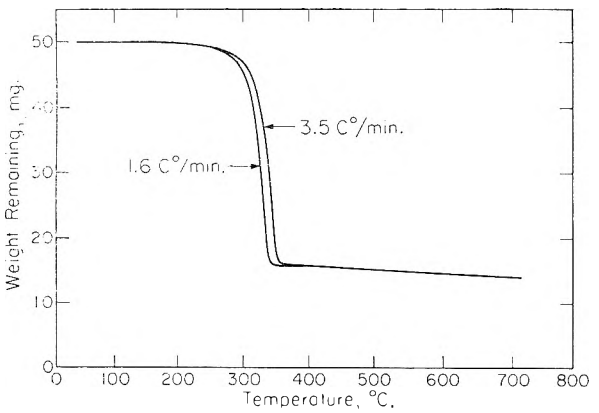

Fig. 3.—Weight loss–temperature curves for a copper tetraacetylethane polymer heated in argon at atmospheric pressure. Fifty mg. samples were used.

For both curves weight losses become detectible above 150° but most of the weight loss occurs between 250 and 350°. This is in agreement with the results plotted in Fig. 1. The total weight loss (to 350°) from Fig. 3, however, is greater than the sum of the weights of the products shown in Fig. 1 by a factor of about five. This indicates that most of the decomposition products are not sufficiently volatile at room temperature to be detected by the mass spectrometer.

Some of the pyrolysis products condensed as a semisolid on the furnace tube above the heated zone. This material was shown, by its infrared absorption spectrum, to contain compound III as a principal component. A strong absorption band at 5.80 μ, not due to III, was also found in the spectrum. At least one other carbonyl compound must therefore be produced in addition to III. Tetraacetylethane, as such, was not detected among these less volatile products.

Freeman and Carroll[18] have proposed a method by which both the order of a reaction and the energy of activation can be determined from a single thermogravimetric curve. When the data obtained here in the temperature region 280 to 325° were plotted in the manner outlined by these authors, good straight lines were obtained. From the intercepts and slopes of these lines, respectively, the order of the reaction and energy of activation (E^*) were calculated. The results of five separate runs showed the reaction to be essentially zero order with an activation energy of 40 ± 1 kcal./mole. There was no significant variation in either reaction order or E^* for separately prepared samples or for different rates of heating (over the range 1.6 to 3.4°/min.). The fact that the reaction is zero order suggests that the rate of weight loss at a given temperature is determined by the surface area available for evaporation of decomposition products rather than by the amount of undecomposed chelate present.

Black powdery residues remained in the sample containers at the conclusion of the thermogravimetric runs. A study was made of the nature of one such residue, heated for 2 hours at 350°. Elemental analyses showed the presence of copper (65.6%), carbon (17.2%), hydrogen (1.0%) and oxygen (16.2%, by difference). The residue contained all the copper initially present in the polymer. No copper-containing species could therefore have volatilized during the thermogravimetric runs.

An X-ray powder diffraction pattern showed only the presence of finely divided copper metal. The residue was paramagnetic with a gram suceptibility of 5.8×10^{-6}. Since both copper metal and copper(I) compounds are diamagnetic, the residue must have contained some (amorphous) copper(II) materials. As nearly as can be judged by the magnetic susceptibility, about one-third of the copper content must remain in the copper(II) state. All copper, in whatever form, could be removed by allowing the residue to stand with 5 M HNO_3 at room temperature for 2 days. A dark brown insoluble material, which did not contain copper, remained from this treatment.

Pyrolysis Mechanism.—On the basis of the evidence presented here it is possible to propose at least one sequence of reactions for the pyrolyses which is consistent with the data. The first step in such a mechanism involves dehydrogenation between adjacent methyl groups to form polymeric materials containing conjugated groupings such as IV. By elimination of methane between IV and II still more highly conjugated structures such as

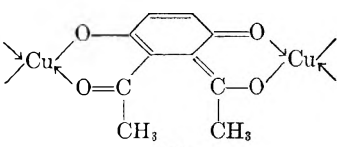

IV

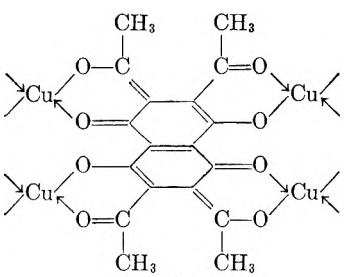

V

V can be built up. Reduction of remaining II, by the hydrogen liberated in the formation of IV, gives copper metal and TAE (I). Reaction of IV and V with hydrogen could also lead to copper metal and the structures corresponding to IV and V in which hydrogen replaces all or part of the copper. The magnetic susceptibility results, however, indicate that some of the metal chelate ring systems such as those in IV and V probably remain intact in the pyrolysis residue.

The presence of the conjugated structures IV and V (and the analogous structures where hydrogen replaces copper) is consistent with both the presence of oxygen in the residues and their dark colors. The percentage of oxygen appears to be somewhat too large, however, to be accounted for by structures IV and V alone. The difference may be due to the presence of some amorphous copper oxide which would not be detected by X-ray diffraction. Since cuprous oxide is diamagnetic and cupric

(18) E. S. Freeman and B. Carroll, THIS JOURNAL, 62, 394 (1958).

oxide has a very low paramagnetism[19] it is still necessary to postulate the presence of other copper(II)-containing materials, such as IV and V, to explain the paramagnetic nature of the residues obtained.

Experimental

Preparation.—Three hundred and ninety-six mg. (2×10^{-3} mole) of tetraacetylethane[20] was dissolved in 100 ml. of tetrahydrofuran. Exactly 10 ml. of 0.200 *M* aqueous cupric acetate was added, at room temperature, dropwise from a buret over a period of one hour. The mixture was stirred with a magnetic stirrer. A green precipitate formed continuously during the addition, after the first few drops of cupric acetate solution had been added. The mixture was allowed to stand for an hour and then the solid was filtered off on a sintered glass crucible. The blue filtrate contained copper but the absence of tetraacetylethane in the filtrate was established by the lack of significant light absorption in the 240 to 300 mμ region of the ultraviolet.[21]

The polymer was washed with water, tetrahydrofuran and acetone, air-dried at room temperature for several days, and finally dried for an hour in a vacuum oven at 100°.

Sealed Tube Experiments.—One hundred mg. of the sample was sealed, under vacuum, into a Pyrex tube and heated for 4 hr. in the same manner as described previously.[3] The experiments were conducted in such a manner that the degradation products remained in the hot zone of the furnace. The tubes were cooled to room temperature and the products volatile at this temperature were analyzed with a mass spectrometer.[3]

Thermogravimetric Experiments.—The thermobalance employed was essentially the same as that previously described.[22] As used here, however, the sample was heated in a stream (50 ml./min.) of argon at atmospheric pressure (*ca.* 730 mm.). Fifty mg. of sample was contained in a platinum crucible. The temperature was raised linearly with time at one of the three rates 1.6, 2.1 or 3.4°/min. Each weight–temperature curve was recorded automatically on a Mosely autograph model 3X X-Y recorder. Weight–time curves were recorded on a Leeds and Northrop Speedomax recorder.

Physical Measurements.—Infrared spectra were obtained with a Perkin–Elmer model 21 spectrophotometer. The samples were dispersed in KBr pellets. Magnetic susceptibility measurements were made by the Faraday method.[23] Ultraviolet absorption measurements were made with a Cary model 14 spectrophotometer.

Acknowledgments.—The author is indebted to Dr. W. M. Hickam for the mass spectrometer analyses, and to Dr. A. Taylor, Dr. J. H. Lady and Mr. P. Piotrowsky for the X-ray diffraction, infrared, and magnetic susceptibility measurements, respectively. Mrs. M. A. Dolan was helpful in several phases of the experimental work.

(19) P. W. Selwood, "Magnetochemistry," Second Edition, Interscience Publishers, Inc., New York, N. Y., 1956, p. 335.

(20) R. G. Charles, *Org. Syntheses*, **39**, 61 (1959).

(21) D. F. Martin, W. C. Fernelius and M. Shamma, *J. Am. Chem. Soc.*, **81**, 130 (1959).

(22) R. G. Charles and A. Langer, THIS JOURNAL, **63**, 603 (1959).

(23) P. W. Selwood, "Magnetochemistry," Second Edition, Interscience Publishers, Inc., New York, N. Y., 1956, p. 11.

TRANSFERENCE NUMBERS FOR CONCENTRATED AQUEOUS SODIUM CHLORIDE SOLUTIONS, AND THE IONIC CONDUCTANCES FOR POTASSIUM AND SODIUM CHLORIDES

BY D. J. CURRIE AND A. R. GORDON

Chemistry Department, University of Toronto, Toronto, Canada

Received June 10, 1960

Transference numbers for concentrated NaCl solutions have been determined by the adjusted indicator technique, the Hittorf values for KCl serving as reference. The transference numbers and the known equivalent conductances give at once the ionic conductances for the two salts. The marked differences between the values of λ_{Cl} for KCl and NaCl in concentrated solution cannot be explained on the basis of viscosity alone.

Although there is considerable information in the literature as to ionic conductances in aqueous solution up to 0.1 *N*, similar data for relatively concentrated solutions are almost non-existent, the reason being the dearth of transference numbers for concentrations greater than decinormal. It was to provide some information for the more concentrated range that the work reported here was undertaken, in the hope that it might prove useful should theoretical treatment of such data become possible.

To obtain the requisite transference numbers, however, the moving boundary method cannot be used owing to the increasing magnitude of the volume correction with rising concentration, with a resultant increasing uncertainty in the corrected transference number.[1] The classical Hittorf procedure is of course applicable to concentrated solutions, but has not in general given results which inspire much confidence. MacInnes and Dole's data for KCl[2] are an exception. Although not of the precision attainable with the moving boundary method, their average values would seem to be reliable to one or two tenth's of a per cent., and (thanks to the adjusted indicator technique[3]) this permits the determination of the transference numbers of any electrolyte having an ion in common with KCl to the precision of the KCl data themselves. We report here results obtained in this way for NaCl since Chambers, Stokes and Stokes[4] have made a careful study of KCl and NaCl conductances in concentrated solution.

Experimental

The general procedure and the preparation of the salts

(1) D. A. MacInnes and L. G. Longsworth, *Chem. Revs.*, **11**, 171 (1932).

(2) D. A. MacInnes and M. Dole, *J. Am. Chem. Soc.*, **53**, 1357 (1931).

(3) D. R. Muir, J. R. Graham and A. R. Gordon, *ibid.*, **76**, 2157 (1954).

(4) J. F. Chambers, J. M. Stokes and R. H. Stokes, THIS JOURNAL, **60**, 985 (1956).

and solutions are essentially those of Muir, Graham and Gordon[3] except for the modifications noted below. For concentrations above 0.5 N, it was not convenient to fuse the salts in nitrogen; instead, stock solutions were made up from the purified salts dried at 120° and conductivity water; aliquots of these were diluted gravimetrically to 0.1 N, and their conductances were compared with those of 0.1 N solutions prepared directly from the fused salt and water. In converting from mass to volume concentrations, the density data from International Critical Tables[5] were employed, and all weights were corrected to vacuum.

Owing to the far higher conductances of the indicator solutions used here as compared with those in the earlier work,[3] a different type of cell had to be used for conductiometric analysis. This consisted of a tube approx. 2 mm. i.d. and 5 cm. long, the ends being fitted with female ground glass joints. Platinum wire electrodes, approx. 1 mm. in diameter, were mounted in the corresponding male parts, and ground flat and flush with the glass. The cell was filled in the vertical position from the sampling pipet with the lower electrode in place, the second electrode was inserted, the cell inverted, and the first electrode removed; additional solution was added from the pipet to remove any air that might have been trapped in the original filling, and the electrode then replaced; circular alignment of the electrodes was by means of etch marks on the male and female parts of the joints. With practice, it was found that repeated fillings of the cell with the same solution gave resistances which checked to 0.05% or better, indicating that the position of the electrodes in the cell was reasonably reproducible. As before, the adjusted indicator concentration was determined by comparing its resistance (as measured at 5000 c.p.s. on the a.c. bridge previously employed) with those of solutions whose known concentrations lay a few per cent. above and below the unknown.

Since for a given wattage dissipation in the moving boundary cell, the current to a rough approximation will vary as the square root of the concentration, it follows that the time required for a given wattage and for a given boundary displacement will also vary as $C^{1/2}$. Since this implies far more lengthy runs than with the dilute solutions previously used, and since the current had only to be known approximately, an Esterline-Angus recording milammeter (operating at its lowest chart speed) was introduced in the circuit, thus eliminating the necessity for constant supervision.

In general, the initial concentration of the indicator when the boundary was formed was from 5 to 10% below the final adjusted value, and for the concentrations obtaining here, the corrections (pipet contamination, solvent conductance, etc.) discussed by Muir, Graham and Gordon are unnecessary.

Results and Discussion

As a check on the procedure, a series of five runs were carried out with 0.1 N KCl as the leading solution. The mean value of the Kohlrausch ratio, r, the ratio of the adjusted concentration of the NaCl indicator to that of the leading solution, was 0.7893, with a mean absolute deviation from the mean of 0.0005. It should also be noted that although the current in this series was varied by a factor of 2, there was no hint of current dependence. Since for 0.1 N KCl[6,7] t_K is 0.4898, $t_{Na} = rt_K$ is 0.3866 ± 0.0003 for 0.0789 N NaCl. Interpolation by means of a large scale deviation plot of the moving boundary data[6,8] for NaCl gives 0.3864. When it is remembered that the conditions for this concentration were far from ideal owing to the characteristics of the conductance cell, it would seem reasonable to conclude that the transference numbers of concentrated NaCl solutions can be determined to the precision of the corresponding KCl data.

The results are summarized in Table I. The first column gives the concentration of the leading solution in equivalents/liter, and the second the selected transference number of potassium ion for the concentration in question. Although the numbers are quoted to four significant figures for numerical accuracy, the choice is somewhat subjective since MacInnes and Dole's experimental results show a scatter for a given concentration of as much, in one case, as ±0.001. The entries in the table and those of Table II (as can easily be verified by plotting) correspond to a curve roughly linear in $C^{1/2}$ for $C > 0.5$, which passes through the moving boundary results for 0.1 and 0.2 N,[6,7,9] and represents the experimental results for higher concentrations within apparent experimental uncertainty. The third column gives the value of r; each entry[10] is in general the mean of three independent measurements in which the current was varied by a factor of 2, the mean deviation for a given concentration being ± 0.0003 or less, except for the last result where it was ±0.0008. The resulting (rounded) values of the adjusted indicator concentration and the corresponding values of t_{Na} are given in the last two columns. We believe the latter are as reliable as the KCl numbers on which they are based; in particular, our value for 0.2 N NaCl may be compared with Longsworth's moving boundary result 0.3821.[9]

Table I

Transference Numbers for NaCl Solutions at 25°

C_{KCl}	t_K	r	t_{Na}	C_{NaCl}
0.257	0.4894	0.7816	0.3825	0.201
0.5	.4889	.7760	.3794	0.388
1.0	.4879	.7710	.3762	0.771
2.0	.4866	.7749	.3771	1.550
3.0	.4857	.7775	.3776	2.333

Table II

Ionic Conductances for KCl and NaCl Solutions at 25°

C	t_K	t_{Na}	Λ_{KCl}	Λ_{NaCl}	$(\lambda_{Cl})_{KCl}$	$(\lambda_{Cl})_{NaCl}$
0.1	0.4898[a]	0.3853[a]	128.96	106.74	65.80	65.60
0.2	.4894[a]	.3823	124.08	101.71	63.35	62.85
0.5	.4889	.3778	117.27	93.62	59.95	58.25
1.0	.4879	.3762	111.87	85.76	57.30	53.50
1.5	.4872	.3767	108.27	80.35	55.50	50.10
2.0	.4866	.3772	105.23	74.71	54.00	46.55
2.5	.4861	.3780	102.38	70.02	52.60	43.55

[a] Moving boundary values.

From a large scale plot of t_{Na} *vs.* $C^{1/2}$, the values of Table II were obtained, the plot representing the experimental points in all cases with a few units in the fourth decimal place. The table also gives the equivalent conductances for the two salts (taken from Table II of ref. 4) and the resulting λ_{Cl} to the nearest 0.05 conductance unit.

One would have expected intuitively that λ_{Cl} would have been definitely less in a concentrated NaCl solution than in the corresponding solution

(5) "International Critical Tables," Vol. 3, McGraw-Hill Book Co., New York, N. Y., p. 79, 87.

(6) L. G. Longsworth, *J. Am. Chem. Soc*, **54**, 2741 (1932).

(7) R. W. Allgood, D. J. LeRoy and A. R. Gordon, *J. Chem. Phys.*, **8**, 418 (1940).

(8) R. W. Allgood and A. R. Gordon, *ibid.*, **10**, 124 (1942).

(9) L. G. Longsworth, *J. Am. Chem. Soc.*, **57**, 1185 (1935).

(10) In computing r, the actual concentrations of the leading and indicator solutions in each measurement were employed; these deviated slightly from the rounded value quoted in Table I, but r itself is insensitive to small changes in concentration. See ref. 3.

of the potassium salt, on account of the markedly greater viscosity of the former. However, a naive attempt to account for the difference in ionic conductance on the basis of macroscopic viscosity grossly over-corrects. For example, the conductance–relative viscosity products[11] for chloride ion at 1.0 *N* are 57.00 and 58.65 for KCl and NaCl, respectively, while at 2.0 *N* they are 54.25 and 56.60.

(11) Ref. 5, Vol. 5, p. 15, 17.

It is possible that similar measurements of the conductance of other ions might suggest a qualitative pattern, but at the moment any quantitative interpretation of transport phenomena under these conditions must await further theoretical development.

In conclusion, we wish to express our thanks to the National Research Council of Canada for a grant in aid of this research.

ISOTOPE EFFECTS IN Hg(6³P₁)-PHOTOSENSITIZED REACTIONS: $H_2 + N_2O$ AND $H_2 + NO$[1]

By Morton Z. Hoffman[2] and Richard B. Bernstein

Department of Chemistry, The University of Michigan, Ann Arbor, Michigan

Received June 10, 1960

The N^{14}/N^{15} and O^{16}/O^{18} isotope effects in the Hg(6³P₁)-photosensitized (MPS) reaction of hydrogen with nitrous oxide and with nitric oxide have been measured. In the MPS reaction of $N_2O + H_2$, then N^{14}/N^{15} isotope effect was independent of the ratio $(H_2)/(N_2O)$ over the range 1.0 to 12, with an average value of $S^0 = 1.018 \pm 0.001$ compared with $S^0 = 1.017 \pm 0.001$ for the MPS decomposition of N_2O. The O^{16}/O^{18} isotope effect was 1.017 ± 0.002 compared with 1.019 ± 0.001 for the decomposition. These observations imply that the rate of H-atom attack on N_2O is a small fraction of the rate of the N_2O decomposition. In the MPS reaction of $NO + H_2$, the N^{14}/N^{15} isotope effect was found to be "inverted," *i.e.*, the first fraction of N_2 produced was *enriched* in N^{15} relative to the original NO. At a ratio $(H_2)/(NO) = 1.0$, the fractionation factor was 1.008, diminishing to the null value of 1.000 at a ratio of 29. The N^{15} enrichment is interpreted on the basis of a postulated isotope exchange equilibrium between NO and HNO.

Introduction

The use of the kinetic isotope effect technique as a means of studying mechanisms of gas phase thermal reactions is well known.[3] Measurements of isotope effects in photolytic reactions have been reported[4] and recently isotopic fractionation in the Hg(6³P₁)-photosensitized (MPS) decomposition of N_2O has been observed[5] and related to differences in the quenching cross section of the isotopic molecules. It was of interest, therefore, to extend the use of kinetic isotope effects in order to elucidate the mechanisms of two MPS reactions.

A detailed kinetic study of the MPS reaction $H_2 + N_2O \rightarrow N_2 + H_2O$ was carried out by Taylor and Zwiebel[6] who found that the reaction rate was affected only slightly by P_{H_2} but significantly by P_{N_2O}. They postulated a mechanism involving a sensitized decomposition of N_2O at a rate roughly 1000 times that of H-atoms with N_2O

$$\begin{aligned} Hg + h\nu &\longrightarrow Hg' && (I_{abs}) \\ Hg' + H_2 &\longrightarrow H + H + Hg && (1) \\ Hg' + N_2O &\longrightarrow N_2 + O + Hg && (2) \\ H_2 + O &\longrightarrow H + OH && (3) \\ H + N_2O &\longrightarrow N_2 + OH && (4) \\ H + O \text{ chain steps} &\longrightarrow H_2O && (5), \text{ etc.} \end{aligned}$$

Since the MPS decomposition could be studied separately,[5] a test of this mechanism, particularly the relative importance of steps 2 and 4, could be achieved using the isotope effect technique.

Taylor and Tanford[7] investigated the MPS reaction $H_2 + NO \rightarrow {}^1/_2\, N_2 + H_2O$. They found that: (1) the rate of reaction was proportional to P_{H_2} at low pressures (with the dependence diminishing at higher pressures); (2) with excess H_2, the rate was essentially independent of P_{NO}; (3) with excess NO, the rate was retarded and the stoichiometry was not simple. They suggested the following mechanism to account qualitatively for their kinetic observations

$$\begin{aligned} Hg + h\nu &\longrightarrow Hg' && (I_{abs}) \\ Hg' + H_2 &\longrightarrow H + H + Hg && (1) \\ Hg' + NO &\longrightarrow NO + Hg && (2) \\ H + NO &\longrightarrow HNO && (3) \\ H + HNO &\longrightarrow H_2 + NO && (4) \\ HNO &\longrightarrow \text{decomposition} && (5) \end{aligned}$$

Harteck[8] had reported that NO reacted with H-atoms (from a discharge tube) to produce a product, $(HNO)_n$, solid at liquid air temperature, which decomposed on warming. The over-all decomposition of HNO in step 5 was expressed[7] as a first-order reaction, although the mode of decomposition was speculated to be dimerization of the HNO to hyponitrous acid with subsequent decomposition to N_2O and H_2O. The N_2O could not accumulate under these experimental conditions and underwent further reaction to produce N_2. They considered that the rate of step 4 was

(1) The authors appreciate financial support from the U. S. Atomic Energy Commission, Division of Research and the Michigan Memorial Phoenix Project.

(2) Receipt of fellowships from the Michigan Memorial-Phoenix Project and the National Science Foundation is gratefully acknowledged.

(3) (a) J. Bigeleisen, This Journal, **56**, 823 (1952); (b) S. Z. Roginsky, "Theoretical Principles of Isotope Methods for Investigating Chemical Reactions," Academy of Sciences, U.S.S.R. Press, Moscow, 1956, Chapters IV and VI; Office of Technical Services, Department of Commerce, Washington 25, D. C. (English translation); (c) D. R. Stranks and R. G. Wilkins, *Chem. Revs.*, **57**, 842 (1957).

(4) A. A. Gordus and R. B. Bernstein, *J. Chem. Phys.*, **30**, 973 (1959).

(5) M. Z. Hoffman and R. B. Bernstein, *ibid.*, **33**, 526 (1960).

(6) H. A. Taylor and N. Zwiebel, *ibid.*, **14**, 539 (1946).

(7) H. A. Taylor and C. Tanford, *ibid.*, **12**, 47 (1944).

(8) P. Harteck, *Ber.*, **66**, 423 (1933).

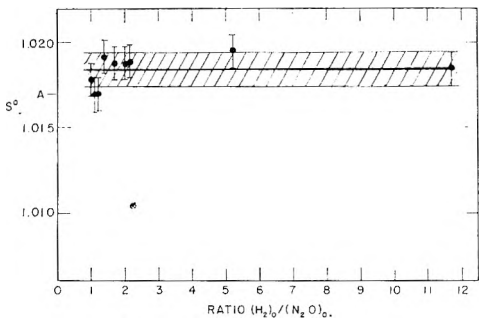

Fig. 1.—N^{14}/N^{15} isotope effect data in the MPS reaction of nitrous oxide and hydrogen. Point A is the value for the MPS decomposition of nitrous oxide.

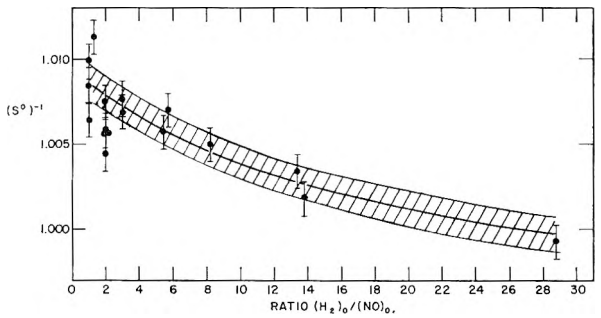

Fig. 2.—N^{14}/N^{15} isotope effect data in the MPS reaction of nitric oxide and hydrogen.

several orders of magnitude faster than the rate of step 5.

The recent interest[9-11] in the HNO molecule has called attention to this reaction; a reinvestigation of it, to understand more fully the role played by the HNO, appeared to be in order.

Experimental[12]

Tank H_2 (Liquid Carbonic Corp.) was purified by passage through a Deoxo unit, a trap at −196°, and a Pd thimble at 370°. Mass spectrometric analysis showed the H_2 to be free of N_2 and O_2.

N_2O (Matheson Co., stated purity: > 98.0%), was purified by repeated distillations from −160 to −196°; the middle fractions were collected and stored over Hg at room temperature. The vapor pressure at the triple point and the infrared spectrum agreed well with the literature.[13,14]

Matheson Co. tank NO (stated purity: > 99.0%) was purified[15] and stored over Hg at room temperature. The vapor pressure at the triple point and the infrared spectrum agreed well with the literature,[16,17] indicating a probable impurity content ≤ 0.1%.

The vacuum apparatus and lamp assembly used have been previously described.[5,12] The reactants were metered into the reaction loop and the reaction (carried out at room temperature) was followed manometrically for a time (*ca.* 1 hr.) corresponding to a small (<0.15) fraction of reaction. The reaction mixtures, containing N_2, H_2O, and unreacted H_2 and nitrogen oxide, were separated by passage through a trap at −78° into a trap at −196° (−210° for the H_2–NO reaction). The volatile gases were cycled through CuO (350°; regenerated after use by heating in air at 600° overnight) and the N_2 remaining was measured and collected for subsequent N^{15} assay. The product H_2O, trapped at −78°, was collected for O^{18} isotopic assay.

By means of the quantitative (± 1%) MPS reduction of the nitrogen oxide with excess H_2, "reference samples" of N_2 and H_2O were obtained for isotopic analysis.

The method of isotopic assay for the N^{14}/N^{15} ratio in the N_2 and O^{16}/O^{18} in the H_2O samples was conventional[5]; the usual definition of the fractionation factor S and the small correction to zero extent of reaction, S^0, have been given previously.[5]

Results

A. H_2 + N_2O.—The qualitative aspects of the reaction reported by Taylor and Zwiebel[6] have been confirmed. The rate of N_2 production was strongly dependent upon P_{N_2O} and only slightly dependent upon P_{H_2}. The reaction rate was not appreciably greater than the rate of N_2 production in the MPS decomposition of N_2O.[12]

The N^{14}/N^{15} isotope effect, S^0, is illustrated in Fig. 1 as a function of the $(H_2)/(N_2O)$ ratio at total pressures in the range 294–434 mm. The bracket on the points represents the probable error due to the mass spectrometric analyses. The average of these points, 1.018, is designated by the horizontal line with the probable error (± 0.001) indicated as the shaded region. The N_2 samples from the first fraction of the reaction were thus *depleted* in N^{15} relative to the original N_2O.

The O^{16}/O^{18} isotope effect at a $(H_2)/(N_2O)$ ratio of 1 had the values 1.016 and 1.014; at a ratio of 5, S^0 was 1.021 and 1.016. The average of these four values is 1.017 ± 0.002, indicating *depletion* of O^{18} in the product H_2O.

Auxiliary experiments to test for the presence of N-isotope exchange between N_2 and N_2O and O-isotope exchange between H_2O and N_2O under MPS conditions indicated such exchange to be absent.

B. H_2 + NO.—The over-all stoichiometry and the qualitative aspects of the reaction corresponded very well to that reported by Taylor and Tanford.[7] The rate of N_2 production decreased sharply as the initial $(H_2)/(NO)$ ratio was increased for a series of experiments at constant total pressure. The over-all rate of the reaction was very similar (*i.e.*, differed by less than a factor of two) to that for the H_2–N_2O case.

The measurement of the N^{14}/N^{15} isotope effected indicated *enrichment* of N^{15} in the product N_2. Figure 2 shows the "inverted" isotope effect $(S^0)^{-1}$ as a function of the initial $(H_2)/(NO)$ ratio at total pressures in the range 284–734 mm. The bracket on the points represents the probable error due to analysis; the shaded area indicates the probable error (± 0.001) of the line drawn through the points.

Nitrogen isotope exchange between N_2 and NO was found to be absent. Oxygen isotope exchange, however, between NO and H_2O, catalyzed by HNO_3 has been reported.[18] The existence of this exchange under the conditions of these experiments was confirmed. Thus the O^{16}/O^{18} isotope effect

(9) F. W. Dalby, *Can. J. Phys.*, **36**, 1336 (1958).

(10) H. W. Brown and G. C. Pimentel, *J. Chem. Phys.*, **29**, 883 (1958).

(11) J. K. Cashion and J. C. Polanyi, *ibid.*, **30**, 317 (1959).

(12) For further details, see Ph.D. dissertation, M. Z. Hoffman, University of Michigan, 1960, available from University Microfilms Ann Arbor, Michigan.

(13) H. Hoge, *J. Research Natl. Bur. Standards*, **34**, 281 (1945).

(14) G. Herzberg, "Infrared and Raman Spectra," D. Van Nostrand Co., Inc., New York, N. Y., 1951, p. 277.

(15) R. E. Nightingale, A. R. Downie, D. L. Rotenberg, B. Crawford, Jr., and R. A. Ogg, Jr., THIS JOURNAL, **58**, 1047 (1954).

(16) H. L. Johnston and W. F. Giauque, *J. Am. Chem. Soc.*, **51**, 3194 (1929).

(17) A. L. Smith, W. E. Keller and H. L. Johnston, *J. Chem. Phys.*, **19**, 189 (1951).

(18) T. I. Taylor and J. C. Clarke, *ibid.*, **31**, 277 (1959).

data,[12] which showed *depletion* of O^{18} in the product H_2O, are not reported here.

Discussion

A. $H_2 + N_2O$.—The kinetic observations have led to the conclusions that the rate of the decomposition of N_2O is appreciably greater than the rate of the H-atom attack upon the N_2O and that the decomposition is the rate-determining step. The measurement of the isotope effect serves as another check on the proposed mechanism. By considering the reactions of the nitrogen isotopic molecules in steps 2 and 4 (assuming these to be the only steps in which N_2 is formed)[19]

$$Hg' + NNO \longrightarrow N_2 + O + Hg \quad (2A)$$
$$Hg' + N^*NO \longrightarrow N^*N + O + Hg \quad (2B)$$
$$Hg' + NN^*O \longrightarrow NN^* + O + Hg \quad (2C)$$
$$H + NNO \longrightarrow N_2 + OH \quad (4A)$$
$$H + N^*NO \longrightarrow N^*N + OH \quad (4B)$$
$$H + NN^*O \longrightarrow NN^* + OH \quad (4C)$$

it can be shown[12] that the nitrogen separation factor is given by

$$S^0 = \frac{\alpha_2\left[1 + \frac{k_{4A}(H)}{k_{2A}(Hg')}\right]}{1 + \frac{k_{4A}(H)\alpha_2}{k_{2A}(Hg')\alpha_4}}$$

where $\alpha_2 = k_{2A}/(k_{2B} + k_{2C})$ and $\alpha_4 = k_{4A}/(k_{4B} + k_{4C})$. Assuming

$$\frac{k_{4A}(H)}{k_{2A}(Hg')} << 1$$

then $S^0 = \alpha_2$, so that the observed isotope effect is that of step 2 and is independent of the concentration of the reactants.

An independent study[5] of the N-isotope effect in the MPS decomposition of N_2O led to the value $S^0 = 1.017 \pm 0.001$ (point A, Fig. 1), to be compared with the average value in Fig. 1 of 1.018 ± 0.001.

The oxygen isotope effect, treated in the same way,[12] results in the same predictions as for the nitrogen isotope effect. The oxygen fractionation factor in the N_2O decomposition[5] was $1.019_5 \pm 0.001$, which is to be compared with the average value here of 1.017 ± 0.002.

It may thus be concluded that the Taylor–Zwiebel[6] mechanism satisfies the kinetic and isotope effect data. The main feature of the mechanism is the slowness of H-atom attack on N_2O compared with the decomposition reaction. This explanation is not incompatible with the observation[20] that the reaction of H-atoms with N_2O has an activation energy of 15–20 kcal. whereas the decomposition of N_2O through the quenching of Hg resonance radiation has a probable activation energy of zero.[21]

B. $H_2 + NO$.—"Inverted" isotope effects, such as the one found here, have been reported for some organic and photochemical systems[22] but are, in general, of rare occurrence. This unusual isotope effect serves to place stringent limitations on any proposed mechanism.

(19) The symbols N and N* represent N^{14} and N^{15}, respectively.

(20) H. W. Melville, *Proc. Roy. Soc.* (*London*), **146A**, 737 (1934).

(21) K. J. Laidler, "The Chemical Kinetics of Excited States," The Clarendon Press, Oxford, England, 1955, p. 97.

(22) P. E. Yankwich and R. W. Buddemeier, *J. Chem. Phys.*, **30**, 861 (1959).

It should first be noted that since the rate of this reaction is very nearly equal to the rate of the MPS H_2–N_2O reaction (which, in turn, has been inferred[12] to be very nearly equal to the rate of the MPS N_2O decomposition, of quantum yield approximately unity[23]), the quantum yield of the H_2–NO reaction must be nearly unity. Any reaction such as step 4 occurring to a large extent would appreciably reduce the quantum yield.

The mechanism of Taylor and Tanford[7] satisfactorily explains the qualitative aspects of the kinetic observations made in this study; unfortunately, the present results have yielded no additional information about the mode of decomposition of the HNO. However, the Taylor–Tanford mechanism does not provide an explanation for the observed nitrogen isotope effect (N^{15} *enrichment*) in the reaction. The assumption that $R_4 << R_5$ leads one to the conclusion that any isotope effect arises from either step 3 (thus probable N^{14} enrichment) or step 2 (yielding excited NO which may undergo further reaction to N_2). A separate study[24] of the MPS decomposition of NO has shown that this isotope effect is in the normal direction (N^{14} enrichment).

However, an N^{15} enrichment could arise from the equilibrium isotope exchange reaction: $N^*O + HNO \rightleftarrows NO + HN^*O$. This equilibrium may arise *via* a direct H-atom transfer mechanism or through the postulated[25,26] step: $H + NO \rightleftarrows HNO$. From a knowledge of the fundamental vibrational frequencies[27] of $N^{14}O$ and $N^{15}O$ and the recent values of the frequencies for HNO,[9,10,28] the equilibrium constant for this reaction was computed[12] to be 1.006 at 300°K. Thus, this equilibrium would result in a 0.6% N^{15} enrichment in the HNO. If one adds this equilibrium step to the mechanism, no change in the rate equation results, but the "inverted" isotope effect is at least qualitatively accounted for. The dependence of the isotope effect on the $(H_2)/(NO)$ ratio might then be explained on the basis of an increase in the rate of step 4 competing with the equilibrium reaction as P_{H_2} is increased.

However, in the absence of more detailed experimental data on the mode of decomposition of HNO in the gas phase, the relationship between the magnitude of the equilibrium isotope effect and the observed isotope effect is not known. The reactions which HNO might undergo after equilibration with the substrate NO will affect the magnitude of the observed isotope effect and its dependence on the experimental parameters. Until further information on the decomposition of HNO in the gas phase is available, the present isotope effect data

(23) R. J. Cvetanovic, *ibid.*, **23**, 1203 (1955).

(24) M. Z. Hoffman and R. B. Bernstein, THIS JOURNAL, **64**, 1769 (1960).

(25) A. Serewicz and W. A. Noyes, Jr., *ibid.*, **63**, 843 (1959).

(26) R. Srinivasan, *ibid.*, **64**, 679 (1960).

(27) H. C. Urey, *J. Chem. Soc.*, 592 (1947).

(28) From the molecular parameters of HNO given in ref. 9 and 10 and the equation[29] for a non-linear XYZ molecule (the assumed structure), the frequencies (in $cm.^{-1}$) of the various isotopic modifications were calculated: $H^1N^{14}O^{16}$: 3300, 1570, 1110; $H^1N^{15}O^{16}$: 3293, 1541, 1107; $H^2N^{14}O^{16}$: 2417, 1557, 840; $H^1N^{14}O^{18}$: 3300, 1532, 1104.

(29) E. B. Wilson, Jr., *J. Chem. Phys.*, **7**, 1047 (1939).

cannot be interpreted in a quantitative way.

Acknowledgment.—The authors thank Mr. J. N. Doshi for his assistance with the mass spectrometric analyses.

ELECTRIC MOMENTS OF THE SIMPLE ALKYL ORTHOVANADATES

BY FRED CARTAN AND CHARLES N. CAUGHLAN

Department of Chemistry, Montana State College, Bozeman, Montana

Received June 27, 1960

The electric moments of a series of alkyl orthovanadates have been determined in benzene solution at 25°. The following moments were found: Et_3VO_4, 1.18 *D.*; $Pr_3^nVO_4$, 1.15 *D.*; $Pr_3^iVO_4$, 1.23 *D.*; $Bu_3^nVO_4$, 1.12 *D.*; $Bu_3^iVO_4$, 1.10 *D.*; $Bu_3^sVO_4$, 1.01 *D.*; $Bu_3^tVO_4$, 1.16 *D.*; $Am_3^tVO_4$, 1.11 *D.* The densities, dielectric constants and refractive indices of the pure esters were also measured. The small electric moments observed show that rotation of the alkoxy groups is considerably restricted.

Introduction

The alkyl orthovanadates (R_3VO_4) are an interesting group of vanadium compounds with "covalent" properties. In 1887, Hall[1] prepared what was apparently ethyl vanadate. In 1913, Prandle and Hess[2] prepared and described several of the alkyl esters.

Since the study by Prandl and Hess, only a few publications have appeared investigating these compounds.[3-5]

This study was conducted to measure the electric moments of these vanadium compounds and to help characterize them. It was hoped that information on the nature of the bonding and structure of these esters could also be obtained.

Experimental

Preparation.—The ethyl ester was prepared by the reaction between $VOCl_3$ and the sodium ethylate

$$VOCl_3 + 3NaOEt \longrightarrow Et_3VO_4 + 3NaCl \quad (I)$$

The other esters were made using either of the following reactions

$$V_2O_5 + 6ROH \rightleftarrows 2R_3VO_4 + 3H_2O \quad (IIa)$$

$$NH_4VO_3 + 3ROH \rightleftarrows R_3VO_4 + NH_3 + 2H_2O \quad (IIb)$$

Prandl and Hess[2] used method IIa. With fused V_2O_5 the reaction is slow and using simple distillation to separate the water the yields were low. It was improved in both respects by using V_2O_5 which had not been fused and an efficient column to remove the azeotrope formed. The substitution of NH_4VO_3 for V_2O_5 (IIb) further increased both speed and yield.

The usual procedure for reaction IIab was as described: A good grade of alcohol was purified by fractionation. The alcohol (in excess) and NH_4VO_3 mixture was refluxed rapidly under a 90 cm. packed column. The azeotrope was removed as formed. After several hours, the majority of the excess alcohol was distilled. The contents of the stillpot were centrifuged to eliminate unreacted solids and decomposition products. The remaining alcohol was removed with a vacuum distillation. The esters were purified by repeated vacuum distillation. Thermal decomposition resulted if distillation was carried out at pressures greater than 1 mm.

With either of the methods, yields of $Bu_3^tVO_4$ were poor. Other esters were produced in yields of 60–90%. Better yields were produced by alcohols with large alkyl groups. $Bu_3^tVO_4$ melts near 45°, Et_3VO_4 near 0° and $Pr_3^iVO_4$ and $Bu_3^sVO_4$ 5–10° below zero. Vapor pressures were not measured but the esters boil from 30 to 140°, depending on the ester, under approximately 1 mm. pressure.

These compounds undergo thermal decomposition, especially when impure. They are also decomposed by exposure to ultraviolet light. Pure samples will keep for several months at 0° in the dark, but slightly impure samples show noticeable decomposition. The branched chain esters are slightly more stable than the straight chain esters. They are rapidly hydrolyzed in the presence of small amounts of moisture and gelatinous V_2O_5 is produced if water is present in excess. The esters are soluble in most organic solvents.

The purified esters were analyzed for vanadium content by titrating samples as VO^{++} with standard $KMnO_4$.

The density, refractive index and dielectric constant were measured on samples of the esters freshly purified by at least a double vacuum distillation. The probable impurities, if present, could be traces of hydrolysis products, silicone hi-vacuum grease or parent alcohol or related substances not removed by vacuum distillation.

Density.—The densities of the pure esters were obtained using a single-necked capillary pycnometer of approximately 30-ml. capacity. The densities obtained should be accurate to ±0.0001.

Refractive Index.—A Zeiss Abbe' refractometer was used for measurement of $n^{25}D$. There was no indication of hydrolysis of the esters during transfer and measurement. The refractive indices thus obtained should be accurate to ±0.0004.

Dielectric Constant.—The apparatus used has been previously described.[6] The cell used had a capacitance in air of approximately 25 $\mu\mu$f. and a cell volume of approximately 10 ml. Benzene and cyclohexane were used to calibrate the cell. The apparatus operated at 4.6 mc. The results should be accurate to ±0.008. The observed dielectric constants were sensitive to traces of moisture and this characteristic provided a convenient criteria of their purity. The results of these measurements are shown in Table I.

TABLE I

PROPERTIES OF THE ALKYL ORTHOVANADATES

Ester	Color and state	d^{25}_4	$n^{25}D$	ϵ^{25}
Et_3VO_4	Yellow-orange liquid	1.1550	1.5059	3.333
$Pr_3^nVO_4$	Yellow liquid	1.0752	1.4953	2.961
$Pr_3^iVO_4$	Colorless liquid	1.0324	1.478	3.299
$Bu_3^nVO_4$	Yellow liquid	1.0335	1.4898	2.780
$Bu_3^iVO_4$	Pale yellow liquid	1.0189	1.4857	2.761
$Bu_3^sVO_4$	Colorless liquid	1.0083	1.4804	2.969
$Bu_3^tVO_4$	Colorless solid	....	....	...
$Am_3^tVO_4$	Colorless liquid	0.9863	1.4805	2.764

Electric Moments.—The total polarizations were obtained using the Hedestrand extrapolation formula.[7]

(1) J. A. Hall, *J. Chem. Soc.*, **51**, 751 (1887).

(2) W. Prandl and L. Hess, *Z. anorg. Chem.*, **82**, 103 (1913).

(3) M. G. Voronkov and Yu. I. Shorik, *Izvest. Akad. Nauk S.S.S.R. Otdel. Khim. Nauk*, 503 (1958).

(4) H. Funk, W. Weiss and M. Zeising, *Z. anorg. allgem. Chem.*, **296**, 36 (1958).

(5) N. F. Orlov and M. G. Voronkov, *Izvest. Akad. Nauk S.S.S.R. Otdel. Khim. Nauk*, 933 (1959).

(6) R. N. Crowe and C. N. Caughlan, *J. Am. Chem. Soc.*, **72**, 1694 (1950).

TABLE II

RESULTS OF ELECTRIC MOMENT CALCULATIONS

Ester	d_1	$\Delta d/\Delta N$	ϵ_1	$\Delta\epsilon/\Delta N$	P_T, cc.	R_D, cc.	$\mu_{soln.}$, D.	$\mu_{monomer}$, D.
Et_3VO_4	0.8735	0.5019	2.2731	2.466	89.86	51.98	1.18	1.16
$Pr_3^nVO_4$	.8736	.4517	2.2748	2.226	102.24	66.27	1.15	1.11
$Pr_3^iVO_4$	.8736	.4074	2.2709	2.427	107.06	66.96	1.23	1.40
$Bu_3^nVO_4$	.8736	.4412	2.2729	2.064	114.50	80.06	1.12	1.09
$Bu_3^iVO_4$	.8736	.4027	2.2703	1.957	114.01	80.55	1.10	1.10
$Bu_3^sVO_4$	.8736	.3990	2.2716	1.698	110.36	80.71	1.10	1.30
$Bu_3^tVO_4$	.8735	.3574	2.2705	2.11	117.63	81.06[a]	1.16	..
$Am_3^tVO_4$	.8735	.3905	2.2731	1.924	128.35	94.66	1.11	1.22

[a] This value calculated from tables of atomic refraction and values of R_D for the other esters.

The electronic polarizations were considered to be an arbitrary fraction (96%) of the molar refractions. The atomic polarizations were estimated as an additive function of bond atomic polarizations. Values for bond atomic polarizations were obtained from calculated atomic polarizations.[8] Estimated atomic polarizations of 11–13 cc./mole were used. Benzene was employed as the solvent.

Solution Densities.—Since the Hedestrand equations requires $\Delta d/\Delta N$, the magnetically controlled float density method was used.[9] This apparatus permitted rapid, precise measurements of density change under nearly anhydrous conditions. $\Delta d/\Delta N$ was obtained by least squares methods.

Solution Dielectric Constant Measurements.—$\Delta\epsilon/\Delta N$ is also needed for the Hedestrand extrapolation. In order to obtain this, a jacketed reservoir of approximately 100 ml. was added to the cell of the apparatus used for measuring the dielectric constants of the esters. Small weighed increments of the esters were added to a weighed quantity of benzene in the cell reservoir. The dielectric constant of the solution was measured after each addition. This provided data needed to calculate $\Delta\epsilon/\Delta N$ by least squares methods.

Densities and dielectric constants of the solvent used in calculations of total polarization were obtained by extrapolation of ϵ^{25} and d^{25}_4 to zero mole fraction.

In addition to calculating the solution electric moments at 25°, these moments were also obtained from ϵ^{25}, d^{25}_4, and $n^{25}D$ using the modified Onsager equation.[10] The results of these measurements are shown in Table II.

Cryoscopic molecular weight measurements were made in benzene. At the concentrations used in the electric moment measurements, the esters were monomeric.

Using the R_D values obtained for the esters and known atomic refractions, a VO group refraction of 15.86 ± 0.3 cc. was calculated.

Discussion

An examination of models of these esters, constructed with tetrahedral vanadium bond angles, indicates the possibility of restricted rotation in these molecules.

A likely configuration (A) and an opposite, less favored, configuration (B) is indicated in Fig. 1. (Only two of the three alkoxy groups are shown.) Bond moments are indicated by labeled arrows, the point indicating the more negative partner.

It should be noted that the less probable configuration (B) results in a combination of bond moments m_2 and m_1 in a direction aiding bond moment m_3. The "A" position, however, shows a resultant moment opposing m_3. Mutual restriction of rotation among the alkoxy groups should result in measured electric moments lower than the moments these molecules would possess if free rotation of the alkoxy groups are possible. Estok[11] has suggested this effect in the orthophosphate esters.

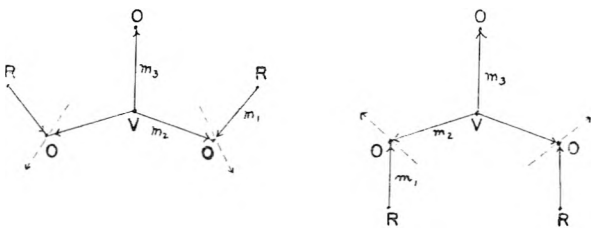

Fig. 1.—Organic vanadate vector model.

The esters can be considered as derivatives of $VOCl_3$ produced by replacing Cl atoms with alkoxy groups. $VOCl_3$ bond angles closely approximate tetrahedral angles.[12] Since the esters are found to be approximately monomeric at the concentrations used for electric moment measurements, it seems probably that the vanadium bond angles of the esters are approximately tetrahedral.

The oxygen bond angle in alcohols and ethers is near 110°.[13] The alkoxy oxygen bond angle in the esters is likely to be close to this value. Since 110° is effectively the tetrahedral angle (109°28′), tetrahedral bond angles may be used to simplify calculation of average free rotation electric moments.

A general expression for the calculation of electric moments assuming free rotation has been developed by Eyring.[14]

Using tetrahedral angles and the notation for bond moments shown in Fig. 1, the simplified equation becomes

$$\bar{\mu}^2 = 3m_1^2 + 3m_2^2 + m_3^2 - 6\cos\phi\,(m_2^2 + m_2m_3 + m_1m_2) + 6\cos^2\phi\,(2m_1m_2 + m_1m_3) - 6\cos^3\phi\,m_1^2$$

ϕ is the supplement of the tetrahedral angle (70°32′).

Lone electron pairs in hybrid orbitals (*e.g.*, NF_3, SF_4) can make sizeable contributions to the electric moment of a molecule. Were this the case for these esters such contributions should be included. Since the vanadium electrons appear to be engaged in bonding, we will assume the above equation to be valid.

Using m_1 equal to 1.14 *D*,[15] and since cos ϕ is

(7) G. Hedestrand, *Z. physik. Chem.*, **2B**, 428 (1929).

(8) C. P. Smyth, "Dielectric Behavior and Structure," McGraw-Hill Book Co., New York, N. Y., 1955, p. 420.

(9) C. N. Caughlan and F. Cartan, *J. Am. Chem. Soc.*, **81**, 3840 (1959).

(10) See ref. 8, p. 226.

(11) G. K. Estok and W. W. Wendlandt, *J. Am. Chem. Soc.*, **77**, 4767 (1955).

(12) J. K. Palmer, *ibid.*, **60**, 2360 (1938).

(13) See ref. 8, p. 297.

(14) H. Eyring, *Phys. Rev.*, **39**, 746 (1932).

(15) See ref. 8, p. 301.

$^1/_3$, this equation simplifies to

$$\bar{\mu}^2 = (m_2 - m_3)^2 - 0.76(m_2 - m_3) + 3.611$$

From this equation, the minimum average electric moment possible, assuming free rotation and irrespective of the values of m_2 and m_3 is 1.86 Debyes. This is evident since a minimum calculated μ will occur when $m_2 - m_3 = +0.38$. The results of the solution measurements (Table II) indicate moments near 1.2 *D*. Considerable restriction to rotation of the alkoxy groups is, therefore, indicated.

Acknowledgment.—We are indebted to the Office of Ordnance Research, U. S. Army, for supporting this work under Contract DA-04-200-ORD-037.

NOTES

THE DECARBOXYLATION OF THE TRICHLOROACETATE ION IN *n*-BUTYL ALCOHOL, *n*-HEXYL ALCOHOL AND *n*-CAPROIC ACID

BY LOUIS WATTS CLARK*

Department of Chemistry, Saint Mary of the Plains College, Dodge City, Kansas

Received April 8, 1960

A large variety of organic reactions takes place as the result of an initial interaction between an electrophilic, polarized, carbonyl carbon atom (in aldehydes, ketones, esters, acids, amides and related compounds) and a nucleophilic agent. The extremely general Claisen condensation may be cited as an outstanding example of this principle.[1] It appears highly probable, also, that a great many reactions of biochemical interest, *e.g.*, enzymic and immunization reactions, are of this same general type.[2]

Two closely related examples of this type of reaction which have been the subject of a great many kinetic studies over a relatively long period of time are the decarboxylations of malonic acid and the trichloroacetate ion in polar solvents. It has been demonstrated convincingly that the rate-determining step for both reactions is the formation, prior to cleavage, of a transition complex involving coördination between the electrophilic carbonyl carbon atom of un-ionized malonic acid on the one hand, and that of the trichloroacetate ion on the other, with an unshared pair of electrons on the nucleophilic atom of the solvent molecule.[3] The decomposition of malonic acid has been studied, to date, in approximately 53 non-aqueous solvents,[4] that of the trichloroacetate ion in more than a dozen.[5]

In those solvents containing mobile electrons in addition to the fixed electron pairs on the nucleophilic atom an interesting difference in electron influence has been observed between these two species. It has been observed that, in the attempted coördination between malonic acid and a polar molecule, the effective positive charge on the carbonyl carbon atom of the malonic acid tends to attract mobile electrons present in the solvent molecule, resulting in a decrease in ΔH^*. On the other hand, the resonating negative ionic charge on the trichloroacetate ion tends to repel mobile electrons present in the solvent molecule, thus decreasing the electron density on the nucleophilic center at the moment of reaction and resulting in an increase in ΔH^*. The solvent molecule responds to the advances of the malonic acid, but resists the advances of the trichloroacetate ion. This phenomenon is not observed in polar solvents containing no mobile electrons.[3b]

Although this principle has been tested already on a considerable number of compounds of various classes it was deemed worthwhile to carry out additional tests to see whether or not any exception could be found to it. For this purpose kinetic studies have been carried out in this Laboratory on the decarboxylation of the trichloroacetate ion in three additional polar solvents, namely, *n*-butyl alcohol, *n*-hexyl alcohol and *n*-caproic acid. The results of this investigation are reported herein.

Experimental

Reagents.—(1) The potassium trichloroacetate used in this research was reagent grade, 100.0% assay. (2) The solvents were reagent grade chemicals which were freshly distilled at atmospheric pressure directly into the reaction flask immediately before the beginning of each decarboxylation experiment.

Apparatus and Technique.—The details of the apparatus and technique have been described previously.[6] Temperatures were controlled to within ±0.01°, and were determined by means of a thermometer calibrated by the U. S. Bureau of Standards. The reaction flask was 100-ml. capacity. Approximately 60 g. of solvent was used in each experiment, along with 330 mg. of potassium trichloroacetate (the amount required to furnish 40.0 ml. of CO_2 at STP on complete reaction).

Results

In the decarboxylation of the trichloroacetate ion in *n*-butyl alcohol and in *n*-hexyl alcohol the log $(V_\infty - V_t)$ was a linear function of time over only approximately the first 75% of the reaction. In any one experiment no more than 85% of the theoretical volume of CO_2 was collected. This probably is attributable to a partial absorption of the evolved CO_2 by the alkoxide ions concomitantly formed. In the decarboxylation of the trichloroacetate ion in *n*-caproic acid, on the other hand,

* Western Carolina College, Cullowhee, N. C.

(1) R. Q. Brewster, "Organic Chemistry," 2nd Ed., Prentice-Hall, Inc., New York, N. Y., 1953, pp. 400 *et seq.*

(2) J. H. Turnbull, *Experientia*, XV/**8**, 304 (1959).

(3) (a) G. Fraenkel, R. L. Belford and P. E. Yankwich, *J. Am. Chem. Soc.*, **76**, 15 (1854); (b) L. W. Clark, THIS JOURNAL, **63**, 99 (1959).

(4) L. W. Clark, *ibid.*, **64**, 692 (1960).

(5) L. W. Clark, *ibid.*, **64**, 917 (1960).

(6) L. W. Clark, *ibid.*, **60**, 1150 (1956).

regular first-order kinetics were observed over the greater part of the experiment, and each experiment went practically to completion. Duplicate experiments were performed in each solvent at four different temperatures over about a 20° interval. The average rate constants calculated in the usual manner from the slopes of the experimental logarithmic plots are brought together in Table I. The parameters of the Eyring Equation,[7] based upon the data in Table I, are shown in Table II. Included in the table for purposes of comparison are corresponding data for the decomposition of the trichloroacetate ion in several other solvents previously studied, as well as data for the malonic acid reaction where available.

TABLE I

APPARENT FIRST-ORDER RATE CONSTANTS FOR THE DECARBOXYLATION OF POTASSIUM TRICHLOROACETATE IN SEVERAL LIQUIDS

Solvent	Temp., °C. cor.	$k \times 10^4$, sec.$^{-1}$	Average deviation
n-Butyl alcohol	96.83	0.080	0.002
	103.04	.166	.002
	107.70	.357	.003
	110.94	.399	.003
n-Hexyl alcohol	77.03	.553	.004
	85.44	1.137	.01
	92.04	5.89	.02
	96.54	11.62	.02
n-Caproic acid	118.71	0.532	.005
	124.54	1.537	.01
	134.23	5.09	.01
	138.86	8.96	.01

TABLE II

KINETIC DATA FOR THE DECARBOXYLATION OF THE TRICHLOROACETATE ION AND OF MALONIC ACID IN VARIOUS LIQUIDS

	Trichloracetate ion		Malonic acid	
Solvent[a]	ΔH^* (kcal./mole)	ΔS^* (e.u.)	ΔH^* (kcal./mole)	ΔS^* (e.u.)
Butanoic acid[5,9]	35.1	+12.7	32.3	+2.5
Hexanoic acid[4]	39.3	+22.1	32.5	+3.2
Decanoic acid[5,4]	41.4	+27.7	26.6	−11.0
Ethanol[10]	31.1	+15.3		
1-Butanol[11]	31.0	+ 1.6	27.2	−4.4
1-Hexanol[11]	39.6	+34.7	26.0	−7.6

[a] The first superscript after the name of the solvent refers to the source of the trichloroacetate ion data, the second to that of malonic acid. In the case of hexanoic acid, 1-butanol and 1-hexanol, the superscript refers to the source of the malonic acid data.

Discussion

It is interesting to note that, in the case of all the aliphatic acids and alcohols listed in Table II, both ΔH^* and ΔS^* for the decomposition of the trichloroacetate ion are generally much higher than they are for that of malonic acid, also, in nearly all cases where the ΔH^* for the trichloroacetate ion reaction increases with changes of solvent, that for malonic acid decreases.

The increase in ΔS^* of approximately 10 e.u. in the case of the trichloroacetate ion reaction on going from butanoic acid to hexanoic acid (lines 1 and 2 of Table II) points to a decrease in the degree of dimerization of the six-carbon acid.

It is highly probable that decanoic acid (line 3) does not exist at all in the dimeric form.[5] The fact that ΔS^* decreases on going from hexanoic acid to decanoic acid in the malonic acid reaction and increases in the trichloroacetate ion reaction probably is connected with the fact that the trichloroacetate ion, because of its electron repelling effect, is able to keep the long hydrocarbon chain of decanoic acid at a distance from the carboxyl group, whereas malonic acid is unable to do this.

Hydrogen bonding (in the case of both acids and alcohols) serves to immobilize or restrain some of the mobile electrons present in a molecule. With the partial or complete destruction of hydrogen bonding these bound electrons are released, and are thereby enabled to retreat to more remote positions within the molecule under the repelling influence of the trichloroacetate ion, or, on the other hand, to respond freely to the attractive influence of the polarized carbonyl carbon atom of malonic acid. The result will be an increase in ΔH^* in the first case, a decrease in ΔH^* in the second. This principle is strikingly illustrated by the data in lines 2 and 3, and again in lines 5 and 6 of Table II.

The large difference in ΔS^* for the trichloroacetate ion reaction on going from ethanol to 1-butanol (lines 4 and 5 of Table II) is commensurate with the relative sizes of the associated complexes of the two alcohols which probably consist of three or four molecules each.[12]

It is interesting to note in Table I that, at about 96°, the trichloroacetate ion decomposes 145 times faster in 1-hexanol than in 1-butanol. The reason for this unexpected result can be deduced readily by studying the data in lines 5 and 6 of Table II. On going from 1-butanol to 1-hexanol the ΔH^* for the trichloroacetate ion reaction increases by about 9 kcal. and the ΔS^* increases by more than 33 e.u. Apparently the association cluster or "supermolecule" of 1-hexanol (but not of 1-butanol) has been broken up by the negatively charged trichloroacetate ion, releasing some of the mobile electrons involved in hydrogen bonding, which then retreat as far as possible from the nucleophilic center. (The malonic acid reaction does not show this kind of behavior.) The great increase in the rate of reaction in 1-hexanol is due largely to the improved entropy factor which more than compensates for the retarding effect of the higher activation energy.

The fact that the ΔH^* for the malonic acid reaction is lower in both alcohols than is that of the trichloroacetate ion indicates that in the malonic acid reaction the alkyl groups of both alcohols produce a +I effect, but in the reaction

(7) S. Gladstone, K. J. Laidler and H. Eyring, "The Theory of Rate Processes," McGraw-Hill Book Co., Inc., New York, N. Y., 1st ed., 1941, p. 195, equation 158.

(8) L. W. Clark, THIS JOURNAL, **63**, 1760 (1959).

(9) L. W. Clark, *ibid.*, **64**, 41 (1960).

(10) F. H. Verhoek, *J. Am. Chem. Soc.*, **56**, 571 (1934).

(11) L. W. Clark, THIS JOURNAL, **64**, 508 (1960).

(12) W. Hückel, "Theoretical Principles of Organic Chemistry," Vol. II, Elsevier Pub. Co., New York, N. Y., 1958, p. 341.

with the trichloroacetate ion the potential +I effect is prevented from taking place.

If decanoic acid and 1-hexanol do not associate through hydrogen bonding the difference of 1.8 kcal. in the ΔH^* of the trichloroacetate ion reaction in these two solvents (lines 3 and 6 of Table II) may be attributed to the additional electron withdrawal due to a −E effect on the carbonyl carbon atom of decanoic acid evoked by the negative charge on the attacking ion. The decrease of 7 e.u. in the ΔS^* of the reaction on going from 1-hexanol to decanoic acid is commensurate with the difference in the number of carbon atoms between the monomers of the two compounds plus the steric effect (screening effect) of the carbonyl oxygen atom in close proximity to the nucleophilic hydroxyl group.

The results of this investigation strengthen the hypothesis that the electron repelling influence of the negative charge on the trichloroacetate ion tends to evoke unfavorable inductive and electromeric effects, and that the electron attracting influence of the electrophilic, carbonyl carbon atom of the un-ionized malonic acid tends to evoke favorable inductive and electromeric effects.

Further work on this problem is contemplated.

Acknowledgments.—(1) The support of this research by the National Science Foundation, Washington, D. C., is gratefully acknowledged. (2) The potassium trichloroacetate used in this research was supplied by Dr. James D. Solomon, Blackburn Laboratories, St. Elizabeth Hospital, Washington, D. C.

ON THE NATURE OF ULTRAVIOLET LIGHT WHICH ACCOMPANIES THE DECOMPOSITION OF SOME AZIDES[1]

BY R. W. NICHOLLS[2]

Department of Physics, University of Western Ontario, London, Ontario, Canada

Received April 29, 1960

Some years ago Audubert and his colleagues reported that a very feeble luminosity accompanied the slow thermal decomposition of NaN_3,[3,4,5,6] KN_3,[3] AgN_3,[3,7] $Pb(N_3)_2$,[3] $Ca(N_3)_2$,[3] $Ba(N_3)_2$,[3] TlN_3.[8] It also occurs near the anode during electrolysis of NaN_3 and HN_3.[9] The spectrum of the luminosity was studied over the wave length range 1800–2600 Å. at very low dispersion using a quartz monochromator and a copper iodide photon counter,[10–12] and was found to be limited to broad bands centered at about 2000, 2150, 2300, 2400 and 2550 Å., with wave length uncertainties which range from ±25 to ±40 Å. His observed wave lengths are listed in Table I and have been claimed to be independent of cation. Audubert suggested in most of the papers cited that the bands could be explained in terms of the known energy levels of N_2, and in one paper[13] specifically compares four of his band wave lengths with those of one band each of four different N_2 band systems.

It is the purpose of this note to suggest that the broad features probably arise from groups of bands of the N_2 Vegard-Kaplan ($A^3\Sigma_u^+ \rightarrow X^1\Sigma_g^+$) system which originate from the $v' = 0, 1, 2, 3$ levels of the $A^3\Sigma_u^+$ state.

The band-head vacuum wave lengths from 1900–2600 Å. of the gas-phase Vegard-Kaplan bands are also given in Table I together with their Franck-Condon factors $q_{v'v''}$[15] which give an indication of the relative band intensities for equal populations in the upper levels. It will be noticed in Table I that strong Vegard-Kaplan bands ($q_{v'v''} \sim 0.1$ or greater) occur in the region of each of the bands reported by Audubert. Positive identifications are, of course, difficult with such large uncertainties on wave lengths but the following points lend strong support to identification of the Vegard-Kaplan system as the most plausible emitter. (A) It is physically more reasonable to attribute all of the bands to one system than to rely on individual wave length coincidences between the bands and those of difference N_2 systems. (B) In considering the mechanisms of dissociation of simple molecules, Henri[16] compared lengths (r_e) and characteristic frequencies (ω_e) of bonds within the molecules with those of the electronic states of diatomic species into which the molecule may decompose. In particular he quotes the values $r_e = 1.13$ Å., $\omega_e = 2060$ cm.$^{-1}$ for the terminal NN bond in NaN_3 to be compared with the values $r_e = 1.144$ Å.; $\omega_e = 2046$ cm.$^{-1}$ for free N_2 in the $C^3\Pi_u$ state. From the close agreement between these data he went on to propose that N_2 is formed in the $C^3\Pi_u$ state in the slow thermal decomposition of NaN_3. The more recent values of $r_e = 1.148$ Å.; $\omega_e = 2035.1$ cm.$^{-1}$ for the $C^3\Pi_u$ state,[17] and the fact that the characteristic frequency $\omega_e = 2141$ cm.$^{-1}$ is now associated with the antisymmetric stretching of the N_3 group as a whole[18] while r_e for the terminal NN bond is 1.128 Å.[19] does not detract from the usefulness of Henri's suggestion which is really based (insofar as rough equality of r_e is concerned) upon the Franck-Condon principle.

If it therefore be supposed that N_2 is formed during slow thermal decomposition of NaN_3 in the $v' = 0$ level of $C^3\Pi_u$, three radiative transitions in cascade will be expected to occur, *viz.*, $C^3\Pi_u \rightarrow$

(1) This work has been supported in part by contracts with the Air Force Office of Scientific Research, The Office of Naval Research, The Air Force Cambridge Research Center and the Department of Defence Production of Canada.

(2) Temporarily on leave of absence at the National Bureau of Standards, Washington, D. C.

(3) R. Audubert and H. Muraow, *Compt. rend.*, **204**, 431 (1937).

(4) R. Audubert, *ibid.*, **204**, 1192 (1937).

(5) R. Audubert, *ibid.*, **206**, 748 (1938).

(6) R. Audubert and J. Mattler, *ibid.*, **206**, 1639 (1938).

(7) R. Audubert, *ibid.*, **205**, 133 (1937).

(8) R. Audubert and C. Racz, *ibid.*, **208**, 1810 (1939).

(9) R. Audubert, *ibid.*, **208**, 1984 (1939).

(10) R. Audubert, *J. Phys. et Rad.*, **6**, 452 (1935).

(11) R. Audubert, *Compt. rend.*, **200**, 389 (1935).

(12) R. Audubert, *ibid.*, **200**, 918 (1935).

(13) R. Audubert, *Trans. Faraday Soc.*, **35**, 197 (1939).

(14) R. W. Nicholls, *Ann. Geophys.*, **14**, 208 (1957).

(15) W. R. Jarmain, P. A. Fraser and R. W. Nicholls, *Astrophy. J.*, **118**, 228 (1953).

(16) V. Henri, *Compt. rend.*, **203**, 67 (1936).

(17) R. S. Mulliken, "The Threshold of Space," Pergamon Press, Inc., New York, N. Y., 1957, p. 169.

(18) E. H. Eyster and R. H. Gillette, *J. Chem. Phys.*, **8**, 369 (1940).

(19) E. H. Eyster, *ibid.*, **8**, 135 (1940).

TABLE I

BAND-HEAD VACUUM WAVE LENGTHS AND FRANCK-CONDON FACTORS FOR VEGARD-KAPLAN BANDS IN THE SPECTRAL REGION 1900–2600 Å., AND AUDUBERT'S BANDS ARISING FROM THERMAL DECOMPOSITION AND ELECTROLYSIS OF SOME AZIDES

Vegard-Kaplan bands			Audubert's features (Å.)				
$v'v''$[a]	λ (Å.)	$q_{v'v''}$[b]	NaN_3 (Thermal)	AgN_3 (Thermal)	TlN_3 (Thermal)	NaN_3 (Elect)	HN_3 (Elect)
2,0	1901	0.009					
3,1	1936	.07					
1,7	1954	.003	1975 ± 25				1950 ± 25
2,1	1990	.043				1990 ± 52	
0,0	2010	.001					
3,2	2027	.099					
1,1	2046	.019			2040 ± 30		
2,2	2085	.096					
0,1	2108	.004					
3,3	2125	.044			2140 ± 30	2130 ± 25	
1,2	2148	.06	2150 ± 25	2150 ± 25			2140 ± 25
2,3	2189	.102					
1,3	2258	.111			2280 ± 35	2270 ± 35	
2,4	2302	.041	2300 ± 35	2300 ± 35			2300 ± 35
0,3	2334	.053					
3,5	2347	.044					
1,4	2379	.124	2400 ± 40	2400 ± 40	2390 ± 40		2450 ± 35
2,5	2425	.000				2425 ± 35	
0,4	2463	.106					
3,6	2474	.07					
1,5	2511	.076			2500 ± 40		
2,6	2561	.041				2550 ± 40	
0,5	2605	.158					2600 ± 40
3,7	2614	.019			(2650)[c]		

[a] The bands predicted as occurring strongly are italicized. [b] $q_{v'v''}$ is the Franck-Condon factor of the band.[14] [c] Audubert cites this band as doubtful.[8]

$B^3\Pi_g$ (Second Positive Bands), $B^3\Pi_g - A^3\Sigma_u^+$ (First Positive Bands), $A^3\Sigma_u^+ \rightarrow X^1\Sigma_g^+$ (Vegard-Kaplan Bands). Tables of Franck-Condon Factors which are available for these transitions[15,20] may then be used to predict which bands will be most strongly radiated. They are

N_2 Second positive bands:	$v' = 0$	$v'' = 0, 1, 2$
N_2 First positive bands:	$v' = 0$	$v'' = 0, 1, 2$
	$v' = 1$	$v'' = 0, 2, 3. 4$
	$v' = 2$	$v'' = 0, 1, 2, 5, 6$
N_2 Vegard-Kaplan bands:	$v' = 0$	$v'' = 4, 5, 6, 7, 8$
	$v' = 1$	$v'' = 3, 4, 5, 9, 10, 11$
(From 1900–2600 Å.)	$v' = 2$	$v'' = 2, 3, 6, 7, 8, 11, 12, 13$
	$v' = 3$	$v'' = 1, 2, 3, 5, 6, 7, 13, 14, 15, 16$

The strong Vegard-Kaplan bands predicted by this scheme, which lie in the wave length range of Table I have been italicized there and it is noted that such strong bands appear in each of the five groups into which the table is divided. Additional Vegard-Kaplan bands can be predicted in a similar fashion if it be assumed that the $v' = 1$, 2, etc., levels of $C^3\Pi_u$ are also populated by thermal dissociation of azides. (C) It is possible that N_2 is formed during the decomposition of the azides directly into the $A^3\Sigma_u^+$ state from which the Vegard-Kaplan system is radiated directly. The primary Franck-Condon parabola for the system passes (in the usual v', v'' array) in the vicinity of the (3, 2), (2, 3), (1, 3), (1, 4) and (0, 5) bands one of each of which is associated in Table I with each of Audubert's spectral features.

(20) W. Jarmain and R. W. Nicholls, *Can. J. Phys.*, **32**, 201 (1954).

The intrinsic weakness of the intercombination Vegard-Kaplan system may account in some part for the very feeble intensities observed by Audubert. The system nevertheless has been excited in the gas phase by electrical discharges of various kinds by Kaplan,[21] Wulf and Melvin,[22] Janin[23] and Herman and Herman,[24] by electron beams by Bernard,[25] and in solid N_2 by Vegard[26] and by Peyron and Broida.[27]

The bands observed during electrolysis of azides probably are excited in electrical discharges inside the small bubbles of N_2 liberated at the anode. Ozonizer-like electrical discharges caused by surface changes in such bubbles are known to give rise to light[28] and as Wulf and Melvin point out[22] such discharges are favorable for the excitation of the Vegard-Kaplan system.

One test for the operation of the cascade mechanism discussed in B above is to observe the predicted strong bands of the N_2 second positive and first positive bands (which lay outside Audubert's range of observation and which are also outside the visible spectrum). Experiments to search for these bands are in preparation. The absence of them will not weaken the case for identification of

(21) J. Kaplan, *Phys. Rev.*, **45**, 675 (1934).
(22) O. R. Wulf and E. H. Melvin, *Phys. Rev.*, **55**, 687 (1939).
(23) J. Janin, *Ann. Phys.*, [12] **1**, 538 (1946).
(24) R. Herman and L. Herman, *J. Phys. et Rad.*, **7**, 203 (1946).
(25) R. Bernard, *Compt. rend.*, **200**, 2074 (1935).
(26) L. Vegard, *Skrifter Norske Videnskaps. Akad. Oslo*, No. 9 (1938).
(27) M. Peyron and H. P. Broida, *J. Chem. Phys.*, **30**, 139 (1959).
(28) P. Jarman, *Proc. Phys. Soc.*, **73**, 628 (1959).

Audubert's features with Vegard–Kaplan bands, but will make the cascade mechanism less likely.

THE GROWTH OF LARGE SINGLE CRYSTALS OF ZINC OXIDE[1]

By J. W. Nielsen[2] and E. F. Dearborn

Bell Telephone Laboratories, Inc., Murray Hill, New Jersey

Received May 3, 1960

Single crystals of hexagonal zinc oxide can be grown from the vapor phase by the method of Scharowsky.[3] Lander[4] has improved upon Scharowsky's method and recently Laudise and Ballman[5] have shown that zinc oxide can be grown hydrothermally. Both of these methods produce crystals which have a needle-like habit with the needle axis and the crystallographic *c*-axis coinciding. Growth perpendicular to the *c*-direction is usually quite slow and seldom exceeds a millimeter. Growth of single crystals from molten salt solution was attempted in the hope crystals large in the *a*-dimension could be obtained which could be used as seeds for the hydrothermal method.

As is usually the case with molten salt systems, insufficient phase equilibrium data were available to choose a solvent for ZnO, and the selection had to be made by trial and error with the help of previous experience. It was quickly discovered that LiCl and KF were very poor solvents for ZnO. PbF_2, however, dissolved appreciable quantities of ZnO, and this solvent was selected. PbF_2 previously had been used by Jona, Shirane and Pepinsky[6] to grow single crystals of lead zirconate, and it had been used by the authors[7] to grow crystals of Mn_2O_3 and $La_{0.7}Pb_{0.3}MnO_3$. ZnO crystals grown from molten PbF_2 between 1050 and 1150° exhibited the desired platey habit, the plane of the plate coinciding with the (001) crystallographic plane.

Experimental

All crystal growth experiments were done in resistance furnaces which have been described previously.[8] The samples were contained in 100 ml. platinum crucibles fitted with lids. They were prepared from reagent grade chemicals or materials prepared from reagent grade salts. Two hundred g. of PbF_2 and 22 g. of ZnO were convenient amounts to use. Temperatures were measured with Pt–10% Rh–Pt thermocouples.

It was found that 1150° was a convenient temperature from which to begin crystal growth. At this temperature the volatility of PbF_2, though high, was not excessive. The samples usually were held at 1150° for from 2 to 4 hours and then cooled at a constant rate of from 1 to 10° per hour. The system reaches a steady state quickly and it is possible a holding time of less than two hours would be satisfactory. The samples usually were withdrawn near 800° and allowed to cool in air. Both air and oxygen atmospheres were used in the growing furnace and no change in growth characteristics resulted.

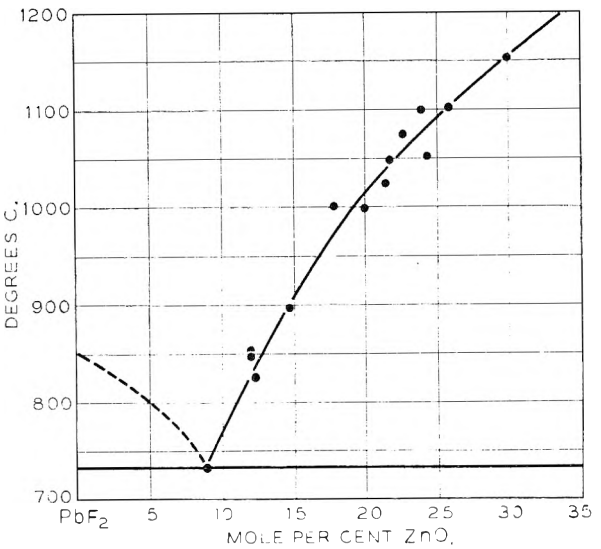

Fig. 1.—Solubility curve of ZnO in PbF_2.

Since no method of chemically separating PbF_2 from ZnO has been found, the crystals must be broken away from the melt. It is still possible, however, to separate crystals which are 1 to 5 cm. in their largest dimension (the *a*-dimension) by tapping the bottom of the crucible containing the sample. It is found that the PbF_2 does not cling very tenaciously to the ZnO crystals.

Solubility Data.—A rather crude solubility curve of ZnO in molten PbF_2 was determined. The system has only a simple eutectic between 0 and 35 mole % ZnO. The curve, which is shown in Fig. 1, was obtained by preparing melts with a large excess of ZnO present, holding them for at least two hours at the desired temperature and quenching them in water as quickly as possible. The excess ZnO which had floated on the surface of the melt was analyzed for zinc and lead. The percentage zinc oxide present was calculated assuming all the zinc was present as ZnO and the lead as PbF_2. The eutectic composition was determined from a crystal run which was allowed to cool to solidification. The eutectic was found to be at 8.8 mole % ZnO and 733°. Two of the points near 850° were determined by approaching the equilibrium from the other side, that is, slowly cooling the melts to that temperature from 1150°, then quenching them. Since these points fell on the curve nicely, it was assumed that two hours is ample time to allow for a steady state condition to be reached by samples held at constant temperature.

The average error in the ZnO concentration determined by this method is ±2% except at the eutectic where the ZnO concentration is known more accurately. It should be pointed out that the quench technique is not as reliable as one might wish when melts are highly fluid, but the great volatility of PbF_2 makes any other technique extremely difficult.

Another possible source of error lies in side reactions. X-Ray powder photographs of quenched melts of ZnO and PbF_2 revealed that only ZnO and β-PbF_2 with a small amount of α-PbF_2, were present. Thus side reactions, if they occur, do not yield products in amounts detectable by X-ray diffraction.

Spectrochemical analyses of the crystals indicated a total impurity content of less than 0.1%.

Discussion

Although the habit of the ZnO crystals on the melt surface was platey, it was discovered that crystals nucleated at temperatures below 1050° tended to be more drum shaped. Thus the ratio of the rate in the *a*-direction to the rate in the *c*-direction varied from about 50 to 1150° to near unity at 1050°. It was also observed that crystals

(1) Presented at the 135th Meeting of the American Chemical Society, Boston, Massachusetts, April 1959.

(2) Now at Airtron, Division of Litton Industries, Morris Plains, N. J.

(3) E. Scharowsky, *Z. physik.*, **135**, 318 (1953).

(4) J. J. Lander (to be published).

(5) R. A. Laudise and A. A. Ballman (to be published).

(6) F. Jona, G. Shirane and R. Pepinsky, *Phys. Rev.*, **97**, 1584 (1955).

(7) J. W. Nielsen and E. F. Dearborn (unpublished work).

(8) J. W. Nielsen and E. F. Dearborn, *Phys. Chem. of Solids*, **5**, 202 (1958).

grown by evaporation of PbF_2 at 1150° were always very thin plates and exhibited the largest ratio of rate in the *a*-direction to rate in the *c*-direction. The reason for this change in habit is not known, but it probably arises from a rather subtle change in the structure of the PbF_2–ZnO melt. The possibility that a buildup of PbO was responsible in some way for the habit change was eliminated by growing crystals in melts to which PbO had been added. No change in growth characteristics was observed. At present, no experimental studies of such melts which could lead to an explanation of the habit change have been made.

In conclusion, large single crystals of ZnO which possess an unusual and convenient habit have been grown from molten lead fluoride. Such crystals already have been used successfully as seeds in hydrothermal crystal growth experiments.[5] The combination of the two methods should lead to growth of the first very large and pure crystals of ZnO.

Acknowledgments.—The authors wish to thank W. Hartmann and E. Bloom for the excellent chemical analyses required for this work.

THE HIGH TEMPERATURE HEAT CONTENT OF SODIUM OXIDE[1]

BY ROBERT T. GRIMLEY[2] AND JOHN L. MARGRAVE

Department of Chemistry, University of Wisconsin, Madison, Wisconsin

Received May 5, 1960

A review of available literature indicates that the only high temperature heat content data reported for the alkali oxides are those of Shomate and Cohen[3] for lithium oxide. In addition, Naylor[4] has estimated the high temperature heat content of sodium oxide by employing the Neumann–Kopp rule in conjunction with experimental data for Na_2TiO_3, $Na_2Ti_2O_5$, $Na_2Ti_3O_7$ and TiO_2. Experimental values for the heat content of sodium oxide are presented in this paper.

Measurements were made using a copper block drop-type calorimeter which has been described previously.[5] The sample of sodium oxide was prepared from commercial grade du Pont sodium oxide by purification according to the method of Klemenc, Ofner and Wirth[6] and X-ray examination of the product showed only the lines of sodium oxide. Analyses were made for Na_2O, Na_2O_2 and Na_2CO_3 and the sample was found to consist of 96.76% Na_2O, 2.33% Na_2CO_3 and 0.91% Na_2O_2. The presence of NaOH was ruled out on the basis of indirect analysis. The sample (9.2728 g. *in vacuo*) was transferred to a gold capsule, the neck of the capsule squeezed shut and then soldered with gold. All operations of preparation or transfer were carried out either *in vacuo* or in a carbon dioxide-free dry box.

The heat content of the capsule was determined by separate experiments over the temperature range investigated. A platinum *vs.* platinum–rhodium thermocouple, previously calibrated against a National Bureau of Standards thermocouple, was used for furnace temperature measurements.

The measured heat contents of Na_2O above 298° K. are given in Table I. The results are based upon a molecular weight of 61.98[7] for Na_2O and are expressed in defined calories per mole (1 cal. = 4.1840 abs. joules). Corrections for the sodium carbonate impurity were made using the integrated heat capacity data of Popov and Ginzberg[8] and for sodium peroxide using the data of Chandrasekharaiah, Grimley and Margrave.[9] It was necessary to extrapolate the data for Na_2CO_3 and Na_2O_2 to higher temperatures in order to correct the sodium oxide data. Measurements at higher temperatures were prevented by the attack on the gold solder used in fabricating the capsule by either the sodium oxide or the impurities.

TABLE I

MEASURED HEAT CONTENT OF SODIUM OXIDE ABOVE 298.15° K. (Na_2O, mol. wt. = 61.98)

T, °K.	$H_T - H_{298.15}$, cal./mole	*T*, °K.	$H_T - H_{298.15}$, cal./mole
380.1	1418	876.0	11,447
477.2	3191	980.4	14,045
577.2	5257	1078.3	16,539
673.5	7190	1174.6	19,409
776.4	9276		

The high temperature heat content data and the heat capacity may be represented by the equations

$$H_T - H_{298.15} = 14.49T + 4.94 \times 10^{-3}T^2 - 4799 \text{ cal./mole}$$
(298–1170°K.; ±2%)

$$C_P = 14.49 + 9.88 \times 10^{-3}T \text{ cal./deg./mole}$$

A plot of the Shomate function[10] using the low temperature heat capacity data of Furukawa[11] gave some evidence of a low energy transition in the range 500–800°K. A study of this range using adiabatic methods on a sample of higher purity would appear to be desirable. Destruction of the capsule during measurements at higher temperatures prevented further study by the drop method.

From the above equations and a value for S_{298} determined by Furukawa[11] to be 17.99 e.u., the heat contents, entropies and the free energy functions were calculated at 100° intervals and the results are listed in Table II. It is interesting to note that the sodium oxide heat content which Naylor[4] estimated by subtracting the α-TiO_2 contribution to the Na_2TiO_3 heat content agrees remarkably well with the experimental values. The agreement with Naylor's mean values obtained from data on additional compounds is somewhat

(1) Presented before the 134th Meeting of the American Chemical Society, Chicago, Illinois, September 8, 1958.

(2) Department of Physics, University of Chicago, Chicago, Illinois.

(3) C. H. Shomate and A. J. Cohen, *J. Am. Chem. Soc.*, **77**, 285 (1955).

(4) B. F. Naylor, *ibid.*, 67, 2120 (1945).

(5) J. L. Margrave and R. T. Grimley, THIS JOURNAL, **62**, 1436 (1958).

(6) A. Klemenc, G. Ofner and H. Wirth, *Z. anorg. Chem.*, **265**, 221 (1951).

(7) E. Wichers, *J. Am. Chem. Soc.*, **80**, 4121 (1958).

(8) M. M. Popov and D. M. Ginzberg, *J. Gen. Chem.* (*U.S.S.R.*), **26**, 1103 (1956).

(9) M. S. Chandrasekharaiah, R. T. Grimley and J. L. Margrave, THIS JOURNAL, **63**, 1505 (1959).

(10) C. H. Shomate, *ibid.*, **58**, 368 (1954).

(11) G. Furukawa, private communication.

poorer, but, in general, does not differ by more than 10%.

TABLE II

SMOOTHED HEAT CONTENTS, ENTROPIES AND FREE ENERGY FUNCTIONS FOR SOLID SODIUM OXIDE (Na_2O, mol. wt. = 61.98)

T, °K.	$H_T - H_{298.16}$, cal./mole	$S_T - S_{298.16}$, cal./deg./mole	$\left(\frac{F_T - H_{298.16}}{T}\right)$ cal./deg./mole
400	1,789	5.27	18.79
500	3,683	9.49	20.11
600	5,676	13.12	21.65
700	7,768	16.34	23.23
800	9,959	19.27	24.81
900	12,247	21.96	26.34
1000	14,636	24.48	27.83
1100	17,122	26.85	29.27

Acknowledgments.—The authors wish to acknowledge the support of this research by the United States Navy through the Callery Chemical Company under a contract with the Bureau of Aeronautics.

HYDROLYSIS OF CADMIUM CHLORIDE AT 25°

BY KARL H. GAYER AND RUDY M. HAAS

Department of Chemistry, Wayne State University, Detroit, Michigan

Received May 9, 1960

The study of the hydrolysis reactions and the evaluation of equilibrium constants for cadmium chloride has been undertaken by other investigators. If a true hydrolysis constant can be obtained for any species of cadmium chloride over a definite concentration range, it can be related to an over-all reaction. The hydrolysis constants (K_h) and the reactions predicted by others are: Kullgren[1] reported a K_h of 3.3×10^{-6} at 100° for the reaction $CdCl^+ + H_2O \rightleftarrows CdClOH + H^+$; Chaberek, Courtney and Martell[2] calculated a K_h of 2.5×10^{-12} at 30° in a 0.1 M potassium chloride medium for the reaction $Cd^{++} + H_2O \rightleftarrows Cd(OH)^+ + H^+$. According to this last reaction it is assumed that the chloride ion from the potassium chloride has no effect on the hydrolysis reaction of the Cd^{++} ion. Doubt is cast on this assumption because it is further assumed that the concentration of the Cd^{++} ion is equal to the total concentration of cadmium chloride used. Our results seem to indicate that the major hydrolysis product at 25° is CdClOH.

Experimental

Purification of Water.—Water was prepared in a manner similar to that described by Gayer and Woontner.[3] Ordinary distilled water was distilled in a Pyrex distillation apparatus from an oxidizing solution of sodium hydroxide and potassium permanganate. The resulting water was then redistilled by adding one drop of orthophosphoric acid per liter of water. Last traces of carbon dioxide were removed by boiling the final distilled water for about 15 minutes.

Purification of Nitrogen.—Purified tank nitrogen was passed through several gas washing bottles of dilute sodium hydroxide, sulfuric acid and water.

Preparation of Cadmium Chloride.—The anhydrous cadmium chloride used was prepared from Baker Chemical Company analytical reagent cadmium chloride containing 2.5 molecules of water. The anhydrous salt was prepared by recrystallizing $CdCl_2 \cdot 2.5H_2O$ from an aqueous solution, slightly acidified with hydrochloric acid. These crystals were dehydrated in a tube oven, heated to 150°, through which was passed a stream of dry hydrogen chloride. The excess hydrogen chloride was removed by means of a current of dry nitrogen. The resulting salt then was evacuated until successive samples, taken at hour intervals, gave a constant pH reading.

Measurement of pH.—The pH was measured with a Beckman Laboratory Model G pH meter using a Beckman general purpose shielded glass electrode and a fiber type sealed calomel Beckman electrode. The hydrolysis cell contained openings for two electrodes, a thermometer, a conductivity water inlet and a nitrogen inlet and outlet. The cell containing the weighed cadmium chloride was flushed with nitrogen gas, before and during the time the purified water was added. A magnetic stirring bar agitated the solution for 15 minutes before the pH readings were taken.

When cadmium chloride is placed in water, these dissociation and association reactions may occur

$$CdCl_2 \rightleftarrows CdCl^+ + Cl^- \quad (1)$$

$$CdCl^+ \rightleftarrows Cd^{++} + Cl^- \quad (2)$$

$$CdCl_2 + Cl^- \rightleftarrows CdCl_3^- \quad (3)$$

$$CdCl_2 + 2Cl^- \rightleftarrows CdCl_4^{=} \quad (4)$$

In order to obtain the activities of these species, it is necessary to know the dissociation constants of the reactions involved. These are not available as such. As an approximation, however, it was assumed by Harned and Fitzgerald that the first reaction goes to completion, the third and fourth do not occur, and the second is the only one in which an equilibrium is involved.[4] By means of electromotive force measurements, they calculated the dissociation constant (K) for this reaction to be 1.1×10^{-2}. Other K_2 values given in the literature, assuming only the presence of Cd^{++}, $CdCl^+$ and Cl^- ions are 0.010[5] and 0.0101.[6]

$$K_2 = \frac{a_{Cd^{++}}\, a_{Cl^-}}{a_{CdCl^+}} = \frac{C_{Cd^{++}}\, C_{Cl^-}}{C_{CdCl^+}} \times \frac{f_{Cd^{++}}\, f_{Cl^-}}{f_{CdCl^+}}$$

Here a, C and f refer to the activity, concentration and activity coefficient, respectively. The various concentrations of $CdCl^+$, Cd^{++} and Cl^- ions can be evaluated by setting $X = Cd$, $X + M = Cl^-$ and $M - X = CdCl^+$, where M is the molar concentration of the cadmium chloride used. The activity coefficients can be obtained by solving the regular form of the Debye–Hückel equation

$$\log f_i = \frac{-AZ_i^2\sqrt{\mu}}{1 + Ba_i\sqrt{\mu}}$$

where Z_i is the charge on the ion, a_i is its effective diameter and u is the ionic strength of the solution. The constants A and B were taken as 0.509 and 0.330, respectively, and the effective diameters[7] of the Cd^{++}, Cl^-, $CdCl^+$ and H^+ ions were taken as 5×10^{-8}, 3×10^{-8}, 4×10^{-8} and 9×10^{-8} cm., respectively.

By the method of successive approximations, the following ionization equation can be solved by successively approximating X, the concentration of the Cd^{++} ion. The activity coefficient of the Cd^{++} ion, f_x is given in the regular form of the Debye–Hückel equation

$$0.011 = \frac{(X)(X + M)}{(M - X)} f_x \text{ where}$$

$$\log f_x = \frac{-2.04\sqrt{4X + M}}{1 + 1.65 \times 10^{-8}\sqrt{4X + M}}$$

(1) C. Kullgren, *Z. physik. Chem.* (*Leipzig*), **85**, 466 (1913).

(2) S. Chaberek, Jr., R. C. Courtney and A. E. Martell, *J. Am. Chem. Soc.*, **74**, 5057 (1952).

(3) K. H. Gayer and L. Woontner, *J. Chem. Ed.*, **33**, 296 (1956).

(4) H. S. Harned and M. Fitzgerald, *J. Am. Chem. Soc.*, **58**, 264 (1936).

(5) H. L. Riley and V. Gallafant, *J. Chem. Soc.*, 514 (1932).

(6) E. C. Righellato and C. W. Davies, *Trans. Faraday Soc.*, **26**, 592 (1930).

(7) J. Kielland, *J. Am. Chem. Soc.*, **59**, 1675 (1937).

$$0.011 = \frac{(X)(X + M)}{(M - X)} \times 10^{-2.04\sqrt{4X + M}/[1 + (1.65 \times 10^{-8}\sqrt{4X + M})]}$$

The hydrolysis constant for cadmium chloride is then calculated from a value of the concentrations of $CdCl^+$, Cd^{++}, Cl^- and H^+ (from *p*H measurements) ions and the activity coefficients of these ions. All the following hydrolysis reactions will probably occur, to some extent; it can however be assumed that one of them predominates over the rest.

$$Cd^{++} + H_2O \rightleftarrows Cd(OH)^+ + H^+ \quad (I)$$

$$Cd^{++} + 2H_2O \rightleftarrows Cd(OH)_2 + 2H^+ \quad (II)$$

$$CdCl^+ + H_2O \rightleftarrows CdClOH + H^+ \quad (III)$$

The K_h equations for the above are given in consecutive order.

$$K_{h_1} = \frac{C_{Cd(OH)^+}\, C_{H^+}}{C_{Cd^{++}}} \frac{f_{Cd(OH)^+} f_{H^+}}{f_{Cd^{++}}} = \frac{C_{(H^+ - H_0^+)} C_{H^+}}{C_{[\overline{Cd}^{++} - (H^+ - H_0^+)]}} \frac{f_{Cd(OH)^+} f_{H^+}}{f_{[\overline{Cd}^{++} - (H^+ - H_0^+)]}}$$

$$K_{h_1} \cong \frac{(A_{H^+} - A_{H_0^+} f_{H^+}) a_{H^+}}{C_{\overline{Cd}^{++}} f_{\overline{Cd}^{++}}}$$

$$K_{h_2} = \frac{C_{Cd(OH)_2}\, C_{H^+}^2}{C_{Cd^{++}}} \frac{f_{Cd(OH)_2} f_{H^+}^2}{f_{Cd^{++}}} = \frac{C_{1/2(H^+ - H_0^+)}\, C_{H^+}^2}{C_{[\overline{Cd}^{++} - 1/2(H^+ - H_0^+)]}} \frac{f_{Cd(OH)_2} f_{H^+}^2}{f_{[\overline{Cd}^{++} - 1/2(H^+ - H_0^+)]}}$$

$$K_{h_2} \cong \frac{(A_{1/2H^+} - A_{1/2H_0^+} f_{H^+}) a_{H^+}^2}{C_{\overline{Cd}^{++}} f_{\overline{Cd}^{++}} f_{H^+}}$$

$$K_{h_3} = \frac{C_{CdClOH}\, C_{H^+}}{C_{CdCl^+}} \frac{f_{CdClOH} f_{H^+}}{f_{CdCl^+}} = \frac{C_{(H^+ - H_0^+)}\, C_{H^+}}{C_{[\overline{CdCl}^{++} - (H^+ - H_0^+)]}} \frac{f_{CdClOH} f_{H^+}}{f_{[\overline{CdCl}^{+} - (H^+ - H_0^+)]}}$$

$$K_{h_3} \cong \frac{(A_{H^+} - A_{H_0^+} f_{H^+}) a_{H^+}}{C_{\overline{CdCl}^+} f_{\overline{CdCl}^+} f_{H^+}}$$

TABLE I

OBSERVED DATA AT 25°

Molarity ($CdCl_2$)	*p*H	$a_{H^+} \times 10^5$
0	6.75	0.18
0.0050	6.40	.40
.0108	6.20	.63
.0242	5.96	1.11
.0371	5.85	1.40
.0542	5.73	1.85
.0734	5.65	2.25
.102	5.55	2.80

Here C_{H^+} is the concentration of the hydrogen ion obtained from *p*H measurements and $C_{H_0^+}$ is the concentration of the hydrogen ion in the pure water before the cadmium chloride was added. The difference $C(H^+ - H_0^+)$ is then the change in the hydrogen ion concentration of the solution due to the hydrolysis of the cadmium chloride. Again assuming that only one of the above reactions occurs, the quantity of $CdClOH$ or $Cd(OH)^+$ formed is equal to the increase in the hydrogen ion concentration, and the quantity of $Cd(OH)_2$ formed is equal to one-half the increase of the hydrogen ion concentration. The concentrations $C_{Cd^{++}}$ and C_{CdCl^+} and the activity coefficients $f_{Cd^{++}}$ and f_{CdCl^+} are the values of these species after hydrolysis has occurred whereas $C_{\overline{Cd}^{++}}$ and $C_{\overline{CdCl}^+}$ and $f_{\overline{Cd}^{++}}$ and $f_{\overline{CdCl}^+}$ are the values of these ions, respectively, before hydrolysis has occurred. The terms $[\overline{Cd}^{++} - {}^1/_2(H^+ - H_0^+)]$, $\overline{CdCl}^+ - (H^+ - H_0^+)$, etc., that is, those containing the bar symbols, simply illustrate how the measured values were corrected to give the equilibrium values used in the calculations.

Approximations.—

$C_{(H^+ - H_0^+)} \ll C_{\overline{Cd}^{++}}$	$\therefore C_{[\overline{Cd}^{++} - (H^+ - H_0^+)]} \cong C_{\overline{Cd}^{++}}$
$C_{1/2(H^+ - H_0^+)} \ll C_{\overline{Cd}^{++}}$	$\therefore C_{[\overline{Cd}^{++} - 1/2(H^+ - H_0^+)]} \cong C_{\overline{Cd}^{++}}$
$C_{(H^+ - H_0^+)} \ll C_{\overline{CdCl}^+}$	$\therefore C_{[\overline{CdCl}^+ - (H^+ - H_0^+)]} \cong C_{\overline{CdCl}^+}$
$C_{H_0^+}$ is very small	$\therefore C_{H_0^+} \cong a_{H_0^+}$
Low ionic strength	$\therefore f_{Cd(OH)_2} \cong 1$, $f_{CdClOH} \cong 1$
Similar effective ionic diameters	$\therefore f_{Cd(OH)^+} \cong f_{H^+}$
Low concn.	$\therefore$ molarity $\cong$ molality

Results

A plot, not reproduced here, was made of experimental values of cadmium chloride. Values of *p*H corresponding to concentrations of (0.01 to 0.10 *M* cadmium chloride) in intervals of 0.01 were obtained. These data were substituted into the three K_h equations. The hydrolysis may be represented by the reaction

$$CdCl^+(aq) + H_2O \rightleftarrows CdClOH(aq) + H^+(aq) \quad (IV)$$

for which the hydrolysis constant varied from 0.8×10^{-10} for a 0.01 molar solution of cadmium chloride to 1.5×10^{-10} for a 0.10 *M* solution of cadmium chloride. A value of 7×10^{-11} is taken for K_{h_3} which was obtained by extrapolating K_{h_2} to zero ionic strength, corresponding to a standard free energy change (ΔF^0 25°) of 1.37×10^4 cal. mole^{-1}. The increasing values of K_{h_2} probably are due to other reactions taking place simultaneously. Over the molar concentration range 0.01 to 0.10, both K_{h_1} and K_{h_2} became constantly larger, K_{h_1} values give a linear graph whereas K_{h_2} values show a non-linear increase. The values of K_{h_1} and K_{h_2} varied from 0.86×10^{-10} and 0.30×10^{-16} to 9.75×10^{-10} and 16.6×10^{-16}, respectively.

The basic dissociation constant (K_b) of $CdClOH$ from the value of K_{h_3}

TABLE II

CALCULATED DATA AT 25°

M (molarity $CdCl_2$)	$C_{Cd^{++}}$	C_{CdCl^+}	C_{Cl^-}	$f_{Cd^{++}}$	f_{CdCl^+}	f_{Cl^-}	f_{H^+}	u	*p*H	$a_{H^+} \times 10^5$	$k_{h_2} \times 10^{10}$	$K_{h_2} \times 10^{16}$	$K_{h_1} \times 10^{10}$
0.01	0.0055	0.0045	0.0155	0.577	0.868	0.862	0.889	0.0210	6.21	0.62	0.79	0.30	0.86
.02	.0087	.0113	.0287	.504	.836	.827	.867	.0374	6.02	0.96	0.91	0.95	1.71
.03	.0111	.0189	.0411	.460	.815	.805	.853	.052	5.90	1.25	1.02	1.92	2.62
.04	.0128	.0272	.0528	.441	.798	.787	.844	.066	5.82	1.50	1.10	3.11	3.52
.05	.0150	.0350	.0650	.420	.785	.769	.834	.080	5.76	1.75	1.21	4.85	4.62
.06	.0165	.0435	.0765	.387	.775	.760	.830	.094	5.70	2.00	1.30	6.85	5.70
.07	.0175	.0525	.0875	.369	.766	.750	.822	.106	5.66	2.20	1.34	9.20	6.88
.08	.0185	.0615	.0985	.356	.759	.741	.818	.118	5.63	2.35	1.33	11.1	7.77
.09	.0200	.0700	.110	.347	.752	.734	.815	.130	5.59	2.55	1.41	13.6	8.70
.10	.0215	.0785	.122	.336	.745	.726	.811	.142	5.56	2.75	1.49	16.6	9.75

$$CdClOH(aq) \rightleftharpoons CdCl^+(aq) + OH^-(aq)$$

$$K_b = \frac{K_w}{K_{h3}} = 1.4 \times 10^{-4}$$

The ΔF^0 25° for this basic dissociation is 5.2×10^3 cal. mole^{-1}.

THE ABSORPTION SPECTRUM OF FERRIC PERCHLORATE AND THE RATE OF THE FERROUS-FERRIC EXCHANGE REACTION IN ISOPROPYL ALCOHOL[1]

BY NORMAN SUTIN

Brookhaven National Laboratory, Upton, Long Island, N. Y.

Received May 10, 1960

The rate of the exchange reaction between Fe(II) and Fe(III) in aqueous solutions has been measured by several workers.[2,3] The measurements have generally been interpreted in terms of electron transfer[4] or atom transfer mechanisms.[5] In both these mechanisms the hydration shells of the ions play an important role in determining the rate of the exchange reaction. Recent measurements of the rate of the Fe(II)–Fe(III) exchange reaction in methyl, ethyl and *n*-propyl alcohol further emphasize the important part played by the solvent.[3] We have extended these measurements to isopropyl alcohol and also determined the spectrum of ferric perchlorate in isopropyl alcohol–water mixtures.

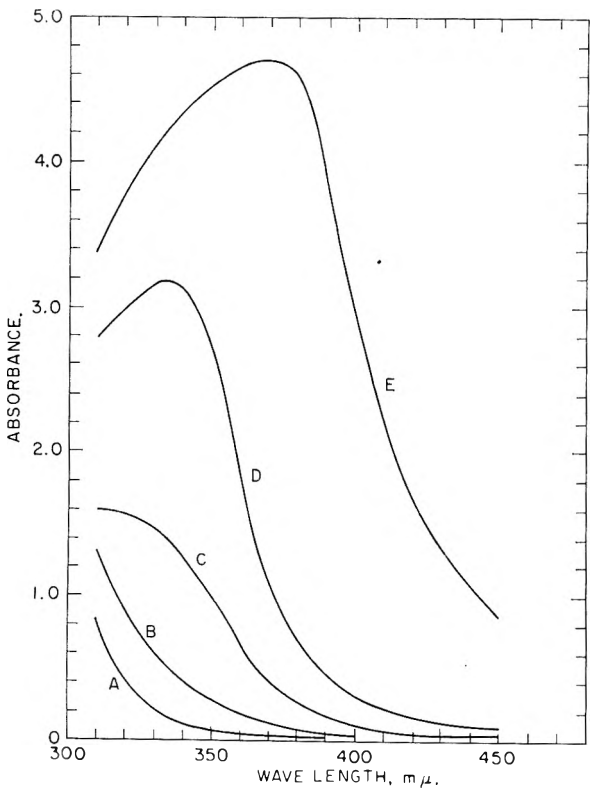

Fig. 1.—Absorption spectrum of ferric perchlorate in isopropyl alcohol–water mixtures: $(H^+) = 0.41\ F$; $(Fe(III)) = 1.50 \times 10^{-2}\ F$; $T = 25°$. The mole fraction of isopropyl alcohol is 0, 0.23, 0.41, 0.55 and 0.75 in A, B, C, D and E, respectively.

The absorption spectrum of ferric perchlorate in isopropyl alcohol–water mixtures at various concentrations of isopropyl alcohol is shown in Fig. 1. It is apparent from these curves that the addition of isopropyl alcohol to aqueous solutions of ferric perchlorate increases the absorbance of the solutions. This increase is similar to that observed on the addition of other alcohols to aqueous solutions of ferric perchlorate.[6] The problem arises as to the extent to which these increases result from changes in the relative concentrations of the Fe^{3+} and $FeOH^{2+}$ ions, changes in the absorption spectra of these ions, or new species such as $Fe_2(OH)_2^{4+}$ ions, higher polymers, etc.

Changes in the relative concentrations of $(H_2O)_6Fe^{3+}$ and $(H_2O)_5FeOH^{2+}$ may result from changes in the dielectric constant of the medium. The addition of isopropyl alcohol to water lowers the dielectric constant and this will tend to increase the equilibrium constant for the reaction

$$Fe(H_2O)_6^{3+} + H_2O \rightleftharpoons (H_2O)_5FeOH^{2+} + H_3O^+$$

While this effect may be largely responsible for the increased absorption at low mole fractions of isopropyl alcohol, the rapid increase in the absorbance and the appearance of a maximum suggest that at higher mole fractions of isopropyl alcohol, additional factors come into play. This is substantiated by the observation that the extinction coefficient of a solution in which the mole fraction of isopropyl alcohol is 0.90 is about 1100 at 350 mμ, which is considerably larger than that of $Fe(H_2O)_6^{3+}$ or of $(H_2O)_5FeOH^{2+}$ in H_2O at this wave length. We thus conclude that the increase in the absorbance of the solutions on adding isopropyl alcohol cannot be due solely to the displacement of the above equilibrium.

It is possible that part of the increased absorbance arises from increases in the extinction coefficient of the ferric and hydrolyzed ferric ions. Such increases are probable if the light absorption is due to an electron transfer process from the solvation shell of the ion to the central ferric ion. Any alteration in the solvation shell of the ion would be expected to have an effect on its absorption spectrum. Such an alteration in the solvation shell could arise from the replacement of water by isopropyl alcohol molecules. Since the ionization potential of isopropyl alcohol is less than that of water, it should be easier to remove an electron from the solvation shell if the shell contains isopropyl alcohol. This would tend to shift the absorption spectrum toward longer wave lengths and thus increase the extinction coefficients at these wave lengths.

Another factor which may contribute to the increased absorbance of these solutions is the presence of dimers and perhaps higher polymers. It is interesting to note that the dimer $(H_2O)_4Fe(OH)_2Fe(H_2O)_4$ or perhaps $(H_2O)_5FeOFe(H_2O)_5$ has been reported to have a maximum at ~335 mμ in

(1) Research performed under the auspices of the U. S. Atomic Energy Commission.

(2) (a) J. Silverman and R. W. Dodson, THIS JOURNAL, **56**, 846 (1952); (b) J. Hudis and A. C. Wahl, *J. Am. Chem. Soc.*, **75**, 4153 (1953).

(3) R. A. Horne, Ph.D. Thesis, Columbia University, 1955.

(4) R. A. Marcus, *J. Chem. Phys.*, **26**, 872 (1957).

(5) H. Taube and H. Myers, *J. Am. Chem. Soc.*, **76**, 2103 (1954).

(6) R. A. Horne, THIS JOURNAL, **62**, 509 (1958).

aqueous solutions.[7] It appears likely that at least part of the increase in the absorbance at about 350 mμ is by species of this type. The shift in this maximum toward longer wave lengths at higher mole fractions of alcohol may be due to the replacement of water by isopropyl alcohol in the solvation shell of the dimer as described above or perhaps to the production of higher polymers.

The above speculations are supported by the results of the exchange measurements which are summarized in Table I. The rate of the exchange reaction in water was calculated from the data of Silverman and Dodson.[2] It will be seen that the exchange reaction proceeds about 10^8 times faster in water than in isopropyl alcohol.

This enormous effect may arise from a variety of causes. The predominant iron species may be quite different in the two solvents, as suggested by the spectrophotometric measurements. If the reactants have larger differences in configuration in isopropyl alcohol than in water, the reorganization energy[4] may be much greater in alcohol. If water plays a specific role in the exchange process as has been suggested,[8] the corresponding mechanism may not be possible in isopropyl alcohol. Finally, we may consider the effect of the change in the dielectric constant of the medium, assuming that the same ionic species (hydrated ions) are present in the two solvents.

TABLE I

RATE OF THE FERROUS–FERRIC EXCHANGE REACTION IN ISOPROPYL ALCOHOL: $HClO_4 < 0.01$ F, $T = 25°$

H_2O, F	Fe(II) $\times 10^2$, F	Fe(III) $\times 10^2$, F	$t_{1/2}$, hr.	$\frac{R \text{ (isopropyl alcohol)}}{R\ (H_2O,\ (H^+) = 0.01\ F)}$
0.53	9.35	5.19	840	0.9×10^{-8}
0.88	6.74	3.14	912	1.2×10^{-8}
2.02	8.00	3.34	412	2.4×10^{-8}

From the relation[9]

$$\ln \frac{k_{alc}}{k_{water}} = \frac{NZ_AZ_Be^2}{RTr}\left[\frac{1}{D_{alc}} - \frac{1}{D_{water}}\right]$$

we calculate $k_{alc}/k_{water} \approx 10^{-9}$ for a charge product of 6 and $\approx 10^{-6}$ for a charge product of 4, taking r, the distance between the reactants in the activated complex, equal to 6.8 Å. More information about the nature of the species present in the alcohol is necessary before a specific explanation can be given with confidence.

The author wishes to thank Dr. R. W. Dodson for suggesting this study and for many helpful discussions.

(7) L. N. Mulay and P. W. Selwood, *J. Am. Chem. Soc.*, **77**, 2369 (1955).

(8) J. Hudis and R. W. Dodson, *ibid.*, **78**, 911 (1956).

(9) G. Scatchard, *Chem. Revs.*, **10**, 229 (1932).

THE X-RAY POWDER PATTERN OF RHOMBOHEDRAL SULFUR

BY AIMERY CARON AND JERRY DONOHUE

Department of Chemistry, University of Southern California, Los Angeles, California

Received May 9, 1960

In connection with our studies of the crystal structure of rhombohedral sulfur[1,2] we have had occasion to record its X-ray powder pattern. In view of the recent interest in the powder diffraction patterns of various forms of sulfur, including orthorhombic,[3] monoclinic,[4,5] "insoluble,"[3] and "nacreous,"[6] we are reporting our results on this additional form.

Experimental

Crystalline rhombohedral sulfur was prepared by the method of Aten,[7] in which both the orthorhombic and rhombohedral varieties appear simultaneously. Individual crystals of rhombohedral sulfur were removed and powdered. The powder photographs were taken in a Straumanis-type camera with CuKα (λ 1.542 Å.) X-radiation. Since X-rays accelerate the decomposition of rhombohedral sulfur into a mixture of plastic and orthorhombic sulfur, the transition being complete in several hours, satisfactory photographs of sufficient intensity could not be obtained by long exposure of a single sample, but were obtained instead by the exposure of a single film to ten different freshly prepared samples, each for one hour. The lines on this multiple exposure photograph were somewhat less sharp than the lines observed on a powder photograph of orthorhombic sulfur which had been taken in the usual way. However, the lines on a one hour exposure of a single sample were at least as sharp, although not as strong, as those in the orthorhombic pattern.

A total of 56 lines was observed on the multiple exposure photograph of rhombohedral sulfur. Of these, fourteen also occurred on a photograph of orthorhombic sulfur, indicating that a fraction of the material had undergone transition during photography. On the basis of preliminary values for the lattice constants obtained from single crystal rotation and Weissenberg photographs[1,8] the remaining lines were indexed. Four lines of rhombohedral sulfur were found to coincide with those of orthorhombic sulfur. Lattice constants were then obtained from thirty-one resolved lines by the method of least squares.[9,10] Hexagonal indexing was used throughout.[11] The lattice constants, and their standard errors, are: $a = 10.818 \pm 0.002$ Å. and $c = 4.280 \pm 0.001$ Å. The coefficient of the Nelson–Riley drift correction[10] is $4.5 \times 10^{-4} \pm 1.1 \times 10^{-4}$. The calculated density is 2.21 g. cm.$^{-3}$.

Results and Discussion

The observed intensities and values of $\sin^2 \theta$ for rhombohedral sulfur are presented in Table I. The calculated values of $\sin^2\theta$, and the values of G^2 as obtained from the refined structure[2] also are shown. Not included in Table I are the observed data for the ten lines which also occurred on the photographs of orthorhombic sulfur, and which could not be indexed as rhombohedral sulfur. Since the calculated values of G^2 for 45 unobserved lines of rhombohedral sulfur having $\sin^2\theta < 0.93$ were all found to be small enough such that their occurrence on the photograph was not expected, these data are likewise not included in Table I.

(1) J. Donohue, A. Caron and E. Goldish, *Nature*, **182**, 518 (1958).

(2) A. Caron, E. Goldish and J. Donohue, to be published.

(3) A. G. Pinkus, J. S. Kim, J. L. McAtee, Jr., and C. B. Concilio, *J. Am. Chem. Soc.*, **79**, 4566 (1957).

(4) A. G. Pinkus, J. S. Kim, J. L. McAtee, Jr., and C. B. Concilio, *ibid.*, **81**, 2652 (1959).

(5) S. R. Das in "IUPAC Colloquium Munster, on Silicon–Sulfur–Phosphates," Verlag Chemie, G.m.b.H., Weinheim/Bergstrasse 1955, p. 103.

(6) A. G. Pinkus, private communication.

(7) A. H. Aten, *Z. physik. Chem.*, **88**, 321 (1914).

(8) C. Frondel and R. E. Whitfield, *Acta Cryst.*, **3**, 242 (1950).

(9) D. P. Shoemaker, R. E. Marsh, F. J. Ewing and L. Pauling, *ibid.*, **5**, 637 (1952).

(10) H. P. Klug and L. E. Alexander, "X-Ray Diffraction Procedures for Polycrystalline and Amorphous Materials," John Wiley and Sons, Inc., New York, N. Y., 1954, p. 486.

(11) M. J. Buerger, "Elementary Crystallography," John Wiley and Sons, Inc., New York, N. Y., 1956, p. 106.

TABLE I

X-RAY DIFFRACTION DATA ON RHOMBOHEDRAL SULFUR

I	$\sin^2\theta$ obsd.	HKL	$\sin^2\theta$ calcd.	G^2 calcd.[a]	I	$\sin^2\theta$ obsd.	HKL	$\sin^2\theta$ calcd.	G^2 calcd.
m	0.0205	110[c]	0.0208	246	vw	0.4351	143	0.4356	876
vs	.0393[b]	101[c]	.0399	2598	w	.4630	072	.4630	972
s	.0612[b]	300[c]	.0618	1410	w	.4831	262	.4831	1452
vs	.0805	211[c]	.0808	9480	m	.5277	104[c]	.5272	330
		220[c]	.0822	1356			811[c]	.5279	1380
w	.1212	131	.1216	672	m	.5487	461	.5487	1344
vw	.1376	012	.1377	258	w	.5578	253	.5573	2052
s	.1449	401[c]	.1419	972	w	.5706	802[c]	.5643	300
		140[c]	.1433	1704			214[c]	.5677	216
w	.1572	202	.1580	384			731[c]	.5685	300
s	.1618	321	.1623	4728			280[c]	.5699	132
s	.1785	122	.1784	4560	w	.6088	134	.6083	912
w	.2012[b]	051[c]	.2030	498	w	.6314	470	.6307	426
s	.2189	312	.2191	6960	vw	.6460	642	.6454	576
m	.2234	241	.2233	3456	vw	.6660	372	.6656	396
s	.2445	042[c]	.2394	636	w	.6897	381	.6901	540
		511[c]	.2437	3696	vvw	.7106	244[c]	.7096	456
		600[c]	.2451	708			10.0.1[c]	.7104	168
w	.2594	232	.2598	1788	vw	.7189	363	.7194	768
s	.2653	250	.2654	3132	vw	.7306	514	.7299	636
m	.3252[b]	161[c]	.3250	2616	m	.7468	562	.7467	1212
		440[c]	.3264	48	vw	.7715	434	.7704	312
vw	.3401	152	.3411	552	vw	.7918	841[c]	.7914	396
w	.3545	033	.3544	726			930[c]	.7928	330
m	.3658	701	.3656	2538	vw	.8399	093	.8410	354
m	.3748	223	.3747	2964	vw	.8719	624	.8717	360
w	.3818	342	.3817	1308	vw	.9223	473	.9220	456
vvw	.3873	621[c]	.3859	480	vvw	.9314	544[c]	.9324	132
		170[c]	.3873	180			491[c]	.9331	216
vw	.4221	612[c]	.4223	294					

[a] Sum of pF_{HKL}^2 for allowed lines of identically equal $\sin^2\theta$. [b] Coincident with lines of orthorhombic sulfur. [c] Not included in determination of lattice constants.

There are no "extra" lines such as were observed for orthorhombic[3] and monoclinic[4] sulfur. It is of interest that the extra lines in these two patterns cannot be accounted for by the presence of rhombohedral sulfur in the preparations from which those data were recorded, as may be seen by a comparison of the several sets of observed data.

Two of the strongest lines of the rhombohedral sulfur pattern occur at very nearly the same values of $\sin^2\theta$ as do two of the strongest lines of the orthorhombic variety, but there are no other striking similarities between the two patterns. There is no resemblance between the patterns of monoclinic and rhombohedral sulfur. Thus there is little chance of mistaking one variety for another if powder patterns are available.

Acknowledgment.—This work was supported in part by the Office of Ordnance Research, U. S. Army, and in part by the National Science Foundation.

THE HEAT OF COMBUSTION OF LUTETIUM[1]

BY ELMER J. HUBER, JR., EARL L. HEAD AND CHARLES E. HOLLEY, JR.

Los Alamos Scientific Laboratory of the University of California, Los Alamos, New Mexico

Received May 16, 1960

The heat of combustion of lutetium metal has been measured in our current series[2] of determining the heats of formation of the rare earth oxides. The method, involving the determination of the heat evolved from the combustion of a weighed sample of the metal in a bomb calorimeter at a known initial pressure of oxygen, has been described.[3] The same units and conventions are used here.

Lutetium Metal.—Lutetium metal was obtained from two sources, Ames Laboratory, A.E.C., Ames, Iowa (Ames) and Michigan Chemical Corp., Saint Louis, Michigan (M.C.). The analyses were made at this Laboratory and the per cent. impurities were as follows: C, 0.048 and 0.082; H, 0.015 and 0.0206; O, 0.320 and 0.125; N, 0.020 and 0.150; Ta, 1.80 and 1.90; Mg, 0.005; Ca, 0.07; Ba, 0.005; Y, 0.05; Al, 0.05. The value given first is for the Ames metal, the second value, if any, for the M.C. metal.

No other metallic impurities were detected spectrochemically. The lutetium metal from Ames thus contained about 2.38% impurities, the M.C. metal, 2.28%. By assuming that the non-metallic impurities are combined with the lutetium as the carbide, hydride, nitride and oxide, one calculates the Ames material to be 94.36 mole % metal and

(1) This work was done under the auspices of the A.E.C.

(2) See E. J. Huber, Jr., E. L. Head and C. E. Holley, Jr., THIS JOURNAL, **61**, 1021 (1957), for reference to earlier papers in this series; also **64**, 379 (1960).

(3) E. J. Huber, Jr., C. O. Mathews and C. E. Holley, Jr., *J. Am. Chem. Soc.*, **77**, 6493 (1955).

the M.C. material, 93.36%. (Atomic weight Lu = 174.99.) The X-ray lattice constants for the M.C. material were slightly greater than expected, possibly indicating the presence of rare earths of lower atomic number in solution.

Combustion of Lutetium.—A 10 mil diameter fuse wire of magnesium was used to ignite the lutetium. The lutetium was burned on sintered discs of lutetium oxide in oxygen at 25 atm. pressure. The metal showed no gain in weight when exposed to O_2 at 25 atm. pressure for one hour. Each combustion product was dissolved in hydrochloric acid to determine the completeness of combustion. The volume of evolved gas was measured and the gas then analyzed with a mass spectrograph. Combustion varied from 93.6 to 99.5% of completion. The average initial temperature was 25.2°. The two series of runs are summarized in Table I.

TABLE I

THE HEAT OF COMBUSTION OF LUTETIUM

Mass Lu burned, g.	Wt. Mg, mg.	Wt. Lu_2O_3, g.	Energy equiv. j./d.[4]	ΔT, °K.	Energy from Firing, j.	Lu, j./g.	Dev. from mean
			Ames Metal				
1.7721	6.80	73.8	10020.1	0.9505	13.4	5272.2	18.3
1.8755	6.16	71.6	10019.6	1.0097	6.2	5309.8	19.3
1.9935	6.18	58.2	10016.3	1.0755	10.0	5322.3	31.8
2.1674	6.55	61.3	10017.0	1.1603	8.5	5284.0	6.5
2.5461	6.07	46.4	10013.3	1.3546	10.5	5264.4	26.1
					Av.	5290.5	20.4
				Stand. dev.			11.05
			Michigan Chemical Metal				
2.3781	7.37	59.2	10016.5	1.2716	11.2	5274.8	5.1
1.9739	7.02	38.3	10011.3	1.0568	11.4	5266.4	3.3
2.2826	6.48	42.0	10012.2	1.2224	11.9	5286.6	16.9
2.2969	6.66	44.8	10012.9	1.2208	11.2	5245.4	24.3
2.2771	6.94	48.7	10013.9	1.2165	14.3	5267.5	2.2
2.2037	6.89	48.7	10013.9	1.1779	8.6	5271.5	1.8
2.0551	5.91	46.6	10013.4	1.1031	13.2	5297.5	27.8
2.2091	6.08	42.8	10012.4	1.1756	11.5	5255.1	14.6
2.1668	6.25	43.4	10012.5	1.1554	12.0	5262.2	7.5
					Av.	5269.7	11.5
				Stand. dev.			5.2

Correction for Impurities.—The calculated percentage composition of the lutetium metal (Ames) by weight is as follows: Lu metal, 93.73; LuH_2, 1.32; Lu_2O_3, 2.65; LuN, 0.27; C, 0.048; Mg, 0.005; Ca, 0.07; Ba, 0.005; Y, 0.05; Al, 0.05; Ta, 1.80. The heat of combustion of this lutetium metal corrected for impurities is 5,393.4 joules/g. or 1.94% higher than the uncorrected value.[5] If the combustion products, H_2O, CO_2, NO_2, are assumed to react with the oxide to form the hydroxide, carbonate and nitrate, the calculated value would be decreased by 0.33%.

The calculated percentage composition of the lutetium (M.C.) is Lu metal, 93.11; C, 0.082; LuH_2, 1.84; Lu_2O_3, 1.04; LuN, 2.02; Ta, 1.90. The heat of combustion of this sample corrected for impurities is 5333.6 joules/g. or 1.21% larger than the uncorrected value. Reactions between the combustion products would decrease this value by 1.12%.

Calculation of the Uncertainty.—The uncertainty to be attached to the corrected values includes the uncertainty in the energy equivalent which is 0.04%, the uncertainty in the calorimetric measurements which is 0.42% (Ames) and 0.20% (M.C.), and the uncertainty introduced in the correction for impurities which is estimated to be 0.62% (Ames) and 0.44% (M.C.). The combined uncertainties become 0.75 and 0.485%.

Composition of the Lutetium Oxide.—The oxide formed was tan in color. An X-ray pattern showed it to have a body-centered cubic structure with a = 10.391 Å.

Heat of Formation of Lu_2O_3.—Using methods of calculation reported elsewhere,[3] the heat of formation of Lu_2O_3 is ΔH_{25} = −1891.8 ± 14.2 and −1870.9 ± 9.1 kjoules/mole for the two samples of lutetium metal used. Combining and weighting these values yields a figure of −1878.4 ± 7.7 kjoules/mole or −448.9 ± 1.8 kcal./mole. This value is close to that recently reported for the heat of formation of thulium oxide (ΔH_f = −451.4 ± 1.4 kcal./mole).[6] No literature values for lutetium are available for comparison.

Acknowledgments.—The authors wish to acknowledge the valuable assistance of F. H. Ellinger, H. D. Cowan and D. Pavone in the analytical work. They also appreciate the courtesy of Dr. F. H. Spedding of the Ames Laboratory, A.E.C., for loaning the oxide and one sample of the metal.

(4) The specific heat of Lu_2O_3 is estimated at 0.25 joule/g./deg.

(5) The heats of formation of LuH_2 and LuN are estimated at −45 and −75 kcal./mole. The heats of combustion of other impurities are taken as follows: graphite (to CO_2), 33,000; Mg (to MgO), 24,670; Ca (to CaO), 15,800; Ba (to BaO), 4050; Y (to Y_2O_3), 10,350; Al (to Al_2O_3), 30,980; and Ta (to Ta_2O_5), 5,760 joules/g. The heats of formation of $H_2O(g)$ and NO_2 are taken as −58 and +8 kcal./mole.

(6) E. J. Huber, Jr., E. L. Head and C. E. Holley, Jr., THIS JOURNAL, **64**, 379 (1960).

THE $Hg(6^3P_1)$-PHOTOSENSITIZED DECOMPOSITION OF NITRIC OXIDE[1]

BY MORTON Z. HOFFMAN[2] AND RICHARD B. BERNSTEIN

Department of Chemistry, The University of Michigan, Ann Arbor, Michigan

Received May 16, 1960

The $Hg(6^3P_1)$-photosensitized (MPS) decomposition of NO was studied by Noyes.[3] The quenching cross section has been found[4] to be large (25 Å.^{2}); recently a new interpretation of the quenching step has been proposed.[5]

Noyes[3] found that in the low pressure range (0.003–0.13 mm.) the rate was proportional to I_{abs} and P_{NO}. He deduced from the pressure change that N_2 was the only gaseous product; the NO_2 formed reacted with the Hg. A possible quenching step giving the proper dependence of the rate upon NO was

$$Hg^* + NO \longrightarrow HgO + N \qquad (1)$$

This was unsatisfactory, however, since no HgO

(1) Financial assistance from the Michigan Memorial-Phoenix Project and the U.S.A.E.C., Div. of Research, is appreciated.

(2) Receipt of fellowships from the Michigan Memorial-Phoenix Project and the National Science Foundation is acknowledged.

(3) W. A. Noyes, Jr., *J. Am. Chem. Soc.*, **53**, 514 (1931).

(4) J. R. Bates, *ibid.*, **54**, 569 (1932).

(5) R. J. Fallon, J. T. Vanderslice and E. A. Mason, THIS JOURNAL, **63**, 2082 (1959).

was detected as a product. This led to the postulate of an alternate quenching step

$$Hg^* + NO \longrightarrow NO^* + Hg \qquad (2)$$

with the suggestion that the NO* is in a highly excited vibrational state. However, the route of NO* to N_2 was not indicated.

The recent interpretation[5] of quenching step (2) was the proposal that the NO* is in the long-lived $^4\pi$ electronic state; this suggestion was based on potential curve calculations[6] and tentative experimental confirmation[7] of the existence of $^4\pi$ NO.

The present note reports data on the rate of formation of N_2 in the MPS decomposition of NO in the pressure range 174–676 mm. as well as measurements of the N^{14}/N^{15} isotope effect in the reaction. Implications of the present results regarding the mechanism of N_2 production are discussed.

Experimental[8]

Matheson Co. NO was purified[9] and stored over Hg. The vapor pressure and the infrared spectrum agreed well with the literature, indicating a probable impurity content $\leq 0.1\%$.

Decomposition (to the extent of 1–5%) in the presence of Hg vapor was effected in a circulating system[8] at room temperature by means of a Hanovia Co. Hg resonance lamp. The illuminated zone consisted of an annulus, 13 cm. long with a width of 2 mm., the outer wall of which was made of type 7910 Vycor (transparent only for $\lambda > 2100$ Å.[10]).

The only gaseous product non-condensable at −196° was N_2 (determined mass spectrometrically). The presence of NO_2 in the final reaction mixture was inferred from the observation of blue N_2O_3 in the condensed, undecomposed NO; corrosion of liquid Hg surfaces also suggested attack by NO_2. No HgO was detected in the reaction zone.[11]

The N^{14}/N^{15} isotope effect in the reaction was determined by mass spectrometric assay of the product N_2. These samples were always compared with N_2 produced by the quantitative MPS reduction of NO with excess H_2[12] to yield the fractionation factor[8] S, defined as $S = (Z_0/Z_f)$, where Z_0 is the N^{15} atom fraction in the N_2 from the total reaction with H_2, and Z_f is the corresponding value for the N_2 from the fractional decomposition.

Table I summarizes the data. The rate of N_2 production shows no systematic dependence upon the initial pressure (P_0) of NO over the range studied. The large scatter in the data may possibly be attributed to variations in the Hg vapor concentration (and thus I_{abs}) as noted in other work.[13]

TABLE I

THE Hg-PHOTOSENSITIZED DECOMPOSITION OF NO

P_0, mm.	t, hr.	$10^8 \times R^a$	S (N^{14}/N^{15})
174	12	6.4	1.009
175	6	5.3	...
175	6	3.9	...
175	12	3.5	1.005
178	12	4.2	1.010
178	12	5.8	1.012
343	12	4.7	1.009
360	12	4.9	1.007
364	12	3.6	1.006
404	6	3.8	...
659	12	5.8	1.008
676	12	3.6	1.005
		Av. 4.6 ± 0.9^b	Av. 1.008 ± 0.002^b

[a] R is the average rate of N_2 production (moles/min.). [b] Average deviation from the mean.

Discussion

A reasonable mechanism for the decomposition must be consistent with Noyes'[3] observation of first-order dependence at low pressures and the observed zero-order dependence[14] in the higher pressure region as well as first power dependence[3] on I_{abs} and the absence of HgO.

One such mechanism is

	I_{abs}
$Hg + h\nu \longrightarrow Hg^*$	
$Hg^* + NO \longrightarrow NO^* + Hg$	1
$Hg^* + NO \longrightarrow NO_v + Hg'$	2
$Hg^* \longrightarrow Hg + h\nu$	3
$Hg^* + NO^* \longrightarrow N + O + Hg$	4
$N + NO \longrightarrow N_2 + O$	5
$O + NO \longrightarrow NO_2$, etc.	6

Here $Hg^* = Hg(6^3P_1)$ atom; $Hg' = Hg(6^3P_0)$ atom; $NO^* = NO(^4\pi)$ molecule; and NO_v = a vibrationally excited NO molecule.

Steady-state treatment yields for the rate of N_2 production

$$R = \frac{k_1 P_{NO} I_{abs}}{(2k_1 + k_2)P_{NO} + k_3} \qquad (3)$$

At high pressures (in the complete quenching region), zero order dependence on the NO is indicated; at low pressures (where deactivation of Hg* occurs mainly by fluorescence), first-order behavior is expected.

Step 4 is here postulated as the route to the formation of N_2, collision of an Hg* atom with an $NO(^4\pi)$ molecule producing a transition to a repulsive state[6] of NO which immediately dissociates.[15] The other steps in the mechanism are well known.[3,16–18]

The slow rate (low quantum yield) is attributable to the small value of k_1/k_2. Comparison of the present rate with that of the MPS decomposition[8] of N_2O (quantum yield: 0.78[13]) measured under identical conditions leads to an estimate for this ratio in the range 10^{-2}–10^{-3}.

A second mechanism satisfying all the previously stated requirements is due to Cvetanović[19]; it involves substituting the following reactions in place of steps 2 and 4 in the first mechanism

$$NO^* + NO \longrightarrow 2NO \qquad 2'$$
$$NO^* + NO \longrightarrow N + NO_2 \qquad 4'$$

The resulting rate equation is

(6) J. T. Vanderslice, E. A. Mason and W. G. Maisch, *J. Chem. Phys.*, **31**, 738 (1959).

(7) M. Ogawa, *Science of Light* (*Tokyo*), **3**, 39 (1954).

(8) For further details see: (a) Ph.D. thesis of M. Z. H., Univ. of Michigan, 1960. Available from Univ. Microfilms, Ann Arbor, Mich.; (b) M. Z. Hoffman and R. B. Bernstein, *J. Chem. Phys.*, **33**, 526 (1960).

(9) R. E. Nightingale, A. R. Downie, D. L. Rotenberg, B. Crawford, Jr., and R. A. Ogg, Jr., THIS JOURNAL, **58**, 1047 (1954).

(10) The absence of any effects attributable to 1849 Å. radiation (*i.e.*, significant change in rate) was demonstrated by employing (a) an additional thickness of this Vycor and (b) a water filter between lamp and reaction zone.

(11) The quantity of HgO that would have formed (assuming quenching step 1) is indeed detectable, having been observed previously in the MPS decomposition of N_2O using the same apparatus.[8]

(12) H. A. Taylor and C. Tanford, *J. Chem. Phys.*, **12**, 47 (1944).

(13) R. J. Cvetanović, *ibid.*, **23**, 1203 (1955).

(14) Noyes[3] observed a significant decrease in the apparent first-order rate constant when P_{NO} was increased to 24 mm., suggestive of an approach to zero order behavior.

(15) It should be noted that step 4 may alternately involve Hg′ or a photon (2537 Å.) from the imprisoned radiation rather than Hg*; the same form of rate equation results.

(16) A. C. G. Mitchell and M. W. Zemansky, "Resonance Radiation and Excited Atoms," Cambridge University Press, England, 1934.

(17) G. B. Kistiakowsky and G. G. Volpi, *J. Chem. Phys.*, **27**, 1141 (1957).

(18) P. Harteck, R. R. Reeves and G. Mannella, *ibid.*, **29**, 1333 (1958).

(19) R. J. Cvetanović, private communication.

$$R = \frac{k_1 P_{NO} I_{abs}}{\left(1 + \frac{k_2'}{k_4'}\right)(k_1 P_{NO} + k_3)} \qquad (3')$$

which is kinetically indistinguishable from eq. 3. An analysis similar to that mentioned in the preceding paragraph leads to an estimate for the ratio k_4'/k_2' in the range 10^{-2}–10^{-3}.

The observed N^{14}/N^{15} isotope effect is in the "normal" direction (*i.e.*, N^{14} enrichment) and shows no systematic dependence on pressure (Table I). The scatter in the isotope data is worse than the precision of any individual analysis (±0.001) and is indicative of some complexity in the reaction not yet understood. Explicit expressions for the observed isotope effect (in terms of kinetic isotope effects for the various elementary steps in the mechanisms) are obtained readily. They are not reported here since data required for their evaluation are not available. Qualitatively, both mechanisms yield isotope effects in the "normal" direction. However, quantitative interpretation of the observed isotope effect is not possible at the present time.

Acknowledgment.—The authors thank Mr. J. N. Doshi for his assistance with the mass spectrometric analyses.

THE PROPERTIES OF THYROGLOBULIN. III. THE TITRATION OF THYROGLOBULIN IN SODIUM DODECYL SULFATE

BY H. EDELHOCH

Clinical Endocrinology Branch, National Institute of Arthritis and Metabolic Diseases, National Institutes of Health, Bethesda, Md.

Received May 23, 1960

Steinhardt,[1] *et al.*, have shown that the acid segments of the titration curves of wool protein are markedly influenced by the nature of the conjugate base of the acid titrant. Putnam and Neurath[2] subsequently demonstrated that the binding of Duponal (a mixture of long chain alkyl sulfates) was observable by a *p*H shift in the protein solution. Scatchard and Black[3] have formulated a relation between *p*H changes and the binding of anions and in this way measured the affinity of a large number of anions to human serum albumin.

Sodium dodecyl sulfate (SDS) increases the *p*H of thyroglobulin solutions. The influence of SDS on the acid segment of the titration curve of thyroglobulin is evaluated in this report. A comparison is also made of the effect of the chain length of the detergent on its interaction with thyroglobulin.

Methods and Materials

A Beckman Model GS *p*H meter, equipped with external electrodes, was used for all *p*H measurements. Water from a constant temperature bath flowed through a water jacket surrounding the titration cell. Nitrogen was blown over the top of the solution when measurements were made above *p*H ~ 7. Titrants were added from a Rehberg microburet of 0.20-ml. capacity which was calibrated in 0.001 ml. units. All *p*H changes were complete in the time required to read the *p*H meter. The *p*H meter was calibrated with buffers recommended by Bates, *et al.*[4]

The preparation and properties of thyroglobulin extracted from calf thyroid tissue have been reported in detail in earlier papers.[5,6] A phosphate-fractionated preparation (1)[6] was used in the observations currently reported.

The sulfate series of alkyl detergents were purified preparations and were a gift from Dr. E. Barthel of E. I. du Pont de Nemours & Co. Other reagents were C.P. grade or equivalent. Fresh glass distilled water was used throughout.

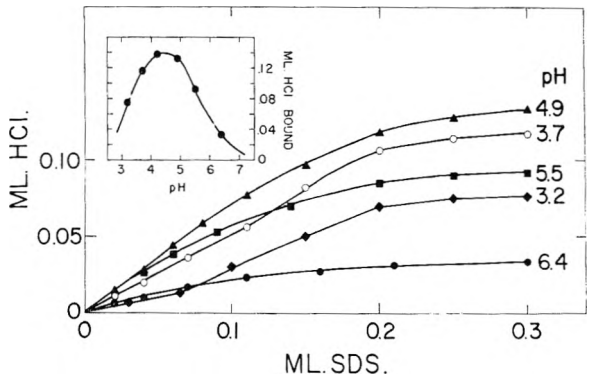

Fig. 1.—The influence of *p*H and detergent concentration on the acid binding properties of thyroglobulin in 0.01 *M* KNO_3. Solutions contain 3.0 ml. of 0.75% protein. Concentration of HCl was 0.097 *M* and SDS was 0.10 *M*. Inset shows effect of *p*H on the maximum acid binding values; $T' = 28.1°$.

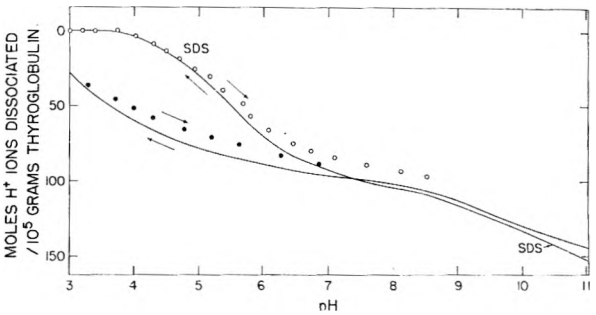

Fig. 2.—The effect of 0.015 *M* SDS on the titration curve of thyroglobulin in 0.01 *M* KNO_3. Neutral solutions of thyroglobulin were titrated with either 0.097 *M* HCl or NaOH.

Experimental Results

When small amounts of SDS were added to a thyroglobulin solution below *p*H ~ 7.5, the *p*H of the solution increased. If the solution then was returned to its original *p*H with HCl, a second aliquot of SDS may be added and another rise in *p*H noted. This procedure then may be continued until the increase in *p*H elicited by the detergent becomes negligible. In this manner a curve can be constructed which shows the influence of detergent on the hydrogen ion binding properties of thyroglobulin. Illustrative H^+ binding curves, obtained at several *p*H values, appear in Fig. 1.[7] Above the isoelectric point of thyroglobulin,[8] *i.e.*, *p*H 4.5, all the curves are of the Langmuir type; below *p*H 4.5 the curves exhibit an inflection point which re-

(1) J. Steinhardt, C. H. Fugitt and M. Harris, *J. Research Natl. Bur. Standards*, **24**, 335 (1940); **25**, 519 (1940); J. Steinhardt, *Ann. N. Y. Acad. Sci.*, **41**, 287 (1941).

(2) F. W. Putnam and H. Neurath, *J. Biol. Chem.*, **159**, 195 (1945).

(3) G. Scatchard and E. S. Black, THIS JOURNAL, **53**, 88 (1949).

(4) R. G. Bates, G. D. Pinching and E. R. Smith, *J. Research Natl. Bur. Standards*. **45**, 418 (1950).

(5) H. Edelhoch, *J. Biol. Chem.*, **235**, 1326 (1960).

(6) H. Edelhoch and R. E. Lippoldt, *ibid.*, **235**, 1335 (1960).

(7) Since the magnitude of these curves is strongly dependent on the ionic strength of the solution the *p*H changes are attributed to electrostatic effects and not to rupture of hydrogen bonds. Moreover at *p*H 5.4 in 0.01 *M* KNO_3 the addition of urea up to a final concentration of 5 *M* produced only a small increase in *p*H; similarly, guanidinium chloride up to 2 *M* produced only a small decrease in *p*H.

(8) M. Heidelberger and K. O. Pedersen, *J. Gen. Physiol.*, **19**, 95 (1935).

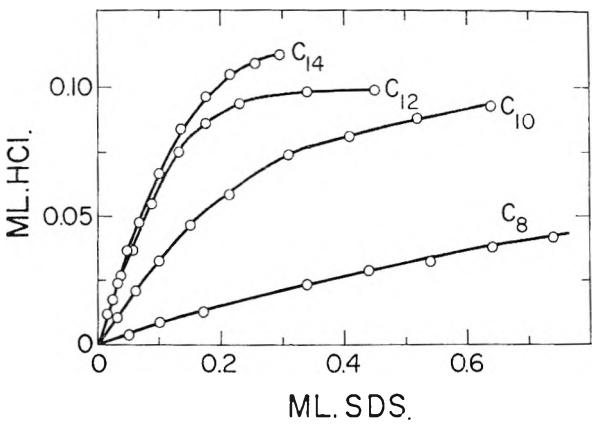

Fig. 3.—The influence of detergent chain length on the binding of hydrogen ions to thyroglobulin at *p*H 5.20: KNO_3 = 0.01 *M*; *T* = 28.1°. Detergents were the sodium salts of: octyl sulfate (C_8); decyl sulfate (C_{10}); dodecyl sulfate (C_{12}) and tetradecyl sulfate (C_{14}); all were in 0.10 *M* solution.

sembles a cooperative interaction. This type of curve could result if an increase in the number of detergent binding sites occurred as a result of detergent binding.

To facilitate evaluation of the curves described above potentiometric titrations of thyroglobulin, with and without SDS, were obtained. The solid lines in Fig. 2 represent the *p*H values observed after adding HCl or NaOH to a solution of thyroglobulin at *p*H ~7. The open and filled circles indicate the *p*H values obtained on back-titrating acidified solutions of thyroglobulin with and without SDS, respectively. It can be seen in Fig. 2 that the back-titration curve without detergent deviates almost immediately from the forward curve. In SDS, however, the reverse curve coincides with the forward curve from *p*H 2.7 to 5.2. Above *p*H ~7.5 the alkaline segment of the titration curve was almost independent of the presence of detergent ions. A small displacement was evident above *p*H 10 (*cf.* Fig. 2).

Karush and Sonenberg[9] have shown that the free energies and enthalpies of binding of alkyl sulfates to serum albumin are decidedly dependent on chain length between 8 and 12 carbon chains. We have observed a similar influence of chain length as evidenced by the H^+ binding curves reproduced in Fig. 3. A marked effect of chain length is apparent between the 8 and 12 unit chains. Apparently the effectiveness of the long chain approaches a limit near the dodecyl size since tetradecyl sulfate interacts only slightly stronger. In fact as shown elsewhere[6] the tetradecyl sulfate produces less dissociation and unfolding of thyroglobulin than does decyl sulfate. The dependence of binding on chain length suggests a van der Waals component to the binding energy.

Discussion

It has been reported[6] that SDS at concentrations below 0.001 *M* dissociates thyroglobulin into halves without much effect on their shape; however, at higher detergent concentrations both thyroglobulin and its subunit swell or unfold appreciably. In 0.015 *M* SDS (in 0.01 *M* KNO_3) thyroglobulin is almost completely dissociated and possesses an effective volume many times that of $\bar{v}c$.

Interpretation of the effects of SDS on the titration curve of thyroglobulin may be attempted in terms of the influence of the binding of anionic detergent on the charge and configuration of the protein molecule. For this purpose the model used by Linderstrøm-Lang[10] to evaluate the electrostatic effects on the titration curves of proteins will be used; however, *w* and *R* are considered as empirical electrostatic and configurational parameters

$$p\mathrm{H} - \log \frac{r_i}{n_i - r_i} = pK_i - 0.868wZ \qquad (1)$$

where

$$w = \frac{N\epsilon^2}{2DkTR}\left(1 - \frac{\kappa R}{1 + \kappa R}\right) \qquad (2)$$

where n_i is the total number of each type of group having an intrinsic dissociation constant pK_i; r_i is the number of groups dissociated at a given *p*H; *w* is the electrostatic work required to remove a proton from a protein molecule which bears the net charge *Z* and has an effective radius of *R*; *A* is the radius of exclusion ($A = R + 2.5$), κ is the reciprocal Debye radius, *D* is the dielectric constant, *k* is the Boltzmann constant and ϵ is the electronic charge.

Near the isoelectric point (*p*H ~4.5) the binding of detergent anions results in the protein acquiring a net negative charge. In accordance with equation 1 an increase in the affinity of proton binding groups results and as a consequence an absorption of protons coupled with a rise in the *p*H of the solution.

Acid to the isoelectric point, the positive charge enhances the protein's affinity for detergent anions. The large shift in the titration curve below *p*H 6 is illustrated in Fig. 2. However, in the acid region, the number of carboxyl groups which can accept protons is progressively reduced. Hence as the SDS titration is performed at lower *p*H values fewer dissociated carboxyl groups remain thereby accounting for the peak in the H^+ binding curves shown in the inset in Fig. 1. This curve may be obtained also from the vertical differences between the two titration curves shown in Fig. 2. In addition to the effect of SDS binding on the net charge (*Z*) configurational changes may also be induced which will affect the value of *R* and therefore the electrostatic interaction term *w*.

On the alkaline side of the isoelectric point the binding of detergent ions would be expected to decrease as the protein (negative) charge increased. The difference between the two thyroglobulin titration curves above *p*H ~7 in Fig. 2 is quite small. Thyroglobulin in 0.01 *M* SDS is more extensively unfolded than the S-15 and S-12 components found below *p*H 11 in the absence of detergent.[11] The greater degree of unfolding and consequently larger effective value of *R* would lead to a smaller value of *w* in equation 2; however the

(9) F. Karush and M. Sonenberg, *J. Am. Chem. Soc.*, **71**, 1369 (1949).

(10) K. Linderstrøm-Lang, *Compt. rend. trav. Lab. Carlsberg*, **15**, No. 7 (1924).

(11) S-15 and S-12 refer to molecules with Svedberg sedimentation constants close to 15 and 12, respectively, which are formed from thyroglobulin (S-19) by raising the *p*H of its solution.

larger value of Z which results from detergent binding appears to compensate so as to leave the net effect (wZ) approximately the same as observed without SDS.

When thyroglobulin is titrated with HCl in 0.015 M SDS, the titration of the carboxyl groups is more than 90% complete at pH 4.0. Moreover, thyroglobulin remains soluble at all pH values in 0.015 M SDS whereas it is insoluble between ~4.6 and 3.6 without detergent. Without SDS less than 50% of the carboxyl groups are titrated at pH 4.0 (see Fig. 2). In the latter instance, the pH must be reduced to below 3 to reach comparable degrees of H^+ binding. It is evident therefore that potentiometric titration in SDS offers a convenient way of obtaining the maximum number of acid binding groups.[12]

It is known that thyroglobulin is readily denatured by reducing the pH to the vicinity of its isoelectric point, *i.e.*, 4.5.[8] As seen in Fig. 2 the difference between the forward and reverse titration curves increases gradually from pH 2.9 to 7.0. When SDS is present, the reverse curve coincides with the forward curve from pH 2.7 to 5.2 and then shifts toward the alkali region. The implication of these experiments is that whatever transformation is occurring in acid solution, it is still incomplete at ~pH 3.0 without SDS, while with detergent present the transformation is complete by pH 5.2. It is apparent, therefore, that SDS can greatly facilitate the disorganization of thyroglobulin to a more elementary form in its structure.

(12) When bovine serum albumin and ovalbumin were titrated in SDS with HCl from neutrality, the forward (acid) and reverse (base) curve were essentially identical and almost all the carboxyl groups were titrated by pH 4.0. It is evident that SDS has the property of shifting the titration range of carboxyl groups in proteins to higher pH values. Moreover, with many insolubie proteins it is possible to keep the protein in solution with detergent. Finally, if acid binding groups are present in the protein which are "masked" or unavailable under normal titration procedures, these groups then may become accessible to titration.

THE EFFECT OF HYDROSTATIC PRESSURE ON THE RATE OF RACEMIZATION OF *l*-6-NITRO-2,2′-CARBOXYBIPHENYL

BY C. C. MCCUNE, F. WM. CAGLE, JR., AND S. S. KISTLER

Departments of Chemical Engineering and Chemistry, University of Utah, Salt Lake City 12, Utah

Received May 31, 1960

It was desired to investigate the effect of hydrostatic pressure on the velocity of a particularly simple chemical reaction. For such a study, one should avoid especially reactions which might involve appreciable differences in ionic character in the initial and activated states, since interpretation of these is complicated by possible solvation differences.[1-3] The pressure effect on the rate of racemization of an optically active biphenyl should provide a particularly simple reaction, and the data obtained should be open to straightforward interpretation. Since such data are apparently not available, a study of the racemization of the sodium salt of *l*-6-nitro-2,2′-carboxybiphenyl at pressures from atmospheric to 12,000 atmospheres was made.

(1) J. Buchanan and S. D. Hamann, *Trans. Faraday Soc.*, **49**, 1425 (1953).

(2) S. D. Hamann, "Physico-Chemical Effects of Pressure," London, Butterworths Scientific Publications, 1957, Chap. 9.

(3) C. T. Burris, Ph.D. Thesis, Catholic University, Washington, D. C., 1955.

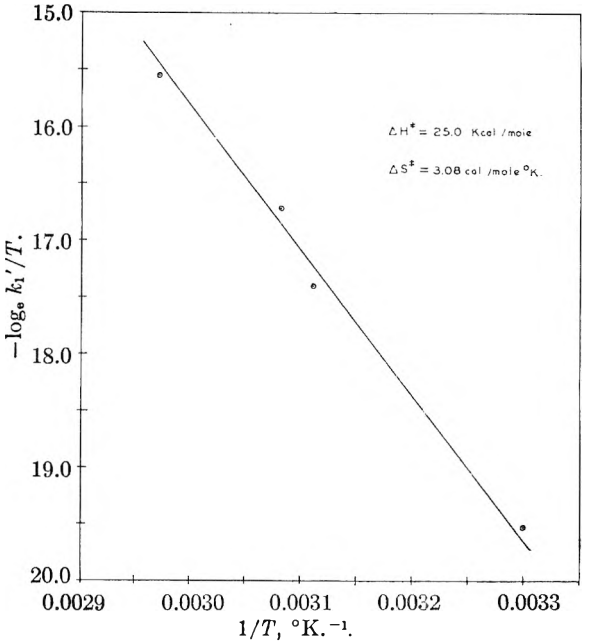

Fig. 1.—A plot of ln (k'/T) *vs.* $1/T$ for the racemization of *l*-6-nitro-2,2′-carboxybiphenyl at one atmosphere pressure.

Over the past 30 years, numerous diphenyl derivatives have been prepared and resolved[4] and it is well known that the optical activity is the result of hindered rotation around the bridging bond. In this study *l*-6-nitro-2,2′-carboxybiphenyl was chosen because of the relative ease of synthesis and the convenient temperature range in which it racemizes at a measurable rate.[5]

Experimental Procedure

For the measurement of the optical rotation of the samples, a Landolt-Lippich Triple Shadow Polarimeter was employed. The polarimeter was calibrated to ± 0.01°, but because of the strong color (amber) of the sample solution, readings were made to ± 0.1°.

The *l*-6-nitro-2,2′-carboxybiphenyl had a specific rotation of α^{25}_{5461} −280°.

Approximately 40 mg. was used in each test, dissolved in 6 ml. of 0.10N NaOH and viewed in semi-micro polarimeter tubes The initial rotation was about 4° when the mercury green line, 5461 Å., was used.

For the transmission of this green line, Wratten filters number 77a and number 58 were used. Filter number 77a transmits 68% of the green line with a negligible per cent. of the yellow line. Filter number 58 eliminates the red line. The rate constant for the reaction $l \underset{k'}{\overset{k'}{\rightleftharpoons}} d$ then could be obtained from

$$2k't = \ln(\alpha_0/\alpha)$$

in which k' is the rate constant in sec.$^{-1}$, t is the time in seconds, α_0 is the initial rotation, and α is the rotation at time t. A plot of $\ln(k_1'/T)$ *vs.* $1/T$ in which T is the absolute temperature and k_1' is the rate constant at one atmosphere, allows one to determine the enthalpy and entropy of acti-

(4) R. Adams and H. C. Yuan, *Chem. Revs.*, **12**, 261 (1933).

(5) F. Bell and P. H. Robinson, *J. Chem. Soc.*, 2234 (1927).

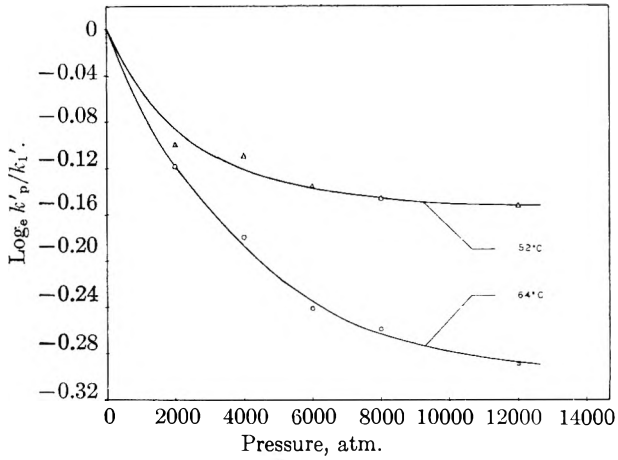

Fig. 2.—A plot of ln (k_p'/k_1') *vs.* $(P - 1)$ for the racemization of *l*-6-nitro-2,2′-carboxybiphenyl at 52 and 64°.

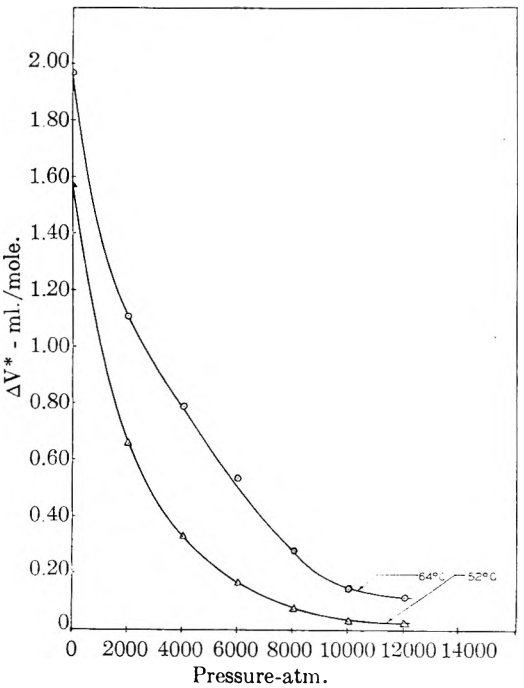

Fig. 3.—Activation volume as a function of pressure for the racemization of *l*-6-nitro-2,2′-carboxybiphenyl at 52 and 64°.

vation (Fig. 1). We have assumed a transmission coefficient of unity.[6]

The effect of pressure is now determined and since we may write[7-9]

$$\left(\frac{\partial \ln k'}{\partial P}\right)_T = \frac{-\Delta V^*}{RT}$$

or on integration from one atmosphere to P atmospheres

$$k_p' = k_1' \exp[-(p - 1)\ \overline{\Delta V^*}/RT]$$

In these expressions ΔV^* is the volume of the activated state less that of the initial state, $\overline{\Delta V^*}$ is the mean value of ΔV^* between P and one atmosphere, and R is the gas constant. A plot of ln (k_p'/k_1') *vs.* $(P - 1)$—actually P within the limits of experimental error—at two temperatures is given in Fig. 2. From the slope of the tangents to these curves values of ΔV^* may be obtained. These values of ΔV^* as a function of pressure are given in Fig. 3.

Discussion

It will be noted that the relations shown in Fig. 3 are not linear. At low pressures they show decided curvature and this is in accord with previous observations for other reactions.[10-13] This effect arises from the different compressibilities of the activated state and the initial state. If one views the activated state as an expanded biphenyl molecule, we would predict that it would be compressed more rapidly than would the initial state. Thus the value of ΔV^*, which is positive as expected for an uncomplicated unimolecular reaction, would decrease with pressure. In the limit $P \rightarrow \infty$, $\Delta V^* \rightarrow 0$ and this condition is indeed approached asymptotically as one sees in Fig. 3.

An interesting second-order reaction has been examined at pressures to 30,000 atmospheres.[11] This was

$$CH_3OH + C_2H_5Cl = CH_3OC_2H_5 + HCl$$

It was observed that ΔV^* decreased beyond 10,000 atmospheres, and that the curve of log (k_1'/k_p') appeared linear in the high pressure range, over a considerable change in pressure. One would expect that since k_p' increases indefinitely with increase in pressure the curve of ln $(k_1'/k_p') \rightarrow -\infty$ (a second order reaction) as $\Delta V^* \rightarrow 0$ and $P \rightarrow \infty$.

The effect of temperature on ΔV^* has been previously observed for other reactions.[3,13] For the racemization reaction, one finds ΔV^* increases with temperature. This one expects if the activated state is more expanded and would thus be expected to increase volume with temperature more rapidly than the initial state. Therefore, one would expect that within the limits of thermal stability of the compound ΔV^* would increase with increasing temperature. It is interesting to note the very small values of ΔV^* compared with the molecular volume of *l*-6-nitro-2,2′-carboxybiphenyl, which is 233 ml.

Pressure Apparatus.—The pressure cell was a thick walled composite cylinder, Fig. 4, of i.d. 0.50 inch and o.d. 2 inches, made from two concentric cylinders of "Alco S" (Universal Cyclops) hardened to Rockwell C50. The two concentric cylinders have an interface tapered to 0.063 inch per foot. The mating surfaces were lubricated with molybdenum sulfide, and were built with such interference that, in order to assemble, the smaller cylinder had to be forced 0.90 inch into the larger one, thus putting a tensile stress in the outer cylinder and a compressive stress in the inner one. By this means, the vessel can withstand very much greater internal pressures than a single thick-walled cylinder of the same dimensions could withstand.

Although reliable seals for pistons in high pressure equipment have been known for many years, some time was spent in an attempt to provide unsupported area seals with a minimum of friction in order to obtain internal pressures from measured thrust on the top piston without the great complication of electrical leads and a manganin pressure

(6) F. W. Cagle, Jr., and H. Eyring, *J. Am. Chem. Soc.*, **73**, 5628 (1951).

(7) S. Glasstone, K. J. Laidler and H. Eyring, "The Theory of Rate Processes," McGraw–Hill Book Co., New York, N. Y., 1941, pp. 470–473.

(8) F. H. Johnson, H. Eyring and M. J. Polissar, "The Kinetic Basis of Molecular Biology," John Wiley and Sons, Inc., New York, N. Y., 1954, Chapts. 9 and 10.

(9) A. E. Stearn and H. Eyring, *Chem. Revs.*, **29**, 509 (1941).

(10) H. G. David and S. D. Hamann, *Trans. Faraday Soc.*, **50**, 1188 (1954).

(11) H. G. David, S. D. Hamann and S. J. Lake, *Australian J. Chem.*, **8**, 285 (1955).

(12) K. E. Weale, *J. Chem. Soc.*, 2959 (1954).

(13) E. G. Williams, M. W. Perrin and R. O. Gibson, *Proc. Roy. Soc. (London)*, **A159**, 162 (1937).

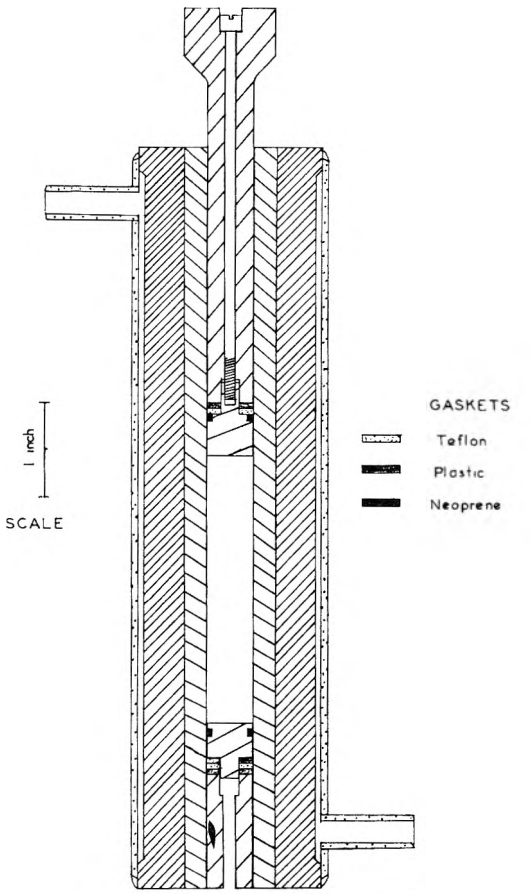

Fig. 4.—Diagram of pressure cell.

cell inside. The seals shown in Fig. 4 were adopted and found satisfactory to 15,000 atmospheres. In this vessel the plastic chosen for the backup rings was fabric reinforced phenol formaldehyde sheet. Its shearing strength is ample to contain the softer Teflon. Teflon shows a very low coefficient of friction against most solids, and it is felt that in this design a thin film of this plastic rubs off onto the steel walls and serves as a lubricant for the phenolic rings.

A novel feature of these closures is the use of Neoprene O rings, both top and bottom, so placed as to reduce to a minimum the danger of necking off the plugs.

The top plug is held in place by means of a concentric screw in the piston while since no movement is required of the bottom plug, the screw is omitted.

In the bottom plug the sandwich of Teflon between phenolic rings worked well. It is probable that the top phenolic ring could be dispensed with although some leakage was observed in the instance when it was tried.

Pistons and plugs were of "Venango Special" steel (Universal Cyclops) hardened to Rockwell C52.

Friction was found to be not greater than 5% of the thrust on the top piston. Each pressure measurement was made by raising the thrust until slight movement of the piston occurred, observed by means of a dial gauge. This thrust was recorded. The thrust then was decreased until again there was movement of the pistons (in the opposite direction) and the reduced thrust was measured. Pressure then was calculated from the average of the two thrusts, and probably was accurate within plus or minus 1%.

From observations that will not be recorded here, it was concluded that the main friction between 0 and 4,000 atmospheres was exerted by the O rings, but as the pressure increased to the range of 5,000 to 7,000 atmospheres the coefficient of friction decreased indicating extrusion of the low friction Teflon ring. At about 7,000 atmospheres the coefficient of friction again increased, which was interpreted to mean that at this higher pressure the harder plastic rings had extruded against the cylinder walls.

A 30 ton hydraulic jack was used to obtain the pressures. The press was made from reinforced 8 inch channel iron welded in the shape of a box with two inch threaded stock as supports. A steel shield was used to cover the front and sides of the press and a heavy wire screen was used in the back. By means of a mirror mounted on the wall behind the press, the pressure cell could be observed during the high pressure tests.

The external pressure in all cases was measured by means of a calibrated load cell. This cell consisted of a hardened steel cylinder with two measuring and two compensating strain gauges cemented onto the cylinder walls.

The samples were maintained at constant temperature by thermostats from which oil was pumped to the copper jacketed pressure cell. A cold temperature bath was used to quickly "freeze" the reaction at the end of each experimental run.

Various methods were tried to contain the sample while under pressure. Both glass and steel tubes with rubber stoppers at both ends were tried, but found unsatisfactory. Finally, a very simple procedure gave good results. This consisted of small polyethylene bags containing the sample solution and tied with string. Methyl alcohol was used as the hydraulic fluid. It was found that even under very high pressures no leakage could be detected. All experimental runs were conducted with these polyethylene bags.

Acknowledgment.—We wish to thank the Office of Naval Research which provided the funds for this project. We are also indebted to Mr. E. L. Hardy and Mr. Arthur Nettleship who constructed the pressure apparatus as well as Mr. W. J. Teerlink and Dr. J. M. Sugihara who synthesized and resolved the hindered biphenyl.

THE POLARIZABILITY OF RADON

BY D. G. TUCK

Department of Chemistry, University of Nottingham, Nottingham, England

Received June 1, 1960

In a recent publication, Miller[1] has given calculated values for the intermolecular force constants of radon; in the course of the calculations, two slightly differing values of 4.50 and 5.86 Å.^{3} are derived for the polarizability of the radon atom. The purpose of the present note is to show that a concordant value of 6.3 Å.^{3} for this parameter can be derived by a quite independent method.

Chackett and the present author[2] have measured the heats of adsorption of the inert gases on charcoal at low equilibrium pressures ($p \leq 10^{-2}$ mm.). From the results, a value of 13.5 ± 1.4 kcal./g. atom was deduced for the heat of adsorption of radon on charcoal under similar conditions; since the periodic behavior of the inert gases is well established (see ref. 2), the limits set on this value are reasonably generous. In the same paper it was shown that for the experimental conditions of negligible interaction between adsorbed atoms, there is a good (semi-empirical) linear relationship between the heat of adsorption (ΔH) and the polarizability (α), which can be expressed as

$$\Delta H = 0.29 + 2.11\alpha$$

where ΔH is in kcal./g. atom and α is 10^{-24} cm.^{3}. Substituting the above value of ΔH for radon into this equation gives

(1) G. A. Miller, THIS JOURNAL, **64**, 163 (1960).

(2) K. F. Chackett and D. G. Tuck, *Trans. Faraday Soc.*, **53**, 1652 (1957).

$$\alpha_{Rn} = 6.3 \pm 0.6 \text{ Å.}^3$$

where the limits are those of the derived value of ΔH.

The agreement with the higher of the two values calculated by Miller is extremely good considering the extrapolations involved.

THE REDUCTION OF OXALATE BY CHROMIUM(II)[1,2]

By Ronald M. Milburn and Henry Taube

George Herbert Jones Laboratory, University of Chicago, Chicago, Illinois

Received June 3, 1960

It has been shown that free oxalate is rather rapidly reduced to glycolate by solutions of Cr(II) perchlorate. Oxalate bound to Cr(III) is reduced only very slowly by Cr(II). The observation that oxalate and Cr(II) undergo an oxidation–reduction reaction is in agreement with Moissan,[3] who reported that on preparation of Cr(II) oxalate, part of the Cr(II) was always oxidized.

We find that in the *p*H range 1–2, with oxalate in moderate excess over Cr(II) and with concentrations of the order of 1/100 *M*, most of the Cr(II) is oxidized within a few minutes at room temperature. The Cr(III) produced is violet-red, of similar color to Cr(III)–oxalato complexes. Some tailing off in the rate of Cr(II) consumption is observed. In a solution which was initially 1.77×10^{-2} *M* in Cr^{+2} and 9.1×10^{-2} *M* in oxalic acid, and which had an initial *p*H of 1.2, the consumptions of Cr(II) at ~23° were: $t = 0$, 0%; $t = 0.10$ hr., 91.4%; $t = 1.0$ hr., 91.2%; $t = 24$ hr., 97.2%. A solution of the same composition was allowed to react to essential completion (> 98% Cr(II) oxidized), and then was exposed to the atmosphere, heated with potassium hydroxide to free ligands attached to the Cr(III), and filtered while hot and again after cooling in an ice-bath.[4] Tests made on portions of the filtrate to determine the nature of the reduced species gave no indication of chloride, formate, formaldehyde, glyoxalate or glyoxal, but gave positive evidence for the presence of glycolate by the deep red-violet color of the 2,7-dihydroxynaphthalene test.[5] Comparison of the absorbance at 540 mμ of the red-violet product with the absorbancies given by solutions of known glycolate concentrations indicated that the original filtrate contained 95% of the amount to be expected for quantitative reduction of oxalate to glycolate by the Cr(II).[6]

In the same range of *p*H and of concentrations of Cr(II) and oxalate, but with the Cr(II) and oxalate in approximately equimolar amounts, the initial rapid reduction of oxalate is soon inhibited by the formation of Cr(III)–oxalato complexes. The tailing off in the rate of Cr(II) consumption is illustrated by the following typical result. In a solution which was initially 0.975×10^{-2} *M* in Cr^{+2} and 1.00×10^{-2} *M* in oxalic acid, and which had a *p*H of 1.6,[7] 29% of the Cr(II) was oxidized after 6 minutes, but only 51% after 10 hours. The amount of oxalate reduced by the initial fast reaction can be greatly increased by introduction into the solution of other chelates, such as pyrophosphate or ethylenediaminetetraacetate, which, while not reduced by Cr(II),[8] compete for coördination positions on the Cr(III). In some typical cases up to 70% reduction of Cr^{+2} was achieved in the first few minutes.

Experimental

Ordinary distilled water was further purified by refluxing with alkaline permanganate for about 12 hours, and redistilling from a tin apparatus. Solutions of Cr^{+2} and Cr_{aq}^{+3} were prepared by standard methods.[9] Except where otherwise indicated, perchlorate was used as the anion in solutions. Reactions of Cr^{+2} were conducted at room temperature (~23°) under an atmosphere of nitrogen. Concentrations of Cr^{+2} were estimated by addition of a deaerated solution of excess iodine (prepared as needed from standard iodate, and iodide and acid) followed by potentiometric titration of the remaining iodine with thiosulfate, using platinum and calomel electrodes.

Glycolate was determined quantitatively by addition to 1 ml. of solution, 1.5×10^{-4} to 5.0×10^{-4} *M* in glycolate, of 10 ml. of a solution containing 0.01 g. of 2,7-dihydroxynaphthalene per 10 ml. of concentrated sulfuric acid. The resulting sample was heated for 1 hour at 90° together with samples prepared from a solution of known concentration in glycolate. On cooling the solutions the optical densities at 540 mμ were measured and compared. Beer's law was found to be obeyed throughout the specified concentration range.

(1) Supported by the A.E.C. under Contract AT(11-1)-378.

(2) The observations reported were made in the course of a study of the catalysis by Cr^{++} of the formation of Cr(III) complexes. Although the research failed in its purpose with oxalate as ligand, a striking effect was demonstrated with pyrophosphate as ligand.

(3) H. Moissan, *Compt. rend.*, **92**, 1051 (1881); *Ann. chim. et phys.*, [5] **25**, 401 (1882).

(4) Much of the perchlorate was removed as $KClO_4$; large amounts of perchlorate interfered with some of the tests made.

(5) On acidification with nitric acid and addition of silver nitrate, no cloudiness from silver chloride was observed. The qualitative tests for the organic compounds were taken from F. Feigl, "Spot Tests in Organic Analysis," D. Van Nostrand Co., Inc., Princeton, N. J., 5th edition, 1954.

(6) The potassium hydroxide treatment may have resulted in at least partial conversion of any glyoxal to glycolate. Tests on the solution before the potassium hydroxide treatment failed to reveal the presence of free glyoxal.

(7) This solution was buffered with HSO_4^- and SO_4^{-2}. Similar tailing off was observed with unbuffered solutions.

(8) Although some oxidation of Cr(II) by ethylenediaminetetraacetate was observed, the amount of oxidation in a few minutes was negligible.

(9) H. Taube and H. Myers, *J. Am. Chem. Soc.*, **76**, 2103 (1954).

THE HEAT OF COMBUSTION OF DICYANOACETYLENE

By George T. Armstrong and Sidney Marantz

The National Bureau of Standards, Washington, D. C.

Received June 6, 1960

Cyanogen, dicyanoacetylene and the dicyanopolyacetylenes are highly unstable thermodynamically. When they are burned with the proper proportions of oxygen, carbon monoxide and nitrogen may be the principal products of combustion. These facts lead to the possibility of obtaining very high temperatures of combustion, a possibility which has been borne out by experiments of Conway, Smith, Liddell and Grosse[1] on the combustion of cyanogen. Kirshenbaum and Grosse[2] have calculated that even higher tempera-

(1) J. B. Conway, W. F. R. Smith, W. J. Liddell and A. V. Grosse, *J. Am. Chem. Soc.*, **77**, 2026 (1955).

(2) A. D. Kirshenbaum and A. V. Grosse, *ibid.*, **78**, 2020 (1956).

tures, above 5000°K., should result from the combustion of dicyanoacetylene, C_4N_2. The heats of formation of C_4N_2 and related cyanoacetylenes are therefore of great interest.

The heat of formation of cyanogen gas has been established to be 73.84 ± 0.43 kcal./mole.[3] The only measurement of the heat of formation of any of the cyanoacetylenes is that by Moureu and Bongrand.[4] The lack of further thermochemical study in spite of their interesting linear conjugated structure probably is the result of the scarcity of materials.

Moureu and Bongrand, using a bomb calorimeter, burned a C_4N_2 sample contained in a glass bulb, which they ignited with a platinum fuse and a naphthalene promoter. Reaction was incomplete, some carbon being formed in all experiments. Carbon deposits were not recovered or their amounts determined in four experiments, in which the heats of combustion ranged from 6426 to 6660 cal. $g.^{-1}$. In a fifth experiment the carbon was collected and burned for analysis, a correction of about 1% was applied for the incompletely burned material and the heat of combustion at constant volume, 6790 cal. $g.^{-1}$ (solid), obtained from this experiment was reported. From this they derived the heat of combustion (solid) at constant pressure to be 515.5 kcal. $mole^{-1}$.

We have redetermined the heat of combustion of C_4N_2 in order to test the value reported by Moureu and Bongrand.

Experimental

Materials.—Two samples of dicyanoacetylene were supplied by Professor A. V. Grosse, of the Research Institute of Temple University. As received, these samples consisted of a 6.0-g. sample (No. 1) and an 8.5-g. sample (No. 2) reportedly melting at 18–20° and 20.0–20.5°, respectively. The infrared spectra had shown no impurities containing C–H or C–OH groupings. Impurities, if present, were believed to be other materials having similar structures.

The samples were refrigerated with Dry Ice to prevent thermal decomposition. During storage some brown coloration developed in the samples. Shortly before use each sample was purified by sublimation into ampoules refrigerated with liquid nitrogen in an evacuated glass apparatus. The material was divided at this step into portions suitable for single combustion determinations and sealed until ready for use. The portions thus obtained were white crystals, quite free of any brown color, which formed a colorless liquid on melting.

Mass spectrometer analysis[5] showed no substances identifiable as impurities.

Samples for the bomb calorimeter were prepared by filling small thin-walled glass sample bulbs of the type commonly used for volatile liquids in this Laboratory.[6] Transfer from ampoule to sample bulb was made by hypodermic syringe in a dry-box filled with nitrogen. The filled bulbs were removed from the dry-box and sealed by torch to permit them to be weighed. Visible charring invariably occurred at the point of the seal, and several samples were lost because the seal could not be made. Where successful seals were obtained, the charred material was considered to be a negligible fraction of the total weight of sample. In the time necessary for weighing, between the time of closure of the bulb and its introduction into the calorimeter, a pale straw color appeared in the liquid.

At no time was there evidence of violent decomposition, even in the near presence of a flame. A deliberate effort to initiate explosion was made by turning a torch directly on a filled bulb which had failed to seal properly. No explosion occurred, but after a brief time of smoky flame, a very vigorous, non-smoking bright blue jet appeared, which, however, was not self sustaining under the conditions of the test.

Combustion Experiments.—Samples were burned in a Dickinson type calorimeter using an Illium bomb, and techniques similar in most respects to our customary practices.[6] The calorimeter was calibrated with benzoic acid, National Bureau of Standards standard sample 39 g, using the certified heat of combustion 26,433.8 $j.g.^{-1}$ (weight *in vacuo*). Absence of hydrogen in the sample required some modification of the ordinary technique. Although no water was to be formed by the combustion, one ml. of water was placed in the bomb as usual in order to dissolve oxides of nitrogen. It was found, however, that practically none of the oxides dissolved in the water when it was on the bottom of the bomb. The difficulty was attributed to the small surface area exposed for solution of the gases. The water was thereafter placed in a shallow platinum pan supported by one electrode and located directly over the flame. Evaporation of the water by the flame during combustion caused a deposit of fine droplets on all walls of the bomb. The oxides were found to be dissolved in the water as nitric acid under these conditions, and were determined by titration.

The carbon dioxide formed in each experiment was measured by absorption in Ascarite. Some carbon was formed during each combustion experiment. The amount was about 1% of the total carbon in experiment 4, the most pronounced case, and was much less in the other experiments. Gases from the bomb were tested for carbon monoxide, but none was found.

Samples used were smaller than necessary to produce a three degree temperature rise of the calorimeter because of (a) the small amount of material available for combustion, (b) the expectation that a very fast reaction would cause an exceptionally high pressure in the bomb, and (c) the experience of Moureu and Bongrand that larger samples tended to produce more carbon.

Heat Measurements.—Of eight experimental measurements made after the technique had been developed for dissolving oxides of nitrogen, one was discarded because of a leak in the bomb, one because of a very large inconsistency in the weights of carbon dioxide and C_4N_2, and one because an unidentifiable black deposit collected in the carbon dioxide absorption tube and because a small leak apparently remained unsealed in the glass sample bulb.

The results of the remaining five experiments are shown in Table I. Two experiments were made on sample No. 1 and three on sample No. 2. In Table I, m_s is the mass of C_4N_2 in grams; m_s' is the mass of C_4N_2 calculated from carbon dioxide collected; $-\Delta E_b$ is the observed energy of the bomb process in joules; $-q_1$ is the correction in joules for nitric acid formed in the reaction; $-q_2$ is the firing energy in joules; $-q_3$ is a correction in joules for the amount of carbon formed; and $-q_4$ is the Washburn correction. The correction $-q_3$ was calculated on the assumption that the difference between m_s and m_s' was due to the conversion of some C_4N_2 to carbon instead of carbon dioxide. ΔE^0_T is the internal energy change in kj. $mole^{-1}$ at the final bomb temperature (300.2 to 301.4°K.) for reaction 1; and ΔH^0_{298} is the enthalpy change at 298°K. for reaction 1

$$C_4N_2(l) + 4O_2 = 4CO_2 + N_2 \qquad (1)$$

The mean value for the enthalpy change of reaction 1 in the standard state is

$$\Delta H^0_{298(l)} = -2078.5 \pm 0.7 \text{ kj. mole}^{-1} = -496.8 \pm 0.2 \text{ kcal. mole}^{-1}$$

The uncertainty given is the standard deviation of the mean. The value found here is about 4% smaller than was found by Moureu and Bongrand.

Discussion

The heat of combustion given above can be used to calculate the standard heat of formation of C_4N_2 liquid. Using $\Delta H^0_{f298}[CO_2] = -94.05$ kcal.

(3) J. W. Knowlton and E. J. Prosen, *J. Research Natl. Bur. Standards*, **46**, 489 (1951).

(4) C. Moureu and J. C. Bongrand, *Ann. chim.*, **14**, 5 (1920).

(5) Mass spectrometer analysis was performed by V. H. Dibeler of the Mass Spectrometry Section at the National Bureau of Standards.

(6) R. S. Jessup, "Precise measurement of heat of combustion with a bomb calorimeter," Natl. Bur. Standards Monograph No. 7, (U. S. Government Printing Office, Washington 25, D. C., 1960).

TABLE I

COMBUSTION DATA AND HEAT OF REACTION 1

Sample	m_s, g.	m_s', g.	$-\Delta E_b$, j.	$-q_1$, j.	$-q_2$, j.	$-q_3$, j.	$-q_4$, j.	$-\Delta E^0_T$, kj. mole^{-1}	$-\Delta H^0_{298}$, kj. mole^{-1}
1	0.65711	0.65667	18019.1	73.6	22.0	2.9	−15.4	2074.6	2077.3
1	.37582	.37421	10282.2	45.9	22.0	10.6	− 8.6	2076.5	2079.1
2	.44996	.44915	12344.0	47.8	22.0	5.4	−10.4	2077.7	2080.3
2	.38954	.38607	10582.5	48.0	22.0	23.0	− 9.4	2073.7	2076.3
2	.23974	.23829	6549.2	24.4	22.0	9.6	− 5.6	2076.9	2079.5
Mean									2078.5
Stand. dev. of the mean									±0.7

mole^{-1},[7] we obtain $\Delta H^0_{f298}[C_4N_2(l)] = 120.6$ kcal. mole^{-1}. The heat of vaporization is given by Saggiomo[8] to be $\Delta H_{vap} = 6.875$ kcal. mole^{-1}. If this is taken as the best approximate value available for the enthalpy difference between gas and liquid in their standard states, the heat of formation of the ideal gas is $\Delta H^0_{f298}[C_4N_2(g)] = 127.5$ kcal. mole^{-1}. Using $\Delta H^0_{f298}[C] = 171.299$ kcal. mole^{-1} [9] and $\Delta H^0_{f298}[N] = 112.96$ kcal. mole^{-1},[10,7] we obtain for the total binding energy of the C_4N_2 molecule 783.6 kcal. mole^{-1} at 298°K.

(7) F. D. Rossini, D. D. Wagman, W. H. Evans, S. Levine and I. Jaffe, "Selected values of chemical thermodynamic properties," Natl. Bur. Standards Circ. 500 (U. S. Government Printing Office, Washington, D. C., 1952)).

(8) A. J. Saggiomo, *J. Org. Chem.*, **22**, 1171 (1957).

(9) W. H. Evans, private communication.

(10) L. Brewer and A. W. Searcy, *Ann. Revs. Phys. Chem.*, **7**, 259 (1956).

NON-RESONANT MICROWAVE ABSORPTION AND RELAXATION FREQUENCY AT ELEVATED PRESSURES

BY A. A. MARYOTT[a] AND G. BIRNBAUM[b]

[a] *National Bureau of Standards, Washington, D. C., and* [b] *The Research Laboratories, Hughes Aircraft Company, Culver City, California*

Received June 10, 1960

The present note is part of a systematic investigation of the non-resonant spectra of symmetric-top molecules in the vapor state. Previous work has dealt with the detailed shape of these spectra,[1] the dependence of relaxation frequency on temperature,[2] and the use of these spectra for precise determinations of values of the electric dipole moment.[3,4] Previous measurements were confined, for the most part, to moderately low pressures (several atmospheres or less). In this region, the relaxation frequency increases in proportion to the pressure, or density, in accord with a mechanism of binary collisions. In the present investigation, data on trifluorochloromethane are extended to much higher densities in order to examine the dependence of relaxation frequency on density in greater detail.

Trifluorochloromethane has a comparatively small dipole moment, 0.50 debye. It was selected because, unlike symmetric tops with large dipole moments, the non-resonant spectrum is characterized by a single relaxation frequency parameter and because reliable compressibility data are available. In addition, certain factors which complicate interpretation, such as dipole association and the problem of the local field, should be minimized.

(1) G. Birnbaum, *J. Chem. Phys.*, **27**, 360 (1957).

(2) A. A. Maryott and G. Birnbaum, *ibid.*, **32**, 1501 (1960).

(3) A. A. Maryott and G. Birnbaum, *ibid.*, **24**, 1022 (1956).

(4) A. A. Maryott and S. J. Kryder, *ibid.*, **27**, 1221 (1957).

Experimental

The method of measuring the dielectric loss in compressed gases with tunable, transmission-type cavities has been described.[1,5] Values of the loss tangent were measured up to 30 atm. (near saturation) with a hybrid-mode cavity (loaded $Q = 4000$) at a frequency of 1190 Mc. (0.0397 cm.$^{-1}$). Values of the dielectric constant ϵ' were measured only with the accuracy needed to convert loss tangent to loss factor.

The $CClF_3$ was part of the sample used previously.[1] The purity indicated by a mass spectrographic analysis was better than 99%. All measurements were made at 30°.

Results and Analysis

The experimental data are given in Table I. The compressibility factor, Z, ($Z = pV/RT$) was obtained by interpolation of data reported by Albright and Martin.[6] Values of the dielectric loss factor were derived from the measured values of the loss tangent according to the relation $\epsilon'' = \epsilon' \tan \delta$, where ϵ' is the real part of the dielectric constant.

TABLE I

DIELECTRIC LOSS FACTOR ϵ'' AND DIELECTRIC CONSTANT ϵ' OF $CClF_3$ AT 1190 MC. AND 30°

p (atm.)	Z	ϵ'	ϵ''
0.355	0.997	1.0088	17.6×10^{-6}
.463	.996	1.0010	27.8
.569	.995	1.0013	38.6
.833	.994	1.0019	64.1
1.028	.992	1.0023	81.6
.1233	.990	1.0027	94.8
1.82	.985	1.0041	124.0
2.90	.975	1.0068	147.4
4.88	.956	1.0118	158.4
7.61	.931	1.019	159.5
10.89	.899	1.029	164.6
14.29	.863	1.040	168.5
17.66	.825	1.052	176.4
21.03	.784	1.065	185.5
24.45	.739	1.080	196.1
27.89	.684	1.097	215.7
30.88	.642	1.116	231.8

The theoretical relations and procedures used to evaluate the parameters characterizing the non-resonant absorption in symmetric-top molecules

(5) H. E. Bussey and G. Birnbaum, *Rev. Sci. Instr.*, **30**, 800 (1959).

(6) L. F. Albright and J. J. Martin, *Ind. Eng. Chem.*, **44**, 188 (1952).

have been described.[1,3] Some modifications, however, are needed in the present case, where the data extend well above atmospheric pressure. In particular, allowance must be made for substantial departures from the ideal gas density and for changes in the local, or polarizing, field when the dielectric constant can no longer be considered as unity. There is also some resonant absorption associated with the pure rotational transitions. The frequencies of the rotational lines are all considerably higher than the applied frequency. However, only at the lower densities, where the lines are comparatively narrow, will their effect on the measured loss be negligible, so that, in general

$$\epsilon'' = \epsilon''\text{ (non-resonant)} + \epsilon''\text{ (resonant)} \qquad (1)$$

The non-resonant loss factor is given by

$$\epsilon''\text{ (non-resonant)} = \frac{4\pi N_0(p/Z)\mu^2 qF}{3kT}\left[\frac{\nu\Delta\nu}{\Delta\nu^2+\nu^2}\right] \qquad (2)$$

where $N_0(p/Z)$ is the molecular density (N_0 being the ideal gas density at 1 atmosphere and p the pressure in atmospheres), μ the total dipole moment, F the local field factor, ν the applied frequency, $\Delta\nu$ the relaxation frequency, and $q = \Sigma_{JK} f_{JK} K^2/(J^2+J)$. The function f_{JK} is the fractional number of molecules in the rotational state designated by the quantum numbers J and K. With $\Delta\nu$ expressed in units of wave number the relaxation time $\tau = 1/2\pi c\Delta\nu$.

Since the dipole moment is small, and F should not differ greatly from unity even at the highest density, an adequate approximation for the local field factor can be obtained from the Clausius–Mossotti relation. If $\epsilon_0 - \epsilon_k$ is the non-resonant contribution to the state dielectric constant, then

$$F = (\epsilon_0 + 2)(\epsilon_k + 2)/9 \backsimeq (\epsilon' + 2)^2/9$$

We shall consider first the data below two atmospheres, where the loss from the rotational lines is quite negligible, to obtain the value of the dipole moment and the relaxation frequency parameter, $\delta = \Delta\nu/(p/Z)$, applicable at lower densities. Equation 2 can be rearranged to give

$$(p/Z)^2F/\epsilon'' = a + b(p/Z)^2 \qquad (3)$$

where

$$\delta = (b/a)^{1/2} \text{ and } \mu^2 = \frac{3kT}{4\pi N_0(ab)^{1/2}q} = \frac{44.9T^2\times 10^{-38}}{(ab)^{1/2}\,q}\ \text{e.s.u.}$$

Figure 1 shows a plot of the data according to eq. 3. The data fit a straight line within the experimental uncertainties of about 2% and give δ = 0.0392 cm.$^{-1}$ atm.$^{-1}$. With the rotational constant A = 1.92 cm.$^{-1}$ and $B = C$ = 1.10 cm.$^{-1}$,[7] the summation q = 0.263. The dipole moment is then 0.496 debye. This value is about 1% lower than previously reported, the difference being due partly to the allowance made here for non-ideal gas behavior.

If $\Delta\nu$ continues to increase in proportion to the density, it is evident from eq. 2 that, when $\Delta\nu^2 >> \nu^2$, ϵ''/F will approach a limiting value provided the absorption from the rotational lines remains negligible. The loss factor computed on the assumption that $\Delta\nu$ is proportional to the density over the entire range is shown by curve 3 of Fig. 2.

(7) D. K. Coles and R. H. Hughes, *Phys. Rev.*, **76**, 858 (1949).

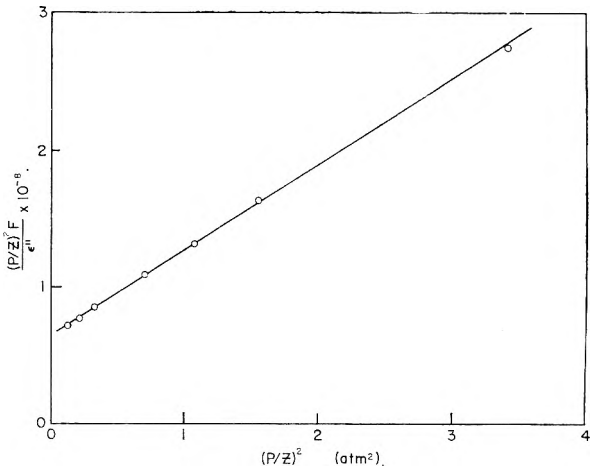

Fig. 1.—Non-resonant loss below 2 atm. plotted according to eq. 3, $(p/Z)^2F/\epsilon''$ as a function of the square of the density, p/Z.

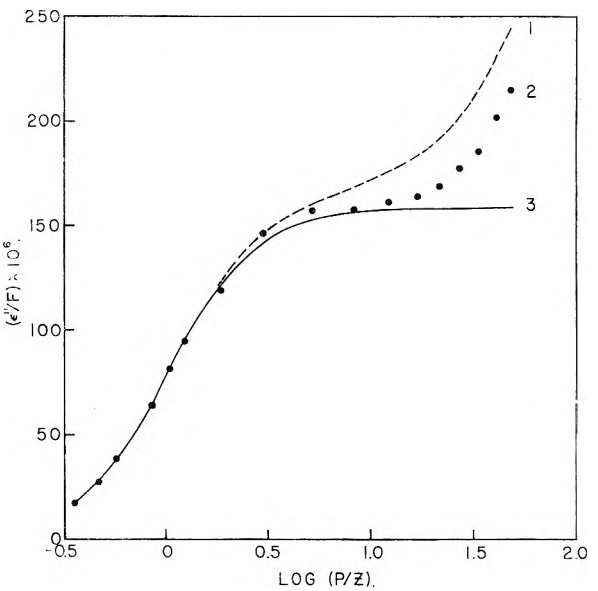

Fig. 2.—Comparison of the total observed loss as a function of log(p/Z) with values computed for the non-resonant contribution from eq. 2: Curve 1, computed with $\Delta\nu$ proportional to the pressure, p; curve 2, observed values; curve 3, computed with $\Delta\nu$ proportional to the density, p/Z.

Below 10 atm. the experimental values of ϵ''/F fit this curve well and lie close to the predicted limiting value of 159 $\times$ 10^{-6} when p/Z is in the neighborhood of 10 atm. At higher densities the data fall above curve 3. The deviation increases roughly as the square of the density and, as shown subsequently, probably derives in large part from the rotational lines, rather than any marked deviation from the assumed proportionality between relaxation frequency and density. If, for example, $\Delta\nu$ were to increase in proportion to the pressure, p, rather than to p/Z, the non-resonant contribution would be given by curve 1 of Fig. 2. As the combined resonant and non-resonant loss is substantially less than this, it is immediately evident that the relaxation frequency must increase more rapidly than the pressure.

It is not possible, for a variety of reasons, to compute with exactness the loss associated with

the rotational transitions. Data on the widths of the individual lines, even at very low pressures, are not available. However, by comparison with other gases where the long-range dipole–dipole interactions are also weak, one might expect line widths of the order of 0.1 to 0.2 cm.$^{-1}$ atm.$^{-1}$. Furthermore, in other gases exhibiting both resonant and non-resonant absorption, it has been generally observed that the resonant line widths are several times larger than the non-resonant widths, or relaxation frequencies. Actually, calculations based on the Van Vleck–Weisskopf line shape indicate that the deviation between curve 3 and the experimental data can be accounted for with an average width for the rotational lines of 0.12 cm.$^{-1}$ atm.$^{-1}$. The loss arising from the rotational transitions would then be insignificant for pressures below 10 atm. and comprise about 25% of the total loss at the highest pressure.

Discussion

It is apparent, by analogy with the liquid state, that pronounced changes in dielectric behavior must occur when the gas is sufficiently compressed. Polar liquids show no rotational quantization and the entire dipolar loss is non-resonant, or Debye type. Such a transition is not yet apparent in $CClF_3$. The loss observed at the highest pressures is consistent with predictions based on the behavior at low pressures. If the entire rotational spectrum had undergone a transition from resonant to non-resonant, the total loss would have been much greater.

The relaxation frequency for the non-resonant loss continues to increase with increasing density throughout the range of this investigation. Below 10 atm. the variation is linear. At higher pressures interference from the rotational lines precludes an exact determination of the functional dependence. However, if a reasonable allowance is made for the effect of the rotational lines, the relaxation frequency appears to vary more or less linearly with the density over the entire range. At the highest density (p/Z = 45 atm.), the relaxation frequency of $CClF_3$ is of about the same magnitude as found for similar substances in the liquid state. In liquids, however, the trend with density is reversed, increasing density causing a decrease in relaxation frequency. The details of the relaxation mechanism are therefore quite different in the two cases. Molecules of the liquid are in almost constant collision, but many collisions are needed to cause random reorientation because of the restraining effect of neighboring molecules. In gases, collisions are less frequent, being directly proportional to the density at lower densities, but their effect on molecular reorientation is much greater. Thus, the relaxation frequency of the gas may approach or exceed that of the liquid.

It probably is fortuitous that the relaxation frequency of $CClF_3$ varies more or less in proportion to the density over such a wide range. The effective collision diameter for molecular reorientation is about 5 Å., or about the same as the molecular diameter. At the maximum density, the mean free path is of the same order. Therefore, the collision frequency will increase faster than the density, since the volume occupied by the molecules is an appreciable part of the total volume. The probability of multiple interactions, which should reduce the effectiveness of collisions, also increases. It would appear that these effects largely compensate each other. At still higher densities the relaxation frequency should reach a maximum and then decrease as the latter effect becomes the determining factor.

Data over a similar range of pressures have been reported by Phillips[8] for chlorodifluoromethane. These results were interpreted in a manner that required the entire loss to be non-resonant for pressures above several atmospheres and led to the conclusion that the relaxation frequency was independent of the pressure. This interpretation is not in accord with the present study. Although $CHClF_2$ is a slightly asymmetric top, its spectrum, from the present standpoint, is qualitatively analogous to that of the symmetric top. The +K, −K degeneracy is removed, but the direct transitions between these levels are of such low frequency that the resulting absorption has the character of a non-resonant spectrum.[9] At the comparatively high frequency (*ca.* 25 kMc.) employed by Phillips, the rotational and non-resonant spectra would overlap strongly and make difficult any detailed analysis.

(8) C. S. G. Phillips, *J. Chem. Phys.*, **23**, 2388 (1955).
(9) E. B. Wilson, Jr., THIS JOURNAL, **63**, 1339 (1959).

NOTE ON THE SOLUTION OF HYDROGEN IN PALLADIUM WIRES

BY JAMES P. HOARE*

Scientific Laboratory, Ford Motor Company, Dearborn, Michigan

Received June 18, 1960

If the open-circuit potential of a clean palladium wire which previously has been anodized in pure hydrogen-stirred 2 *N* H_2SO_4 solution is followed as a function of time, one observes a curve having a plateau at 50 mv. more noble than a Pt/H_2 electrode in the same solution.[1] It was suggested that Frumkin and Aladjalova[2] did not observe this plateau because they mounted their palladium electrodes in platinum holders sealed in glass.[3] The local cell action due to the contact of two dissimilar metals in acid solution charged the Pd to β-Pd and the potential fell rapidly to a value of zero volt. It was suggested recently[4] that the platinum holder did not have any effect on the rate of solution of hydrogen and that metastable states causing plateaus in the potential–time curves were due to the extreme inactivity of the palladium surface of the electrodes used by Hoare and Schuldiner.

Evidence is presented here to show a very marked

* General Motors Research Laboratories, General Motors Corporation, Warren, Michigan.

(1) J. P. Hoare and S. Schuldiner, THIS JOURNAL, **61**, 399 (1957); J. P. Hoare, *J. Electrochem. Soc.*, **106**, 640 (1959).
(2) A. Frumkin and N. Aladjalova, *Acta Physicochim. U.R.S.S.*, **19**, 1 (1944).
(3) S. Schuldiner and J. P. Hoare, *J. Chem. Phys.*, **23**, 1551 (1955); S. Schuldiner, G. W. Castellan and J. P. Hoare, *ibid.*, **28**, 16 (1958).
(4) J. O'M. Bockris, *Chem. Revs.*, **43**, 525 (1948); J. P. Hoare and S. Schuldiner, *J. Electrochem. Soc.*, **103**, 237 (1956); *J. Chem. Phys.*, **26**, 1771 (1957).

effect on the rate of solution of hydrogen in Pd by the electrical contact of Pt with Pd in acid solution.

A palladium wire 10.5 cm. long and 0.38 cm. in diameter was mounted in a Teflon cell filled with 2 N H_2SO_4 solution. All purification, electrode preparation and measurement procedures were identical to those found in the literature.[1,3] Both the resistance of the wire and the potential against a Pt/H_2 electrode in the same solution were recorded as a function of time while the Pd wire absorbed hydrogen from the acid solution. The solution is stirred with hydrogen flowing at a rate of 230 ± 10 cc./min. Zero time is taken when the hydrogen flow is first started and all potentials are measured against a Pt/H_2 electrode in the same solution.

The A-curves in Fig. 1 are plots of the data taken on the wire described above. The filled symbols are the potential–time points and the open symbols are the resistance–time points. The symbols represent points taken directly from the meters while the smooth curves were obtained from the recorder chart. After these data were collected, the wire was removed from the cell and annealed at red heat in a flame for five minutes to remove the dissolved hydrogen. A piece of platinum gauze about 0.5 $cm.^2$ in area was spotwelded to the center of the palladium wire. After this wire had been mounted in the cell, the same procedures which had been used in obtaining the data for the A-curves were repeated. The B-curves in Fig. 1 are a plot of these data. The C-curves were obtained in the same way except that a platinum gauze 7 cm. long and 3 mm. wide was spot-welded at about 10 points along the center of the Pd wire.

From Fig. 1 it is seen that, as the contact with platinum is increased, the length of the 50-mv. plateau is shortened and the steady-state value is lowered for the potential–time curves. The length of the α-Pd-plateau[1] on the resistance–time curves is reduced and the slopes of these curves are increased as contact with platinum is increased. This may be explained by an increased rate of solution of hydrogen due to local cell action at the points of contact with platinum as suggested before.[2] The reason why the points on the resistance–time curve in the case of the C-curve are lower than what might be expected may be traced to the parallel resistance of the platinum gauze.

These data support the contention that conditions of high purity with regard to electrode materials, cell construction materials, solutions and gases are of the utmost importance[4] in investigations of this kind. It is suggested that these data show why a 50 mv. plateau was not observed[2] and why Frumkin and co-workers[5] seem to have more active electrodes than Hoare and Schuldiner since the criterion for surface activity may be taken as the rate at which a Pd/H_2 electrode reaches the equilibrium value of zero volt *vs.* Pt/H_2 or the rate at which palladium dissolves hydrogen.

An interesting feature of the potential–time curves in Fig. 1 is the increase in the amount of initial overshoot of the plateau value with increasing rate of the solution of hydrogen due to contact with platinum. These data may provide supporting evidence for the existence of a supersaturated α-Pd–H phase.[6]

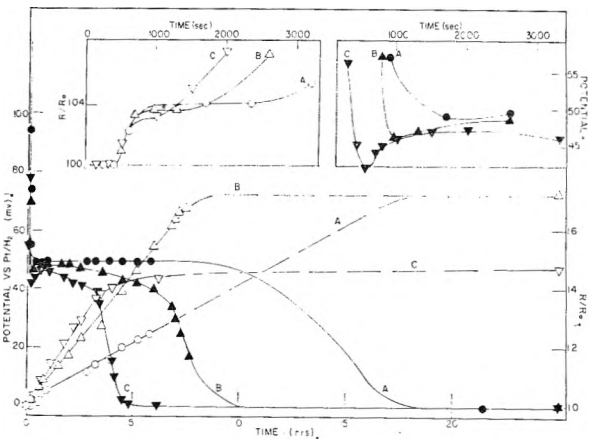

Fig. 1.—Potential *vs.* time (filled symbols) and relative resistance, R/R_0, *vs.* time (open symbols) curves for Pd wires in H_2-stirred 2 N H_2SO_4 solution. Smooth potential–time curves are taken from recorder chart but broken resistance–time curves were not recorded. T = 24 ± 1°, H_2-flow = 230 ± 10 cc./min. A curves for pure Pd wire; B curves for same Pd wire with one contact to Pt; C curves same Pd wire with about ten contacts to Pt (see text). The insets show curves on expanded time scale.

(5) Private communication; A. Fedorova and A. Frumkin, *Zhur. Fiz. Khim. U.S.S.R.*, to be published.

(6) R. J. Ratchford and G. W. Castellan, THIS JOURNAL, **62**, 1123 (1958).

MECHANISM OF THE ISOTHERMAL DECOMPOSITION OF POTASSIUM PERCHLORATE[1]

BY KURT H. STERN[2] AND MARIJON BUFALINI

Department of Chemistry, University of Arkansas, Fayetteville, Arkansas

Received June 13, 1960

Recently considerable evidence has been presented[3] that both the liquid and solid phase decomposition of $KClO_4$ proceeds according to the mechanism

$$KClO_4 \longrightarrow KClO_3 + {}^1/_2O_2 \quad (1)$$
$$KClO_3 \longrightarrow KCl + {}^3/_2O_2 \quad (2)$$
$$KClO_3 \longrightarrow {}^3/_4KClO_4 + {}^1/_4KCl \quad (3)$$

The first reaction is the slowest and activation energies and enthalpies suggest that the abstraction of atomic oxygen from the perchlorate ion is the rate-determining step. Exchange of Cl^{36} between $KClO_3$ and $KClO_4$ provides evidence for reaction (3). The mechanism is also consistent with the observation of Bosch and Aten[4] that no appreciable exchange of labelled chlorine occurs between chloride ion and either chlorate or perchlorate ions.

Glasner and Weidenfeld[5] have suggested that

(1) This work was supported by the United States Office of Scientific Research under contract AF49(638)-653.

(2) Electrochemistry Section, National Bureau of Standards, Washington 25, D. C.

(3) A. E. Harvey, C. J. Wassink, T. A. Rodgers and K. H. Stern, *Annals N. Y. Acad. Sci.*, **79**, 971 (1960).

(4) A. V. Bosch and A. H. W. Aten, *J. Am. Chem. Soc.*, **75**, 3835 (1953).

(5) A. Glasner and L. Weidenfeld, *J. Am. Chem. Soc.*, **74**, 2464, 2467 (1952).

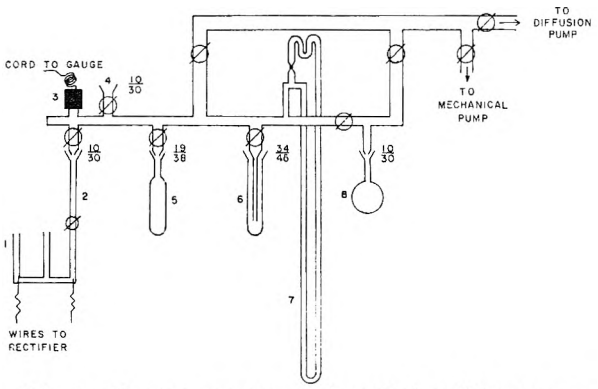

Fig. 1.—Vacuum system: 1, electrolysis cell for preparation of enriched O_2; 2, $CaCl_2$ drying tube; 3, vacuum thermocouple gauge; 4, flush gas inlet; 5, reaction vessel; 6, liquid air cold trap; 7, Hg manometer; 8, sample collector.

oxygen is involved in a reversible reaction, *e.g.*, $KCl + 4[O] \rightleftarrows KClO_4$. Our mechanism does not include such a step because we consider it unlikely on the basis of more recent results. However, no study of oxygen exchange in this system has yet been carried out. In this note we report a study of such an exchange.

Experimental

Apparatus.—The vacuum line used in the exchange experiments is shown in Fig. 1. An electrical multiple unit furnace was used to heat the $KClO_4$ sample. Furnace temperature was measured with a chromel–alumel thermocouple. All pressure readings were made with a Gaertner cathetometer.

Preparation of Enriched Oxygen.—Enriched oxygen was prepared by electrolysis of water which was 5.7% O^{18} and 0.45% O^{17}. Water vapor was removed by passing the gas through a $CaCl_2$ drying tube before it entered the vacuum system.

Purification of Flush Gas.—Argon was used as flush gas for the $KClO_4$ samples. It was dried by passage through two H_2SO_4 wash bottles and a $MgClO_4$ drying tube before entering the system. A mercury bottle open to air served as pressure valve.

Determination of O^{18} Taken up by the Reaction Mixture.—Approximately 1 g. of C.P. grade $KClO_4$ was put in the reaction vessel which then was connected to the vacuum system and evacuated to 0.3 μ. The preheated furnace was raised to the reaction vessel with a small scissor jack and the salt decomposed at 580–585° for about 40 minutes. The reaction next was stopped by lowering the furnace and a sample of the evolved oxygen taken for analysis (sample 1). The remaining oxygen was pumped out and the system flushed with argon three times. The reaction vessel was then isolated from the rest of the vacuum system and the oxygen enriched in O^{18} introduced into it. A sample of this gas, prepared by electrolysis, was taken for analysis (sample 2). The salt mixture ($KClO_4$, $KClO_3$, KCl) now was further decomposed for 5–15 minutes. After stopping the reaction again a further sample of oxygen was taken (sample 3). The remaining oxygen then was pumped out and the system flushed with argon. The remaining residue was decomposed completely at 580–585° and the resulting gas sampled (sample 4). The above experiment was repeated several times. The various samples were analyzed in a mass spectrometer. The results of two representative runs are shown in Table I.

Determination of O^{18} in $KClO_4$ and $KClO_3$.—An attempt was made to separate $KClO_4$ from $KClO_3$ after exchange had occurred and to measure the oxygen enrichment in each as a function of time. The experiment was carried out as above except that the reaction was stopped after the reaction mixture had been in contact with enriched oxygen for a certain period. The mixture then was dissolved in water and the perchlorate precipitated as tetraphenylarsonium perchlorate.[6] The filtrate, containing chlorate and chloride, then was dried (variously) with or without prior removal of the chloride. The perchlorate and chlorate fractions were both converted to CO_2 for mass spectrometric analysis by a procedure similar to that of Anbar and Gutman.[7] Neither fraction showed any enrichment when compared to normal CO_2. However, the accuracy of the method is rather low (0.02–0.05), the experimental error being as great as the enrichment found by direct determination of O^{18}.

(6) H. H. Willard and G. M. Smith, *Ind. Eng. Chem., Anal. Ed.*, **11**, 186, 269, 305 (1939).

TABLE I

Run	Sample	34/32	Atom % O^{18}	Enrichment[a]
3	1	0.0040	0.1996	0.0398
	2	.0870	4.1687	
	3	.0787	3.7860	
	4	.0048	0.2394	
4	1	.0040	0.1996	0.0597
	2	.0782	3.7629	
	3	.0572	2.7805	
	4	.0052	0.2593	

[a] Enrichment = % O^{18} (sample 4) − % O^{18} (sample 1).

Discussion

The results strongly suggest that oxygen exchange in this system, if it occurs at all, is rather small. Thus takeup of molecular oxygen by KCl is unlikely. These experiments do not entirely rule out the possibility that atomic oxygen first liberated in reaction 1 is then taken up by either KCl or $KClO_3$. However, since the recombination of oxygen atoms is quite rapid such takeup must either occur very rapidly or only to a slight extent. The slight enrichment observed may be used to account for the known formation of $KClO_4$ from decomposing $KClO_3$, *i.e.*, reaction 3 in the above mechanism should be replaced by the reverse of (1) which then gives for the mechanism

$$KClO_4 \rightleftarrows KClO_3 + {}^1/_2O_2 \quad (1)$$

$$KClO_3 \longrightarrow KCl + {}^3/_2O_2 \quad (2)$$

(7) M. Anbar and S. Gutman, *J. Appl. Rad. Isotopes*, **5**, 233 (1959).

CHELATES OF β-DIKETONES. IV. ACIDITY OF DIBENZOYLMETHANES

BY GEORGE S. HAMMOND, ALBRECHT W. MOSCHEL AND WILFRED G. BORDIUN

Gates and Crellin Laboratories of Chemistry (No. 2572), California Institute of Technology, Pasadena, Cal., from the Ames Laboratory of the Atomic Energy Commission and from the Chemical Laboratory of Iowa State University, Ames, Iowa

Received June 14, 1960

Determination of formation constants for metal chelates by the method of Bjerrum[1,3] requires accurate data for the ionization constants of the conjugate acids of the ligands. As part of a program for the systematic study of effects of ligand structure on chelate stability, we have measured the ionization constants of a number of *meta*- and *para*-substituted dibenzoylmethanes. Comparison of the results with dibenzoylmethane itself to those reported by Van Uitert, *et al.*,[4] showed a significant disagreement. For this reason, the measurements

(1) J. Bjerrum, "Metal Amine Formation in Aqueous Solution," P. Haase and Sons, Copenhagen, 1941.

(2) M. Calvin and K. Wilson, *J. Am. Chem. Soc.*, **67**, 2003 (1945).

(3) A. E. Martell and M. Calvin, "The Metal Chelate Compounds," Prentice–Hall, Inc., New York, N. Y., 1952, p. 87.

(4) L. G. Van Uitert, C. G. Haas, W. C. Fernelius and B. E. Douglas, *J. Am. Chem. Soc.*, **75**, 455 (1953).

with dibenzoylmethane were repeated independently and very carefully.

Results and Discussion

Data for the ionization constants of dibenzoylmethane are summarized in Table I. The two series of measurements, indicated as series A and B, were carried out by different workers in different laboratories after an interval of eight years. Essentially the same results are obtained with either tetramethylammonium bromide or potassium perchlorate as the leveling electrolyte. The results are obtained directly in terms of concentration quotients, Q_A, and were measured at higher electrolyte concentrations than was the case with the measurements made at Penn State.[4] Comparison of the results can be made by using our data to estimate the thermodynamic ionization constants as was done by Van Uitert and co-workers. The mean ionic-activity coefficient for 0.05 N HCl in 75% dioxane–water[5] is estimated by interpolation to be 0.168; therefore, addition of 1.55 to the $-\log Q_A$ values in Table I should give pK_A if the method of extrapolation is valid. Application of the correction gives a value of 13.06 for pK_A; this should be compared to the value of 13.76 calculated from the equation reported by the earlier workers.[4] The method of extrapolation was applied to data reported earlier[6] for acetylacetone and gave a value of pK_A, which agrees very well with that reported[4] by the group at Pennsylvania State University. We do not understand the source of this discrepancy. It may be that the validity of the extrapolation is not equally good for dibenzoylmethane and for acetylacetone. Van Uitert, *et al.*,[4] observed that the apparent values of pK_D for diketones were different when measured in the presence of sodium chloride and quaternary ammonium iodides. The difference was reasonably attributed to binding of diacylmethide ions by sodium ions and it was found that classical association constants for sodium chelates could be evaluated. The effects were much larger with diaroylmethides than with acetylacetonate. The "inert" electrolytes used in our study were tetramethylammonium bromide and potassium perchlorate. Neither of these would be expected to give trouble because of chelate formation; it is clear that ion-pair formation not involving the enolate ions would affect data for dibenzoylmethide and acetylacetonate in a similar manner. However, it is still possible that the activity coefficients of diacylmethide ions are subject to anomalous electrolyte effects of a less specific nature than is implied by the chelation model. It is interesting that the fairly large difference between our estimated value of pK_A and that of Van Uitert is still smaller than the differences between measurements made by the latter in the presence of two different electrolytes. We have not investigated the matter further as our principal objective was to obtain a consistent set of data for use in the measurement of substituent effects on the acidity of dibenzoylmethanes.

(5) H. S. Harned and B. B. Owen, "The Physical Chemistry of Electrolyte Solutions," Reinhold Publ. Corp., New York, N. Y., 1943, p. 581.

(6) G. S. Hammond, W. G. Bordiun and G. A. Guter, *J. Am. Chem. Soc.*, **81**, 4682 (1959).

TABLE I

ACIDITY CONSTANT OF DIBENZOYLMETHANE IN 75% BY VOLUME DIOXANE AT 25°

Expt. no.	Series	Inert electrolyte[a]	$-\log Q_A$[b]
1	A	Me_4NBr	11.49
2	A	$KClO_4$	11.51
3	B	$KClO_4$	11.53
4	B	$KClO_4$	11.54
5	B	$KClO_4$	11.51
6	B	$KClO_4$	11.50
7	B	$KClO_4$	11.50
8	B	$KClO_4$	11.50
		Av.	11.51

[a] Total ionic strength in half-neutralized solution is 0.050. [b] $Q_A = [H^+][A^-]/[HA]$.

Further indication of probable accuracy of our measurements is obtained by comparison of the data, reported in Table II, for the ionization constants of a series of substituted benzoic acids in 75% dioxane. Using a potentiometric method, Elliott and Kilpatrick[7] measured the ionization constants of a series of benzoic acids in a very similar medium, 73.5% by weight dioxane at an ionic strength of 0.05. Their values for $-\log Q_A$ are included in Table II for purposes of comparison to ours. It is obvious that the agreement is excellent, essentially precluding the possibility that there is a repeating error in our method. Specifically the agreement indicates that, barring some remarkable coincidences, our values for the ion-product characterizing autoprotolysis in the medium must be quite accurate.

TABLE II

ACIDITY CONSTANTS OF DIAROYLMETHANES AND BENZOIC ACIDS IN 75% BY VOLUME DIOXANE–WATER AT 25°

X	$-\log Q_A$[a] $(XC_6H_4CO)_2CH_2$	$-\log Q_A$[a] $XC_6H_4CO_2H$ (this study)	$-\log Q_A$[b] $XC_6H_4CO_2H$ (ref. 7)
p-OCH_3	12.31	7.36	7.39
p-CH_3	12.12	7.32	7.25
m-CH_3	11.55	7.22	7.17
H	11.51	7.02	7.04
m-OCH_3	11.43	6.98	..
p-Cl	10.80	6.67	6.64
m-Br	10.62	6.60	6.50
p-$CH_3OC_6H_4COCH_2COC_6H_5$	12.11		

[a] Ionic strength in half-neutralized solution is 0.050. [b] Measured in 73.5% by weight dioxane.

Data for the acidity constants of dibenzoylmethane and its derivatives, the principal objective in this research, are listed in Table II. The data are reported in terms of Q_A, the concentration quotient at ionic strength of 0.05. Approximate values of pK_A may be obtained by adding 1.55 to the values of $-\log Q_A$.

Discussion

The values of $-\log Q_A$ for the diketones fit the Hammett equation[8] with no more than the usual scattering of points. Figure 1 is a Hammett

(7) J. H. Elliott and M. Kilpatrick, *J. Chem. Phys.*, **45**, 454 (1941).

(8) L. P. Hammett, "Physical Organic Chemistry," McGraw-Hill Book Co., New York, N. Y., 1940, p. 184.

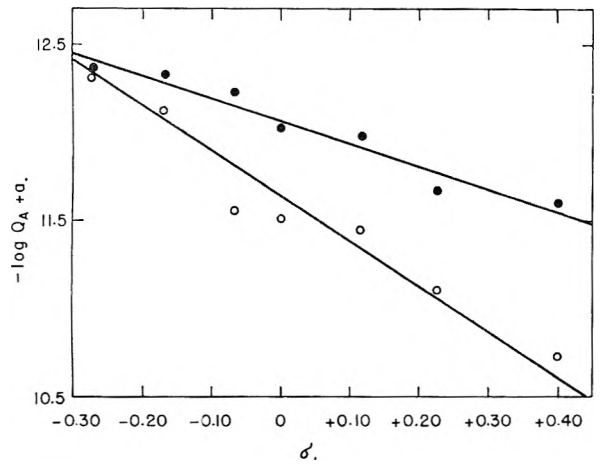

Fig. 1.—Hammett plots of ionization constants of dibenzoylmethanes and benzoic acids in 75% dioxane–water at 25°: dibenzoylmethanes, O—O—O, a = 0.00; benzoic acids, ●—●—●, a = 5.00.

plot of the data, and the values for the ionization of the corresponding benzoic acids are also plotted for purpose of comparison. The value of ρ for ionization of the diaroylmethanes is 2.63 (r = 0.33) and that for the benzoic acids is 1.28 (r = 0.15). Since the diketones are each symmetrically di-substituted, the effect *per substituent* is the same for the two reactions with a precision better than those of the fits to the Hammett equation. The implication is that interactions between the substituents and the functional groups are similar in the two series of compounds. This, in turn, implies that internal interactions within the functional groups are probably much more important than are conjugated interactions with the adjacent benzene rings. If the effects of substituents in the diketones were cumulative, one would expect that a single substituent would have half the effect of two. Actually, a single *p*-methoxy group decreases the acidity constant by 0.62 log unit and a second methoxy group gives an additional decrease of only 0.20 unit. Mecke and Funk[9] have analyzed the infrared spectrum of the enol of acetylacetone and have concluded that the compound is symmetrical. This is a view with which we have agreed, but present data suggest that *p*-methoxydibenzoylmethane is stabilized to some extent by interactions such as those shown in I. This may induce significant asymmetry in the C–O bonds and in the position of the bridge hydrogen.

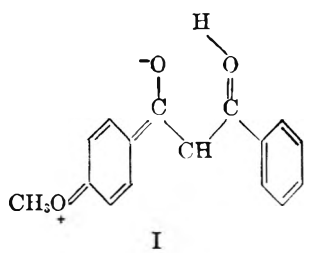

I

Experimental

Materials.—Preparation and purification of the diaroylmethanes were described earlier.[6] A new sample of dibenzoylmethane was used and purified for the measurements listed as series B in Table I. Other materials and solutions were prepared as described earlier.[6] During series B measurements the usual troubles with dioxane, due to development of acidity by oxidation, were experienced even though the solutions were protected rather carefully by a nitrogen atmosphere at all times. The solvent was repurified and the solutions were made up freshly several times during the study.

Procedures.—The measurements have been described in detail previously.[4,6] In series B the *p*H-meter calibration and estimation of the ion product of the medium by titration of perchloric acid with potassium hydroxide were repeated before every determination of the acidity of dibenzoylmethane. Values of U_H in the equation $-\log [H^+]$ = meter reading + $\log U_H$ varied slightly from one series of experiments to another, despite the fact that the electrodes were carefully conditioned and that the meter was always set to read *p*H 7.00 in the appropriate, standard Beckman buffer. Small variations also were noted in the apparent values of $-\log [H^+][OH^-]$: The average value from six runs was 16.77 ± 0.16. The apparent values for the individual runs were used in calculating the values of $-\log Q_A$ reported in Table I, and the values reported in Table II were calculated using a single, average value of 16.9 obtained by a series of calibration measurements in the early phase of the study.

Acknowledgment.—The later part of this study was supported by a grant from the Film Department of the du Pont Company.

(9) R. Mecke and E. Funk, *Z. Elektrochem.*, **60**, 1124 (1956).

THE REACTION BETWEEN $B_2O_3(l)$ AND C(s): HEAT OF FORMATION OF $B_2O_2(g)$*

BY PETER RENTZEPIS, DAVID WHITE AND PATRICK N. WALSH

Cryogenic Laboratory, Department of Chemistry, The Ohio State University, Columbus 10, Ohio

Received June 15, 1960

During the past few years it has been demonstrated that, under reducing conditions, boron suboxide, B_2O_2, is an important species in the vapor in the B–O system. Inghram, *et al.*,[1] and Scheer[2] identified the species and measured its partial pressure in the system B(s) + $B_2O_3(l)$, the former by mass spectrometric and the latter by torsion effusion techniques. Searcy and Myers[3] measured the effusion of B_2O_2 and Mg vapors from a mixture of MgO and B at elevated temperature. Evans, *et al.*,[4] in a review of the properties of B–O–H vapor species, concluded that the results of these three investigations lead to the following values of the heat of formation (ΔH_0^0 (f)) of $B_2O_2(g)$, −103.6 ± 5, −109.6 ± 6 and −105 ± 5 kcal./mole, respectively. From the above figures a "best" value of −105 ± 5 kcal./mole was chosen.

Scheer[2] has suggested that the attainment of equilibrium in the reaction of $B_2O_3(l)$ with B(s) in his experiments and those of Inghram, *et al.*, might have been impeded by the formation of a condensed polymer $(BO)_x$, with the result that the observed pressures of B_2O_2 may be lower than the true equilibrium pressures. Similarly, Searcy and Myers[3] suggest that poor contact between their solid react-

* This work was supported by the Office of Naval Research, Washington, D. C.

(1) M. G. Inghram, R. F. Porter and W. A. Chupka, *J. Chem. Phys.*, **25**, 498 (1956).

(2) M. D. Scheer, THIS JOURNAL, **62**, 490 (1958).

(3) A. W. Searcy and C. E. Myers, *ibid.*, **61**, 957 (1957).

(4) W. H. Evans, E. J. Prosen and D. D. Wagman in "Thermodynamic and Transport Properties of Gases, Liquids, and Solids," Y. S. Touloukian (Editor), McGraw-Hill Book Co., New York, N. Y., 1959.

ants may have resulted in a lowering of the partial pressures of the gaseous products. Hence, all the above investigations may have led to an upper limit for the heat of formation of $B_2O_2(g)$.

In order to avoid some of the difficulties mentioned above, and establish possibly a lower limit for the heat of formation of $B_2O_2(g)$, the reaction of $B_2O_3(l)$ with carbon has been studied.

B_2O_3–C Reaction.—Consider the vaporization of $B_2O_3(l)$, to which carbon has been added, from a carbon Knudsen cell, in the temperature range 1350-1650°K. Only two reactions are of importance[5]

$$B_2O_3(l) + 3C(s) \longrightarrow 3CO(g) + 2B(s) \quad (1)$$
$$B_2O_3(l) + C(s) \longrightarrow B_2O_2(g) + CO(g) \quad (2)$$

At the lowest temperatures, assuming a reasonable value for the heat of formation of $B_2O_2(g)$, reaction 1 should predominate. As the equilibrium constant for this reaction can be calculated from available thermodynamic data, one can determine, (a) under what conditions equilibrium can be established in the Knudsen cell, and (b) whether any new condensed phases (say $(BO)_x$), which would appreciably affect the equilibrium pressure of CO, are formed. If the reaction then is studied at higher temperatures, where reaction 2 cannot be neglected, it can be shown that

$$RT \ln (P_{CO}/P_{B_2O_2}) = \Delta F^0_f(B_2O_2(g)) - \Delta F^0_f(CO(g)) - 1/3\Delta F^0_f(B_2O_3(l)) \quad (3)$$

where ΔF^0_f represents the standard free energy of formation at temperature T. The heat of formation of $B_2O_2(g)$ thus can be obtained from the ratio of pressures, using the appropriate thermodynamic data.

Experimental

The effusion experiments were performed in an apparatus similar to that described by Skinner, Edwards and Johnston[6] with a demountable silica gel trap cooled to 77°K. in the vacuum line when CO samples were collected. For rate of effusion measurements, the system was pumped continuously and no absorbent was used in the trap. The temperature in the induction-heated cells was measured by sighting through the effusion orifice with a calibrated Leeds and Northrup optical pyrometer.

The boric oxide was prepared by vacuum dehydration, at approximately 1100°, of reagent grade Matheson, Coleman and Bell boric acid. The graphite effusion cells and lids, and the graphite particles placed in the cell, were made from material of spectroscopic purity obtained from the National Carbon Company. The graphite was thoroughly degassed at 2000° *in vacuo* before being used in any of the experiments.

The effusion cells were short cylinders, with internal diameter approximately 0.3 cm. and height approximately 1.1 cm. The orifice was drilled axially through the tight-fitting lid. When the ratio of orifice area to area of the evaporating surface was greater than 0.008, it was found that the CO pressures (calculated by the method of Motzfeldt[7]) were not independent of the orifice area, but decreased with increasing area. This probably came from a reduction in the effective area of the evaporating surface caused by floating graphite particles. The results in Table I and II were obtained using orifice-to-cell area ratios of about 0.005. The diameter of the orifice was, on the average, approximately 0.02 cm. and its length approximately 0.04 cm.

Results

It was found that, at temperatures below 1550° K., only very small quantities of $B_2O_2(g)$ were evolved from the effusion cell for any appreciable rate of weight loss (5–20 mg./hr.). This was readily detectable because B_2O_2 condenses to a deep brown amorphous solid on the cold walls of the condenser. Within experimental error, therefore, the only gas effusing from the cell below 1550°K. is CO, and reaction 1 is predominant. In Table I, the observed CO pressures are compared with those calculated for this reaction. The free energy functions used in the calculations were taken from these several sources: B(s) and C(s), the compilation of Stull and Sinke[8]; $B_2O_3(l)$, reference 4; CO(g), free energy of formation[9] combined with free energy functions of C(s) and $O_2(g)$.[8]

TABLE I

COMPARISON OF EXPERIMENTAL AND CALCULATED CO PRESSURES FOR REACTION $B_2O_3(l) + 3C(s) \rightarrow 3CO(g) + 2B(s)$

T, °K.	P_{CO}, atm. × 10^3, exptl.	ΔF^0, kcal. calcd.	P_{CO}, atm. × 10^3, calcd.
1376	1.03	58.1	0.836
1389	1.08	57.5	0.964
1468	5.24	48.7	3.82
1473	3.81	48.2	4.12
1476	8.60	47.8	4.36
1525	23.9	42.4	9.43
1563	41.4	38.1	16.8
1593	71.1	34.9	25.4
1603	73.4	33.8	29.0

It is evident from Table I that there is good agreement between the experimental and calculated CO pressures at the lower temperatures. At higher temperatures, the apparent divergence probably arises from the fact that the equation for molecular flow[7] used in calculating the pressure is no longer applicable. The magnitude of the error arising from viscous flow in these experiments can be approximated from the relationship between a/L and F/F_t tabulated by Dushman.[10] If F is the actual flow through the orifice, F_t, the calculated molecular flow, a, the orifice radius and L, the mean free path at the average pressure across the orifice, then for $a/L = 1.0$, which corresponds approximately to the case when the CO pressure is 5×10^{-3} atm., $F/F_t = 1.00$. For $a/L = 10$ (CO pressure approximately 5×10^{-2} atm.), $F/F_t = 2.29$. Considering the approximations involved in the Dushman table and the uncertainties inherent in Knudsen effusion studies, the experimental data appear consistent over the entire temperature range. It is therefore concluded that no significant lowering of the activity of $B_2O_3(l)$ takes place.

It is only at temperatures in excess of 1600°K. that the vapor contains enough B_2O_2 to permit a reliable determination of the ratio of the partial pressure of CO to that of B_2O_2. It is evident from the foregoing discussion, however, that the classical

(5) $B_2O_2(g)$ comprises a maximum of 10% of the boron-containing species in the vapor at any temperature. X-Ray analysis of the solid phase disclosed no B_4C or B–C solid solution. Even if these were present, their free energies of formation are so small that they would have a negligible effect on the observed pressures.

(6) G. B. Skinner, J. W. Edwards and H. L. Johnston, *J. Am. Chem. Soc.*, **73**, 174 (1951).

(7) K. Motzfeldt, THIS JOURNAL **59**, 139 (1955).

(8) D. R. Stull and G. C. Sinke, "Thermodynamic Properties of the Elements," American Chemical Society, Washington, D. C., 1956.

(9) J. P. Coughlin, *Bur. Mines Bull.*, 542 (1954).

(10) S. Dushman, "Vacuum Technique," John Wiley and Sons, Inc., New York, N. Y., 1949, p. 114.

TABLE II

HEAT OF FORMATION OF $B_2O_2(g)$

T, °K.	Initial B_2O_3, mmoles	Total CO evolved, mmoles	Total B_2O_2 evolved, mmoles	Total wt. loss, mg. exptl.	Total wt. loss, mg. calcd.	$P_{CO}/P_{B_2O_2}$	$\Delta H_0^{0f}(B_2O_2)$, kcal./mole
1603	1.763	5.14	0.075	148.0	148.3	69	−110.6
1616	2.868	8.41	.095	240.6	241.3	89	−109.6
1626	2.191	6.40	.085	183.9	184.2	75	−110.1
1651	5.270	15.19	.31	442.0	441.7	49	−111.3
1656	3.471	9.86	.27	290.8	290.6	37	−112.1
						Av.	−110.7 ± 1.5

Knudsen technique cannot be applied under these conditions; a different technique therefore was employed. A known weight of $B_2O_3(l)$ was introduced into the cell, along with some graphite particles, and the reaction allowed to go to completion at a constant temperature. The CO evolved was collected on a silica gel bed which previously had been cycled with CO. The amount of CO was determined by desorption into calibrated volumes. On the assumption that only reactions 1 and 2 were involved in the depletion of the B_2O_3, the amount of B_2O_2 evolved was computed.

The experimental data and the derived heat of formation of $B_2O_2(g)$ are given in Table II. From a comparison of columns 5 and 6, it would appear that the assumption that reactions 1 and 2 are predominant in the depletion of the liquid boric oxide is justified. The ratio of $P_{CO}/P_{B_2O_2}$ was calculated from columns 3 and 4 assuming viscous flow. In calculating the heat of formation, the thermal functions cited above were used for $B_2O_3(l)$, B(s), C(s) and CO(g). For $B_2O_2(g)$, those reported by White, *et al.*, were employed.[11]

Discussion

From the nature of the experiment, it is felt that the heat of formation of gaseous B_2O_2 given in the last column of Table II probably represents a lower limit. The experimental uncertainties are unquestionably large in this type of determination, because of the large $P_{CO}/P_{B_2O_2}$ ratios and the small quantities of B_2O_2 evolved. The lower limit is suggested because the largest uncertainties arise from (a) the extent of incomplete desorption of the CO, which is estimated as 0.002 mmole, and (b) the presence of B_2O_3 in the vapor, which, though small, may appreciably diminish the $P_{CO}/P_{B_2O_2}$ ratio.

In order that a comparison of this work with that of the previous investigators be meaningful, it is essential that the same values for the thermal functions of each of the species should be used throughout. The heat of formation of $B_2O_2(g)$ has therefore been recomputed from the experimental data of references 1, 2 and 3.

The free energies of reaction 4 reported by Inghram, Porter and Chupka[1] have been used in conjunction with the thermodynamic data listed to calculate ΔH_0^0 of formation of $B_2O_2(g)$. Free energy functions of the vapor species were taken from White, *et al.*,[11] while the compilation of Stull and Sinke was used for boron. Together with the heat of formation of $B_2O_3(g)$, $\Delta H_0^0 = -209.5 \pm 2$ kcal./mole,[12] the data yield $\Delta H^0(f) = -111.6 \pm 3$ kcal./mole for $B_2O_2(g)$.

$$2/3B_2O_3(g) + 2/3B(s) \longrightarrow B_2O_2(g) \qquad (4)$$

Scheer[2] studied reaction 5

$$2/3B_2O_3(l) + 2/3B(s) \longrightarrow B_2O_2(g) \qquad (5)$$

by the torsion effusion method. The slope of a Clausius–Clapeyron plot of his data yields −108.2 kcal./mole for $\Delta H_0^0(f)$ of $B_2O_2(g)$ while applications of the third law, using free energy functions already discussed, give a value of −112.7 ± 4 kcal./mole. Despite a small but definite variation of the "third law" heat with temperature, the latter value is probably more reliable. It is interesting to note the good agreement between the two sets of investigators, despite the factor of 6 to 8 difference in their reported pressures at a given temperature. The probable explanation is that the mass spectrometric technique[1] gives better relative than absolute pressures.

Searcy and Myers[3] studied the reaction

$$2MgO(s) + 2B(s) \longrightarrow 2Mg(g) + B_2O_2(g) \qquad (6)$$

by conventional Knudsen effusion procedures. Their reported pressures, which are not in accord with the stoichiometry of reaction 6 corrected for differences in rates of flow of the two vapor species, have been recomputed. The thermodynamic properties of B(s) and $B_2O_2(g)$ were taken from the sources previously cited; those of Mg(g) were derived from Stull and Sinke.[8] The free energy functions of MgO were calculated from the high temperature heat content data of Victor and Douglas.[16] These differ little from those computed using Coughlin's table.[9] The average of all experimental points yields −105.7 ± 5 kcal./mole for the heat of formation of $B_2O_2(g)$. The authors, however, point out[3] that poor contact between the solid reactants may be responsible for the rather large average deviation of their heats, and suggest that the single determination carried out with a compacted sample and very small effusion orifice probably represents a more reliable value than the average. From this point, we calculate a heat of formation of $B_2O_2(g)$ of −111.9 kcal./mole at 0°K.

(11) D. White, D. E. Mann, P. N. Walsh and A. Sommer, *J. Chem. Phys.* **32**, 481 (1960).

(12) Computed as follows: The vapor pressure data[13,14] yield 94.4 ± 2 kcal./mole for the heat of sublimation of crystalline B_2O_3 at 0°K. when the free energy functions of ref. 11 are used for $B_2O_3(g)$. This value was combined with $\Delta H_0^0(f)$ of crystalline B_2O_3[15] to obtain $\Delta H_0^0(f)$ of $B_2O_3(g)$.

(13) R. Speiser, S. Naiditch and H. L. Johnston, *J. Am. Chem. Soc.*, **72**, 2578 (1950).

(14) (a) M. D. Scheer, THIS JOURNAL, **61**, 1184 (1957); (b) J. R. Soulen, P. Sthapitanonda and J. L. Margrave, *ibid.*, **59**, 132 (1955).

(15) E. J. Prosen, W. H. Johnson and F. Y. Pergiel, *J. Research, Natl. Bur. Standards*, **62**, 43 (1959).

(16) Unpublished data by A. C. Victor and T. B. Douglas.

It is evident that all the values, some of which should be lower and some upper limits, agree within experimental error. This strongly indicates that the average, *viz.*, -111.7 ± 2 kcal./mole, is a reliable value for the heat of formation of $B_2O_2(g)$ at 0°K.

THERMOCHEMISTRY OF SULFUR TETRAFLUORIDE

By J. D. Vaughn and E. L. Muetterties

Contribution No. 537 from the Central Research Department Experimental Station, E. I. du Pont de Nemours and Company, Wilmington, Delaware

Received June 28, 1960

Sulfur tetrafluoride is strikingly reactive in comparison to sulfur hexafluoride and we have sought a comparison of their thermochemical properties. Yost and Claussen[1] have determined the heat of formation of SF_6 by direct reaction of sulfur and fluorine, but nothing has been reported on the heat of formation of SF_4. In the investigation described herein, the heat of formation of SF_4 was estimated calorimetrically by use of the hydrogenation of SF_4

$$SF_4(g) + 2H_2(g) \longrightarrow 4HF(l) + S(s)$$
$$SF_4(g) + 3H_2(g) \longrightarrow 4HF(l) + H_2S(g)$$

Only the former reaction occurred with SF_4 in stoichiometric excess, but both occurred with H_2 in excess.

Experimental

Purity of Sulfur Tetrafluoride.—SF_4 was passed through an oxy-hydrogen flame and then fluorine was determined by thorium nitrate titration of fluoride ion and sulfur by precipitation as barium sulfate. The results of two analyses are given in Table I.

Table I

Chemical Analysis of SF_4

Sample	S, %	F, %	% S + % F
1	31.06	69.32	100.38
2	30.82	69.71	100.53
Theoretical	29.60	70.40	100.00

Mass spectrophotometric analysis gave the following results: 95.6% SF_4, 3.8% SOF_2, 0.3% SiF_4, 0.2% CS_2, and 0.2% N_2. Preconditioning of the mass spectrometer led to higher values (>98%) for the SF_4 content. The presence of SOF_2 was assumed to be due to hydrolysis within the mass spectrometer in view of the implied absence of other elemental species in the chemical analyses.

Calorimeter.—A Parr double-valve isothermal oxygen bomb calorimeter was adapted for the hydrogenation reaction by replacement of the rubber sealing ring and the mica electrode insulator with "Teflon." A hot platinum wire was used for initiation of the calorimeter reaction both for the calibration combustion and the hydrogenation of SF_4. The calorimeter was calibrated by combustion of benzoic acid; thirteen such combustions gave an average calorimeter heat capacity of 2488 cal./deg.

General Procedure.—The bomb was flushed several times with hydrogen before SF_4 was added under pressure. In three of the experiments, SF_4 was added in excess, and in three others, H_2 was added in excess. At completion of the calorimeter reaction, 2.5 *M* NaOH was added to the calorimeter bomb contents under external hydrogen pressure. Excess unreacted SF_4 was determined as the hydrolysis product, sulfite ion, by titration with standard iodine solution. H_2S was determined by addition of excess iodine solution and back-titration with standard thiosulfate solution. HF was analyzed by thorium nitrate titration of fluoride ion. It was necessary to determine sulfite at various time intervals because of the slow autoöxidation to sulfate; the initial $SO_3^=$ was taken as that found by extrapolation of the observed linear relation to zero time of exposure of the bomb contents to air. Sulfur was determined indirectly from the HF, $SO_3^=$ and/or H_2S values; preliminary experiments showed that the weighed quantity of free sulfur was in good agreement with the amount expected from the weighed initial quantities of SF_4 and H_2.

Results and Discussion

The heat effects accompanying the bomb reaction included the heat of hydrogenation of SF_4, the heat of condensation of the product HF, and the heat of formation of H_2S (when H_2 was in excess). To compute the heat of condensation of HF, the extent of condensation was estimated. The saturation vapor pressure of liquid HF at 298°K. is 908 mm.,[2] corresponding to an average molecular weight of 60.6 g.; the vapor density of HF under these conditions is given by $d = MP/RT = 0.00295$ g./ml. The weight of HF in the gaseous state in the bomb of 360 ml. is, therefore, 1.062 g., and the fraction of HF that becomes liquid $(1 - 1.062/W)$, where W is the total weight of HF found in the bomb at the completion of the hydrogenation. The heat evolved due to condensation is given by the product of the fraction of liquid HF and the heat of condensation per gram HF.[3]

The heat of formation of HF of molecular weight 60.6 g. was required for computation of the heat of hydrogenation of SF_4. Simons and Hildebrand[2] indicated that the apparent molecular weight is due to incomplete polymerization of HF to the hexamer $(HF)_6$. Long, Hildebrand and Morrell[4] gave the heat of polymerization of HF as -6800 cal./20 g. A molecular weight of 60.6 corresponds to 50.5% polymerization, such that the heat evolved because of polymerization at 298°K. is -3434 cal. The heat of formation of HF under the experimental conditions then equals the heat of formation of monomer plus the heat evolved in polymerization, that is, -67.6 kcal./20 g. The heat of formation of HF monomer, as well as the heat of formation of H_2S, were taken from the National Bureau of Standards Circular 500.[3]

The experimental results are summarized in Table II. Consideration was given to the following uncertainties: solubility of H_2, H_2S and SF_4 in condensed HF, polymerization of HF in the vapor phase, the effect of final reaction temperature other than 298°K., calibration error, extent of autoöxidation of $SO_3^=$ to $SO_4^=$, and purity of SF_4. First approximation estimates of these uncertainties indicated them to be smaller than the average deviation from the mean value of the standard heat of formation of SF_4. Because of the difficulty of precise estimation of these uncertainties, and the uncertainties arising from the extreme nonideal behavior of HF in vapor condensed phases, the over-all uncertainty is taken as the sum of the average deviation from the mean (2.3 kcal./mole) and the calibration error (0.3 kcal./mole).

(1) D. M. Yost and W. H. Claussen, *J. Am. Chem. Soc.*, **55**, 885 (1933).

(2) J. H. Simons and J. H. Hildebrand, *ibid.*, **46**, 2185 (1924).

(3) N.B.S. Circular 500, Washington, D. C., 1952.

(4) R. W. Long, J. H. Hildebrand and W. E. Morrell, *J. Am. Chem. Soc.*, **66**, 182 (1943).

TABLE II

RESULTS OF CALORIMETER EXPERIMENTS

	Experiment 1	2	3	4	5	6
Initial SF_4 (mmoles)	102	104.1	96.8	73.4	68.2	82.1
Initial H_2 (mmoles)	~150	~90	~150	~150	~150	~150
Initial T (°C.)	24.7	24.5	22.2	24.3	23.5	23.7
HF (mmoles)	417.7	421.7	385.3	306.6	288.4	328.7
$SO_3^=$ (mmoles) (from SF_4)	10.33	14.3	3.7	0	0	0
$S^=$ (mmoles) (from H_2S)	0	0	0	35.42	22.98	23.58
HF from hydrogenation of SF_4	376.5	364.5	370.5	306.6	288.4	328.7
HF from alkaline hydrolysis of SF_4	41.2	57.2	14.8	0	0	0
Obsd. temp. rise (°C.)	3.734	3.614	3.972	3.152	2.978	3.396
Final T (°C.)	28.4	28.1	26.0	27.5	26.5	27.1
Heat evolved (cal.)	−9239	−8896	−9742	−7737	−7334	−8468
Heat of reaction per mole SF_4	−98.18	−97.62	−105.2	−100.9	−101.7	−103.0
$-\Delta H^\circ SF_4$ (kcal./mole)	173.8	174.4	166.8	173.2	171.8	170.4

Mean stand. heat of formation of SF_4 = −171.7 ± 2.5.

The mean S–F bond energy[5] was calculated to be ~78 kcal./mole in SF_4 and ~72 kcal./mole in SF_6. These nearly identical bond energies support the thesis that kinetic factors and not energetic factors are responsible for the inert character of SF_6 in comparison to the high reactivity of SF_4.

(5) A value of 37 kcal./mole was used for the heat of dissociation of F_2.

ELECTRIC MOMENTS AND ROTATIONAL CONFORMATIONS OF HALOGENATED PROPANES AND RELATED COMPOUNDS[1]

BY H. BRADFORD THOMPSON AND CRAIG W. LAWSON

Department of Chemistry, Gustavus Adolphus College, St. Peter, Minnesota

Received June 20, 1960

The very small electric moments of the pentaerythrityl halides, $C(CH_2X)_4$, have been explained on the basis of threefold barriers to internal rotations, plus steric exclusion of certain rotational isomers (rotomers).[2] Specifically, in a structure such as 1,3-dichloropropane, rotomers in which the two C–Cl bonds would be parallel would bring the chlorine nuclei to within 2.51 Å., while the sum of the non-bonded (van der Waals) radii should be about 3.6 Å. Accordingly, these rotomers may be disregarded. In many small molecules it may be shown that the remaining rotomers would have the same electric moment, so that the observed moment may be predicted readily. It is our purpose here to report further tests of this model.

Experimental

Electric moments were calculated by the procedure of Halverstadt and Kumler.[3] Apparatus and method have been described previously.[2] Results are reported in Tables I and II.

The bromides were prepared from PBr_3 and the appropriate alcohols by published procedures.[4] 1,3-Dibromo-2,2-dimethylpropane was fractionated twice: b.p. 89° at 29–30 mm., 52° at 5 mm., $n^{25}D$ 1.5000, d^{25}_4 1.6631. 1,3-Dibromo-2-bromoethyl-2-methylpropane was also fractionated twice: b.p. 105.5° at 5 mm., $n^{25}D$ 1.5562, n^{25}_4 2.0870.

1,1,1,3-Tetrachloropropane, obtained in about 20% yield as by-product in a previous synthesis of 1,1,3,3-tetrachloropropane,[2] was again fractionated: b.p. 54.6–54.8° at 20 mm., $n^{25}D$ 1.4790, d^{25}_4 1.4463. 1,3-Dichloropropane was fractionated twice at 740 mm. pressure: b.p. 119.2–119.6°, $n^{20}D$ 1.4488, d^{20}_4 1.1794.

Discussion

The brominated neopentanes both have moments much more in accord with our model than with the assumption of free rotation. Our moment for 1,3-dibromo-2-bromomethyl-2-methylpropane differs somewhat from that of Gur'yanova, 1.83 *D*.[5] The latter value is, however, in even better accord with our model.

TABLE I

EMPIRICAL CONSTANTS FOR CALCULATION OF ELECTRIC MOMENTS[a] (BENZENE SOLUTION, 25°)

Compound	ϵ_1	α	ν_1	β
$CMe_2(CH_2Br)_2$	2.2745	2.60	1.1447	−0.561
$CMe(CH_2Br)_3$	2.2740	1.58	1.1438	− .685
$CCl_3CH_2CH_2Cl$	2.2745	1.03	1.1445	− .571
$CH_2(CH_2Cl)_2$	2.2750	4.13	1.1444	− .310

[a] Symbols are as defined by Halverstadt and Kumler.[2] α and β are weight fraction coefficients.

TABLE II

MOLAR REFRACTIONS AND POLARIZATIONS AND ELECTRIC MOMENTS

Compound	P_{20}	MR_D	Electric moments: Obsd.	Our model	Free rotation
$CMe_2(CH_2Br)_2$	152.4	40.67	2.34	2.23	2.67
$CMe(CH_2Br)_3$	133.9	47.58	2.05	1.93	3.22
$CCl_3CH_2CH_2Cl$	66.3	35.66	1.22	0.40	2.45
$CH_2(CH_2Cl)_2$	115.8	25.86	2.10	2.27	2.73

1,3-Dichloropropane exists as a mixture of rotomers each of which should have a moment 1.155 times that associated with each C–Cl bond. A group moment of 1.8 *D*, as suggested by Smyth,[6] rather than the 1.97 *D* we have used,[2] would lead to the observed value. The excluded rotomer

(1) Presented in part before the Division of Physical Chemistry at the 137th meeting of the American Chemical Society, Cleveland, Ohio, April, 1960.

(2) H. B. Thompson and C. C. Sweeney, THIS JOURNAL, **64**, 211 (1960).

(3) I. F. Halverstadt and W. D. Kumler, *J. Am. Chem. Soc.*, **64**, 2988 (1942).

(4) H. B. Schurink, *Org. Syntheses*, **17**, 73 (1937).

(5) E. N. Gur'yanova, *Zhur. Fiz. Khim.*, **24**, 470 (1950); *C. A.*, **44**, 8181 (1950).

(6) C. P. Smyth, "Dielectric Behavior and Structure," McGraw-Hill Book Co., Inc., New York, N. Y., 1955, p. 253.

would have a much higher moment, twice that for each C–Cl. That this makes no contribution to the observed moment is, of course, in accord with the observation of Smyth and McAlpine,[7] that the vapor-phase electric moment of this compound is temperature-independent.

The predicted moment for 1,1,1,3-tetrachloropropane was obtained by subtracting the moment for 1,1,1-trichloroethane,[8] 1.57 *D*, from that for the single C–Cl bond. The moment of the $-CCl_3$ group is assumed to lie along the C–C bond. In the only non-excluded rotomer the two group moments are opposed.

The observed moment in this case is significantly larger than that predicted. The explanation here is probably the same as in the case of 1,1,3,3-tetrachloropropane,[2] calculated moment zero, observed, 0.75 *D*. Torsional oscillations create an additional polarization which becomes highly important in a case where a small or zero moment results from opposition of large group moments. In addition, the C–H moments in the terminal $-CH_2Cl$ group probably differ somewhat from those in the central methylene, adding another small component to the total moment.

Acknowledgment.—This work was supported by Research Corporation, and by an undergraduate research participation grant from the National Science Foundation.

(7) C. P. Smyth and K. B. McAlpine, *J. Am. Chem. Soc.*, **57**, 979 (1955).

(8) L. E. Sutton, *Proc. Roy. Soc.* (*London*), **113A**, 668 (1931).

PYROLYSIS OF ALLYL CHLORIDE

BY L. J. HUGHES AND W. F. YATES

Plastics Division Research Department, Monsanto Chemical Co., Texas City, Texas

Received July 11, 1960

Earlier work on the pyrolysis of allyl chloride has been concerned with the kinetics of dehydrochlorination[1,2] and identification of the products of the decomposition.[3] Goodall and Howlett[1] studied the pyrolysis at 370–475° and concluded that the reaction was a complex homogeneous, heterogeneous process. They found an activation energy for the over-all process of about 32 and 46 kcal./mole for the homogeneous component. The activation energy of the heterogeneous component was estimated to be 25 kcal.

Shilov[2] found an activation energy of 59.3 kcal./mole at 623° for the primary decomposition of allyl chloride.

Both of these authors indicate that the primary reaction is the loss of HCl to form allene. The allene then undergoes further reaction to give the liquid products described by Meinert and Hurd.[4]

Porter and Rust[3] on the other hand propose a mechanism based on positive identification of products which involves formation of the allyl radical as the primary step and subsequent reactions of the allyl radical by coupling or hydrogen extraction from another molecule, *i.e.*

$$CH_2{=}CHCH_2Cl \longrightarrow CH_2{=}CH{-}CH_2\cdot + Cl\cdot$$
$$2CH_2{=}CH{-}CH_2\cdot \longrightarrow CH_2{=}CHCH_2CH_2CH{=}CH_2$$
$$CH_2{=}CH{-}CH_2\cdot + RH \longrightarrow CH_2{=}CHCH_3 + R\cdot$$

These authors indicate that a change in mechanism may have taken place as the temperature of the reaction increased to 540°. However, Shilov indicates that allene and methylacetylene are the major products of the pyrolysis at a still higher temperature of 625°.

One is thus led to wonder whether there has been confusion as a result of inadequate identification of products by earlier workers or there is multiplicity of primary reactions occurring simultaneously.

Experimental

Allyl chloride from Shell Chemical Co. was distilled before use.

Dry nitrogen was passed through a rotameter to an allyl chloride reservoir which was immersed in a constant temperature bath set at 27°. The nitrogen was saturated with allyl chloride vapor by passing the gas through a sintered glass tip below the liquid surface. The resulting mixture, containing 400 mm. partial pressure of allyl chloride, was passed through a short preheater at 150° into the pyrolysis tube. The reactor was a 22 mm. i.d. quartz tube 23 inches long fitted with a 6 mm. o.d. thermowell and filled with 8–12 mesh, porous silicon carbide. The reactor was wrapped with a nichrome ribbon and insulated with high temperature pipe insulation.

The reactor was heated to the desired temperature while a stream of dry nitrogen was passed through. When the temperature had become stabilized the reactant mixture was started. The effluent was conducted through a cold water condenser, a water scrubber, a Dry Ice trap and a liquid nitrogen trap. The contents of the traps and any organic phase from the water scrubber were combined, weighed and analyzed by use of a gas-liquid partition chromatograph. The solution from the water scrubber was diluted to a standard volume and an aliquot titrated for HCl content. It may be appropriate to point out the great utility of the gas–liquid partition chromatograph in this type of study for both the analysis and isolation of the reaction products. For example by use of the chromatograph and infrared spectroscopy we found in addition to the major products, trace amounts of methane, acetylene, butenes, allene, methylacetylene, butadiene, chloropropenes, chlorobutadiene, toluene and styrene.

Results and Discussions

In the present investigation reaction products essentially identical with those of Porter and Rust were obtained when the pyrolysis was carried out at 540–725°. However by use of lower contact times, 0.8–1.0 sec., and a large surface to volume ratio, it was possible to substantially decrease the formation of tars and carbonaceous deposits.

The effect of the temperature on the relative yields of biallyl, 1,3-cyclohexadiene and benzene is shown in Table I. It can be seen that at low temperature, 540–575°, biallyl (1,5-hexadiene) is the major product. As the temperature is increased 1,3-cyclohexadiene becomes the major product and reaches a maximum between 600 and 630°. At temperatures above 630° the benzene yield increases until it is the major product. It is also significant that the yield of propylene increases rapidly and closely parallels the increase in benzene yield at higher temperature, see Table I.

(1) A. M. Goodall and K. E. Howlett, *J. Chem. Soc.*, 2596 (1954).

(2) A. E. Shilov, *Doklady Akad. Nauk, SSR*, **98**, 601 (1954); *C. A.*, **49**, 11605*f* (1955).

(3) L. M. Porter and F. F. Rust, *J. Am. Chem. Soc.*, **78**, 557 (1956).

(4) R. N. Meinert and C. D. Hurd, *ibid.*, **52**, 4540 (1930).

TABLE I

PYROLYSIS OF ALLYL CHLORIDE

Temp., °C.	Cont., sec.	Conv., %	% Yields[c] C_3H_6	C_6H_{10}	C_6H_8	C_6H_6
540–50[a]	1.04	15	0.5	16.5	5.5	2.3
570–80	1.00	8.9	..	20.0	7.1	3.1
600–10	0.97	17.0	..	11.5	18.5	10.7
630	.94	27.4	16.9	10.0	21.8	25.6
660–70	.90	47.2	15.2	3.2	4.1	35.3
720–65[b]	.83	99.5	41.6	..	..	58.0

[a] The pyrolysis tube was clean and "unseasoned." [b] Reaction too exothermic for good temperature control. [c] Based on allyl chloride. C_6H_{10}—biallyl; C_6H_8—cyclohexadiene.

The mechanism proposed by Porter and Rust may be used very well to explain the data presented in this paper.

$$CH_2{=}CHCH_2Cl \xrightarrow{\Delta} CH_2{=}CHCH_2\cdot + Cl\cdot \quad (1)$$

$$2CH_2{=}CH{-}CH_2\cdot \longrightarrow CH_2{=}CHCH_2CH_2CH{=}CH_2 \quad (2)$$

$$Cl\cdot + CH_2{=}CHCH_2Cl \longrightarrow CH_2{=}CH\dot{C}HCl + HCl \quad (3)$$

$$2CH_2{=}CH{-}\dot{C}HCl \longrightarrow C_6H_6 + 2HCl \quad (4)$$

$$CH_2{=}CHCH_2\cdot + CH_2{=}CH\dot{C}HCl \longrightarrow C_6H_8 + HCl \quad (5)$$

$$C_6H_8 \longrightarrow C_6H_6 + H_2 \quad (6)$$

$$CH_2{=}CHCH_2\cdot + RH \longrightarrow CH_2{=}CHCH_3 + R\cdot \quad (7)$$

At low temperatures the scission of allyl chloride to allyl radicals and chlorine atoms followed by coupling of two allyl radicals would be expected to play an important role in determining the products.

As the temperature is increased reaction 2 should be reversed. In fact reaction 2 may be written as a reversible process since the work of Hurd and Bollman[5] has shown that biallyl decomposes to propylene. Porter and Rust found the same reaction to give mainly propylene with about 10% of benzene and 2% of cyclohexene.

At moderate and high temperatures reaction 3 should become increasingly important from the increase in total Cl atom concentration and the increased energy of the system which will favor cleaving the C–H bond in allyl chloride. This in turn will increase the contribution of reactions 4 and 5.

Thermally and catalytically cyclohexadiene is reported to disproportionate to benzene and cyclohexane.[6] It is significant that in neither this work nor earlier work has there been an indication of cyclohexane as a product of the pyrolysis of allyl chloride, or the presence of enough hydrogen.

It seems likely therefore that the dehydrogenation of cyclohexadiene to benzene must proceed

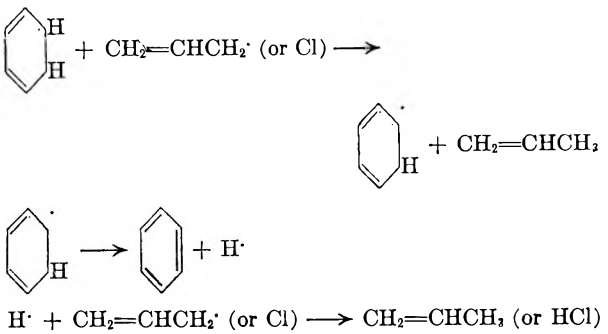

$$H\cdot + CH_2{=}CHCH_2\cdot \text{ (or Cl)} \longrightarrow CH_2{=}CHCH_3 \text{ (or HCl)}$$

This portion of the mechanism is also indicated by the fact that the production of propylene increases rapidly at higher temperatures where benzene becomes the major product.

A rough estimate of the activation energy for the over-all process was made using our data at 570–670°. A plot of log k *vs.* $1/T$ gave a straight line indicating that our data were consistent. The value of the activation energy obtained was 34.7 kcal./mole, which is in good agreement with the value of 32 kcal./mole found by Goodall and Howlett.[1]

(5) C. D. Hurd and H. T. Bollman, *ibid.*, **55**, 699 (1933).

(6) M. Ya. Kagan, *Problemy Kinetiki i Kataliza Akad Nauk SSSR*, **6**, *Geterogennyi Kataliz*, 232 (1949); *C. A.*, **49**, 15217b (1955).

COMMUNICATIONS TO THE EDITOR

POLYELECTROLYTE CONCENTRATION ON A POLARIZED MERCURY SURFACE

Sir:

It is not practical to employ the Gibbs adsorption isotherm in order to determine the polymer surface excess in the water–mercury interface. The area occupied by one polymeric molecule is very high and therefore the surface excess and the variation of the surface tension with the chemical potential of the polymer is too small to be determined with adequate accuracy. Moreover, as mercury surface cannot, because of contamination, be exposed for periods of time larger than about a minute, one often is unsure whether equilibrium has been reached. In the case of charged polyelectrolytes in the presence of salt, additional difficulties occur as a result of the contribution of the small ions to the surface tension. An alternative procedure to obtain the surface concentrations, based on the kinetics of adsorption, was tried on a series of polyelectrolytes and some of the results are presented in this communication.

For all the polymer investigated it was found that the equilibrium bulk concentration required to saturate the mercury surface is lower in order of magnitude than the polymer concentration used experimentally. If equilibrium between the surface and the adjacent layer is maintained at all times, the concentration near the surface $c_{x=0} \ll c_{bulk}$ while the droplet is growing and polymer is transfered into the surface. Under those conditions[1]

(1) P. Delahay and I. Trachtenberg, *J. Am. Chem. Soc.*, **79**, 2355 (1957); J. Koryta, *Coll. Czechoslov. Chem. Commun.*, **18**, 206 (1953).

i.e., in the case of a growing mercury droplet, the relation (1) holds

$$\Gamma_t = 0.745 c_b D^{1/2} t^{1/2} \qquad (1)$$

In the case of all the polymers examined, namely: polymethacrylic acid (PMA), polylysine (PL), sodium polyacrylate and polymethacrylate (NaPM) and poly 2- and 4-vinylpyridinium nitrate (PVP), a linear variation of differential capacity, surface charge density and surface tension with the square root of the age of the mercury droplet $t^{1/2}$ was found.

Assuming that eq. (1) holds, it follows that the mentioned surface properties are proportional to Γ_t. This suggests that in the case of incomplete polymer adsorption the surface can be subdivided into microphases of covered and uncovered areas.

The surface concentration Γ_{lim} of a fully packed but non-compressed surface can be obtained by considering the plot of one of the surface properties against bulk concentration, under various conditions of the surface, from the partly covered state to high concentrations, when the surface is fully occupied. In Fig. 1 and 2 the surface tension and differential capacity, respectively, are plotted *versus* bulk concentration of PMA $z = 3900$ at a given age "t" of the surface. A break in the curve is evident. The point where the first break in the curve occurs gives the critical bulk concentration at which the surface just becomes fully covered. From here and with the aid of eq. (1), the minimal concentration of the fully covered surface is obtained.

An estimate of the number of segments anchored in the mercury surface in the case of uncharged polymers was obtained from the differential capacity of surface charge density values by a procedure used in a previous publication.[2] In the case of fully ionized polyelectrolytes the number of segments anchored in the surface is related to the increment in surface charge density.

The fraction p (p = Number of anchored segments/Total number of segments in the surface) of segments anchored in the surface varies in most cases between about 0.1 and 1 depending on the polymer and on the surface potential. Only on the verge of desorption lower values of p than 0.1 are observed.

Some of the p values for different polymers at 25° are given in Table I.

TABLE I

Polymer	z	$-E$ relative to 1 N cal. electr.	Monomoles/cm.^{2} × 10^{10} lim	p
PMA	2900	0.6	13.4	0.41
		0.3		0.13
		1.0		0.25
	3900–9000	0.6	17–19	0.28–0.31
		0.3		0.1–0.11
		1.0		0.165–0.18
NaPM	3900	More positive than 0.35	2.1	0.5
4 PVP	1200	1.0	9	0.2
PL	40	0.4–0.6	2.4	1
		0.1		0.75
		1.0		0.75

(2) I. R. Miller and D. C. Grahame, *J. Am. Chem. Soc.*, **78**, 3577 (1956).

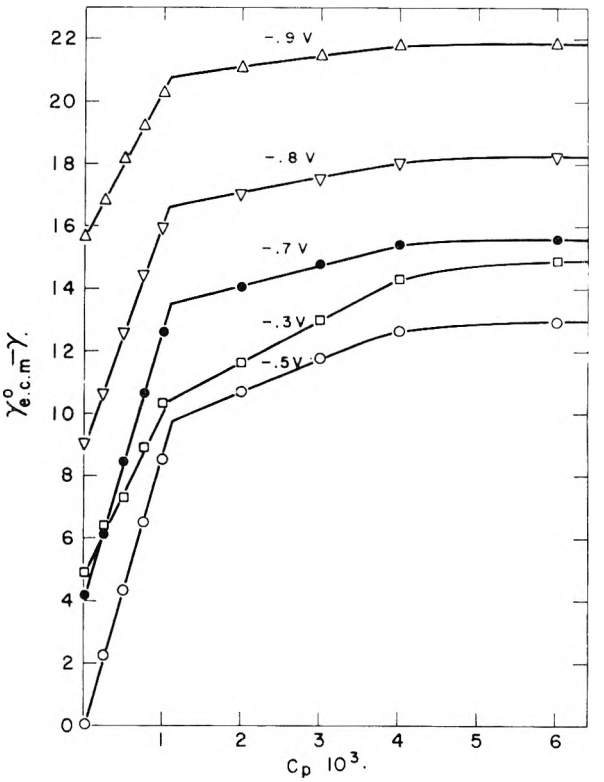

Fig. 1.—($\gamma^{\circ}_{c.c.m} - \gamma$) surface tension at electrocapillary maximum (supporting electrolyte only) minus surface tension under experimental conditions, against PMA concentration c_p; $z = 3900$, $T = 61°$, $t = 4.25$ sec.

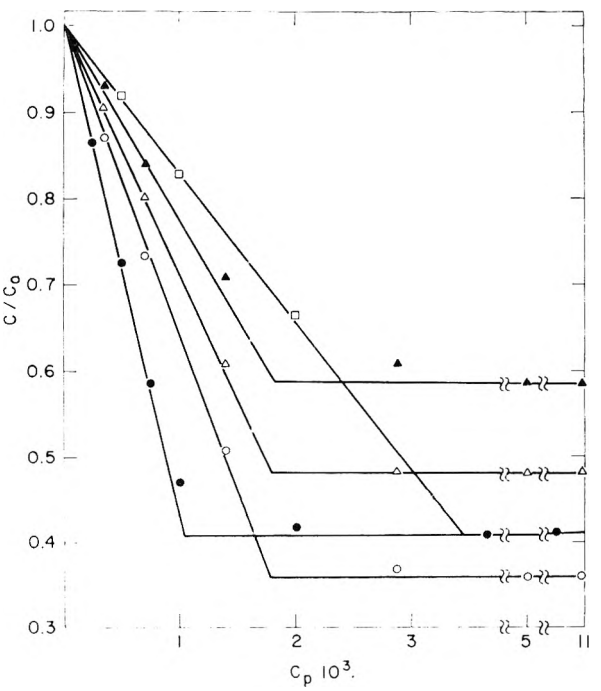

Fig. 2.—Differential capacity relative to differential capacity of supporting electrolyte (C/C_0) *versus* c_p: PMA $z = 3900$, $t = 3.75$ sec.

	T, °C.	$-E$ relative to N calomel electrode
○	25	0.60
△	25	0.40
▲	25	0.90
●	61	0.60
□	0	0.60

The anchored fractions p found in the present experiments are considerably higher than the fraction of anchored segments postulated by the theory of Simha, Frisch and Eirich.[3] A later theoretical treatment[4] for the case of appreciable adsorption energies shows much better agreement with our experimental results. The order of magnitude of the adsorption energy ϵ_0 can be estimated roughly by analogy with corresponding monomeric substances, at least for the case of un-ionized polymers near the electrocapillary maximum. The estimated ϵ_0 per methacrylic acid residue is 4–5 kT and per lysine residue is about 8–10 kT. The effective range of the forces R under these conditions is narrow and the approximate solution of eq. 14 in reference 4 which gives $\langle p \rangle$ = const. $\times$ $(1 - \theta)\alpha/R$ seems only of limited validity. Here α is the probability of a successful contact between segment and surface, and θ is the fraction of the surface covered. Close to the adsorption potentials, ϵ_0 is of the order of kT. $\langle p \rangle$, as postulated in reference 4 for this case, is $2\alpha(1 - \theta)(1 + \epsilon_0/kT)/(\pi f Z)^{1/2}$. The p's found in our experiments under these conditions are considerably higher and they depend very little on the molecular weight.

POLYMER DEPARTMENT
WEIZMANN INSTITUTE OF SCIENCE
REHOVOTH, ISRAEL I. R. MILLER

RECEIVED JULY 7, 1960

(3) R. Simha, H. L. Frisch and E. R. Eirich, *J. Phys. Chem.*, **57**, 584 (1953).

(4) H. L. Frisch, *ibid.*, **59**, 633 (1955).

SELF-DIFFUSION IN MOLTEN $PbCl_2$

Sir:

We have had occasion recently to repeat an earlier measurement of the self-diffusion coefficients of Pb^{210} and Cl^{36} in molten $PbCl_2$. The original paper[1] reported anomalous results for these quantities. The present results, although generally similar, are more nearly what might be expected for this system in the light of corresponding data for other systems. The experimental procedure employed in this work is described in detail in an earlier paper.[2] Since this procedure uses doubly labeled $PbCl_2$ as tracer, the two ions experience identical environments during the experiment and the measurement should be ideal for comparing the coefficients of the two species. This fact, together with the generally improved accuracy, leads us to prefer the present results, which are presented in Table I.

TABLE I

THE DIFFUSION COEFFICIENTS OF Pb^{210} AND Cl^{36} IN MOLTEN $PbCl_2$

Temp., °C.	$D_{Pb} \times 10^5$ cm.^{2} sec.$^{-1}$	$D_{Cl} \times 10^5$ cm.^{2} sec.$^{-1}$
510	0.997 ± 0.02	1.80 ± 0.05
518	1.05 ± 0.004	1.90 ± 0.03
533	1.12 ± 0.07	1.92 ± 0.07
546	1.13 ± 0.01	2.09 ± 0.07
556	1.26 ± 0.03	2.26 ± 0.03
566	1.37 ± 0.02	2.34 ± 0.03

It will be seen that a plot of log D *vs* $1/T$ for these data does not give the apparent discontinuity found in the earlier work.[1] These data fit very well a relationship of the form

$$D = A \exp(-\Delta H^*/RT), \text{ with}$$

$$D_{Pb} = 7.73 \times 10^{-4} \exp(-6777 \pm 643/RT)$$

and

$$D_{Cl} = 8.95 \times 10^{-4} \exp(-6099 \pm 483/RT)$$

ΔH is the energy of activation for diffusion, which shows no significant difference for the two ions within experimental error. This corresponds to the results reported for other systems.[3] However, there is no immediately apparent correlation between the diffusion coefficient and either the ionic radius or the ionic weight, as has been reported variously for other systems. As was the earlier experience, and as is usual in molten salts, neither the Nernst–Einstein nor Stokes–Einstein relations hold for this system. We are, at present, investigating the influence of a variety of factors on the diffusion coefficient and this work will be published within the coming year. We gratefully acknowledge the continuing financial support given this work by the Robert A. Welch Foundation.

GERALD PERKINS, JR.
NORTH TEXAS STATE COLLEGE R. B. ESCUE
DENTON, TEXAS JAMES F. LAMB
J. WAYNE WIMBERLEY

RECEIVED AUGUST 26, 1960

(1) G. Perkins, Jr., R. B. Escue, J. F. Lamb and T. H. Tidwell, THIS JOURNAL, **64**, 495 (1960).

(2) G. Perkins, Jr., R. B. Escue, J. F. Lamb, T. H. Tidwell and J. W. Wimberley, THIS JOURNAL, to be published.

(3) A. S. Dworkin, R. B. Escue and E. R. VanArtsdalen, THIS JOURNAL, **64**, 872 (1960).

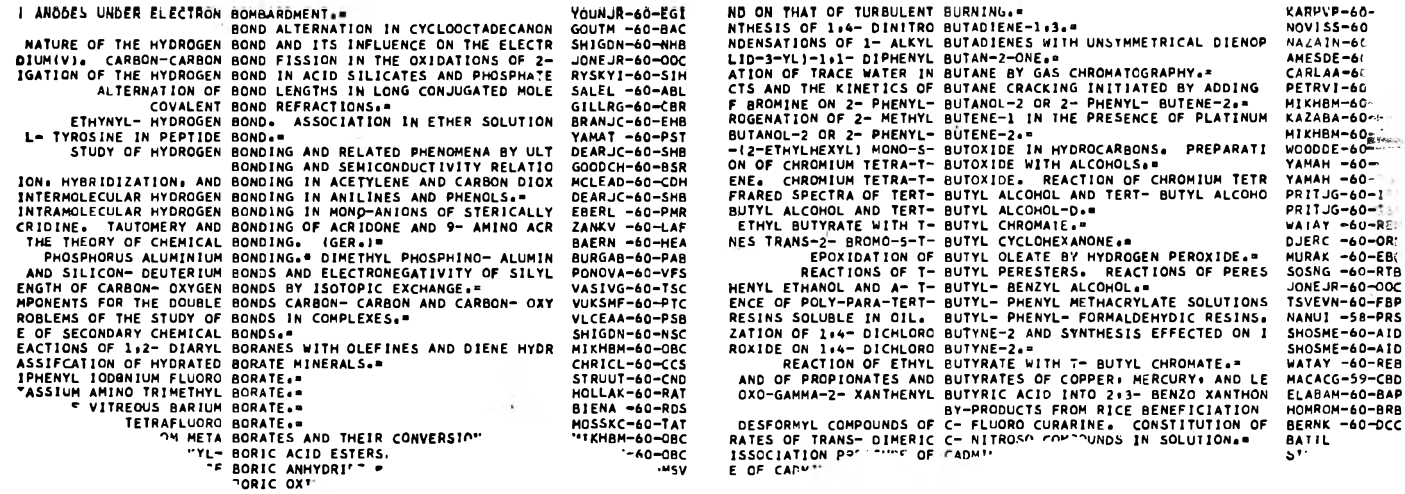

SAMPLE OF KEYWORD INDEX

announcing a new publication

CHEMICAL TITLES

the express service for increasing "current awareness" of new chemical research

● Starting in January 1961, CHEMICAL TITLES will be issued twice each month with each issue reporting approximately 3000 titles from the most recent chemical research. This service provides a current author and keyword index to selected chemical journals and is intended to fill the void between primary publication and the appearance of abstracts.

Taken from 575 journals—110 Russian—of pure and applied chemistry, these titles are listed for maximum convenience of use. The first part is a permuted title index in which keywords from each title are arranged alphabetically with each keyword in full or partial context. The second part is an alphabetical index of authors together with full titles of papers and journals in which they appear. You can find a source in a minute.

Timeliness matches ease of use. All titles are found in the listing *within two weeks of the time they are received* in the offices of The Chemical Abstracts Service, the publisher. No other index or alerting service provides such prompt and complete coverage.

Prices and discounts follow:

	Base Rate	Rate per Volume College and University	ACS Member
1st–10th subscriptions (each)	$65	$50	$50*
Additional 11th–25th subscriptions (each)	45	45	...
26th and each succeeding subscription	30	30	...

*Single subscription only

ORDER FROM: CIRCULATION DEPARTMENT • AMERICAN CHEMICAL SOCIETY
1155 SIXTEENTH STREET, N.W. • WASHINGTON 6, D.C.